AD-A070 535 NAVAL UNDERSEA CENTER SAN DIEGO CA F/G 11/9
ACRYLIC PLASTIC VIEWPOINT FOR OCEAN ENGINEERING APPLICATIONS. V--ETC(U)
FEB 77 J D STACHIW
UNCLASSIFIED NUC-TP-562-VOL-1 NL

1 OF 5
AD
A070535

AD A070535

DDC FILE COPY

TP 562

Volume I

Acrylic Plastic Viewports For Ocean Engineering Applications

LEVEL II

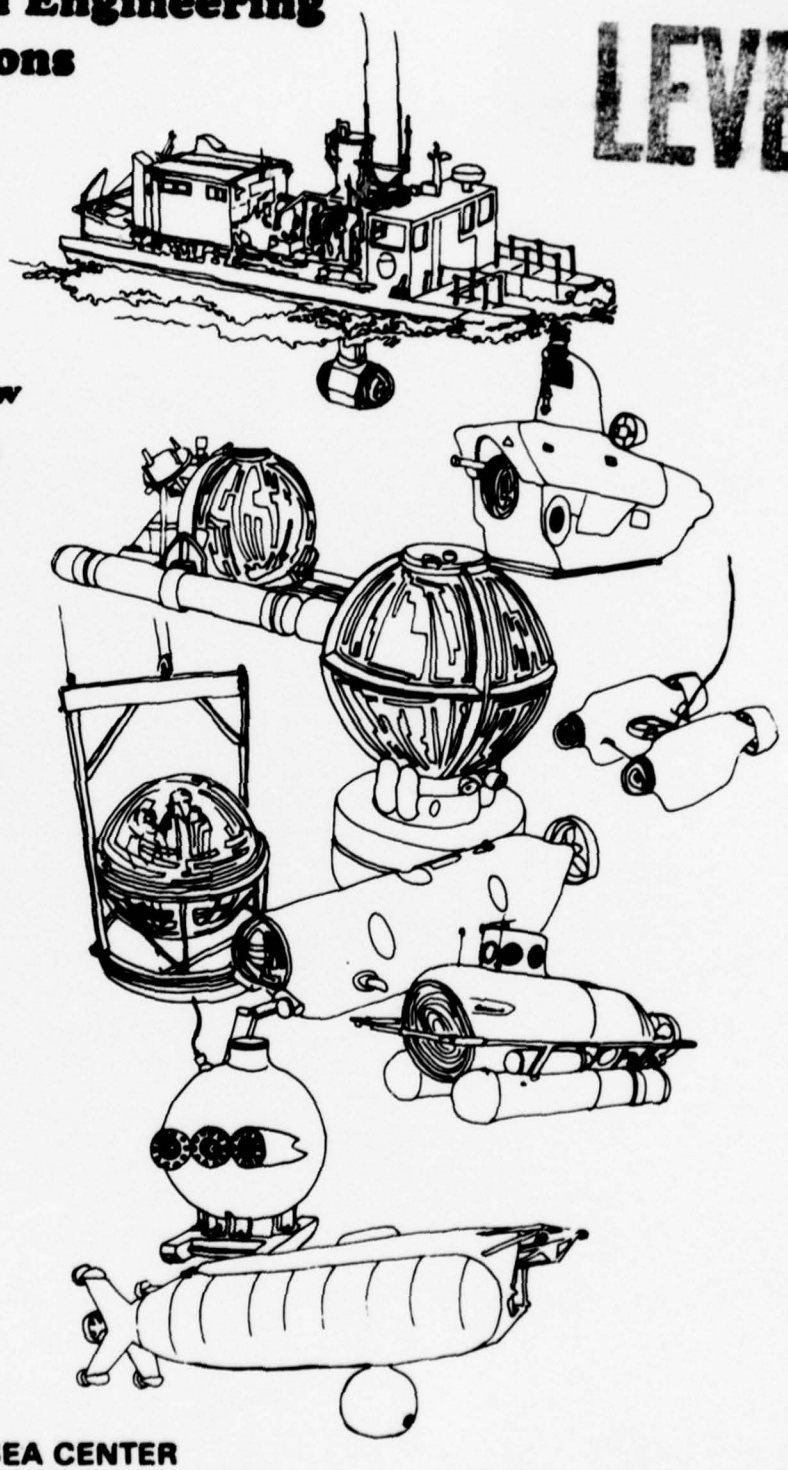

by J.D. Stachiw

February 1977

DD
JUN 28
A

NAVAL UNDERSEA CENTER
SAN DIEGO, CALIFORNIA 92132

Approved for public release; distribution unlimited.

LEVEL II (12)

ACRYLIC PLASTIC VIEWPORTS FOR OCEAN ENGINEERING APPLICATIONS

by

J. D. Stachiw

AD70-537 appendices
V. 2 - AD70 536

DDC
RECEIVED
JUN 28 1979
A

February 1977

Sponsored By

Naval Facilities Engineering Command
Alexandria, Virginia 22332

79 06 28 015

NAVAL UNDERSEA CENTER, SAN DIEGO, CA. 92132

AN ACTIVITY OF THE NAVAL MATERIAL COMMAND

R. B. GILCHRIST, CAPT, USN
Commander

HOWARD L. BLOOD, PhD
Technical Director

ADMINISTRATIVE INFORMATION

This design handbook summarizes research on viewports with acrylic plastic windows. Its preparation was supported by the Naval Facilities Engineering Command and the Director of Navy Laboratories.

Released by

H. R. Talkington, Head
Ocean Technology Department

ACKNOWLEDGEMENTS

This handbook represents not only the efforts of the author but also those of researchers without whose data the formulation of the design guidelines would not have been feasible. Section 1 was authored by J. L. Atkerson of the New York Historical Society; section 2 by H. Mukamal, N. G. Nixon, and W. Yamaguchi of Swedlow, Inc.; section 5 by J. L. Stachiw of San Diego City Schools; section 14 by J. J. Lones of Adroit Engineering; and section 15 by the Committee on Viewports, Ocean Engineering Division, American Society of Mechanical Engineers. All other sections and appendices are the work of J. D. Stachiw of the Ocean Technology Department.

UNCLASSIFIED

SECURITY CLASSIFICATION OF THIS PAGE *(When Data Entered)*

REPORT DOCUMENTATION PAGE		READ INSTRUCTIONS BEFORE COMPLETING FORM
1. REPORT NUMBER NUC TP 562	2. GOVT ACCESSION NO.	3. RECIPIENT'S CATALOG NUMBER
4. TITLE *(and Subtitle)* (6) ACRYLIC PLASTIC VIEWPORTS FOR OCEAN ENGINEERING APPLICATIONS. Volume I.		5. TYPE OF REPORT & PERIOD COVERED (9) Research Report. 6. PERFORMING ORG. REPORT NUMBER
7. AUTHOR(s) (10) J. D. Stachiw		8. CONTRACT OR GRANT NUMBER(s)
9. PERFORMING ORGANIZATION NAME AND ADDRESS Naval Undersea Center San Diego, CA		10. PROGRAM ELEMENT, PROJECT, TASK AREA & WORK UNIT NUMBERS
11. CONTROLLING OFFICE NAME AND ADDRESS Naval Facilities Engineering Command Alexandria, VA 22332		(11) 12. REPORT DATE February 1977 13. NUMBER OF PAGES 38
14. MONITORING AGENCY NAME & ADDRESS *(if different from Controlling Office)* (14) NUC-TP-562-Vol-1		15. SECURITY CLASS. *(of this report)* UNCLASSIFIED 15a. DECLASSIFICATION/DOWNGRADING SCHEDULE

16. DISTRIBUTION STATEMENT *(of this Report)*

Approved for public release; distribution unlimited. (12) 459 p.

17. DISTRIBUTION STATEMENT *(of the abstract entered in Block 20, if different from Report)*

18. SUPPLEMENTARY NOTES

19. KEY WORDS *(Continue on reverse side if necessary and identify by block number)*

20. ABSTRACT *(Continue on reverse side if necessary and identify by block number)*

For safe performance, viewports in pressure vessels for human occupancy require windows that are designed according to conservative engineering principles and fabricated from optical material with proven structural properties. This design handbook presents to the prospective viewport designer a succinct summary of existing data and recommended guidelines for using these data in the design, fabrication, and acceptance testing of acrylic plastic windows.

390 458

DD FORM 1 JAN 73 1473 EDITION OF 1 NOV 65 IS OBSOLETE
S/N 0102-LF-014-6601

UNCLASSIFIED

SECURITY CLASSIFICATION OF THIS PAGE *(When Data Entered)*

70 06 28 015

20. ABSTRACT (continued)

Guidelines are presented for windows operating in the range of -15 to +20,000 pounds per square inch and -40 to 151°F. By utilizing these guidelines a cyclic fatigue life of 10,000 cycles with 40,000 hours of sustained pressurization over a period of 10 years can be assured. Greater cyclic fatigue life or longer sustained loading durations can also be achieved, but the designer must develop design criteria whose safety factors exceed those incorporated in the design guidelines of this handbook.

Specifications for acrylic plastic are given to ensure procurement of material whose performance will satisfy the structural, optical, and longevity criteria of this handbook. Samples of quality control forms are also included which, when filled completely out, will constitute acceptable documentation for subsequent safety design review and certification procedures.

SUMMARY

For safe performance, viewports in pressure vessels for human occupancy require windows that are designed according to conservative engineering principles and fabricated from optical material with proven structural properties. This design handbook presents to the prospective viewport designer a succinct summary of existing data and recommended guidelines for using these data in the design, fabrication, and acceptance testing of acrylic plastic windows.

Guidelines are presented for windows operating in the range of -15 to +20,000 pounds per square inch and -40 to 151°F. By utilizing these guidelines a cyclic fatigue life of 10,000 cycles with 40,000 hours of sustained pressurization over a period of 10 years can be assured. Greater cyclic fatigue life or longer sustained loading durations can also be achieved, but the designer must develop design criteria whose safety factors exceed those incorporated in the design guidelines of this handbook.

Specifications for acrylic plastic are given to ensure procurement of material whose performance will satisfy the structural, optical, and longevity criteria of this handbook. Samples of quality control forms are also included which, when filled completely out, will constitute acceptable documentation for subsequent safety design review and certification procedures.

Accession For
NTIS GRA&I
DDC TAB
Unannounced
Justification
By
Distribution/
Availability Codes
Dist. | Avail and/or special
A

PREFACE

In the early era of submersibles, each component of the system, including viewports, had to be subjected to an extensive test program before its incorporation into a manned submersible system.

Ocean engineers had to repeat this design validation process for each viewport design. Some published the results of their test programs; however, others because of lack of initiative, shortage of resources, or restrictive company policy did not and thus hampered the development of viewport technology.

After approximately three decades of viewport development, there are sufficient published data to warrant a brief summary and review of this technology. It is the purpose of this review, i.e., this handbook, to highlight areas where adequate information is lacking. It is hoped that such an approach will be of value both to designers, i.e., the design of pressure hulls will be expedited by using proven viewport configurations, and to researchers, i.e., significant progress in unresearched areas will be achieved with a minimum of time needed for a literature search.

Several approaches could have been used in summarizing and reviewing published studies on viewport development. The approach chosen is a design handbook rather than a research monograph. The selection of this approach was based on the premise that the viewport designer is the key element in providing safe viewports for pressure-resistant hulls of submersible habitats, personnel transfer capsules, and deck compression and medical treatment chambers. If the designer is aware of all factors that affect the performance of an acrylic plastic window, a sound engineering appraisal of these factors can be used as the basis for a safe viewport design.

This report particularly reflects this design handbook philosophy in section 12 and the three appendices. Factors such as materials, fabrication processes, distribution of stresses and strains in selected window shapes, critical pressures, and surface finishes are discussed from the viewpoint of a designer. Since this is the person ultimately responsible for the performance of the viewport in service, all pertinent information is presented in a manner that will make the designer's decision valid. To help achieve this, an attempt has been made to differentiate between guidelines based on facts and guidelines based on postulates. Guidelines based on facts represent firm conclusions that can be applied with confidence, while guidelines based on the author's postulates must be applied with caution as they represent only informed engineering opinions that future studies may prove inaccurate.

Although there is adequate information in the book for the design of any viewport shape by a competent ocean engineer, a special chapter has been included that makes the design of standard viewport shapes a "cookbook" approach. The fifteenth chapter is a reprint of the sixteenth draft of appendix A in the ANSI/ASME Safety Standard for Pressure Vessels for Human Occupancy (PVHO). It represents in a condensed form the engineering judgment of experts on the proper design, materials, fabrication, and acceptance test procedures for acrylic windows in viewports of manned submersibles.

Windows designed on the basis of rules specified by ANSI/ASME Safety Standard PVHO-1, Appendix A, have amassed an enviable safety record, i.e., there has been no loss of life because of window failure. Because the safety standard is accepted by many domestic and foreign regulatory agencies, insurance societies, and classification societies, it is highly recommended as a design basis for prospective viewport designers. The designer must remember, however, that the safety standard is subject to periodic revisions by ASME and that it is

always necessary to ascertain what changes have been made. As a rule, these revisions tend to make the safety standard less, rather than more, conservative; thus section 15 will probably remain a reliable and conservative design guide for standard acrylic window shapes.

Two sections in this book are not directly applicable to design, but are background material. Section 1 is a historical discussion of the development of viewport technology, and section 3 introduces the sources of data subsequently utilized as the basis for the design guidelines. It is believed that the designer who develops a historical perspective of viewport technology and understands the limitations of the data sources is in a good position to apply the information within this book to design standard, or to develop, viewport shapes.

In addition to the 15 sections, this book also contains three appendices with detailed experimental and fabrication data. These data have been placed in appendices to make basic data available to the designer without the use of reference materials. The appendices become especially valuable for the design of windows whose operational requirements differ drastically from those forming the basis of the ANSI/ASME Safety Standard PVHO-1. In such a case, the designer must consult the basic data contained in the appendices and formulate safety factors that surpass those in the ANSI/ASME Safety Standard PVHO-1.

It is hoped that this handbook will satisfy an existing need on the part of designers, researchers, and students for an overview of acrylic plastic viewport technology. Hopefully the field of viewport technology will continue to grow rapidly and thus make this book obsolete in a rather short time. Perhaps at that time the information contained in this book will be updated, expanded, and rearranged to reflect the higher level of sophistication in the field of viewport technology.

CONTENTS

SECTION 1. THE QUEST FOR PANORAMIC VISION UNDERWATER . . . 1-1

1.1 INTRODUCTION . . . 1-1

1.2 BATHYSPHERE . . . 1-2

1.3 TRIESTE . . . 1-3

1.4 WINDOW DESIGN (TRIESTE TYPE) . . . 1-4

1.5 MORAY, DEEP JEEP, AND DOWB . . . 1-5

1.5.1 MORAY . . . 1-5
1.5.2 DEEP JEEP . . . 1-5
1.5.3 DOWB . . . 1-6

1.6 PANORAMIC WINDOWS . . . 1-6

1.7 ACRYLIC PLASTIC SUBMERSIBLES . . . 1-8

1.8 SUMMARY . . . 1-10

1.9 REFERENCES . . . 1-11

1.10 BIBLIOGRAPHY . . . 1-11

SECTION 2. INTRODUCTION TO ACRYLIC PLASTIC . . . 2-1

2.1 INTRODUCTION TO PLASTICS . . . 2-1

2.2 INTRODUCTION TO ACRYLIC . . . 2-2

2.3 MANUFACTURE OF ACRYLIC MONOMER . . . 2-3

2.4 ACRYLIC POLYMERIZATION . . . 2-3

2.5 MODIFICATION OF ACRYLIC . . . 2-5

2.6 CONVERSION OF ACRYLIC RESIN . . . 2-7

2.7 ACRYLIC PROPERTIES . . . 2-17

2.8 COMPARISON OF ACRYLICS . . . 2-20

2.9 CHEMICAL RESISTANCE . . . 2-26

2.10 PRODUCTS MADE FROM ACRYLICS . . . 2-27

2.11 DESIGN CONSIDERATIONS . . . 2-38

2.12 THERMOFORMING ACRYLIC . . . 2-38

2.13 MACHINING ACRYLIC . . . 2-42

2.14 SANDING, POLISHING, AND CLEANING ACRYLIC . . . 2-46

2.15 SURFACE COATINGS AND TEXTURING . . . 2–46

2.16 JOINING ACRYLICS . . . 2-51

2.17 LAMINATION . . . 2-53

2.18 SUMMARY . . . 2-57

SECTION 3. SOURCES OF WINDOW DESIGN DATA . . . 3-1

3.1 INTRODUCTION . . . 3-1

3.2 EVALUATION OF STRUCTURES . . . 3-2

3.2.1 Viewports . . . 3-2
3.2.2 Pressure Hulls . . . 3-8

3.3 EVALUATION OF MATERIAL . . . 3-9

3.3.1 Short-Term Data . . . 3-10
3.3.2 Long-Term Data . . . 3-13

SECTION 4. STRUCTURAL PROPERTIES OF MONOLITHIC CAST ACRYLIC PLASTIC . . . 4-1

4.1 INTRODUCTION . . . 4-1

4.2 PLASTIC DESIGN CONSIDERATIONS . . . 4-2

4.2.1 General Comments . . . 4-2
4.2.2 Strength Values Permitted by Design . . . 4-2
4.2.3 Notch Sensitivity and Crazing . . . 4-2
4.2.4 Factors Affecting Structural Properties . . . 4-9

4.3 SHORT-TERM MECHANICAL PROPERTIES . . . 4-11

4.3.1 Tensile Loading . . . 4-11
4.3.2 Flexural Loading . . . 4-12

4.3.3 Shear Loading . . . 4-13
4.3.4 Impact Loading . . . 4-13
4.3.5 Compressive Loading . . . 4-15
4.3.6 Flammability . . . 4-16

4.4 LONG-TERM MECHANICAL PROPERTIES . . . 4-16

4.4.1 Tensile Loading . . . 4-18
4.4.2 Flexural Loading . . . 4-19
4.4.3 Compressive Loading . . . 4-20
4.4.4 Intermittent Loading . . . 4-22

4.5 CONCLUSIONS . . . 4-24

4.6 REFERENCES . . . 4-26

SECTION 5. FOULING AND WEATHERING OF ACRYLIC PLASTIC . . . 5-1

5.1 INTRODUCTION . . . 5-1

5.2 FOULING . . . 5-1

5.3 WEATHERING . . . 5-4

5.4 SUBMERGENCE . . . 5-7

5.5 REFERENCES . . . 5-8

SECTION 6. PRESSURE-RESISTANT WINDOWS . . . 6-1

6.1 INTRODUCTION . . . 6-1

6.2 WINDOW CLASSIFICATIONS . . . 6-1

6.2.1 Window Shapes . . . 6-2
6.2.2 Window Curvatures . . . 6-2
6.2.3 Bearing Surfaces . . . 6-2

6.3 SUMMARY . . . 6-3

SECTION 7. PLANE DISC WINDOWS WITH FLAT BEARING SURFACES . . . 7-1

7.1 INTRODUCTION . . . 7-1

7.2 STRUCTURAL PERFORMANCE . . . 7-2

7.3 MODES OF FAILURE . . . 7-2

7.4 PREDICTION OF CRITICAL PRESSURES . . . 7-3

7.5 SEATING . . . 7-5

7.5.1 Bearing Support . . . 7-5
7.5.2 Bearing Gasket(s) . . . 7-5
7.5.3 Sealing . . . 7-6
7.5.4 Retainer Ring . . . 7-6
7.5.5 Window Mounting . . . 7-6

7.6 FABRICATION OF WINDOWS . . . 7-6

7.7 RESISTANCE TO IMPULSE AND POINT-IMPACT LOADING . . . 7-7

7.8 REFERENCES . . . 7-8

SECTION 8. PLANE RECTANGULAR WINDOWS . . . 8-1

8.1 INTRODUCTION . . . 8-1

8.2 STRUCTURAL PERFORMANCE . . . 8-1

8.3 MODE OF FAILURE . . . 8-1

8.4 PREDICTION OF CRITICAL PRESSURES . . . 8-2

8.5 SEATING . . . 8-4

8.5.1 Bearing Support . . . 8-4
8.5.2 Bearing Gaskets . . . 8-4
8.5.3 Sealing . . . 8-5
8.5.4 Retaining Methods . . . 8-5
8.5.5 Window Cavity . . . 8-5

8.6 FABRICATION . . . 8-5

8.7 RESISTANCE TO IMPULSE AND POINT LOADING . . . 8-6

8.8 CONCLUSION . . . 8-6

8.9 REFERENCES . . . 8-6

SECTION 9. PLANE DISC WINDOWS WITH CONICAL BEARING SURFACES . . . 9-1

9.1 INTRODUCTION . . . 9-1

9.2 STRUCTURAL PERFORMANCE . . . 9-2

9.3 MODES OF FAILURE . . . 9-3

9.3.1 Short-Term Loading . . . 9-3

9.3.1.1 Critical Pressure . . . 9-3
9.3.1.2 Displacement and Deformation . . . 9-5

9.3.2 Long-Term Loading . . . 9-6

9.3.2.1 Critical Pressure . . . 9-6
9.3.2.2 Displacement and Deformation . . . 9-7
9.3.2.3 Bearing Surface Deterioration . . . 9-11

9.3.3 Cyclic Loading . . . 9-12

9.3.3.1 Critical Pressure . . . 9-12
9.3.3.2 Displacement and Distortion . . . 9-12
9.3.3.3 Bearing Surface Deterioration . . . 9-13

9.4 PREDICTION OF CRITICAL PRESSURES . . . 9-13

9.5 SEATING OF WINDOWS . . . 9-17

9.5.1 Conical Angle . . . 9-17
9.5.2 Bearing Surfaces . . . 9-18

9.5.2.1 Friction . . . 9-18
9.5.2.2 Crack Initiation . . . 9-18
9.5.2.3 Rotation of Bearing Surfaces . . . 9-19

9.5.3 Sealing and Retaining . . . 9-20

9.6 FABRICATION . . . 9-21

9.6.1 Dimensional Tolerances . . . 9-21
9.6.2 Surface Finish . . . 9-22
9.6.3 Chamfering . . . 9-22

9.7 RESISTANCE TO IMPULSE AND POINT LOADING . . . 9-23

9.7.1 Impulse Loading . . . 9-23
9.7.2 Point-Impact Loading . . . 9-24

9.7.2.1 Resistance to Fracture . . . 9-24
9.7.2.2 Failure Mode . . . 9-26

9.8 NONSTANDARD WINDOWS . . . 9-27

9.9 CONCLUSION . . . 9-27

9.10 REFERENCES . . . 9-27

SECTION 10. PLANE DISC WINDOWS WITH TWIN CONICAL BEARING SURFACES . . . 10-1

10.1 INTRODUCTION . . . 10-1

10.2 STRUCTURAL PERFORMANCE . . . 10-2

10.3 MODES OF FAILURE . . . 10-3

10.4 CRITICAL PRESSURES . . . 10-3

10.4.1 Short-Term Loading . . . 10-3
10.4.2 Long-Term Loading . . . 10-3
10.4.3 Cyclic Loading . . . 10-6

10.5 SEATING . . . 10-6

10.6 SEALING . . . 10-8

10.6.1 Design A . . . 10-8
10.6.2 Design B . . . 10-8
10.6.3 Design C . . . 10-8
10.6.4 Design D . . . 10-8

10.7 FABRICATION . . . 10-9

10.8 RESISTANCE TO UNDERWATER EXPLOSIONS AND POINT-IMPACT LOADING . . . 10-9

10.9 CONCLUSION . . . 10-9

10.10 REFERENCE . . . 10-10

SECTION 11. SPHERICAL SECTOR WINDOWS . . . 11-1

11.1 INTRODUCTION . . . 11-1

11.2 SPHERICAL SHELL SECTORS WITH CONICAL BEARING SURFACES . . . 11-2

11.2.1 Structural Performance . . . 11-3

11.2.1.1 Distribution of Stresses . . . 11-3
11.2.1.2 Buckling . . . 11-4

11.2.2 Modes of Failure . . . 11-6

11.2.2.1 Short-Term Loading . . . 11-6
11.2.2.2 Long-Term Loading . . . 11-8

11.2.2.3 Cyclic Pressurization . . . 11-10
11.2.2.4 Impact Loading . . . 11-13
11.2.2.5 Dynamic Pressure Loading . . . 11-15

11.2.3 Prediction of Implosion Pressure . . . 11-16
11.2.4 Mounting of Sectors in Flanges . . . 11-17

11.2.4.1 Seating . . . 11-17
11.2.4.2 Attachment . . . 11-18
11.2.4.3 Sealing . . . 11-18

11.2.5 Fabrication . . . 11-19

11.2.5.1 Free-Form Blowing . . . 11-19
11.2.5.2 Vacuum Forming . . . 11-20
11.2.5.3 Casting . . . 11-20

11.3 MODIFIED SPHERICAL SHELL SECTORS . . . 11-21

11.3.1 Spherical Shell Sectors with Restrained Edges . . . 11-21

11.3.1.1 Design . . . 11-21
11.3.1.2 Sealing . . . 11-21
11.3.1.3 Structural Performance . . . 11-21
11.3.1.4 Operational Performance . . . 11-22

11.3.2 Spherical Sector with Equatorial Flange . . . 11-23

11.3.2.1 Design . . . 11-23
11.3.2.2 Structural Performance . . . 11-23
11.3.2.3 Operational Performance . . . 11-24

11.3.3 Spherical Sector with Spherical Bearing Surface . . . 11-25

11.3.3.1 Design . . . 11-25
11.3.3.2 Structural Performance . . . 11-25

11.3.4 Spherical Sector with Toroidal Bearing Surface . . . 11-26

11.4 CONCLUSION . . . 11-27

11.5 REFERENCES . . . 11-27

SECTION 12. SPHERICAL PRESSURE HULLS . . . 12-1

12.1 INTRODUCTION . . . 12-1

12.2 STRUCTURAL PERFORMANCE . . . 12-2

12.2.1 Internal Pressure . . . 12-2
12.2.2 External Pressure . . . 12-3

12.2.2.1 Definition of Ideal Spheres . . . 12-3
12.2.2.2 Short-Term Pressurization . . . 12-4

12.2.2.2.1 Critical Pressure . . . 12-4
12.2.2.2.2 Deformations . . . 12-6

12.2.2.3 Long-Term Pressurization . . . 12-7

12.2.2.3.1 Critical Pressure . . . 12-7
12.2.2.3.2 Mechanism of Implosion . . . 12-8
12.2.2.3.3 Deformations . . . 12-9

12.2.2.4 Cyclic Pressurization . . . 12-10

12.2.3 Spheres With Penetrations Under External Pressure . . . 12-12

12.2.3.1 Definition of Spheres with Penetrations . . . 12-12
12.2.3.2 Design Characteristics of Spherical Cone Penetrations with Removable Closures . . . 12-13
12.2.3.3 Structural Performance of Ideal Spheres with Penetrations . . . 12-13

12.2.3.3.1 Short-Term Pressurization . . . 12-13
12.2.3.3.2 Long-Term Pressurization . . . 12-14
12.2.3.3.3 Cyclic Pressurization . . . 12-16
12.2.3.3.4 Dynamic Pressurization . . . 12-18

12.2.3.4 Design of Spherical Acrylic Pressure Vessels for Human Occupancy . . . 12-19

12.2.3.4.1 Structural Design . . . 12-19
12.2.3.4.2 Attachments . . . 12-20

12.2.3.5 Fabrication of Acrylic Spheres . . . 12-22

12.2.3.5.1 Thermoforming . . . 12-22
12.2.3.5.2 Casting . . . 12-23

12.2.3.6 Repair of Damaged Acrylic Spheres . . . 12-23

12.3 REFERENCES . . . 12-25

SECTION 13. CYLINDRICAL WINDOWS . . . 13-1

13.1 INTRODUCTION . . . 13-1

13.2 INTERNAL PRESSURE . . . 13-2

13.2.1 Structural Response . . . 13-2
13.2.2 Mode of Failure . . . 13-4
13.2.3 Design . . . 13-5
13.2.4 Mounting and Sealing . . . 13-6
13.2.5 Impact Protection . . . 13-7

13.3 EXTERNAL PRESSURE . . . 13-7

13.3.1 Structural Response . . . 13-7
13.3.2 Modes of Failure . . . 13-8
13.3.3 Design . . . 13-10
13.3.4 Mounting . . . 13-17
13.3.5 Sealing . . . 13-17
13.3.6 Attachment . . . 13-18

13.4 FABRICATION . . . 13-18

13.4.1 Monocoque Cylinders . . . 13-18
13.4.2 Stiffened Cylinders . . . 13-19

13.5 CONCLUSION . . . 13-20

13.6 REFERENCES . . . 13-20

13.7 BIBLIOGRAPHY . . . 13-20

SECTION 14. OPTICAL CHARACTERISTICS OF ACRYLIC WINDOWS . . . 14-1

14.1 OPTICAL PROPERTIES OF MATERIALS . . . 14-1

14.2 IMAGERY IN VIEWING MEDIA . . . 14-6

14.2.1 Photographic Sensing . . . 14-6
14.2.2 Refractive Index of Water . . . 14-7

14.3 OPTICAL GEOMETRY OF VIEWPORTS . . . 14-8

14.3.1 Plane Window . . . 14-8
14.3.2 Dome Window . . . 14-10
14.3.3 Binocular Viewing with a Single-Dome Viewport . . . 14-14

14.4 RAY TRACING AND LIGHT PIPES . . . 14-16

14.4.1 Dowell Ray Trace . . . 14-17
14.4.2 Light Pipes . . . 14-18

14.5 COMPARISONS AND CONCLUSIONS . . . 14-19

14.6 REFERENCES . . . 14-19

SECTION 15. SAFETY STANDARD FOR VIEWPORTS IN PRESSURE VESSELS FOR HUMAN OCCUPANCY . . . 15-1

15.1 INTRODUCTION . . . 15-1

15.2 DISCUSSION . . . 15-1

15.3 ANSI/ASME SAFETY STANDARD PVHO-1, APPENDIX A . . . 15-4

15.4 IN-SERVICE INSPECTION OF VIEWPORTS . . . 15-79

APPENDIX A. CONSTRUCTION OF ACRYLIC SPHERES . . . A-1

A.1 CONSTRUCTION BY BONDING THERMOFORMED SPHERICAL PENTAGONS . . . A-1

A.1.1 Fabrication . . . A-1
A.1.2 Construction . . . A-2
A.1.3 Quality Control . . . A-3
A.1.4 Conclusion . . . A-5
A.1.5 Bibliography . . . A-5

A.2 CONSTRUCTION BY BONDING OF CAST HEMISPHERES . . . A-19

A.2.1 Tooling . . . A-19
A.2.2 Casting Process . . . A-20
A.2.3 Inspection of Castings . . . A-21
A.2.4 Fabrication of Spherical Hull . . . A-22
A.2.5 Inspection of Assembled Sphere . . . A-23
A.2.6 Findings . . . A-24
A.2.7 Conclusion . . . A-24
A.2.8 Bibliography . . . A-24

APPENDIX B. CRITICAL PRESSURES AND DISPLACEMENTS OF CONICAL FRUSTUMS . . . B-1

B-1 SHORT-TERM PRESSURE LOADING . . . B-1

B.1.1 Critical Pressures (Varying Included Angle) . . . B-3
B.1.2 Axial Displacements (Varying Included Angle) . . . B-11
B.1.3 Critical Pressures (Varying Temperatures) . . . B-19
B.1.4 Axial Displacements (Varying Temperatures) . . . B-30

B-2 LONG-TERM PRESSURE LOADING . . . B-52

B.2.1 Axial Displacements (5000 Pounds Per Square Inch) . . . B-54
B.2.2 Axial Displacements (10,000 Pounds Per Square Inch) . . . B-63
B.2.3 Axial Displacements (20,000 Pounds Per Square Inch) . . . B-73
B.2.4 Permanent Deformations . . . B-91

APPENDIX C. CRITICAL PRESSURES AND DISPLACEMENTS OF SPHERICAL SECTORS . . . C-1

C.1 SHORT-TERM PRESSURE LOADING . . . C-1

C.1.1 Critical Pressures . . . C-2
C.1.2 Sliding Displacement . . . C-15
C.1.3 Axial Displacement . . . C-22

C.2 LONG-TERM PRESSURE LOADING . . . C-29

C.2.1 Time-Dependent Sliding Displacement . . . C-30
C.2.2 Time-Dependent Axial Displacement . . . C-37

SECTION 1. THE QUEST FOR PANORAMIC VISION UNDERWATER . . . 1-1

1.1 INTRODUCTION . . . 1-1

1.2 BATHYSPHERE . . . 1-2

1.3 TRIESTE . . . 1-3

1.4 WINDOW DESIGN (TRIESTE TYPE) . . . 1-4

1.5 MORAY, DEEP JEEP, AND DOWB . . . 1-5

1.5.1 MORAY . . . 1-5
1.5.2 DEEP JEEP . . . 1-5
1.5.3 DOWB . . . 1-6

1.6 PANORAMIC WINDOWS . . . 1-6

1.7 ACRYLIC PLASTIC SUBMERSIBLES . . . 1-8

1.8 SUMMARY . . . 1-10

1.9 REFERENCES . . . 1-11

1.10 BIBLIOGRAPHY . . . 1-11

SECTION 1.
THE QUEST FOR PANORAMIC VISION UNDERWATER*

1.1 INTRODUCTION

The history of submersibles and submarines has been written many times. In each case, the emphasis has been on describing the particular system in terms of its depth capability, submergence time, and work tasks. Only peripheral attention has been directed to what could well be the most important element in the design – the means by which the ocean's depths are visually studied. From the days of Alexander the Great and his "glass barrel" submersible to today's most sophisticated system, man has wanted to examine visually the ocean depths. To achieve this objective, windows for submergence systems, submersibles with panoramic visibility, highly sophisticated television cameras and receivers, and ingenious optical arrangements have been developed.

Many of the approaches are now only of historical value, while some are as technically and operationally viable as when they were invented. If there is any generalization that can be made concerning them and their designers, it is that man will not cease to invent new optical systems until submersibles can provide at any depth the same visibility now possible with automobiles and aircraft.

The earliest reliable record of the actual use of a diving apparatus is that contained in a book written by Francisco de Marchi and published in 1599. The apparatus, designed and built by Guglielmo de Lorena, was first used in 1531 in an attempt to raise Caligula's pleasure galleys which had sunk in Lake Nemi. The most interesting thing about this diving bell was that it contained a glass window directly in front of the operator's face (reference 1.1). From the sketch available, it appears that the window was simply a flat piece of glass sealed, probably with pitch, into the wall of the bell. As the diving bell was used in shallow water, the window presented no significant problems.

Another approach to reaching the ocean floor was attempted with the "Aquatic Corselet" which can best be described as a forerunner of a diving helmet and suit. According to Father Schott, this device was made of leather and contained tiny panes of glass (reference 1.2).

In both these early devices, the windows were used for visual contact. In 1690, Dr. Edmund Halley, who later became an astronomer, designed and built a wooden diving bell with a large glass window in the top. This window was included so that light from the surface could enter the bell (reference 1.1). Halley himself, on several occasions, stayed on the bottom at a depth of 9 or 10 fathoms for over an hour.

---

* *This section was contributed by J. L. Atkerson of the New York Historical Society.*

As the years went on, refinements and advances were made on all these basic designs: Metal instead of wood or leather was used; different shapes were tried; and the depths to which the various devices were employed were extended.

In 1903, Giuseppe Pino designed his sophistocated hydroscope which allowed an observer to remain on the surface while viewing the seabed through a series of telescopic tubes; the lower end of the device was an optical chamber containing 12 lenses (reference 1.1). In this, as in the previous windows, glass was used.

At the depths to which these diving machines were used, it was possible to use glass because the state-of-the-art was sufficiently advanced to make safe designs feasible. To reach greater depths, it became necessary to design more elaborate vehicles, to improve the materials used to provide visibility, and to increase knowledge of window and flange designs.

1.2 BATHYSPHERE

In the 1930s, the zoologist, William Beebe, and his associate, Otis Barton, reached the unprecedented depth of 1426 feet (435 meters) in the "bathysphere." The old style of rigid diving suits, i.e., a steel cylinder furnished with portholes and hung from a cable, was the basis for the design of this system (reference 1.3).

The vehicle was a sphere which weighed 5000 pounds (2268 kilograms), measured 57 inches (145 centimeters) in diameter, and had steel walls that were 1.5 inches thick (3.8 centimeters) (reference 1.1). It contained three plane circular windows made of fused quartz; the windows were 8 inches in diameter (20 centimeters) and 3 inches thick (8 centimeters) (reference 1.2). The pieces of fused quartz, manufactured by General Electric, were the largest pieces made to this time (reference 1.4).

From the standpoint of the evaluation of underwater visibility, these windows were the first serious attempt at what is now called "window technology." There are three reasons for this claim. First, both Beebe and Barton believed that sight is the most important of the senses, as approximately 85 percent of all knowledge is acquired through sight. Beebe, as a zoologist, felt that he had to be able to select his samples under visual control and, therefore, the bathysphere had to have accommodating windows. Since windows had traditionally caused the greatest difficulty for all deep-diving bells and helmets (reference 1.2), they started the discipline of window technology by attempting to solve this problem. Second, they designed the windows from an engineering standpoint. Fused quartz was recommended by Dr. E. E. Free, an authority on optometrics in the 1930s (reference 1.4). There were two reasons for the selection of fused quartz: (1) it was the strongest transparent substance known at that time and (2) it would transmit all wavelengths of light (reference 1.2). Third, these windows departed from past tradition, as various gaskets, flanges, sealants, and retaining frames were tried and the optimum approach selected. Previous windows had tended to be plane rectangular plates of glass held in place by caulking. The fused-quartz windows were fitted into cylindrical projections in the front of the sphere, sealed in the mounting with a paper gasket and white lead paste, and secured in place with a light steel frame bolted over each window (reference 1.2). Six inches (15 centimeters) of the window's diameter were free of the supporting flange (reference 1.2), and the windows were so arranged that a shaft of light thrown out of one could be viewed from another (reference 1.4).

In 1934, Beebe and Barton had to dispose of all three windows, since they had developed cracks and one had broken under dangerously low-pressure tests. In addition, the windows had developed peculiar smokey patches which affected their usefulness for light transmission (reference 1.2).

During the numerous dives made with bathysphere there were times when the windows leaked. However, each time it was found that the window had not been seated correctly. The soundness of the window's design, material, flange, and gasket was proven many times. The ultimate success for the system, and for the windows in particular, came when Beebe and Barton reached their maximum depth of 3028 feet (923 meters) and showed that life was found at this depth (figure 1.1) (reference 1.5).

The bathysphere was the culmination of knowledge concerning pressure-resistant windows. There were some experiments, especially in regard to the windows, which were basically a break with the past. However, based on their works, the author believes that Beebe and Barton were not as concerned with the windows as with other aspects of their system, i.e., they believed that visual contact was critical but once their design was proven, there was no further experimentation. This is verified by the fact that when the benthoscope (Barton's successor to the bathysphere) was built fused quartz was again used with the same thickness but with a somewhat smaller diameter (figure 1.2) (reference 1.4).

The contribution to window technology made by Beebe and Barton was significant. By showing an interest in engineering details, they convinced designers of later submersible windows to experiment with materials, designs, shapes, flanges, and sealants.

1.3 TRIESTE

In the late 1920s and early 1930s, Auguste Piccard became interested in the stratosphere and began experimenting with the effects of pressure, or lack of pressure, on various bodies, materials, and designs. In 1931 he ascended in his balloon into the stratosphere to a height of approximately 10.5 miles (17 kilometers) (reference 1.1). He then experimented with new materials and designs that were related to exploration of the atmosphere. Having shown the validity of his theories concerning atmospheric pressure, he turned his attention to the ocean – the other source of great pressure differentials.

In studying the ocean, Piccard realized that there are "so many questions, so many mysteries, it is only by going down to the depths of the sea that we can hope to clear them up" (reference 1.3). He began his study of the ocean by reviewing all that was known concerning submersible design. It was at this time that Barton and Beebe were making their dives in the bathysphere. Piccard noted that "it is no exaggeration to say that it is he (Professor Beebe) who opened the doors of the abyss to man" (reference 1.3). Piccard, however, did not like several things about the bathysphere:

1. The ocean bottom could not be studied using a tethered assembly, since the wave-induced motion of the support vessel would make the bathysphere bounce, making the occupants sick and possibly striking the bottom (reference 1.3).

2. The possibility of the cable breaking could not be completely eliminated (reference 1.3).

3. The window material was subject to brittle fracturing (reference 1.6).

4. The shape of the window had to be changed to eliminate the possibility of leaks at great depths.

When TRIESTE I was launched (figures 1.3 and 1.4), Piccard said, "These windows are perhaps the finest feature of the bathysphere" (reference 1.3). Made of acrylic plastic (Plexiglas), the windows were truncated cones with 90-degree (1.57 radians) included angles that measured 5.91 inches thick (15 centimeters), 3.94 inches (10 centimeters) at the inside diameter, and 15.75 inches (40 centimeters) at the external diameter (reference 1.3). The window was directly set against a conical metal seat machined into the pressure hull. Lubricant was generously applied to the window and acted like a high-pressure seal (reference 1.6). Through experimentation, Piccard found that the windows would withstand a pressure equal to 18.6 miles (29.9 kilometers) of water (reference 1.3). The windows were conical frustums (plane discs with conical bearing surfaces). Piccard selected this shape because the window seated more securely as the pressure on the exterior face increased, which reduced the need for sophisticated gaskets or retaining rings. Acrylic plastic was used since it, unlike glass or fused quartz, is plastic and yields under compression without fracturing. Piccard found that if a window became overloaded beyond its limit of elasticity, it bent slightly and passed the excess load to the adjacent parts, in this case the pressure hull (reference 1.3). According to Piccard, it was this last feature that explained the success of the windows.

When TRIESTE II was built, the same basic design was used for the windows. The windows were made by laminating two sheets of acrylic plastic, and the thickness-to-interior-diameter ratio was set at 1.56 (reference 1.7). Eventually it became necessary to replace the TRIESTE II windows because of scratches on the viewing surface and apparant discoloration. However, no window ever failed in service or were there any leakage problems.

Auguste Piccard and his son Jacques contributed significantly both to submersible design and window technology. By experimenting with materials and design, they provided a standard of excellence with which to measure the next generation of submersible windows. In addition, they caused the nonmilitary submersible community to realize the importance of visual observations.

1.4 WINDOW DESIGN (TRIESTE TYPE)

Following Piccard's successes with the conical frustrum acrylic plastic window, most submersible designers adapted both the design and the material to their own requirements. Hence, most commercial submersibles had conical windows of some size that allowed the aquanauts visual contact with the ocean. In some submersibles, the aquanauts were given windows only 2 to 3 inches in diameter (5 to 8 centimeters); in others, they were as large as in TRIESTE.

There were, however, drawbacks to the TRIESTE-type windows. First, they were limited in size. It became increasingly obvious to those experimenting with window design that to increase the diameter of the window for panoramic observation at even a moderate depth, e.g., 5000 feet (1524 meters), the window thickness had to increase significantly.

This introduced several problems. Since it was very difficult to obtain thick enough material, the only possibility was lamination which also introduced problems. In addition, if the window's thickness was increased, it was also necessary to increase the mounting flange thickness, thus significantly increasing the weight of the pressure hulls. The resulting decrease in buoyancy in turn decreased the payload and thus operational value of the submersible. A second problem was that the aquanauts were not satisfied with viewing the ocean through what was a tiny "peephole." They wanted windows in many places so that the sea bottom could be seen from all planes and in all directions. To satisfy this need, it was necessary to cut window holes at numerous locations in the hull, which meant a greater hull thickness, stronger areas around the windows, additional stress concentrations, and elastic stability discontinuities. Nevertheless, submersibles with multiple windows were successfully designed, built, and operated to depths in excess of 1000 feet (305 meters) (figure 1.5). Today, submersibles with multiple viewports operate successfully at depths in excess of 10,000 feet (3048 meters) (figure 1.6).

1.5 MORAY, DEEP JEEP, AND DOWB

Submersible designers next began to think of other ways to achieve visibility which would not include a viewport for direct use by an aquanaut. Three examples are provided by MORAY, DEEP JEEP, and DOWB.

1.5.1 MORAY

MORAY was a test vehicle built by the Naval Ordnance Test Station (NOTS), China Lake, California. It had an operational depth capability to 2000 feet (610 meters) (figure 1.7). The pressure hull was a 5-foot-diameter (1.5 meters) cast aluminum sphere which contained no viewports (figure 1.8). All visual contact was maintained via television and sonar (reference 1.10). This system, however, did not provide ideal observation, i.e., the direct line-of-sight vision was negated, the cost was high, it required much power to operate, panoramic visibility was not available, and it was subject to power failure which made the operators virtually blind. For an unmanned vehicle, MORAY's approach would have been acceptable, but when carrying aquanauts this lack of visual stimulus led to claustrophobia and seasickness. Thus, while an interesting approach, MORAY was not adopted by the commercial hydrospace engineering community.

1.5.2 DEEP JEEP

DEEP JEEP, like MORAY, was designed and built by NOTS, China Lake. A small two-man submersible, DEEP JEEP was a 5-foot-diameter (1.5 meters) steel sphere with a maximum depth of 2000 feet (610 meters) (figure 1.9). The acrylic plastic viewing port was a conical frustrum 5 inches in diameter (13 centimeters) and 2 inches (5 centimeters) thick; however, it was not used directly by the aquanauts. Instead, observations were made through monocular viewing scopes (one per operator) (figure 1.10). The scope allowed the operator to view hydrospace without placing his face close to the window. This optical arrangement provided a field-of-view of 40 degrees (0.7 radian). However, panning could only be achieved by rotating the vehicle. In addition, DEEP JEEP contained a closed-circuit, black-and-white television system with the camera mounted outside. The combined viewing systems provided a degree of visual contact, but as the principal designer and operator, Will Forman, pointed out, in future submersible designs the emphasis had to be placed on maximum visibility instead of the tunnel vision approach provided by this system (reference 1.8).

1.5.3 DOWB

DOWB was built for the General Motors Defense Research Laboratory. It was a three-man submersible with an 80-inch (203 centimeters) steel pressure sphere and a unique optical system designed by Kollmorgen (figure 1.11). The system had two, external, 180-degree (3.14 radians), objective lenses that were served by eyepieces inside the pressure sphere (figures 1.12 and 1.13). Two eyepieces were available for each lens system so that at any time two of the three aquanauts could use them. One optical system was oriented directly down under the vehicle and provided an undistorted view of a 90-degree cone (1.57 radians). The other had the objective lens located forward on the bow and was oriented so that its axis pointed downward 35 degrees (0.6 radian) below the horizontal. Thus, a view of the bottom approximately 10 feet (3 meters) ahead of the bow was provided (reference 1.9).

The problems with such an optical system were those associated with all complex optical systems: There was less than panoramic visibility; claustrophobia and seasickness were easily induced; and there was a significant loss of light intensity because of internal reflections in the optical train. In addition, the DOWB system had a tendency to defocus at operational depths, the result of deflections of the acrylic plastic windows that were used as transparent bulkheads on the externally located, image transmission tubes. This necessitated the use in the eyepiece assembly of corrective lenses especially designed for various depths. These lenses were manually inserted by the pilot or copilot at the appropriate depth. The need for several corrective lenses was later eliminated by placing a single lens in a mounting whose location, relative to the eyepiece, could be adjusted with a rack and pinion adjustment.

1.6 PANORAMIC WINDOWS

The U. S. Navy became interested during the 1960s in the problem of visibility, not because of any need for visual observation from combat submarines but because of the need for a hydrospace exploration effort paralleling the outer-space exploration program conducted by NASA. The key to hydrospace exploration lay in the development of deep-ocean technology which would allow man to study the ocean bottom at any depth, first on the continental shelf and later at greater depths. As a result, projects and programs were initiated and supported, the objective of which was the development of deep-ocean technology for both the Navy and the ocean-engineering community. All naval laboratories participated in this program according to their technological specialties. One key laboratory was the Naval Civil Engineering Laboratory (NCEL) at Port Hueneme, California. Because of NCEL's interest in materials, structures, and soils, a Deep-Ocean Simulation Facility was constructed in 1964 to study the behavior of materials, structures, and soils in a deep-ocean environment. The presence of the facility and the availability of funding for research attracted a group of engineers interested in deep-ocean technology. Among them was Jerry Stachiw, a recent graduate of Pennsylvania State University who became intrigued by the structural potential of acrylic plastic while utilizing this material for construction of torpedo shell models during his doctoral research program. His long range plans were to (1) complete research on the conical frustum acrylic plastic windows initiated by Piccard, (2) standardize the design of flat disc windows proposed by diving contractors, and (3) invent and qualify for manned diving systems an optimized window design that would maximize the field-of-vision while at the same time decrease the weight of the window-flange assembly. His experiments included conical frustum windows with other

than 90-degree (1.57 radians) included angles. As a result he was able to establish the design parameters for windows with included angles of 30, 60, 120, and 150 degrees (0.5, 1.04, 2.09 and 2.6 radians). Although adding to data on the design of conical frustum windows for deep submergence vehicles, these experiments did not solve the need for significantly larger windows.

Flat disc acrylic windows were also extensively investigated by him since they have several desirable features for use in shallow-diving submersibles and hyperbaric chambers. These features include easy fabrication from commercially available flat stock by simple machine shop tools and ease of mounting in the pressure hull. The flanges required for such windows are very simple, and the window itself can be seated and sealed in the flange with ordinary gaskets or rings held in compression by the window which, in turn, is securely attached to the flange with bolts and a simple retaining flange. However, no significant increase in panoramic visibility resulted from this research, and the windows could only be used by submersibles and diving bells in the depth range of the continental shelf.

The window that finally began to provide panoramic visibility was the spherical shell sector acrylic window (figure 1.14). These windows had been considered by Stachiw for hydrospace only since the late 1960s as they represented a considerably more complex shape than conical frustums or flat disc windows. Numerous experimental tests showed that acrylic under uniformly distributed biaxial or triaxial compressive stresses can withstand considerably higher stresses than if the distribution of stresses is nonuniform, as in a conical frustum or flat disc window. Stachiw also showed that a spherical shell sector window, although not a complete sphere, retains the high-critical-pressure attribute of a spherical shell even in the presence of new restraints, e.g., unyielding steel window flanges not present in complete spheres. The spherical shell sector window with parallel convex and concave surfaces also has decided optical advantages: (1) it gives the aquanaut a larger field-of-vision for a given diameter opening in the steel flange; (2) it acts as a lens with a magnification of less than one, which provides the aquanaut an undistorted view if he remains in the center of the window's curvature; (3) and it permits the aquanaut, if the opening of the flange is sufficiently large, to place his head inside the window and use the window as an observation cupola.

However, before large spherical shell sector windows could be designed for safe use, four empirically established relationships had to be developed:

a. The relationship between the window's critical pressure and its t/D_i ratio.

b. The relationship between the window's critical pressure and its t/R_i ratio.

c. The relationship between the hydrostatic pressure and magnitude of axial displacement for windows of different sector angles and t/R_i ratios.

d. The relationship between test results obtained with scale models machined from blocks of acrylic plastic and results obtained from full-size spherical sector windows fabricated by thermoforming of thick acrylic plastic sheets

In August 1969, Stachiw published his findings on these relationships for acrylic spherical sector shell windows in the *Transactions of the American Society of Mechanical Engineers.* It was now possible to design and build windows of almost any size that could function as the entire nose section of a cylindrical-bodied submersible and provide vastly increased visibility.

The first submersible to incorporate findings of his experimental studies, and thus the first working submersible to have a large spherical sector acrylic window, was PC-8B which had an 800-foot (244 meters) operational depth capability. Built by Perry Ocean Engineering, PC-8B had a pressure hull 104 inches (264 centimeters) long, an inside diameter of 42 inches (107 centimeters), and a 114-degree (1.9 radians) spherical sector acrylic plastic bow window (figure 1.15) (reference 1.5).

Today most commercially produced submersibles with a continental shelf depth capability have acrylic spherical sector windows in their bows (figure 1.16) and even old submersibles have had their bows remodeled to accept these windows, e.g., BEAVER and MERMAID II. Spherical sector windows have basically satisfied all three conditions for the acceptance of a new design: (1) they are reasonably economical; (2) they provide unobstructed forward visibility; and (3) they are safe. The U. S. Navy, American Bureau of Shipping, and the Norwegian ship classification society (Det Norske Veritas) accept these windows, if they are built according to the design criteria established by Stachiw and codified in the American Standards Institute's ASME PVHO-1 Safety Standard on Pressure Vessels for Human Occupancy (section 15).

Commercial users of submersibles are very satisfied with these large bow windows. In most cases, the single spherical sector window located in the bow provides all visibility needed to operate a working submersible at continental shelf depths for half the cost of multiple conical frustum windows. However, regardless of the size of a spherical sector bow window, it still remains only a transparent discontinuity in an otherwise opaque enclosure. Only when a transparent material is substituted for the opaque metal as the only load-carrying material of the pressure hull will the search for panoramic visibility be ended (figure 1.17). Such a hull now exists and it, like the spherical, conical, and flat disc windows, is made of acrylic.

1.7 ACRYLIC PLASTIC SUBMERSIBLES

The first reaction to acrylic plastic is that it does not appear to be a feasible material for constructing pressure hulls. Its low compressive strength, low fracture toughness, and sensitivity to stress risers in tension make it a poor replacement for metal. Fortunately, however, its strength-to-weight ratio makes it equivalent to low carbon steel; its plasticity permits it to tolerate large stress concentrations in compression; and its ability to adhere well to specially formulated adhesives makes it feasible to join acrylic structural shapes by bonding. In addition, because acrylic has desirable optical qualities, it is an ideal hull material for submersibles working above the 3000-foot (914 meters) level.

Pioneering work in the development of acrylic plastic submersible hulls was initiated by Stachiw in 1961 and continued for many years until spherical acrylic pressure hulls for submersibles became a reality. While at the Ordnance Research Laboratory, Pennsylvania State University, Stachiw built several torpedo-shaped, acrylic plastic, instrumentation capsules that performed exceedingly well in a sea environment. The opportunity to apply this experience to large submersible hulls presented itself at NCEL. While investigating the performance of acrylic plastic in windows for submersibles, he was approached by Moldenhauer of the Naval Missile Center to assist the Center in the design and construction of a tethered undersea observatory. Sensing the opportunity to match the transparency

of acrylic plastic to a system requiring panoramic visibility, he submitted to NMC a revolutionary hull design in which the use of acrylic plastic was maximized and steel minimized. The design called for an acrylic sphere with a 1000-foot (305 meters) design depth and a 4200-foot (1280 meters) implosion depth.

At this time (1964), there were no data available on the mechanical properties of the thick acrylic castings needed for man-sized pressure hulls, the strength of bonded joints between thick castings, and the corrosive effects of seawater on acrylic. In addition, there was no engineering design or fabrication technique available for making a thick-walled pressure hull of acrylic and data were needed to make performance predictions.

It took until 1970 to develop the data and fabrication techniques necessary to certify NEMO (Naval Experimental Manned Observatory) (figures 1.18 and 1.19). Sponsored by the Naval Facilities Engineering Command, NEMO was the first transparent submersible to be approved for manned service and it overcame many obstacles inherent in an experimental approach: By choosing the spherical shape, resistance to crushing was maximized, the design was simplified, and the utilization of interior space was optimized. Using the modular assembly technique (12 spherical pentagons bonded to form a sphere), the fabrication process was made reliable, and by thermoforming the pentagonal modules from flat sheets the fabrication technique was made economical. By placing all penetrations in the top and bottom poles of the capsule, the aquanauts had a panoramic view of the exterior.

To establish the applicability of such an acrylic pressure hull for manned submersible operations, it was experimentally proven that the acrylic hull possessed an adequate safety margin for the chosen operational depth and that failure of the hull in a submersible could be predicted accurately and reliably on the basis of model- and full-scale acrylic hulls tested to destruction in deep-ocean simulation facilities. Both points were proven by hydrostatic testing of 23 model-scale capsules, 15 inches (38 centimeters) in diameter, and two full-scale capsules, 66 inches (168 centimeters) in diameter, in the pressure vessels of the Deep-Ocean Simulation Facility at NCEL. During the approximately 100,000 hours of hydrostatic testing, all model- and full-scale hulls were tested to failure, yielding the data that subsequently became the basis for the certification of acrylic hulls for submersibles by the U. S. Navy, the American Bureau of Shipping, and Det Norske Veritas.

Since panoramic visibility had become a reality with NEMO, the evaluation process now began to focus on the incorporation of the hull in other submersible designs and the determination of its depth capability.

The second submersible to utilize an acrylic hull with the same modular construction as NEMO was JOHNSON-SEA-LINK (figure 1.20). Conceived by Edwin A. Link as a self-propelled, undersea, diver-decompression chamber, it combined the best features of a 1-atmosphere, transparent submersible with that of a roomy, diver-compression chamber with undersea lockout capability. The acrylic cockpit for the pilot and scientific observer allowed them to guide the submersible to its objective through visual contact (figure 1.21).

Since the Smithsonian Institution, which owned the JOHNSON-SEA-LINK, was interested in exploring the entire continental shelf, the submersible was fitted in 1971 with a 4-inch-thick (10 centimeters) acrylic hull which gave it a 1000-foot (305 meters) operational depth capability.

The third submersible to use a NEMO-type hull was the MAKAKAI built by the Naval Undersea Research and Development Center, Kaneohe, Hawaii (figure 1.22). Conceived by Wm. B. McLean, the submersible represented an answer to the needs of the ocean explorer with high agility requirements. The mounting of the acrylic hull above the catamaran-like structure insured unlimited visibility while a pair of pi-pitch cycloidal propellers mounted behind the acrylic sphere gave the submersible maneuverability in any direction. In addition, one of the novel features of MAKAKAI was the ability to transmit command signals from the interior of the capsule to the propulsion and guidance systems outside the sphere by means of amplitude-modulated light beams, rather than by the customary wire transmission lines.

It is possible to state that these were the first generation of acrylic submersibles. Their depth capabilities, based on certification, varied from 600 to 2000 feet (183 to 609 meters). They showed the versatility of acrylic hulls and opened the doors to their unlimited use. However, increased depth capability, as well as panoramic visibility at lower cost, was still being sought. With this in mind, McLean and Stachiw began to study other fabrication processes which not only would make the hulls less costly but would also allow the acrylic submersible to reach 3000 feet (914 meters). Combining research efforts with those of a producer of large cast acrylic structures, Bruce Beasley, a new hull cast in two hemispheres and bonded together with a cast-in-place acrylic layer was introduced (figure 1.23). The hull had the same diameter as NEMO, 66 inches (168 centimeters) outside diameter, and a wall thickness of 4.25 inches (10.8 centimeters). After extensive tests, the hull was approved to depth of 3000 feet (914 meters) and is being used on JOHNSON-SEA-LINK III.

The possibilities for using acrylic hulls at continental shelf depths are unlimited, e.g., observation bells, inspection vehicles, and underwater work vehicles, (underwater tractors, manned transfer capsules, and exploration submersibles) (figure 1.24). All of these are commercially feasible, and several are now in various planning stages.

1.8 SUMMARY

The transition from tiny glass windows placed directly in front of the observer's face to totally transparent submersibles has taken many years and much engineering effort. However, the search for panoramic visibility at all depths is not complete. Acrylic is definitely depth limited. New materials, like transparent glass ceramics and chemically tempered glass, promise to extend the depth capability of spherical windows and pressures hulls from 3000 feet (914 meters) to the bottom of the abyssal depths. The exploratory work conducted by Stachiw at the Naval Undersea Center, San Diego, California, has already resulted in small glass ceramic and chemically tempered glass spherical sector windows with a 40,000-foot (12,192 meters) depth capability (figure 1.25) (reference 1.11). Only the lack of funding presently prevents the application of glass ceramic and chemically tempered glass to full-scale sector windows with abyssal depth capabilities (figure 1.26).

1.9 REFERENCES

1.1 Davis, Robert H., *Deep Diving and Submarine Operations, Parts I and II,* Sixth Edition, London: Siebe, Gorman & Co., Ltd., 1955.

1.2 Beebe, William, *Half Mile Down,* London: John Lane the Godley Head, 1935.

1.3 Piccard, Auguste, *Earth, Sky and Sea,* New York: Oxford University Press, 1956.

1.4 Barton, Otis, *The World Beneath the Sea,* New York: Thomas Y. Crowell Company, 1953.

1.5 Wright, Christopher, "Development of a Large Spherical Acrylic Viewport for the PC-8B Submarine," ASME Paper, WAC, 1972.

1.6 Piccard, Jacques, and Robert S. Dietz, *Seven Miles Down,* New York: G. P. Putnam's Sons, 1961.

1.7 Naval Ship Research and Development Center, Bethesda, Maryland, "Material Characterization Studies of a Trieste-II (DSV-I) Sphere Window after Deep Submergence Service," by Frank M. Schwartz, May 1972.

1.8 Forman, W. R., "DEEP JEEP from Design Through Operation," Marine Technology Society Publication, pp. 17–23.

1.9 Lankes, L. Richard, "Viewing Systems for Submersibles," *Optical Spectra,* pp. 62–67, May 1970.

1.10 Marine Technology Society, "Small Research Submersibles," October 1968.

1.11 Stachiw, J. D., "Transparent Structural Materials for Underwater Research and Exploration," *Industries Atomiques and Spatiales,* pp. 1–24, 1974.

1.10 BIBLIOGRAPHY

1.1 Cousteau, Jacques Yves, *The Living Sea,* New York: Harper and Row, 1963.

1.2 Stachiw, J. D., *Window in the Sea,* Washington, DC: Smithsonian Institution Press, 1971.

1.3 Sweeney, James B., *A Pictorial History of Oceanographic Submersibles,* New York: Crown Publishers, Inc., 1970.

Figure 1.1. Otis Barton's bathysphere, an early deep-diving observation bell, is shown with the explorer William Beebe. During 1934, the bathysphere with Beebe and Barton aboard established the world's depth record at 3028 feet (923 meters). (New York Zoological Society photograph.)

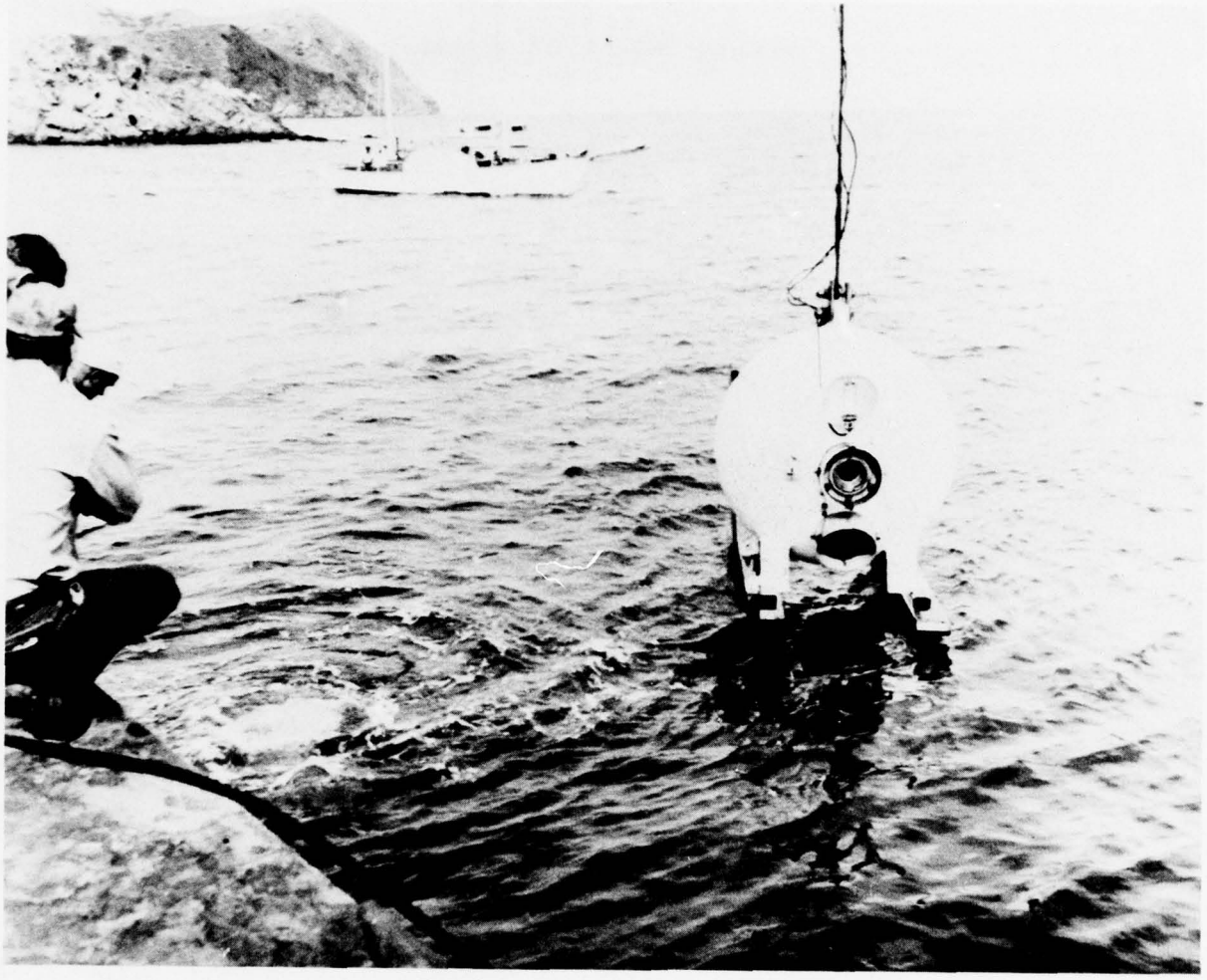

Figure 1.2. Otis Barton's benthoscope, the second deep-diving observation bell for undersea exploration. During 1949, it established the world's depth record at 4500 feet (1372 meters). (Maurice Nelles photograph.)

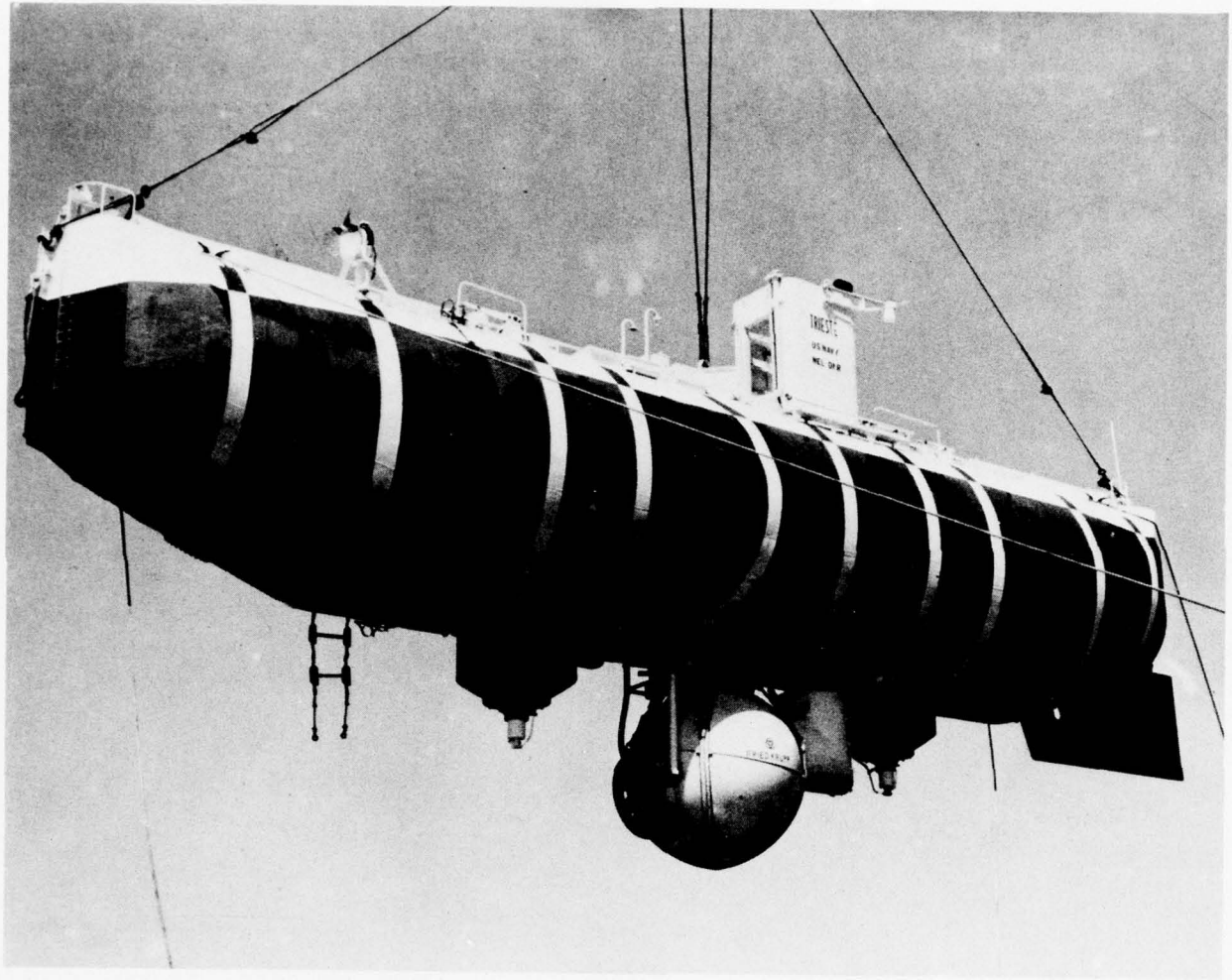

Figure 1.3. Auguste Piccard's TRIESTE I.

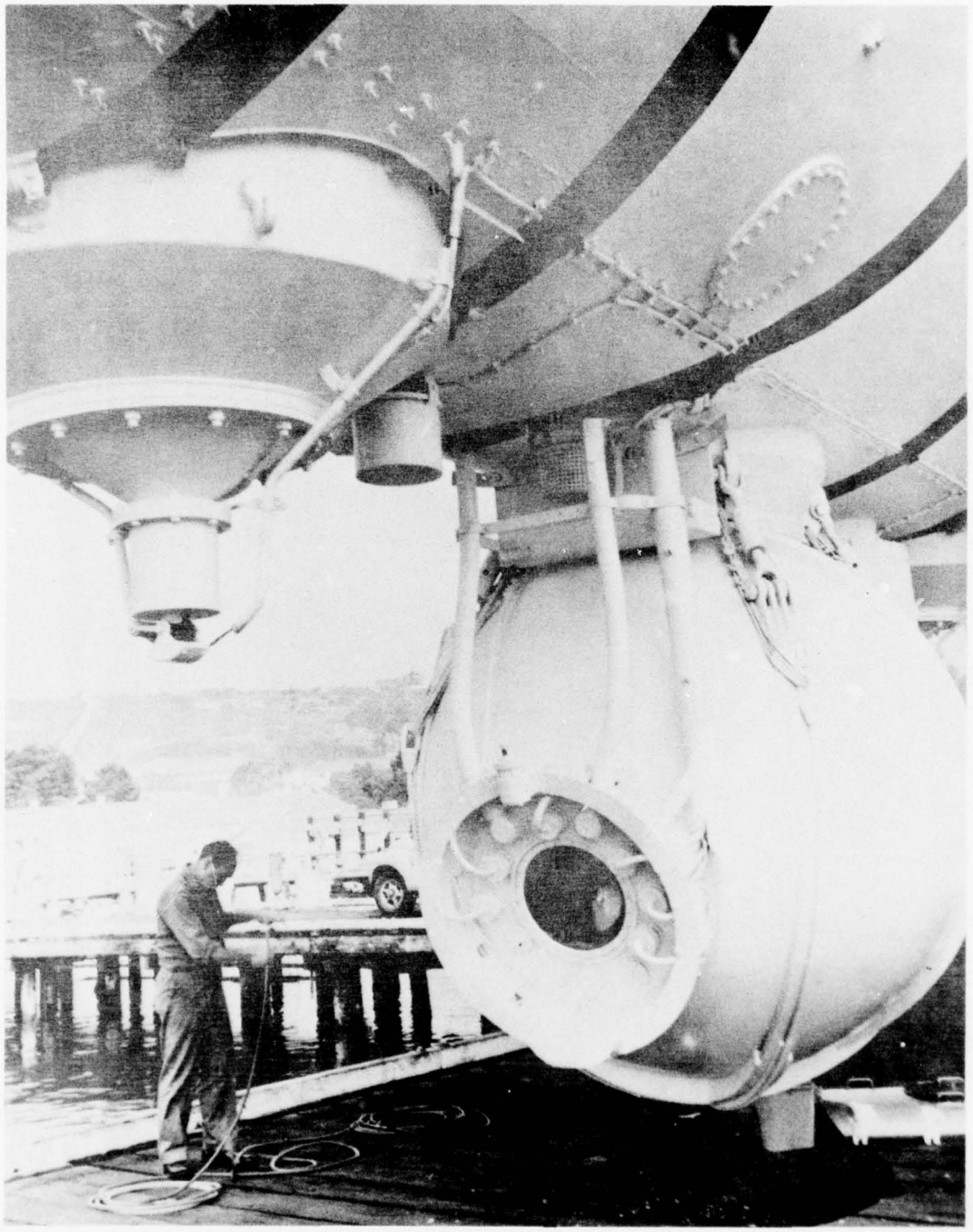

Figure 1.4. Viewport in TRIESTE I through which D. Walsh and Jacques Piccard were the first men to observe the bottom of the Mariana's Trench at 35,800 feet (10,912 meters) during 1960.

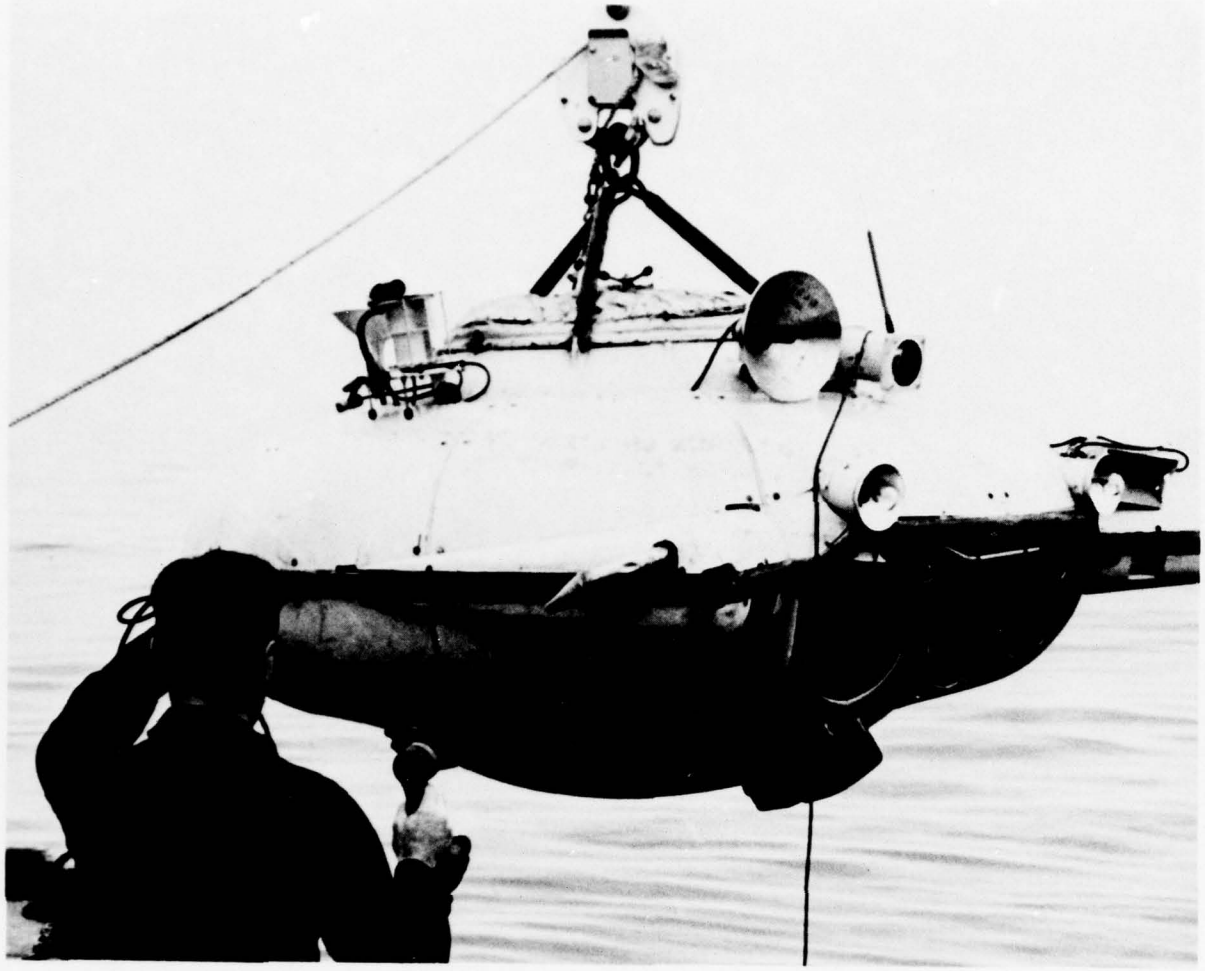

Figure 1.5. Jacques Cousteau's SOUCOUP, a modern shallow-depth submersible that used twin viewports to provide the pilot and observer with separate viewports.

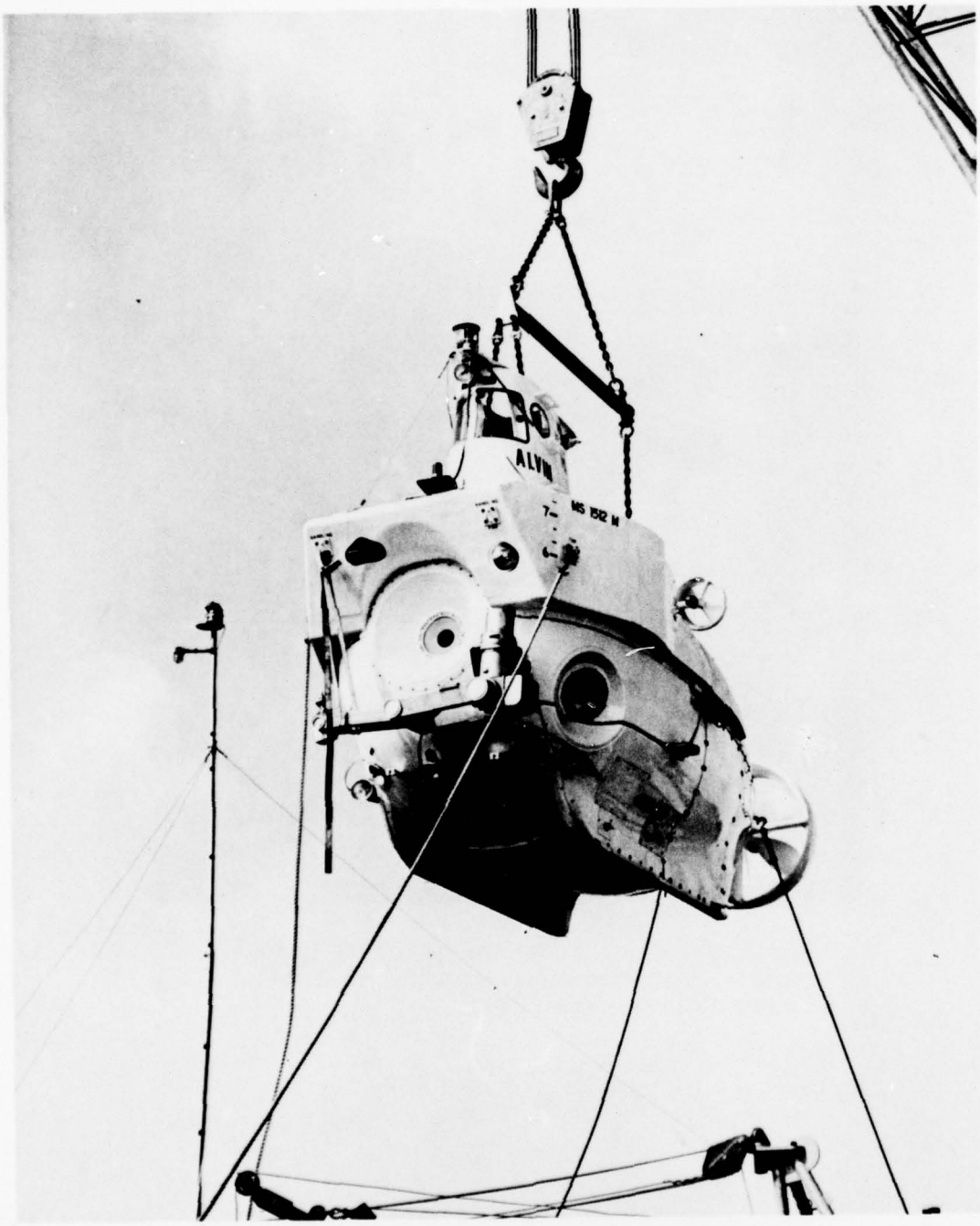

Figure 1.6. A. Vine's ALVIN, a modern deep-submergence submersible with a 12,000-foot (3658 meters) depth capability. The multiple-conical-frustum, acrylic plastic viewport is based on Piccard's engineering efforts. (Woods Hole Oceanographic Institution photograph.)

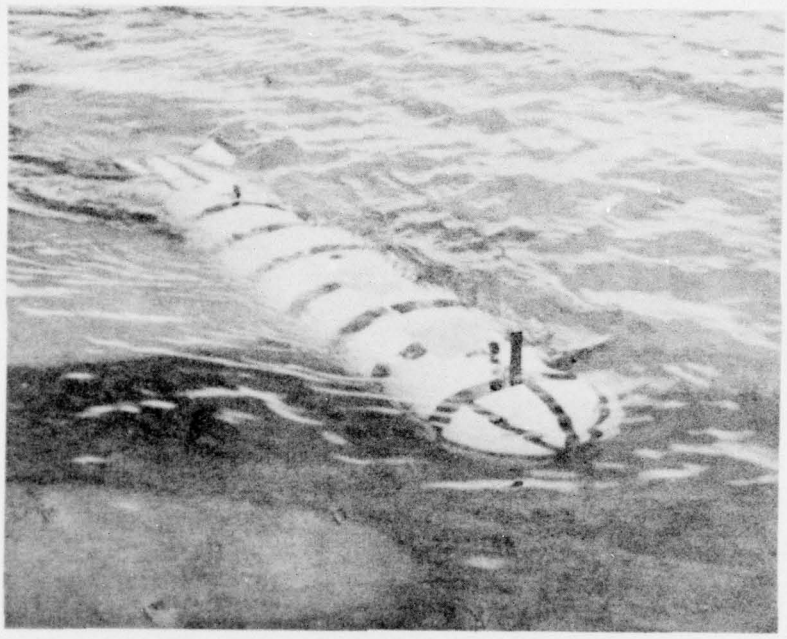

Figure 1.7. Wm. B. McLean's MORAY submersible with a 2000-foot (610 meters) operational depth capability. Closed-circuit television and sonar were used for underwater observation.

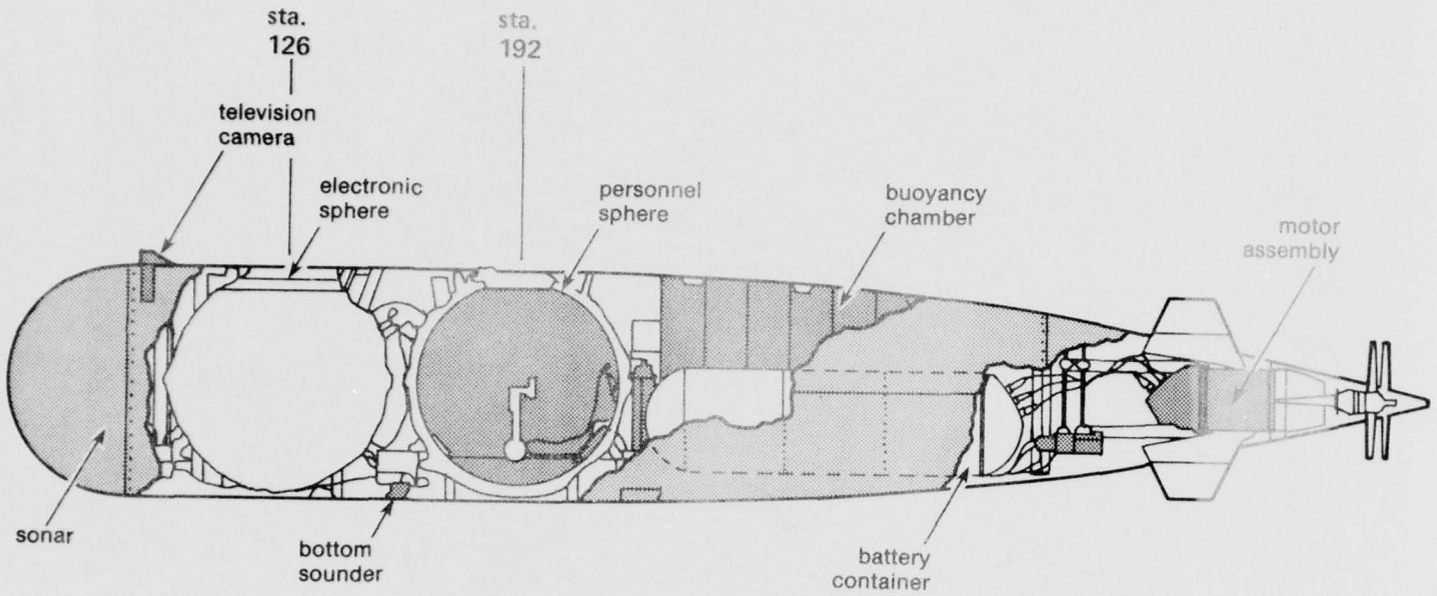

Figure 1.8. Schematic of the MORAY's interior. Note the windowless crew compartment served by an outboard television camera.

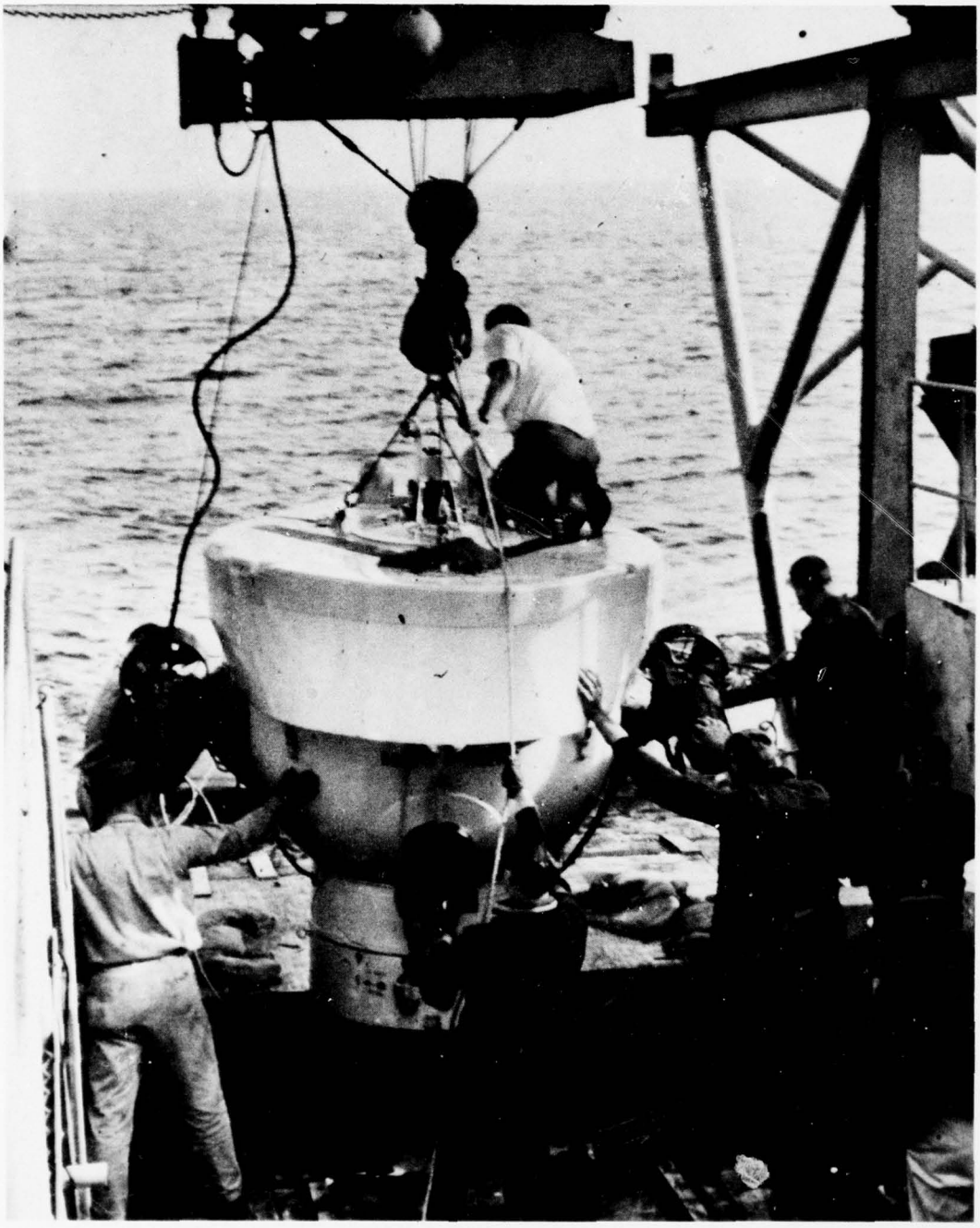

Figure 1.9. W. Forman's DEEP JEEP submersible with a 2000-foot (610 meters) operational depth capability. Monocular telescopes and periscopes were used for underwater viewing.

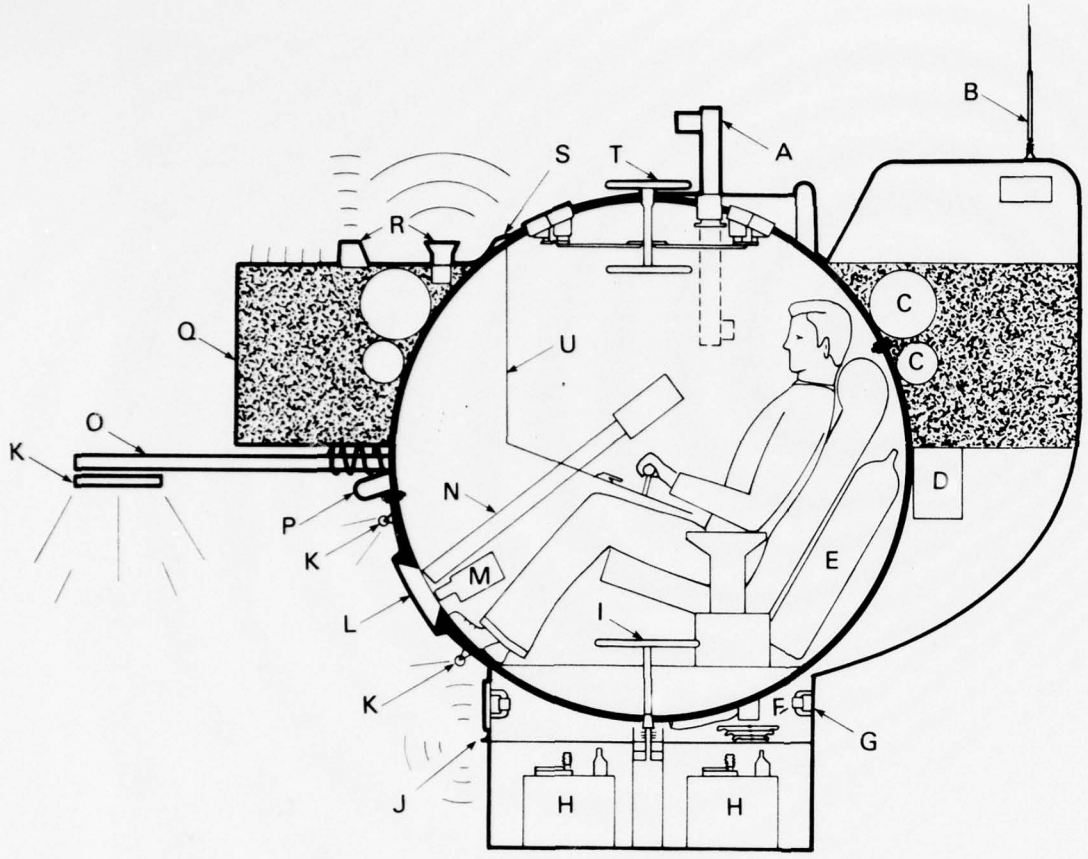

A periscope
B radio antenna
C buoyancy tanks
D motor
E compressed air
F electromagnets
G ballast plates
H batteries
I battery release
J depth sounder
K lights
L viewport
M movie camera
N viewing optic
O lighting arm
P movie light
Q flotation
R sonarphone heads
S lifting eye
T hatch wheel
U instrument panel

Figure 1.10. Schematic of the equipment carried by DEEP JEEP. Note the perioscope for viewing on the ocean surface and the viewport telescope assembly for underwater observation.

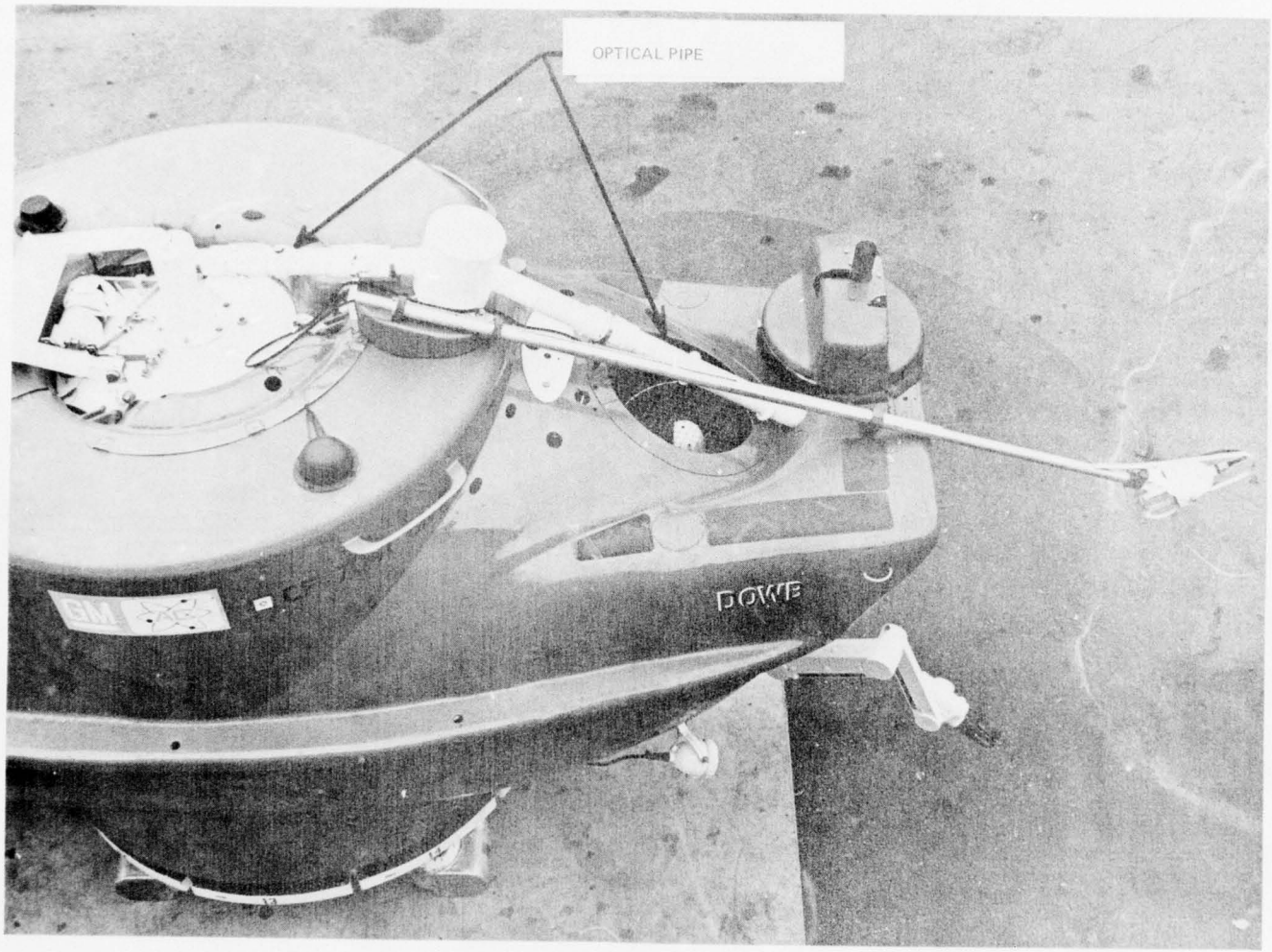

Figure 1.11. Daubin's DOWB submersible with a 6000-foot (1829 meters) operational depth capability. Wide-angle lenses and external telescopes provided panoramic underwater observation. An optical pipe connected the windows in the upper hatch with the forward optical dome in the bow of the submersible. (General Motor's Defense Research Laboratory photograph.)

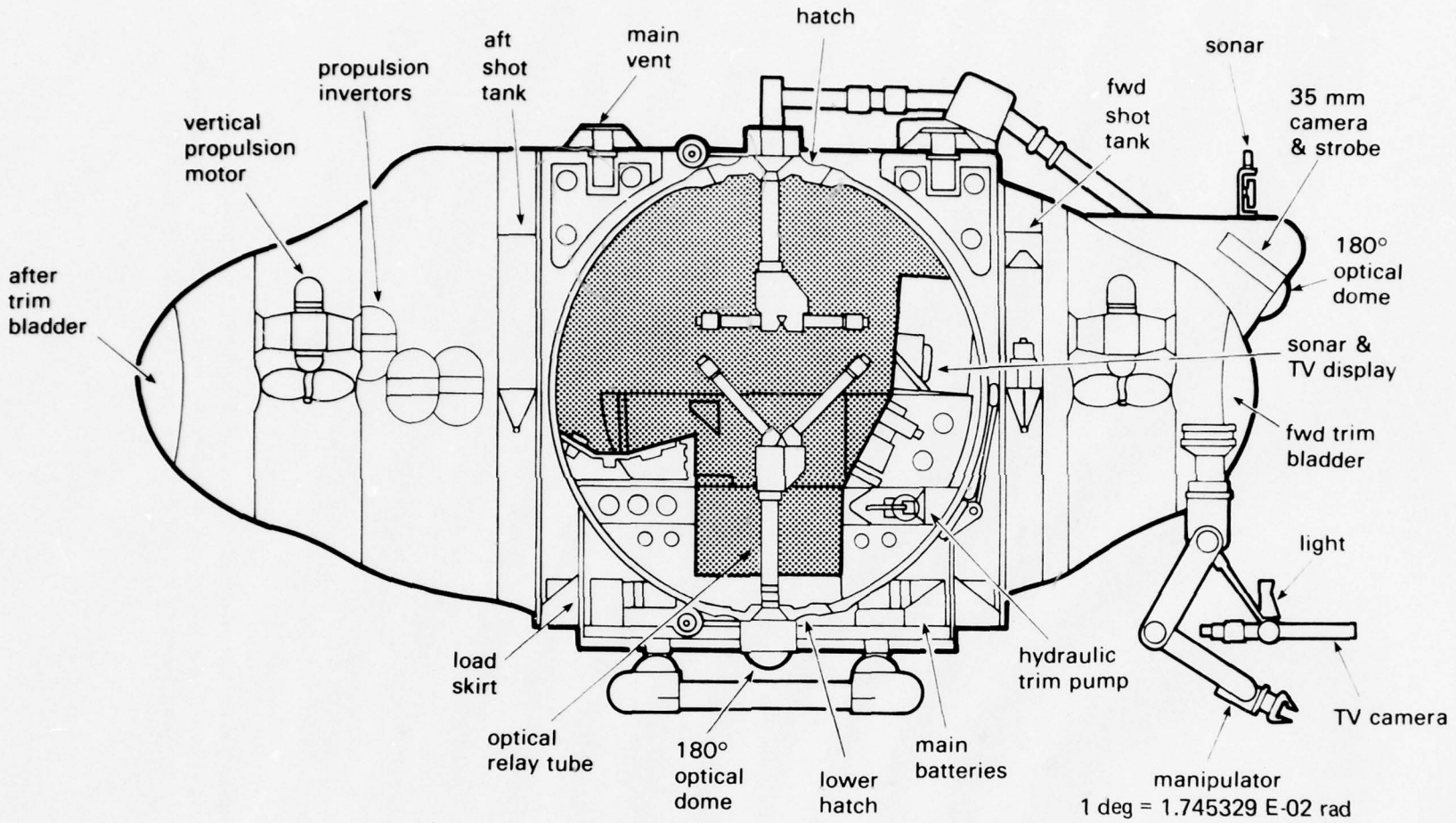

Figure 1.12. Schematic of the wide-angle telescope system on DOWB (reference 1.9).

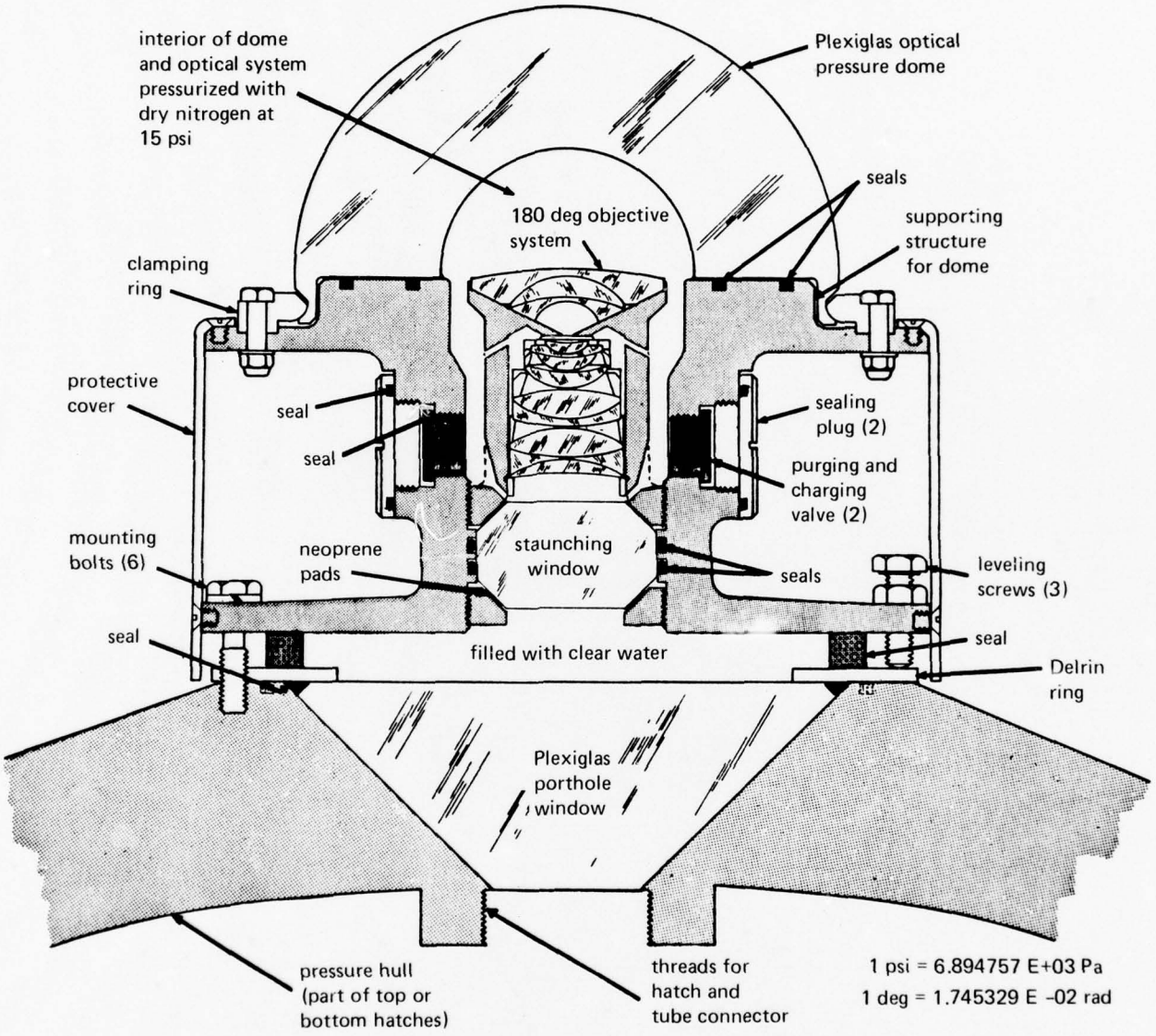

Figure 1.13. Cross-section through the optical dome on DOWB providing it with panoramic vision (reference 1.9). One dome was located in the bottom hatch while the other was located in the bow, an arrangement which provided the crew with panoramic visibility directly below and in front of the submersible.

Figure 1.14. Experimental prototype of full-scale spherical sector windows for undersea applications. Developed for the U. S. Navy by Stachiw in 1968 at the Naval Civil Engineering Laboratory.

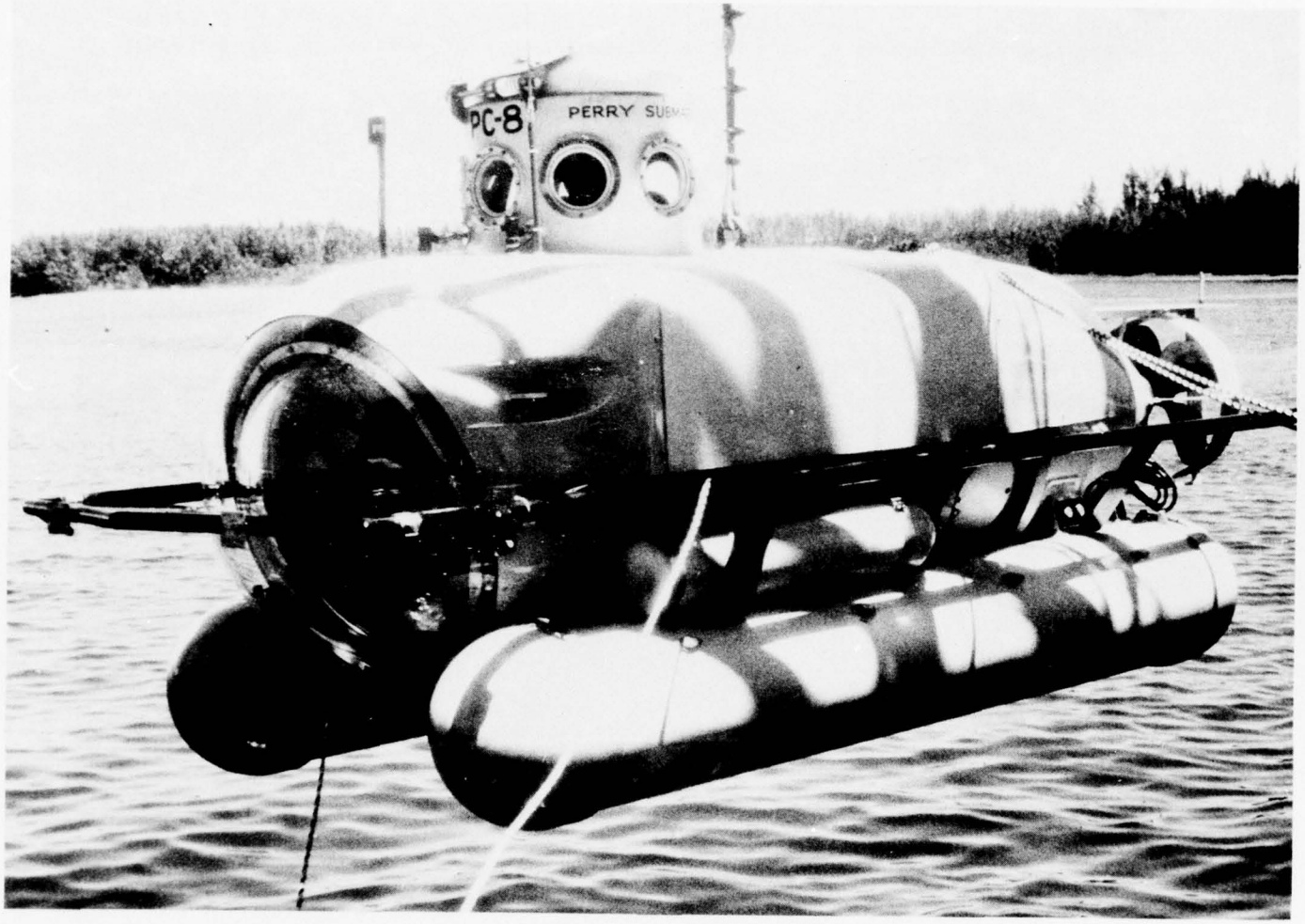

Figure 1.15. PC-8B submersible with 800-foot (244 meters) depth capability built by Perry Oceanographics in 1970. Acrylic plastic spherical sector windows are integrated into the pressure hulls of the submersible. (Perry Ocean Engineering, Inc., photograph.)

Figure 1.16. PC-16, a typical modern work submersible with a large bow window for service to 3000 feet (914 meters). Spherical sector bow windows are now standard on all modern work submersibles with continental shelf depth capabilities. (Perry Ocean Engineering, Inc., photograph.)

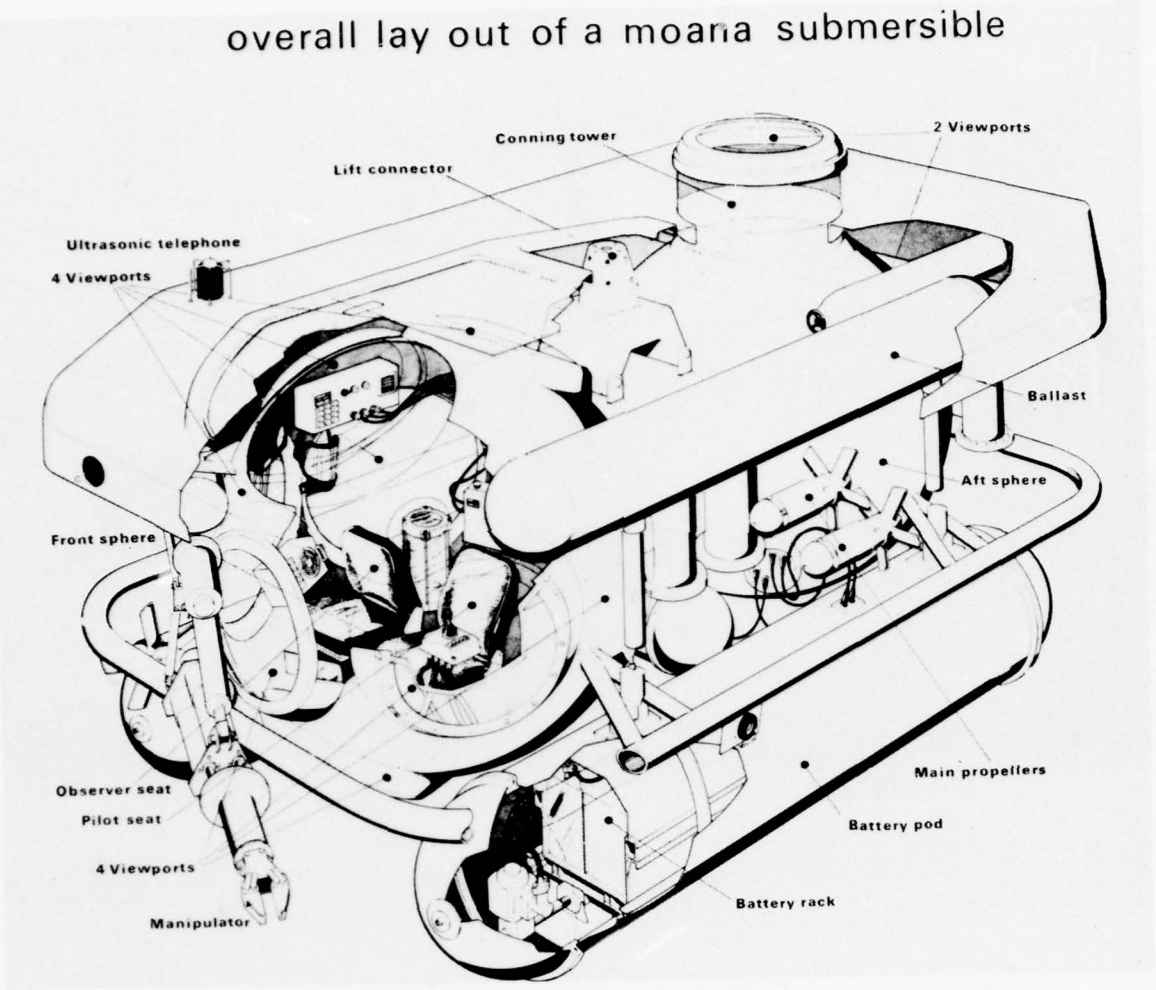

Figure 1.17. MOANA submersible built in 1975 by COMEX using multiple spherical sector windows with panoramic visibility. The presence of the windows increases the ability of the crew to operate the lockout submersible close to offshore platforms or other underwater structures. (COMEX photograph.)

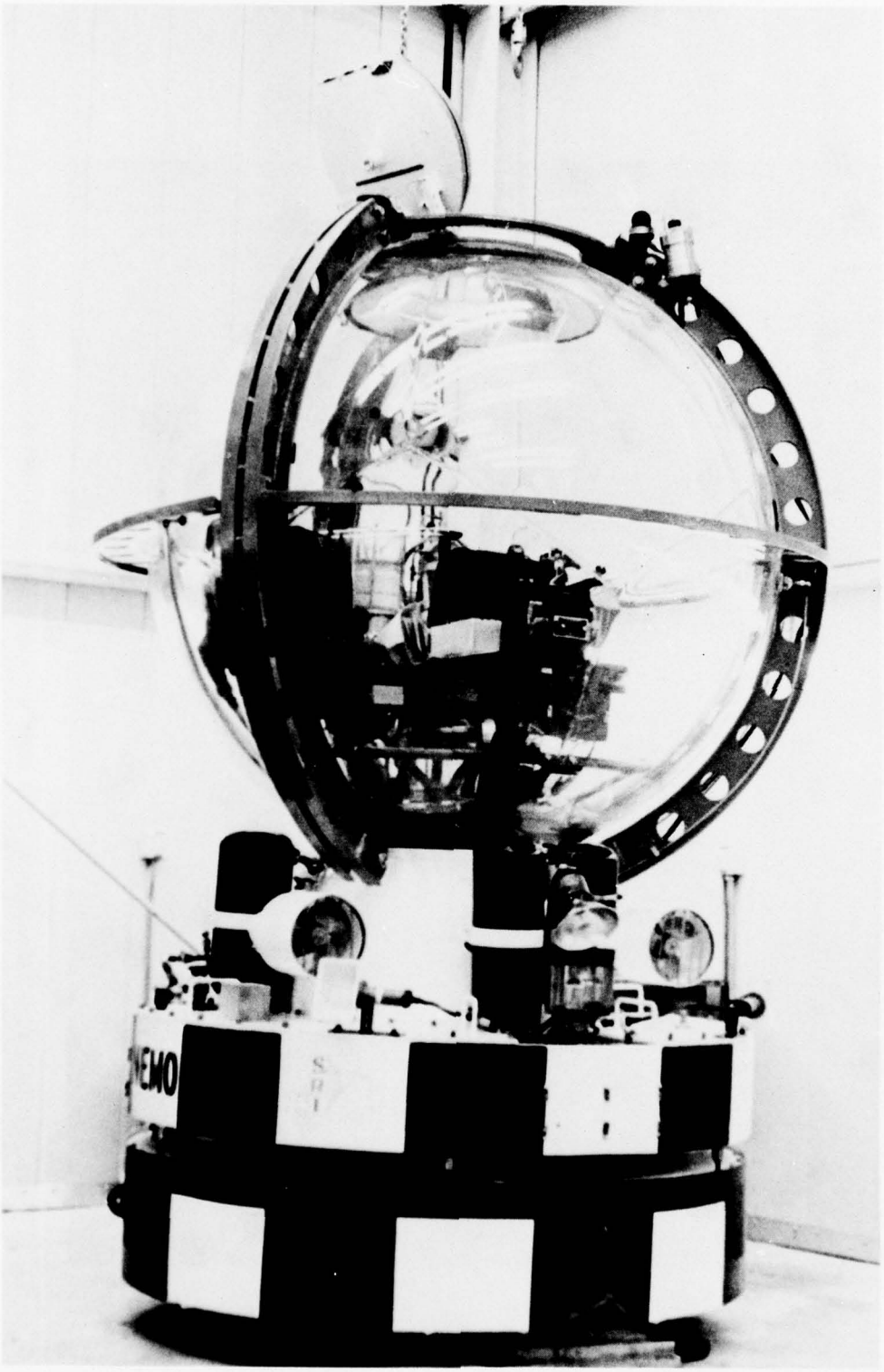

Figure 1.18. Stachiw's NEMO submersible, the first submersible with a transparent pressure hull. NEMO was developed at the Naval Civil Engineering Laboratory and approved by the U. S. Navy in 1970 for service to 600 feet (183 meters).

Figure 1.19. Typical full- and model-scale acrylic plastic pressure hulls used from 1964 through 1970 by Stachiw for destructive testing in the Deep-Ocean Simulation Facility at NCEL during the development of certification criteria for acrylic pressure hulls.

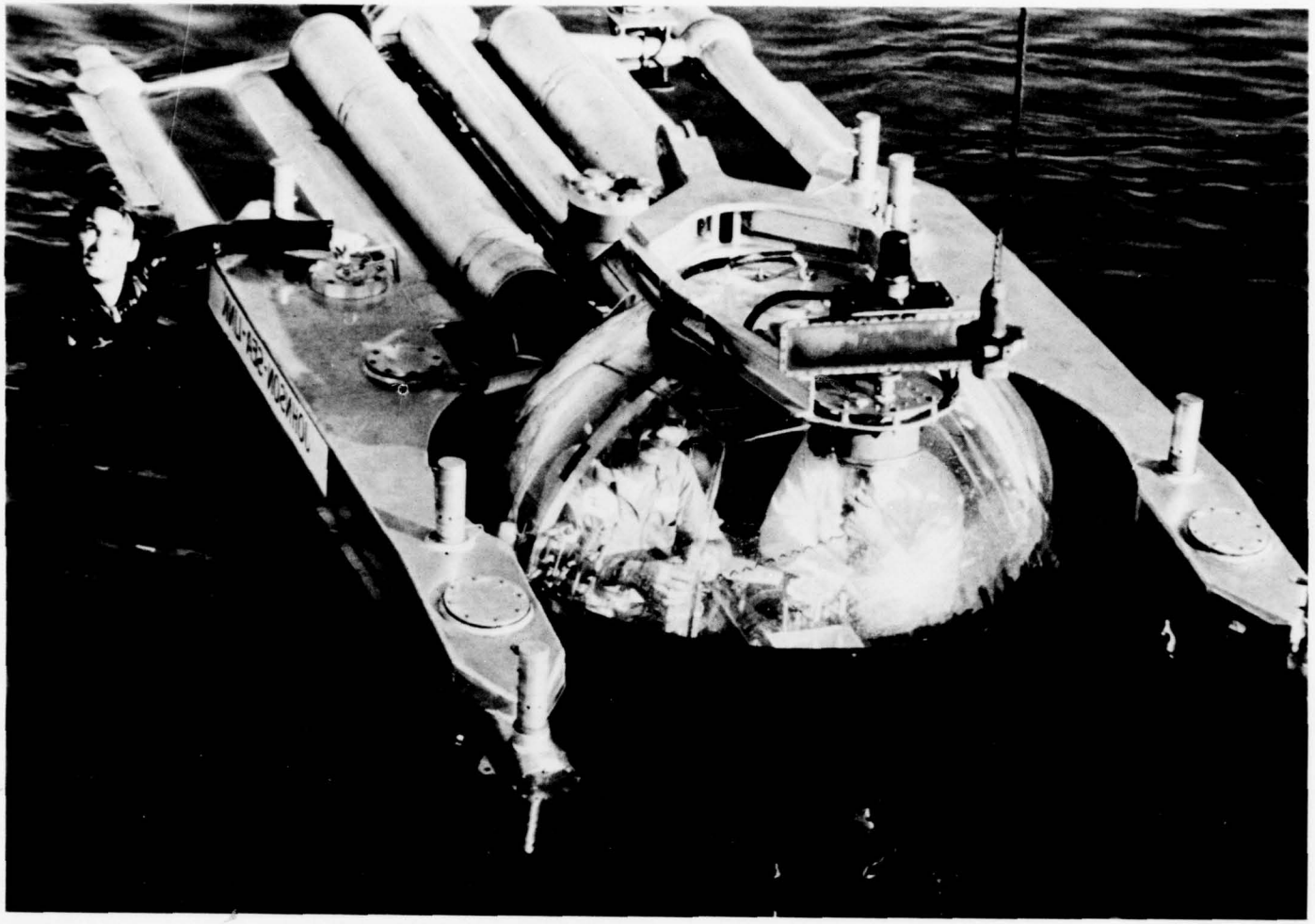

Figure 1.20. Link's JOHNSON-SEA-LINK submersible with a 3000-foot (914 meters) operational depth capability. This submersible represents a successful union between the acrylic plastic hull, chosen for its panoramic visibility, and the aluminum diver lockout chamber, chosen for its corrosion resistance and high strength-to-weight ratio. (Harbor Branch Foundation, Inc., photograph.)

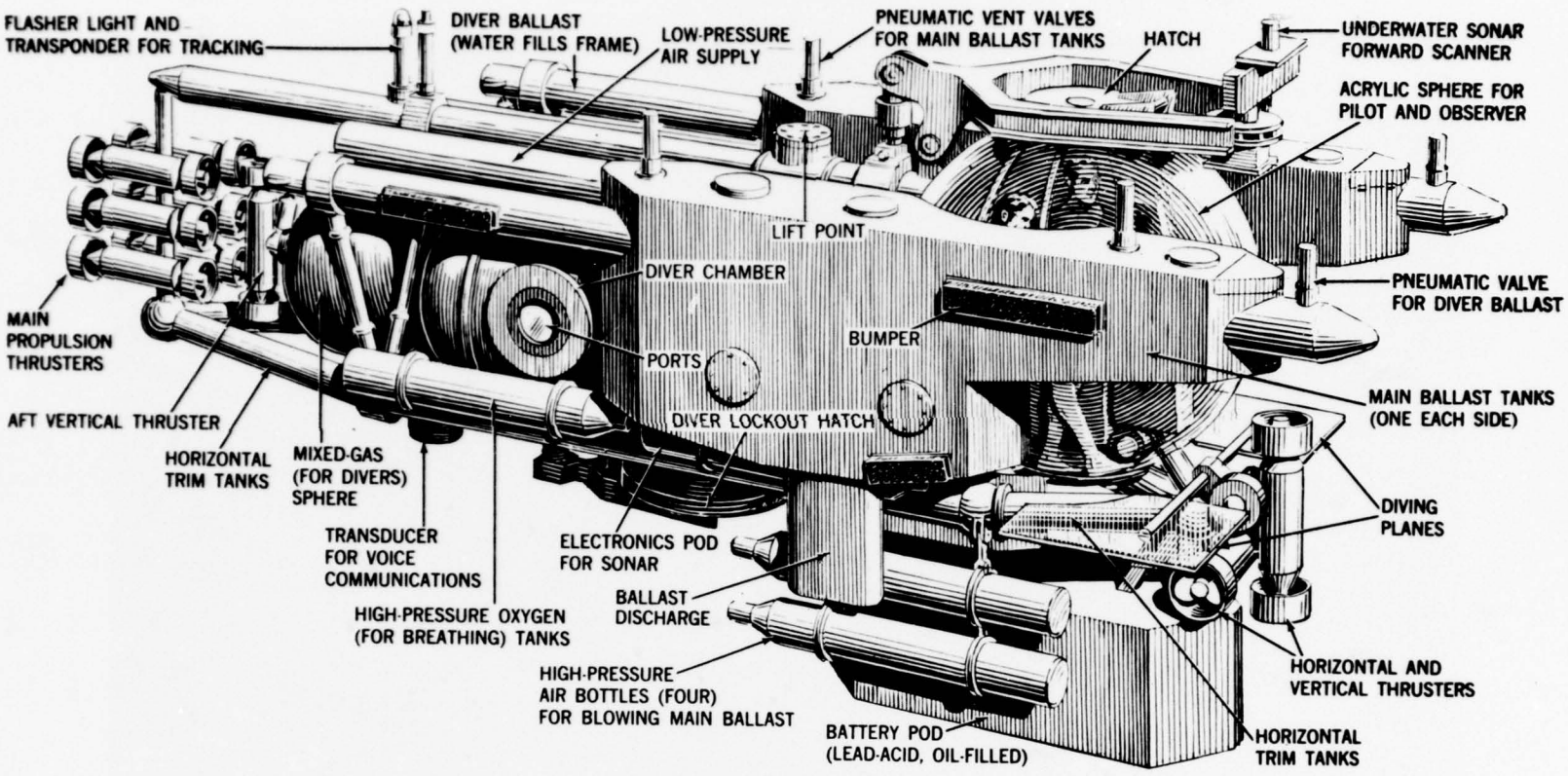

Figure 1.21. JOHNSON-SEA-LINK. The high elevation of the acrylic capsule in relationship to the ballast tanks allows the occupants to have panoramic visibility when floating on the ocean surface. (Photograph by Harbor Branch Foundation, Inc.)

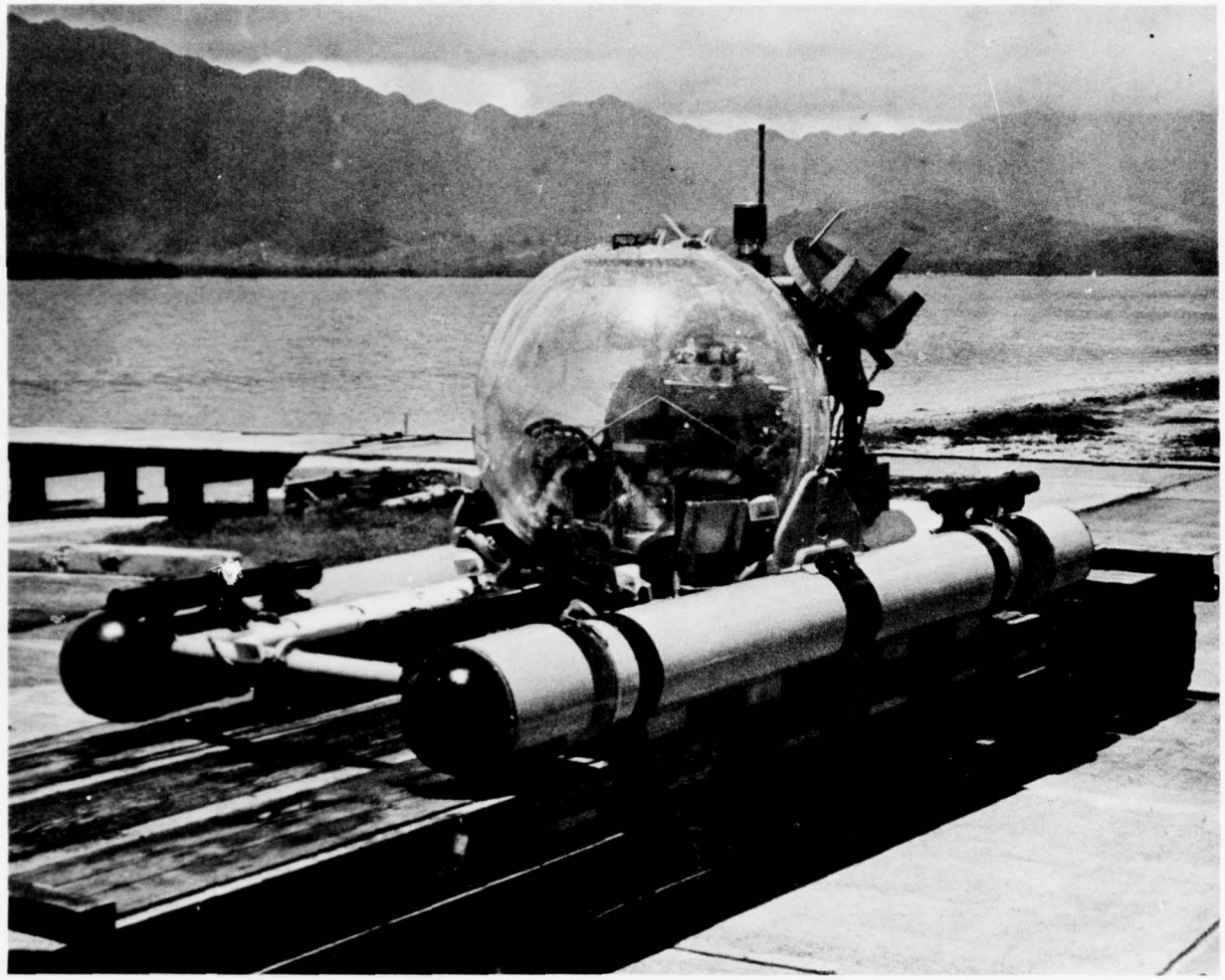

Figure 1.22. Wm. B. McLean's MAKAKAI submersible with a 600-foot (183 meters) operational depth capability. Built in 1974, it matched a panoramic visibility pressure hull to a control system by using a modulated light beam transmitted from the interior of the hull to an externally located receiver.

Figure 1.23. Acrylic plastic hull for 3000-foot (914 meters) service. The hull is made by bonding two precision-cast hemispheres. The presence of only a single equatorial bonded joint gives the cast hull undistorted visibility and lowers the fabrication costs significantly. (Applied Polymetrics photograph.)

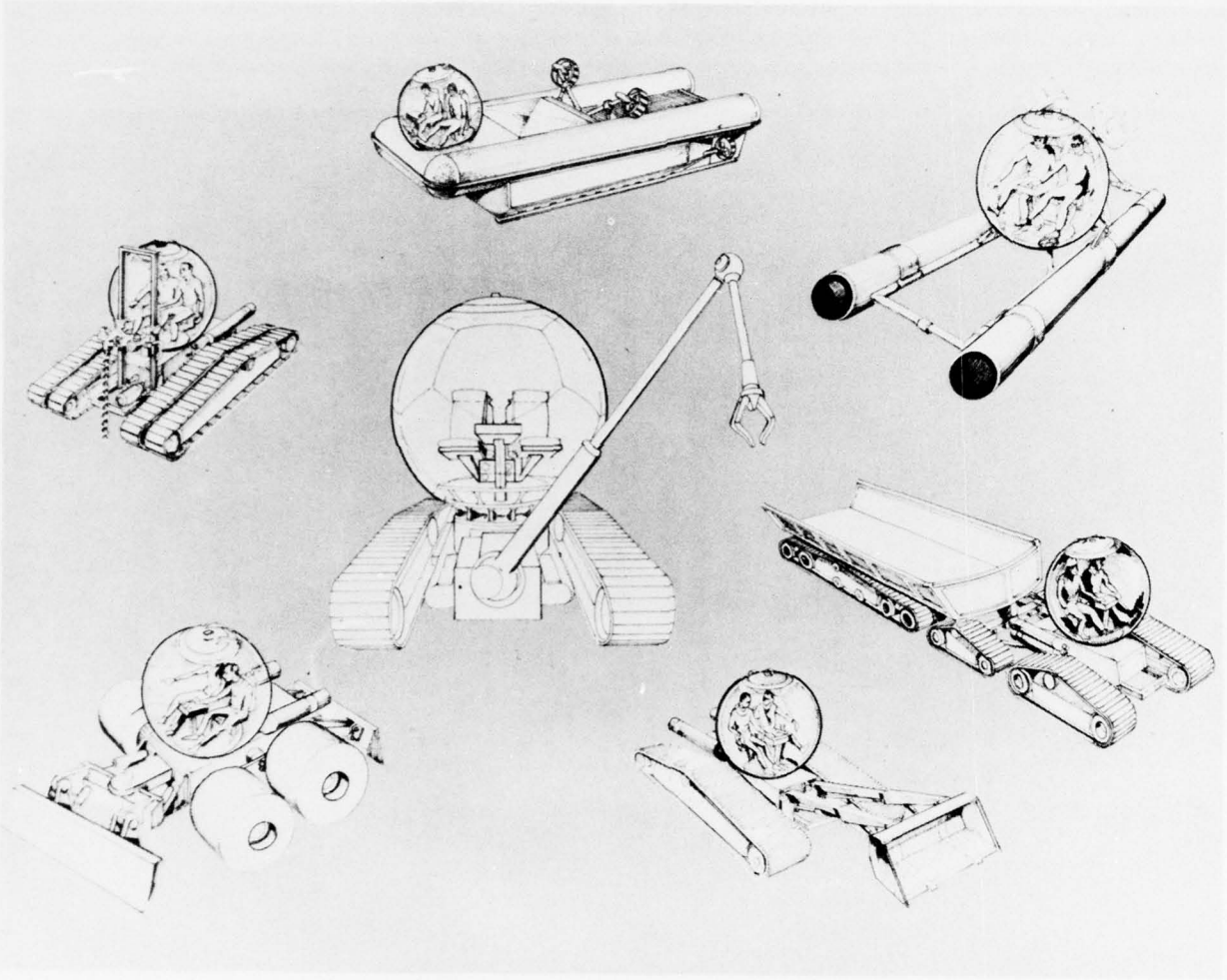

Figure 1.24. Projected future undersea applications for acrylic plastic pressure hulls in the 0- to 3000-foot (0 to 914 meters) depth range. The hulls will function as 1-atmosphere crew cabs for undersea work and exploration systems.

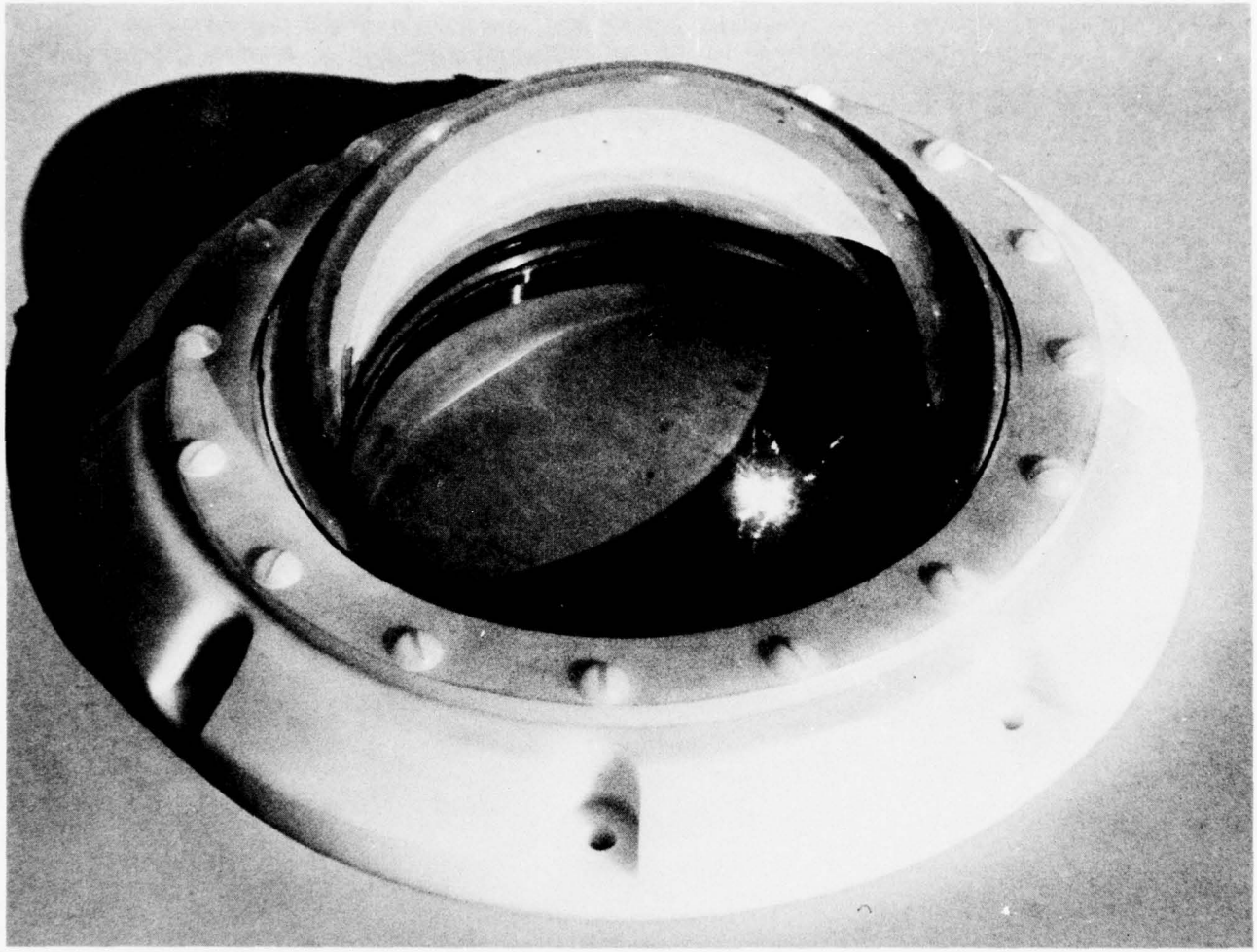

Figure 1.25. Model scale of chemically-surface-compressed glass, spherical sector window assembly with a proven operational depth capability to 40,000 feet (12,192 meters). The window assembly uses a conical bearing seat and a patented KEVLAR-49 fiber-reinforced epoxy bearing gasket developed by Stachiw at the Naval Undersea Center for spherical windows made of brittle materials.

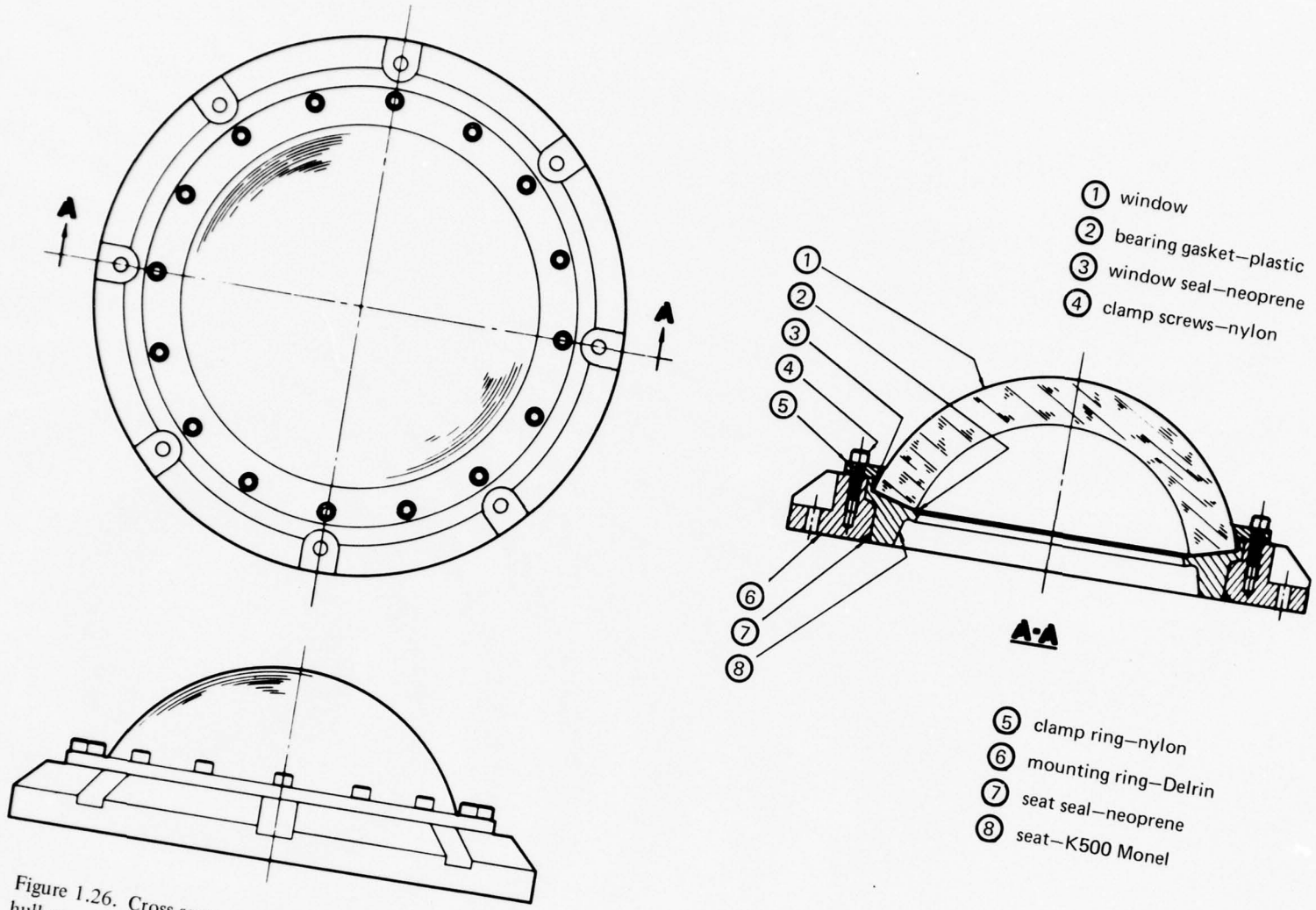

Figure 1.26. Cross-section of the viewport assembly utilizing glass or glass ceramic windows. Note that the assembly can be bolted onto any hull penetration with a plane mating surface.

SECTION 2. INTRODUCTION TO ACRYLIC PLASTIC . . . 2-1

2.1 INTRODUCTION TO PLASTICS . . . 2-1

2.2 INTRODUCTION TO ACRYLIC . . . 2-2

2.3 MANUFACTURE OF ACRYLIC MONOMER . . . 2-3

2.4 ACRYLIC POLYMERIZATION . . . 2-3

2.5 MODIFICATION OF ACRYLIC . . . 2-5

2.6 CONVERSION OF ACRYLIC RESIN . . . 2-7

2.7 ACRYLIC PROPERTIES . . . 2-17

2.8 COMPARISON OF ACRYLICS . . . 2-20

2.9 CHEMICAL RESISTANCE . . . 2-26

2.10 PRODUCTS MADE FROM ACRYLICS . . . 2-27

2.11 DESIGN CONSIDERATIONS . . . 2-38

2.12 THERMOFORMING ACRYLIC . . . 2-38

2.13 MACHINING ACRYLIC . . . 2-42

2.14 SANDING, POLISHING, AND CLEANING ACRYLIC . . . 2-46

2.15 SURFACE COATINGS AND TEXTURING . . . 2-46

2.16 JOINING ACRYLICS . . . 2-51

2.17 LAMINATION . . . 2-53

2.18 SUMMARY . . . 2-57

SECTION 2.
INTRODUCTION TO ACRYLIC PLASTIC*

2.1 INTRODUCTION TO PLASTICS

Plastics are synthetic organic materials consisting of combinations of carbon with oxygen, hydrogen, nitrogen, and other organic and inorganic elements. Although solid in their finished state, at some point in the processing they are liquid and thus capable of being formed into various shapes by the application of heat and pressure. Plastics in finished form consist of long chain molecules (polymers) that result from combining single molecules (monomers). There are approximately 30 distinct families of plastics (table 2.1), and within each family there are many different types, each capable of being produced in a variety of forms. Thousands of plastic types and formulations exist; however, in practice, selection for a given application is limited to a relatively small number.

Table 2.1. Plastic families.

Thermoplastics	Thermosets
ABS	Alkyd
Acetal	Allylic
Acrylic	Casein
Cellulosic	Epoxy
Chlorinated polyether	Melamine
Fluoroplastic	Phenolic
Ionomer	Polyester
Nylon	Silicone
Phenoxy	Urea
Polyallomer	Urethane
Polycarbonate	
Polyimide	
Polyphenelene oxide	
Polysulphone	
Polyethylene	
Polypropylene	
Polystyrene	
Vinyl	

* *This section was contributed by H. Mukamal, N. G. Nixon, and W. Yamaguchi of Swedlow, Inc.*

Plastics are divided into one of two groups: thermoplastics or thermosets. The thermoplastics become soft when heated and then harden when cooled (this process occurs regardless of the number of times it is repeated). Thermosetting resins, conversely, undergo a chemical change when heat and pressure are applied but cannot be resoftened. Thermoplastics can be generally grouped by their load-bearing abilities, capabilities to withstand various weather conditions, and general-purpose qualities; they are normally used in an unfilled state. In contrast, thermosets are generally used in conjunction with fillers and reinforcements which are added to enhance a normally weak and easily fractured polymeric structure. Compression molding is the most common method of forming thermosets, whereas injection molding is the principal process for forming thermoplastics.

Each family has identifying characteristics, which render it most suitable for specific applications. The characteristics of these materials, as well as general physical properties, are contained in numerous references and can be used in conjunction with information on cost and method of manufacture to select a plastic for a specific application.

Acrylic is a material family within the thermoplastic group and is distinct from all other members because of its chemical structure and unique physical properties and characteristics. A study of acrylic not only provides the necessary tools for its successful use, but it also provides a framework for evaluating and understanding other families.

The information which will be presented in this section is necessarily brief and generalized. Specific processes and material properties should be considered as approximations and verified prior to application. Physical properties, in particular, are typical values and must not be applied as minima.

2.2 INTRODUCTION TO ACRYLIC

The term "acrylic" is generally used to describe that group of glass-like thermoplastic resins and resulting derivatives that is made by polymerizing esters of acrylic or methacrylic acid. The most common interpretation of the term is a polymer known as polymethyl methacrylate which has been sold in sheet form under the trade names of Acrivue, Lucite, Plexiglas, and Swedcast. In a general sense, acrylic monomers can be polymerized to form materials which range from soft and rubbery to hard crystal-like substances with properties that can be tailored to fit a variety of applications and requirements.

While evaluating acrylate polymers and copolymers of methyl methacrylate for application as an interlayer or laminating medium between sheets of glass, the unique nature of polymethyl methacrylate – a rigid glass-like thermoplastic material – was discovered by Dr. Ottom Rohm. In 1933, he patented a process for the manufacture of structures, such as panels or sheets, from this new resin. This original work formed the foundation for current acrylic technology, and polymethyl methacrylate usefulness has subsequently predominated in the acrylic family. Several companies have continued to extend this technology and the processing of acrylics. United States firms such as American Cyanamid Co., E. I. du Pont de Nemours & Co., Rohm & Haas Co., and Swedlow, Inc., have provided significant technical advancements and material production capabilities along with contributions from several European and Asian firms. Innumerable fabricators have provided important product and processing innovations that were necessary to achieve the currently expanding product base for acrylics.

2.3 MANUFACTURE OF ACRYLIC MONOMER

A methyl methacrylate monomer is industrially produced by reacting hydrogen cyanide with acetone to yield acetone cyanhydrin. This acetone cyanhydrin is mixed with concentrated sulfuric acid and heated to form a crude methacrylamide sulfate which is reacted with methanol and water, yielding methyl methacrylate and ammonium bisulfate:

$$CH_3-\overset{\overset{O}{\|}}{C}-CH_3 \xrightarrow{HCN} CH_3-\overset{\overset{OH}{|}}{\underset{\underset{CN}{|}}{C}}-CH_3 \xrightarrow[H_2SO_4]{CH_3OH} CH_2=\overset{\overset{CH_3}{|}}{C}-COOR + (NH_4HSO_4)$$

This process has its origin in natural gas which yields propane to form propylene, then isopropyl alcohol, and finally the necessary acetone for subsequent reactions. The major producers of methyl methacrylate monomers in the United States are E. I. du Pont de Nemours & Co. and Rohm & Haas Co.

2.4 ACRYLIC POLYMERIZATION

Most acrylic monomers are polymerized commercially by a mechanism of free radical induction* which occurs in one of three basic polymerization processes: bulk, single-phase dilute solution, and multiphase dilute solution (figure 2.1). The selection of a particular polymerization process is determined by the necessary requirements of the derived polymeric material. In addition to the effect of the process selected, the resultant physical properties depend on the process conditions and are modified by the use of different acrylic monomers or monomer mixes. The wide range of properties obtainable has been significant in the constantly increasing scope of acrylic applications. The bulk process yields material in sheet form; the single-phase dilute solution process yields liquid materials like cements, adhesives, and impregnating resins and coatings; and the multiphase dilute solution process, which is further subdivided, yields extrusion-type pellets in the case of the suspension method and paints in the case of the emulsion method. The general character of materials derived from these processes can be more clearly understood by examining the key features of each polymerization method.

Bulk polymerization (figure 2.2) is accomplished without any diluents, i.e., with the monomer acting as the solvent medium. This process accounts for the majority of sheet stock, rods, and tubes and is achieved by pouring monomers or monomer-polymer mixtures into suitable molds. Control of the chemical reaction rate which occurs during the cure cycle (the Traumsdorff period) is an important key to this process. At this time there is a high concentration of growing polymer chains and thus high exothermic heat generation. Success in bulk polymerization requires a careful reaction rate control (slowing down) to avoid bubble formation and other problems. During this polymerization process a volumetric shrinkage of about 21 percent occurs with an accompanying increase in specific gravity. The chief advantages of bulk polymerization are (1) the outstanding optical quality of the transparent grades of this material, (2) the possiblity for attainment of high molecular weight polymers, and (3) the capability to achieve highly cross-linked structures through the use of additives.

**An initiator such as a peroxide or azo compound is usually used.*

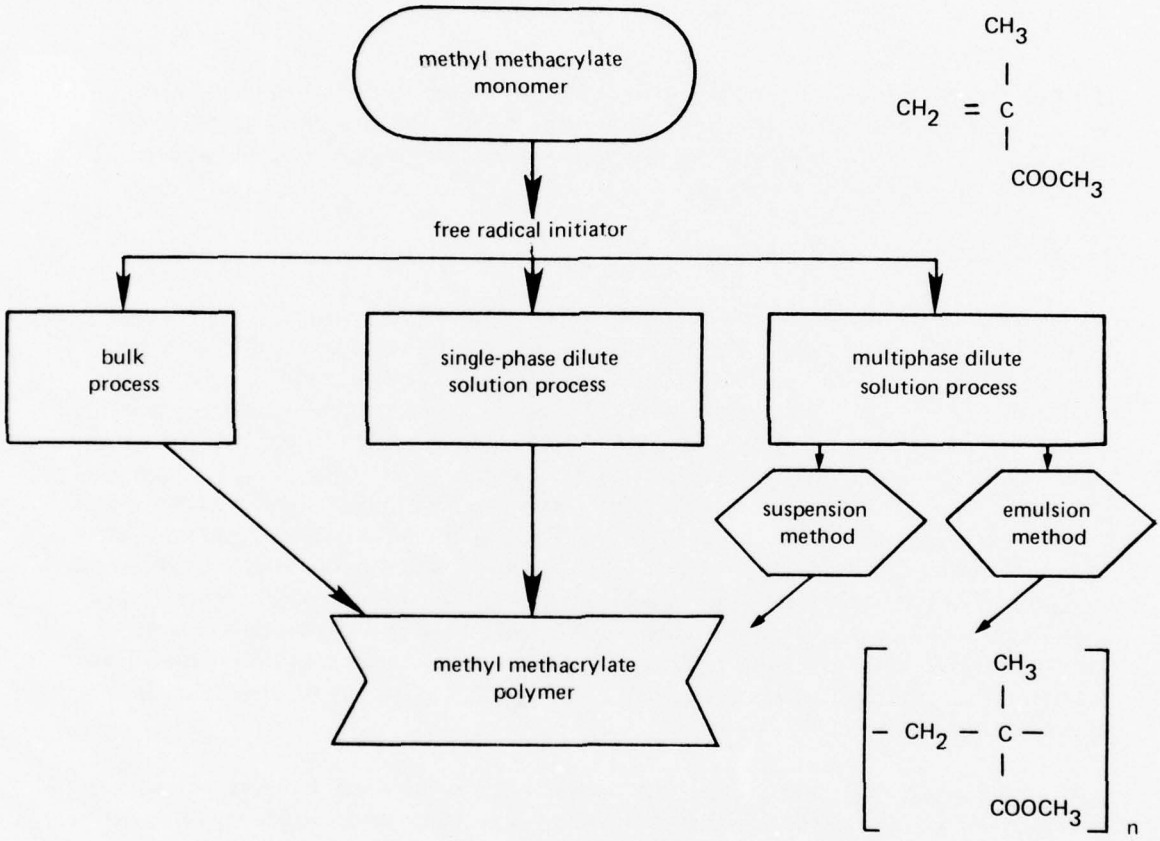

Figure 2.1. Methyl methacrylate polymerization processes.

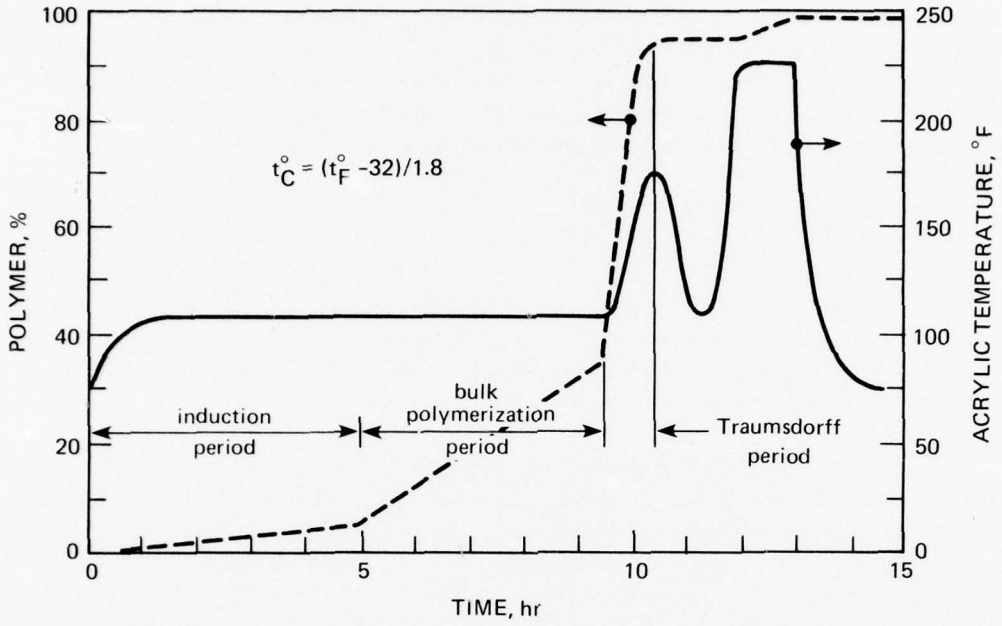

Figure 2.2. Typical bulk polymerization cycle.

Single-phase solution polymerization uses a nonpolymerizable solvent in conjunction with the monomer to reduce viscosity and control the rate of heat production. The process is carried out in a chemical reactor or kettle and directly produces materials such as coatings, adhesives, and cements, i.e., acrylic polymer solutions. These materials are usually formulated to be of low molecular weight.

Multiphase solution polymerization is performed using a monomer insoluble phase, such as water, as a carrier, and is divided into suspension and emulsion methods. In the emulsion method the polymer remains dispersed in the water mixture, and in the suspension method polymeric beads are formed and extracted from the water mixture. The advantage of this process lies in the economy and safety derived from the use of water as the polymerization medium and the completeness of the polymerization reaction. Again, material of a fairly low molecular weight is usually derived.

2.5 MODIFICATION OF ACRYLIC

During polymerization, acrylic can be modified to produce optimum combinations of properties. These modifications include molecular weight control, crosslinking, molecular modification, and the incorporation of additives.

The molecular weight of polymethyl methacrylate is the most important property that must be defined for the polymer. The use of chain regulators (usually mercaptans) results in lower molecular weight. Low molecular weight polymers are extensively used as the pellets for extrusion and compression molding. Such a material results in reduced levels of melt viscosities and hence easier extrusion or capability to be molded. When the molecular weight

is reduced, however, there is an attendant reduction in weatherability and allowable usage temperature. High molecular weight polymers, produced by low rates of polymerization, are generally fabricated from monomeric percursors, i.e., a bulk polymerization process. These materials usually have improved resistance to weathering and solvent attack and improved physical properties when compared with extruded parts.

Incorporation of crosslinking in polymethyl methacrylate is accomplished by the use of either a difunctional monomer such as ethylene glycol dimethacrylate or by a chemical reactant involving a reactive monomer incorporated in the polymer. The first results in a crosslinked product during formation of the shape, e.g., cell casting; the second can be made to occur after the formation of the shape, e.g., during thermal treatment. In either case, the resulting polymer has improved thermal resistance, excellent resistance to solvents, and improved physical properties.

Polymethyl methacrylate can also be modified by using comonomers to alter specific properties. The incorporation of acrylate comonomers in small quantities in the polymer formation is useful in increasing the thermal stability of polymers. In large quantities, however, these comonomers lower the ceiling temperature and increase the softness of the polymethyl methacrylate. The impact strength of polymethyl methacrylate can be increased by the incorporation of polymeric rubbers to produce two-phase systems, in which the polymeric rubber is uniformly dispersed in the polymethyl methacrylate matrix.

Additives also play a significant role in modifying the basic properties of polymethyl methacrylate. Some additives and their effects on the resulting material are in table 2.2.

Table 2.2. Additives used to modify polymethyl methacrylate.

Additive	Approximate Usage Quantity, %	Effect
Dyes	0.001 to 0.1	Coloring and reduction of light transmission
Polymers	0.01 to 1	Diffusion of light
Pigments	0.01 to 5	Translucency, opacity, and color
Glass spheres	0.01 to 10	Translucency and density reduction
Inorganic fillers	0.1 to 70	Increased hardness and decreased flammability, opacity, and translucency
Flame retardants	0.01 to 10	Retarded flammability
Ultraviolet stabilizers	0.0001 to 0.1	Light stability

By selective modification, specific properties of polymethyl methacrylate can be enhanced to satisfy the needs of new markets. Modification can be done by the use of additives or copolymerization with other resins during the polymer formation stage. In both solution and emulsion polymerization, endless specific formulations can be obtained for specialty products, such as inks, adhesives, binders, coatings, and paints. Modification during polymer formation in suspension polymerization is more limited than for solution or emulsion polymerization. However, the powder or granules can be blended with other resins to achieve specific objectives; high-impact-resistant extrusion and molding materials are good examples. In general, however, some property is sacrificed to obtain the selected improvement, e.g., for impact-resistant acrylic products of copolymers there is usually a lower thermal deformation limit than for those made of acrylic homopolymers. Specific additives can also be included in the polymer formulation to increase temperature and craze resistance, which are important in aircraft-grade acrylic sheeting.

Modifications in catalysts and casting techniques offer the potential in bulk polymerization for casting massive acrylic shapes. Techniques have been developed to produce such castings using a monomer-polymer slurry in conjunction with the modification of conventional cell-casting techniques. Although these do not have the physical properties of conventional castings, they are quite acceptable for applications where increased weight is tolerable and the use of normal cell-cast acrylic material would be precluded.

2.6 CONVERSION OF ACRYLIC RESIN

The bulk polymerization process produces sheets, rods, and shapes through batch cell casting, continuous casting, and slush casting.

The procedure for cell casting is shown in figure 2.3.

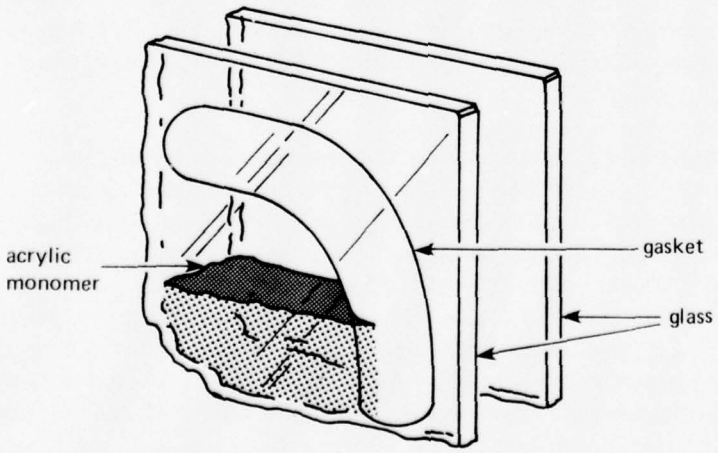

Figure 2.3. Cell casting process.

The cell is prepared from two pieces of tempered glass which are larger than the desired finished casting size. The plates are separated at the periphery by a flexible gasket, such as plasticized polyvinyl-chloride tubing. The gasket is held in place by spring clamps or similar devices which permit continuous contraction of thickness as polymerization proceeds. When the cell is prepared, a corner is left open to allow filling with a predetermined quantity of monomer or syrup (monomer-polymer mixture) (see figure 2.4). The monomer or syrup is formulated with all necessary modifiers and ingredients, such as the catalyst, chain regulators, crosslinkers, colorants, and mold-release agents. After cell filling, the corner is sealed and clamped. The material in the filled cell is polymerized by placing the cell in water tanks, air ovens, or pressurized autoclaves for a specified temperature/time cycle which depends upon the material's composition and thickness. After cooling the cell and stripping the glass molds from the sheet, the polymerized acrylic can be annealed to relieve internal strains or possibly post-cured to further chemical reactions within the sheet.

In the late 1960s, Swedlow, Inc., developed a continuous casting process (figures 2.5, 2.6, and 2.7). This process utilizes two endless, polished, stainless-steel belts which are vertically separated by the pressure exerted through a continuously injected and polymerizing syrup. The syrup is confined to the belts by two flexible polyvinyl-chloride gaskets at each side of the belt. The upper and lower belts move at the same speed and at a rate determined by the nature of the product produced and the thickness of the desired casting. The material held between the belts proceeds at a constant speed through temperature zones of varying lengths and emerges from the belts as a completely cured sheet. The only size limitation is the belt width.

Another approach is to use a slush-casting process. A polymer-catalyzed monomer slurry containing 50- to 90-percent polymer is mixed and placed in a mold, which may be a stationary or rotating type (figure 2.8). Because of the presence of the preformed polymer in the mixture, the heat generated by the polymerizing monomer is reduced and more easily dissipated. If the formulations of the preformed polymer and catalyzed monomer are similar and if the preformed polymer is not crosslinked, then a totally clear homogeneous product results. Extremely large castings, such as clear submarine nosecones, tubular hyperbaric chambers, and massive diamond-quality art objects, have been prepared using this approach (figures 2.9, 2.10, and 2.11).

The extrusion and compression molding processes use pellets prepared through suspension polymerization (figure 2.12). These pellets are heated and pressures applied within a die until the material is in a molten state and capable of flowing within the control cavity. In the case of extrusion, both heating and pressure applications are developed within a barrel by means of a screw that runs inside its length. The molten material is extruded out of the end of the barrel and into a mold cavity. Compression molding relies on a moveable section of the mold cavity for pressure application and the material is heated within the mold. Because the resulting products are normally formulated to be of low molecular weight, the mechanical properties are generally lower than those for bulk polymerized products.

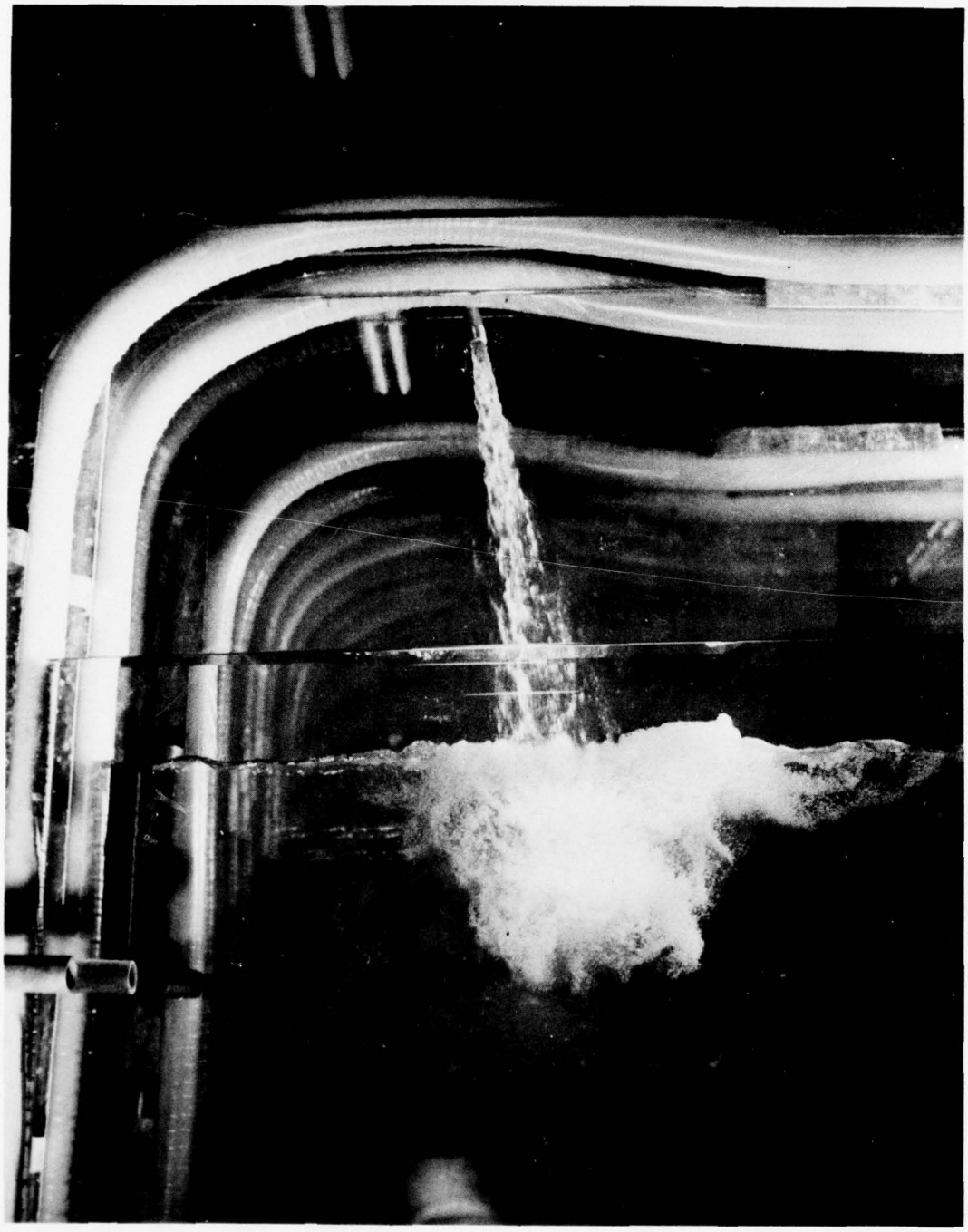

Figure 2.4. Filling of casting cell with acrylic monomer mixture. Cell is composed of two pieces of glass spaced apart at the edges by an elastomeric tube gasket. (Photograph by Swedlow, Inc.)

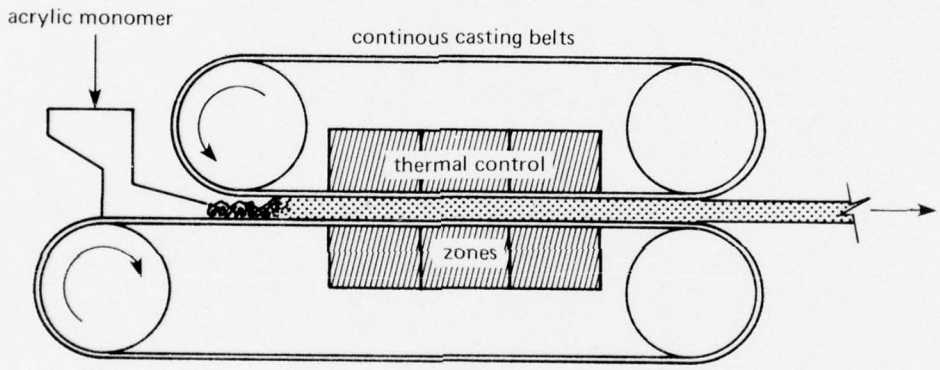

Figure 2.5. Continuous casting method.

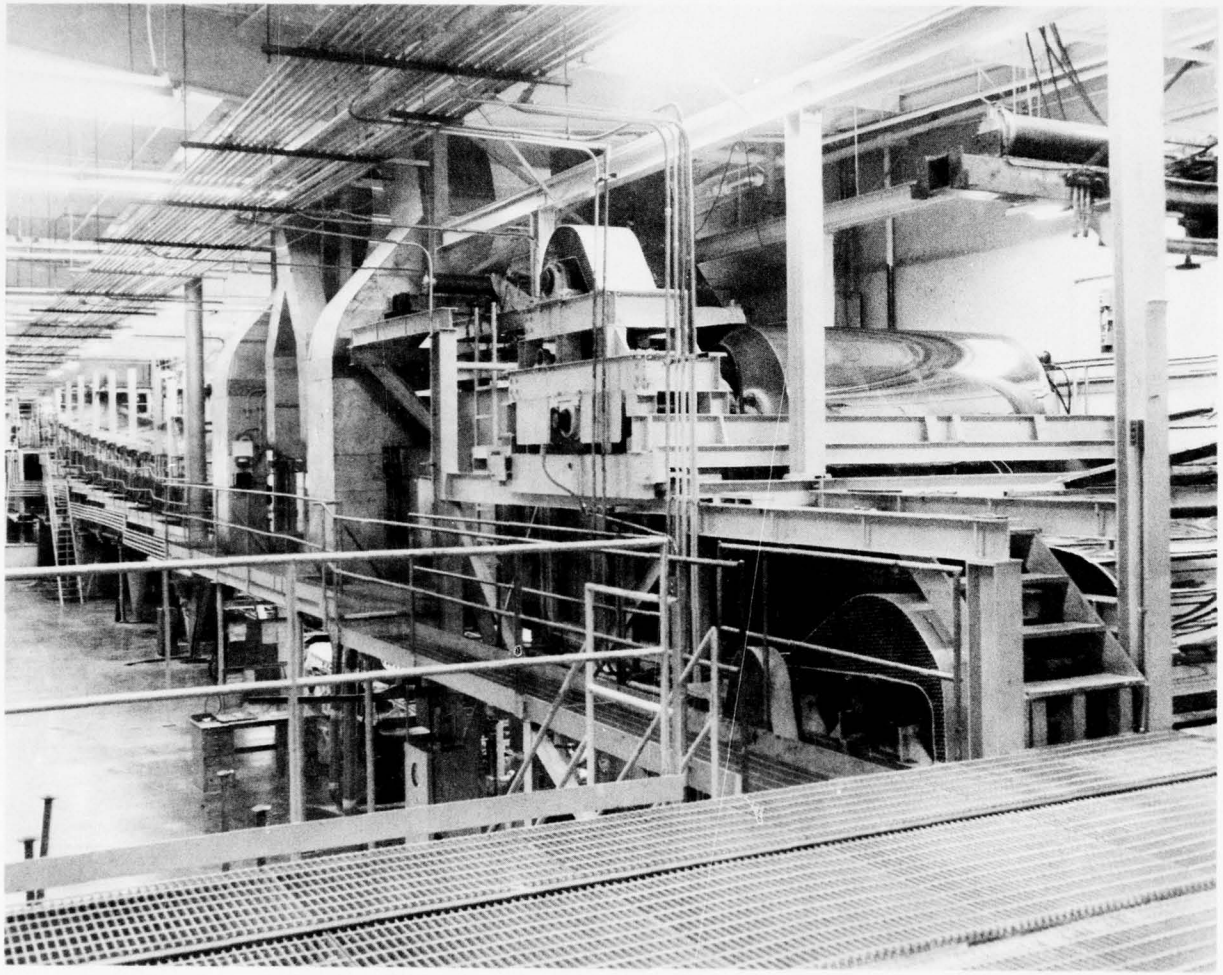

Figure 2.6. Machine developed by Swedlow, Inc., for continuous casting of acrylic sheeting. (Photograph by Swedlow, Inc.)

Figure 2.7. Rolls of acrylic sheeting, a product of the continuous casting process. (Photograph by Swedlow, Inc.)

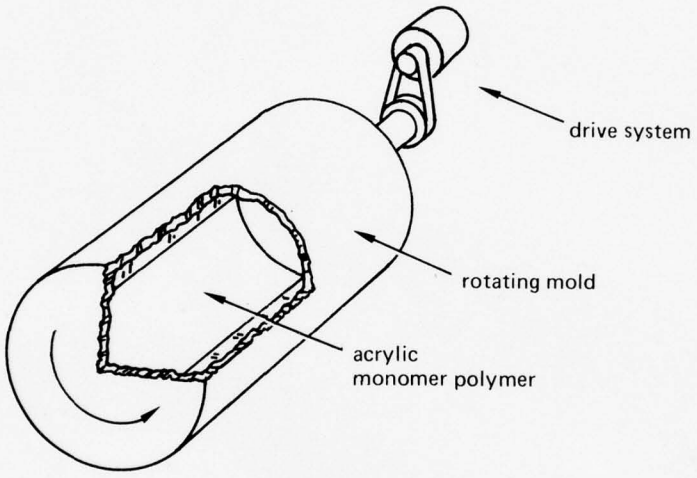

Figure 2.8. Rotary slush-casting method.

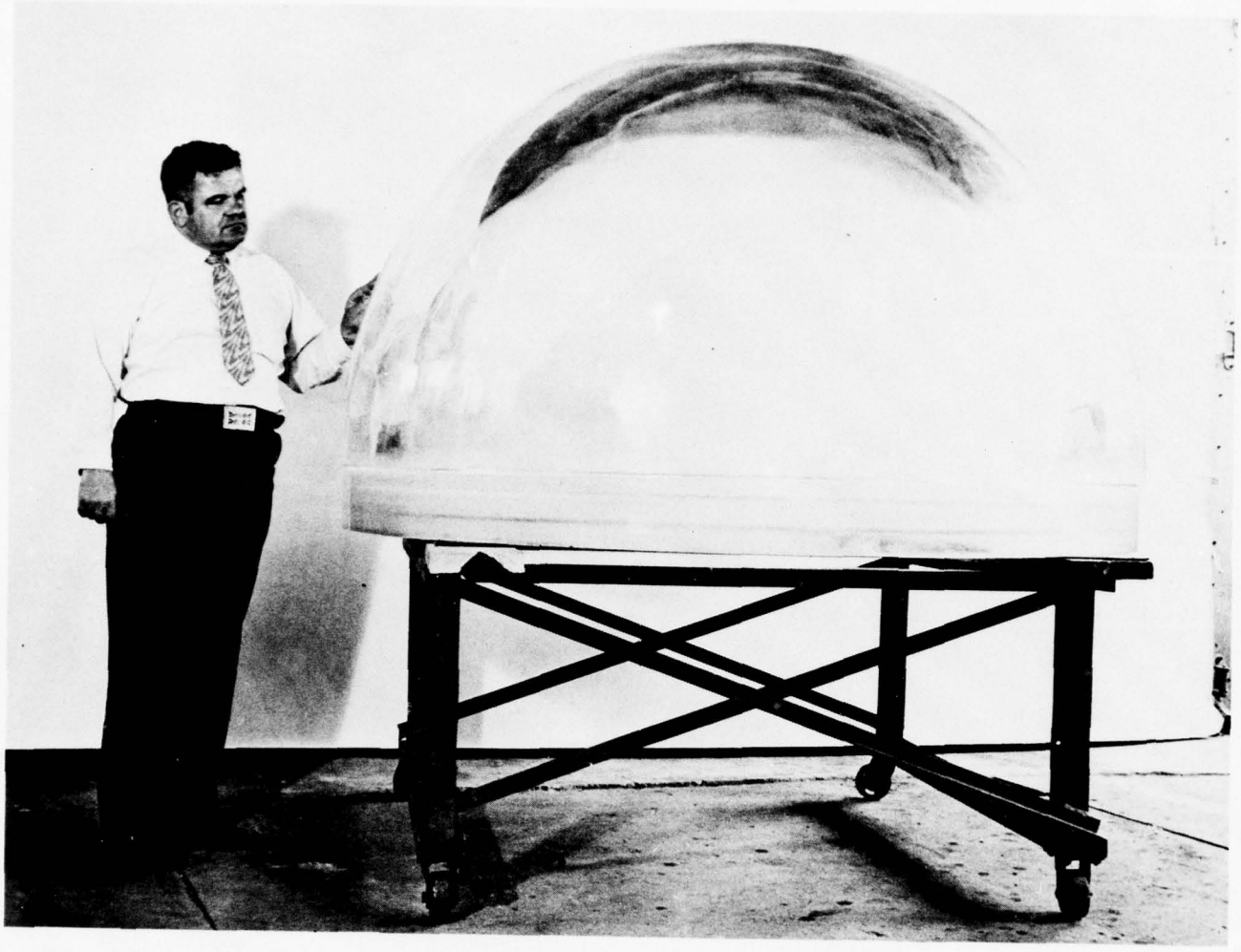

Figure 2.9. Massive casting for the observation dome on the semisubmersible SSP KAIMALINO. (Photograph by Cadillac Plastic and Chemical Co.)

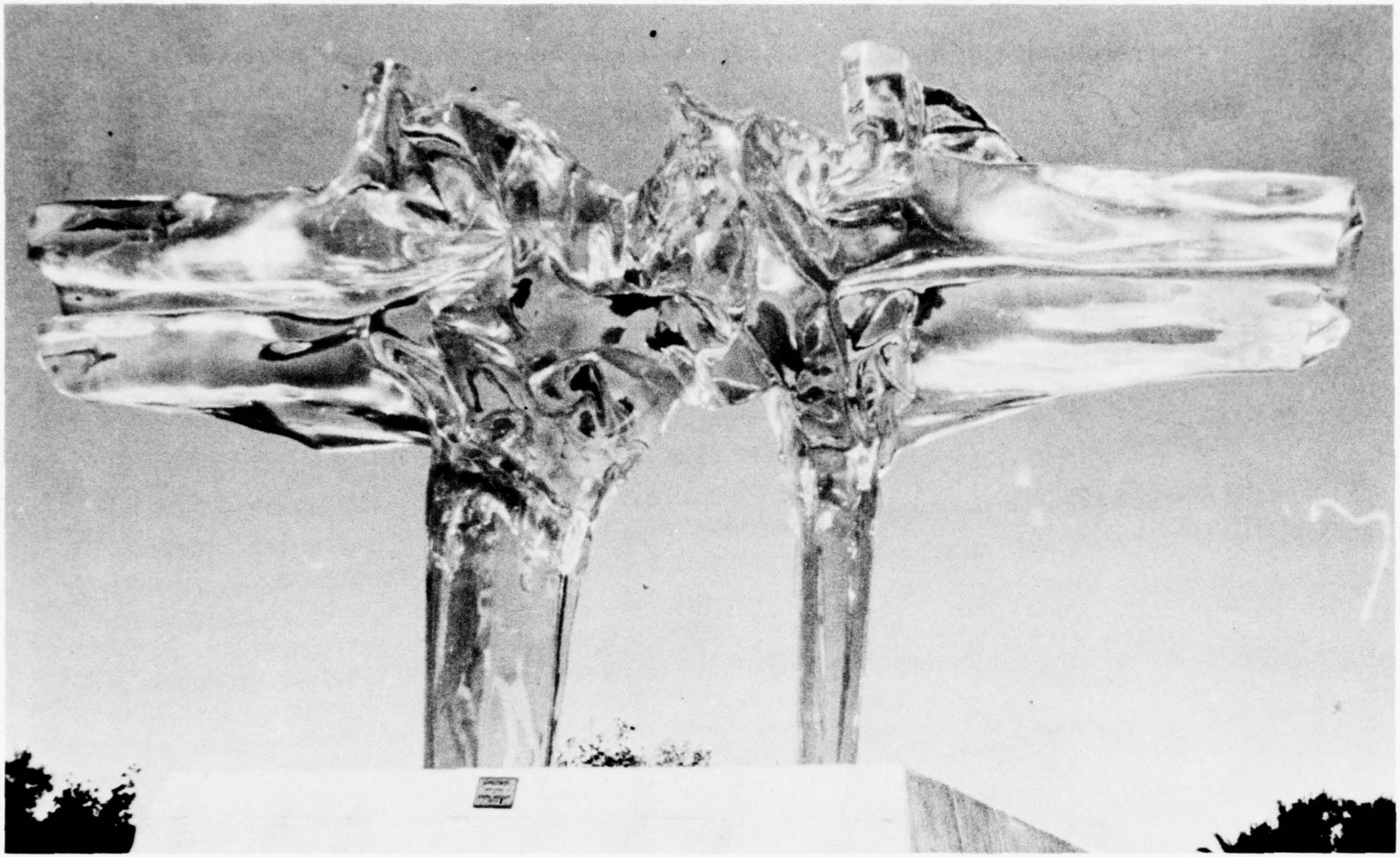

Figure 2.10. Modern sculpture cast in acrylic plastic by Bruce Beasley. (Photograph by Western Statuary.)

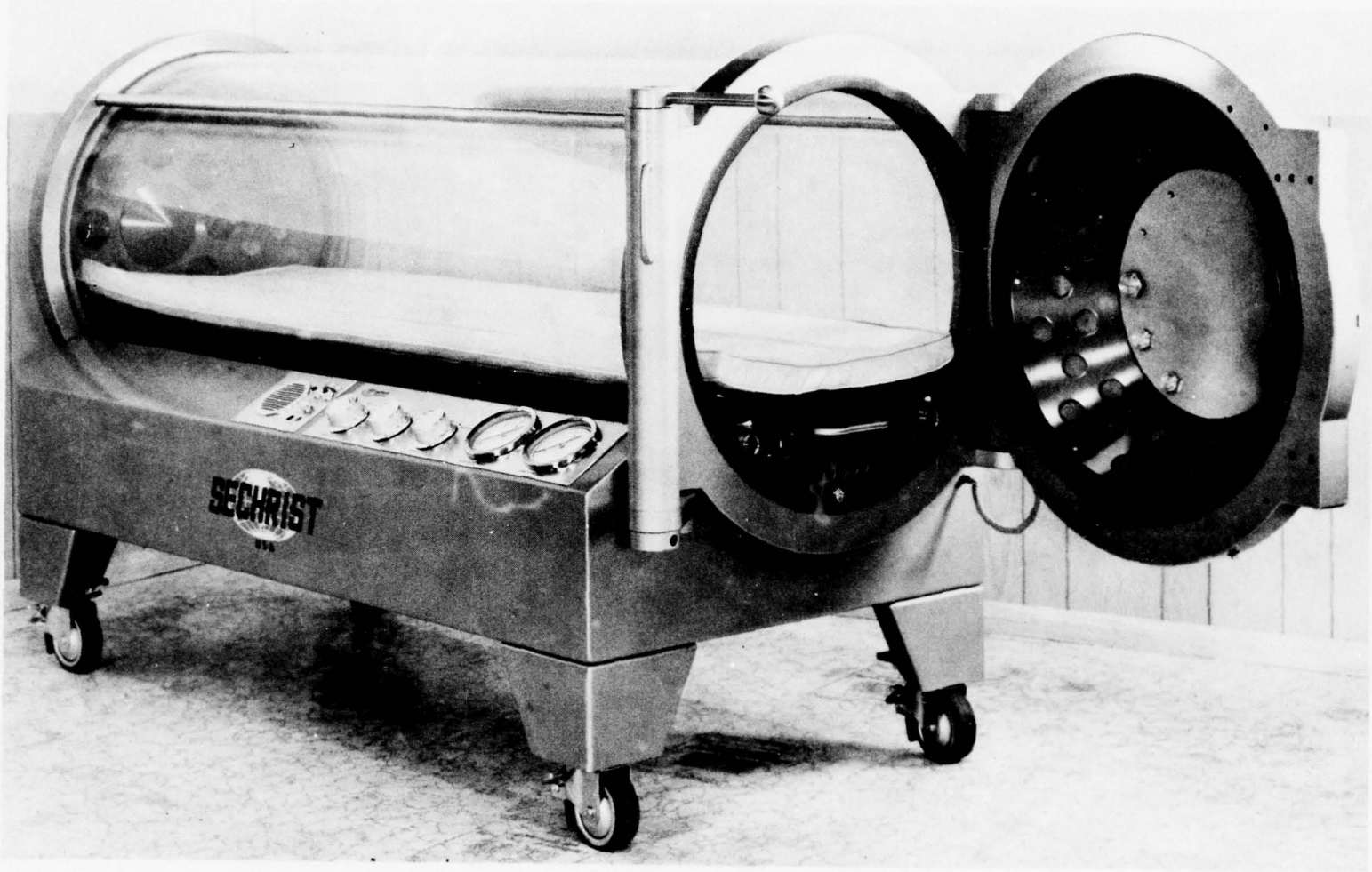

Figure 2.11. Hyperbaric chamber for hospital utilizing spin-cast acrylic tubes. (Photograph by Sechrist Industries.)

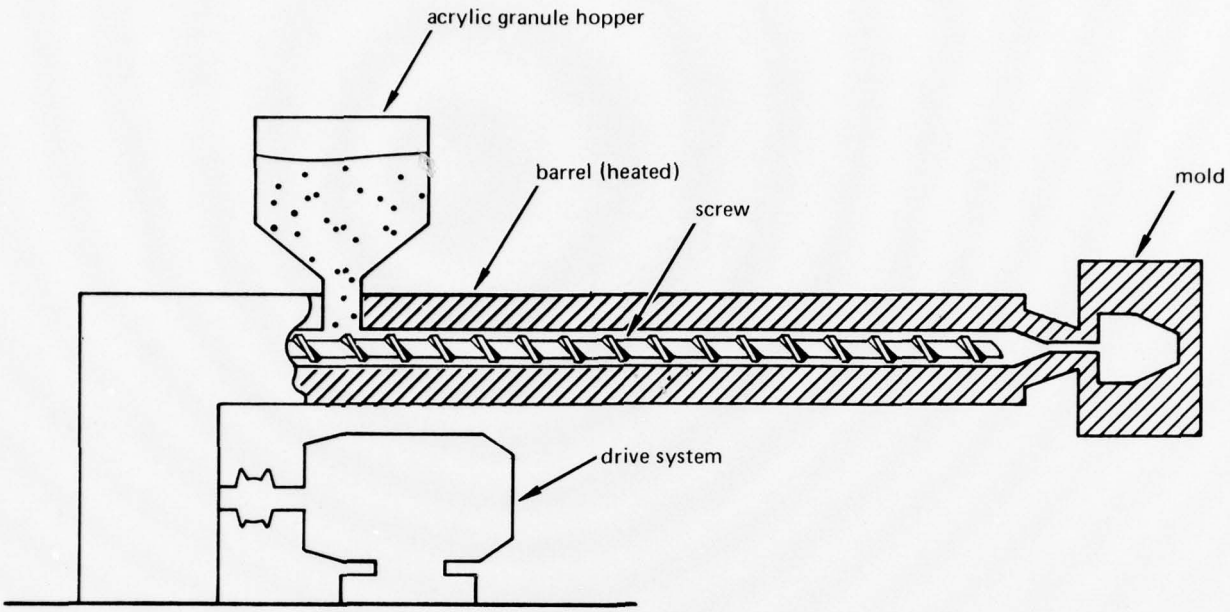

Figure 2.12. Injection molding method.

2.7 ACRYLIC PROPERTIES

The three main product performance requirements which are satisfied through the use of acrylic and which usually account for its selection in preference to competing plastic materials are its outstanding weather resistance, excellent optical clarity, and superb colorability and color retention.

Bulk-polymerized methyl methacrylate is virtually unsurpassed in its resistance to outdoor weathering. This property, coupled with color retention, accounts for acrylic's dominance in the outdoor sign market (figure 2.13). Signs of acrylic are commonly guaranteed to be weather resistant for more than 15 years. In addition, acrylic paint finishes and coatings are well known for their long and durable life.

In the visual range of light, the transmission of acrylic approaches perfection (figure 2.14). Transmission of 91 to 92 percent is normal for material thicknesses less than 1/2 inch (1.27 centimeters) with 92 percent the maximum achievable for a material with an index of refraction of 1.5. The transmission is reduced slightly as the thickness is increased because of absorption (figure 2.15).

Acrylic sheets, paints, and moldings are virtually unlimited in the variety of colors which can be achieved. Sheet stock is available from most suppliers in a broad range of standard colors with special colors available on request. The resistance to color change with time, or color stability, is dependent upon the pigments used, but it is generally outstanding.

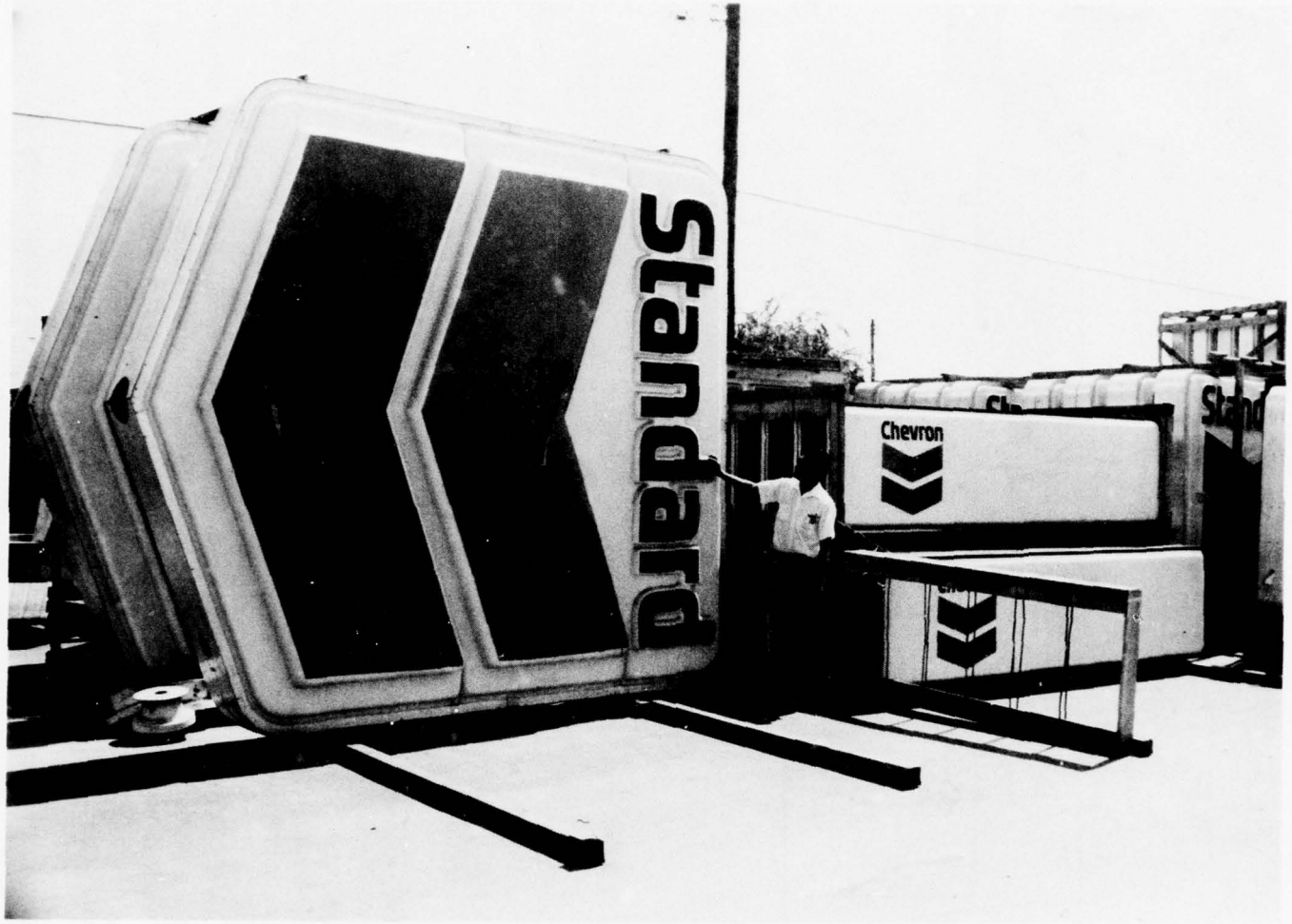

Figure 2.13. Typical outdoor advertising sign fabricated from vacuum-formed acrylic plastic. (Photograph by Swedlow, Inc.)

Figure 2.14. Crystal clarity and optical quality of acrylic plastic is readily apparent in this spherical viewport for submersibles. (Photograph by Swedlow, Inc.)

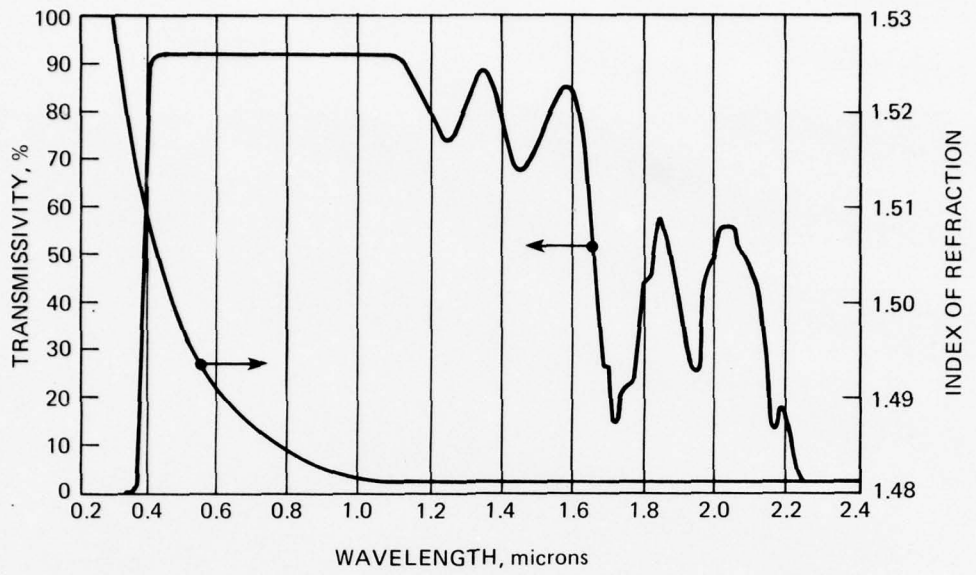

Figure 2.15. Typical optical properties of acrylic.

2.8 COMPARISON OF ACRYLICS

Bulk-polymerized acrylic sheets, plates, and custom castings are available in various government specification grades (table 2.3). The most common is the unshrunk utility grade which conforms to federal specification LP-391. It is available in sheets and plates of 1/16 to 4 inches (0.15 to 10.16 centimeters) in thickness and a variety of sizes. This material's length and width dimensions will decrease about 2.2 percent, while the thickness will increase about 4 percent, when the sheet is heated to forming temperature. Acrylic conforming to MIL-P-5425 is the preshrunk grade of acrylic, which is used in products that demand improved dimensional stability. It can also be obtained in a wide range of thicknesses and sizes. Acrylic conforming to MIL-P-8184 is a crosslinked grade. When this material is biaxially stretched (figure 2.16), it conforms to MIL-P-25690 and has improved crack-propagation-resistance properties. These latter two grades are used in structural applications, such as aircraft canopies and seaquarium windows. Other available acrylic materials, although not qualified to these standards, can be discussed on the basis of these grades.

Acrylic material properties can be examined by using molecular weight as a frame of reference. This categorization can be established by considering the grouping of material in table 2.4, which is based on approximated molecular weights. As noted previously, weatherability and resistance to chemical attack improve with increased weight and the heat distortion also increases, i.e., the upper service temperature improves. However, the capability of being processed is also affected, with increasing weight resulting in a reduced capability.

Table 2.5 lists the proposed minimum acceptable values for acrylic sheeting to be used in man-rated hyperbaric chambers, and tables 2.6 and 2.7 compare the properties of the various grades of acrylic. It should be noted that these properties are average values and do not define minima or ranges of values. As such, they should be used with care and the appropriate safety factors applied or more detailed testing for specific properties undertaken.

Table 2.3. Government specifications for acrylic.

Qualified Acrylic Grade	General Characteristics	Frame of Reference, molecular weight*
LP-391	Noncrosslinked, low molecular weight, dimensionally unstable at elevated temperatures	1,000,000
MIL-P-5425	Noncrosslinked, low molecular weight, improved high temperature dimensional stability	1,000,000
MIL-P-8184	Crosslinked, high effective molecular weight, high heat distortion temperature	4,000,000
MIL-P-25690	Crosslinked, high effective molecular weight, improved general properties developed through biaxial stretching	4,000,000

improving properties ↓

* These are only approximations; molecular weight definitions do not apply to crosslinked-type materials, but the concept of large molecular sizes or matrices is useful in judging general material characteristics.

Table 2.4. Grades of acrylic and molecular weights.

Grade of Acrylic	Frame of Reference, molecular weight
Extruded and compression molded acrylic	190,000
Continuous cast acrylic	400,000
Utility-grade acrylic MIL-P-21105 and MIL-P-5425	1,000,000
Highly crosslinked acrylics MIL-P-8184 and MIL-P-25690	4,000,000

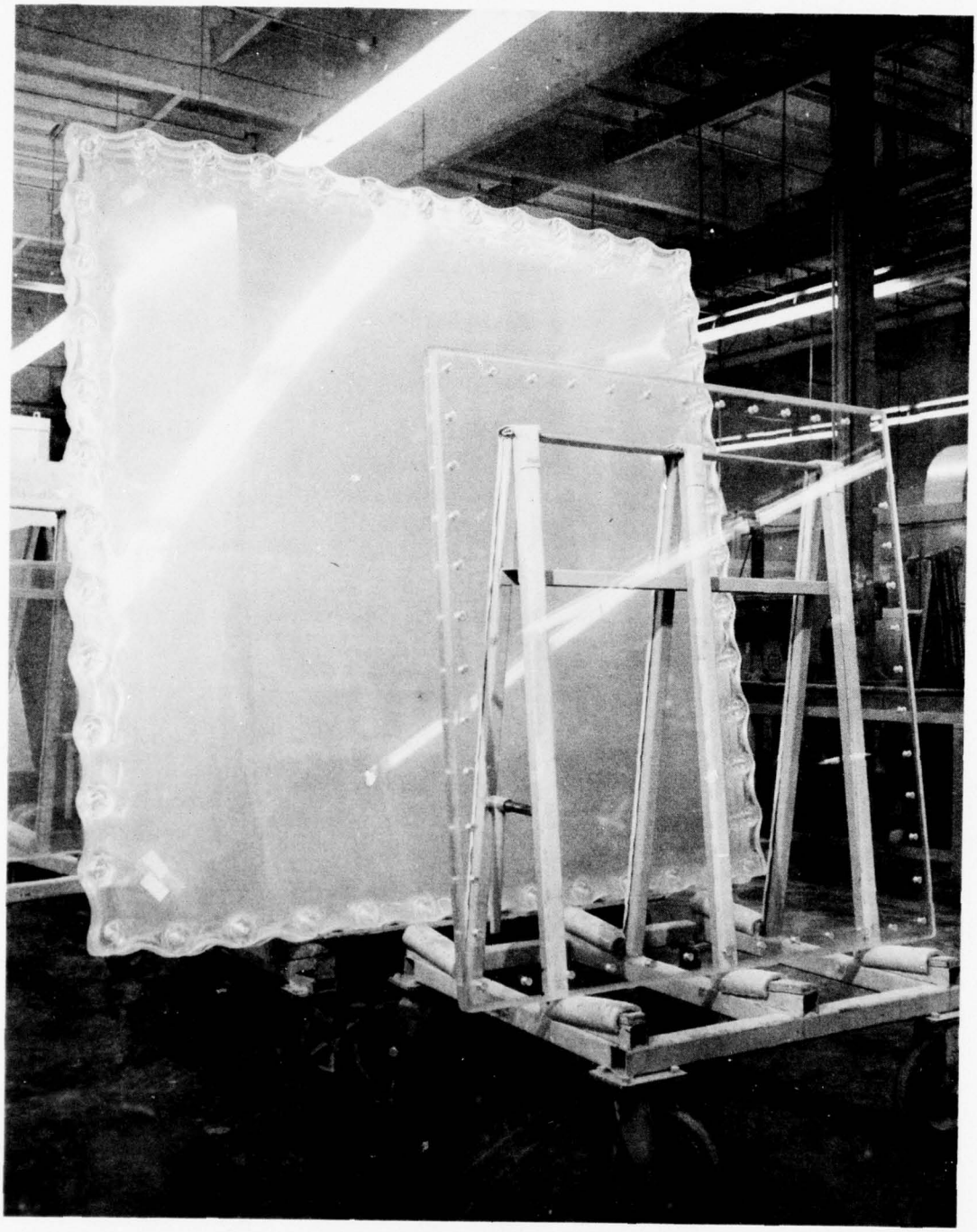

Figure 2.16. A typical acrylic sheet prior to and after thermal stretching to conform to MIL-P-25690 material, which is highly resistant to fracture propagation and stress-solvent crazing. (Photograph by Swedlow, Inc.)

Table 2.5. Proposed minimum requirements for acrylic sheeting for man-rated hyperbaric chambers.*

Property	Required Value
Izod-notched impact strength	0.3 ft-lb/in minimum
Refractive index	1.49 ±0.01
Water absorption, 24 hr	0.25% maximum
Compressive deformation, 4000 psi at 122°F	1.0% maximum
Tensile	
Ultimate strength	9000-psi minimum
Elongation at break	2% minimum
Modulus	400,000-psi minimum
Compression, yield strength	15,000-psi minimum
Modulus	400,000-psi minimum
Shear, ultimate strength	8000-psi minimum
Rockwell hardness	M scale, 90 minimum
Flexure, ultimate strength	14,000-psi minimum
Specific gravity	1.19 ±0.01
Residual monomer	
Methyl methacrylate	1.5% maximum
Ethyl acrylate	0.01% maximum
Ultraviolet (290–330 nm) light transmittance	5% maximum
Clarity, visually rated	Must pass readability
Coefficient of linear thermal expansion at	
–40°F	2.8 maximum (in 10^{-5}/°F)
–20°F	3.0
– 0°F	3.2
+20°F	3.5
+40°F	3.7
+60°F	4.0
+80°F	4.3
+100°F	4.7

* Reference table A1 of ANSI/ASME PVHO-1, Pressure Vessels for Human Occupancy, Appendix A – Acrylic Viewports.

Notes:

1 psi = 6.894757 E+03 Pa

$t_C^\circ = (t_F^\circ - 32)/1.8$

1 ft-lb = 1.355818 E+00 N-m

1 in = 2.540000 E-02 m

Table 2.6. Typical properties of various grades of acrylic sheet stock.

Type of Test	Test Method	Units	ASTM D-702-68	LP-391-C	MIL-P-5425C	ANSI/ASME PVHO-1	MIL-P-8184
Mechanical Tests							
Tensile strength	ASTM D-638	psi	9000	9000	9800-10,500	9000	9000 minimum
Tensile elongation	ASTM D-638	psi	2.0 minimum	2.0 minimum	4.9-6.4	2.0 minimum	20% minimum
Tensile modulus	ASTM D-638	psi			$4.5\text{-}4.6 \times 10^5$	4.0×10^5	
Flexural strength	ASTM D-790	psi			16,000	14,000	14,000 minimum
Flexural modulus	ASTM D-790	psi			4.5×10^5		
Compressive strength	ASTM D-695	psi			18,000	15,000	
Shear strength	FTMS 1041	psi			9000-10,000		
Physical Tests							
Rockwell hardness	ASTM D-785(M)				92	90	
Moisture absorption	ASTM D-570	%	0.2%		0.2% maximum	0.25%	1.0% maximum
Specific gravity	ASTM D-792		1.18	1.18-1.20	1.19-1.20	1.19 ±0.01	1.18-1.20
Craze resistance	FTMS-6043			No craze		No craze	No craze
Refractive index	ASTM D-542		1.49	1.49-1.50	1.491	1.49-1.50	1.48-1.50
Thermal Tests							
Thermal stability	MIL-LP-391C					No blisters, crazing, etc.	No blisters, crazing, etc.
Heat distortion temperature	ASTM D-648	°F		188.6	204-205	190	
Specific heat	ASTM C-351	BTU/lb/°F			0.35		
Thermal expansion	ASTM D-696	in/in/°F			4.1×10^{-5}	0.00010 maximum	0.00010 maximum
Internal strain	FTMS-6052	%	1.0				1.0% maximum
Impact Tests							
Izod – notched	ASTM D-256	ft-lb/in-N	0.3		0.3-0.9	0.3	
Izod – unnotched	ASTM D-256	ft-lb/in-N			1.5-3.0		
Flammability							
Burning rate	ASTM D-635	in/min			1.1		
Optical Tests							
Light transmission	ASTM D-1003	%		87 minimum	91	87	
Haze	ASTM D-1003	%	91.0	3.0 maximum	1.0	3.0	
Spectral transmission (290-700 mu)	ASTM D-725	%	3.0				5.0 maximum
Δ yellowness index	ASTM D-1925	%Δ	5.0				21
Electrical Strength							
Dielectric strength	ASTM D-150-70	ohm/cm			500		530

Table 2.7. Material properties and structural efficiencies for various grades of acrylic.

Material	F_{TU}, psi $\times 10^3$	F_{TY}, psi $\times 10^3$	E_T, psi $\times 10^6$	F_{CY}, psi $\times 10^3$	E_C, psi $\times 10^6$	W, lb/in^3	FTU/W, $\times 10^{-3}$	$\sqrt{E_C}/W$, $\times 10^{-3}$	$\sqrt[3]{EC}/W$, $\times 10^{-2}$	$/lb
Metals										
Aluminum (2024-T3)	64.0	42.0	10.60	40.0	10.60	0.100	640	33	22	0.65
Alloy steel (1025)	55.0	36.0	29.00	36.0	29.00	0.284	194	19	11	0.20
Magnesium (AZ31B-H24)	38.0	26.0	6.50	20.0	6.50	0.064	610	40	29	1.10
Titanium (Ti-6AL-4V)	130.0	120.0	16.00	126.0	16.40	0.160	1000	25	16	4.35
Woods										
White ash (hardwood)	13.2	7.2		4.3	1.40	0.022	1000	54	51	5.80
Sitka spruce (softwood)	9.4	5.3		3.5	1.40	0.015	626	79	74	0.70
Reinforced Plastics										
181E – glass cloth/epoxy	45.0				3.30	0.070	643	26	21	2.00
Chopped E – glass/polyester	20.0				2.00	0.070	286	20	18	0.65
Thermoplastics										
ABS	10.5	7.8	0.35		0.35	0.038	276	16	14	0.90
Polycarbonate	9.5	8.5	0.34		0.35	0.043	221	14	16	1.90
Acrylic (as cast)	10.0		0.45		0.45	0.043	232	16	18	2.00
Acrylic (stretched)	10.5	9.0	0.50		0.55	0.043	232	17	18	12.00
Glass										
Soda lime plate (annealed)	1.5		10.00		10.00	0.089	17	36	24	0.45

Notes:

1 psi = 6.894757 E+03 Pa

1 in = 2.540000 E-02 m

1 lb = 0.04536 kg

2.9 CHEMICAL RESISTANCE

Acrylic is generally unaffected by most inorganic solutions. High concentrations of oxidizing acids and concentrated basic solutions attack acrylic, and acrylics are soluble in harsh organic materials such as ketones, low esters, and aromatic and chlorinated hydrocarbons. Organic solvents which can be used to clean acrylic surfaces include aliphatic naphtha (200 thinner) and isopropyl alcohol.

Chemical resistance does not consider the combined effect of stress acting on the material. Tensile stresses acting in combination with chemicals which otherwise show no attack on the acrylic can result in crazing.

Table 2.8 shows the effect of various chemicals on general-purpose acrylic.

Table 2.8. Effect of chemicals on acrylics.

Chemical	Negligible Attack	Strong Attack
Acids		
Weak		
Acetic (5%)	X	
Chromic (40%)	X	
Citric (10%)	X	
Hydrochloric (10%)	X	
Nitric (10%)	X	
Sulphuric (30%)	X	
Strong		
Hydrochloric (40%)		X
Hydrofluoric (40%)		X
Nitric (40%)		X
Sulphuric (98%)		X
Bases		
Weak		
Ammonium hydroxide (28%)	X	
Sodium carbonate (20%)	X	
Sodium hydroxide (60%)	X	
Strong		X

Table 2.8. Continued.

Chemical	Negligible Attack	Strong Attack
Organics		
Weak		
Naphtha (aliphatic)	X	
Isopropyl alcohol	X	
Heptane	X	
Strong		
Chlorinated hydrocarbons		
Chloroform		X
Trichlorethylene		X
Methylene chloride		X
Carbon tetrachloride		X
Ketones		
Acetone		X
Methyl ethyl ketone		X
Alcohols		
Methyl		X
Ethyl		X
Butyl		X
Toluene		X

2.10 PRODUCTS MADE FROM ACRYLICS

A wide range of products is manufactured from acrylic materials because of its resistance to outdoor weathering and its resulting long-term material beauty, or in the case of transparent acrylic, its retention of visual clarity. Examples of the diversity of acrylic products are given in the following list:

Aircraft transparencies (figure 2.17)

- Canopies
- Windshields
- Windows

Architecture (figure 2.18)

- Signs
- Facia
- Glazings

- Naval transparencies (figures 2.19 and 2.20)
  - Gunshield windows
  - NEMO-type submersibles
  - Viewports for pressure vessels
- Automotive recreational (figure 2.21)
  - Automobile bodies
  - Camper shells
  - Boat hulls
- Armor transparencies (figure 2.22)
  - Tank vision blocks
  - Windows
- Decoration (figure 2.23)
  - Infinite variety, usually selected for visual clarity
- Molded and extruded shapes
  - Rods, tubes
  - Tail-light covers
  - Lenses
- Paints, adhesives, and coatings
- Furniture (figures 2.24 and 2.25)
  - Chairs
  - Tables
  - Shelves
  - Partitions
  - Sinks, bathtubs, and showers

The size, form, and functional needs of these products vary over a wide spectrum, and, as such, the manufacturing methods must be tailored to product demands. Acrylic material must be shaped, machined, finished, and joined in various ways on its way to becoming a product. However, underlying the processing are two fundamental concepts: (1) acrylic is a thermoplastic material and may, therefore, be shaped when heated (thermoformed) and (2) acrylic may be machined by using wood-working or machine-shop equipment and basic machining techniques with only minor modifications.

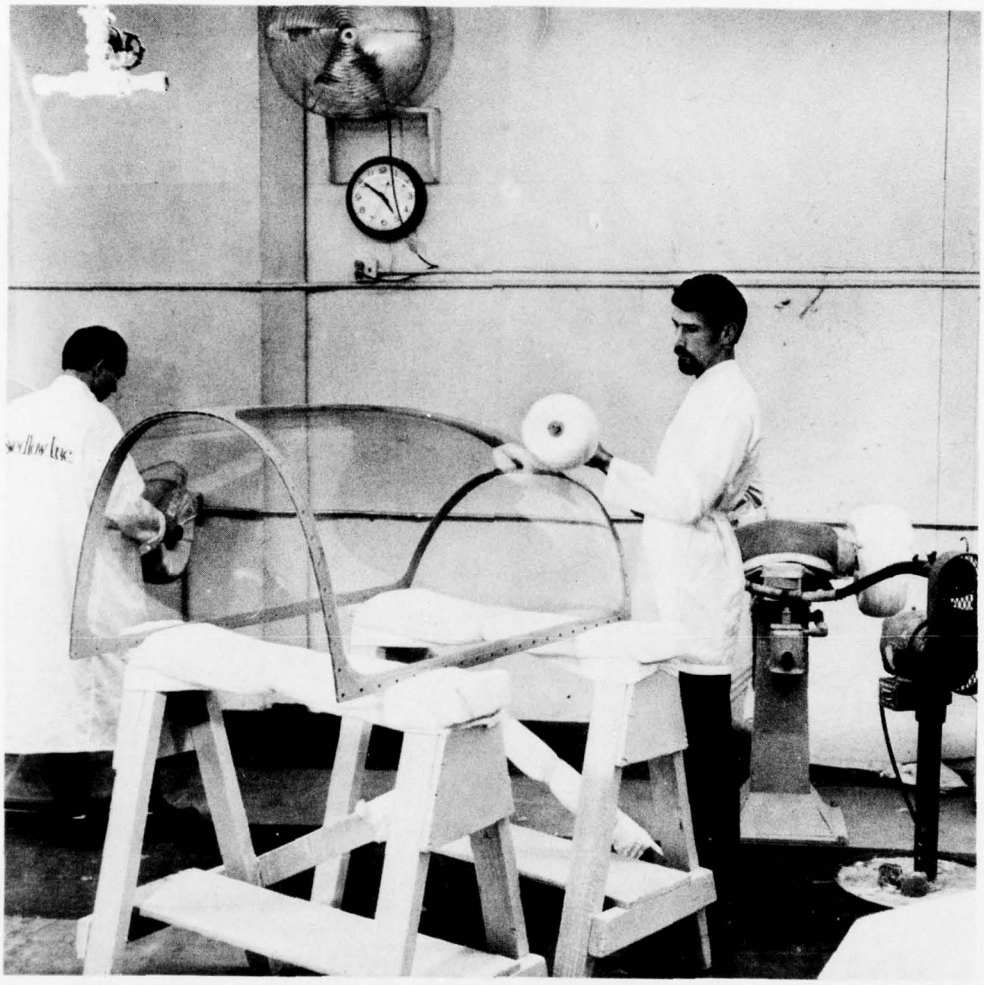

Figure 2.17. Aircraft canopy during final buffing operation. Note the edge attachment for bolting the canopy to the aircraft. (Photograph by Swedlow, Inc.)

Figure 2.18. Acrylic glazing on the roof of a car showroom. (Photograph by U. S. Navy.)

Figure 2.19. NEMO-type pressure hull for a submersible with 1000-meter depth service. Hull built from adhesive-bonded thermoformed spherical pentagons. (Photograph by Swedlow, Inc.)

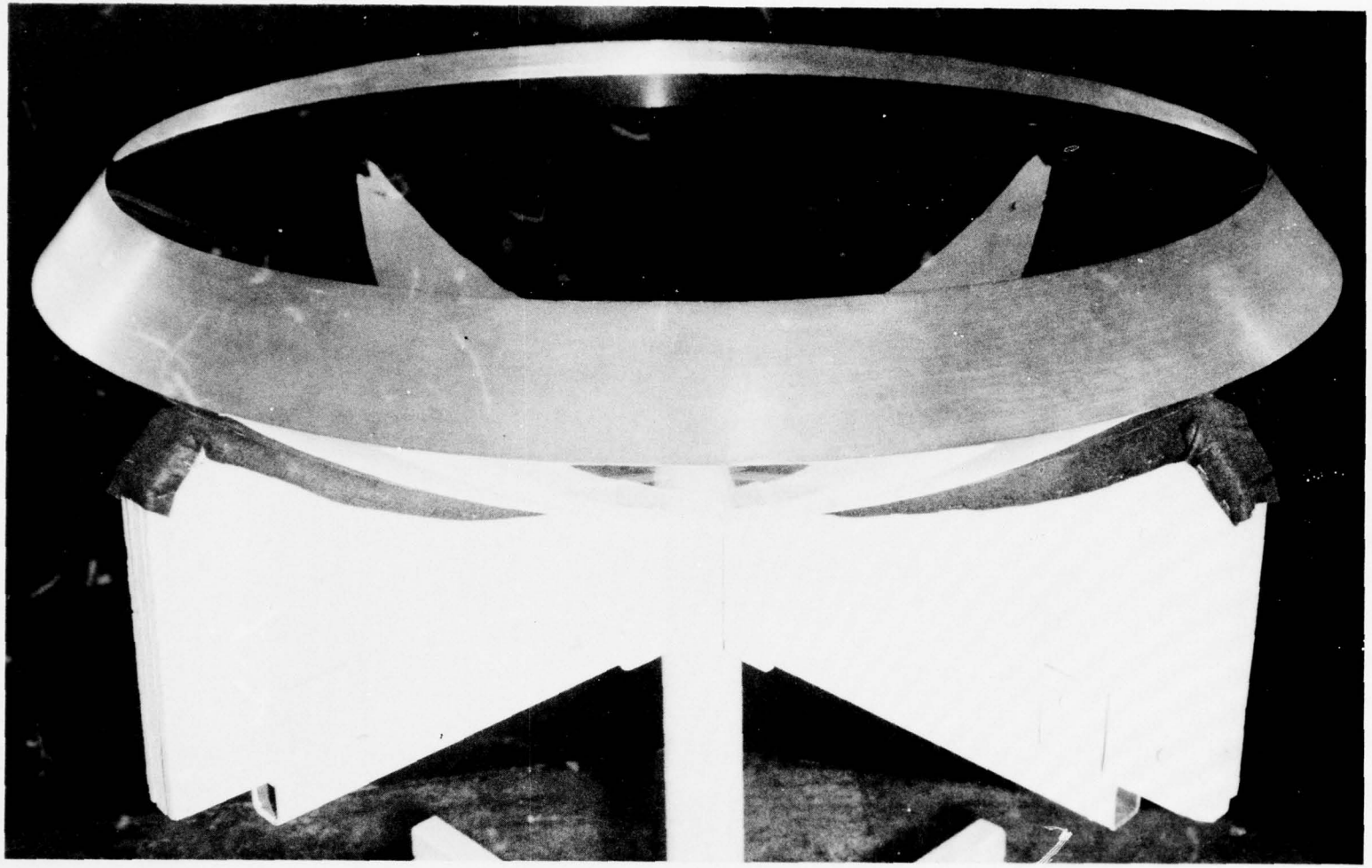

Figure 2.20. Spherical sector bow window for a submersible with 1000-meter depth service. Window is vacuum-formed from thick, cast acrylic sheet. (Photograph by Swedlow, Inc.)

Figure 2.21. Complete exterior car body fabricated from rigidized acrylic panels thermoformed from acrylic sheets. (Photograph by Swedlow, Inc.)

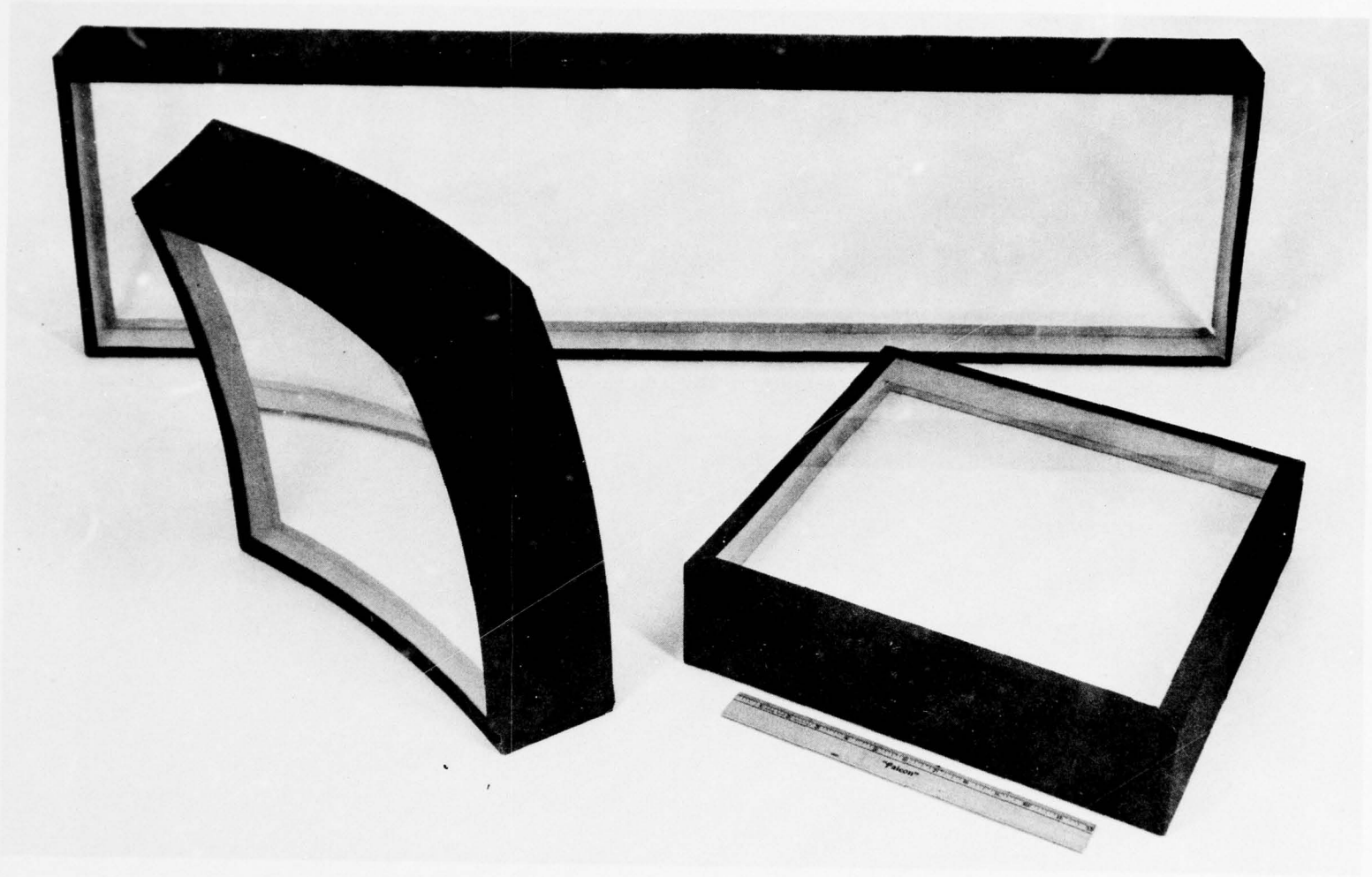

Figure 2.22. Laminated bulletproof windows for commercial or military applications. (Photograph by Swedlow, Inc.)

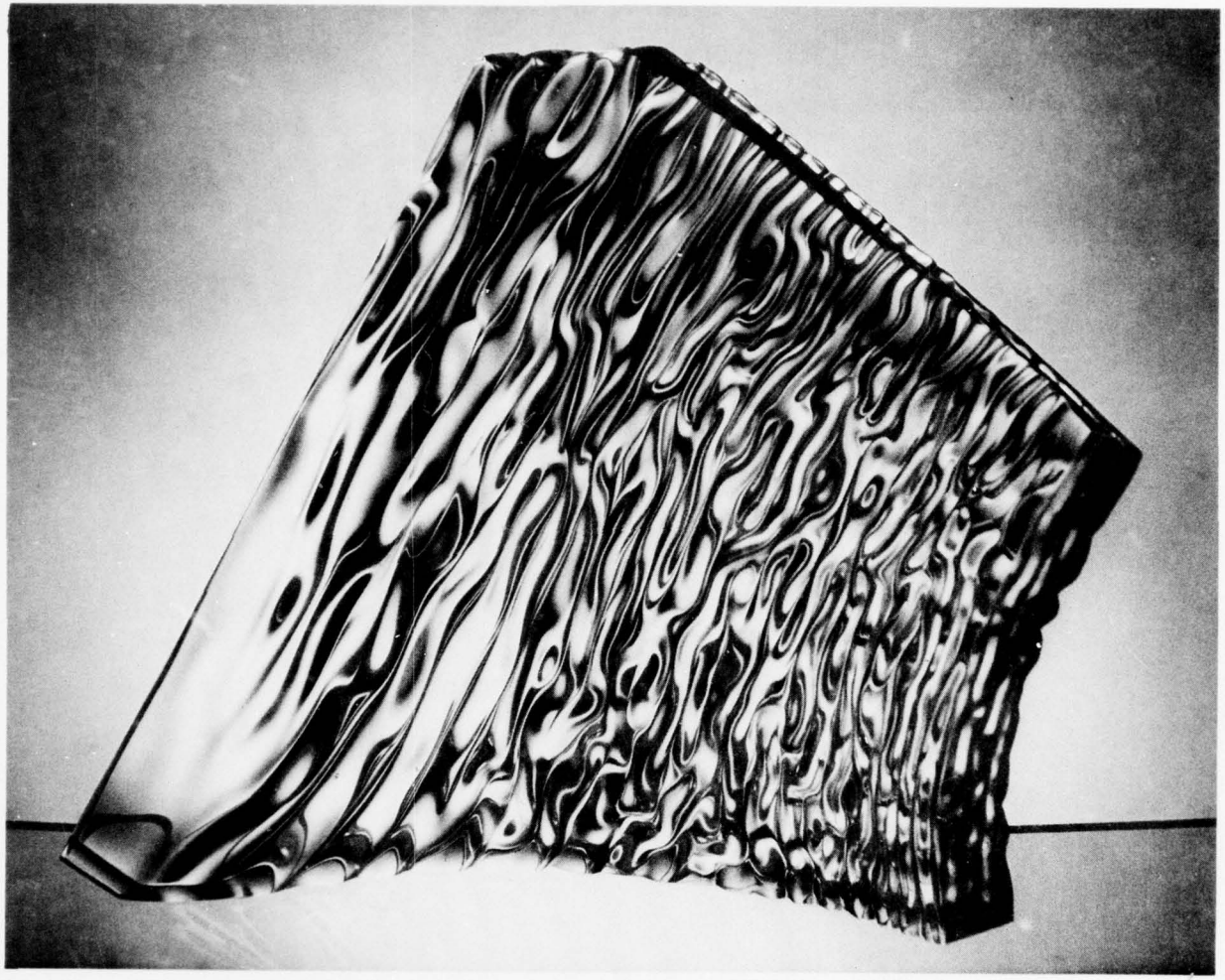

Figure 2.23. Unique artistic quality of acrylic is demonstrated in this modernistic free-flow sculpture. (Photograph by Swedlow, Inc.)

Figure 2.24. Modern chair vacuum-formed from acrylic plastic that has been rigidized with reinforced thermoset plastic. (Photograph by Swedlow, Inc.)

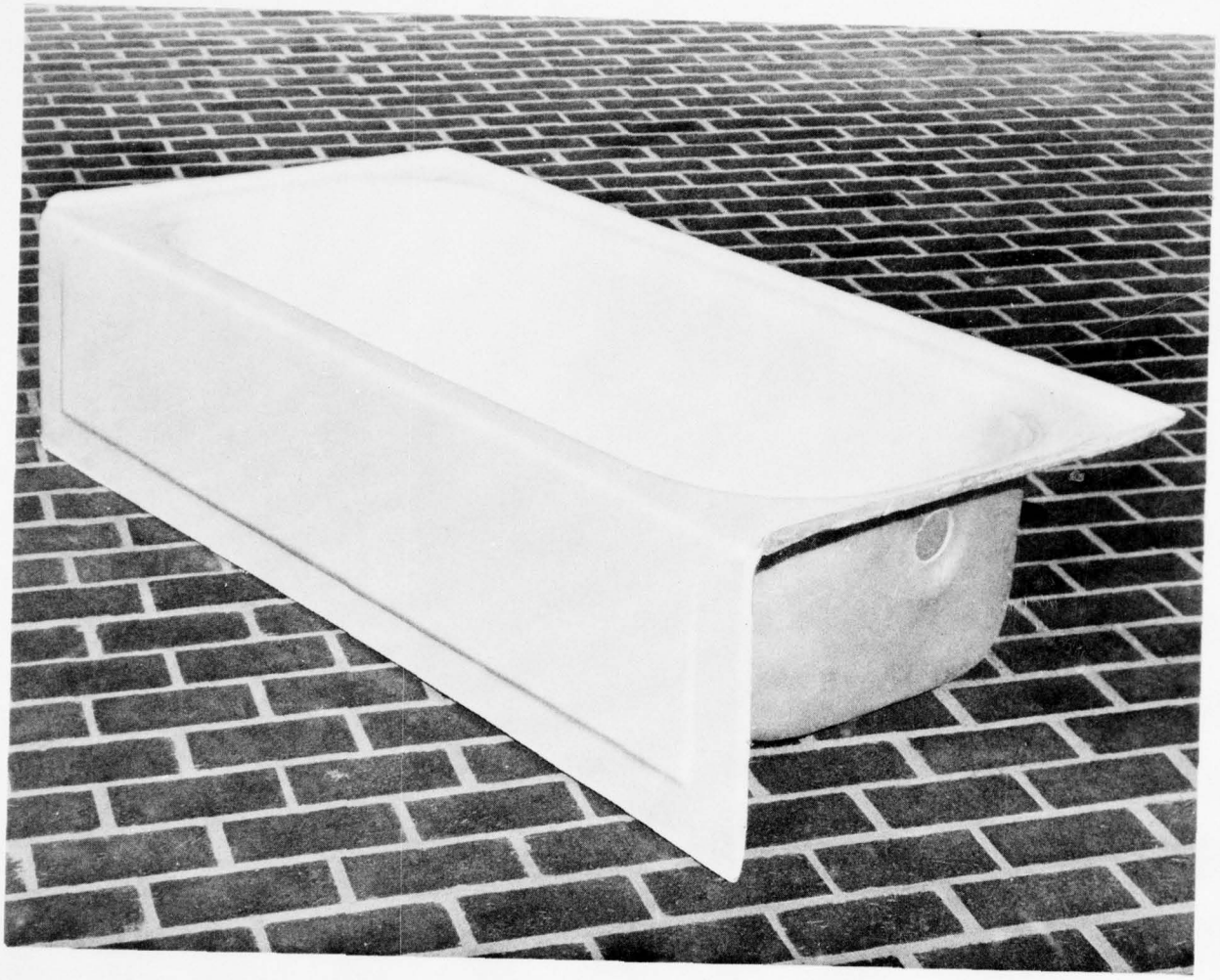

Figure 2.25. Bathtub made of vacuum-formed acrylic which has been rigidized on the undersurface with reinforced thermoset plastic. (Photograph by Swedlow, Inc.)

2.11 DESIGN CONSIDERATIONS

As with the conversion of nearly all materials into products, it is necessary to understand the physical properties of the material and observe the recommended practices for its use. With plastics, in particular, it is necessary to give careful consideration to the methods or processes which are used to shape and join the materials, as the possibilities are quite diverse and the material's performance can be altered by the selected process. Design of the process is often as important as the design of the product itself. Other consideration include the following.

1. Thermal changes must be given careful attention, as properties of plastic are much more sensitive to such changes than are most other materials.

2. Properties of plastics are time dependent, and parameters such as load duration and load-application rate in combination with thermal changes must be carefully evaluated.

3. Plastics exhibit a rather unique failure mechanism known as crazing, which can be attributed to the action of stress, solvents, and environmental exposure. This degradation can result in failure by fracture of the part and, as such, it must be understood if the problem is to be avoided. Crazing is defined as the formation of fine cracks which can extend over or under the surface of a plastic. The cracks are difficult to see, and when magnified they appear as a three-dimensional lacy network (figure 2.26). They appear on the tension surface of an object and are normally oriented perpendicular to the direction of maximum tensile stress. When crazing occurs in a random fashion, it is normally the result of solvent action and is known as solvent crazing. Crazing reduces the load-carrying capability of a material and acts as a stress riser. Residual monomer can act as a solvent and result in crazing. It is an irreversible process and cannot be eliminated, except by the physical removal of the crazed material through grinding and polishing. To salvage a part which has been crazed, the part can be annealed and the craze physically removed. This results in an overall thickness reduction, but it has the advantage of removing the stress concentration caused by a residual tensile stress developed during fabrication.

There are many examples of the improper design of products made of plastic: the radio case which becomes distorted when left in the sun or the plastic case which takes abusive treatment when first purchased but which breaks after a few months. These problems can be avoided through cautious and considered application of good design principles, which are developed through a good understanding of the material's properties and are available from suppliers, either in written form or through direct contact.

2.12 THERMOFORMING ACRYLIC

Thermoforming of acrylic requires heating the material above its glass transition temperature and applying sufficient pressures and load while hot to obtain the desired shape. While maintaining the application of load, the part is cooled and the shape is thereby retained.

Forming temperatures vary considerably and are related to the grade of acrylic. Temperatures are usually from 230 to 360°F (110 to 182°C), with the exception of stretched acrylic which is formed at 220°F (104°C) or slightly lower. The forming temperature for a particular acrylic and the required shape must be carefully controlled in most cases. If it is

AD-A070 535 NAVAL UNDERSEA CENTER SAN DIEGO CA F/G 11/9
ACRYLIC PLASTIC VIEWPOINT FOR OCEAN ENGINEERING APPLICATIONS. V--ETC(U)
FEB 77 J D STACHIW
UNCLASSIFIED NUC-TP-562-VOL-1 NL

2 OF 5
AD
A070535

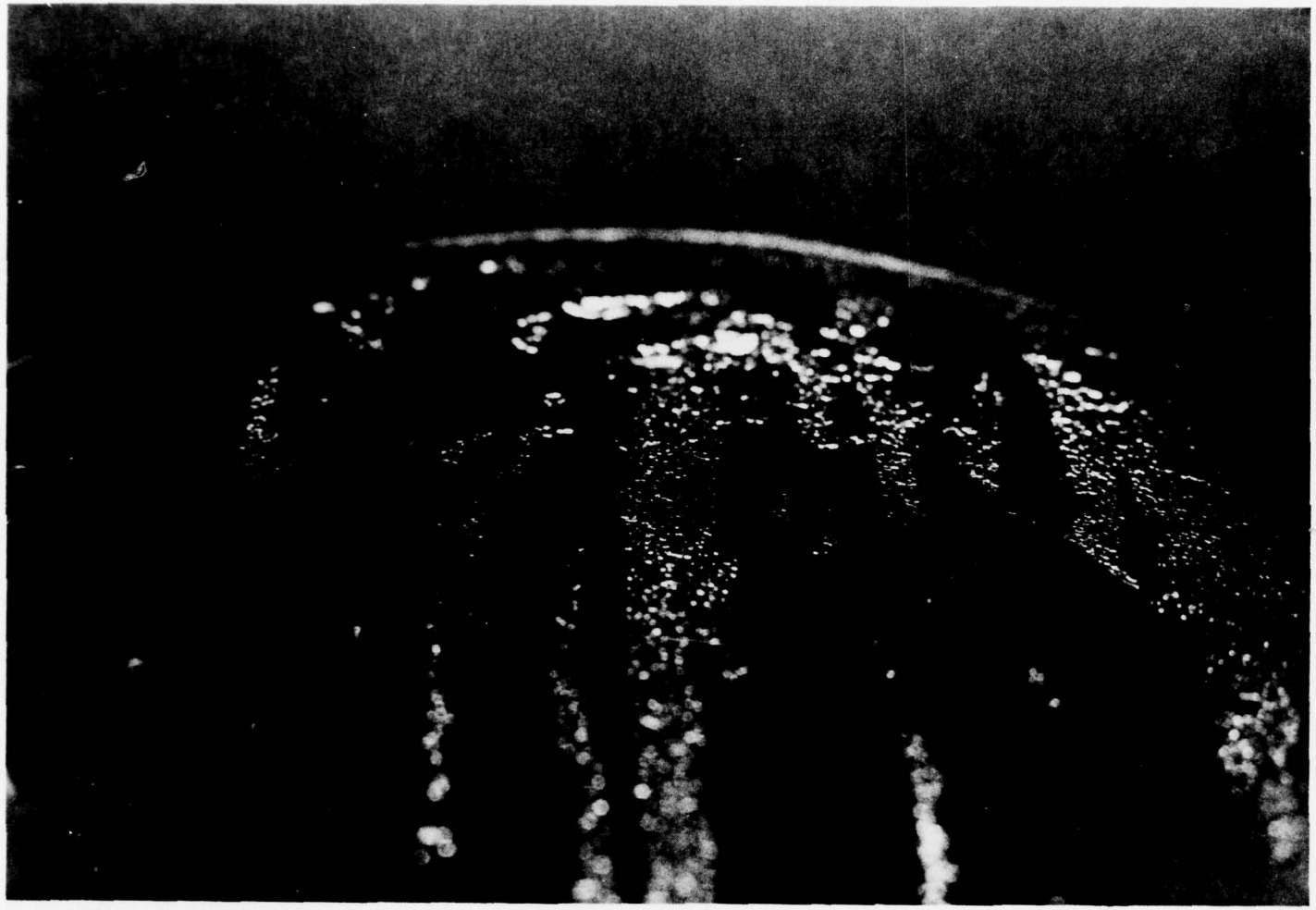

Figure 2.26. Crazing of acrylic surface on a submersible viewport after several years of weathering and periodic cleanups with solvent-type cleaners. (Photograph by U.S. Navy.)

too low, the shape may not be retained because of the high residual stresses which can also cause crazing in service; if it is too high, the acrylic can tear during formation. An optimum forming temperature is dependent upon the grade of acrylic, the thickness of the material,* the method of formation, and the required shape. Forming temperatures are commonly derived from test data defining the tensile modulus of elasticity as a function of temperature and are subsequently refined on the basis of forming experience (figure 2.27).

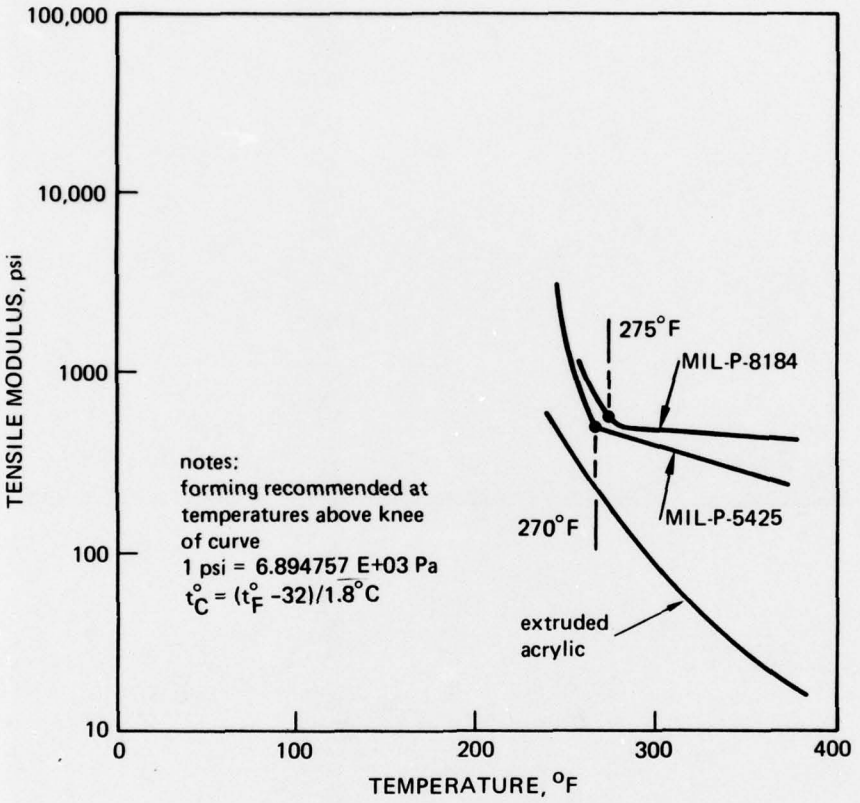

Figure 2.27. Tensile modulus of elasticity as a function of temperature.

In many cases, the desired shape is a free-formed surface which requires only periphery contour control, while the body contour is developed through the application of pressure and the free movement of the material. More complex shapes may require the use of full-surface dies for either a single surface or a matched two-surface configuration (figure 2.28).

Application of the loads necessary to move the acrylic to the desired shape can be achieved by pressing a die surface against the material through the reaction of a matched die, applying a vacuum pressure between the material and the die, or applying pressures greater

** Thin material is normally heated slightly more than thick material because of its more rapid cool-down during the formation operation.*

Figure 2.28. Vacuum-formed acrylic door panel being removed from forming die. (Photograph by Swedlow, Inc.)

than ambient to the surface of the acrylic away from the die. In the case of free forming, either vacuum or positive pressures are used. Some instances require combinations of these loads and variations in material temperatures.

The rate at which the shape is developed and the rate of cool-down are important to the quality of the product. As previously noted, residual strains, which can cause surface crazing, result if careful control is not exercised. These strains can also cause the part to distort in shape, resulting in either an inherent deficiency or a mismatch when the mating surfaces are joined.

If a temperature which exceeds the forming temperature is experienced subsequent to forming the acrylic, the part will relax and tend to return to its original flat sheet form.

2.13 MACHINING ACRYLIC

Routers, band saws, table saws, shapers, lathes, milling machines, and drill motors, as needed for woodworking or metalworking, can be used to machine acrylic (figure 2.29). Experienced woodworkers or machinists should have no trouble in working acrylic shapes; however, they must understand the properties of the material being shaped to achieve good quality finishes and to avoid damage. The coefficient of thermal conductivity, coefficient of thermal expansion, and tensile modulus of elasticity are the most important properties affecting the machining of acrylic (table 2.9). The low thermal conductivity prevents heat generated by the cutting tool from effectively flowing away from the cutting zone; the high thermal expansion causes reductions in the clearances of the cutting tools in the machining zone, which can result in tool binding; and the low modulus of elasticity results in material deflection at the cutting point, if proper precautions are not taken.

Table 2.9. Thermal conductivity, thermal expansion, and tensile modulus of elasticity.

Material	Thermal Conductivity, BTU · in/hr · ft^2 · °F	Thermal Expansion, in/in · °F	Tensile Modulus of Elasticity, lb/in^2
Silver	2900.0	11.0×10^{-6}	11.0×10^6
Aluminum	1570.0	12.6×10^{-6}	10.0×10^6
Yellow brass (65-35)	830.0	11.3×10^{-6}	16.0×10^6
Nickel	420.0	7.2×10^{-6}	32.0×10^6
Mild steel (1020)	360.0	8.4×10^{-6}	30.0×10^6
Stainless steel (304)	155.0	9.9×10^{-6}	28.0×10^6
Acrylic	1.2	35.0×10^{-6}	0.5×10^6

Notes:

1 BTU · in/ft^2 · °F = 1.441314 E-01 W/m · K

1 in = 2.540000 E-02 m

1 in · °F = 1 in/in · °F = 1.8°C

1 lb = 0.04536 kg

1 in^2 = 6.451600 E-04 m^2

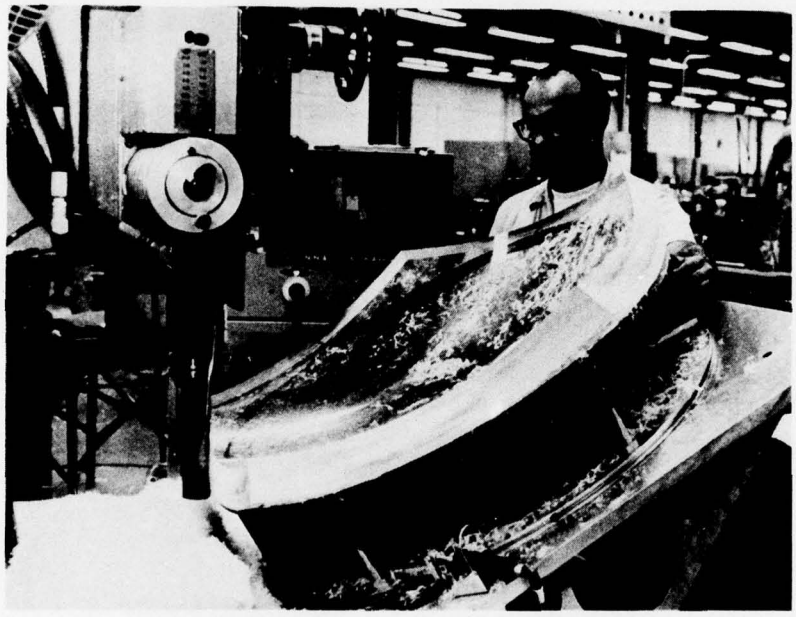

Figure 2.29. Milling of edges on spherical pentagons used in the assembly of NEMO-type pressure hulls for submersibles. (Photograph by U.S. Navy.)

Routers are commonly used in edge-finishing operations. These machines should have a minimum no-load spindle speed of 10,000 revolutions per minute. Cutters used with these machines should have a back clearance of 10 degrees (0.17 radian) and 15 degrees (0.26 radian) of rake. Two or three flute cutters smaller than 1-1/2 inches (3.81 centimeters) in diameter produce very smooth cuts. At slower surface speeds for the cutter, more flutes may be desired. The direction of cutting tool movement can be either conventional (up) or climb (down), depending on the desired cut geometry and chip formation (figure 2.30).

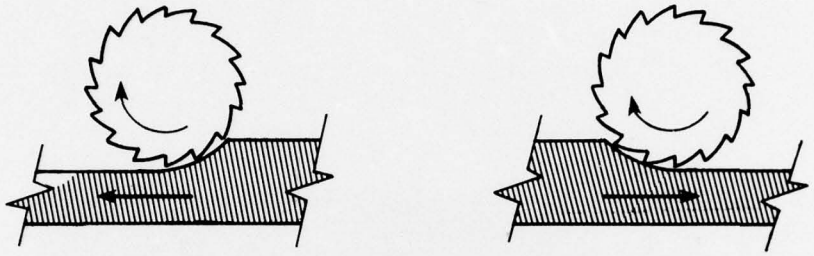

Part A. Climb cutting.

Part B. Conventional cutting.

Figure 2.30. Cutting tool movement for routing acrylic.

Drills should be operated at 1000 to 5000 revolutions per minute, depending on the bit diameter. The larger diameter holes should use a reduced speed. High-speed, standard-steel, twist drill bits are recommended, but should be modified to a 60-degree (1.04 radian) tip angle, 0-degree (0 radian) rake angle, and a 12- to 15-degree (0.21 to 0.26 radian) clearance angle (see figure 2.31). The material being drilled should be backed with wood or

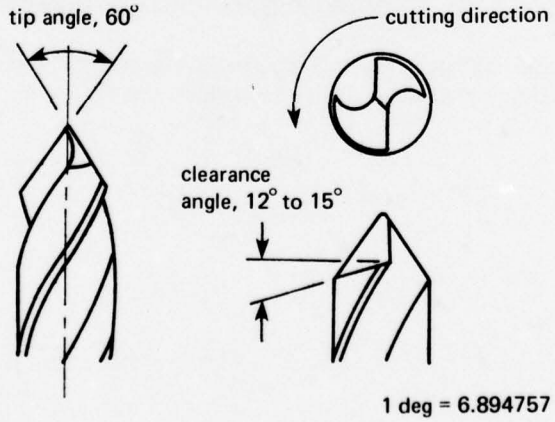

1 deg = 6.894757 E+03 rad

Figure 2.31. Drill bit dimensions for machining acrylics.

acrylic on the bit-exiting surface to prevent spalling. The bit should be fed and backed off periodically to insure chip removal and to provide cooling time. As in all drilling operations, the bit must not wobble and the workpiece must be held securely to insure quality holes.

Acrylic can be saw[illegible]on circular, band, jig, or saber saws, depending on the desired cut. Circular saws should o[illegible]ate at 8000 to 12,000 surface feet per minute. Blades should be hollow ground with slightly set teeth (0.010- to 0.015-inch (0.03 to 0.04 centimeter) clearance kerf-to-blade) and have a 0- to 10-degree (0 to 0.17 radian) rake angle. If possible, the blades should be slotted to prevent heat warping. The number of teeth per inch decreases as the workpiece thickness increases. As in the cutting of wood, a chip breaker plate should be used to prevent spalling. Band saws should be operated at 3000 to 5000 surface feet per minute. Metal-cutting blades are preferred, and uniform feed rates should be observed with caution exercised to prevent binding. When using jig or saber saws, the workpiece must be held securely to prevent cracking. This is especially true in the case of thin material. As in all cutting operations, sharp tools are required if problems are to be avoided and quality and efficiency achieved. In many cases, carbide-tipped cutting tools should be considered. Single-point cutting of acrylic should be done at about 500 surface feet per minute. The cutting tool should be ground as shown in figure 2.32.

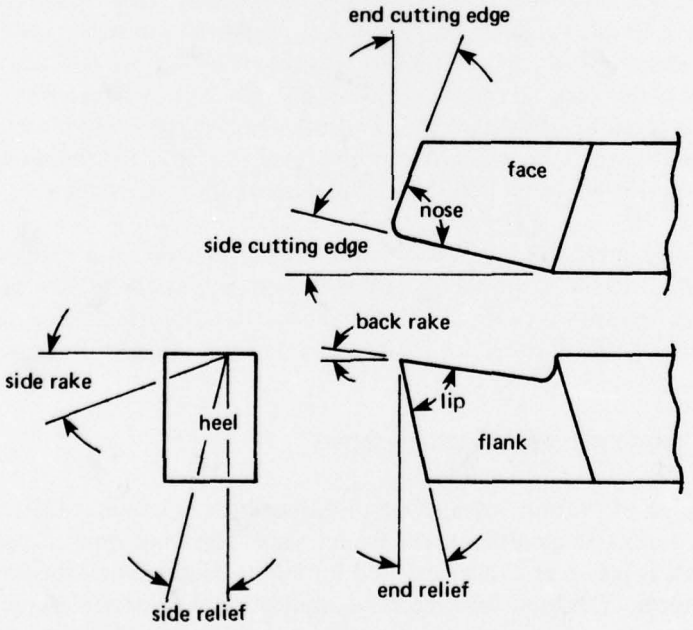

Figure 2.32. Single-point cutting tool.

Cutting fluids can be used to help machine acrylic. These fluids primarily act as a coolant, secondarily provide lubrication for chip removal, and finally act as a chip removal medium. The preferred fluid, when used, is water with some wetting agent, such as a detergent, as an additive. Other cutting fluids should be used with caution to avoid acrylic crazing.

It should be noted that unshrunk acrylic undergoes a 2.2-percent shrinkage when heated to forming temperature. This factor must be allowed for in trimming acrylic. Under these same conditions, the thickness increases approximately 4 percent.

2.14 SANDING, POLISHING, AND CLEANING ACRYLIC

Scratches, gouges, and marks on acrylic surfaces can be removed by hand or machine sanding. Wet or dry sandpaper should be used, with a coarse enough grit to remove the blemish and progressively finer grits to finish the process. The sanding surface should be kept wet with water to minimize generated heat and to prevent clogging of the sandpaper. A uniform and flexible back-up pad, such as neoprene foam, can be used behind the sandpaper to help distribute pressure. A slightly larger area should be covered with each finer grade of paper to prevent localized sanding distortions.

Scratches left by the sanding, or hairline surface scratches developed in service, can be removed by buffing and polishing (figure 2.33). Such finishing can be done for purely aesthetic reasons or, in the case of transparencies, to improve optical quality. Used first is an abrasive wheel, which consists of a buffing pad made of stitched cotton or flannel and an abrasive compound composed of very fine alumina, or similar material, combined with tallow or wax binders. The wheel should run at about 1800 surface feet per minute. After this operation, a buff of only tallow is used to refine the acrylic surface further. A high luster is finally achieved by carefully buffing with a wheel without abrasive or tallow. These operations should be done with extreme care to prevent overheating the acrylic surface and the developing of a rippled surface which has the potential for subsequent crazing.

The preferred method of cleaning acrylic is washing with mild detergent and water. A soft, clean cloth or chamois should be used with only a light application of pressure. Oil or grease spots can be removed with aliphatic naphtha. Do not use alcohol, gasoline, acetone, benzene, chlorinated hydrocarbons, strong caustics, lacquer thinner, or household window cleaning compounds.

2.15 SURFACE COATINGS AND TEXTURING

Several types of coatings are applied to the surfaces of acrylic to improve resistance to abrasion, provide reflective qualities, and enhance visual transmission and electrical conductivity. Films, such as paints and inks, are used for either decorative purposes or to provide special optical effects. The basis for successful application is substrate preparation, cleaning, and a compatible coating chemistry. Each coating is usually intended for a limited range of acrylic grades.

Figure 2.33. Machine polishing of stretched acrylic sheet. (Photograph by Swedlow, Inc.)

Acrylic sheets are made significantly more resistant to abrasion through the application of special coatings (figures 2.34 and 2.35). One coating is described by its manufacturer as crosslinked fluoroplastic polymer containing silica. Other manufacturers are working to develop coatings based on different polymer systems. In general, these coatings improve light transmission, reduce haze, and improve the solvent resistance of coated surfaces. They are characterized by excellent resistance to weather and environment, and are finding application in the areas of public transportation, buildings, and display windows.

Vacuum-deposited and chemically plated thin films of aluminum, silver, chromium, or gold are routinely applied to acrylics. Film thicknesses range from 1 to 1000 microinches (2.54 to 2540 meters $^{-8}$). In the case of very thin films (approximately 1 microinch (2.54 meters^{-8})), the materials can be transparent and are used in heater elements, radio-frequency shields, passband filters, and antireflective devices. Thick films (approximately 1000 microinches (2540 meters^{-8})) are opaque and are used in decorative products or reflective items.

Acrylic can be easily painted. A special application involves back painting clear acrylic material, a procedure which protects the paint from damage and provides a unique beauty, Inherent in this application is the need for clean acrylic surfaces. Oils or greases can be removed by using aliphatic naptha, isopropyl alcohol, hexane, kerosene, or white gasoline. For general cleaning, water and a mild detergent, followed by a thorough rinsing, is preferred. Acrylic-based paints are recommended for outdoor applications with alkyd paints acceptable for indoor items.

Acrylic can also be effectively silk-screened, a process widely used in the sign industry. It is possible, using this process to form shapes from flat silk-screened material, thereby simplifying the color application process.

It is also possible to obtain acrylics with various textured surfaces. These textures are applied either during polymerization of the stock or as a secondary operation by using embossing techniques.

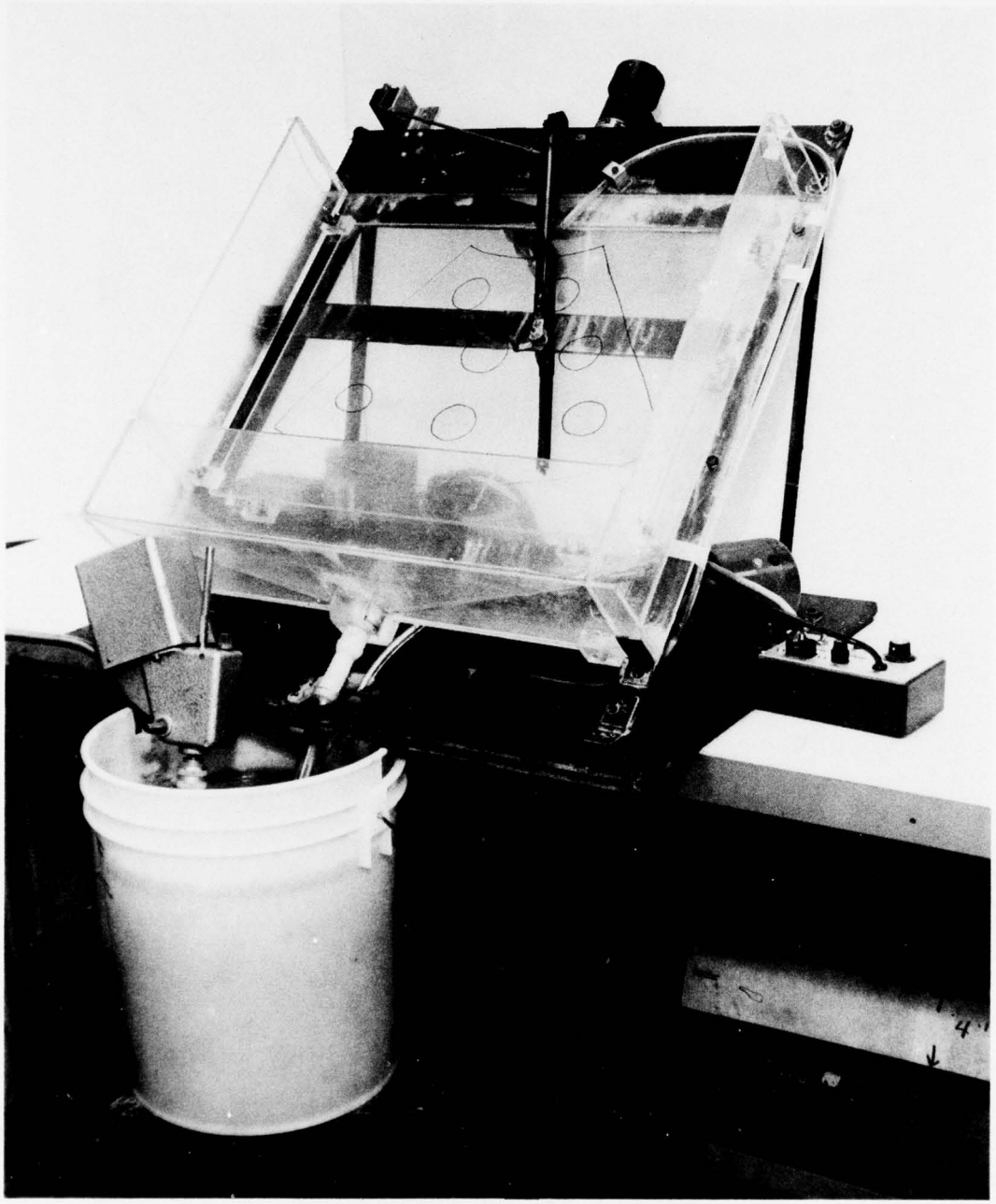

Figure 2.34. Windshield-wiper test used to evaluate the quality of abrasion-resistant coatings applied to acrylic plastic. (Photograph by Swedlow, Inc.)

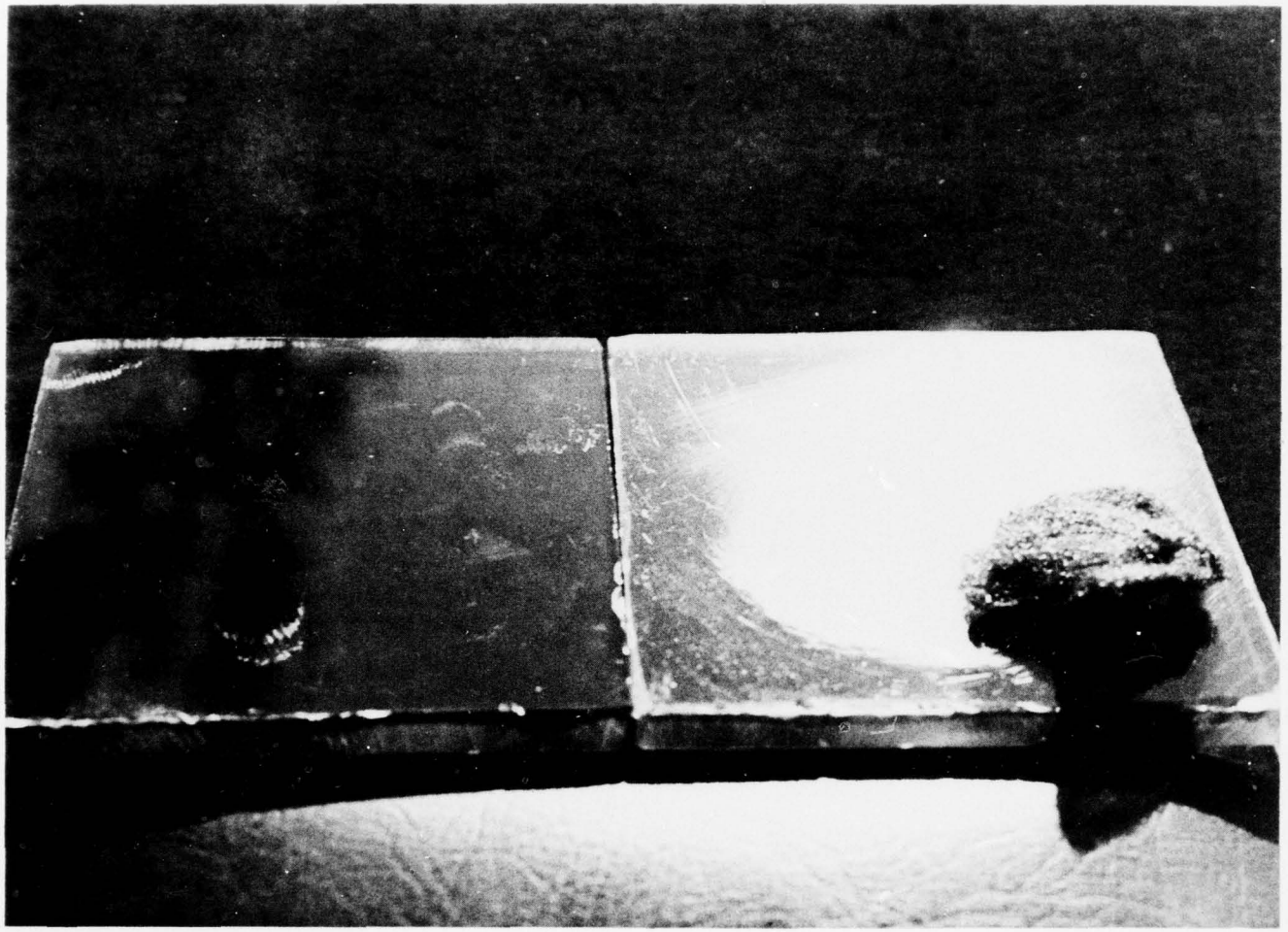

Figure 2.35. Protection provided the surface of acrylic plastic by an abrasion-resistant coating. The coated area of the specimen does not show as many scratches as the uncoated area, although both were exposed to the same surface wear by scuffing with a pad of steel wool. (Photograph by U.S. Navy.)

2.16 JOINING ACRYLICS

In most applications, acrylics are joined to some other structure by conventional bolting or riveting, clamping, or adhesive bonding. The effects of the differential thermal expansion between members and the basic mechanical properties which affect structural performance must be considered if the bond is to hold.

Acrylic can also be joined to other acrylic elements to form complex shapes by direct bonding to form butt, scarf, lap, or offset joints (figure 2.36). Acrylic adhesives or solvent-based cements are used. Each joint has features which make it particularly suitable for special types of loading (figure 2.37).

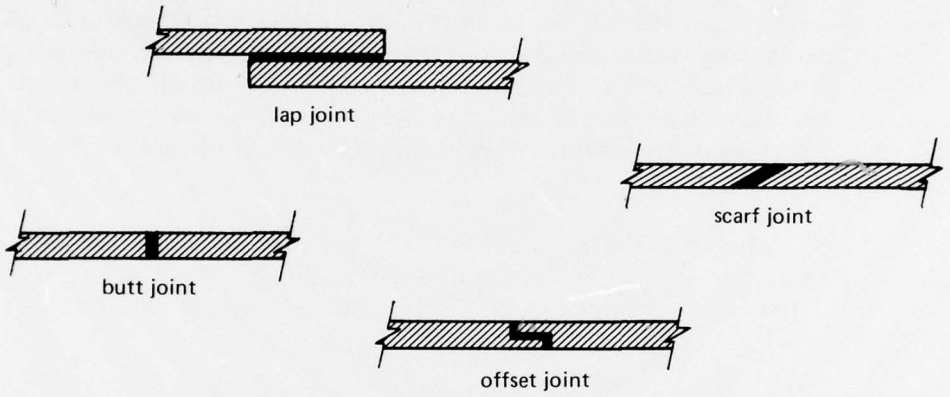

Figure 2.36. Different joints used to bond acrylic.

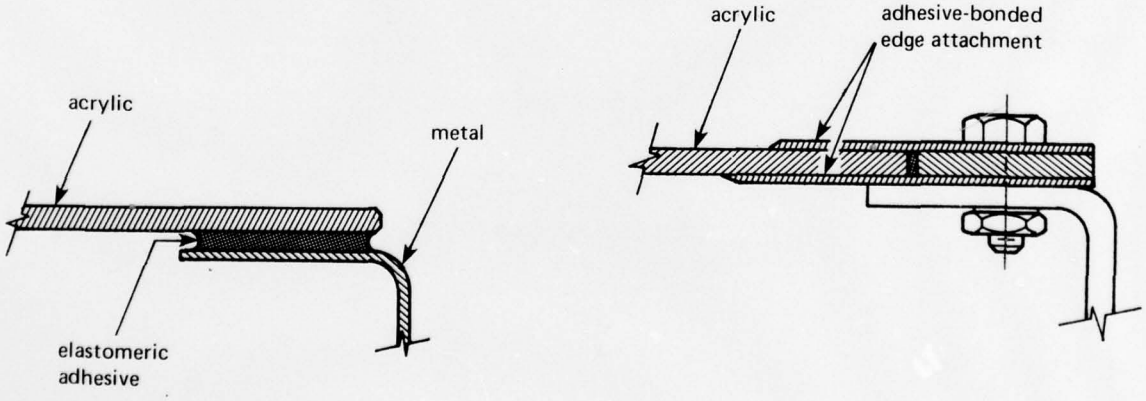

Part A. Acrylic directly to structure.

Part B. Attachment materials bonded to acrylic.

Figure 2.37. Bonding of acrylic.

The adhesives used to form these joints can be either reactive or solvent and are selected on the basis of the grade of acrylic being bonded. Reactive adhesives are commonly acrylic based and are used on crosslinked grades. Solvent adhesives rely on their ability to soften the parent material and are used with low molecular weight, noncrosslinked grades. The solvent adhesives can be used as either straight solvents or as combinations of solvent and acrylic materials. These adhesives have varying degrees of strength and can be optically transparent; however, in most cases they yellow or otherwise discolor with age.

Before and after bonding, it is recommended that the acrylic be annealed to remove stresses and absorbed moisture. If this is not done, the joints will degrade with time. Annealing is a time-at-temperature phenomenon and is dependent upon the thickness and grade of the acrylic: the thicker the sheet, the longer the annealing time. Annealing temperatures are normally above the heat-distortion temperature of the material, i.e., from 200 to 230°F (93 to 110°C), and the time is that period necessary to bring the material to thermal equilibrium. Cooling is a necessary part of the operation and must be controlled to prevent part warpage caused by residual stress formation. The cooling period is normally considered to be complete when the midplane temperature is below the glass transition temperature of the material.

Acrylic can be bolted or riveted to substructures, but normally edge attachment materials are first bonded to the acrylic to provide a way to distribute the fastener load. Acrylic is somewhat "notch" sensitive and differential thermal expansion must be considered (figure 2.38).

In summary, the weak link in the structural chain is usually the joining mechanism, which means that careful attention must be given to the method used, the structural design, the acrylic's notch sensitivity, and the effects of differential thermal expansion.

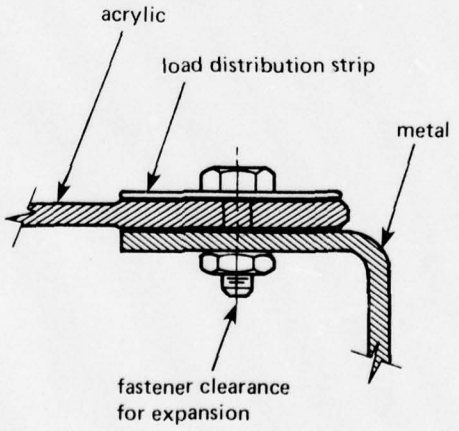

Figure 2.38. Normal bolted or riveted edge attachment.

2.17 LAMINATION

In many applications, it is necessary to laminate acrylic to other acrylic layers or different materials, such as glass or reinforced plastic. This need arises when the properties or the acrylic composite structure offer design advantages which cannot be achieved when a single material is used. One example is an aircraft windshield which is composed of glass, a flexible interlayer, acrylic, an interlayer, and acrylic (figure 2.39). This provides a structure which is lightweight, resistant to bird impacts and windshield-wiper abrasion, and fail-safe (figure 2.40). Another example is the use of as-cast acrylic, an interlayer, and stretched acrylic to form a window which can tolerate high temperatures on the as-cast acrylic face while experiencing only moderate temperatures on the stretched acrylic side. Many times it is desirable to place decorative films, wire grids, reflective coatings, or other elements within an acrylic composite to achieve various effects.

Laminating materials or interlayers can be rigid (high modulus) or extremely flexible (low modulus), depending upon the service environment and the materials. Two important considerations in selecting an interlayer are the differential loads being carried by each structural element and the differential thermal expansion of each element. The difference in deformations of these elements must be reacted by the selected interlayer material. Examples of materials commonly used for interlayers are modified acrylics, urethanes, polyvinyl butyrals, and silicones. Some are manufactured in sheet form and are laminated through the application of heat and pressure in an autoclave. Other materials are cast in liquid form between the members to be joined and polymerized in place, normally with the application of heat.

Table 2.10 lists general characteristics of some common interlayer materials used in laminating acrylic to other materials.

Figure 2.39. Laminated windshield for jet aircraft. (Photograph by Swedlow, Inc.)

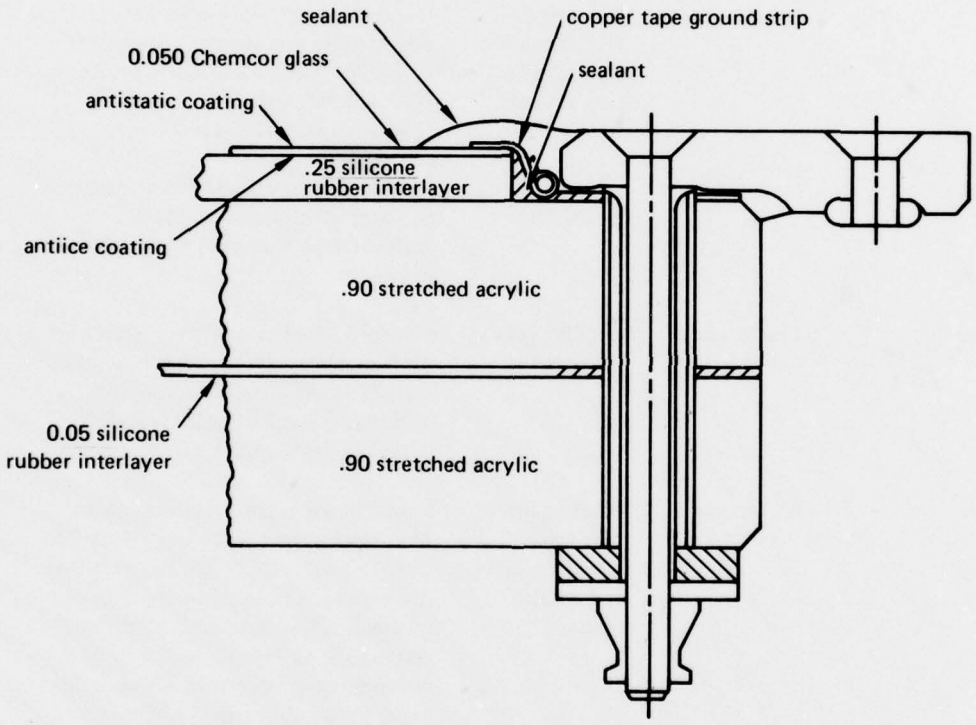

Figure 2.40. Cross-section through an impact-resistant windshield for modern, high-speed, aerospace vehicles.

Table 2.10. Interlayer materials.

Identification	Type	Typical Usage	Comments
Polyvinyl butyral (BGH plasticizer)	Sheet	Bonding glass face sheets	Has good optical properties above +32°F (0°C). Helps prevent shattering of the laminate when impacted.
Polyvinyl butyral (LBS plasticizer)	Sheet	Bonding glass face sheets	Adhesion of the face ply to the interlayer minimizes particle scattering. Sensitive to water ingress. Delamination from face sheet at edges. Limited to +160°F (71°C).
Silicone	Sheet	Bonding glass face sheets for high temperature applications	Has good optical properties and good elevated temperature properties (300° to 400°F) (149 to 204°C). Sensitive to H_2O and SO_2 with severe cracking. High cost. Availability unknown.
Acrylic	Cast-in-place	Bonding acrylic face sheets	Provides laminates with flexural properties equivalent to a monolithic configuration. Will not provide fail-safe capability.
Polyester	Cast-in-place	Bonding plastic face sheets	One of the first cast-in-place interlayers developed. Permits lamination of plastic materials with different processing cycles. Improved thermal capability over polyvinyl butyral.
Silicone	Cast-in-place	Bonding plastic face sheets, glass face sheets, and glass to plastic	Excellent for applications requiring a wide temperature capability: -100°F to +450°F (-73 to +232°C). Has excellent toughness and optical quality. Provides excellent adhesion to both plastic and glass. Does not become brittle or rigid at depressed temperature. Maintains its excellent tensile strength and elongation characteristics over broad temperature range. Excellent compatibility with conductive coatings.
Polyurethane	Cast-in-place or sheet	Bonding plastic face sheets, glass face sheets, and glass to plastic	Most recent of interlayer materials. Characterized by higher tensile strength with respect to temperature. Has natural tenacity to most materials.

2.18 SUMMARY

As the previous sections have shown, acrylic plastic is a many-faceted material whose properties can be custom-tailored to meet the requirements of different applications. Still, it has not found the wide application to which it is entitled. The reasons are not high cost, lack of fabrication capabilities, or absence of requirements for transparent materials with structural integrity. Rather, the absence of acrylic structures, or large structural components in otherwise opaque structures, can be explained only by lack of confidence and experience on the part of architects, structural engineers, designers, and building inspectors. Only if these people acquire the needed confidence and experience will the use of structural members fabricated from acrylic plastic increase significantly. It is hoped that this chapter contributes in a small measure to this goal.

SECTION 3. SOURCES OF WINDOW DESIGN DATA . . . 3-1

3.1 INTRODUCTION . . . 3-1

3.2 EVALUATION OF STRUCTURES . . . 3-2

3.2.1 Viewports . . . 3-2
3.2.2 Pressure Hulls . . . 3-8

3.3 EVALUATION OF MATERIAL . . . 3-9

3.3.1 Short-Term Data . . . 3-10
3.3.2 Long-Term Data . . . 3-13

SECTION 3.
SOURCES OF WINDOW DESIGN DATA

3.1 INTRODUCTION

Most engineering fields basically rely on two sources of data: analytical and experimental. The unusual aspect of acrylic plastic structural engineering is the preponderance of experimental data, the reasons for which are rooted in the history of viewport development and the inability to predict analytically the viscoelastic behavior of acrylic plastic. In 1948 when Professor A. Piccard introduced both acrylic plastic and the conical frustum shape to viewports in submersibles, the analytic tools and the material science necessary for accurately calculating the distribution of stresses in an acrylic plastic window shaped like a conical frustum did not exist. Therefore, the selection of appropriate window dimensions was based solely on experiments conducted in Piccard's high-pressure laboratory. These data now form the cornerstone of all experimental data generated for acrylic viewports.

Since 1948, the sciences of both material behavior and stress analysis have made enormous strides. The response of materials to triaxial stress fields is well understood for most materials and numerous theories exist for the prediction of their failure. Stresses can be calculated for structures of almost any conceivable shape by utilizing finite-element stress analysis techniques. However, the prediction of stresses in acrylic plastic structures under long-term or cyclic loadings is still less than satisfactory for two reasons: First, the response of acrylic plastic to complex three-dimensional stress fields is not completely understood, particularly its creep and relaxation functions. Second, finite-element analysis has not yet been sufficiently refined to consider creep and relaxation rates that are not only functions of time and temperature, but also of the stress-field configuration and magnitude of individual stresses.

As a result, experimental evaluation of acrylic structures and structural elements must be performed whether analytic calculations or general engineering experiences are used to determine the dimensions, particularly when the structures are used to house men. Thus, experimental data generated by testing full- or model-scale structures are the majority of the structural data used in the design of standard-shaped windows and pressure hulls. These data are augmented by results from tests under standard loading conditions, e.g., tension, compression, flexure, impact, and fatigue, on material specimens. Since these data are general in nature, they are often used to expand the applicability of existing exmerimental data.

Analytic stress analysis techniques should be utilized wherever feasible to arrive at the proper dimensions of acrylic structures. However, until they are used more often and the response of acrylic structures to complex stress fields is fully understood and the initiation of fracture predictable, existing experimental data from testing of acrylic structures and material specimens remain the basis of design and the ultimate way to compare the performance of operational structures.

3.2 EVALUATION OF STRUCTURES

3.2.1 Viewports

The acrylic plastic windows for viewports are generally tested to obtain four types of data: critical pressures, displacements, strains, and crack sensitivity. All are important for the proper understanding of window behavior, but only the first two are absolutely essential for adequate design of the viewport assembly and evaluation of its performance. Other data that should be considered include impact and dynamic shock resistances.

3.2.1.1 **CRITICAL PRESSURES.** Critical pressures are experimentally generated by placing a full- or model-scale window in a mounting and subjecting its high-pressure face to hydrostatic loading until the window loses its structural integrity, i.e., until it leaks or disintegrates catastrophically (figures 3.1 and 3.2). Since acrylic plastic is a temperature-sensitive viscoelastic material, the magnitude of critical pressure varies significantly with the ambient temperature and type of hydrostatic loading to which it is subjected. For this reason, the ambient temperature must always be maintained within a specified range during testing.

Destructive testing of acrylic plastic windows is usually accomplished by placing the viewport in the pressure vessel's end closure with the high-pressure face of the window facing the interior of the vessel (figure 3.3). To eliminate any undesirable restraint on the window by back pressure, the low-pressure face is always directly in contact with external atmospheric pressure through an opening in the vessel's end closure. Upon failure, the window fragments are ejected with explosive force through this opening. For this reason, pressure vessels used to generate critical pressure data are generally placed outside in a barricaded area. When this is not feasible, a container is placed around the low-pressure face of the viewport mounting and the entire assembly is placed inside the vessel. The interior of the container is vented to the atmosphere by a long tube with a small orifice restrictor that immediately becomes plugged by fragments when the window fails, thus preventing any damage to the immediate environment of the vessel.

The magnitude of critical pressure and the associated displacement of the window through the mounting prior to failure largely depend on the design of the window's mounting. Therefore, it is always necessary to describe the mounting arrangement used to generate critical pressure or displacement data (figure 3.4).

3.2.1.1.1 **Short-Term Critical Pressure.** This is always numerically higher than the critical pressures generated by long-term or cyclic loadings. Since these pressures are operationally easy to generate, they predominate in the published data. The Navy has generated the majority of short-term critical pressures by pressurizing windows at 650 pounds per square inch (4.48 megapascals) per minute in a room temperature environment. Since the magnitude of the critical pressure varies with the pressurization rate, ambient temperature, and type of mounting, these characteristics must be known when comparing or combining data from different sources.

If comparisons must be made between data from different sources with different test conditions, it is preferable to match them by ranking the effects of different test parameters on the critical pressure. For such purposes, temperature is ranked first; type

of mounting, second; and rate of pressurization, last. The following ranges of variation in test parameters between different sources of data are considered acceptable, as their effect on the critical pressure is probably less than 10 percent: ±5°F (2.5°C) for temperature and ±300 pounds per square inch (2.07 megapascals) per minute for rate of pressurization. Higher pressurization rates and lower temperatures produce higher critical pressures and smaller displacements, while lower pressurization rates and higher temperatures produce lower critical pressures and larger displacements. Since the effect of the mounting is a very complex subject and varies significantly with each type of window, it will be discussed later in the sections on the appropriate window shapes.

3.2.1.1.2 **Long-Term Critical Pressure.** These pressures are always lower than short-term critical pressures. Since the magnitude is a function of sustained loading duration and temperature, it is best represented as a family of static fatigue curves for a given window design (figure 3.5). The curves are generated by individually subjecting a series of identical windows to different levels of sustained constant loading until failure occurs. Since temperature is an important factor, a series of tests must be conducted not only at room temperature but also at other ambient temperatures. Long-term critical pressures are essential for the design of windows in underwater habitats, deep ocean simulators, and saturated diving chambers, where the magnitude of hydrostatic pressure is constant and applied for long periods of time.

Since long-term critical pressure is very sensitive to temperature, comparison of data from different sources is only feasible when the ambient test temperatures are identical. A difference of 5°F (2.5°C) can generate at least an order of magnitude difference in the duration of sustained loading prior to failure. The pressurization rate to sustained loading, however, can be ignored, as its effect on durations in excess of 1 day prior to failure is insignificant. The effect of the mounting is as important as it is for short-term critical pressures, and for this reason only data tested in similar mountings can be compared.

3.2.1.1.3 **Cyclic Loading Critical Pressure.** Such data are generated by individually subjecting a series of identical windows to pressure cycles with different maximum pressure levels and different ambient temperatures. This generates a family of cyclic fatigue curves for a given window design (figure 3.6). A typical cycle consists of pressurizing the window to a given pressure level, maintaining this pressure for a fixed period of time, depressurizing the window, and then allowing the window to relax for a fixed period of time. Pressure cycling usually continues until the window begins to leak or fails catastrophically. The cyclic fatigue life, expressed in number of cycles at a given pressure, is a function of pressure level, temperature, duration of individual pressure periods, and duration of relaxation periods. The fatigue life is decreased by increasing the pressure level, increasing the temperature, lengthening the duration of individual pressure periods, and shortening the relaxation periods.

Because the length of pressure cycles varies significantly with investigators, care must be used in comparing or combining data from different sources, since little is known quantitatively on the relationship between the length of the sustained loading period in a pressure cycle and the cyclic loading's critical pressure for a fixed number of cycles. Thus,

for example, there is no proven way to compare the cyclic critical pressures of two window designs when one was pressure cycled at 1 minute per cycle while the other was cycled at 100 minutes per cycle, even if the ambient temperature were the same. If, however, a comparison must be made, the duration of all sustained loading periods should be added and used instead of the total number of cycles. This recommendation is based on experimental evidence that the total duration of the sustained loadings in a pressure cycling program has a larger effect on the cyclic fatigue life of an acrylic plastic window than does the number of cycles.

From an operational viewpoint, the only cyclic fatigue data that are directly applicable are those based on pressure cycles of approximately the same duration as those for a typical operational pressure loading. Since these loadings vary in duration and the cyclic fatigue lives of different window designs must be compared, a typical pressure cycle has been established for experimental studies, i.e., a cycle that consists of 7 hours of sustained loading at maximum pressure followed by a relaxation period of at least 7 hours.

3.2.1.2 DISPLACEMENTS. Displacement data are generally the byproduct of tests for critical pressures. Only in isolated cases have tests been conducted with the sole purpose of measuring displacement. In either case, the window is mounted in the pressure vessel's end closure with the low-pressure face exposed to the atmosphere.* Measurements are usually made only along the axis of the seat; displacement has been measured along the bevel angle of the seat surface in only a few instances. The basic approach consists of mounting the bodies of displacement transducers on some rigid benchmark surface while the active elements of the transducer contact the low-pressure face at one or several locations. In arrangements where the face is visible to the observer, the displacement can be easily measured with mechanical dial indicators. Because of cost of these indicators, measurements are generally performed only at the center of the low-pressure face; only in a few cases have measurements been performed at enough locations to provide a reasonably accurate topography of the window's low-pressure face under operational loading (figure 3.7).

The most reliable measurement technique consists of a very thin wire anchored at one end to the low-pressure face and on the other to a small weight that rests atop a mechanical dial indicator (figures 3.8, 3.9, and 3.10). To minimize the effect of experimental errors the wire is attached to the window's face via an acrylic post bonded to the window's surface with room-temperature-vulcanizing silicone adhesive. Because of the large weight on the other end of the wire, the friction of the pulleys does not introduce any error. Another advantage of this technique is its insensitivity to distortion and cracking of the low-pressure face, as the flexible adhesive retains its bond even in the presence of surface cracks and flexing. Thus, this instrumentation technique is used exclusively for measurement of displacements on windows undergoing destructive hydrostatic testing.

Another technique consists of mechanical dial indicators clamped to the end closure with the contact points resting directly against the window's low-pressure face. Absence of pulleys, weight, wire, and anchor post makes this an elegant displacement measurement technique. Its accuracy is very high, if cracking or major flexing of the low-pressure faces does not occur (figure 3.7).

---

* *Because of experimental difficulties posed by measuring displacements on the high-pressure face, measurements are usually done only on the low-pressure face.*

Electrical transducers in the form of linear potentiometers or transformers have been used only rarely for measuring axial displacements. The basic reasons are the high cost, calibration requirements, waterproofing, and requirement for accurate readout instrumentation. Linear potentiometers are usually used only for measuring the axial displacement of the high-pressure face, which is inaccessible to mechanical means of measuring displacement (figure 3.11).

3.2.1.3 STRAINS. Strain, defined as unit deformation of material, is experimentally measured with photoelastic techniques or with electric-resistance straingages that are bonded to the surface of an acrylic window. Which technique is chosen depends on whether the strains are to be measured only on the window's face or also in its interior. Since maximum strains occur only on the exterior of the window, measurement with the straingages generally suffices. It is only when the engineer must see the complete strain pattern that the photoelastic investigation is used.

3.2.1.3.1 Electric-Resistance Straingages. These gages provide satisfactory data for engineering investigations, if certain precautions are taken in attaching gages, selecting readout equipment, and recording the readings (figure 3.12).

Gages have been satisfactorily bonded to acrylic with many types of cement with results that varied from excellent to disastrous. Eastman 910 contact cement provides consistently good results and is preferred. The wrong choice of cement can result in low strain readings because of slippage between the gage and acrylic and can also initiate stress cracking under the gage, resulting in high strain readings and premature failure of the window. Most adhesives containing solvents will attack acrylic plastic and for this reason should be avoided.

The same problem is encountered with waterproofing the gages, where the use of coatings that attack acrylic plastic can initiate stress-corrosion cracking in the plastic when it is subjected to hydrostatic loading. Room-temperature-vulcanizing silicone rubber (RTV), a very effective adhesive and waterproofing compound, initiates such cracking at very low stress levels and should not be used for waterproofing of straingages on acrylic plastic. Gagecotes 2 and 5 (manufactured by Bean) provide excellent waterproofing without initiating stress-corrosion cracking.

Heat generated by the gage is another source of error in strain readings. As the energizing current flows through the straingage it generates heat that causes the surface of the material to expand and thus generates false positive strain readings. For this reason, strain switch-and-balance units that energize the individual straingages only at the moment the strains are read are preferred. Rapid switching from one gage to another also accomplishes another objective: it allows the investigator to obtain a complete surface-strain distribution pattern for the window in real time. Thus switch-and-balance units that balance and record at rates of 0.01 to 0.1 second per channel should be used. These are particularly valuable during measurement of strains under short-term loading conditions where, at any one pressure level, the strains change rapidly because of creep, e.g., 2000 microinches per inch per minute (0.2-percent strain per minute). Data from short-term tests where the recording rate was slower than 1 second per channel should be viewed with suspicion, as the magnitude of recorded strains can be off 10 to 20 percent, particularly if the window was

instrumented with many gages. During long-term loading, the reading of strains is not as much of a problem, since the creep rate finally stabilizes itself at a slow rate and real-time distribution of strains can be obtained, even with manually operated switch-and-balance units.

3.2.1.3.2 **Photoelastic Strain Measurement.** This technique is generally used when it is necessary to determine the distribution of strains not only upon the surface of the window but also within its interior. This three-dimensional method consists of (1) fabricating in epoxy a scale model of the acrylic window; (2) generating a three-dimensional pattern of photoelastic fringes by pressurizing it in a proper mounting at an ambient temperature range of 290 to 310°F (143 to 154°C); (3) freezing the photoelastic fringe pattern inside the epoxy window by cooling the window to ambient room temperature without reducing the magnitude of hydrostatic loading; (4) cutting the epoxy window into thin slices along the directions of principal stresses; and (5) plotting the distribution and magnitude of strains by noting their location and counting the number of photoelastic fringes. Because this technique is very expensive compared to straingage instrumentation and because it requires a new test specimen for each pressure level investigated, it has been used only in a few cases where the criticality of the window's application warranted the additional expense.

Where it is necessary to determine three-dimensional strains inside a window along a single plane, a composite optical system incorporating a bonded polariscope is built inside the window (figure 3.13). This optical system is arranged around a central slice of epoxy material in which the stresses are to be analyzed. Straddling the slice of epoxy are polarizers that form a light-field circular polariscope. On one side of the polariscope is a two-piece segment incorporating a vapor-deposited aluminum mirror; the other side is a segment of the window whose upper surface has been roughened to form a light diffuser. The six components of the optical system are bonded together with epoxy cement to form a unit that can be illuminated and viewed through the high-pressure face of the window. The composite window is then placed in the appropriate mounting and pressurized on the high-pressure face with gas. During the test, the high-pressure face is illuminated with monochromatic light while the behavior of the epoxy slice in the window is observed and photographed through a window in the pressure chamber directly above the test specimen (figure 3.14). This technique is economically more attractive than freezing the photoelastic fringes, as it allows the use of a single test specimen for determination of stresses at several pressure locations. The generated data are not as complete as those produced by the freezing technique, but they still are more extensive than data generated by straingage instrumentation.

3.2.1.4 **CRACK SUSCEPTIBILITY.** Crack susceptibility is numerically defined by the same experimental parameters used for critical pressures, i.e., pressure, time, and temperature. The pressures required to initiate a crack also vary with the type of loading: Under short-term pressure loading the magnitude of pressure required for crack initiation is higher than it is for long-term or cyclic loading conditions.

Initiation of cracks is studied experimentally by placing the window in a pressure vessel's end closure with the high-pressure face facing the interior of the vessel and the low-pressure face vented to ambient atmospheric pressure. During application of pressure, the condition of the low-pressure face is observed using a mirror and telescope arrangement or

a closed-circuit television. Since in many cases the cracks first originate on the bearing surface rather than on the low-pressure face, pressurization of the vessel must be periodically interrupted and the window removed for detailed inspection of the bearing surfaces. The pressure or time intervals chosen for removal of the window for observation must be small, or the crack can grow to a significant length without being noticed.

After the test parameters at which crack was initiated have been recorded, the test is usually continued to determine the rate of crack growth. For some window shapes and dimensions the rate is high, leading to catastrophic window failure within a small load or duration of loading increments. For other shapes the rate is very low, making the load or time interval between initiation of cracks and catastrophic failure very large. Windows with a high rate are considered to be crack sensitive, while those with low rate are considered to be crack insensitive. Crack sensitivity is generally defined as the ratio of pressure that initiates the crack to critical pressure under short-term pressurization. Another quantitative measurement of crack sensitivity is the ratio of pressure cycles at crack initiation to the number of cycles when catastrophic failure occurs.

3.2.1.5 **IMPACT RESISTANCE.** The resistance of windows to mechanical impacts is generally determined experimentally, since acrylic plastic is not only sensitive to the magnitude of dynamic stresses but also to the rate at which they are generated, a situation which makes the analytic solution to this problem prohibitively expensive. Some analytic predictions that correlate reasonably well with experimental data have been made, but they were done only for low velocity impacts where the effect of the high stress application rate was minimal.

Most experimental impact data are produced by mounting the window in the pressure vessel's end closure with the high-pressure face turned to the interior of the vessel and the low-pressure face vented to ambient atmospheric pressure. If the window is too large for the mounting, a pressure-proof enclosure is used to keep the low-pressure face at ambient pressure, while the high-pressure face is exposed to hydrostatic loading. To insure axial impact loading, the impactor is also mounted on the pressure-proof enclosure. The actual tests consist of dropping a steel impactor from a predetermined height on the low- or high-pressure face (figure 3.15). The impact resistance of the window is then recorded as the velocity and/or kinetic energy at which the first crack is initiated (figure 3.16). The choice of the high- or low-pressure face depends on the operational use of the window. For submersibles, habitats, and 1-atmosphere diving bells, the resistance is determined by impacting the high-pressure face, while for deck- and land-mounted hyperbaric chambers the low-pressure face is impacted.

Impact resistance data for acrylic windows cannot be directly used for assigning ratings to windows with shapes or proportions different from those tested for two reasons: (1) there is a multitude of variables that affect the results of impact testing and (2) investigators have not yet agreed upon a standard set of test parameters. In addition to the typical test parameters, e.g., temperature and pressure, there are others found only in impact testing, e.g., the radius of the impactor, the ratio of impactor diameter to window diameter, angle of impact, and location of impact. In addition, to economize a window may be tested repeatedly with increasing impact velocities until a crack is initiated. Such repeated testing probably fatigues the material and generates microscopic cracks in the acrylic that eventually

cause premature failure. As a result, impact data must be used only with the greatest caution. Basic rules for establishing the validity of the data for operational requirements are

1. The range of the terminal impactor velocities should overlap the range of the impact velocities predicted by the operational scenario.

2. The ratio of the impactor's diameter to the minor diameter of the test specimen should be less than or equal to 0.25.

3. The impactor should contact the center of the window's face at right angles.

4. The ambient temperature and pressure should closely match those of the predicted operational environment.

5. The impactor's curvature radius should be greater than or equal to 0.125 times the minor diameter of the window.

3.2.1.6 DYNAMIC SHOCK RESISTANCE. Dynamic shock resistance is defined as the maximum dynamic overpressure which a window can withstand at a given depth and temperature. It is usually established experimentally by mounting the window in the pressure vessel's end closure and subjecting the high-pressure face to dynamic impulses generated by underwater explosions in the vessel. However, such an arrangement often creates a hazard to the personnel outside the vessel. In such cases the test specimen is mounted in a pressure-proof housing with only the high-pressure face of the specimen exposed to dynamic overpressure (figure 3.17A). In either case, the magnitude of the dynamic overpressure is controlled by changing the weight of the explosive or the standoff distance. The minimum overpressure causing the window to crack is recorded as the dynamic shock resistance of the window (figure 3.17B).

Comparison of data from different sources is almost impossible, since dynamic shock resistance is a function of both dynamic overpressure and its duration. In addition, the simple, spherical, dynamic pressure wave generated by an explosion inside the pressure vessel is invariably augmented by reflections from the walls of the vessel. Thus, depending on the size of the vessel, the effect of an explosive charge will vary with the window. It has also been found that the effect of dynamic overpressure can be mitigated or augmented by static pressure, depending on the shape of the window. Thus a meaningful comparison of experimental data from different sources requires that the static pressure and temperature used for testing be identical, as there is insufficient knowledge to assign numerical values to the effects of these variables.

3.2.2 Pressure Hulls

Most existing data on the structural performance of acrylic pressure hulls have been experimentally generated* by placing the hulls inside a pressure vessel with a minimum of physical restraint. Such restraint generally consists of a ballasted external cage and a crush-proof, flexible, tubular conduit between the interior of the hull and the exterior of the vessel (figures 3.18 and 3.19). The external cage keeps the buoyant hull from striking the top end closure of the pressure vessel, while the conduit serves as both a waterproof raceway for instrumentation wires and as a way to maintain the interior of the acrylic hull at atmospheric pressure. In some cases the cage is eliminated and the flexible conduit is replaced by a rigid pipe that holds the hull in a fixed position relative to the vessel's end closure (figure 3.20).

* *See section 3.2.1 for reasons why data are generated experimentally.*

The experimental data are basically the same type as generated for viewpoints, and are produced in the same manner. The structural performance is defined during the tests in terms of short-term critical pressure, long-term critical pressure, cyclic loading critical pressure, crack susceptibility, impact resistance, and dynamic shock resistance.

The instrumentation used for testing the hulls is basically the same used for testing the viewports, except for the water-displacement technique which has been successfully used to measure average radial displacement and average membrane shell strains. Because of its low cost, high reliability, and ability to measure very large strains, it is used in hydrostatic tests where the hull is being pressurized to implosion (figure 3.21). Although electric-resistance straingages are routinely used to measure strains on acrylic pressure hulls, they rarely remain functional at levels above 0.02 inch per inch (2-percent strain). For this reason the ability of the water displacement technique to obtain some quantitative indication of strain magnitudes at implosion is of inestimable value. Furthermore, the presence of water inside the pressure vessel eliminates the need for external ballast during testing and also mitigates the shock generated by catastrophic failure of the hull. Because water acts as a cushion, the fragments of the failed hull do not develop the same velocity as if the hull were filled only with air; thus there is less damage to the remainder of the hull. As a result, inspections of imploded acrylic hulls filled with water are useful in determining the origin of failure (figure 3.22).

In some instances manned acrylic hulls have been experimentally evaluated. Such tests were generally not conducted for structural reasons, but for establishing heat-transfer and human-performance parameters (figure 3.23). This practice has been also followed in evaluating the performance of a complete submersible system in a deep ocean simulator prior to diving (figure 3.24).

3.3 EVALUATION OF MATERIAL

Material specimens are tested to establish the suitability of the material for its intended application and to control its quality. It is important to remember this when discussing such tests, since test results are not necessarily interchangeable. The basic difference in testing philosophies is that the objective of the former is to simulate operational conditions, while the objective of the latter is to generate data rapidly and economically. However, since most tests established for quality control also apply to a large degree to tests for material suitability, they will be discussed together.

Acrylic plastic specimens are usually tested to establish short-term, long-term, and environmental effect data. Since short-term data can be rapidly and economically generated, they predominate in the literature and are often used for quality control in the production of acrylic plastic. Long-term data generated in a laboratory environment are an order of magnitude less available than are short-term data because of their expense; for this reason they are not routinely used for quality control. The data describing the effect of the environment on the structural and optical performance of acrylic plastic are almost nonexistent. Because of this scarcity and the time and expense of their generation, they are never used for quality control. Their value for establishing the suitability of acrylic plastic for its intended applications as pressure-resistant structures or as structural elements is, however, inestimable.

3.3.1 Short-Term Data

This category includes all tests that require less than 1 day for completion. The majority of standard tests for mechanical, optical, electrical, and physical properties fall into this category. Only tests customarily used by window designers and users in procurement specifications will be discussed in this section. A complete list of standard short-term tests applicable to acrylic plastic is in section 15.

3.3.1.1 TENSILE STRENGTH, TENSILE MODULUS OF ELASTICITY, AND ELONGATION AT BREAK. These values are established by pulling a tensile test specimen in the shape of a "dogbone" at a specified rate in a room temperature environment until fracture of the specimen occurs (ASTM-D-638) (figure 3.25). Because acrylic plastic is sensitive to straining rate, temperature, surface condition, and ambient environment, the generated values of tensile strength, tensile modulus, and elongation at break are valid only for the set of experimental parameters present during the test, i.e., a 70 to 77°F (21 to 25°C) temperature range, 0.2-inch-per-minute (5 millimeters per minute) overall strain rate, uniaxial stress field, polished surface, and clean air environment with 50-percent relative humidity. If any parameters change, so do the test values in a significant manner, particularly if the surface is scratched and the environment is at a higher temperature and contains vapors of organic substances that act as solvents for acrylic plastic.

Because the standard ASTM test parameters cover such a narrow and operationally unrealistic range, the ASTM tensile strength of material is primarily applicable only for quality control and procurement specifications. Since tensile strength is considered a basic property and the ASTM-D-638 test can be performed rapidly and economically, it forms the basis for all specifications for acrylic plastic used in pressure-resistant structures. However, if the designer wishes to utilize short-term tensile strength for predicting the response of an acrylic structure to momentary overloads, i.e., impact loading, dynamic shock loading, momentary increases in static pressure because of loss of pressure control, etc., he must specify nonstandard test parameters that reflect the temperature, rate of loading, surface condition, and environment and that simulate the operational overload of the structure.

3.3.1.2 COMPRESSIVE YIELD STRENGTH AND COMPRESSIVE MODULUS OF ELASTICITY. These values are established by compressing a test specimen in the shape of a cylinder or prism at a specified rate in a room temperature environment until an increase in strain occurs without an increase in stress (ASTM-D-695) (figure 3.26). The values generated by this test are valid only for a 70 to 77°F (21 to 25°C) temperature range, 0.05-inch-per-minute (1.25 millimeters per minute) overall strain rate, uniaxial stress field, and clean air environment with 50-percent relative humidity.

Because the test for compressive yield strength is conducted under a very narrow set of experimental parameters, it is primarily applicable for quality control and procurement specifications. Since compressive yield is considered a basic property and the ASTM-D-695 test can be performed rapidly and economically, it is included in all specifications for acrylic plastic utilized in pressure-resistant structures. However, if the designer wishes to utilize short-term yield strength for predicting the response of the acrylic structure to momentary overloads, i.e., momentary increase in static pressure because of loss of pressure control, nonstandard test parameters that reflect the expected rate of loading and ambient

temperature at which overload of the structure will take place must be specified. Because the compressive yield strength is not sensitive to the shape and surface quality of the specimen or the presence of harmful chemicals in the ambient atmosphere, it is not necessary to specify ambient atmospheres other than the one provided in the standard test.

3.3.1.2 FLEXIBLE STRENGTH AND FLEXURAL MODULUS OF ELASTICITY. These values are established by subjecting a test specimem in the shape of a rectangular bar to bending, applied with a 3- or 4-point loading system, at a specified rate in a room temperature environment until fracture of the specimen takes place (ASTM-D-790). Because acrylic plastic is sensitive to the rate of straining, temperature, surface condition, and ambient environment, the values of this test are valid only for a 70 to 77°F (21 to 25°C) temperature range, a deflection rate that is a function of the specimen's proportions, uniaxial stress field, polished surface, and clean air environment with 50-percent relative humidity. Because of the narrow range of test parameters, the values generated by ASTM-D-790 are primarily utilized for quality control and procurement specifications. The flexural strength test ASTM-D-790 is not as frequently used in such specifications as are the tests for tensile and compressive yield strengths, since flexural strength is not a basic, but rather a derived, property, i.e., tension on top and compression on bottom of specimen, and a larger test specimen is usually required. However, if the designer wishes to utilize short-term flexural strength for predicting the response of an acrylic structure to momentary overload, nonstandard test parameters that reflect the temperature, rate of loading, surface condition, and ambient environment present during a projected momentary overload must be specified.

3.3.1.4 DEFORMATION OF PLASTIC UNDER LOAD. This value is established by subjecting a test specimen in the form of a cube to axially applied, sustained, compressive stress at a specified temperature (ASTM-D-621). Because deformation of acrylic plastic is a function of temperature, stress level, humidity, and time, the generated values are valid only for the set of experimental parameters present during the test. This means that the recorded deformation is valid only for a sustained loading of 24 hours at stress levels of 1000, 2000, or 4000 pounds per square inch (6.89, 13.7, or 27.5 megapascals) at 73.5, 122, or 158°F (23, 50, or 70°C).

The generated deformation values are primarily used in quality control and procurement specifications. For these purposes, any stress level or ambient temperature may be selected. As a rule, those which best match the intended working stress level and maximum expected ambient temperature are chosen. For acrylic plastic windows and pressure hulls, those that best correspond with operational conditions are 4000 pounds per squre inch (27.5 megapascals) and 122°F (50°C). If the material has a propensity to creep excessively, such parameters will accentuate this tendency. Because the standard test for deformation under load performs a valuable function in differentiating between grades of acrylic with acceptable and unacceptable levels of creep, it is widely used in quality control and procurement specifications. This test is also one of the few short-term tests that is of any value to the designer, as it provides valid design data for acrylic structures that are subjected to loading cycles shorter than 24 hours.

3.3.1.5 IMPACT RESISTANCE OF PLASTICS. This characteristic is determined by subjecting a test specimen in the form of a notched bar to dynamic flexure loading (ASTM-D-256). In one case (Izod test method), the specimen is held by a vise at one end while the

dynamic load is applied to the other end of the cantilevered specimen (figure 3.27); in the other case (Charpy test method), the specimen is supported at the ends while the dynamic load is applied at the center directly over the notch in the bar (figure 3.28). The dynamic loading is generated by a pendulum that strikes the specimen at preset locations. The velocity of the pendulum at the moment of impact is set to be just sufficiently high enough to break the specimen. Unless otherwise specified, the ambient test temperature is 70 to 77°F (21 to 25°C).

The impact energy required to break the notched test specimen is primarily utilized in quality control and only secondarily in design, as the test parameters have only a very remote relationship to operational conditions. It is also impossible to translate the impact energy at fracture during the test into useful criteria for prediction of fracture in an acrylic structure when subjected to point-impact or dynamic pressure loading.

The test results are very useful, however, for the designer when selecting material for applications where there is a high probability of impact damage to the acrylic structure. By choosing a grade with a higher Izod or Charpy number, i.e., requiring more impact energy to break it at the notch, the designer is assured that the impact resistance of the acrylic structure will be increased.

3.3.1.6 DEFLECTION TEMPERATURE OF PLASTICS UNDER LOAD. This characteristic is determined by subjecting a bar specimen to 3-point flexural loading while the ambient temperature is increased at a uniform rate (ASTM-D-648). The flexural loading is of such magnitude that it maintains a constant maximum tensile stress of 264 pounds per square inch (1.8 megapascals) while the temperature of the oil bath is increased from 73°F (23°C), at a rate of 35°F (1.6°C) per minute, until the deflection at the flexed bar increases by 0.01 inch (0.25 millimeter). The temperature reading at which the deflection of the bar increases by 0.01 inch (0.25 millimeter) is a measure of the plastic's ability to retain its mechanical properties at elevated temperatures, i.e., the higher the temperature at which the deflection is recorded, the higher is the resistance of the material to thermally induced plasticity.

The temperature at which the specified deflection occurs is utilized exclusively in quality control and procurement specifications. It is of particular value in procurement of material for acrylic structures that will operate at temperatures above 122°F (50°C). It is also useful in the procurement of materials for structures that will operate at room temperature, since the appropriate minimum temperature value for ASTM-D-648 insures a superior grade of material with lower creep properties even at room temperature.

3.3.1.7 RESIDUAL ACRYLIC MONOMER PERCENTAGE. This value is determined by using gas liquid chromatographic techniques.* The test is primarlly used for quality control of the casting process and for material procurement specifications. The percentage of unpolymerized methyl methacrylate and ethyl acrylate monomers serves as an indication of how much of the polymerization process has been completed. A low percentage indicates that the process is essentially complete and the physical properties of the material will not undergo any significant change in a short period of time when exposed to solar radiation or heat.

---

* *See, for example, Snell and Otto, "Encyclopedia of Industrial Chemical Analysis," Interscience Publisher, 1972, Vol. 4, pp. 211-217, and Vol. 16, p. 99.*

3.3.1.8 **CLARITY OF MATERIAL.** This characteristic is determined by viewing a printed pate (7 lines per column inch and 16 letters to the linear inch) from a distance of 20 inches (51 centimeters) through the full thickness of the casting with the opposite faces polished. The ability to read the print indicates that the clarity of the casting is acceptable for general use as an optically transparent material. This test is primarily utilized in material procurement specifications to insure that the acrylic casting has only a minimum of optical imperfections in the form of haze, porosity, striae, and inclusions.

3.3.2 Long-Term Data

Long term data are generally produced in nonstandard tests conducted by investigators in government and academic research laboratories rather than by investigators in commercial material testing laboratories. Because the data have been generated by nonstandard tests, they do not readily lend themselves to correlation studies. Each researcher generally uses a different set of test parameters that are either chosen because of their similarity to projected operational conditions or because of their applicability to material properties under investigation. However, even with all the shortcomings accompanying data generated by nonstandard tests, they are the basis for predicting the performance of acrylic plastic structures under the long-term loading that is typical of all engineering structures.

3.3.2.1 **LONG-TERM TENSILE PROPERTIES.** These properties, e.g., tensile rupture strength, creep, effective modulus of elasticity, and resistance to crazing, are functions of temperature, applied stress level, duration of stress application, and environment. The data are generated by subjecting a test specimen to a constant tensile stress or known magnitude in a rigidly controlled ambient environment. Periodically the strains are measured and the surfaces of the specimen are inspected for crazing. Also the time is noted at which a test specimen fails.

The results for a given ambient temperature are usually plotted as (1) a family of strain curves on stress as a function of time coordinates (figure 3.29), (2) a family of stress curves on strain as a function of time coordinates (figure 3.30), (3) a family of effective modulus curves on stress as a function of time coordinates (figure 3.31), (4) a family of stress curves on effective modulus as a function of time coordinates (figure 3.32), and (5) crazing and rupture curves on stress as a function of time coordinates (figure 3.33). Since most tests are only for 1000 hours duration, the results must be extrapolated for structures where loading is measured in years rather than in hours. Extrapolation can be performed with reasonable confidence, if (1) the extrapolation does not exceed by more than one order of magnitude the time period for which data are available and (2) the coordinates chosen for plotting the existing data allow the data to be represented by a straight line. Extrapolations exceeding a period of 10 years should be avoided, since it is not known how much the physical and optical properties deteriorate over such a long time span, i.e., data on deterioration of thin acrylic plastic are available only for periods less than 10 years. Wherever possible, extrapolation should be performed with data collected in the same type of environment for which the extrapolation is being performed, i.e., if performance of acrylic is to be predicted for 10 years of continuous tensile loading in an outdoor environment, the basis of prediction should be data generated over a period of 10 years by tensile specimens in an outdoor environment.

3.3.2.2 **LONG-TERM FLEXURAL PROPERTIES.** These properties, e.g., flexural rupture strength, creep, effective modulus of elasticity, and resistance to crazing are functions of temperature, applied stress level, duration of stress application, and environment. The data are usually generated by subjecting flexure test specimens to constant moments of known magnitude in a controlled laboratory environment or in uncontrolled outdoor weathering exposure (figure 3.34). Periodically the strains are measured and the surfaces of the specimens are inspected for crazing. If fracture occurs, the time of failure is noted.

The resulting data are plotted in a fashion similar to that used for tensile data's long-term tensile properties (section 3.3.2.1). Since some data are generated with scratched or notched specimens, they are very valuable to the designer since they provide an opportunity to compare performances of acrylic plastic with polished and scratched surfaces. If data are available for both surface conditions, it is best to base the design on the data generated by the scratched specimens, as after several years of service the surface of any acrylic structure will become scratched.

3.3.2.3 **LONG-TERM COMPRESSIVE PROPERTIES.** These properties, e.g., creep and effective modulus of elasticity, are functions of temperature, applied stress level, duration of stress application, and environment. The data are generated by round cylinders or square prisms subjected to constant compressive loading. The strains are read periodically and noted.

The resulting data are plotted in a fashion similar to that described in section 3.3.2.1. Because long-term compressive properties are insensitive to the condition of the material surface, the available data can be applied to any acrylic structure whose structural members are in compression, regardless of the condition of its surfaces.

There is one other attractive characteristic of the long-term compression data. Because the data are generated in uniaxial stress field, their values are conservative when applied by a designer to a structure with biaxial or triaxial compressive stress fields. How much the creep decreases and how much the compressive strength increases under different ratios of biaxial and triaxial compressive loadings when compared to uniaxial compression is only known for a few biaxial stress ratios at ambient room temperature. Exploratory studies indicate that the decrease of creep and associated increase in effective modulus and compressive strength for some biaxial and triaxial compressive stress fields are significant.

The conservatism of uniaxial compression data represents a departure from the character of uniaxial tensile and flexural data, which are less than conservative for the prediction of rupture in biaxial and triaxial tensile stress fields. There the designer must discount the rupture strength values by some factor, if the structure being designed encompasses biaxial or triaxial tensile stress fields.

Figure 3.1 Setup for long-term testing of multiple windows under the same temperature and pressure. Each test jig consists of two test flanges with the windows mounted back-to-back. Each jig is pressurized from a common pressure manifold and cooled from a common refrigeration manifold. In this test facility, six conical frustum windows can be tested at the same time inside the three pressure vessels. Each vessel consists of two viewport flanges mounted back-to-back.

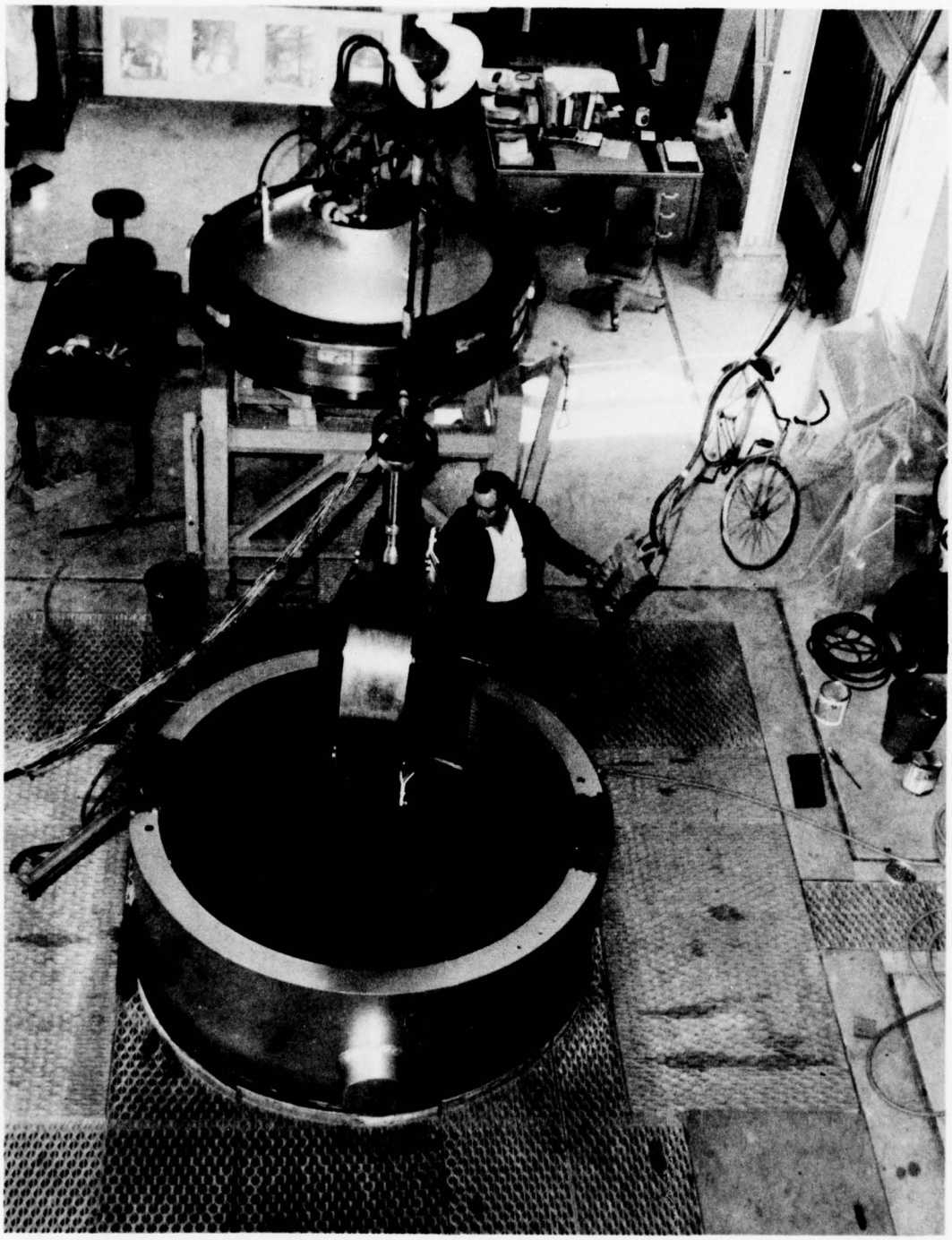

Figure 3.2. Setup for testing two large spherical shell sector windows at the same time inside a pressure vessel. The windows are mounted back-to-back in a common test flange. The interior of the test jig is vented to atmospheric pressure through a rigid pipe that is threaded into an opening in the vessel's end closure.

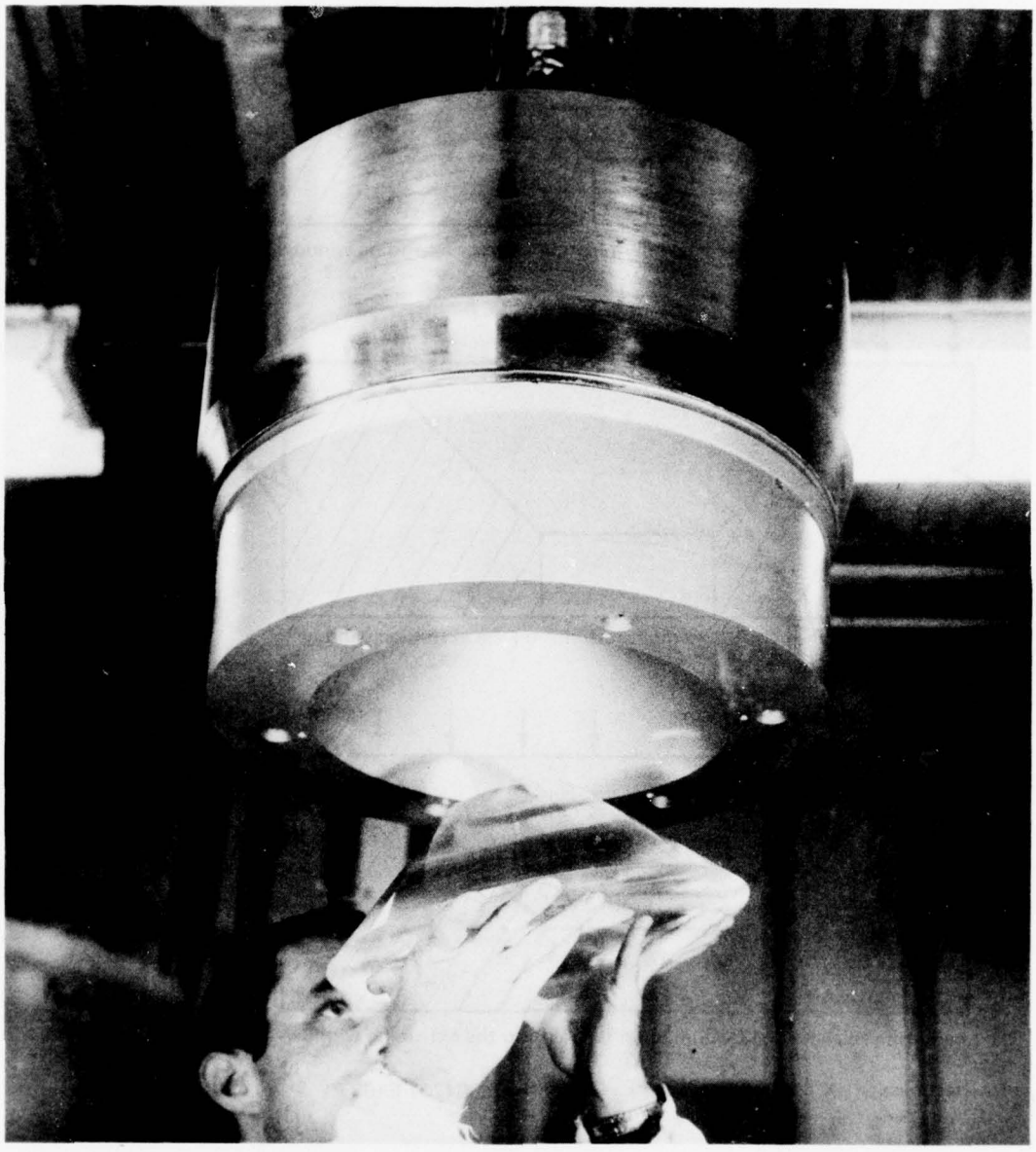

Figure 3.3. Installation of a conical frustum window in a test flange mounted on the pressure vessel's end closure. The back of the test flange is vented to atmospheric pressure through an opening in the end closure. This test set has the capability of pressurizing the window to 20,000 pounds per square inch (137.8 megapascals) in a simulated ambient ocean environment.

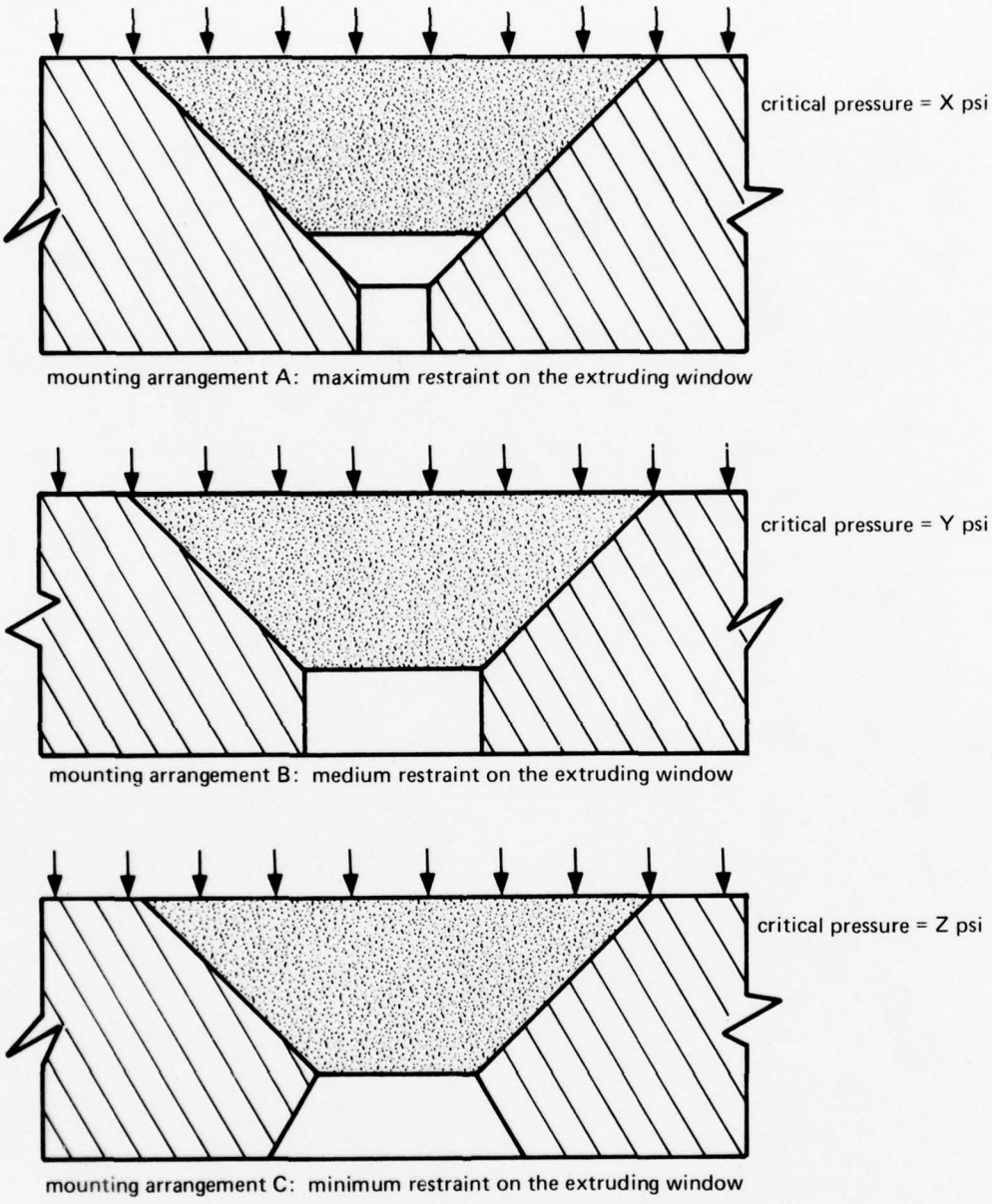

Figure 3.4. Test flanges for conical frustum windows with different degrees of axial and radial restraint upon the window. The critical pressures on which the design criteria of section 15 are based were generated in mounting arrangement B.

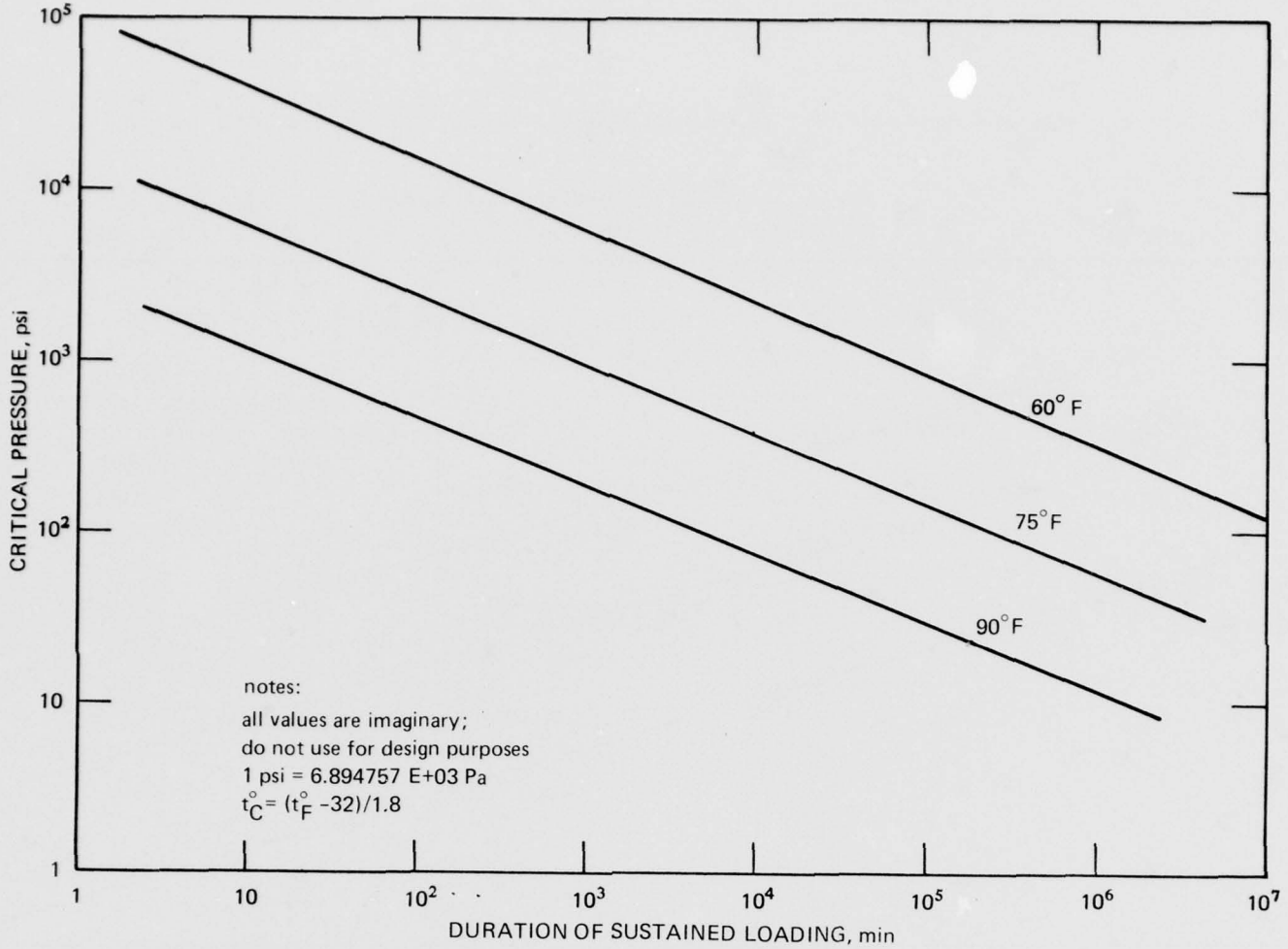

Figure 3.5. Empirical static fatigue life curves based on critical pressure and duration of loading for a given window design.

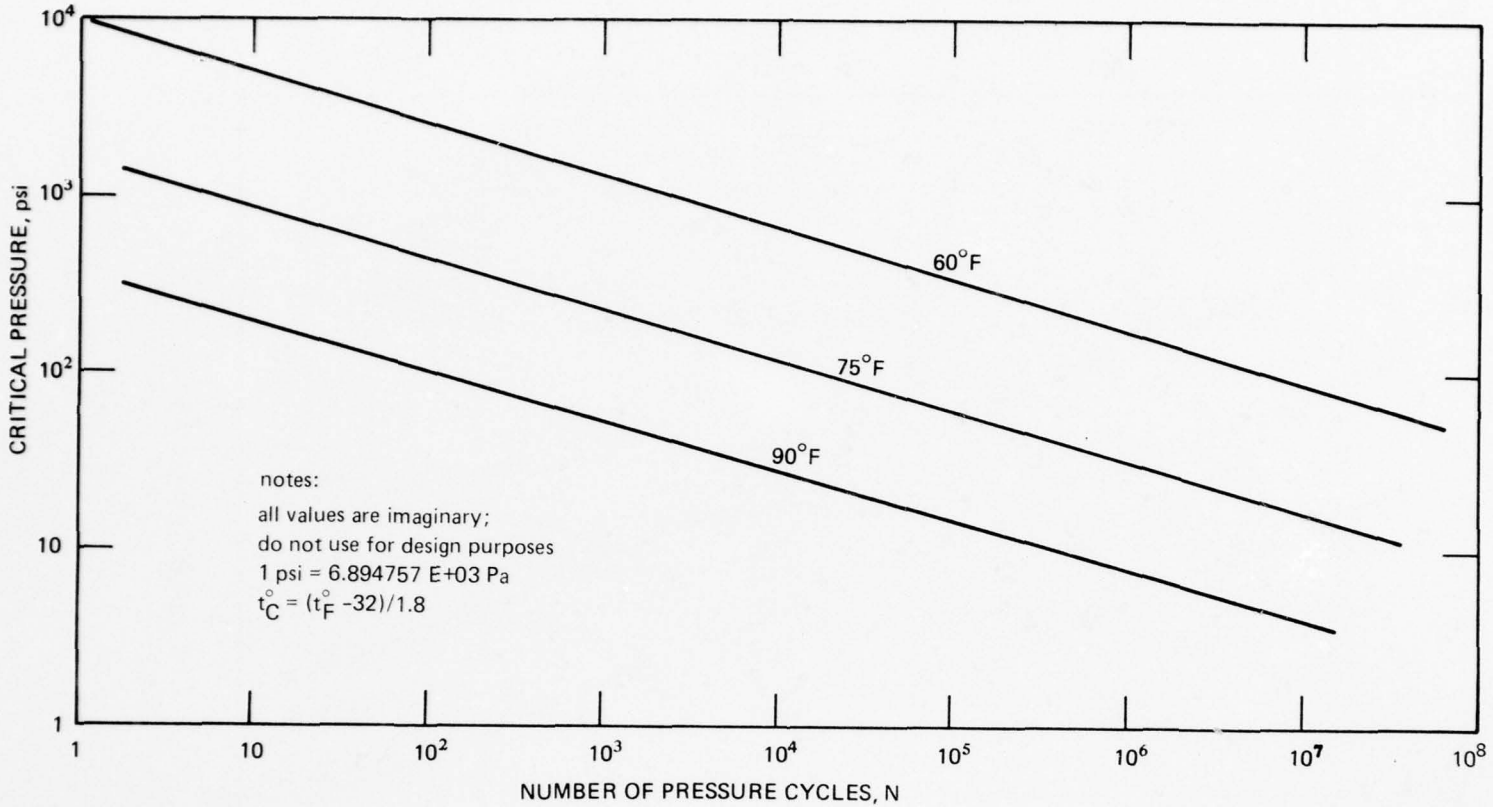

Figure 3.6. Empirical static fatigue life curves based on critical pressure and number of pressure cycles.

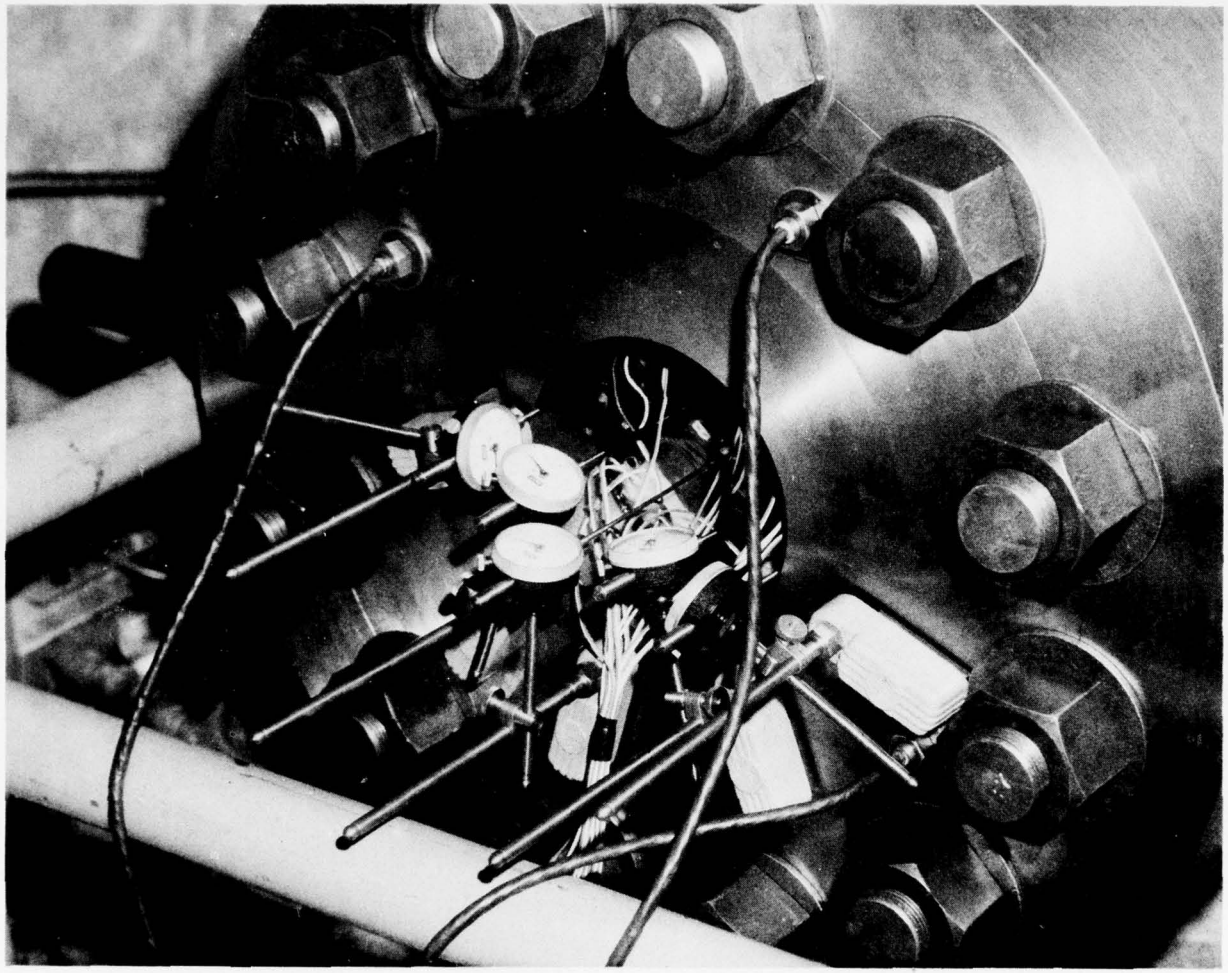

Figure 3.7. Arrangement for measuring the axial displacement of window's low-pressure face, where the window is not pressurized to destruction. The bases of the mechanical dial indicators are magnetically attached to the vessel's end closure, while the tips of the indicator rods touch the low-pressure face at different locations. By utilizing this approach, the topography of the face can be established.

Figure 3.8. Typical arrangement for testing to destruction small acrylic windows that are mounted in the end closure of a pressure vessel and for measuring the axial displacement of the window's low-pressure face. The television camera is used for remotely reading the magnitude of displacement on the dial indicator.

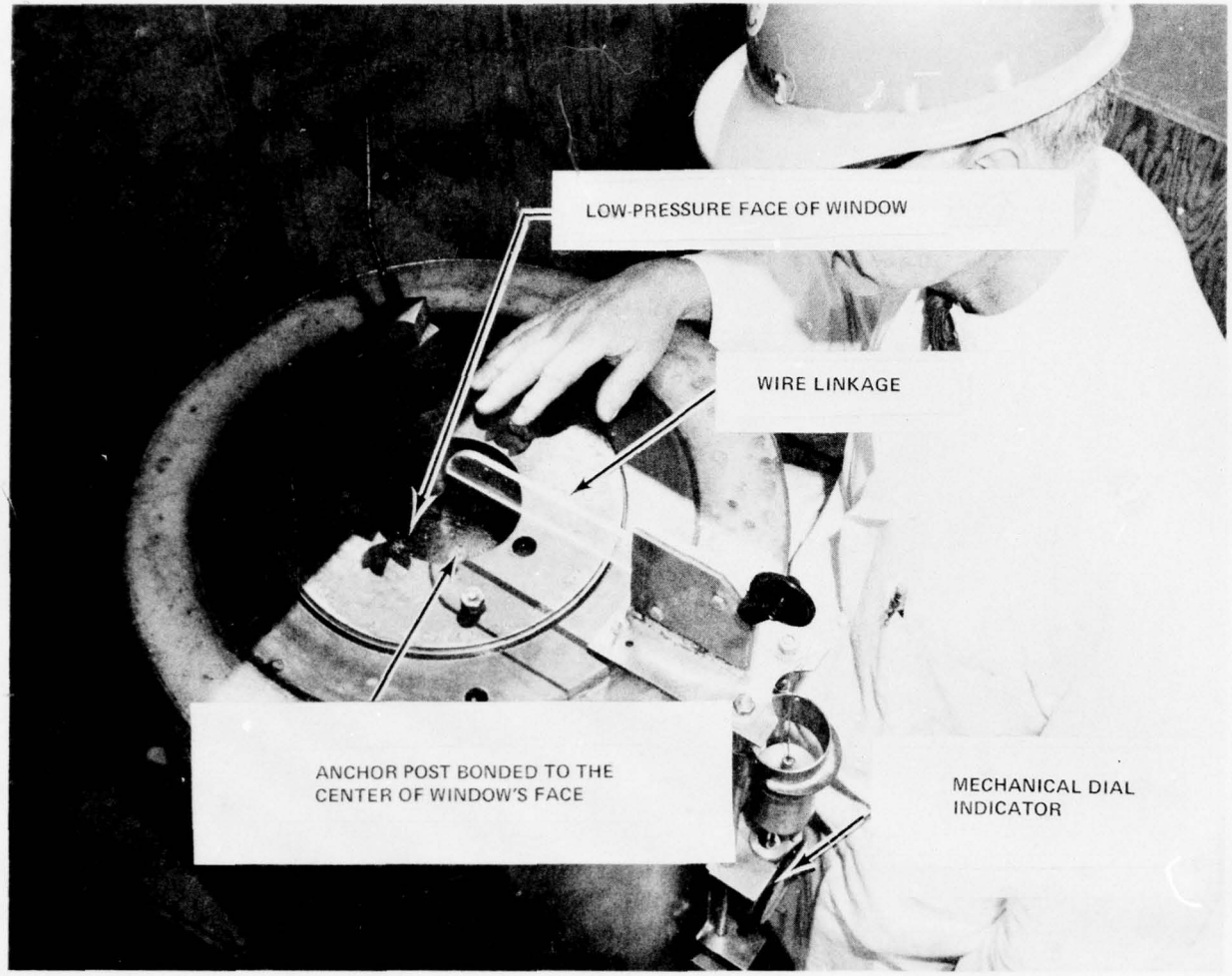

Figure 3.9. Components of the mechanical device used to measure the window's low-pressure face displacement. The window is mounted directly in the vessel's closure so that its low-pressure face can be observed with a mirror during pressurization and the initiation of cracks can be noted.

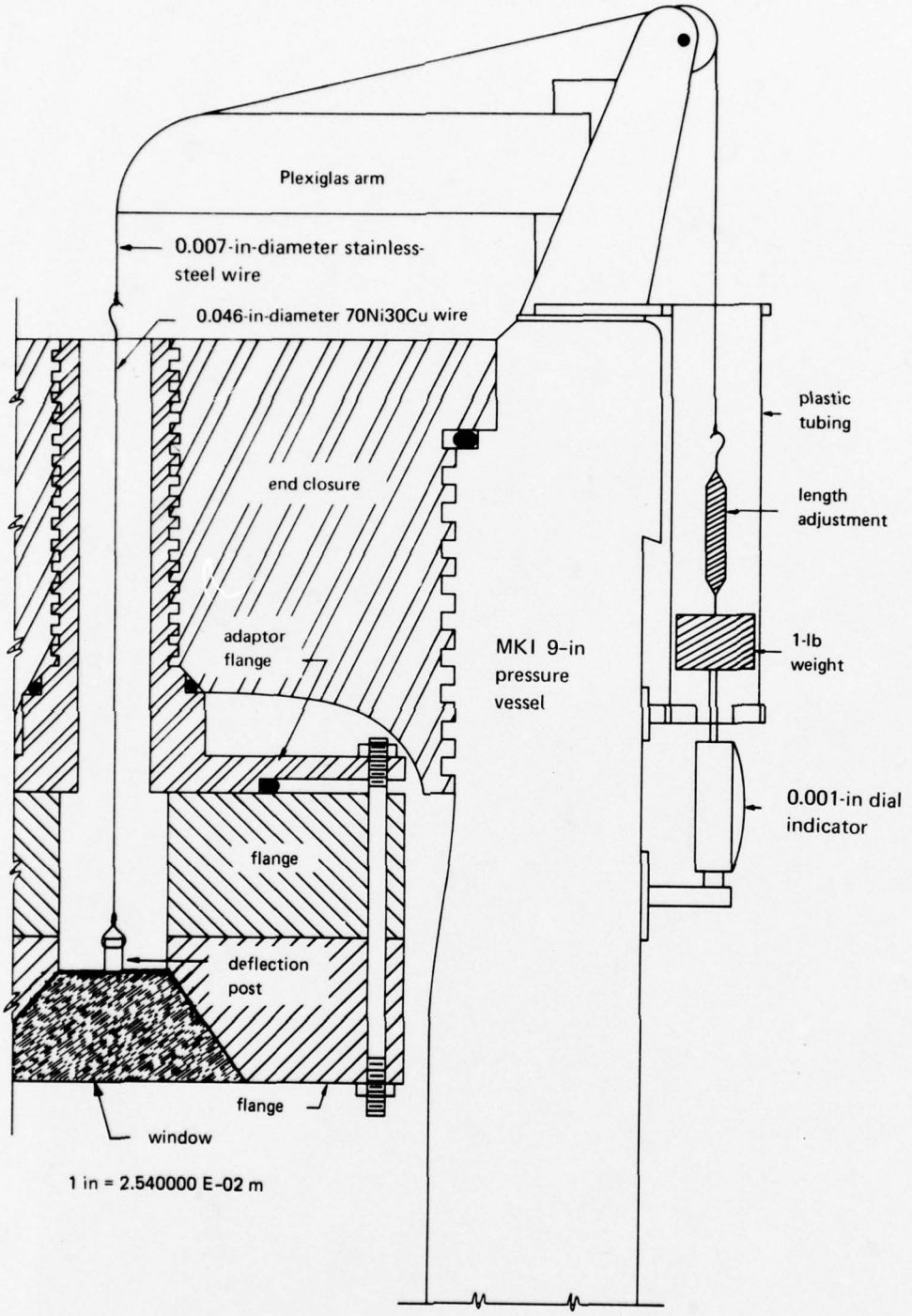

Figure 3.10. Test arrangement for measuring displacement without observation of the low-pressure face. For destructive tests, a restrictor with an opening just large enough for the wire is placed inside the passage to prevent ejection of window fragments into the atmosphere.

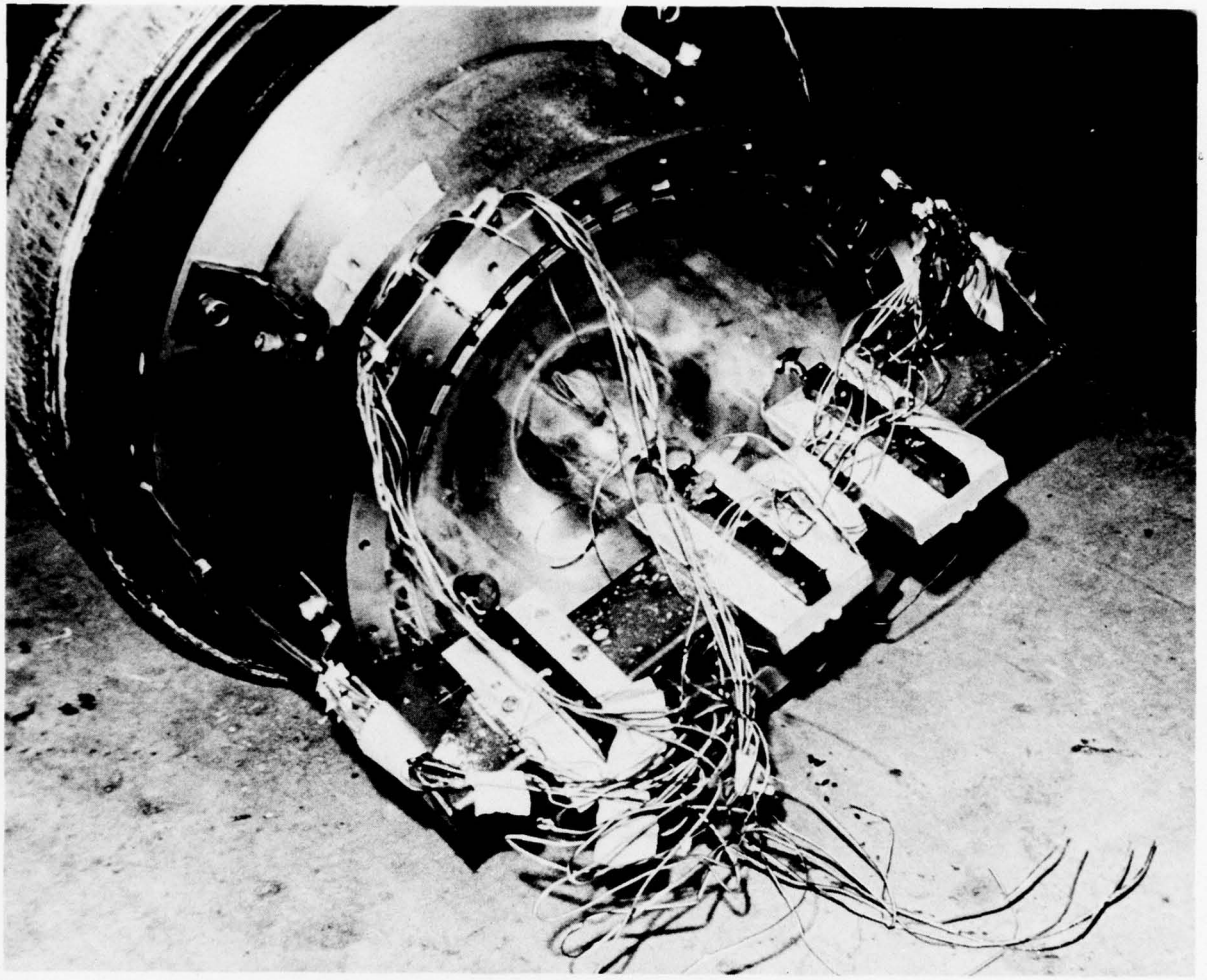

Figure 3.11. Arrangement for measuring the displacement of the window's high-pressure face during hydrostatic pressurization by using linear potentiometers.

Part A. Typical installation of staingages on conical frustum windows.

Figure 3.12. Measuring the strains on windows during pressurization.

Part B. Typical data generated by straingages during short-term hydrostatic loading

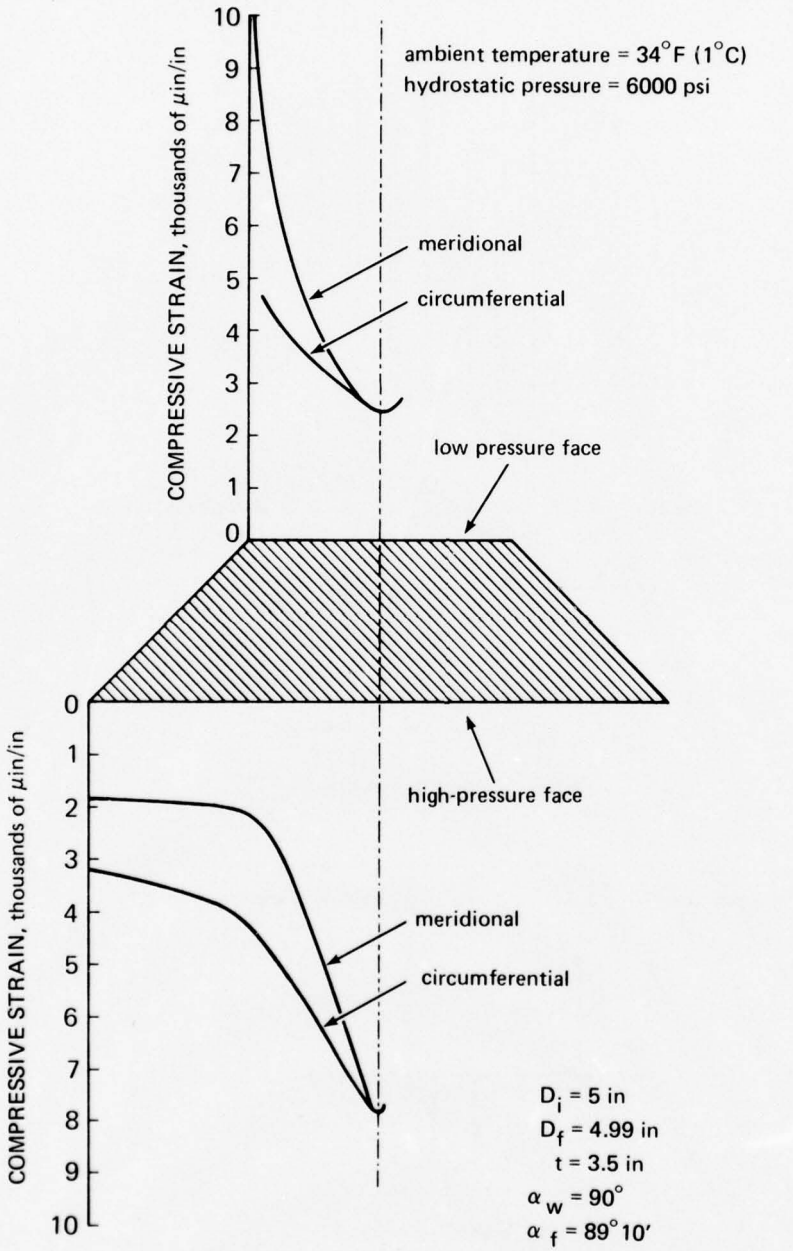

Figure 3.12. Continued.

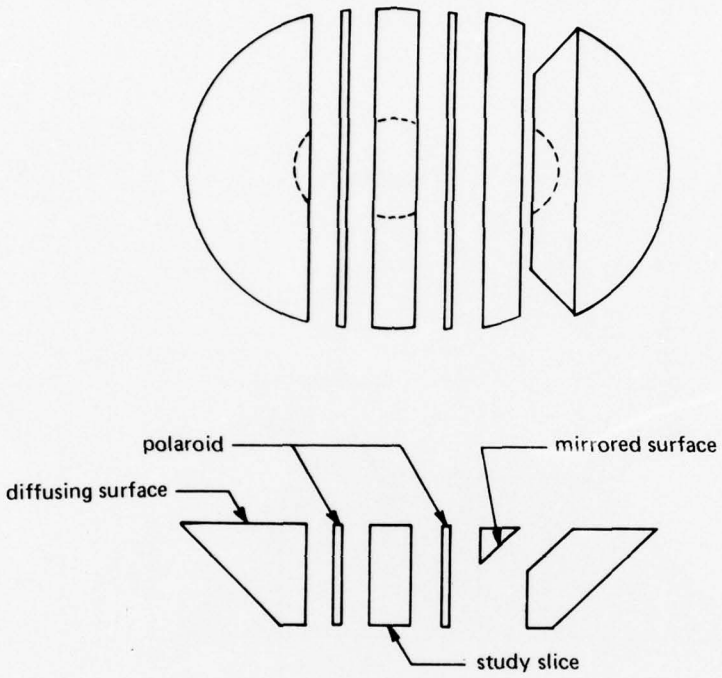

Part A. Window components

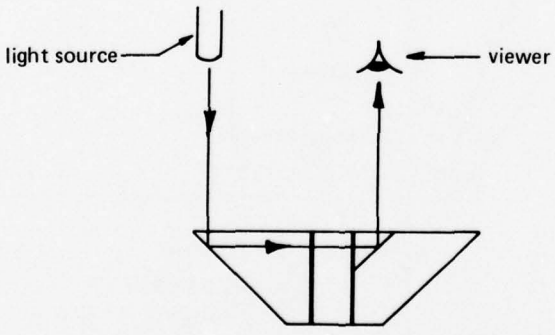

Part B. Assembled window

Figure 3.13. *Optical system incorporated into a conical frustum* window for observation of photoelastic fringes generated by hydrostatic loading.

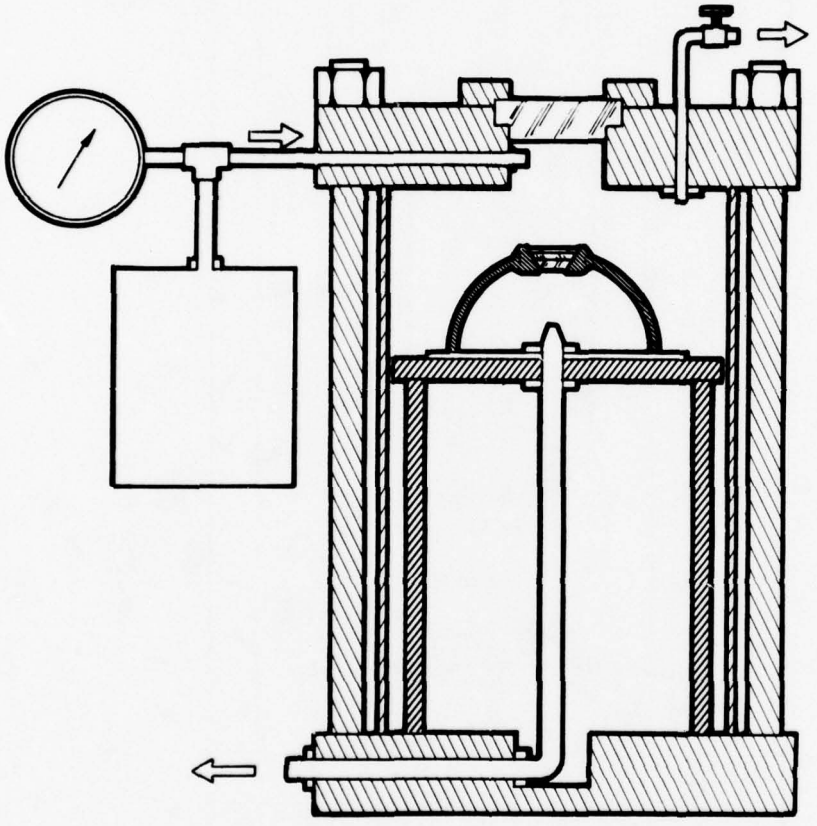

Figure 3.14. High-pressure test apparatus for observation of photoelastic fringes in a conical acrylic window under pneumatic pressure. Note that the low-pressure face of the window is under ambient atmospheric pressure.

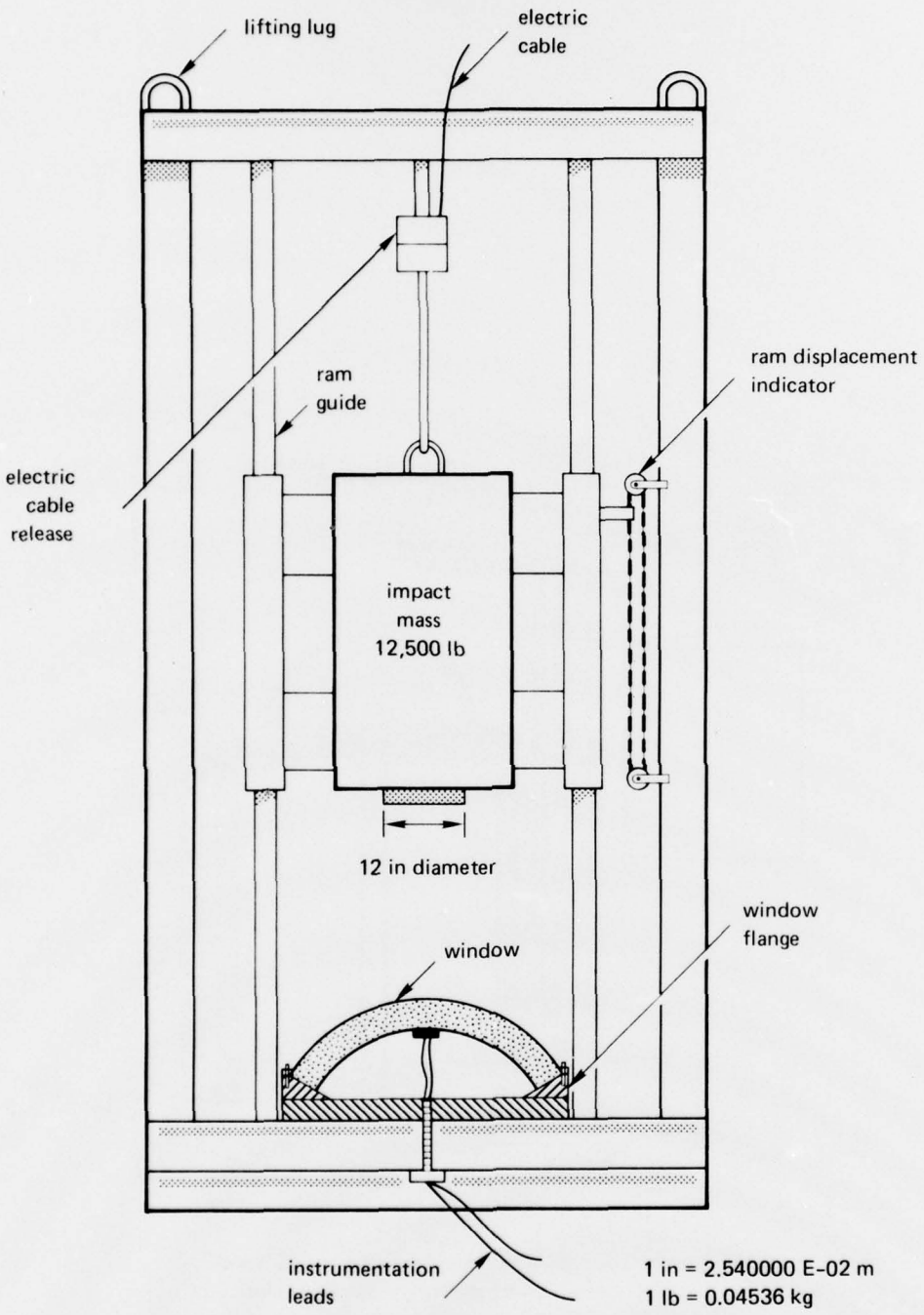

Figure 3.15. Test jig for impact testing of large, spherical shell, sector windows inside a pressure vessel. The test jig is placed inside a pressure vessel and the impactor released remotely. The interior of the window is under atmospheric pressure.

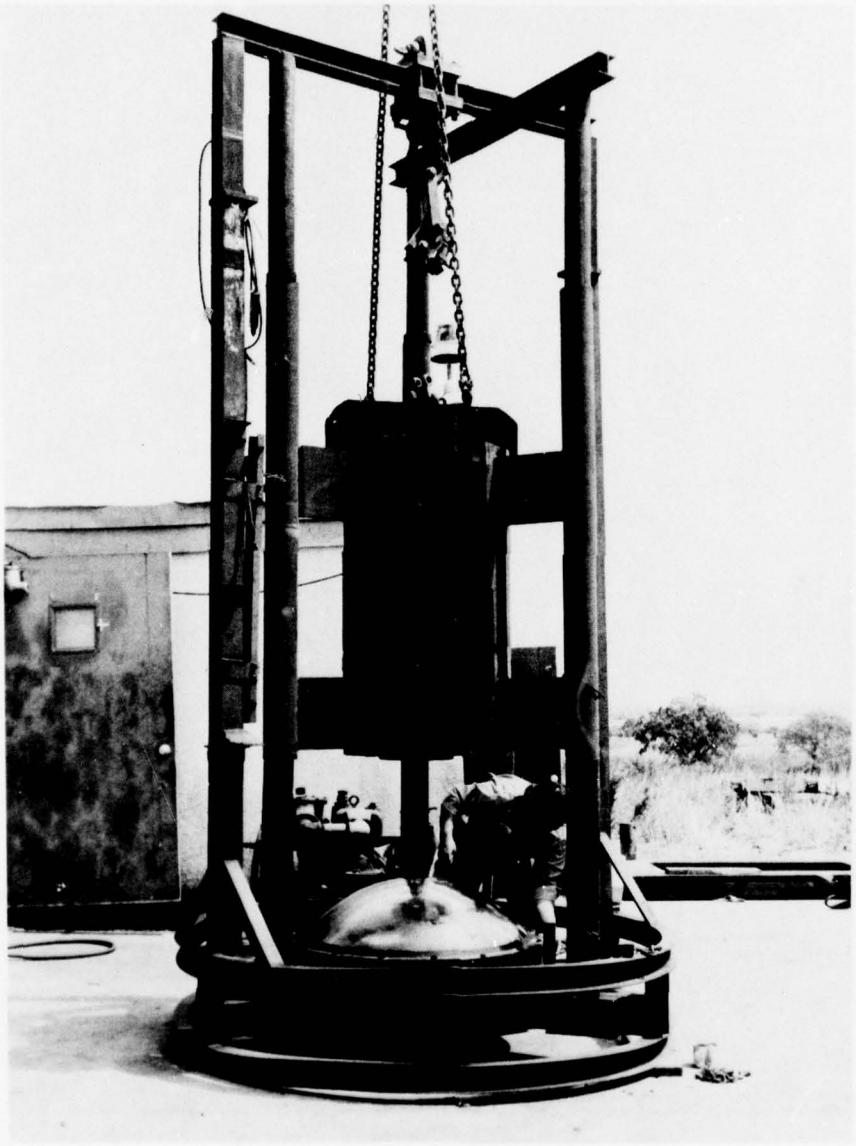

Figure 3.16. Test jig utilized in impact testing of large spherical shell sector windows. Tests performed at the Southwest Research Institute for the Naval Undersea Center.

Part A. Test jig with the spherical sector window mounted on a pressure-proof housing.

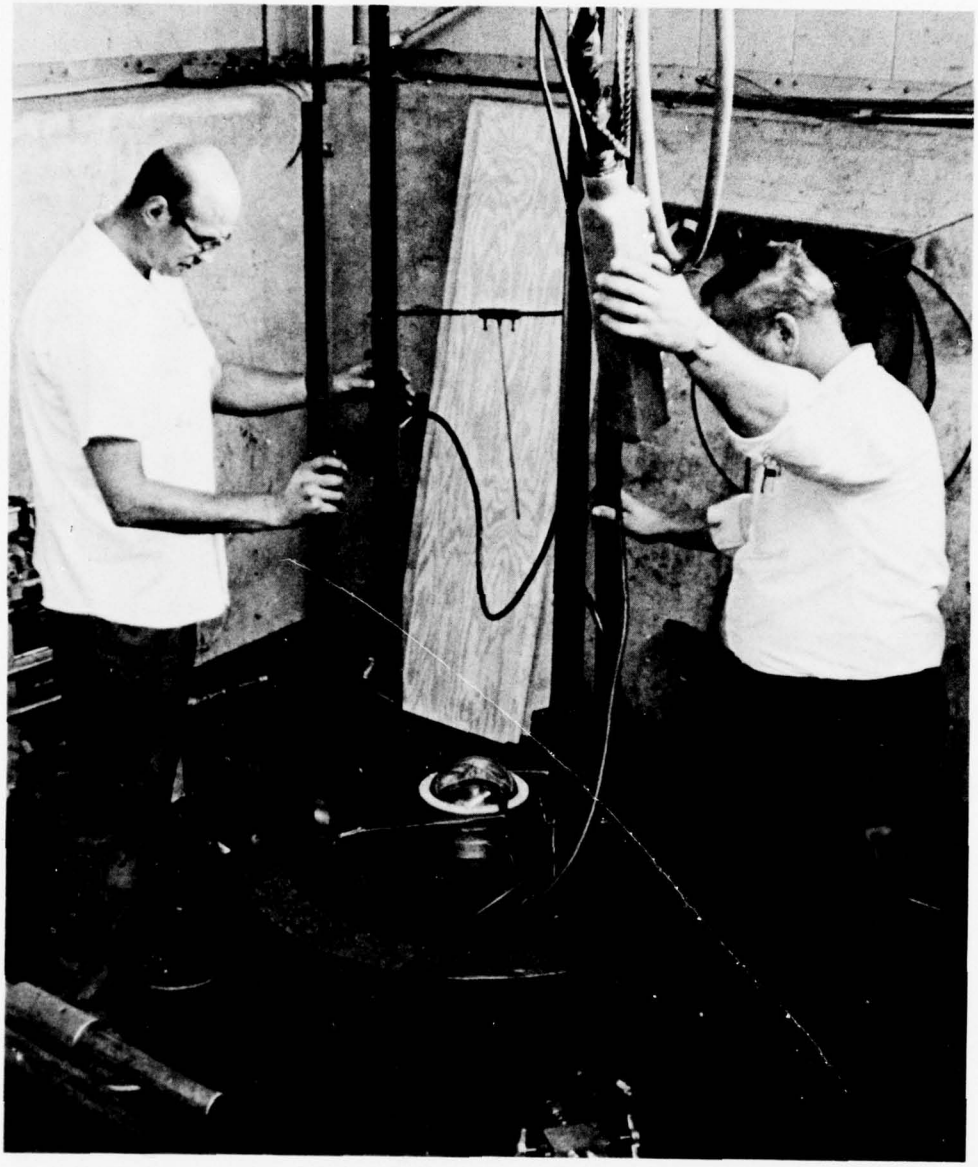

Figure 3.17. Test arrangements for dynamic shock resistance.

Part B. Test setup for hydrodynamic impulse testing of windows or pressure hulls inside a pressure vessel.

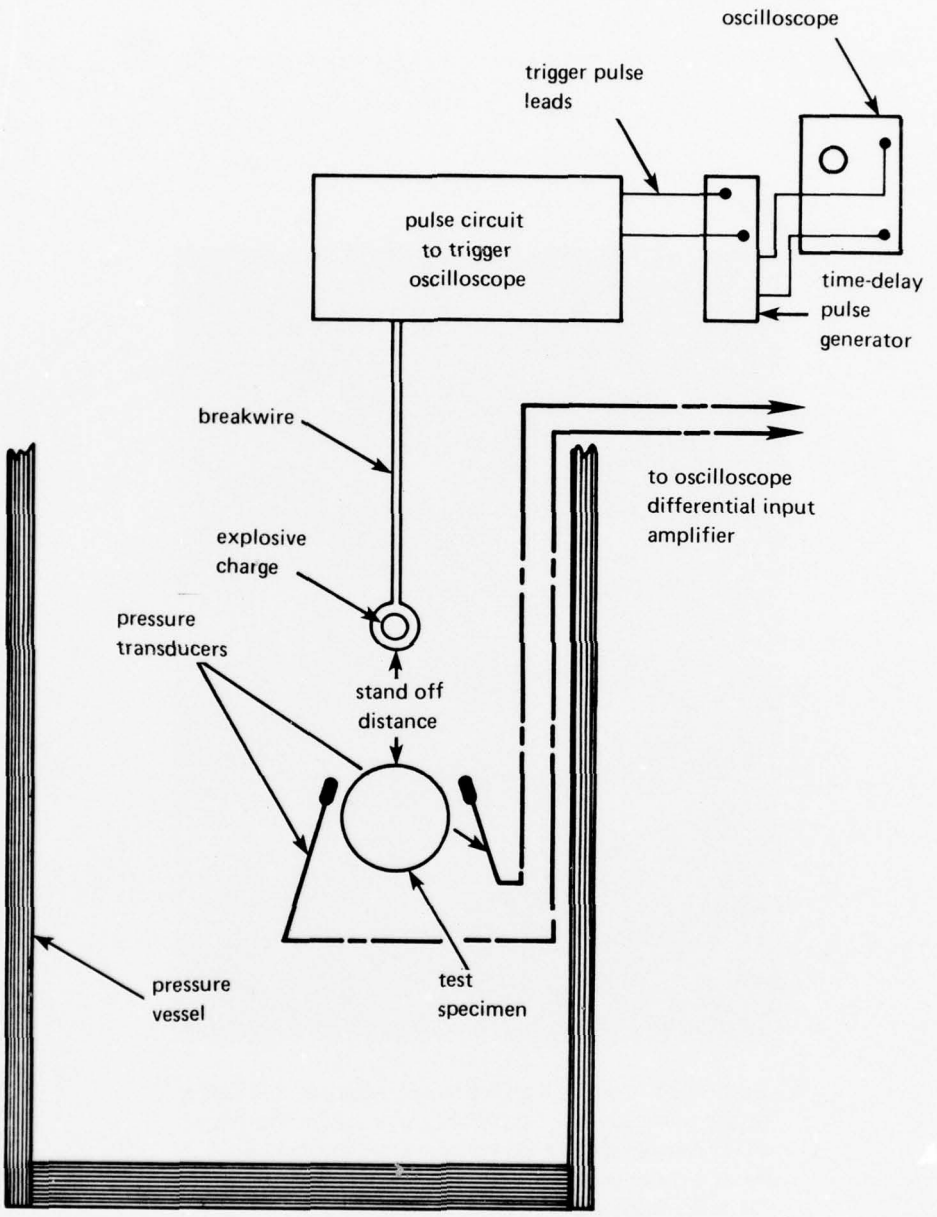

Figure 3.17. Continued

Figure 3.18. Cage used for restraining an acrylic hull during testing inside a pressure vessel filled with water. The buoyant hull does not strike the pressure vessel's end closure because the bottom hatch on the hull is rigidly bolted to the cage's framework, which serves as ballast.

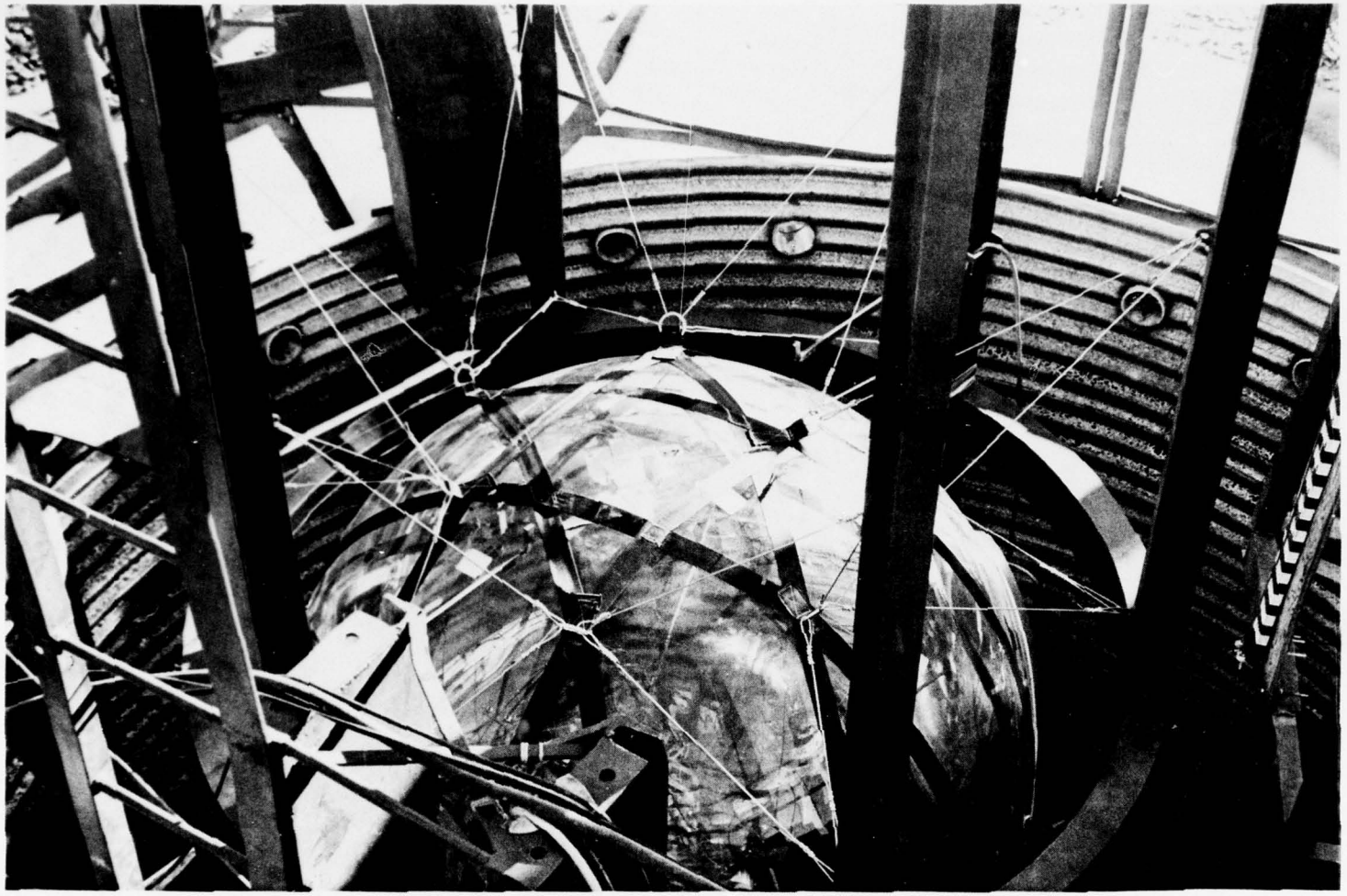

Figure 3.19. Another arrangement for caging the hull inside a water-filled vessel. The hull is held in place with a compliant system of nylon straps and cables. The compliant restraint is primarily used in dynamic overpressure tests, where a lateral movement of the hull under the action of a shockwave simulates the reaction of a free-swimming submersible to an underwater explosion.

Figure 3.20. Rigid tubular member for hanging the hull from the pressure vessel's end closure when the end closure is being placed on the vessel. The rigid tube also serves as a spacer that restrains the buoyant hull from rising to the top of the vessel when it is filled with water and thus striking the end closure.

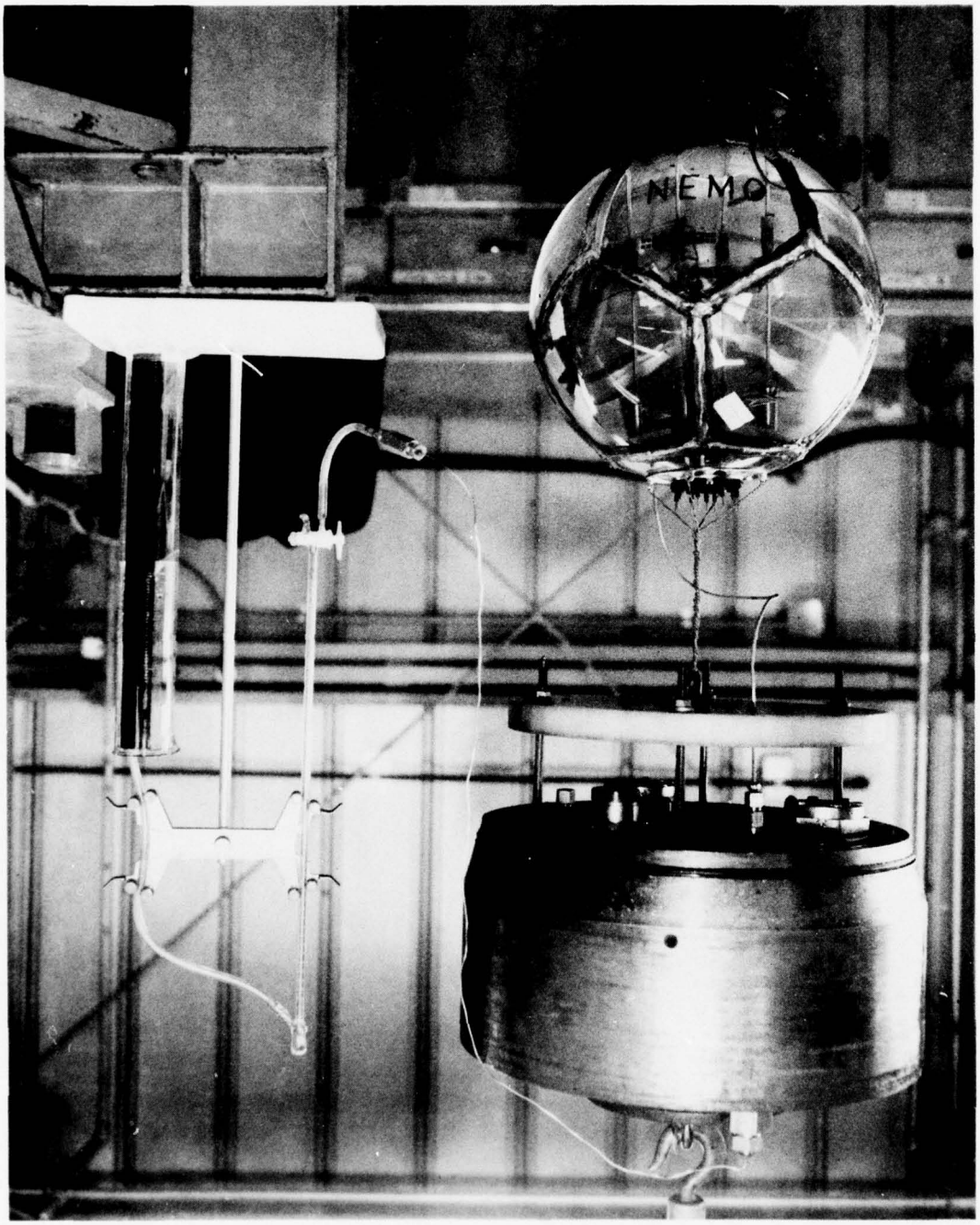

Figure 3.21. Arrangement for measuring the volumetric change of the hull under external hydrostatic loading inside a pressure vessel. The water inside the hull also mitigates the force of implosion.

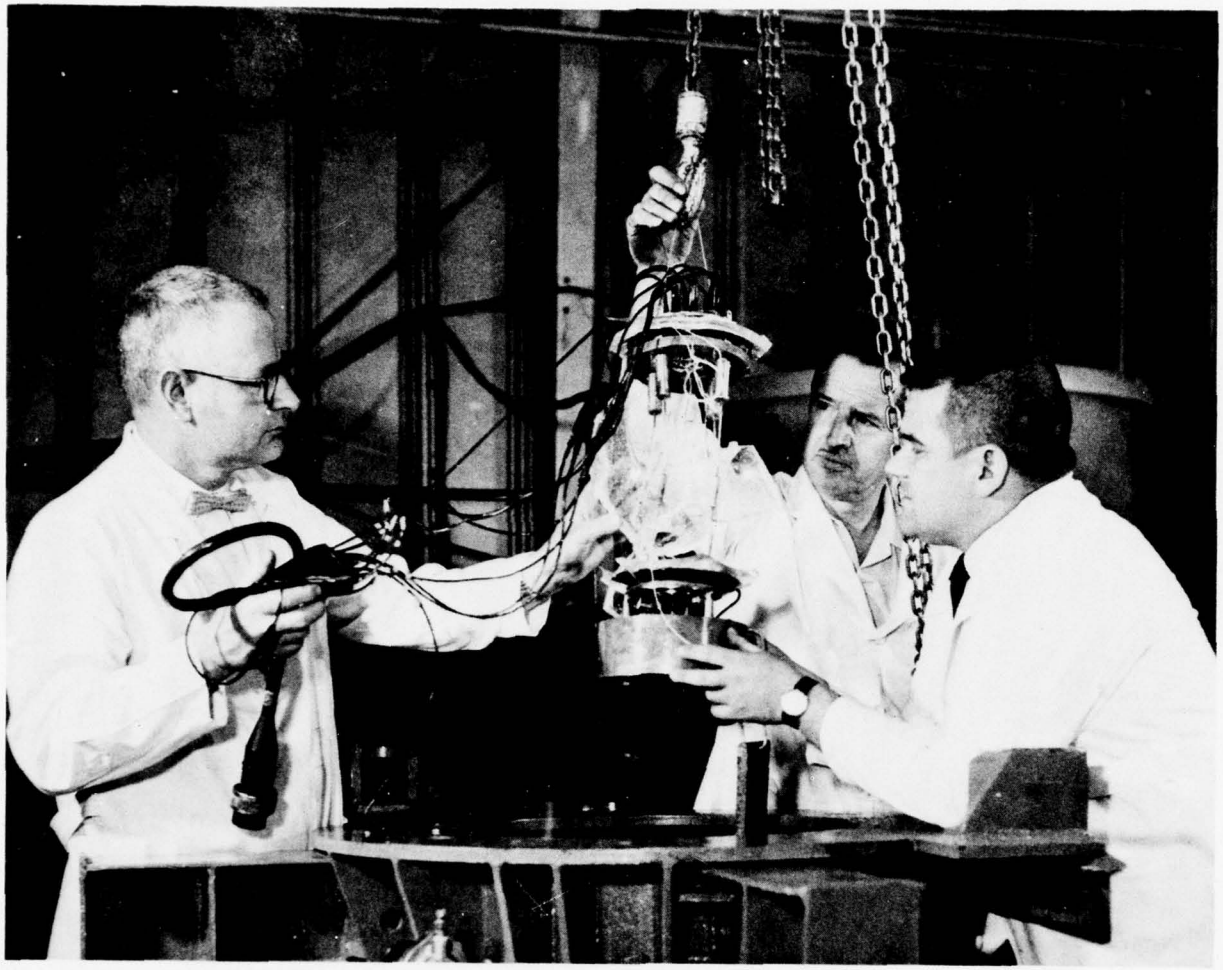

Figure 3.22. Remains of the hull shown in figure 3.21. The large fragments of the hull are still attached to the internal framework. If the hull had not been filled with water during the test, the implosion would have minutely fragmented the hull, making it impossible to pinpoint the origin and to reconstruct the mode of failure.

Figure 3.23. Experimental evaluation of life-support system and measurement of gasses given off by the acrylic plastic hull prior to installation in a submersible.

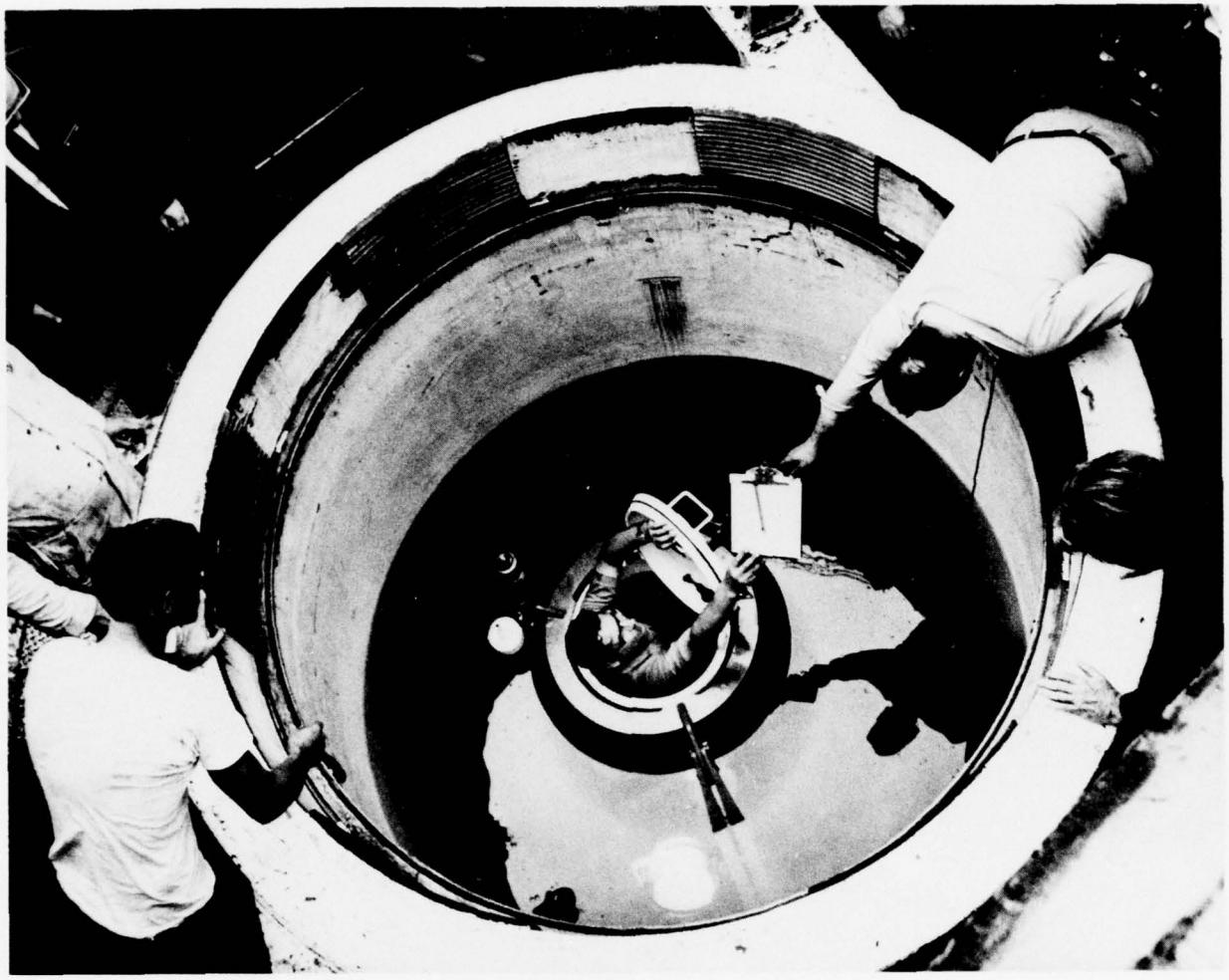

Figure 3.24. Check out of the complete NEMO submersible system in a deep-ocean simulator at Southwest Research Institute. The manned simulated dive to 1000 feet (305 meters) was performed in 1970 by submersible pilots Briggs and Poirer of the Southwest Research Institute.

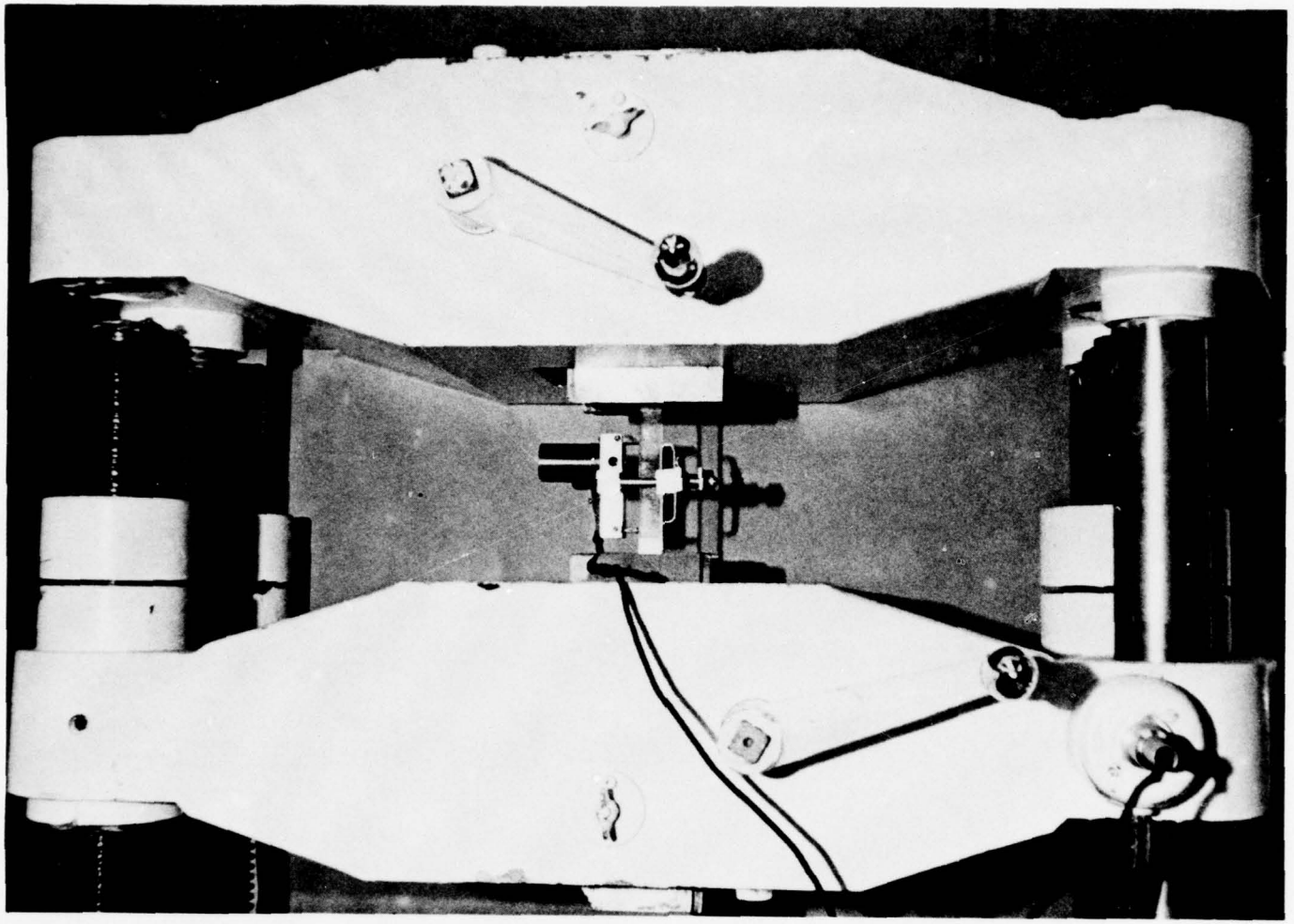

Figure 3.25. Pulling an acrylic plastic tensile test specimen to determine the material's extension, modulus of elasticity, and ultimate strength.

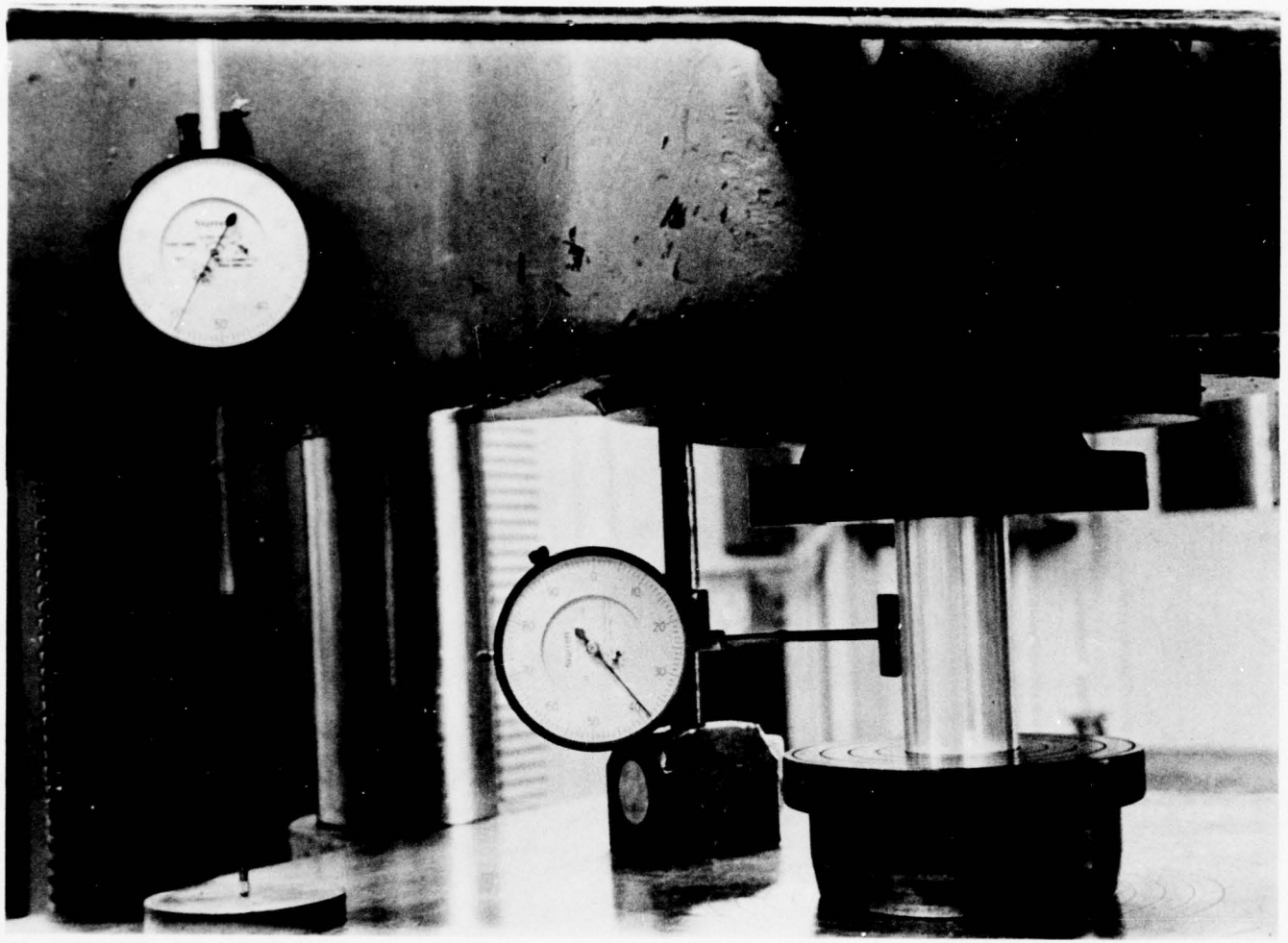

Figure 3.26. Squeezing a compressive test specimen to determine the material's compressibility, modulus of elasticity, yield point, Poisson's ratio, and ultimate compressive strength.

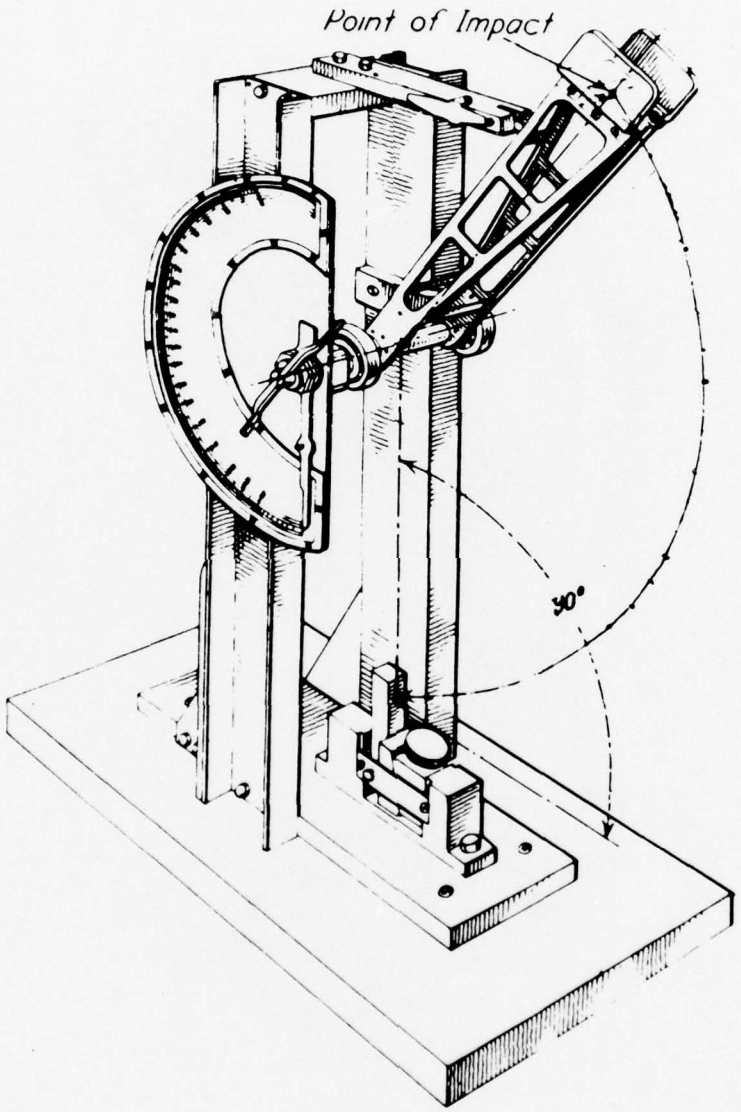

Figure 3.27. Impacting a notched Izod test specimen to determine its toughness.

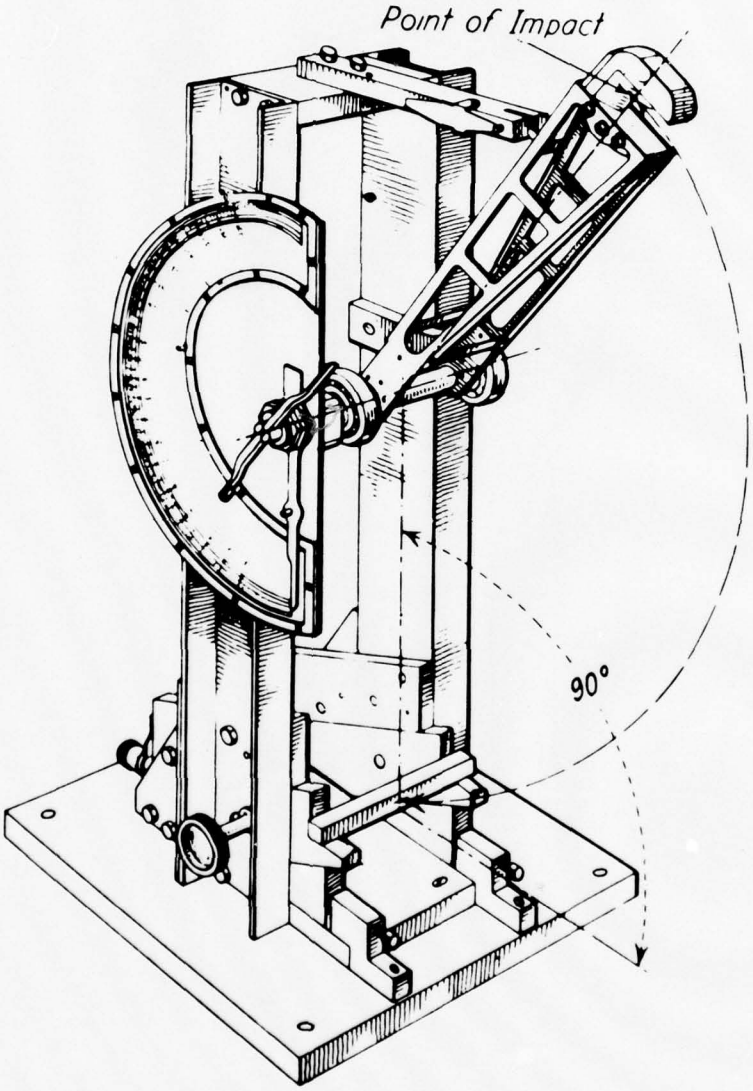

Figure 3.28. Impacting a notched Charpy test specimen to determine its toughness.

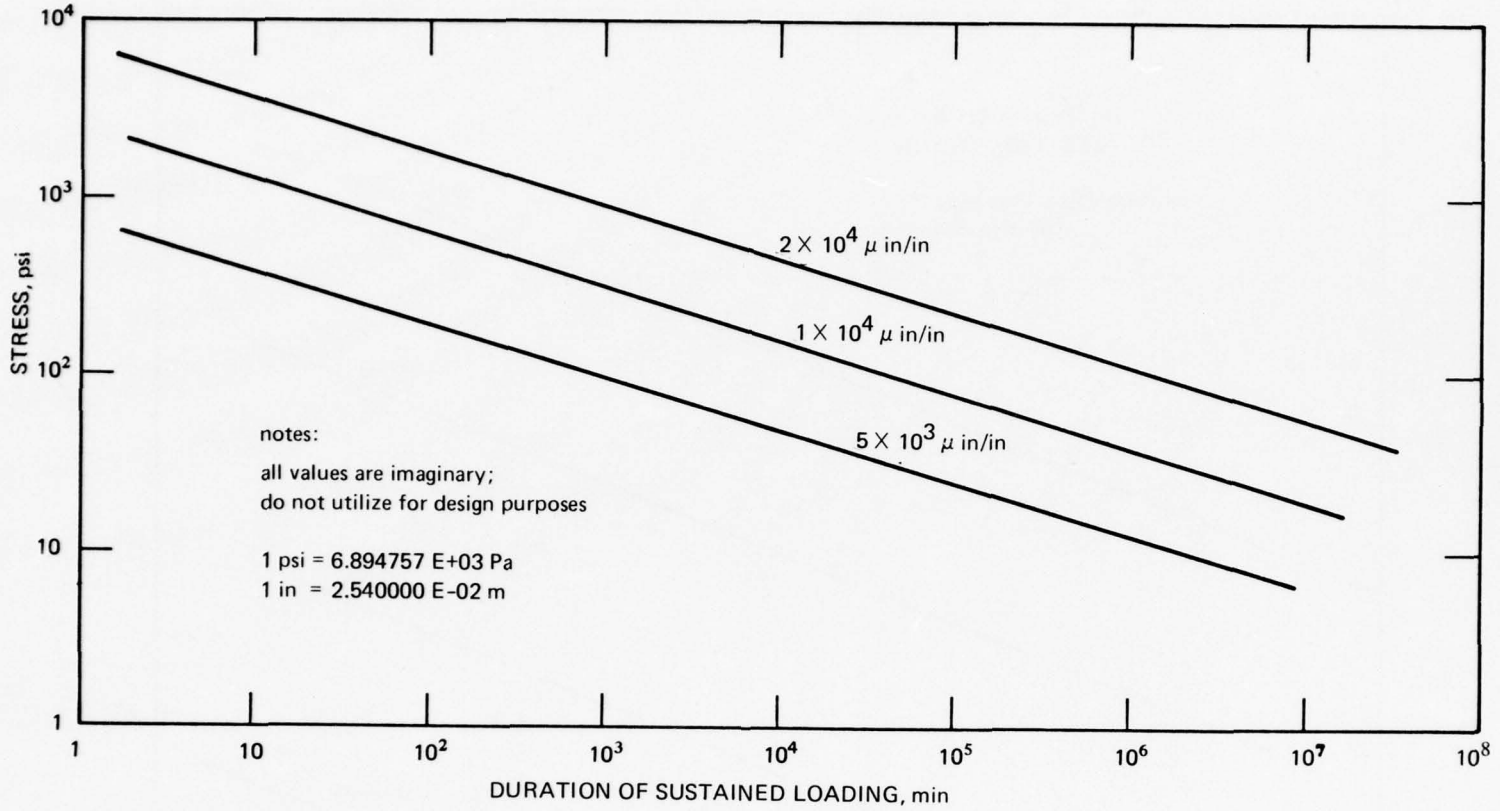

Figure 3.29. Typical presentation of strain data resulting from long-term sustained loading of acrylic plastic test specimens. A family of constant strain curves is plotted against applied stress and duration of loading.

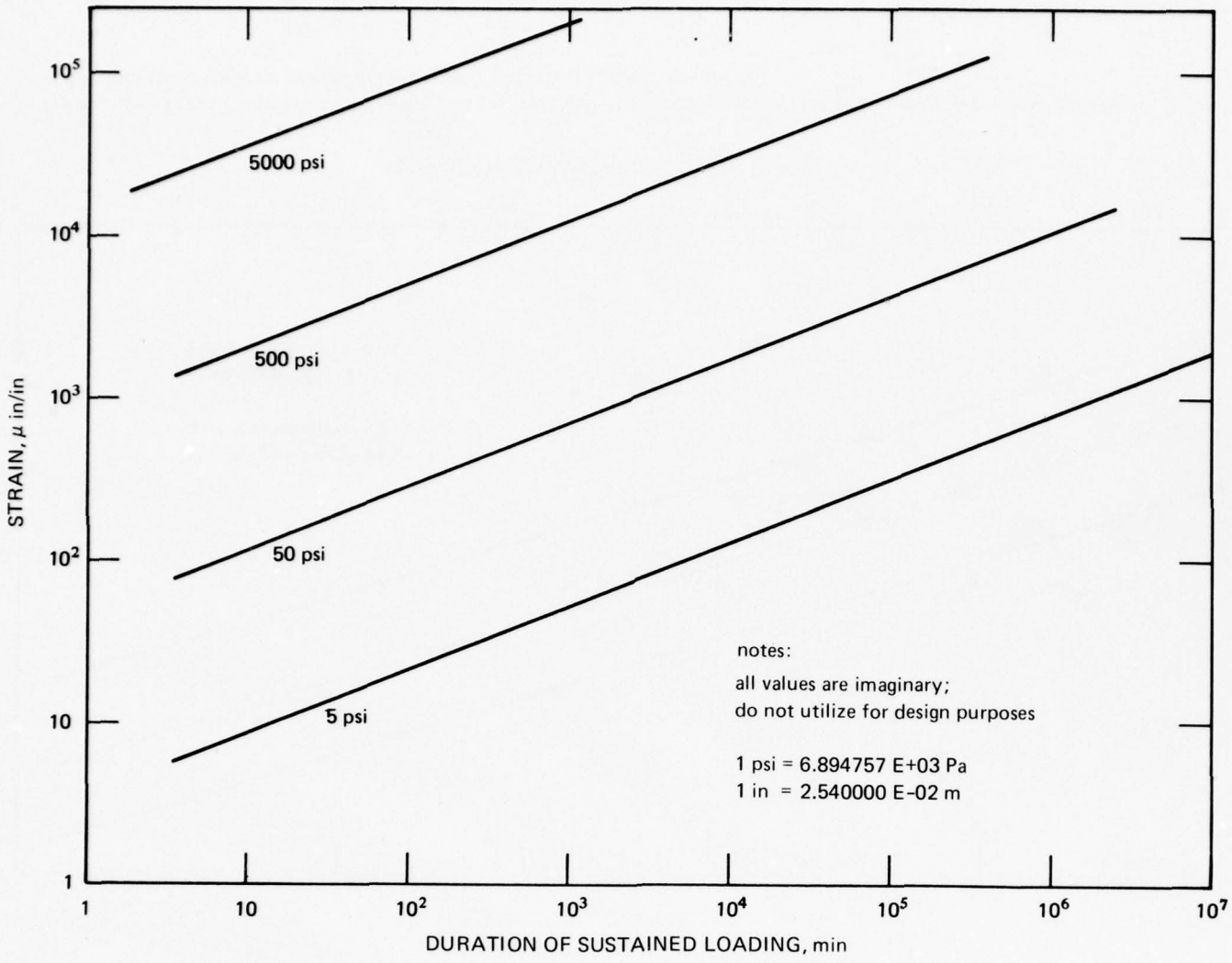

Figure 3.30. Typical presentation of strain data resulting from long-term sustained loading of acrylic plastic. A family of constant applied stress curves is plotted against strain and duration of loading.

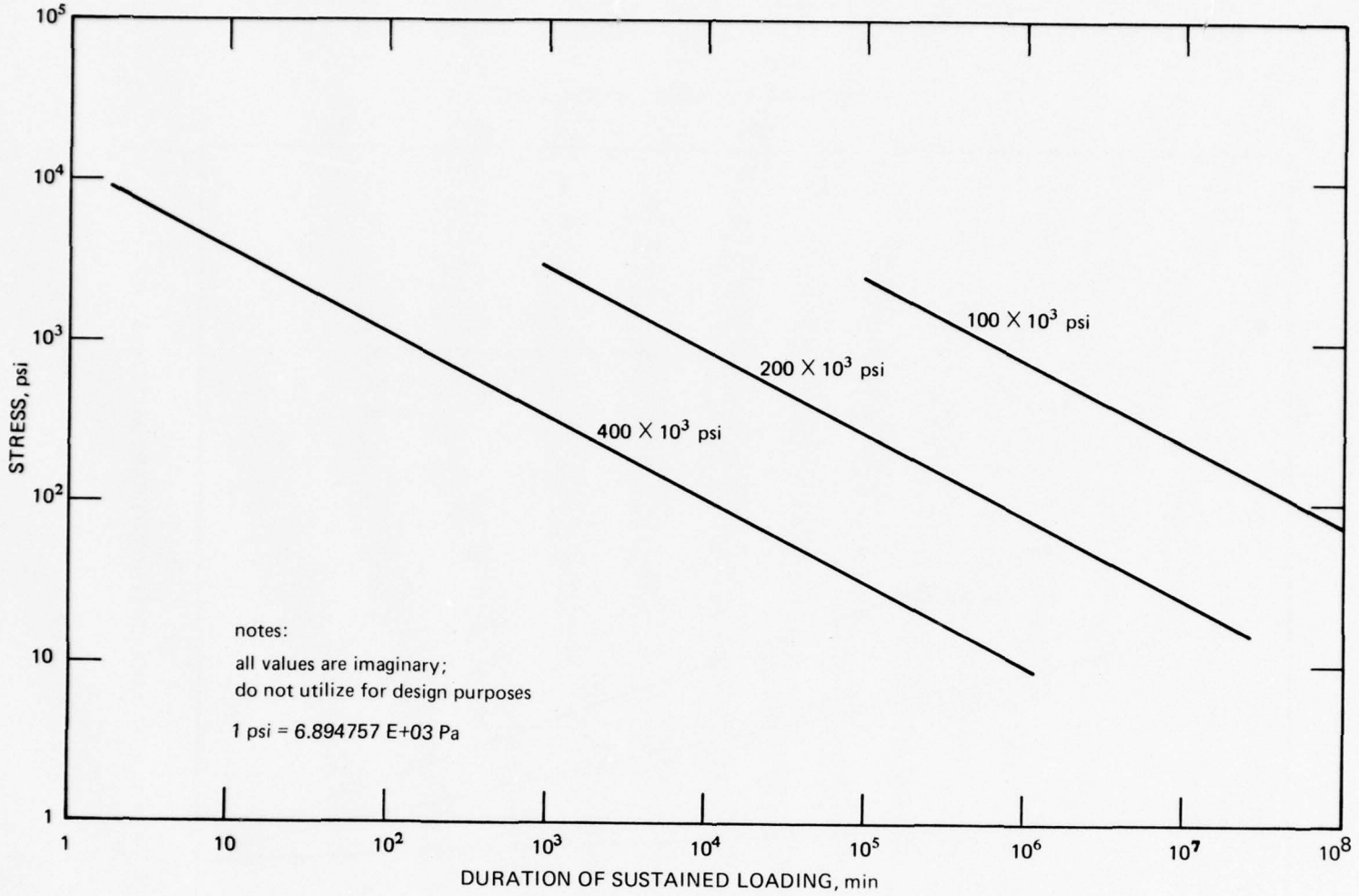

Figure 3.31. Typical presentation of effective modulus of elasticity data resulting from long-term sustained loading of acrylic plastic. A family of constant effective modulus of elasticity curves is plotted against applied stress and duration of loading.

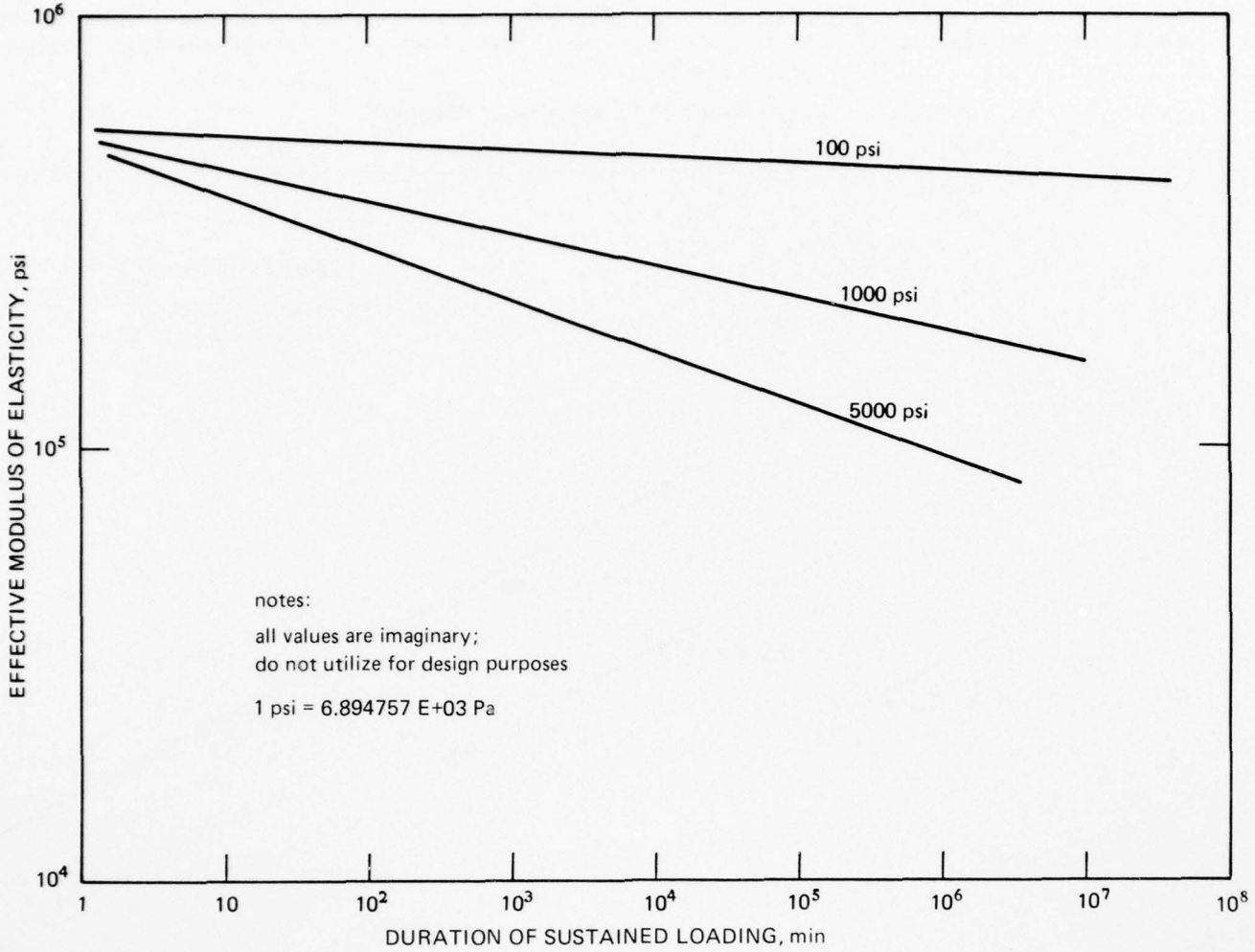

Figure 3.32. Method of presenting effective modulus of elasticity data resulting from long-term sustained loading of acrylic plastic. A family of constant applied stress curves is plotted against effective modulus of elasticity and duration of sustained loading.

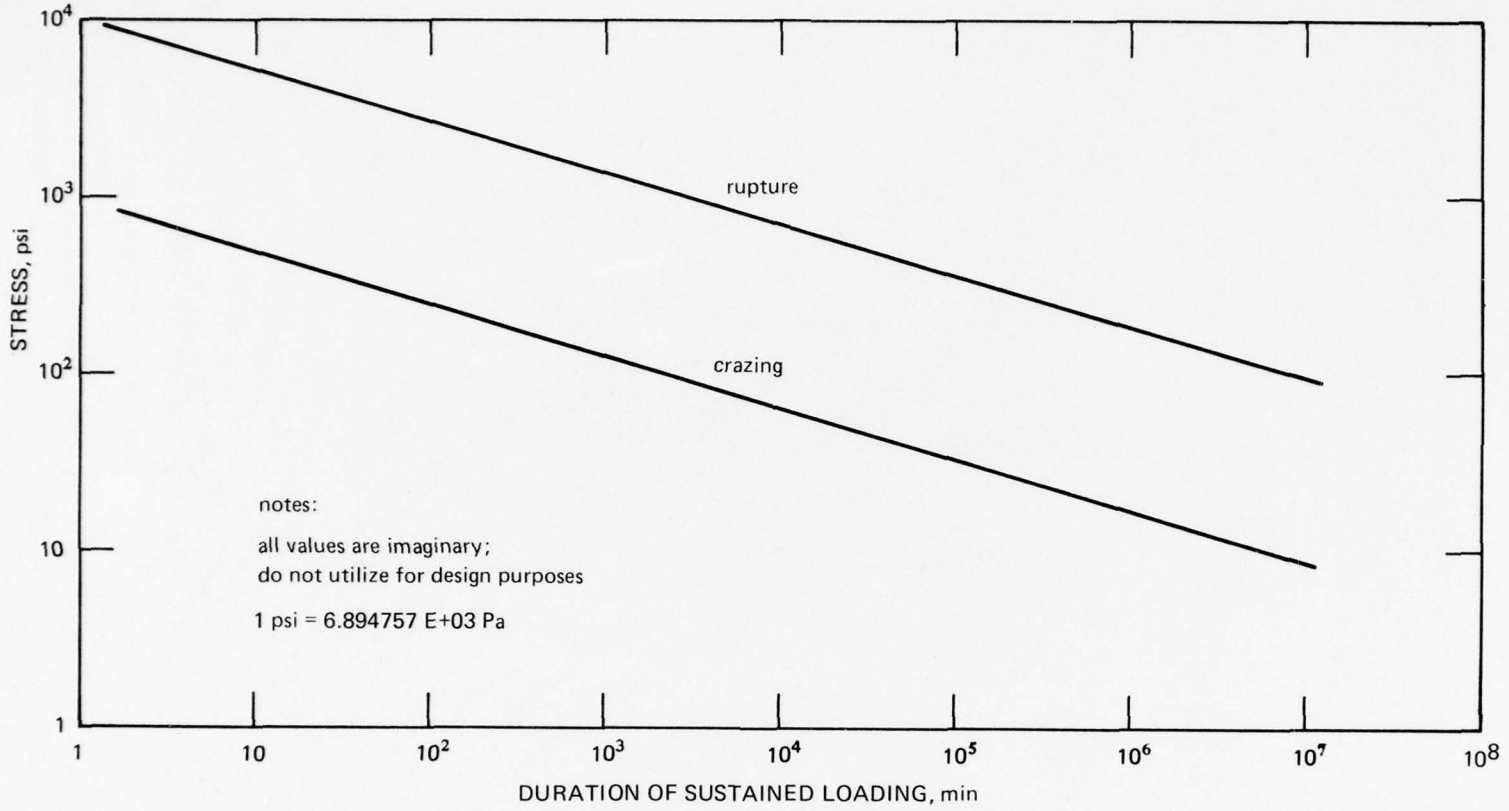

Figure 3.33. Typical presentation of data from long-term sustained tensile loading of acrylic plastic specimens. This type of data is very valuable to the designer, as it provides information on the magnitude of sustained uniaxial stress that will cause an acrylic plastic structure to fail after a defined period of time.

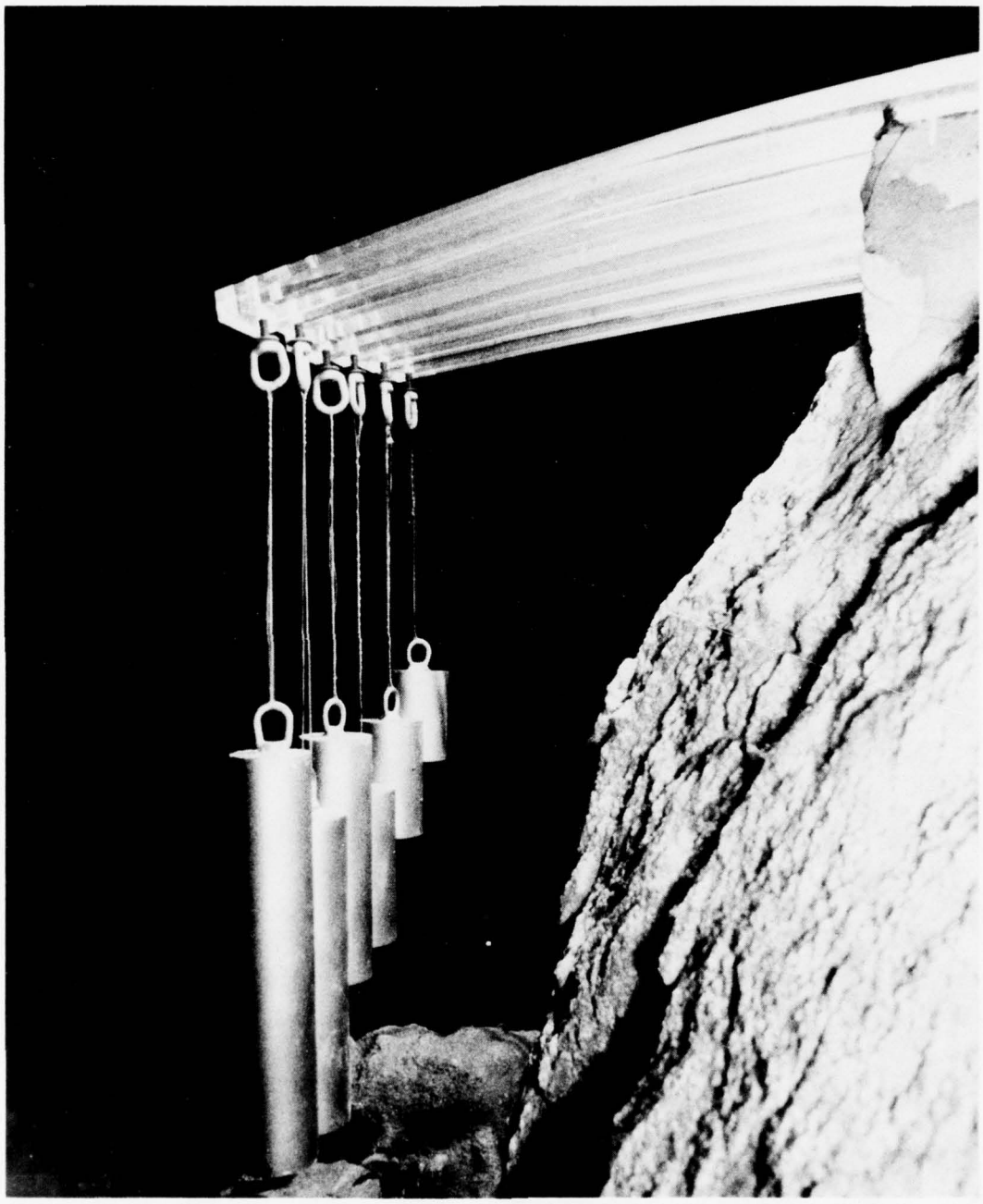

Figure 3.34. Typical setup for long-term sustained flexure testing of thick acrylic plastic specimens exposed to the effects of weather. Each specimen shown in this photograph is subjected to a different loading. The maximum flexure stresses in these specimens correspond to 24, 17, 12.5, 10, and 6 percent of the ultimate short-term tensile strength of acrylic plastic. Test site is located in El Cajon, California.

SECTION 4. STRUCTURAL PROPERTIES OF MONOLITHIC CAST ACRYLIC PLASTIC . . . 4-1

4.1 INTRODUCTION . . . 4-1

4.2 PLASTIC DESIGN CONSIDERATIONS . . . 4-2

- 4.2.1 General Comments . . . 4-2
- 4.2.2 Strength Values Permitted by Design . . . 4-2
- 4.2.3 Notch Sensitivity and Crazing . . . 4-2
- 4.2.4 Factors Affecting Structural Properties . . . 4-9

4.3 SHORT-TERM MECHANICAL PROPERTIES . . . 4-11

- 4.3.1 Tensile Loading . . . 4-11
- 4.3.2 Flexural Loading . . . 4-12
- 4.3.3 Shear Loading . . . 4-13
- 4.3.4 Impact Loading . . . 4-13
- 4.3.5 Compressive Loading . . . 4-15
- 4.3.6 Flammability . . . 4-16

4.4 LONG-TERM MECHANICAL PROPERTIES . . . 4-16

- 4.4.1 Tensile Loading . . . 4-18
- 4.4.2 Flexural Loading . . . 4-19
- 4.4.3 Compressive Loading . . . 4-20
- 4.4.4 Intermittent Loading . . . 4-22

4.5 CONCLUSIONS . . . 4-24

4.6 REFERENCES . . . 4-26

SECTION 4.
STRUCTURAL PROPERTIES OF MONOLITHIC CAST ACRYLIC PLASTIC

4.1 INTRODUCTION

Although many grades of acrylic plastic are available on the market, only the general-purpose, heat-resistant, cast polymethyl methacrylate* will be discussed in great depth in this section, i.e., this is the grade used for most windows in submersibles and hyperbaric chambers.

There are other grades of acrylic plastic from which windows could be made, resulting in improved resistance to crazing and impact loading. However, because of the significantly increased cost and unavailability of such grades in thicknesses above 1 inch (2.54 centimeters), they apply only to a minority of window installations and thus are not of sufficient interest to the general window designer and user.

There are also grades with less strength, resistance to crazing, deformation under load, and resistance to elevated temperatures. However, unless there is an overriding engineering requirement for their use, they should not be used for fabrication of windows in pressure-resistant structures. A valid reason for their use may be the unavailability of large custom castings that meet the physical properties of section 15. In this case, the designer must take into account the lower values of the mechanical properties. In practice this means that the material performance curves shown in this section and the structural performance curves described in the rest of this handbook must be discounted by appropriate factors. Since the magnitude of these factors has, in most cases, not been established, the designer must rely on his or her judgment.

Although there is extensive information on the common mechanical properties of acrylic plastic, it is insufficient to establish reliable statistical minimum values under all foreseeable conditions of loading and ambient environments. For this reason, the only available and logical approach to discussion of acrylic plastics is in terms of typical properties. Thus the data on structural properties in this handbook represent only typical test values. They are conservative to the extent that when a range of published data was available the lower values were selected for presentation.

One of the very desirable features of acrylic plastic castings is that the physical properties are the same in all orientations, i.e., the material is isotropic. Furthermore, basic mechanical properties, e.g., tensile, compressive, and shear strengths, are not a function of material thickness or volume. Thus such properties established with typical ASTM test specimens, cut from any location or along any orientation in the casting, are valid for full-scale structural members or pressure hulls.

** Conforming to MIL-P-5425 and ASME Safety Standard for Pressure Vessels for Human Occupancy PVHO-1.*

Because mechanical properties of acrylic plastic are usually a function of time, their discussion has been arbitrarily divided into two categories: short-term and long-term mechanical properties. The knowledge of short-term properties is important to the designer because it provides both a general understanding of material behavior and the necessary background required for writing and interpreting quality-control criteria and procurement specifications. The long-term mechanical properties, on the other hand, form the basis of all designs for acrylic structures. Having access to data covering both short-term and long-term mechanical properties in the same chapter will also provide the designer with the opportunity to visualize their quantitative relationship and thus permit translation of the long-term mechanical strength requirements into short-term specifications.

4.2 PLASTIC DESIGN CONSIDERATIONS

4.2.1 General Comments

Three design considerations important for the utilization of plastic glazing materials are discussed in this section: the strength values permitted by the design; notch sensitivity and crazing susceptibility; and factors, such as environmental, that affect the structural properties.

4.2.2 Strength Values Permitted by Design

Specifications for plastics generally do not specify minimum guaranteed values of the usual mechanical properties. The tremendous number of individual tests that would be required to establish reliable statistical minimum values makes the "typical property" approach the only logical one. Thus the data on structural properties presented in this handbook represent typical test values. They are conservative to the extent that when a range of data was available the lower values were selected. The amount that the typical test value is reduced for use in design is dependent on the material and application.

4.2.3 Notch Sensitivity and Crazing

Two phenomena exhibited by transparent plastics that should receive special attention for good design are notch sensitivity and crazing. Unstretched acrylic plastics are moderately notch sensitive and particularly susceptible to crazing. Lamination of the acrylics, done partially to decrease notch sensitivity, increases their susceptibility to crazing, an effect caused by the solvent action of the plasticizer in the interlayer. Stretched acrylic plastics, particularly those in excess of 50 percent, possess greater resistance to notch effects than do unstretched acrylics, monolithic or laminated, and the stretched acrylics also have considerably greater resistance to crazing.

4.2.3.1 NOTCH SENSITIVITY. Unstretched plastic glazing materials are very sensitive to stress concentrations and have little resistance to crack propagation, i.e., once a crack starts, little energy is needed to cause complete failure. Internal stresses and common service damage, such as scratches, nicks, and star fractures, can appreciably reduce tensile and flexural strengths. The amount of strength reduction varies widely with the type, size, shape, direction, and spacing of the defects. Since this damage can occur in random fashion, no precise evaluation of strength reductions can be made.

Shallow, smooth-bottomed scratches and nicks have little effect on plastic materials. However, deeper scratches or nicks – especially those with sudden discontinuities of surface– and cracks – even those of microscopic nature – may reduce the strength of plastic materials considerably. Star fractures can reduce the tensile and flexural strengths of unstretched acrylics by 50 percent. Stretched acrylics are practically immune to star fractures and possess good crack-propagation resistance.

Some measure of the notch sensitivity of a glazing material can be determined by means of flexural and impact tests with controlled notches on the tension side of the specimens (table 4.1). The strength of the notched specimen is usually constant over a wide temperature range, but notch sensitivity, being a ratio of the unnotched and notched strengths, increases with decreasing temperature because the unnotched strength tends to increase with decreasing temperature.

Table 4.1. Effect of surface condition on impact strength of MIL-P-6886 material.*

Condition of Tension Surface	Charpy Impact Strength
Polished to remove scratches	3.2
Sawed	2.9
Passed through planer so that scratches are parallel to long dimension	3.4
Passed through planer so that scratches are perpendicular to long dimension	3.1
Sanded on belt sander so that scratches are parallel to long dimension	3.5
Sanded on belt sander so that scratches are all at 45-deg angle to long dimension	3.0
Sanded on belt sander so that scratches are perpendicular to long dimension	1.6
Tension side sanded so that scratches are parallel to long dimension, compression side sanded so that scratches are perpendicular to long dimension	3.2
Tension side sanded perpendicular, compression side sanded parallel to long dimension	1.6
Sanded on belt sander so that scratches were perpendicular to long dimension, then resanded so that scratches are parallel to long dimension	3.3

* Data from reference 4.1.

Methods have been developed to evaluate the crack-propagation resistance of stretched acrylic plastics for use in quality control; these methods have also been occasionally used with other materials for information and comparison. The most commonly accepted method is to determine the K-value (references 4.1, 4.2, and 4.3):

$$K = \frac{P}{t}\sqrt{\frac{\pi Z}{B}} \text{ lb/in}^{3/2} \tag{4.1}$$

where

P = failure load in pounds

t = thickness of specimen in inches

B = width of specimen in inches

π = 3.14

$$Z = \frac{y(2 - y^4)}{(2 - y^3 - y^4)^2}$$

$$Y = \frac{X}{B}$$

X = crack length in inches at onset of fast fracture.

Some typical K-values are in table 4.2.

Table 4.2. Relative crack propagation resistance (K-value) of various materials.

Material	K-Value, 10^3 lb/in$^{3/2}$
Brittle steel	54.8
24 St 6 aluminum	63.2
As-cast MIL-P-5425	1.2
Stretched MIL-P-5425	3.2
As-cast MIL-P-8184	1.3
Stretched MIL-P-8184	3.2
Glass in air	.6
Glass in low humidity	.9

Note:

1 lb/in = 1.129848 E-01 N-m

4.2.3.2 CRAZING. All transparent plastic materials currently available are susceptible to crazing, although in varying degrees. Crazing is defined as the fine cracks which may extend in a network over or under the surface or through a plastic. These cracks are often difficult to discern, since they are approximately perpendicular to the surface, very narrow in width, and usually not more than 0.001 inch (0.003 centimeter) deep. They can be seen by reflection from their surfaces and appear as bright lines when the specimen is viewed at varying angles to the incident light (figures 4.1, 4.2, and 4.3).

Crazing results from a variety of causes, the more prominent of which are (1) residual stresses caused by the uneven stretching and cooling that occur during thermoforming of acrylic sheets to complex shapes; (2) contact with solvents and solvent vapors in the manufacture, operation, and servicing of vehicles (these include the adhesives used in making joints with acrylic plastics); and (3) stresses induced in the material by machining, buffing, polishing, mounting, and other fabricating operations. When the cracks are in a random pattern, crazing can usually be ascribed to the action of solvent-vapors and is referred to as solvent crazing. When the cracks are approximately parallel, the crazing is usually the result of the application of mechanical stresses and is referred to as stress crazing. These two types are not mutually exclusive, i.e., the effect may be produced by the simultaneous action of both stress and solvent crazing. In this instance, the cracks appear perpendicular to the applied stress. Only tensile and flexural stresses cause crazing, whereas purely compressive stresses do not. Crazing is not a reversible property of acrylic plastics, although visible crazing may disappear. Experiments show that craze cracks produced by flexural stresses become invisible to the naked eye when the specimens are heated at 212°F (100°C); however, after cooling and restressing, the crazing is rapid and the original pattern reappears (references 4.3 and 4.5).

Crazing reduces the luminous transmittance of the transparent plastic material, affects the structural properties, and interferes with vision. Crazing cracks 0.006 inch (0.015 centimeter) deep resulted in a 30-percent loss in tensile strength of MIL-P-5425 material in one investigation. The extreme stress concentration at the bases of the fissures results in propagation of the crazing with time and under load. Small changes in the depths of the cracks are accompanied by large decreases in the impact strength. In extreme cases, crazing can reduce tensile, flexural, and impact strengths to virtually zero.

Monomer present in acrylic plastic sheets prior to forming acts as a solvent and produces crazing. It has therefore become the practice of some manufacturers to anneal the finshed sheets to remove this monomer and relieve residual casting stresses.

Proper annealing of formed and finished acrylic plastics is the most effective preventive measure against crazing in unstretched acrylic plastics. It consists of prolonged heating at an elevated temperature followed by slow cooling. Recommended annealing times are given in table 4.3. The internal stresses set up during fabrication and machining are reduced or eliminated by this treatment. It also results in greater dimensional stability and resistance to crazing. To obtain these benefits, it is necessary that the procedure be performed after all other fabrication procedures, including polishing, are completed. After elevated temperature annealing, the part must be cooled at an even rate. The cooling rate must be slower for thick sections than it is for thin sections. The parts can be cooled by turning off the oven heat or by placing them where they will be subjected to room temperature in still air. Recommended cooling times are in table 4.4.

Table 4.3. Optimized annealing schedule for acrylic plastic windows. Recommended heating times and temperatures.

Maximum Thickness, in	Heating Time in Forced Circulating Air Ovens Maintained at Indicated Temperature, hr			
	230°F	221°F	212°F	203°F
0.060 to 0.187	1½	3½	7½	24½
0.250 to 0.375	2	4	8	25
0.500 to 0.750	3	5	9	26
0.875 to 1.250	4	6	10	27
1.500 to 1.750	7	9	13	30
2.000	9	11	15	32
2.500	12	14	18	35
3.000	15	17	21	38
3.500	19	21	25	42
4.000	23	25	29	46

Notes:

1. Anneal parts at highest temperature for indicated time. If distortion occurs, use the next lowest temperature. If distortion still occurs, shift the temperature heading to the left and use these combinations.

2. The cycles given will be satisfactory for most formed parts. For extreme forming, such as 100-percent biaxial stretching, the lower temperatures should be used. Another example is a free-blown hemisphere, where the middle temperatures will probably be used.

3. Airshould circulate around each part during annealing.

4. The calculations for these heating times assume an air velocity of 175 feet (53 meters) per minute. Other heating conditions require different heating times.

5. $t_C^\circ = (t_F^\circ - 32)/1.8$

6. 1 in = 2.540000 E-20 m.

Table 4.4. Optimized annealing schedule for acrylic plastic windows. Recommended cooling times and rates.

Maximum Thickness, in	Cooling Rate, ^{o}F/hr	Time Needed to Cool Fabricated Part from Indicated Temperature to 120^{o}F, hr			
		230^{o}F	221^{o}F	212^{o}F	203^{o}F
0.060 to 0.187	140	0.75	0.75	0.50	0.50
0.250 to 0.375	54	2.00	1.75	1.75	1.50
0.500 to 0.750	25	4.50	4.00	3.75	3.25
0.875 to 1.250	18	6.00	5.50	5.00	4.50
1.500 to 1.750	12	9.00	8.00	8.00	7.00
2.000	10	11.00	10.00	9.00	8.00
2.500	8	14.00	13.00	11.00	10.00
3.000	7	16.00	14.00	13.00	12.00
3.500	6	18.00	17.00	15.00	14.00
4.000	5	22.00	20.00	18.00	17.00

Notes:

1. Parts are usually held in the forced-circulation-air oven and the temperature of the oven is dropped at the cooling rate.
2. The air should circulate about each part.
3. Parts must cool evenly or distortion caused by differential cooling can result.
4. 1 in = 2.540000 E-02 m.
5. $t_C^{\circ} = (t_F^{\circ} - 32)/1.8$.

Improved annealing can be attained by twice heat-treating the fabricated acrylic plastic window. The first cycle – a shrinking cycle (table 4.5) – should be done after rough machining operations have been completed. The second cycle – a shortened annealing cycle (table 4.6) – should be done after all fabrication procedures, including polishing, have been completed.

Stretching of acrylic plastic represents the most effective preventive measure against crazing. Since the resistance of stretched acrylic plastic to crazing is directly related to the amount of stretching, it is desirable, whenever feasible, to use acrylic with biaxial prestretch in excess of 100 percent.

Table 4.5. Shrinking cycles for cast acrylic plastic sheets.

Thickness, in	Time Required for Shrinking Cycle			Dimensional Change, %	
	130°C to 80°C	80°C to 35°C	35°C	Decrease in Length and Width	Increase in Thickness
0.500	4 hr 20 min	2 hr 20 min	1 hr	2.2	4.8
0.625 to 1.000	5 hr 20 min	2 hr 20 min	1 hr	2.1 to 1.9	4.4 to 3.6
1.125 to 2.000	6 hr 20 min	2 hr 20 min	1 hr	1.8 to 1.5	3.2 to 2.2
2.125 to 3.000	7 hr 20 min	2 hr 20 min	1 hr	1.5	2.2
3.250 to 4.250	8 hr 20 min	3 hr 20 min	1 hr	≤1.5	≤2.2

Notes:

1. The time shown is from the instant that the plastic sheet is placed in an oven preheated to 266°F.
2. $t_C^\circ = (t_F^\circ - 32)/1.8$.
3. 1 in = 2.540000 E-02 m.

Table 4.6. Short annealing schedule for acrylic plastic windows.

Recommended Heating Times and Temperatures			
	Heating Time for Acrylic Placed in a Forced-Circulation-Air Oven Maintained at Indicated Temperature, hr		
Thickness, in	212°F	194°F	185°F
0.500 to 0.750	4.0	6.0	11.0
0.875 to 1.125	4.5	6.5	11.5
1.250 to 1.500	5.0	7.0	12.0
1.750	5.0	7.0	12.0
2.000	6.0	8.0	13.0
2.250	7.0	9.0	14.0
2.500	9.0	11.0	15.0
3.000	11.0	12.0	17.0
3.250	13.0	14.0	17.0
3.500	13.0	14.0	19.0
3.750	14.0	16.0	20.0
4.000	17.0	18.0	22.0

Table 4.6. Continued.

Recommended Cooling Rates and Times				
Thickness, in	Maximum Cooling Rate, °F/hr	Time Needed to Cool Acrylic from Indicated Annealing Temperature at the Maximum Permissible Rate to the Minimum Removal Temperature of 160°F, hr		
		212°F	194°F	185°F
0.500 to 0.750	25	2.00	1.25	1.00
0.875 to 1.125	18	3.00	2.00	1.75
1.250 to 1.500	13	4.00	2.50	2.00
1.750	11	4.50	2.75	2.00
2.000	10	5.25	3.50	2.50
2.250	9	6.00	4.00	3.00
2.500	8	6.50	4.25	3.25
3.000	7	7.25	4.75	3.50
3.250	6	8.00	5.25	4.00
3.500	6	8.75	5.75	4.25
3.750	6	9.25	6.25	4.50
4.000	5	10.50	6.75	5.00

Notes:

1. $t_C^\circ = (t_F^\circ - 32/1.8$.

2. 1 in = 2.540000 E-02 m.

Long-time cantilever loading of test specimens, with and without various solvents applied to the tensile surface, has been used to estimate threshold crazing stress under various conditions. However, a more realistic test of craze resistance is long-term weathering under load.

4.2.4 Factors Affecting Structural Properties

The physical properties of plastic glazing materials are greatly influenced by factors such as temperature, rate of loading, duration of loading, and environment. This behavior is not unique to plastics, although it is much more pronounced than in metals.

4.2.4.1 TEMPERATURE. Throughout the range of service temperatures, increasing temperature is usually accomplished by decreasing physical properties, except for elongation and, in the case of acrylics, impact strength. As the temperature is increased, acrylic plastic changes from a hard, brittle state to a rubber-like solid state. This change is evident in the elastic behavior of the material at different temperatures. Below 160°F (71°C) the ultimate

elongation of MIL-P-5425 material is low and the mechanism of deformation is mainly that of ordinary elastic deformation. At room temperature, tensile test specimens show brittle failure and no necking in the region of fracture. As the temperature is increased above 160°F (71°C) the deformation becomes highly plastic or rubber like. Between −70 and +160°F (−56 and +71°C) the tensile strength may decrease 85 percent and the elongation may increase 5000 percent.

4.2.4.2 RATE OF LOADING. An increase in the rate of loading increases the values obtained for the physical strength of plastic. This is especially true of unnotched thermoplastics, where an increase in the speed of the cross-head motion of the testing maching from 0.05 to 0.5 inch (0.127 to 1.27 centimeter) per minute may increase the tensile strength by 35 percent.

4.2.4.3 DURATION OF LOADING. Most structural materials are subject to creep deformation and creep rupture effects, i.e., they will gradually suffer increasing permanent deformation and eventual failure from a constant load that is only a fraction of the normal static strength. Plastic materials exhibit this effect to a marked degree, particularly at elevated temperatures. The creep rupture strength of a thermoplastic after 1000 hours of sustained stress may be only 50 percent of the strength found in the usual static tests.

Creep deformation usually becomes objectionable before the danger of creep rupture develops, particularly with acrylic plastics, so that such characteristics in a plastic material are important in design.

Considerable work has been done to determine the creep rates and rupture times of several materials under various conditions of temperature and stress. Results show that the creep rupture times of all materials are reduced, sometimes drastically, if the tests are conducted outdoors. Very little is known about the effects of creep under intermittent loading.

4.2.4.4 SOLVENTS AND SOLVENT-VAPOR. The physical properties of plastic glazing materials, especially acrylics, may be reduced by exposure to a variety of solvents and solvent-vapors. Reduction is especially noticeable in the threshold crazing stress of acrylic materials. The decrease caused by some solvents (including water) is of finite extent and continued exposure does not cause any further decrease in the physical properties. The decrease caused by the majority of solvents, however, is continuous, and prolonged exposure results in complete loss of strength. Fuels, lubricating and hydraulic oils, deicing fluids, sealing compounds, adhesives, and vehicle cleaning compounds usually fall in the latter category.

4.2.4.5 AGING. Indoor storage normally has no appreciable effect on the physical properties of plastic glazing materials. Thermoplastics should not be exposed to high temperatures, but should be stored in a cool place. Outdoor exposure causes a decrease in physical properties, the extent depending on the time and conditions of exposure and the chemical structure of the glazing material.

4.2.4.6 WEATHERING. In the past, the materials used for vehicle glazing were chosen, in part, because of their good weathering resistance. For a time it was believed that outside exposure had no appreciable effect on stressed plastic materials. However, results of recent outside creep tests, when compared with the results of inside creep tests, indicate that outside exposure does affect the physical properties of acrylic plastic materials, sometimes drastically.

4.3 SHORT-TERM MECHANICAL PROPERTIES

4.3.1 Tensile Loading

Response of acrylic plastic to tensile loading is a function of temperature, rate of stress application, character of stress field, amount of prestretch, and composition of ambient atmosphere (figures 4.4 through 4.11).

4.3.1.1 TENSILE STRENGTH. This property increases with a drop in temperature, high stress application rate, and the absence of solvent-vapors in the atmosphere (figures 4.4, 4.5, and 4.6). At standard test conditions (ASTM-D-638) the values for tensile strength are between 9000 and 10,000 pounds per square inch (62 and 69 megapascals). Tensile strength values are independent of casting thickness or volume, and thermal prestretching of the material has no significant effect (figure 4.11). Inclusions in the form of widely scattered voids ($0.1 \leqslant 5$ millimeters) decrease tensile strength by approximately 30 percent. If the total cross-sectional area of voids in a plane at right angles to the direction of the tensile load exceeds 10 percent, the tensile strength of the member decreases further in direct proportion to the decrease in the load-carrying area.

4.3.1.2 TENSILE-MODULUS OF ELASTICITY. Similar to tensile strength, this increases with a drop in temperature and a high stress application rate (figures 4.4 and 4.7). At standard test conditions (ASTM-D-638) the values for tensile modulus of elasticity are between 400,000 and 450,000 pounds per square inch (2758 and 3103 megapascals). Values are independent of casting thickness or volume, and thermal prestretching of the material has no significant effect (figure 4.10).

4.3.1.3 STRAIN AT FAILURE. This value decreases with a drop in temperature, high stress application rate, and the presence of a multiaxial tensile stress field (figures 4.4, 4.8, and 4.9). At standard test conditions (ASTM-D-638) the strain values at failure are between 3 and 6 percent. Thermal prestretching of acrylic plastic significantly increases the magnitude of strain at failure (figure 4.10), and the magnitude of strain at failure is independent of casting thickness or volume. The presence of biaxial tensile stress fields, however, significantly decreases the magnitude of strain at failure (figure 4.9).

4.3.1.4 STRESS CRAZING INITIATION THRESHOLD. Similar to tensile strength, this value increases with a drop in temperature, high stress application rate, and the absence of solvent-vapors in the ambient atmosphere. Crazing is a mode of plastic deformation, peculiar to glassy polymers, that is competitive with conventional shear ductility in reducing stress. Crazes contain polymer materials that interconnect the polymer above and below the craze and appear continuous under observation in a microscope. This is supported by the observation that under compression, or upon annealing, crazes tend to retract and disappear. Craze reflects the light very strongly because the rarefaction characteristic of craze formation produces a large decrease in the refractive index. The craze surface surrounded by normal polymer can be optically likened to a thin layer of liquid of low refractive index that is between two pieces of glass of high refractive index in a refractometer. The craze formation process is one of plastic deformation in the tensile stress direction without lateral contraction.

In well annealed material, crazing initiates at the surface and each craze tends to increase in planar area by growing both along the surface and into the specimen. For materials with internal tensile strains, crazes can initiate internally and grow to a large size without making contact with the surface. As the tensile stress applied to the material increases past the crazing initiation threshold, the craze tends to enlarge until it ruptures. Thus the craze is the flaw that serves as the ultimate limitation on the fracture strength of acrylic plastic.

Crazing is usually initiated under short-term loading at 80 to 90 percent of tensile strength. For temperatures less than 50°F (10°C), fracture can occur before crazing, since the crazing initiation strain increases with a drop in temperature while the strain at failure increases with temperature.

4.3.1.5 SOLVENT CRAZING. In appearance and composition, this is identical to tensile stress crazing, except that it is initiated by contact with solvents or their vapors at a stress level that is well below the threshold for stress crazing initiation. Solvent crazing will appear even on material that is not under applied tensile loading, since residual tensile stresses, caused by machining, buffing, polishing, mounting, and other fabrication processes, are usually present in any material.

Substitution of modified acrylic plastic or thermally prestretched plastic for the general-purpose, heat-resistant material increases resistance to stress solvent crazing.

4.3.2 Flexural Loading

The response of acrylic plastic to flexural loading is a function of temperature, rate of stress application, character of stress field, amount of prestretch, and composition of ambient atmosphere (figure 4.12).

4.3.2.1 FLEXURAL STRENGTH. This value increases with a drop in temperature, high stress application rate, fine surface finish, and the absence of solvent-vapors in the ambient atmosphere. At standard test conditions (ASTM-D-790) values are between 14,000 to 16,000 pounds per square inch (96 to 110 megapascals). The presence of notches, even very shallow ones, lowers the strength value by approximately 50 percent, i.e., to 7000 to 8000 pounds per square inch (48 to 55 megapascals). The flexural strength values of unnotched material increase slightly with material thickness, while those of notched material are independent of the thickness. Thermal prestretching of the material has no significant effect.

4.3.2.2 FLEXURAL MODULUS OF ELASTICITY. Similar to flexural strength, this increases with a drop in temperature and high stress application rate. At standard test conditions (ASTM-D-790) the values are between 420,000 and 500,000 pounds per square inch (2896 and 3448 megapascals). Thermal prestretching of the material has no significant effect.

4.3.2.3 DEFLECTION AT FLEXURE FAILURE. This increases with temperature and slow bending rates. At standard test conditions (ASTM-D-790), the deflections are from 0.6 to 1.0 inch (1.52 to 2.54 centimeters). Thermal prestretching of the material has no significant effect on deflection at failure (100-percent prestretching increases deflection by more than 1.7 inches (4.3 centimeters)).

4.3.2.4 DEFLECTION TEMPERATURE. This is a function of the acrylic plastic's casting composition. Under standard test conditions (ASTM-D-648, 264-pound-per-square-inch (1.8 megapascals) flexural loading), the temperature range at which deflection of the test beam reaches the specified magnitude is between 200 and 212°F (93 and 100°C). A deflection temperature less than 200°F (93°C) indicates that the acrylic plastic is not heat resistant.

4.3.3 Shear Loading

Response of acrylic plastic to shear loading is a function of temperature and rate of stress application. Only the shear strength is usually measured, since the associated strain and modulus of elasticity are of little practical value.

Shear strength increases with a drop in temperature, high stress application rate, and the presence of compressive stresses acting at right angles to the shear loading application. At standard test conditions (ASTM-D-732), values are between 8000 and 10,000 pounds per square inch (55.2 and 68.9 megapascals).

4.3.4 Impact Loading

Response of acrylic plastic to impact loading is a function of surface finish condition, rate of stress application, character of stress field, amount of prestretch, and composition of the ambient atmosphere. Since acrylic plastic is very sensitive* to impact loading, understanding the parameters that cause such sensitivity is a necessity for window designers and users.

The impact strength is a function of surface finish, thickness of material, magnitude and character of static stresses in a multiaxial stress field, rate of dynamic stress application, and magnitude of thermal prestress. Of these, the quality of the surface finish is the most important. Although compressive strength is not affected by surface finish and tensile and flexural strengths are affected only moderately, the impact strength depends almost totally upon it. The Charpy test method (ASTM-D-256) has shown the impact strength to vary from 0.2 to 3.2 foot-pounds per inch (0.02 to 0.4 Newton-meters per meter) of specimen width, depending on the surface finish (tables 4.6 and 4.7). A similar variation has been established with the Izod test method (ASTM-D-256), where a notch only 0.01 inch (0.25 millimeter) deep decreased the impact strength by 75 percent (figures 4.13 and 4.14). Because temperature has no effect on the impact strength of notched acrylic plastic (−80 to +80°C), it does not have to be considered (figure 4.15).

The impact strength of acrylic plastic as measured by Izod, Charpy, or ball-impact (USAS 726.1) methods is very much a function of specimen thickness. Increasing the thickness of the material increases the impact energy required for its fracture. For a specimen with polished surfaces, the increase in impact energy required for fracture falls into the range of values where the minimum is a linear function of thickness and the maximum is a function of the thickness squared.

** The sensitivity is approximately the same as that for thermally tempered glass with the same thickness.*

Another effective way to increase the impact strength of a window is to use thermally prestretched material. For materials that are prestretched over 100 percent, the impact resistance is an order of magnitude higher than for as-cast materials (figure 4.16). In applications where pressurized windows may be impacted with high-velocity projectiles, for example, bullets, the use of thermally prestretched acrylic plastic will preclude catastrophic disintegration of the window. Because thermally prestretched acrylic is available only in thicknesses less than 1 inch (2.54 centimeters), its applicability to pressure-resistant windows, which are generally thicker than 1 inch (2.54 centimeters), is rather limited.

Table 4.7. Impact strength of acrylic plastic with different notch configurations.

Shape of Notch	Charpy Impact Strength
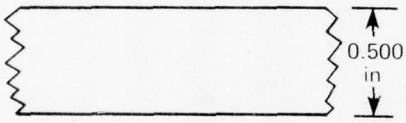	3.3 ft-lb for standard ½ in x ½ in bar
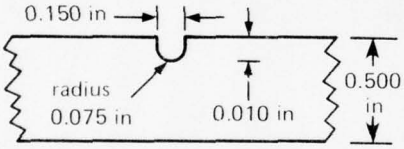	notch filed only: 0.49 ft-lb notch sanded and polished: 0.38 ft-lb
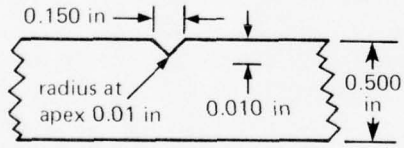	0.33 ft-lb
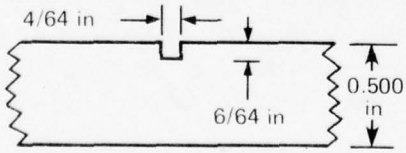	0.20 ft-lb

Notes:
1 in = 2.540000 E-02 m

4.3.5 Compressive Loading

Response of acrylic plastic to compressive loading is a function of temperature, rate of stress application, character of stress field, amount of prestretch, and composition of ambient atmosphere. Since compressive properties of acrylic plastic are not influenced by surface finish and only very moderately by the presence of solvents, acrylic structures should be designed so that they will only experience compressive stresses under operational loading. Furthermore, since the initiation of impact-generated fracture requires the presence of dynamic tensile stresses at the point of fracture, the superposition of a static compressive stress field significantly increases the impact resistance of the structure.

4.3.5.1 **COMPRESSIVE STRENGTH.** This value increases with a drop in temperature, high stress application rate, and the presence of multiaxial compressive stress fields (figure 4.17). At standard test conditions (ASTM-D-695), the yield strength values are between 15,000 and 18,000 pounds per square inch (103 to 124 megapascals). The compressive strength values at the same standard test conditions are significantly higher than those for yield strength, generally between 45,000 and 50,000 pounds per square inch (310 to 344 megapascals). Surface finish and presence of solvent vapors have no significant effect, although the presence of internal discontinuities in the form of gas bubbles will initiate tensile fractures under internal compressive stress when the uniaxial compressive strain exceeds 5 percent. These fractures are oriented along the axis of maximum principal compressive stress. In multiaxial compressive stress fields, the compressive strength increases significantly until it becomes infinite in a uniform triaxial compressive stress field (figure 4.18).

4.3.5.2 **COMPRESSIVE MODULUS OF ELASTICITY.** Similar to compressive strength, this increases with a drop in temperature, high stress application rate, and the presence of multiaxial compressive stress fields (figures 4.19 and 4.20). At standard test conditions (ASTM-D-695), the values are between 420,000 and 550,000 pounds per square inch (2896 and 3793 megapascals). Since the stress-strain relationship of acrylic plastic is not linear, both the tangent and secant moduli of elasticity vary inversely with stress magnitude (figures 4.21 and 4.22). Knowledge of both is very important, as it forms the basis of calculations that predict elastico-plastic buckling of acrylic plastic structures under conditions of momentary overload.

4.3.5.3 **COMPRESSIVE STRAIN AT ANY STRESS LEVEL.** This value decreases with a drop in temperature, high stress application rate, and the presence of multiaxial compressive stress fields (figures 4.23 and 4.24). At standard test conditions (ASTM-D-695), the values at yield point are between 7 and 10 percent. The presence of a multiaxial compressive stress field significantly decreases the magnitude of strain at any stress level.

4.3.5.4 **POISSON'S RATIO.** This value decreases with a drop in temperature, high stress application rate, and the presence of multiaxial compressive stress fields (figure 4.25). In addition, the magnitude of the ratio varies with the applied compressive stress level, with higher ratios associated with higher stress levels. Under standard test conditions (ASTM-D-695), Poisson's ratios increase from approximately 0.3 at 4000 pounds per square inch (27.6 megapascals) to 0.6 at yield point.

4.3.5.5 COMPRESSIVE DEFORMATION UNDER LOAD. This value decreases with a drop in temperature and the presence of multiaxial compressive stress fields. In addition, it varies with the duration of sustained loading, i.e., longer periods of loading produce larger deformations. Under standard test conditions of 4000 pounds per square inch (27.6 megapascals), 122°F (50°C), and 24-hour duration, the values are between 0.5 and 1.0 percent.

4.3.6 Flammability

Ignition temperature, rate of flame propagation, and time to autonomous extinction of flame are functions of atmospheric pressure and composition of the atmosphere. Furthermore, the rate of flame propagation and time to autonomous extinction also depend on the orientation of the material specimen, i.e., a specimen oriented vertically has a higher flame propagation rate than one oriented horizontally.

4.3.6.1 IGNITION TEMPERATURE. This is a function of pressure, composition of the atmosphere, and partial pressure of oxygen. At standard atmospheric pressure and air composition, the minimum ignition temperature by heated air (ASTM-D-2155) is 842°F (450°C), while by contact with a hot plate it is 1103°F (595°C). Ignition temperature is more sensitive to an increase in the partial pressure of oxygen than to an increase in the total pressure of the oxygen-nitrogen mixture; however, if both increase at the same time, the reduction in ignition temperature is dramatic (figures 4.26 and 4.27).

4.3.6.2 FLAME-SPREAD RATE OF ACRYLIC. This is a function of pressure, composition of the atmosphere, partial pressure of oxygen, and orientation of the test specimen. In standard air atmosphere at atmospheric pressure, the flame is not self-propagating from the origin of ignition when the material is oriented horizontally. When the material is oriented vertically, the rate of propagation is a function of the amount of time that the igniter maintains contact with the material at point of ignition. For an igniter contact of less then 60 seconds, flame spread is so slow that autonomous extinction of the flame results. The associated burn lengths and flame times appear to be a function of exposure time to the 1550°F (843°C) igniter flame (figures 4.28 through 4.31).

When the pressure in air atmosphere is raised above 1 atmosphere, the flame spread rate becomes positive and the burning continues until all material is consumed. Increased partial pressure of oxygen achieves similar results (figure 4.32).

4.4 LONG-TERM MECHANICAL PROPERTIES

Long-term mechanical properties of acrylic plastic are a result of complex chemical and physical actions that occur in the material (figure 4.33A and 4.33B). The first increment of deformation is instantaneous, truly elastic, and instantly recoverable (figure 4.34). It is believed that it is caused by a change in bond angles. The second, third, and fourth stages of deformation are time dependent, and depending on the magnitude of deformation they can cause permanent set. These deformations are thought to be caused by uncoiling and slippage of the polymer chains.

The first stage of deformation is usually completed when the load ceases to increase. The second stage is characterized by a rapid increase in deformation, lasting approximately 30 to 45 minutes. The third stage is characterized by a linear range of creep lasting from

1 to 10,000 or more hours, depending on the stress level and temperature of environment. The fourth stage is characterized by rapid acceleration of the deformation, ultimately terminating in rupture. The first, second, and fourth stages, although contributing significantly to the magnitude of deformation, are of little interest to the designer, as the durations of most loadings are within the third stage.

To predict the magnitude of deformation, the designer must know the effective modulus for a given environmental temperature and the projected maximum duration of loading. Effective modulus, like the deformation that it represents, can also be broken down into four stages (figure 4.34). Only the third stage is of interest, as it represents loading durations of practical concern.

The general equation for effective modulus during stage three of material deformation is

$$E_T = E_1 T^{-M} \quad , \tag{4.2}$$

where

E_T = calculated variable effective modulus for a given temperature at designated time T

E_1 = effective mudulus at time = 1 day

T = time, days

M = slope constant, expressing modulus decay for a given temperature.

It can be represented as a straight line on log-log coordinates (figure 4.33).

Values of E_1 and M have been experimentally derived for flexural and tensile loadings from 68 to 194°F (20 to 90°C) under laboratory test conditions (figures 4.44 and 4.45). For other temperatures or types of loading, values can be readily generated in several days of sustained loading by using the following relationships:

$$M = \frac{\log (E_1/E_2)}{\log (T_2 - T_1)} \quad , \tag{4.3}$$

where

E_1 = effective modulus at T_1 (generally 1 day)

E_2 = effective modulus at T_2 (generally 10 days)

T_1, T_2 = time, days,

or

$$M = \frac{\log (\delta_2/\delta_1)}{\log (T_2 - T_1)} \quad , \tag{4.4}$$

where

δ_1 = deflection or displacement at T_1

δ_2 = deflection or displacement at T_2

T_1, T_2 = time, days.

In addition to the physical reaction of acrylic plastic to sustained loading, there is also its chemical reaction to solar or nuclear radiation, moisture, and chemical reagents. Their cumulative effect is to degrade the surface of the material and as a result cause deformation and rupture sooner than predicted by extrapolation of data generated in the laboratory environments. For this reason, it is preferable to base the design of acrylic structures on long-term experimental data generated in operational environments and to limit the extrapolation of values to a maximum time factor of 10. If this is not feasible, appropriate safety factors should be applied to the extrapolated laboratory data.

4.4.1 Tensile Loading

Response of acrylic plastic to long-term tensile loading is a function of temperature, magnitude of stress, character of stress field, composition of ambient atmosphere, and environmental factors.

4.4.1.1 TENSILE STRENGTH. This decreases with an increase in loading duration, increase in temperature, increase in stress level, exposure to weather, and surface abrasion. Because of the expenses associated with generation of long-term tensile data, most available data cover only 1 to 1000 hours. Fortunately, when the data are plotted, straight lines that can be extrapolated with reasonable confidence to at least 10,000 hours result. From these graphs (figure 4.35), it is apparent that the tensile rupture of acrylic plastic after 10,000 hours of loading occurs at 5000 pounds per square inch and 80°F (34.5 megapascals and 27°C), 3500 pounds per square inch and 120°F (24.1 megapascals and 49°C), 1500 pounds per square inch and 160°F (10.3 megapascals and 71°C), and 750 pounds per square inch and 200°F (5.2 megapascals and 93°C). When these values are compared with short-term tensile strengths at identical temperatures, the magnitude of decrease is from 40 to 50 percent.

Long-term experiments have discovered a time-temperature equivalency concept for acrylic plastic under tension (figure 4.36). Utilizing this concept, it is feasible to substitute higher temperature for time in long-term tensile rupture tests. This concept permits, for example, using rupture data from tests of one day at 70°C to predict acrylic plastic rupture after 10 years at 10°C (figure 4.37). Engineering judgement must be exercised, however, when extrapolating data for more than 1 month for structures exposed to weather, as the data in figure 4.37 were generated in laboratories with carefully controlled ambient atmospheres and temperatures.

When exposed to weather, acrylic plastic ruptures after 10,000 hours at a stress level (2250 pounds per square inch (15.5 megapascals)) lower than the one encountered in a laboratory environment at room temperature (5000 pounds per square inch (34.4 megapascals)) (figures 4.38 and 4.39). This decreased capability is probably caused by the chemical deterioration of the acrylic surface under the action of ultraviolet rays and smog, the abrasive action of dust, and the superposition of tensile stresses caused by daily differential thermal expansions.

The best method for design of structures exposed to weathering is to use rupture data from long-term tests conducted in an outdoor environment that are discounted by at least a factor of two. If such data are not available, the design should be based on laboratory long-term tensile rupture data, generated at the maximum expected environmental temperature, discounted by at least a factor of four.

The substitution of thermally prestretched acrylic plastic can significantly increase the ability of the acrylic structure by approximately a factor of two to carry tensile stresses for long periods of time when exposed to weather (figures 4.38 and 4.39).

4.4.1.2 TENSILE EFFECTIVE MODULUS. This decreases with increases in loading duration, temperature, and stress level. However, data do not exist for all stress, temperature, and duration of loading ranges. For stress levels that generate only 1 percent of strain (approximately 50 percent of tensile rupture stress for a given loading duration) the effective modulus is only a fraction (figure 4.40) of the short-term modulus of elasticity discussed in section 4.3.1.2. Because the data generally plot as a straight line on log-log coordinates for modulus as a function of time, the value at 10 years of sustained loading can be graphically extrapolated from data generated by tests lasting only several days. Mathematical expressions can also be developed that relate the effective time-dependent modulus at time T to the experimentally determined 1-day effective modulus and its rate of decay. Such mathematical relationships, based on 1 hour and 1 day of experimentally determined effective moduli, have been experimentally validated for long-term flexural loading and are described in greater detail in section 4.4.2.2. These relationships appear to apply conservatively without any modification of contents to long-term tensile loadings.

4.4.2 Flexural Loading

The response of acrylic plastic to long-term flexural loading is a function of temperature, magnitude of stress, character of stress field, composition of ambient atmosphere, and environmental factors. The experimental data generated in test laboratories and outdoor test facilities with narrow test specimens are somewhat conservative, as the deflections of wide acrylic beams or sheets are significantly less.

4.4.2.1 FLEXURAL STRENGTH. This decreases with increases in loading duration, temperature, and stress level, exposure to weathering, and surface abrasion. Most available experimental data cover only a time period of less than 10,000 hours, but because they plot as a straight line on log-log coordinates they can be safely extrapolated to a longer time period.

Ultimate strength of acrylic plastic under long-term flexural loading appears to decrease with time at about the same rate that it does under tensile loading. Thus, after 10,000 hours of sustained flexural loading at 80°F (27°C) in a laboratory environment, rupture will occur under a sustained flexure stress of 9000 pounds per square inch (62 megapascals), an approximate decrease of 44 percent from the short-term flexural strength of 16,000 pounds per square inch (110 megapascals) (figure 4.41). The decrease in long-term strength becomes greater when the convex surface of the test specimen is scratched* at

** ARTC scratch is between 0.004 to 0.007 inch (0.01 to 0.02 centimeter) deep and is produced with a phonograph needle whose tip has a 0.002-inch (0.005 centimeter) radius.*

right angles to the direction of principal stress; at 10,000 hours the rupture of a scratched specimen occurs under a sustained flexure stress of 5500 pounds per square inch (38 megapascals) at 80°F (27°C). When compared, however, to the short-term flexure strength of acrylic plastic with an identical scratch* (approximately 12,000 pounds per square inch (83 megapascals)), the decrease in strength is also only about 50 percent.

When the acrylic plastic is subjected to long-term flexure loading outdoors, the unscratched specimen after 10,000 hours of sustained loading ruptures under a sustained flexure stress of 3000 pounds per square inch (21 megapascals), which represents an 81-percent decrease from the short-term strength (figure 4.42). Based on these data, it appears prudent in the design of outdoor structures to use only rupture data from specimens exposed to weathering that are discounted by at least a factor of two or rupture data from specimens tested in a laboratory environment at the maximum expected environmental temperatures that are discounted by at least a factor of four.

4.4.2.2 FLEXURAL EFFECTIVE MODULUS. Similar to long-term flexural strength, the flexural effective modulus decreases with increased loading duration, temperature, stress level, and exposure to weathering. Most existing data were produced in a laboratory environment and apply only to loadings of less then 100 days (figure 4.43). However, since the data for different ambient temperatures plot as straight lines on log-log coordinates representing E_T and T, they can be readily extrapolated to cover durations in excess of 10,000 hours.

The relationship between E_T and T has been reduced to a mathematical relationship, shown in equations 4.2, 4.3, and 4.4, that simplifies the calculation of E_T for any T of interest to the designer. For flexural long-term sustained loading, the E_1 and M terms required for solution of the equations have been experimentally determined for the temperature range of 68 to 194°F (20 to 90°C) and can be used with confidence for the calculation of E_T and subsequently the total deflection of the structure (figures 4.44 and 4.45). The calculated values of E_T are valid only for flexural stress values from 0 to 3000 pounds per square inch (0 to 20.7 megapascals).

The effective modulus of acrylic plastic under long term flexural loading E_T is not only very useful for predicting the deflection of the structure at time T but also for predicting the maximum surface strain ϵ_t whose magnitude determines whether the surface of the plastic will craze during its useful design life. Some idea on the relationship between surface strain and crazing initiation can be obtained from outdoor test data lasting from 1 to 1000 days: For sustained flexural loadings up to 1 year, design strains should be kept below 0.5 percent, while for sustained loadings up to 10 years, the strain value should not exceed 0.25 percent.

4.4.3 Compressive Loading

Response of acrylic plastic to long-term compressive loading is a function of temperature, magnitude of stress, character of stress field, and environmental factors. Compressive loading differs somewhat from tensile and flexural loadings in that the material never ruptures at right angles to the direction of the uniaxial compressive stress, but is parallel to it. The accepted explanation is that when the lateral positive strain exceeds a certain value, the material ruptures in tension. Lateral restraint in the form of compressive stress decreases the lateral positive strain, thus in effect raising the compressive yield and ultimate compressive strengths of acrylic plastic.

** ARTC scratch is between 0.004 to 0.007 inch (0.01 to 0.02 centimeter) deep and is produced with a phonograph needle whose tip has a 0.002-inch (0.005 centimeter) radius.*

Since surfaces under compressive strain are immune to crazing, no provisions must be made by the designer to eliminate crazing. As a result, surfaces under compression can be subjected to higher strain and stress levels than surfaces under positive strain, i.e., those under tensile or flexural loadings. Similarly, the effect of weathering is only minor on structures whose surfaces are in compression.

Because of the many structural benefits associated with the placement of acrylic plastic under compression, all efforts should be made to design the structure so that all, or at least the highest, stresses on the surfaces occur when the structure is undergoing compression rather than tension.

4.4.3.1 COMPRESSIVE YIELD STRENGTH. The compressive yield strength decreases with increases in loading duration and ambient temperature. The presence of biaxial or triaxial compressive stress fields raises the yield strength; in a hydrostatic stress field, the yield strength approaches infinity. There are presently no experimental data that relate yield strength to the duration of loading at different temperatures. However, sufficient experimental data have been produced from 60 to 80°F (15 to 27°C) to indicate that in a uniaxial stress field it is in excess of 3000 pounds per square inch (20.7 megapascals) for durations up to 10,000 hours. From 30 to 40°F (−1 to +4°C), the compressive yield strength for 10,000 hours appears to be in excess of 6000 pounds per square inch (41.3 megapascals). In a biaxial stress field, where $\sigma_y/\sigma_x = 1$, the compressive yield strength at room temperature is in excess of 6000 pounds per square inch (41.3 megapascals) and from 30 to 40°F (−1 to +4°C), it exceeds 9000 pounds per square inch (62.1 megapascals).

4.4.3.2 COMPRESSIVE STRAIN. This value increases with magnitude of compressive stress, duration of loading, and temperature, and it decreases with the magnitude of compressive stress acting at right angles to the principal compressive stress. Because acrylic is a viscoelastic material, the magnitude of strain at any particular time during sustained loading is the sum of instantaneous strain, observed immediately after load application, and creep, the time-dependent strain.

It appears that under uniaxial compression at room temperature creep becomes excessive only at stress levels exceeding 7000 pounds per square inch (48.3 megapascals) while at near-freezing temperatures it becomes excessive at stress levels above 9000 pounds per square inch (62.1 megapascals) (figures 4.46 through 4.49). The presence of a biaxial stress field significantly decreases the magnitude of creep (figures 4.50 through 4.52). Thus, for example, the magnitude of creep under 7500 pounds per square inch (51.7 megapascals) of uniaxial compressive stress at room temperature is approximately equal to 0.0001 microinch per inch per hour, while under biaxial loading of the same magnitude it is only 0.00001 microinch per inch per hour, an order of magnitude less. If the principal stresses in a compressive biaxial stress field are not of equal magnitude, the magnitude of creep will increase somewhat along the axis of the larger principal stress.

Thus it can be concluded that the most effective design tool is a biaxial stress field, where both principal stresses are of equal magnitude. A structure designed on this principle can tolerate much higher compressive stresses without excessive creep.

4.4.3.3 COMPRESSIVE EFFECTIVE MODULUS. Similar to the long-term compressive yield strength, the compressive effective modulus decreases with increases in loading duration, temperature, and stress level and increases with the presence of multiaxial compressive stress fields.

Experimental data describing the effective axial modulus of acrylic under compression at room temperature exist (figure 4.53). When a comparison is made between the effective axial modulus under compression with the effective modulus under tension at the same temperature (figure 4.35A), the magnitude of the effective axial modulus under compression in acrylic plastic appears to be significantly less than that under tension, or for that matter, under flexure.

The effective modulus of acrylic plastic E_T can be calculated by using equation 4.2, if the proper 1-day values for effective compressive modulus E_1 and modulus decay M are used. Although the available experimental data are not extensive, it appears that in a uniaxial stress field under compressive stress in the range of 0 to 3000 pounds per square inch (0 to 20.7 megapascals) and at room temperature E_1 equals 380,000 pounds per square inch (2620 megapascals) and M equals 0.035. In the 30 to 40°F (-1 to +4°C) temperature range E_1 equals 500,000 pounds per square inch (3447 megapascals) and M equals 0.025.

4.4.3.4 COMPRESSIVE EFFECTIVE POISSON'S RATIO. The Poisson's ratio under sustained compressive loading has been found to increase with the magnitude of stress, increase in temperature, and duration of loading. Since duration of loading significantly affects magnitude, the Poisson's ratios may readily exceed values of 0.5 (figure 4.54).

4.4.4 Intermittent Loading

Intermittent loading often occurs in acrylic structures that are used as pressure-resistant members in submersibles and hyperbaric chambers. There are basically two types of intermittent loading: (1) a load that is always applied from the same direction and (2) a load that reverses direction between succeeding applications causing the maximum stress to alternate between compression and tension.

Intermittent loading presents the greatest challenge to the designer because of the scarcity of experimental data and the multitude of design variables. When reviewing available data, the designer must be aware of test parameters that influenced the test results and also know how to discount published values, i.e., design requirements can differ substantially from the test parameters.

The major parameters that influence such test results are temperature, environment, duration of loading phases, duration of relaxation phases, rate of loading, rate of unloading, and the presence or absence of load-direction reversals. Of these, the effect of temperature is best understood, as it affects the ultimate strength and effective modulus of elasticity in the same manner that it does under constant long-term loading, i.e., longer fatigue life and effective modulus of elasticity values are associated with lower ambient temperatures. The absence of sunlight and of industrial pollutants in the ambient atmosphere are also known to increase the fatigue life significantly. However, the effects of either continuous or intermittent immersion in seawater are not known.

Rapid loading and unloading, typical of commercial fatigue testing machines, tend to raise the temperature of the test specimen and as a result lower the fatigue life. Thus data generated by fatigue test specimens in a rapid-loading test machine without the benefit of forced-air blowers are suspect. If the specimens are cooled by blowers, the fatigue life of acrylic plastic, as tested in a commercial rapid cycling machine, is approximately 5000 pounds per square inch (34.7 megapascals) for 10^7 complete stress reversal cycles (cycles of mean zero stress) (figure 4.55). This value can be confidently used with the appropriate safety factors only for acrylic plastic structural components subjected to fatigue cycle rates of 100 to 2000 cycles per minute (a typical application would be components for a pump). For applications where the individual cycles last hours or days, these data are inappropriate. These latter cycles have not been sufficiently studied to permit definite theories on the fatigue mechanism of acrylic plastic under lengthy cycles. The only reliable prediction method is to subject either a full- or scale-size model to fatigue cycles which are either identical to, or at least representative of, the loadings that the structure will experience. This is a very expensive and time-consuming operation, as it ties up a test machine or facility for years.

Only a few acrylic structures have been subjected to the operational type of fatigue testing. These structures were windows and pressure hulls for submersibles, where the potential loss of life justified the expense. Tests conducted in water at room temperature on spherical acrylic pressure hulls, where the stresses varied from zero to the maximum compression values, showed that for an acrylic plastic structure with a projected craze-free life of 1000 cycles,* the peak and nominal compressive working stresses in a biaxial stress field should not exceed 7900 and 5500 pounds per square inch (54.5 and 37.9 megapascals), respectively. Operational fatigue testing in water of flat disc acrylic windows, where both compressive and tensile stresses were present, showed that the peak tensile working stress in a biaxial stress field should not exceed 1500 pounds per square inch (10.3 megapascals), if the window is to have a craze-free life of at least 1000 cycles in room temperature range.*

It is not positively known whether cyclic loading where the relaxation phases of the cycles are shorter than the sustained loading phases is more or less severe than cyclic loading where the length of succeeding phases in each individual cycle is the same. However, there are indications that, for acrylic structures whose load or pressure rating is based on peak tensile stresses present during the sustained loading phase, shortening the relaxation phases decreases fatigue life. As the length of relaxation phases between applied tensile stress phases is progressively shortened, the effect of tensile stress becomes the same as that of a continuous sustained tensile stress. Similar reasoning applies to acrylic plastic structures whose load, or pressure rating, is based on peak or nominal compressive stresses, except that the continuous sustained compressive stress application is the limiting effect.

A peculiar effect of intermittently applied compressive stresses on thick acrylic structural members is the generation of tensile stresses at some locations during the relaxation phases between load application phases. As a result, the member may fail because of the magnitude of these tensile stresses generated during relaxation phases rather than because of the compressive stresses generated by the application of the external load during sustained loading phases. For this to occur, two basic conditions must be present: (1) there must be a

** Each cycle consists of 1 to 8 hours of sustained loading phases followed by relaxation phases of equal or longer durations.*

substantial gradient in compressive stress across the thickness of the structural member with the maximum compressive stress on one face and the minimum compressive stress on the opposite face at the same location and (2) significant creep must take place at the location of maximum compressive stress. Experimental data generated with thick-walled spheres and hemispheres under external hydrostatic loading indicate that tensile stresses effecting tensile fatigue failure in less than 100 intermittent load cycles can be produced during the sustained loading phase by as little as 10,000-microinches-per-inch (1.0 percent) difference in compressive strains between the outer and inner surfaces of the shell. To preclude tensile fatigue failures in acrylic plastic structural members that are under compressive strain during loading phases, and that are restrained from changing curvature or length during the relaxation phases, the difference in compressive strains on opposite faces of the structural member at the end of individual loading phases should not exceed 5000 microinches per inch (0.50 percent). Unrestrained structural members that can adjust their length or curvature during the relaxation phases can probably tolerate larger strain differences between the opposite faces of the structural member.

4.5 CONCLUSIONS

The task facing the designer of acrylic plastic structures is formidable, not only because adequate experimental data do not exist but also because of the complex response of acrylic plastic to sustained or intermittent loading that generates multiaxial stress fields in structural members. There are basically three approaches for the design of safe acrylic structures.

The shortest and most reliable approach is to use or slightly modify a design that has already been fabricated and evaluated. Such designs are discussed in sections 5 through 14 of this handbook and are summarized in section 15.

The second approach is somewhat longer, but it is reliable and capable of producing original designs. The resulting structures are, however, not optimized in weight or cost. This approach is based on the use of very conservative allowable working stress levels (table 4.8).

The third approach is also reliable, but very long. It is capable of producing original designs that are optimized in weight and cost for the intended operational life of the structure. It is based on the discussion of experimental data and engineering recommendations presented in this section. This approach is particularly cost-effective, if the operational conditions are well defined and the specified useful life of the structure is short, i.e., an expendable item or one with a projected life of less than 1 year.

Table 4.8. Allowable nominal working stress levels for acrylic plastic design.

	Maximum Allowable Working Stress Level, psi	
Temperature, ^{O}F	Compression	Tension
77	3000	1500
104	2400	1200
122	2200	1100
140	2000	1000
158	1600	800
176	1200	600
194	600	300

Notes:

$t_C^o = (t_F^o - 32)/1.8$

1 psi = 6.894757 E+03 Pa

AD-A070 535 NAVAL UNDERSEA CENTER SAN DIEGO CA F/G 11/9
ACRYLIC PLASTIC VIEWPOINT FOR OCEAN ENGINEERING APPLICATIONS. V--ETC(U)
FEB 77 J D STACHIW
UNCLASSIFIED NUC-TP-562-VOL-1 NL

3 OF 5
AD
A070535

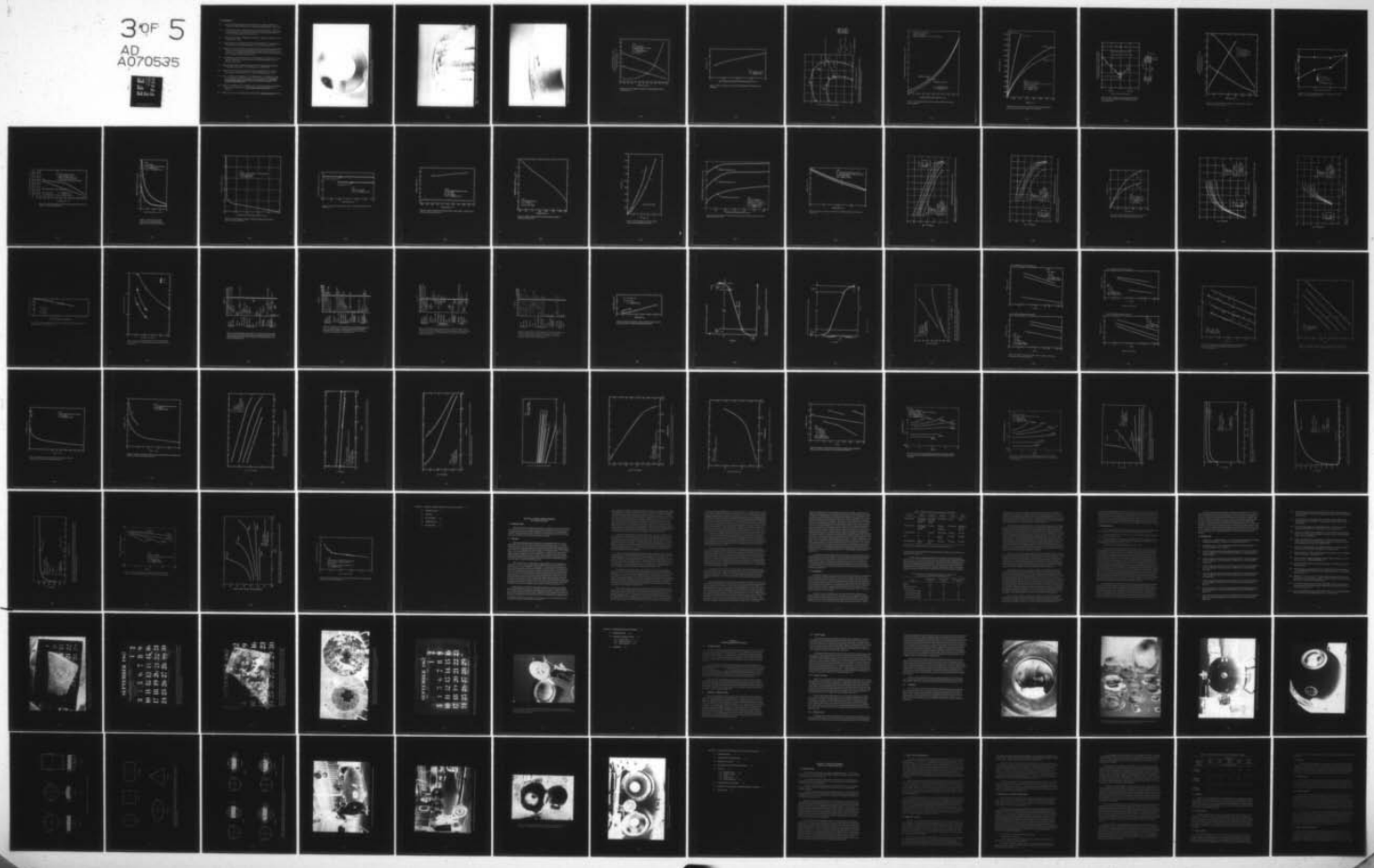

4.6 REFERENCES

4.1 Armed Forces Supply Support Center, Washington, D.C., Military Handbook 17, "Plastics for Flight Vehicles; Part II – Transparent Glazing Materials," August 1961.

4.2 General Electric Company, Schenectady, New York, Report 61GL181, "The Effects of Biaxial Stresses on the Deformation and Fracture of Polymethylmethacrylate," by R. L. Thorkildsen and Olszewski, April 1962.

4.3 Rohm and Haas Company, Philadelphia, Pennsylvania, "Plexiglas: Handbook for Aircraft Engineers," 1952.

4.4 Naval Ordnance Laboratory, White Oak, Maryland, NOLTR 66-45, "The Compressibility of Polymers to 20,000 Atmospheres," by R. W. Warfield, June 1966.

4.5 Naval Civil Engineering Laboratory, Port Hueneme, California, Technical Report R631, "Windows for External or Internal Hydrostatic Pressure Vessels – Part III: Critical Pressure of Acrylic Spherical Shell Windows under Short-Term Pressure Applications," by J. D. Stachiw and F. W. Brier, June 1969.

4.6 Naval Ship Research and Development Center, Washington, D.C., Report 3167, "The Structural Performance of Acrylic Viewports for Deep Submersibles," by F. M. Schwartz, August 1969.

4.7 Bureau of Mines, Bruceton, Pennsylvania, PB 176528, "Flammability of Materials in Hyperbaric Atmospheres," by J. M. Kuchta, et al., August 1969.

4.8 Douglas Aircraft Company, Long Beach, California, Douglas Paper 5733, "Plastics and Fire Safety in Commericial Aircraft," by E. M. Kunreuther, May 1970.

4.9. Lohr, J. J., Wilson, D. E., Hameker, F. M., and Stewart, W. J., "Accelerated Testing of the Mechanical and Thermal Integrity of Polymeric Materials," Proceedings of the AIAA/ASME Eighth Structural Dynamics and Materials Conference, Palm Springs, California, March 1967.

4.10 Weber, C. H., Robertson, E. N., and Bartoe, W. F., "Time and Temperature Dependent Modulus Concept for Plastics," Industrial and Engineering Chemistry, vol. 47, July 1955.

4.11 Rondeau, H. R., "You can Predict Creep in Plastic Parts," Machine Design, March 1976.

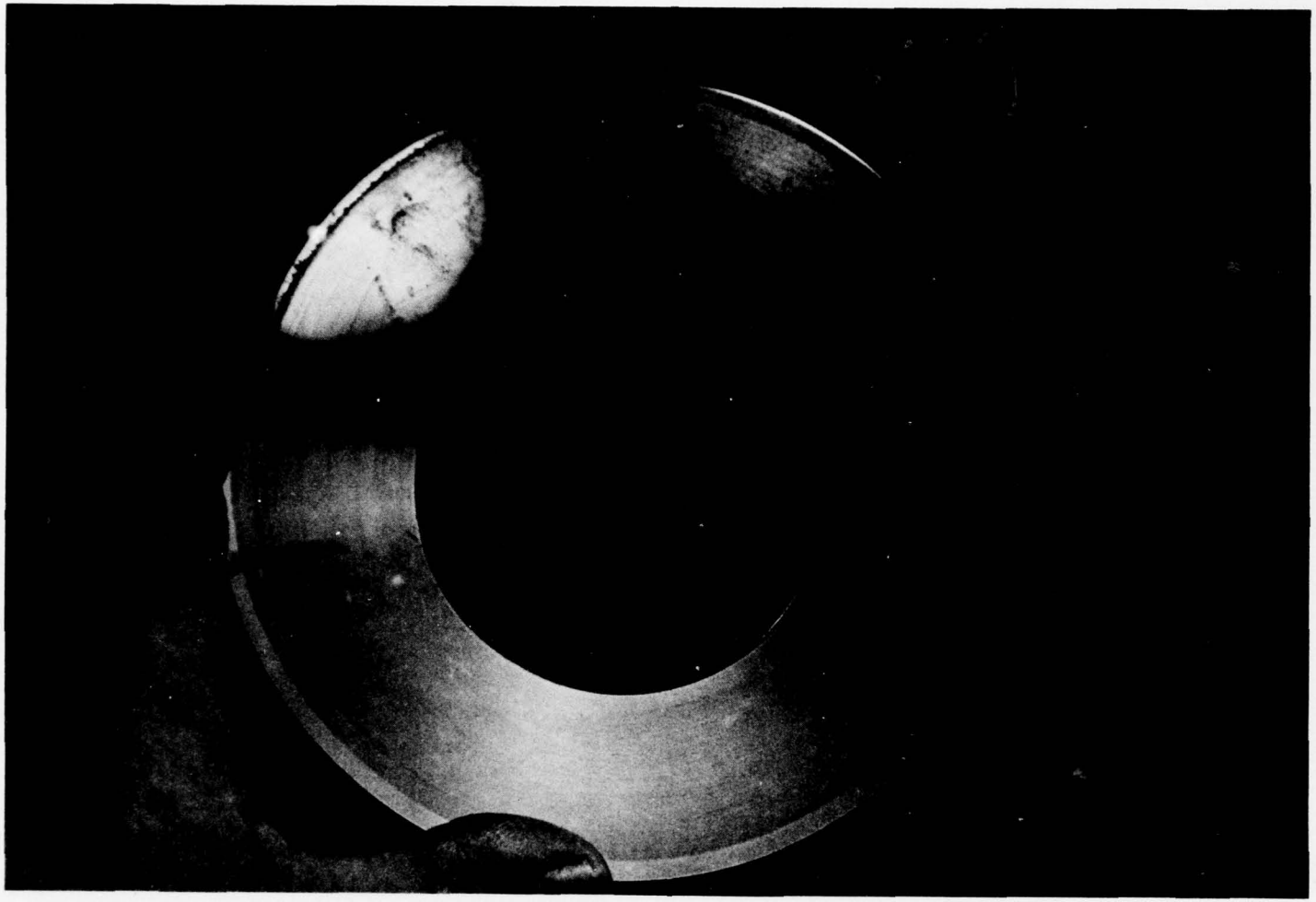

Figure 4.1. Typical plane disc window with conical bearing surface. Window was removed from service after crazing was detected on the high-pressure face. Note that the crazing is not visible in transmitted light.

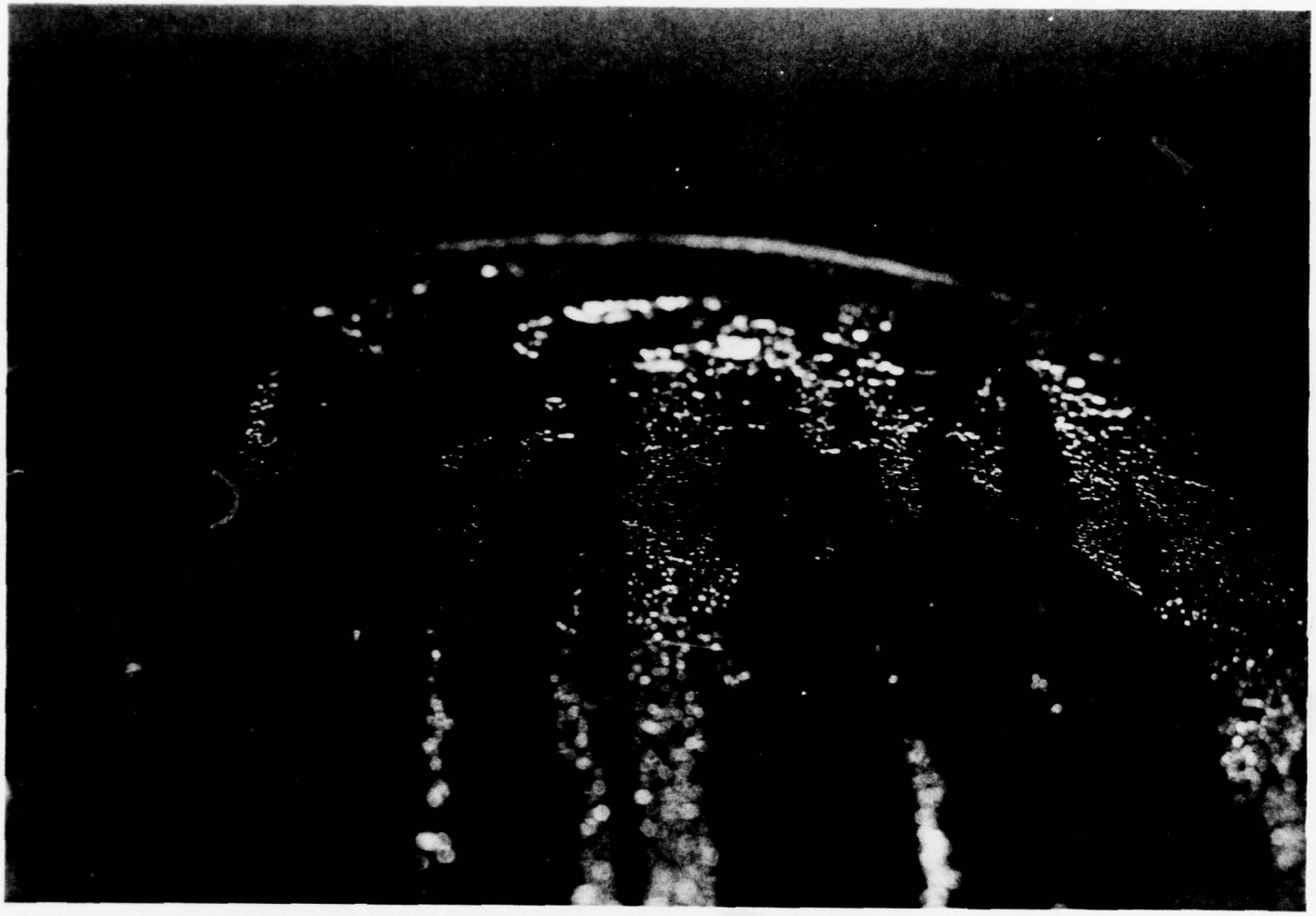

Figure 4.2. Oblique lighting falling upon the high-pressure face of window shown in figure 4.1 provides information on the extent of crazing.

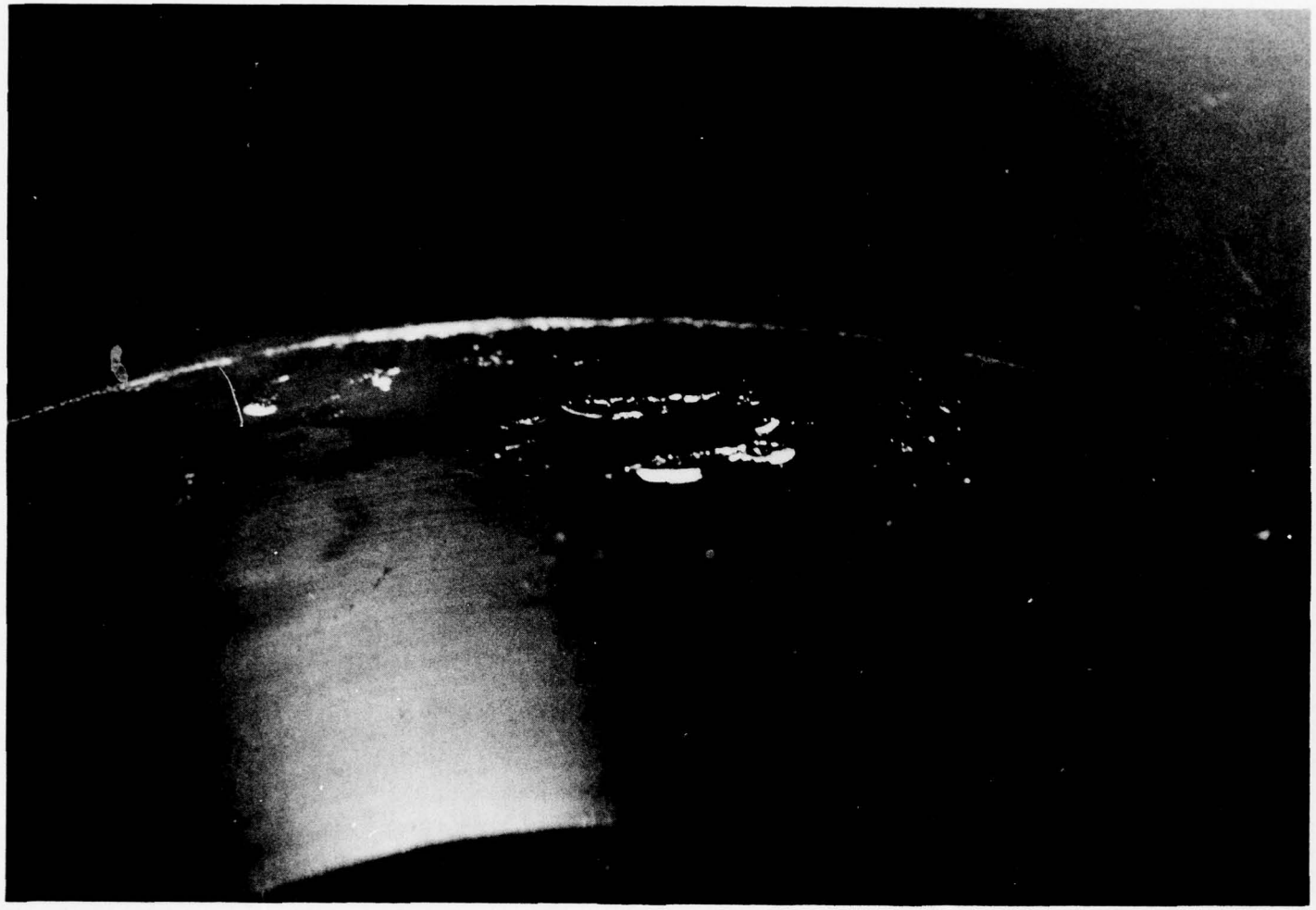

Figure 4.3. Oblique lighting falling upon the backside of window shown in figure 4.1 provides information on the depth of crazing.

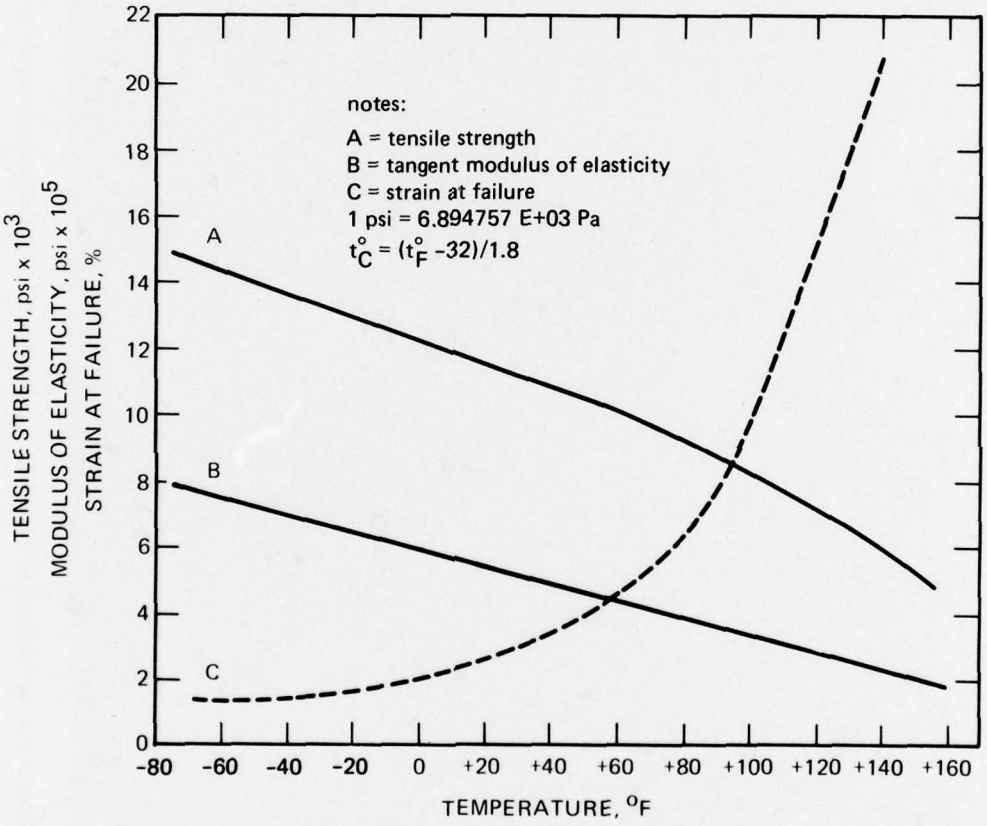

Figure 4.4. Effect of temperature on short-term tensile properties of acrylic plastic (reference 4.1).

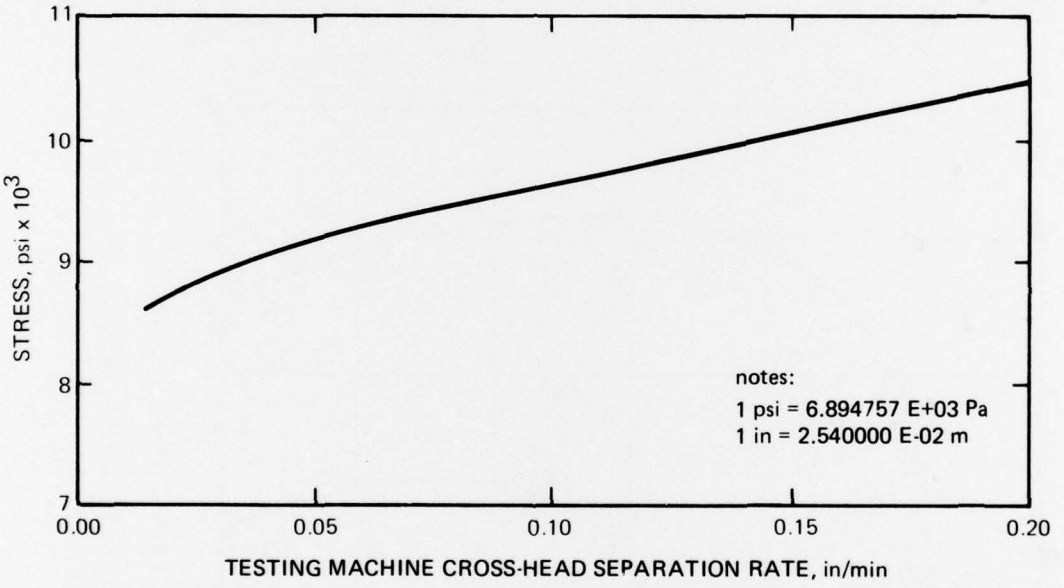

Figure 4.5. Effect of testing rate on short-term tensile strength of acrylic plastic at room temperature.

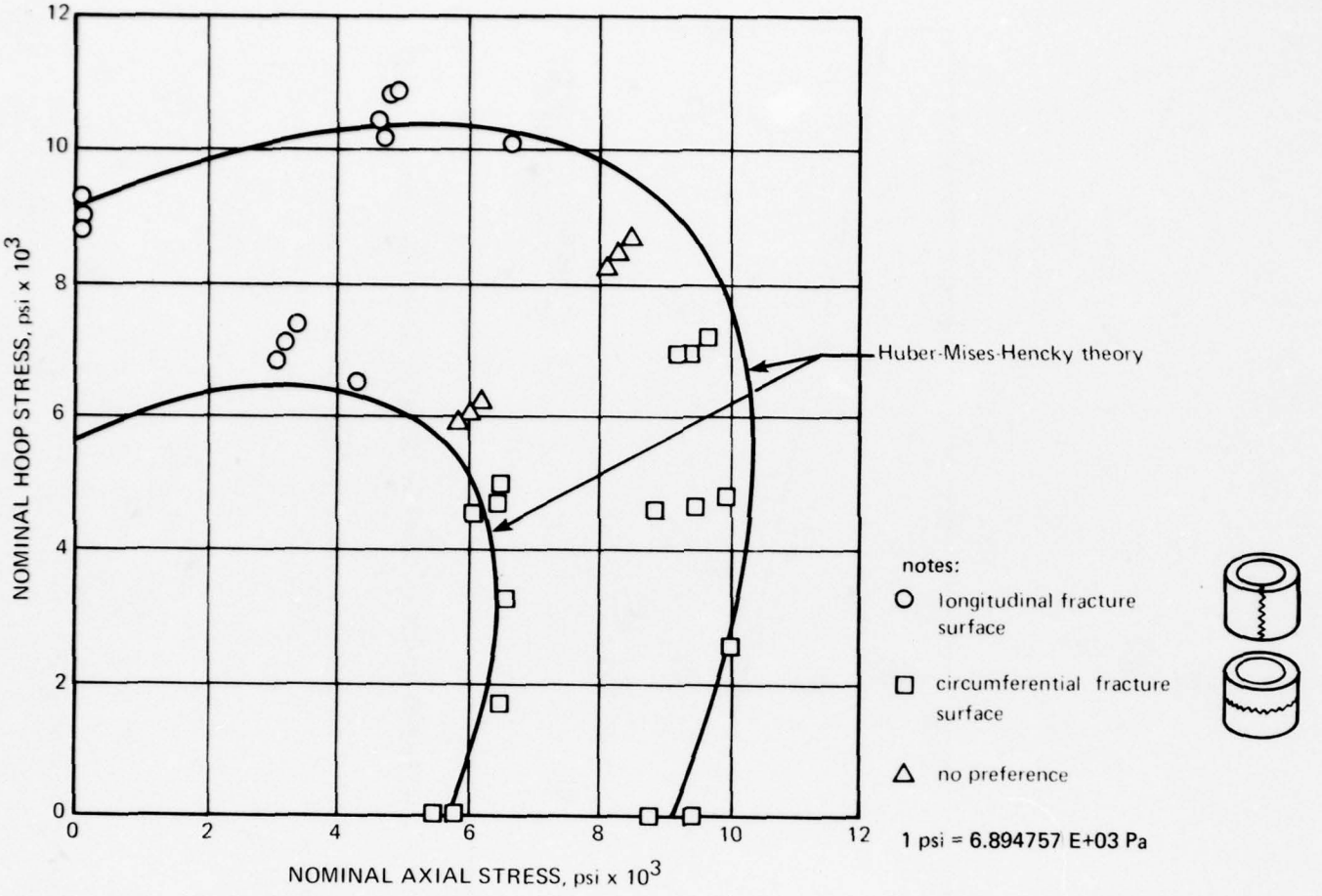

Figure 4.6. Effect of biaxial stress distribution on the magnitude of short-term nominal tensile yield and fracture stresses (reference 4.2).

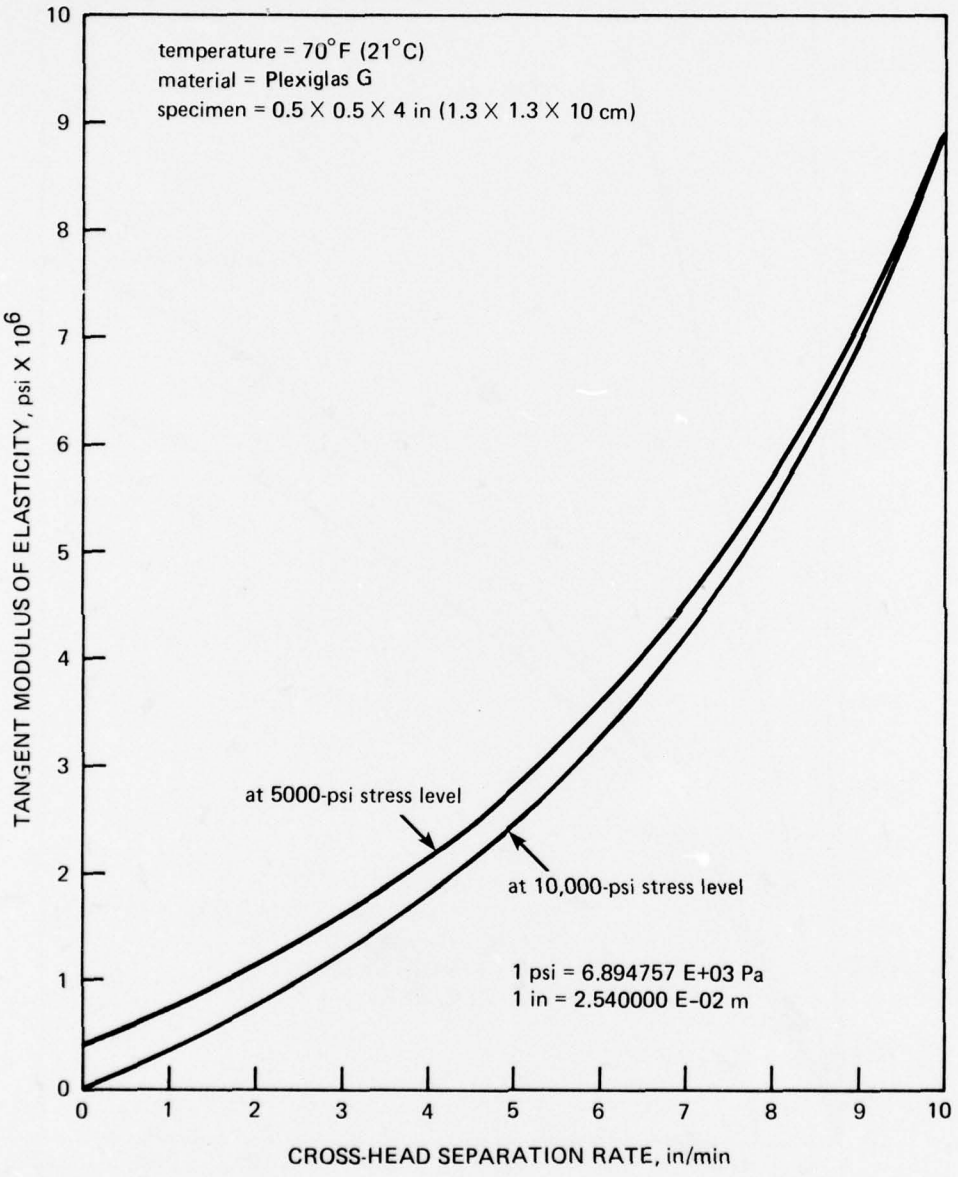

Figure 4.7. Effect of testing rate on short-term tensile modulus of acrylic plastic at room temperature.

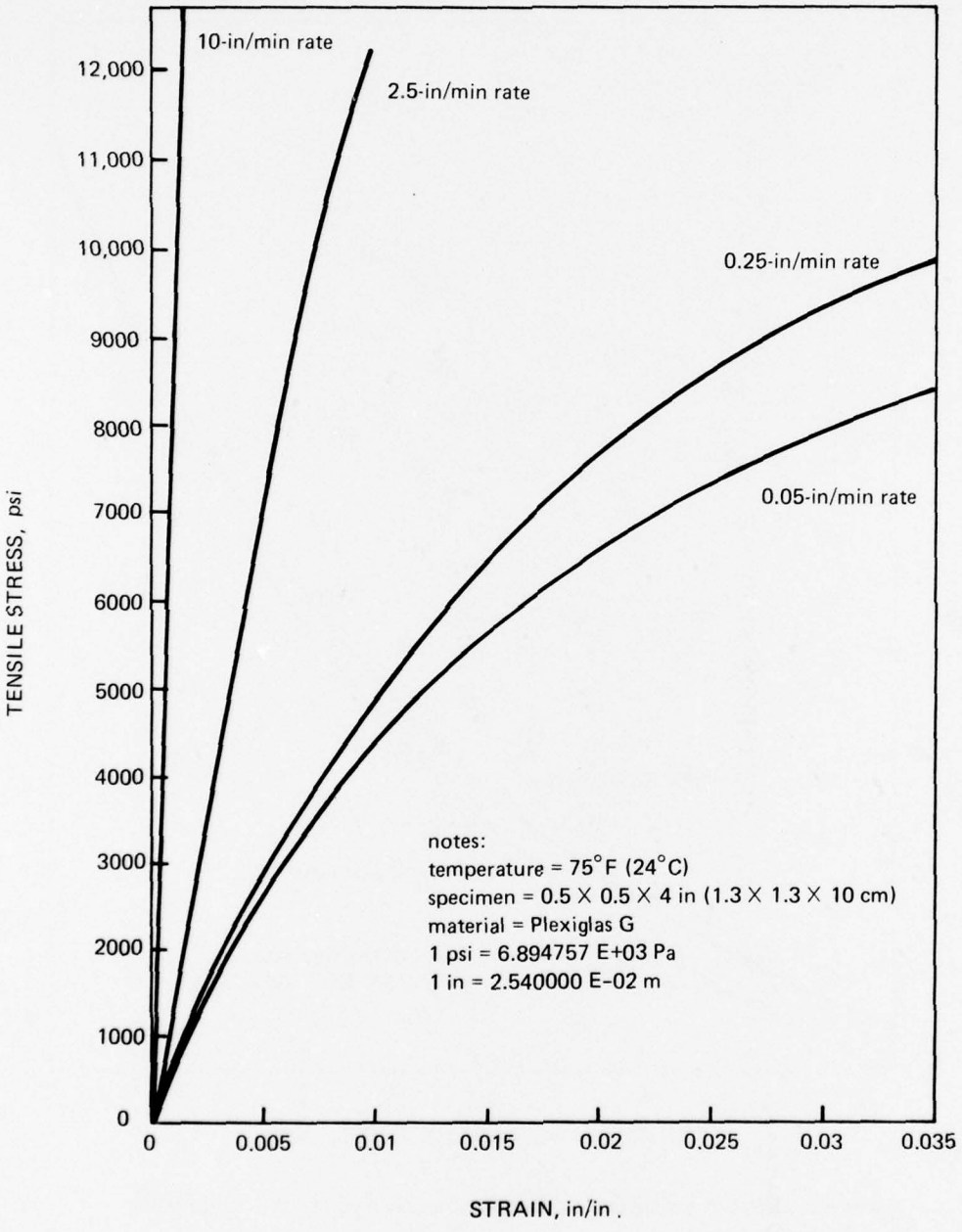

Figure 4.8. Effect of testing rate on the short-term stress-strain relationship of acrylic plastic under short-term loading at room temperature.

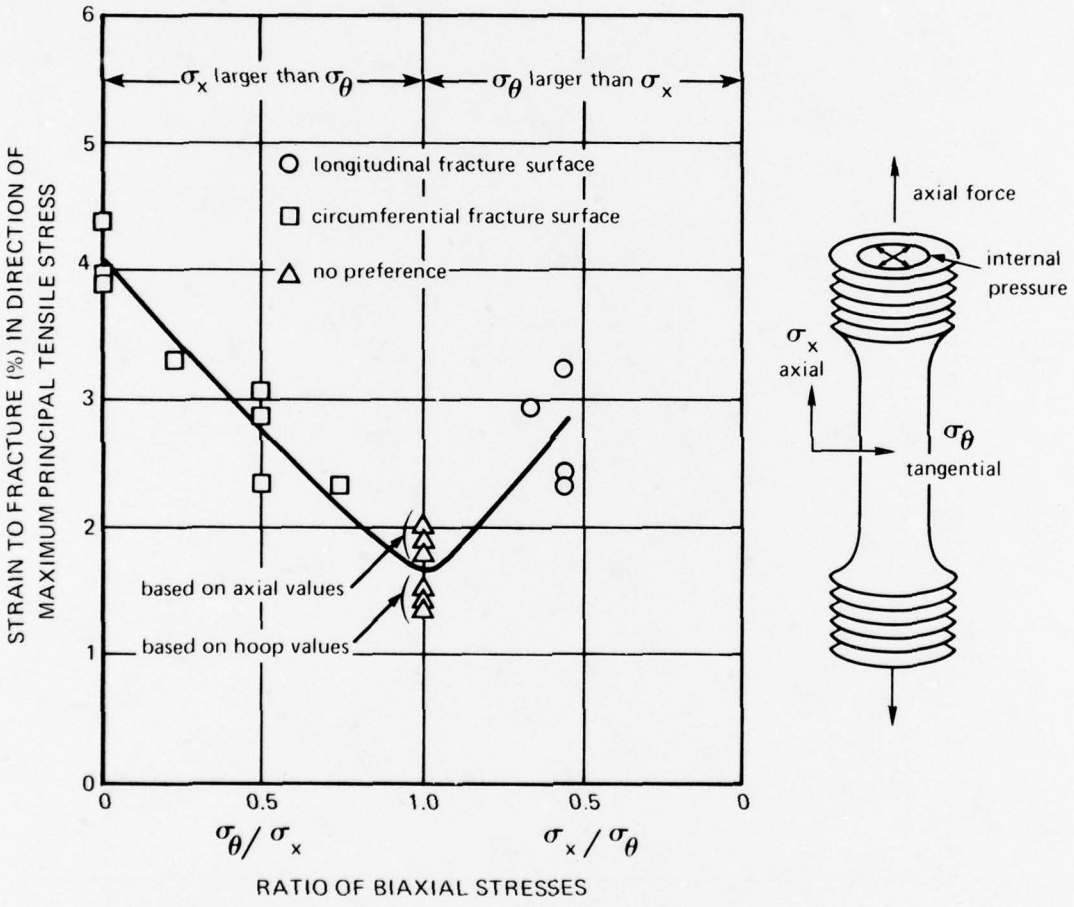

Figure 4.9. Effect of biaxial stress distribution on the magnitude of short-term strain at fracture in a room temperature environment (reference 4.2).

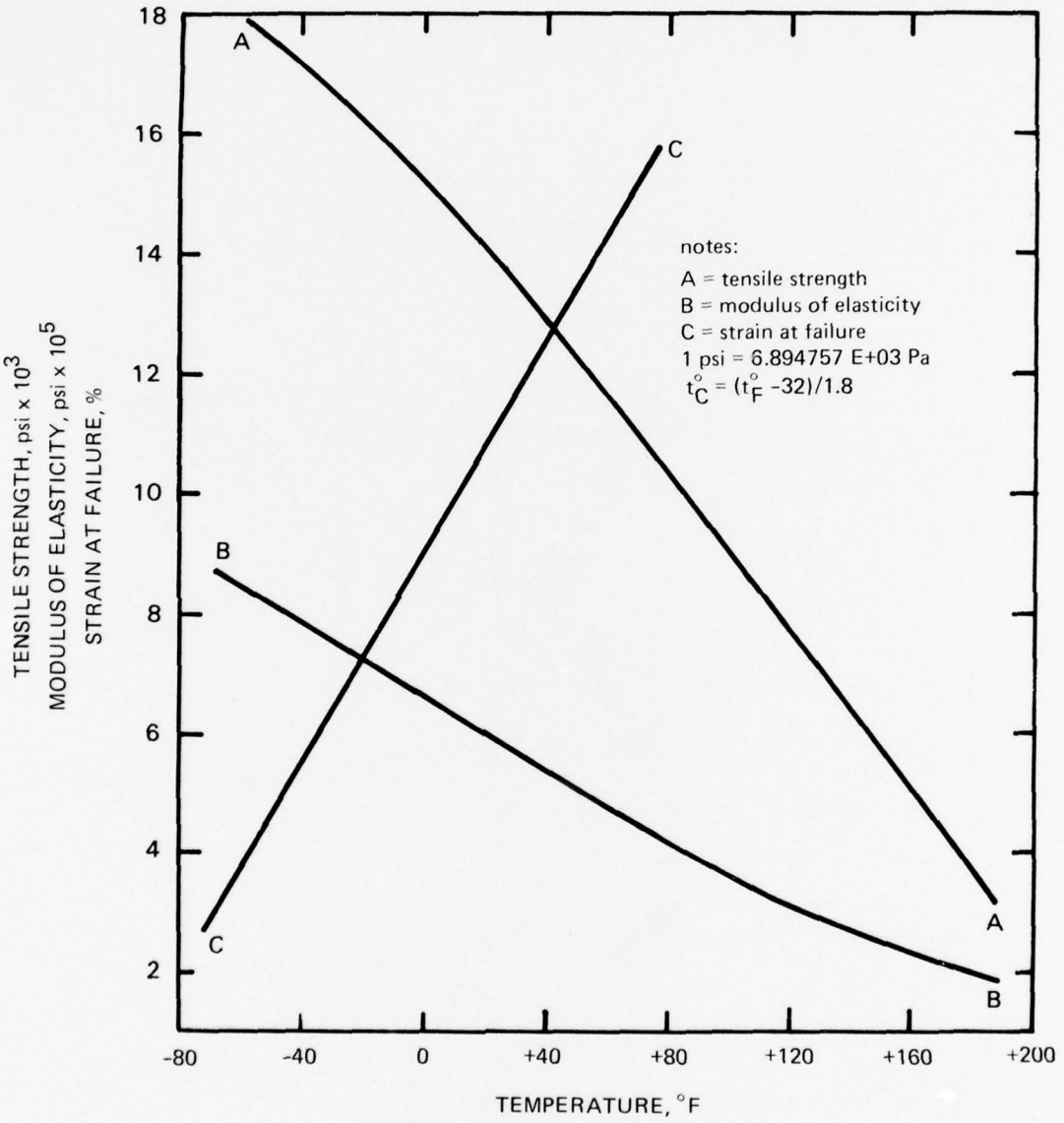

Figure 4.10. Effect of temperature on short-term tensile properties of 100-percent stretched acrylic plastic (reference 4.1).

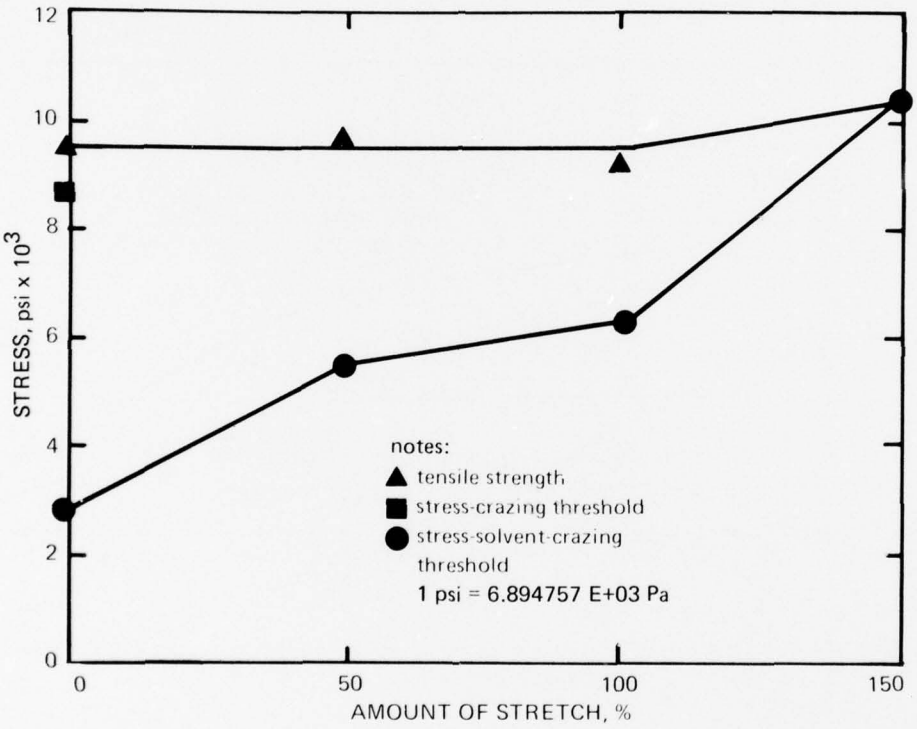

Figure 4.11. Effect of stretching on short-term tensile properties of acrylic plastic at room temperature (reference 4.1).

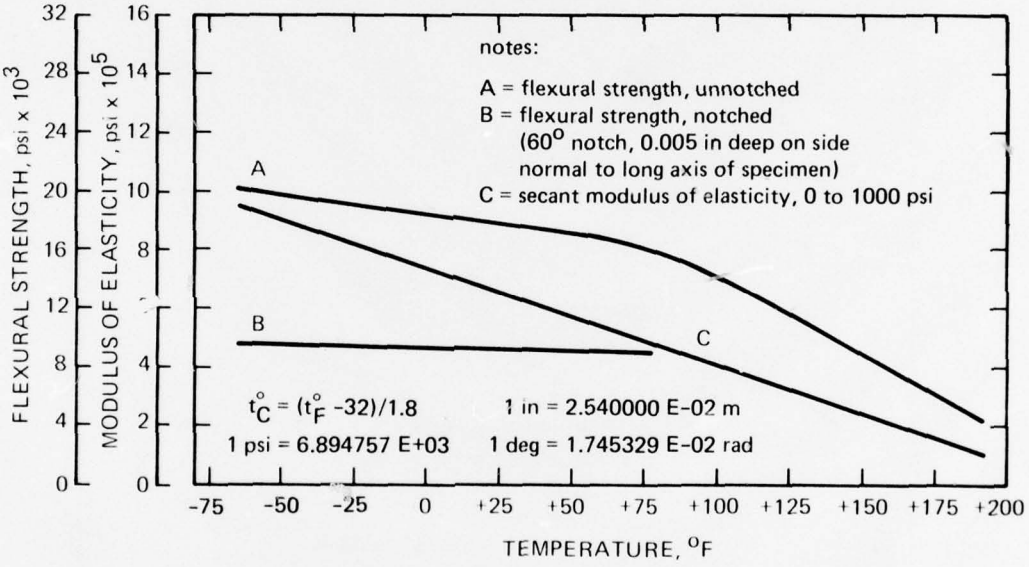

Figure 4.12. Effect of temperature on short-term flexural properties of notched and unnotched acrylic plastic (reference 4.1).

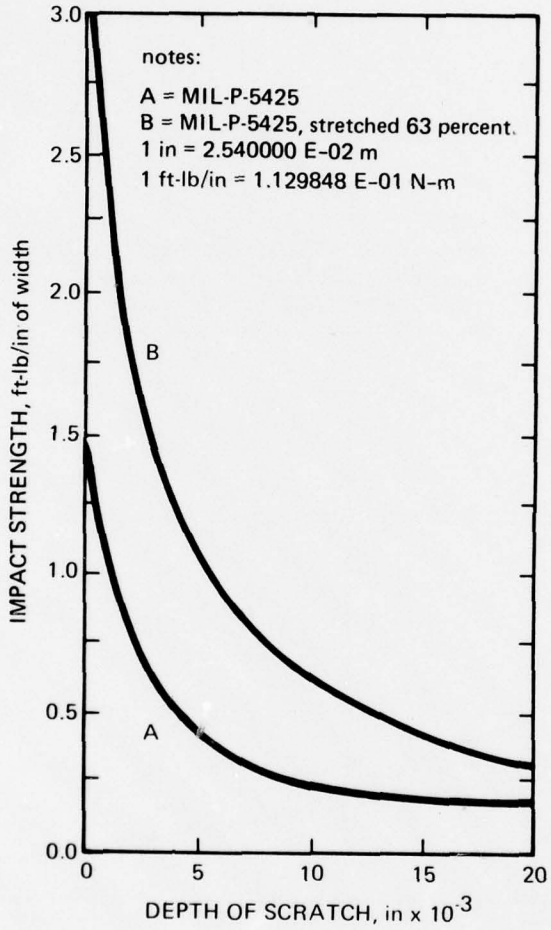

Figure 4.13. Effect of depth of ARTC needle scratch on Izod impact strength plastic at room temperature (reference 4.1).

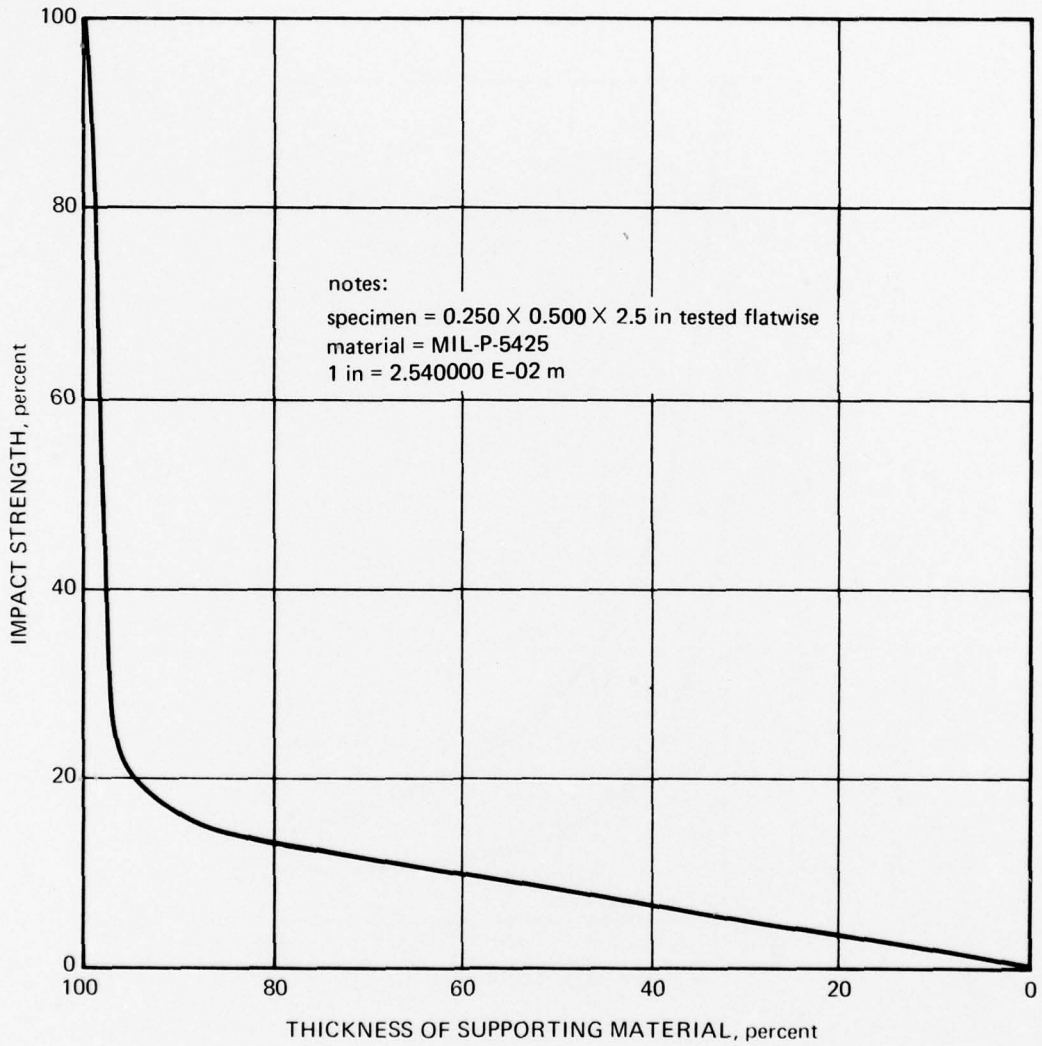

Figure 4.14. Impact strength as a function of thickness of supporting material below a deep surface scratch (reference 4.3).

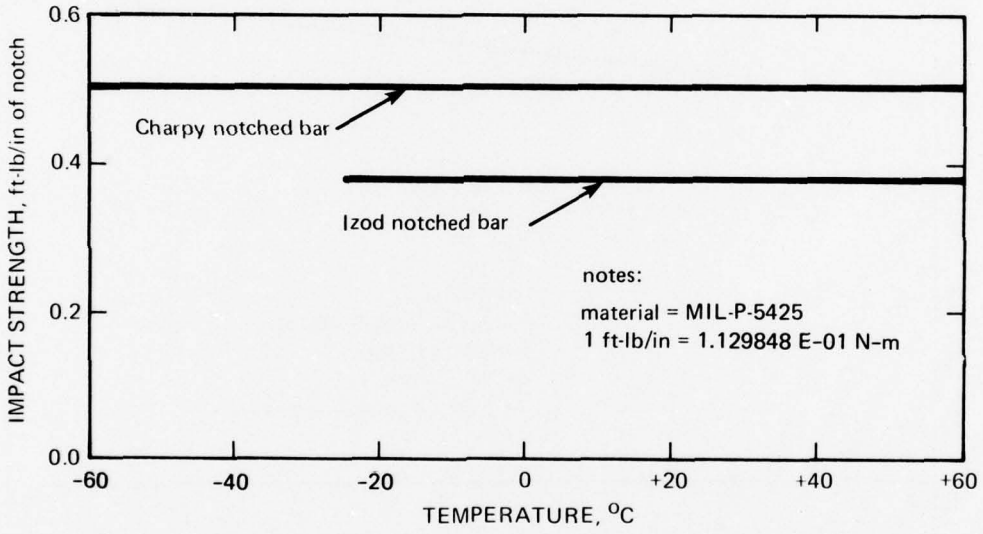

Figure 4.15. Effect of temperature on the impact strength of notched acrylic plastic (reference 4.3)

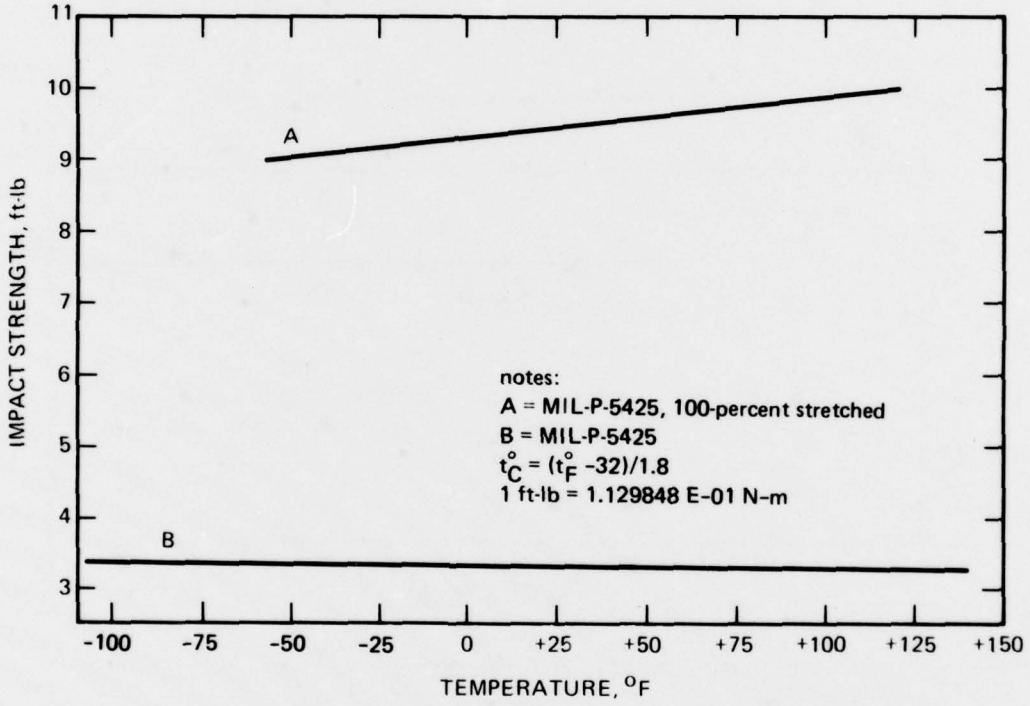

Figure 4.16. Effect of temperature on unnotched Charpy impact strength of stretched and unstretched acrylic plastic (reference 4.1).

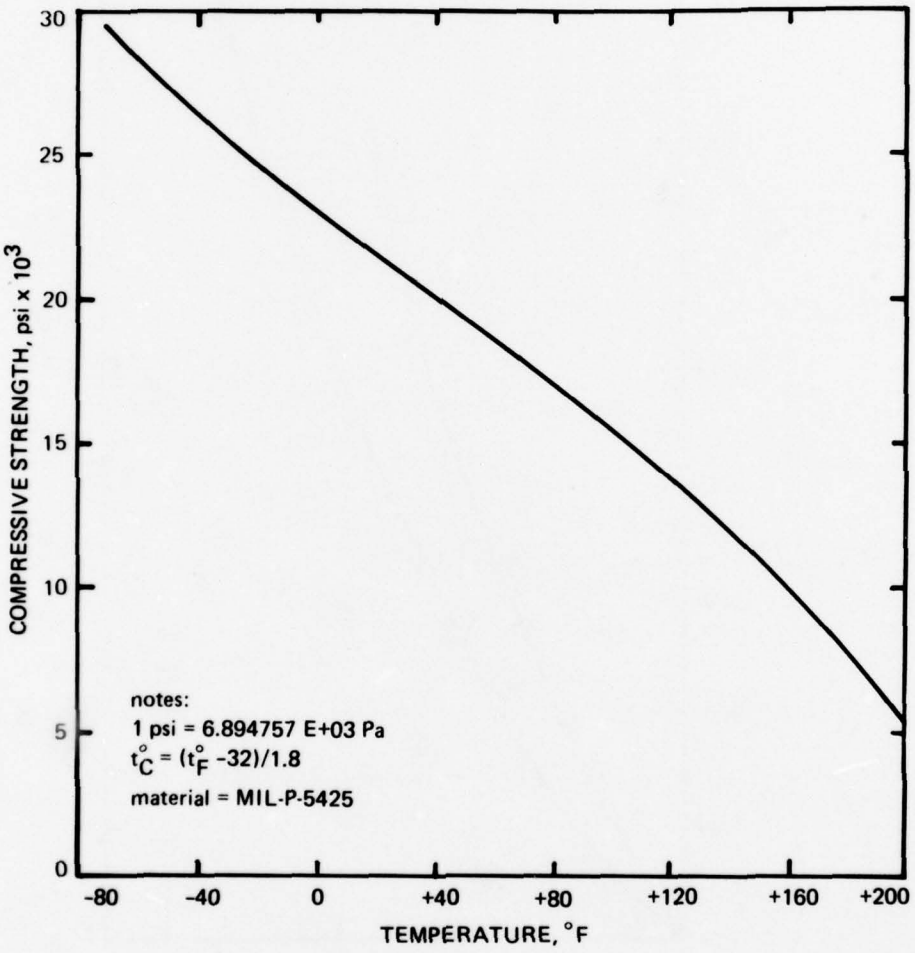

Figure 4.17. Effect of temperature on short-term compressive strength of acrylic plastic (reference 4.1).

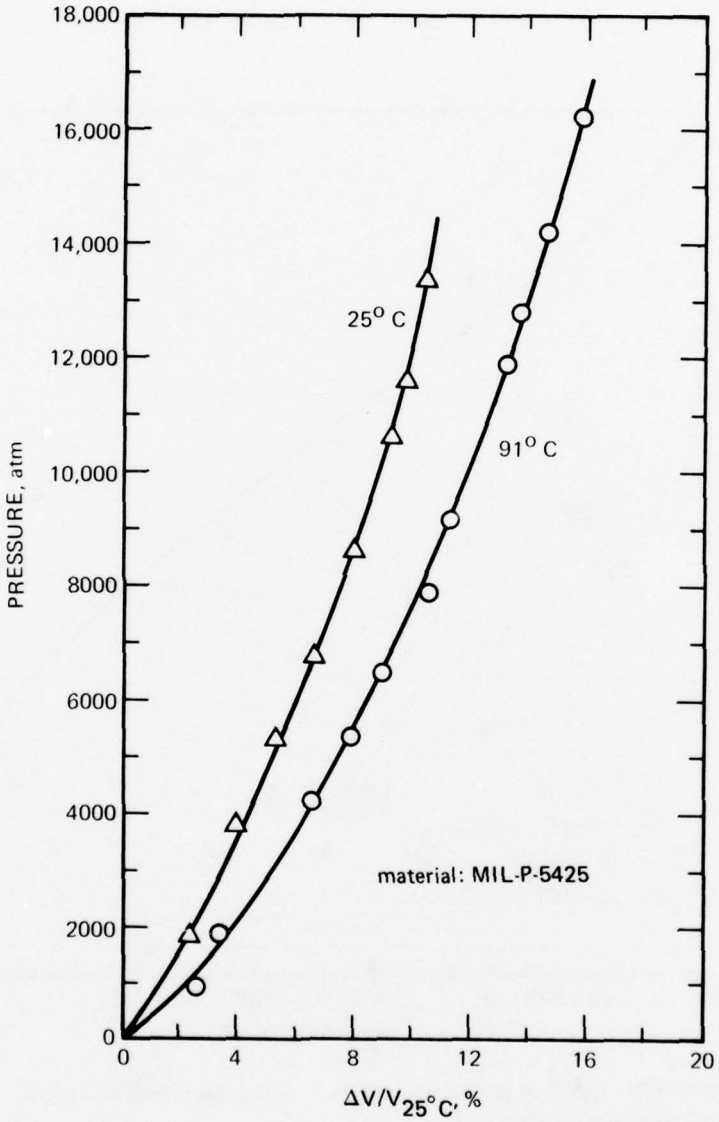

Figure 4.18. Compressibility of acrylic plastic under triaxial compressive loading (reference 4.4).

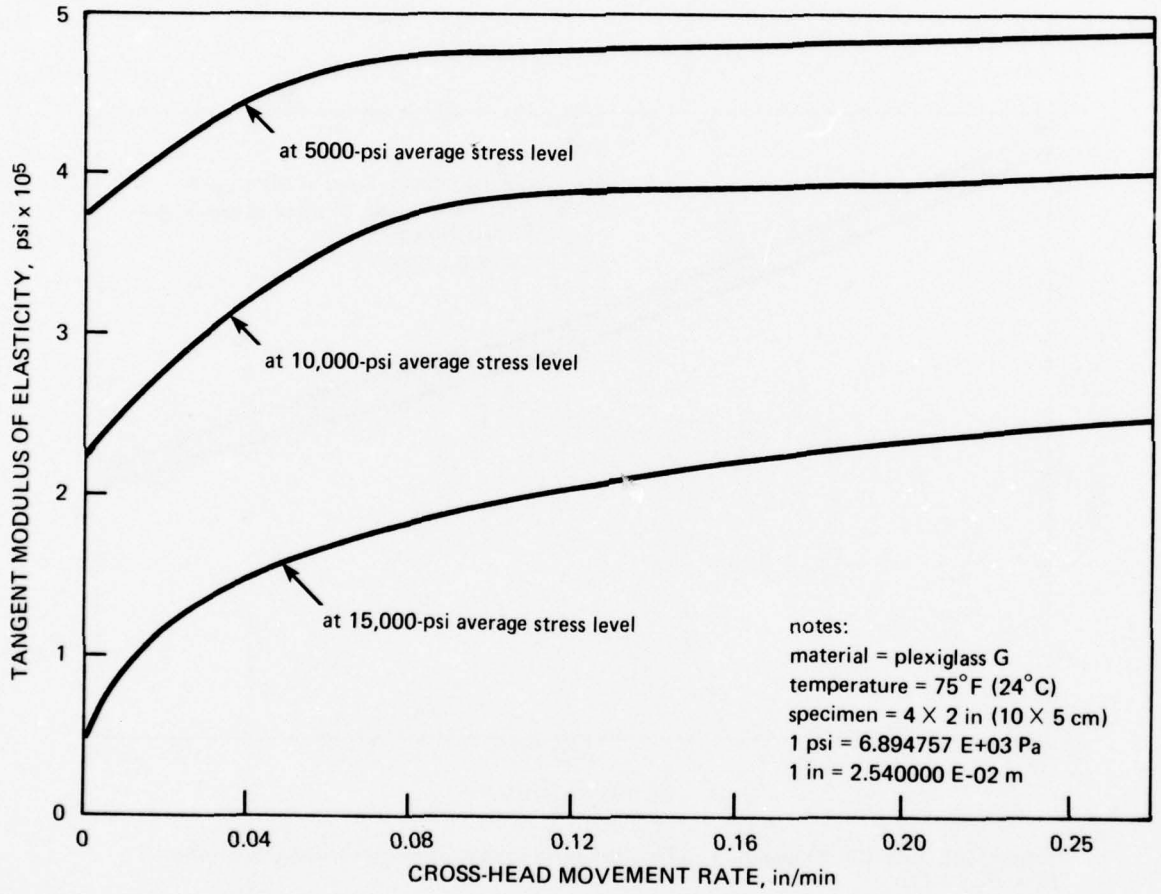

Figure 4.19. Effect of loading rate on the short-term compressive modulus of acrylic plastic at room temperature (reference 4.5).

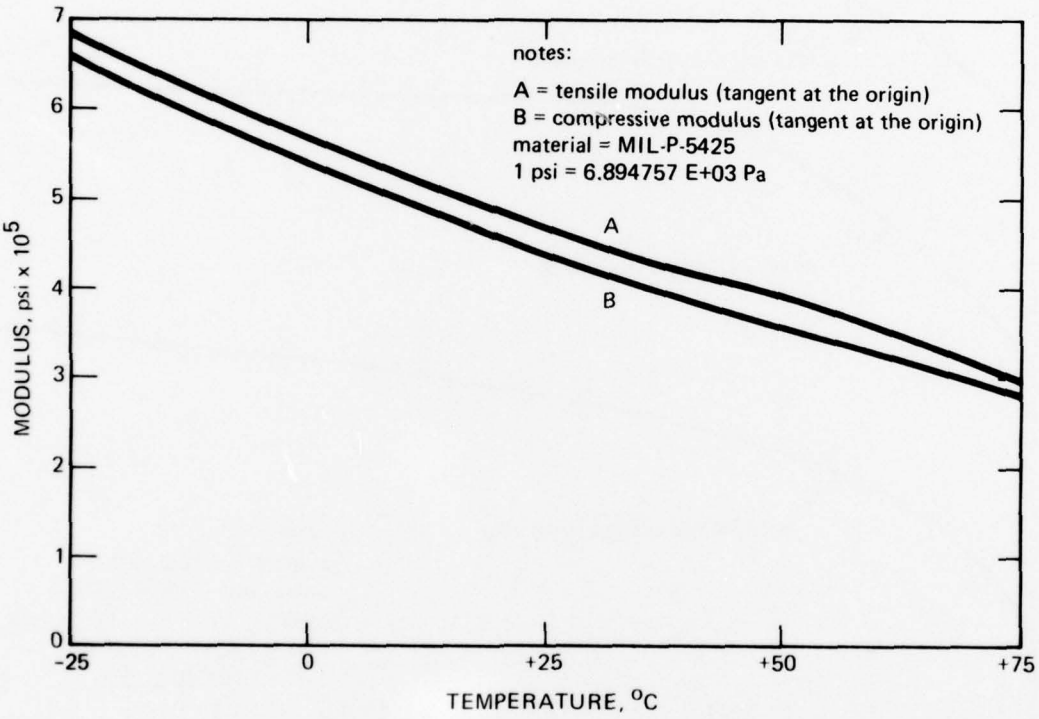

Figure 4.20. Effect of temperature on the short-term compressive modulus of acrylic plastic (reference 4.1).

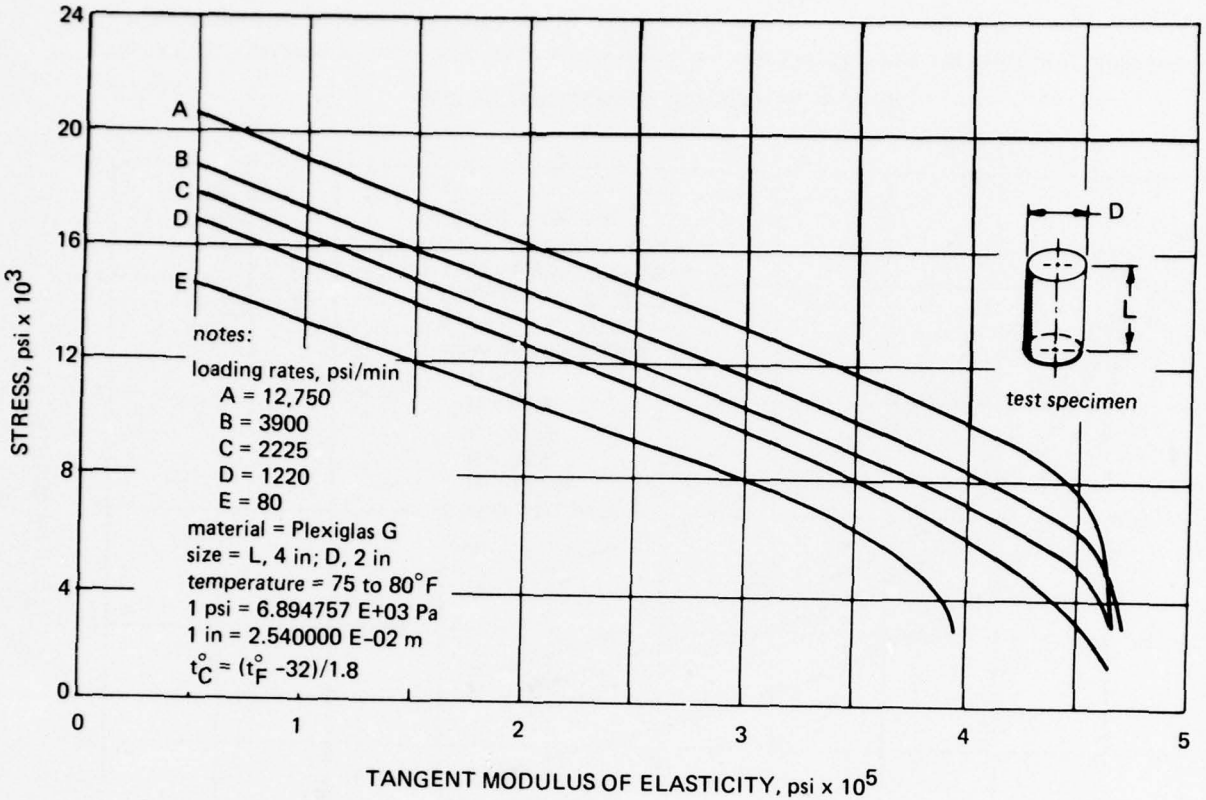

Figure 4.21. Compressive tangent modulus of acrylic plastic as a function of compressive stress under short-term loading at room temperature (reference 4.5).

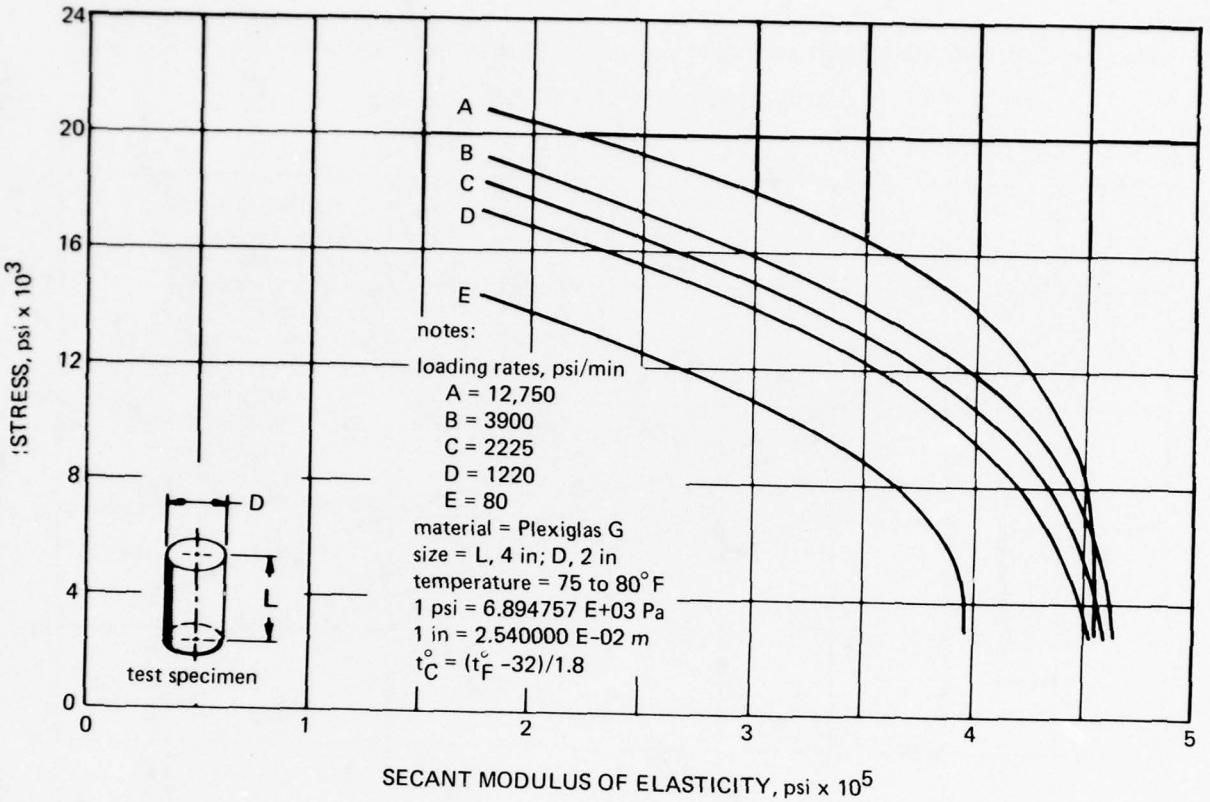

Figure 4.22. Compressive secant modulus of acrylic plastic as a function of compressive stress under short-term loading at room temperature (reference 4.5).

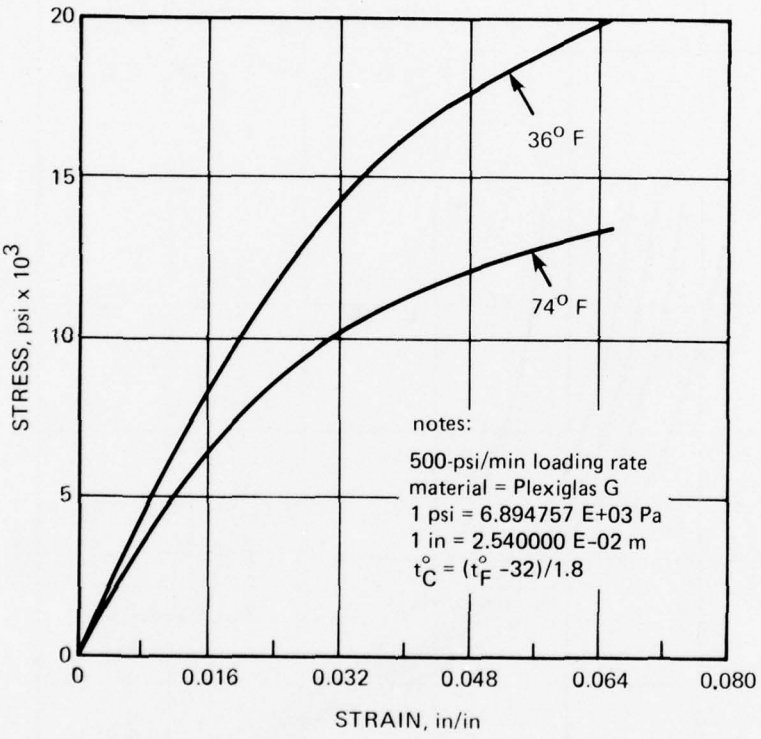

Figure 4.23. Effect of temperature on the short-term strain of acrylic plastic under compressive loading (reference 4.6).

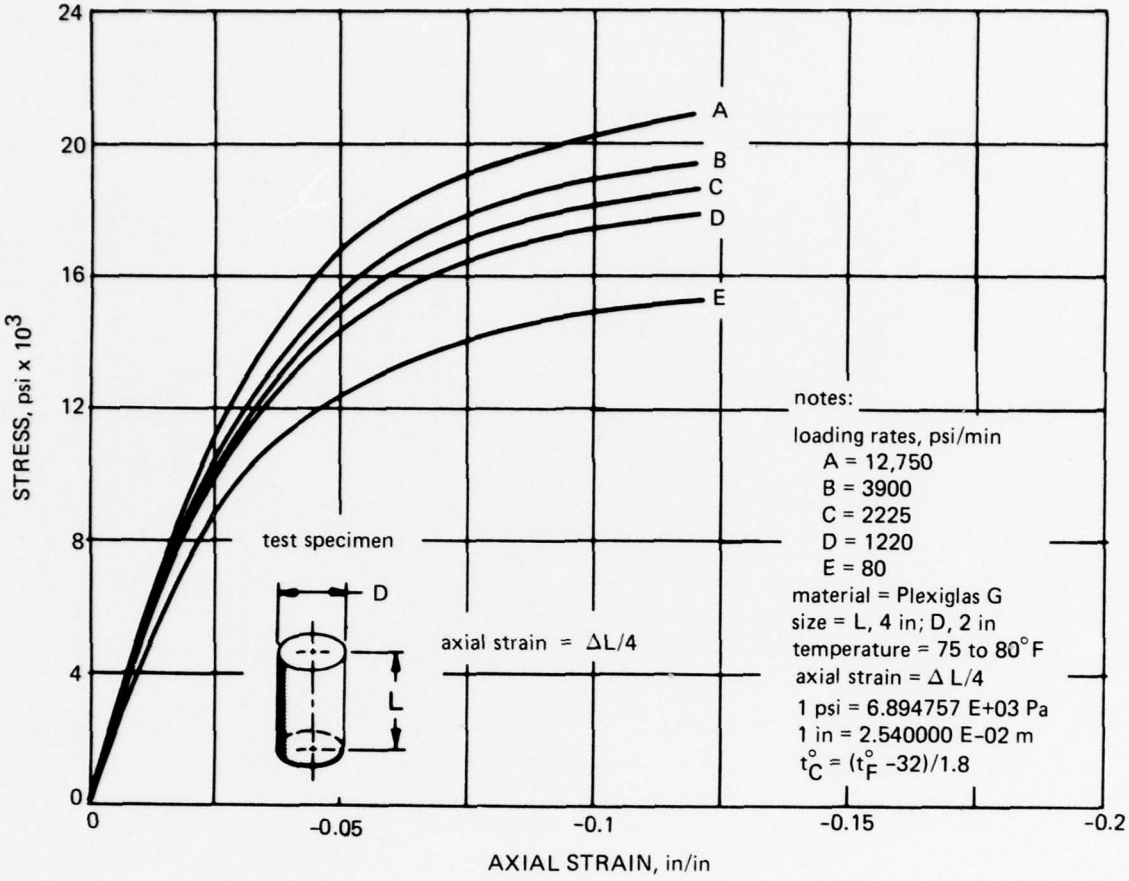

Figure 4.24. Effect of loading rate on the short-term compressive strain of acrylic plastic under compressive loading at room temperature (reference 4.5).

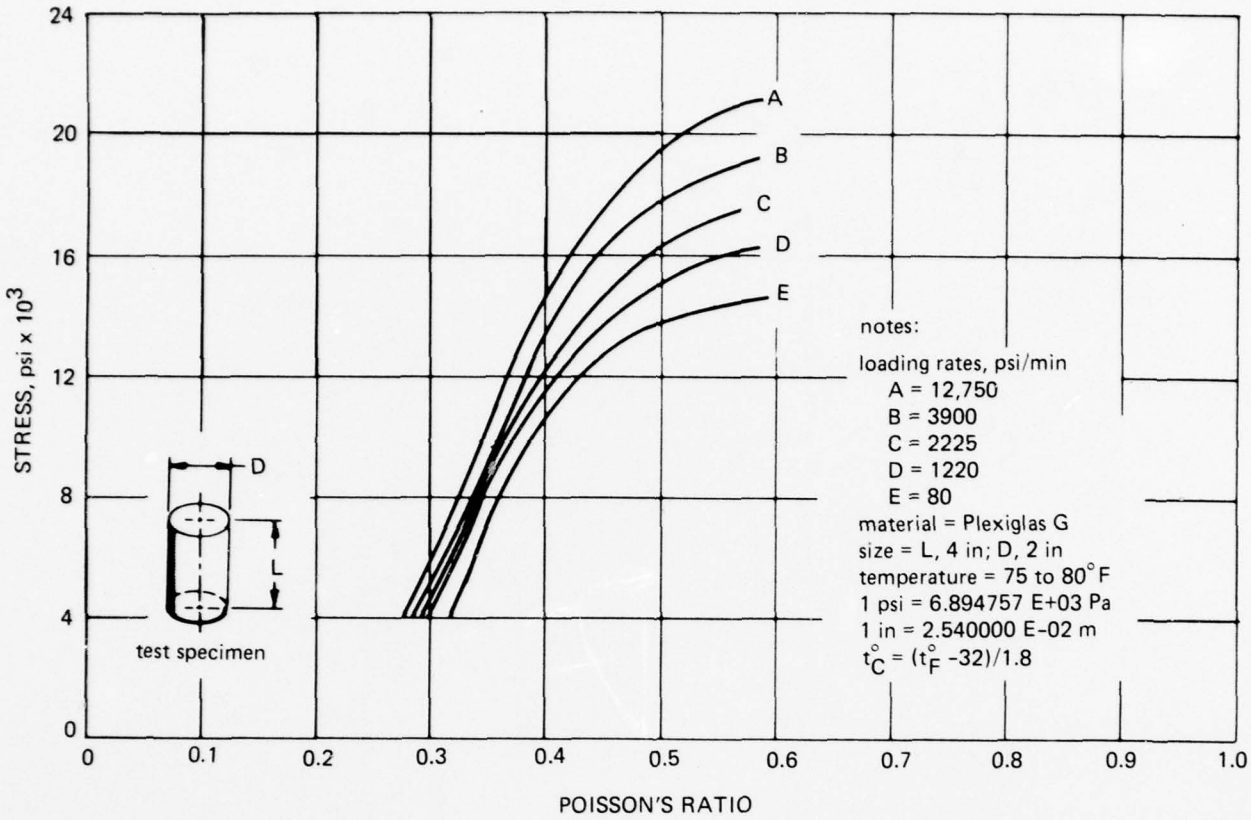

Figure 4.25. Effect of loading rate on the short-term Poisson's ratio under compressive loading at room temperature (reference 4.5).

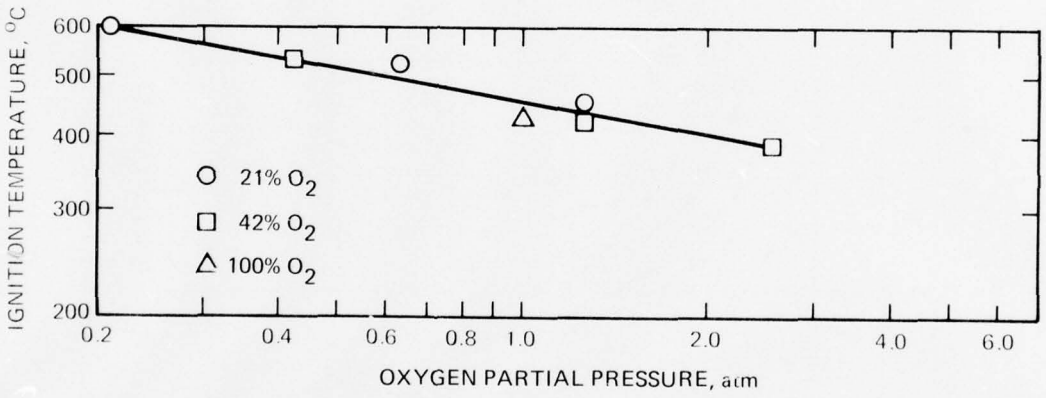

Figure 4.26. Effect of partial pressure of oxygen on the hot-plate minimum ignition temperature in oxygen-nitrogen mixtures (reference 4.7).

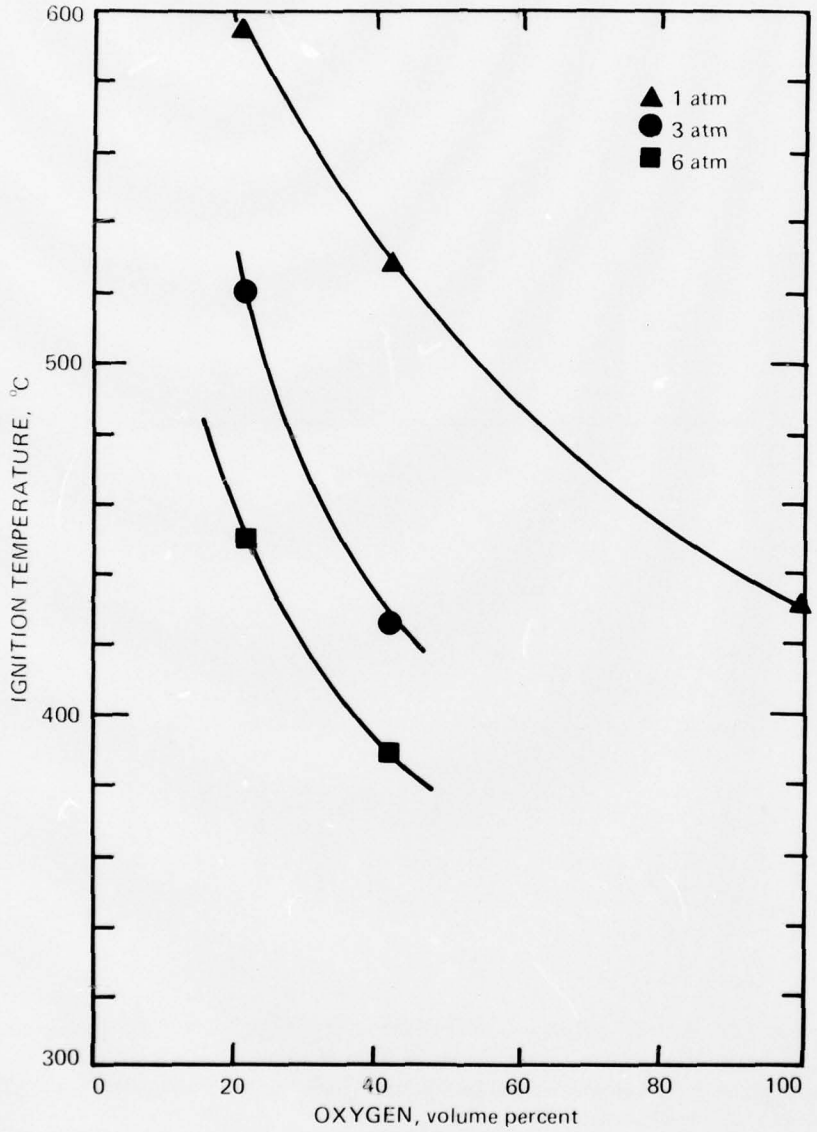

Figure 4.27. Effect of total ambient pressure on the minimum hot-plate ignition temperature of acrylic plastic in various oxygen-nitrogen mixtures (reference 4.7).

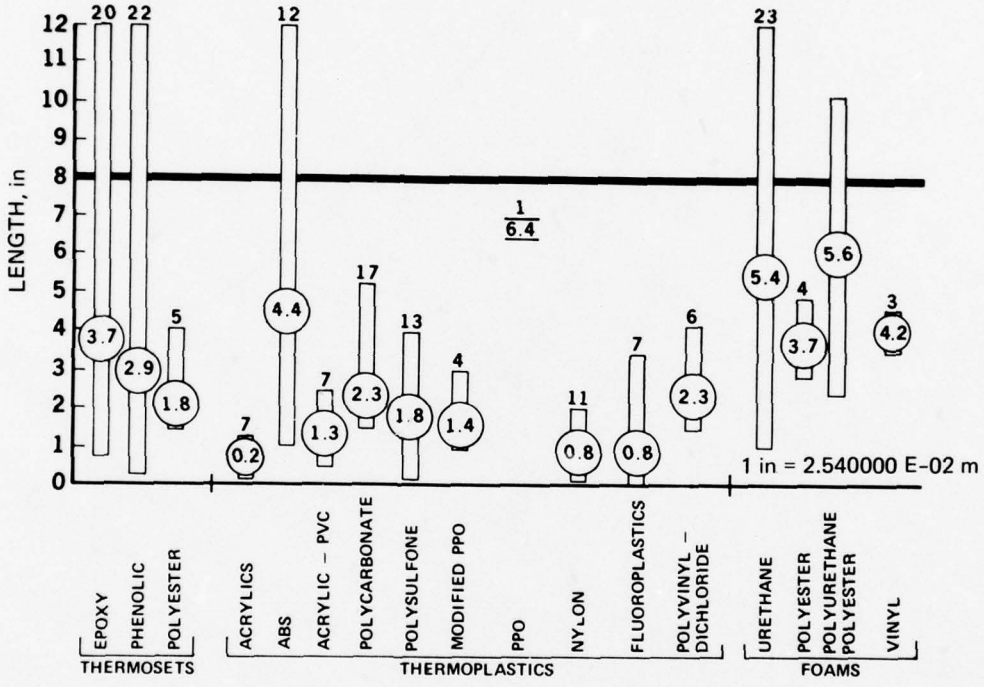

Figure 4.28. Burn length prior to self extinction of a vertical acrylic plastic strip after 12 seconds exposure to a Bunsen burner flame in an atmospheric environment. Mean readings are given inside circles, while the total number of specimens tested is shown above each bar (reference 4.8).

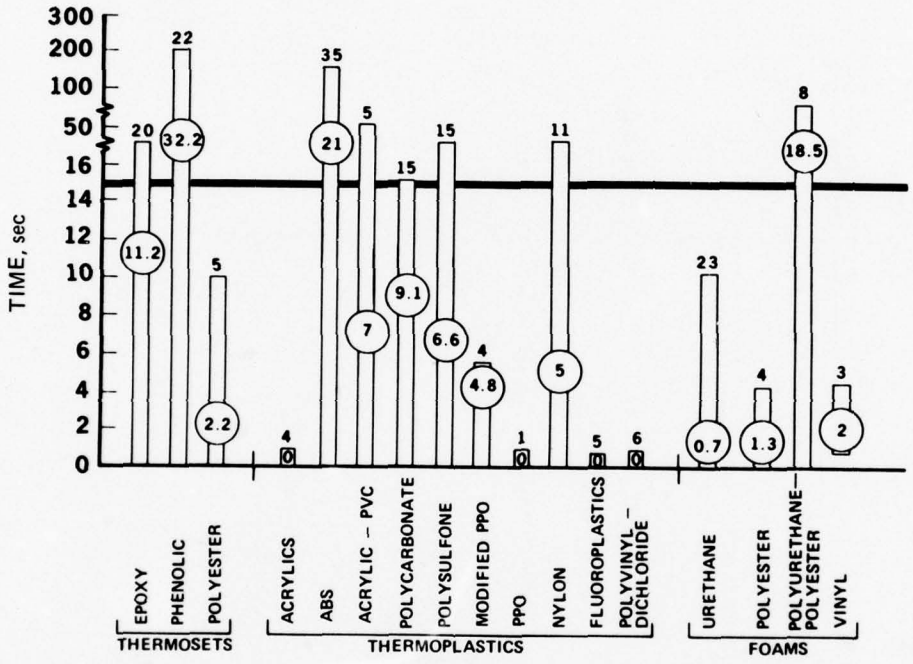

Figure 4.29. Flame time prior to self extinction of a vertical acrylic plastic strip after 12 seconds of exposure to a Bunsen burner flame in an atmospheric environment. Mean readings are given inside circles, while the total number of specimens is shown above each bar (reference 4.8).

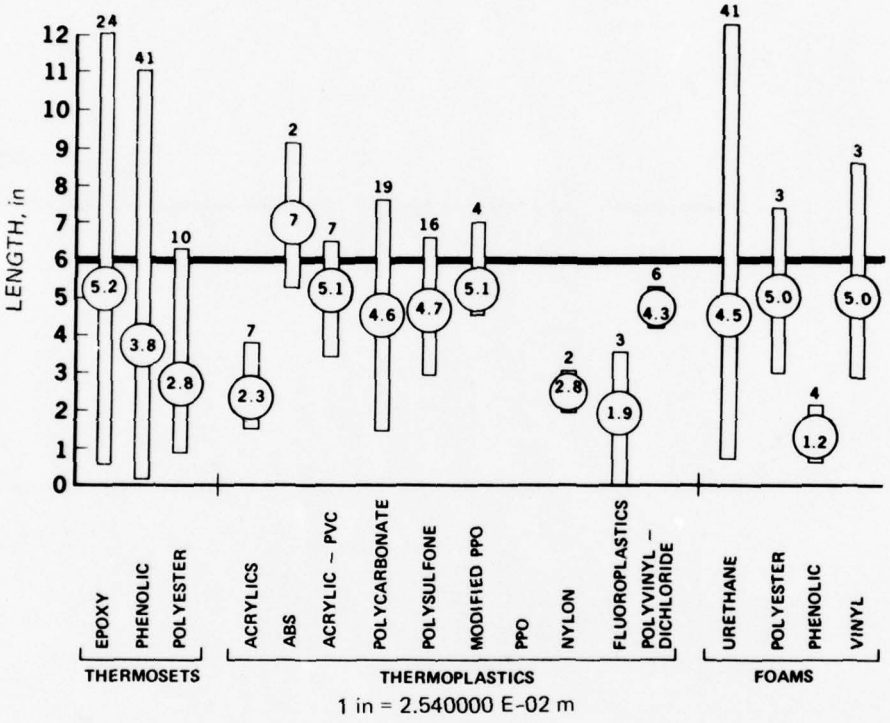

Figure 4.30. Burn length prior to self extinction of a vertical acrylic plastic strip after 60 seconds of exposure to a Bunsen burner flame in an atmospheric environment. Mean readings are given inside circles, while the total number of specimens is shown above each bar (reference 4.8).

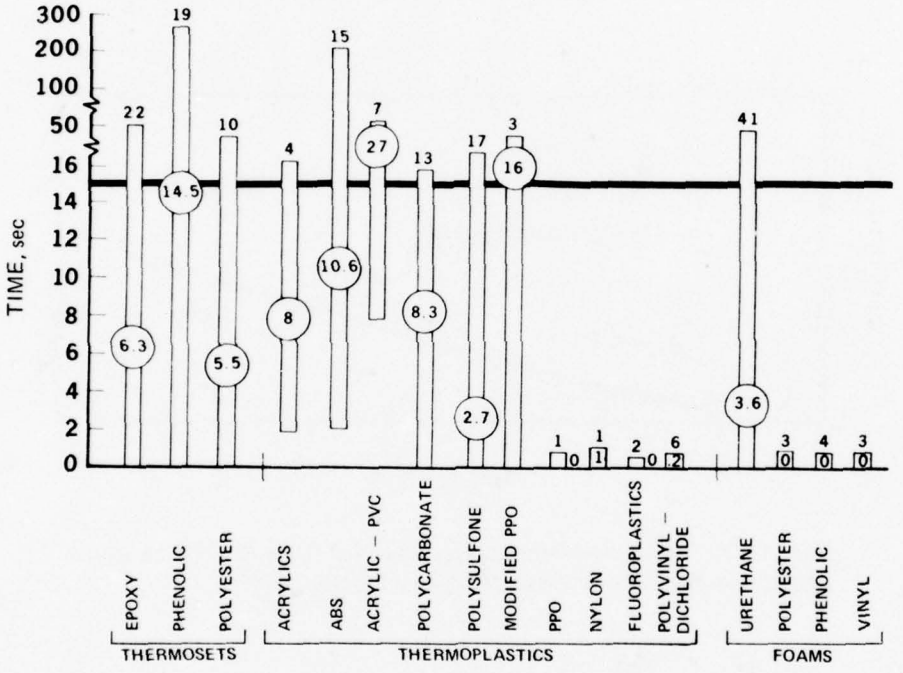

Figure 4.31. Flame time prior to self extinction of a vertical acrylic plastic strip after 60 seconds of exposure to a Bunsen burner flame in an atmospheric environment. Mean readings are inside circles, while the total number of specimens is shown above each bar (reference 4.3).

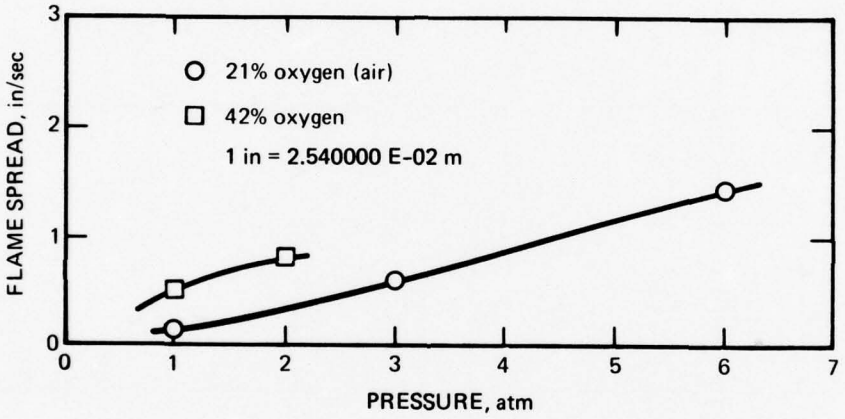

Figure 4.32. Effect of total pressure on the rate of flame spread of an acrylic plastic strip inclined at 45 degrees (0.8 radian) (reference 4.7).

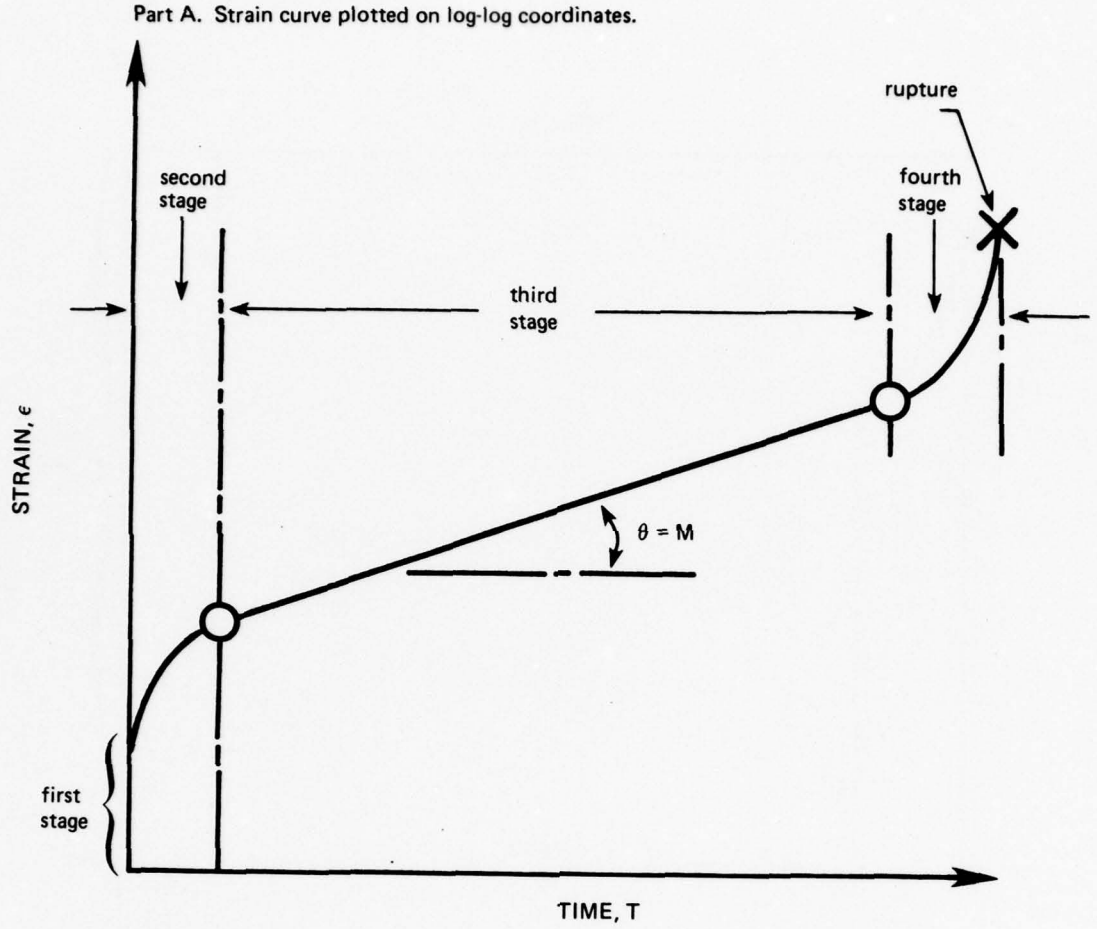

Figure 4.33. Curves for strain and effective modulus for acrylic plastic subjected to long-term sustained loading (reference 4.11).

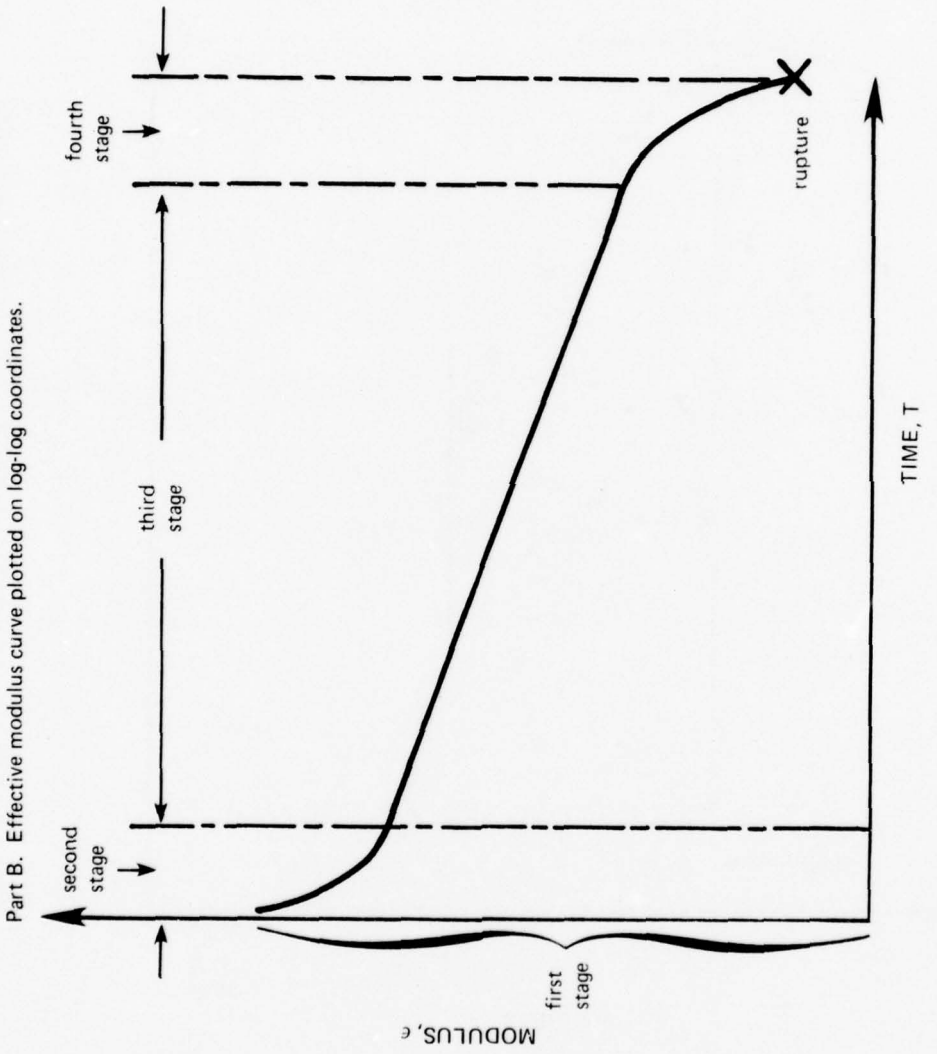

Figure 4.33. Continued

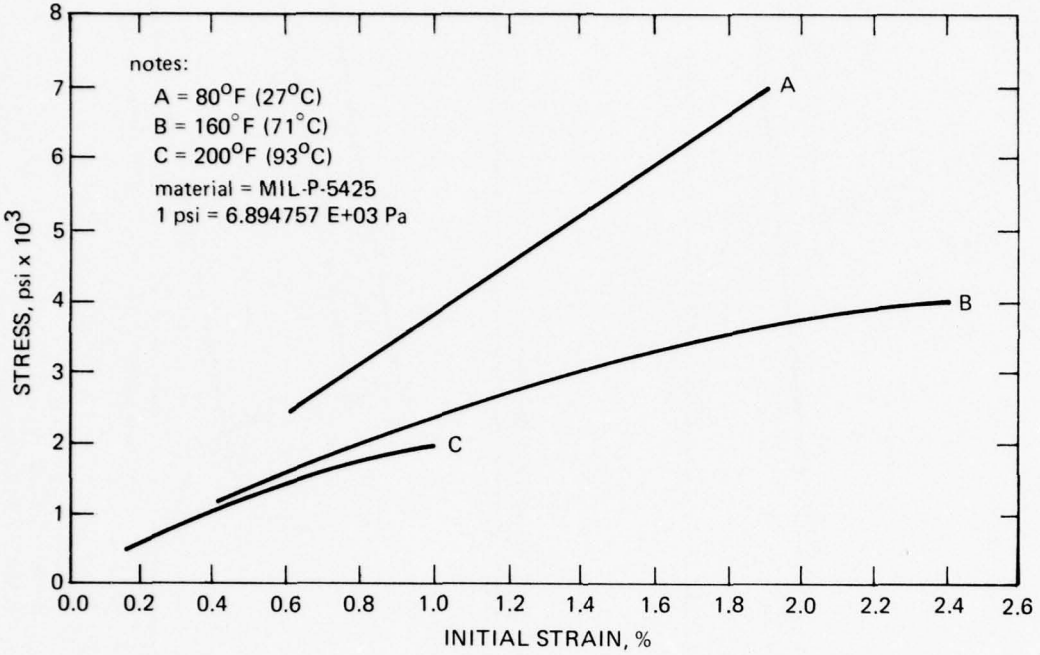

Figure 4.34. Effect of stress and temperature on initial strain during the first (instantaneous) stage of deformation in acrylic plastic under sustained tensile loading. The third stage of deformation for the same specimens is shown on figure 4.35.

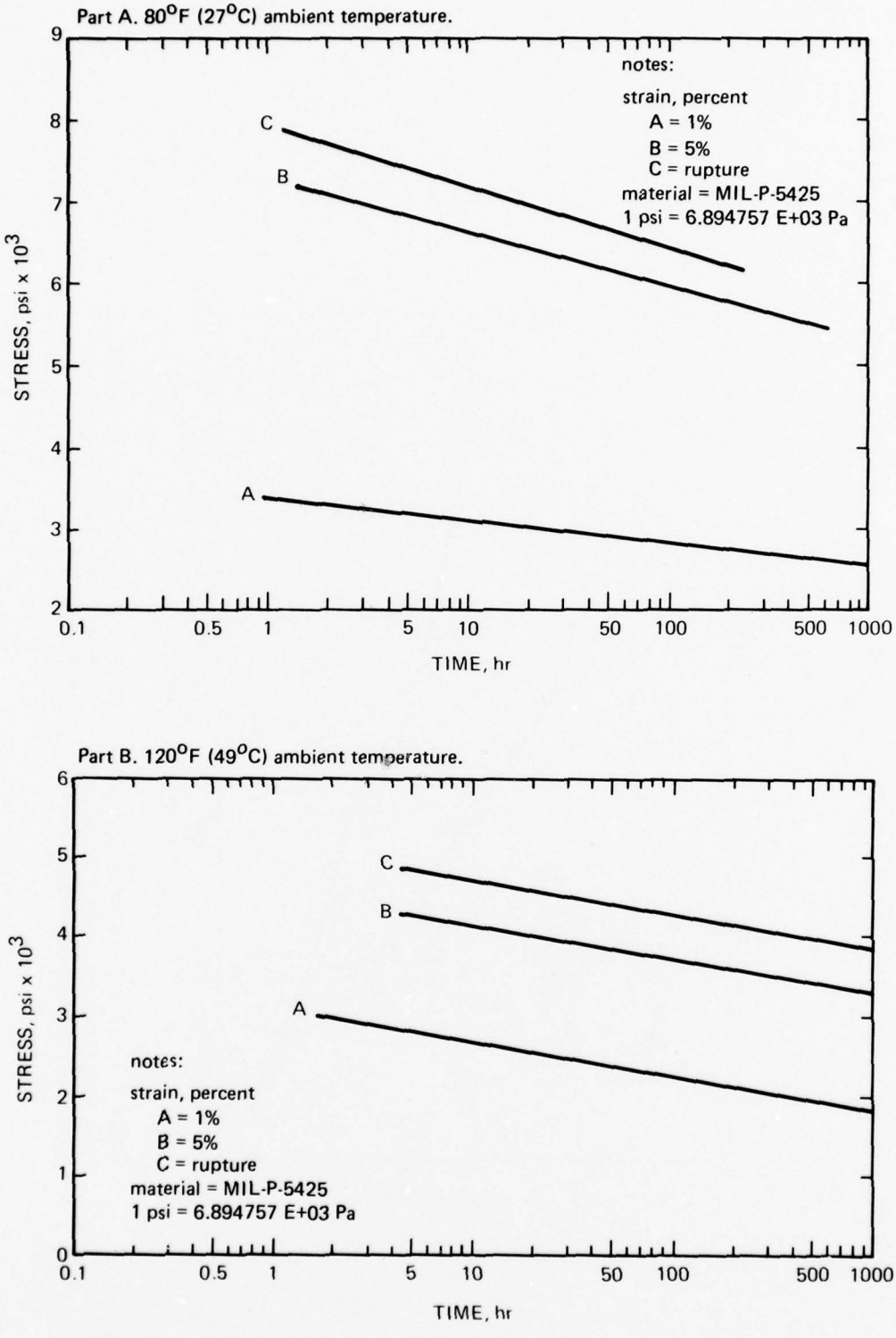

Figure 4.35. Behavior of acrylic plastic under long-term sustained tensile loading in laboratory environment (reference 4.1).

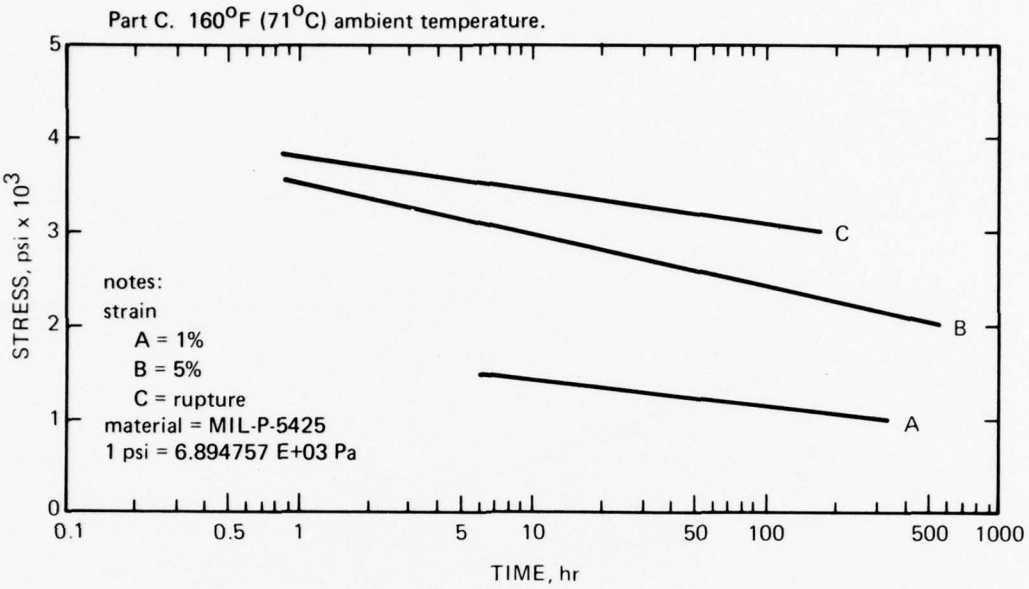

Figure 4.35. Continued.

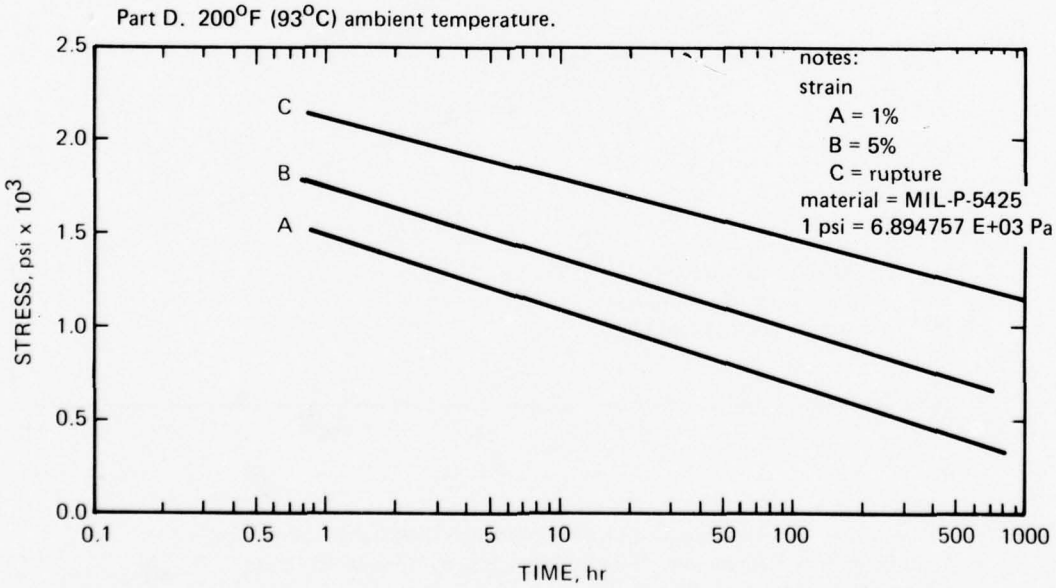

Figure 4.35. Continued.

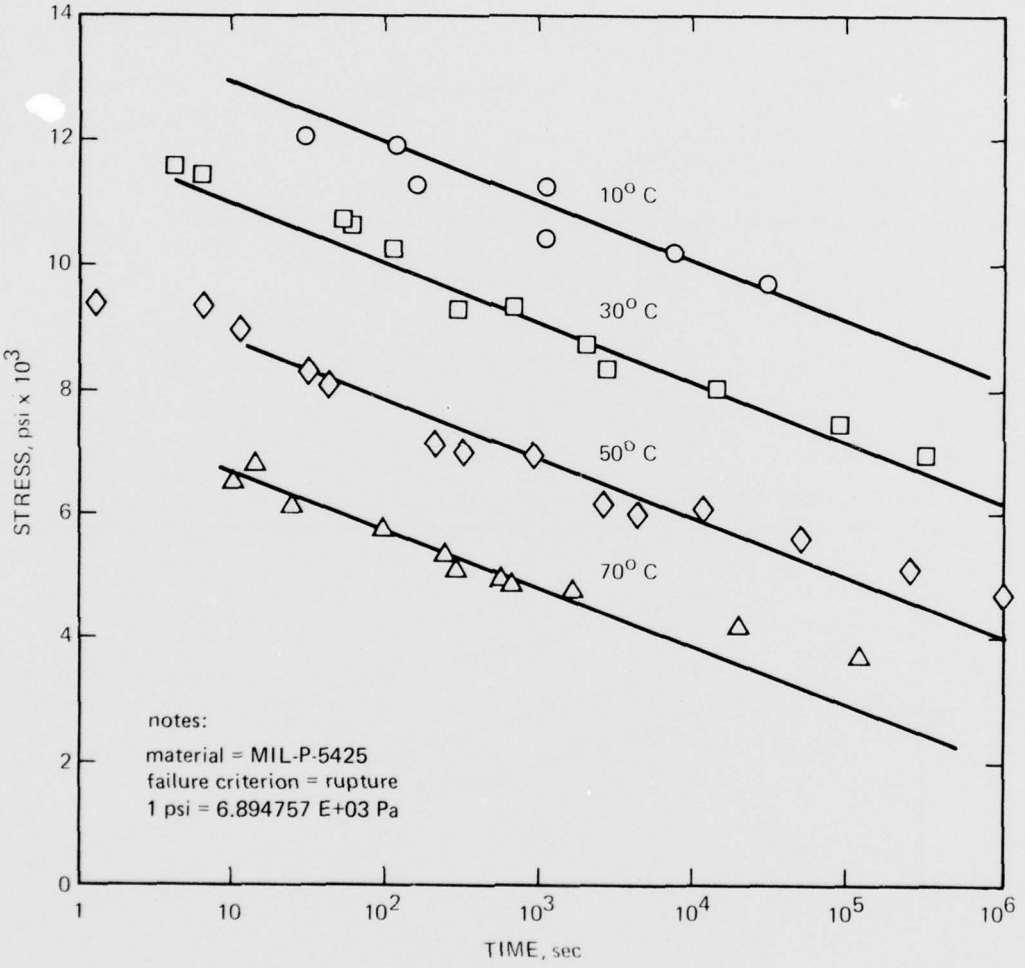

Figure 4.36. Rupture stresses of acrylic plastic under sustained tensile loading in a laboratory environment whose ambient temperature can vary from 10 to 70°C (reference 4.9).

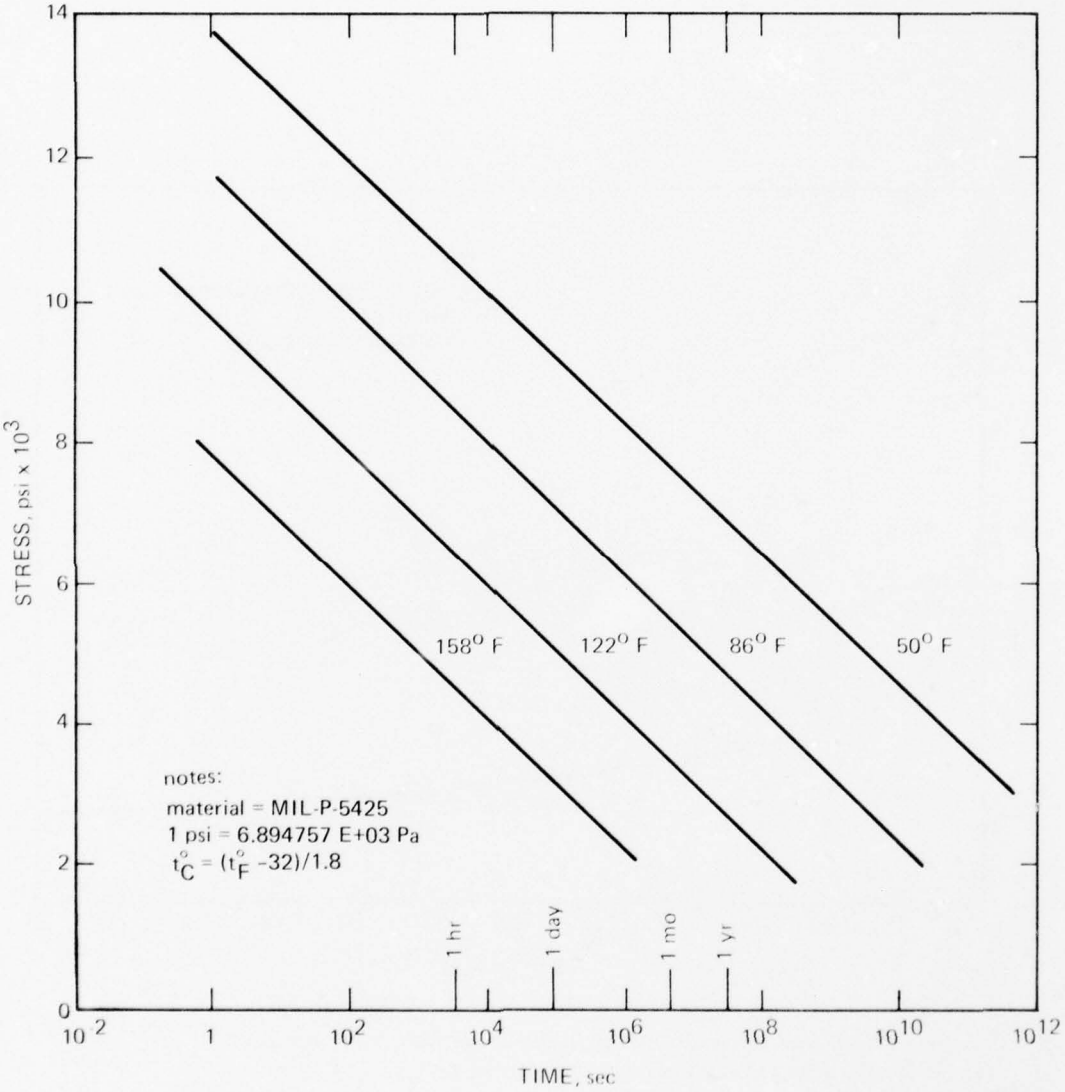

Figure 4.37. Extrapolated rupture stresses of acrylic plastic under sustained tensile loading in a laboratory environment at different ambient temperatures (reference 4.9).

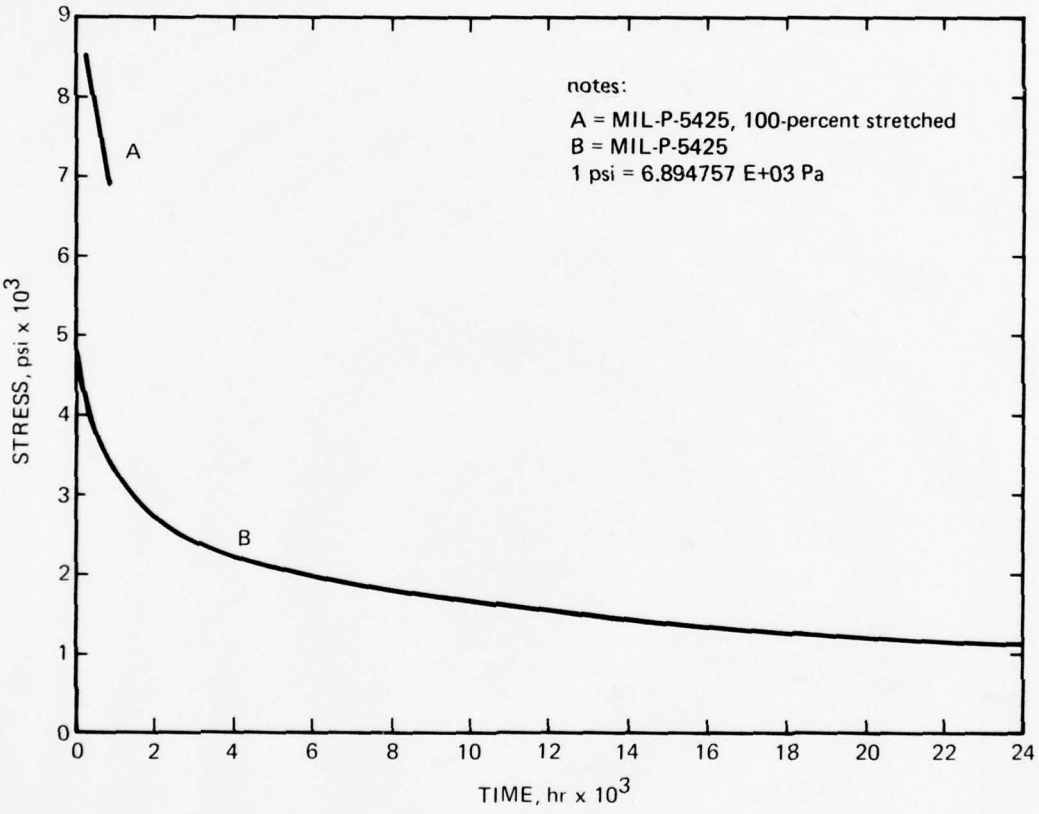

Figure 4.38. Rupture stress level of acrylic plastic under long-term sustained tensile loading in an outdoor environment (reference 4.1).

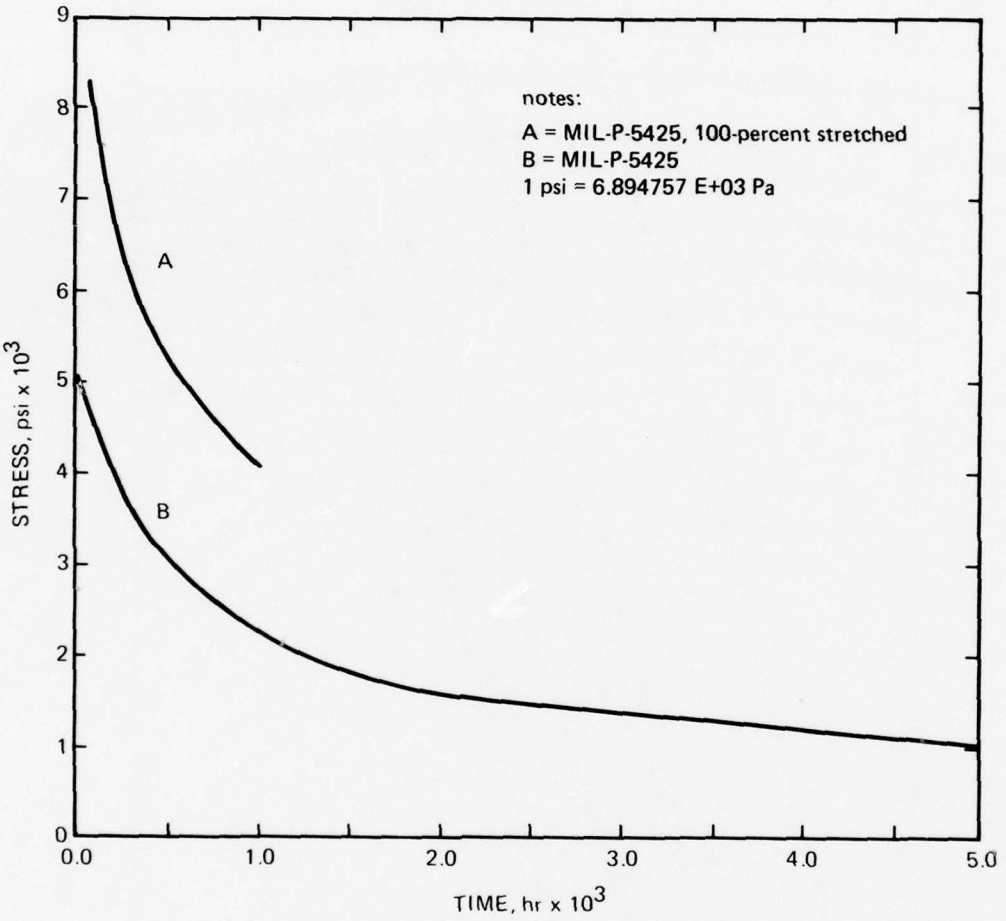

Figure 4.39. Initiation of crazing on surfaces of acrylic plastic under long-term sustained tensile loading in an outdoor environment (reference 4.1).

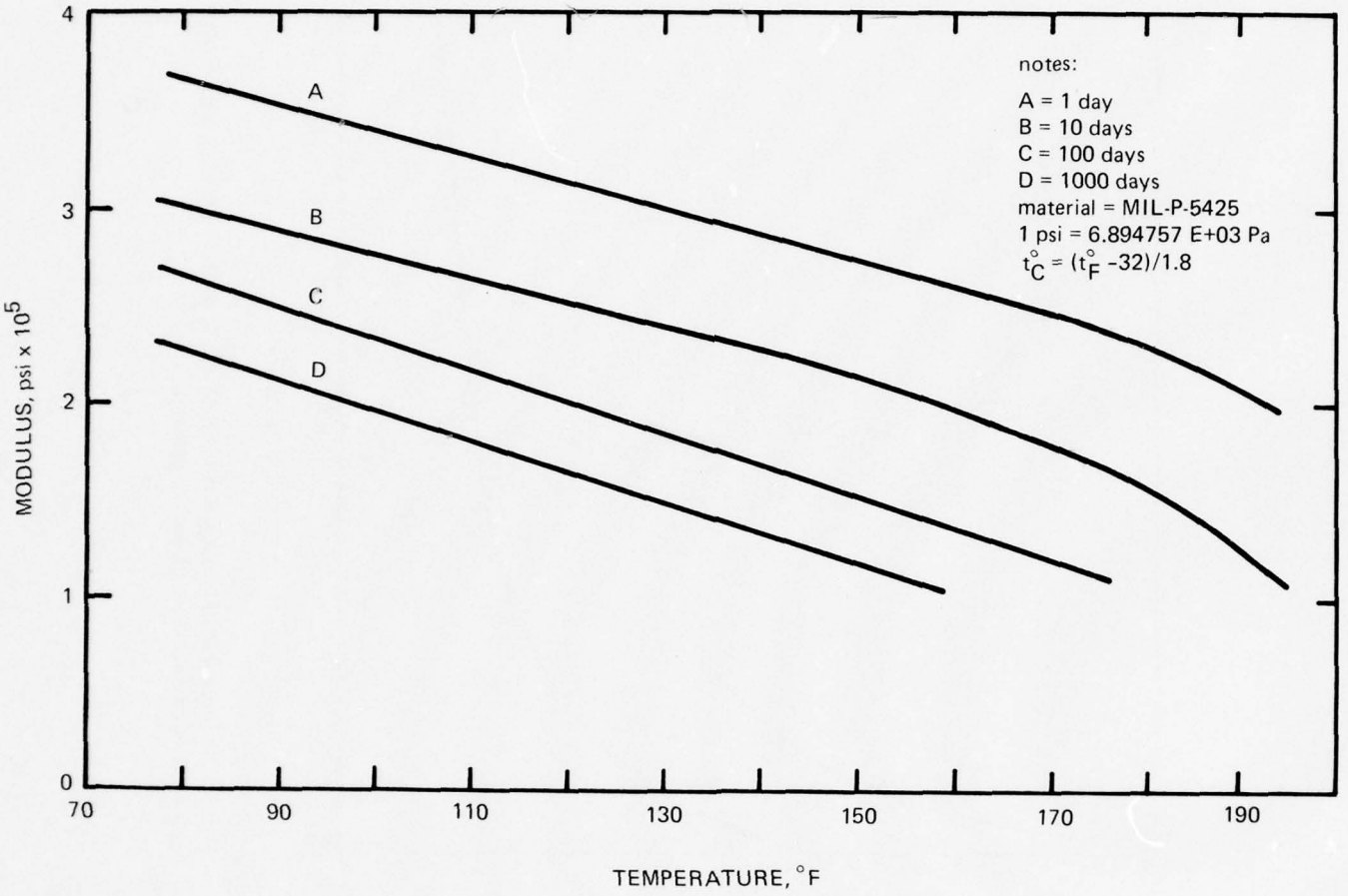

Figure 4.40. Effective modulus of acrylic plastic under long-term sustained tensile loading in a laboratory environment whose ambient temperature can vary from 70° to 190° F (21 to 88° C) (reference 4.1).

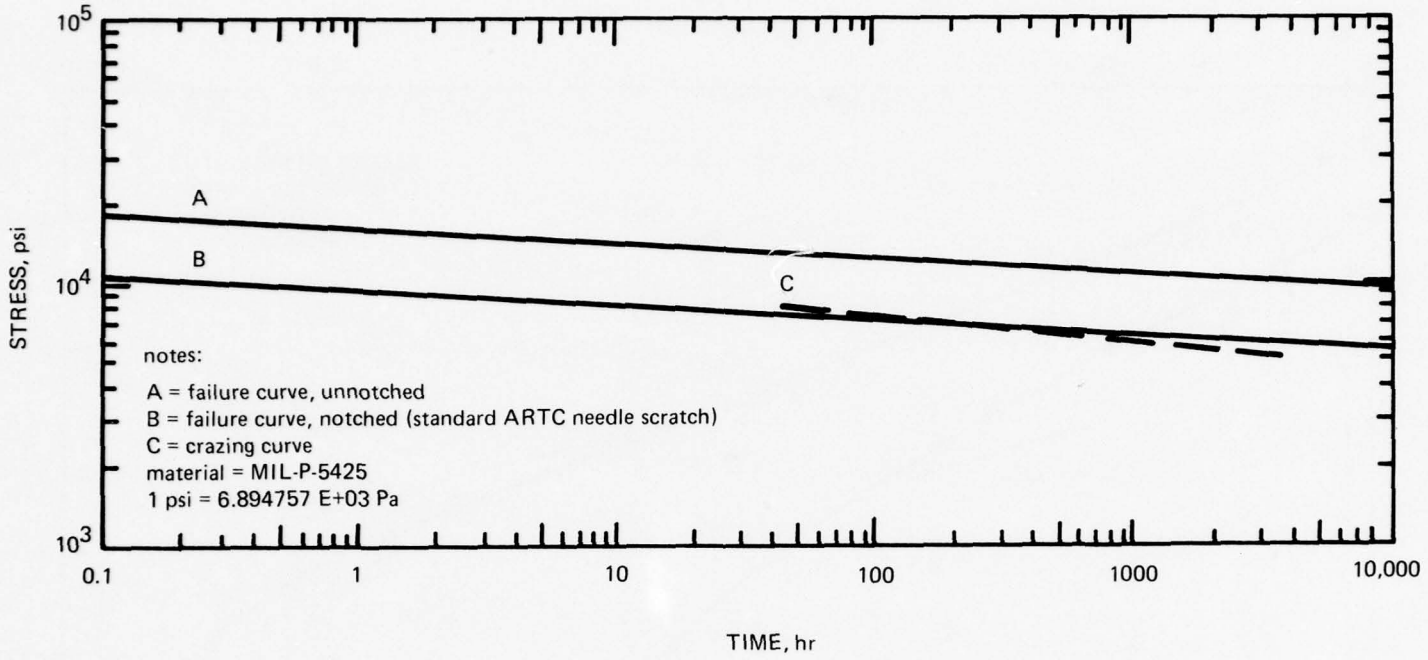

Figure 4.41. Rupture stress and initiation of surface crazing on acrylic plastic with notched and unnotched surfaces. Long-term sustained flexural loading in a laboratory environment at room temperature (reference 4.1).

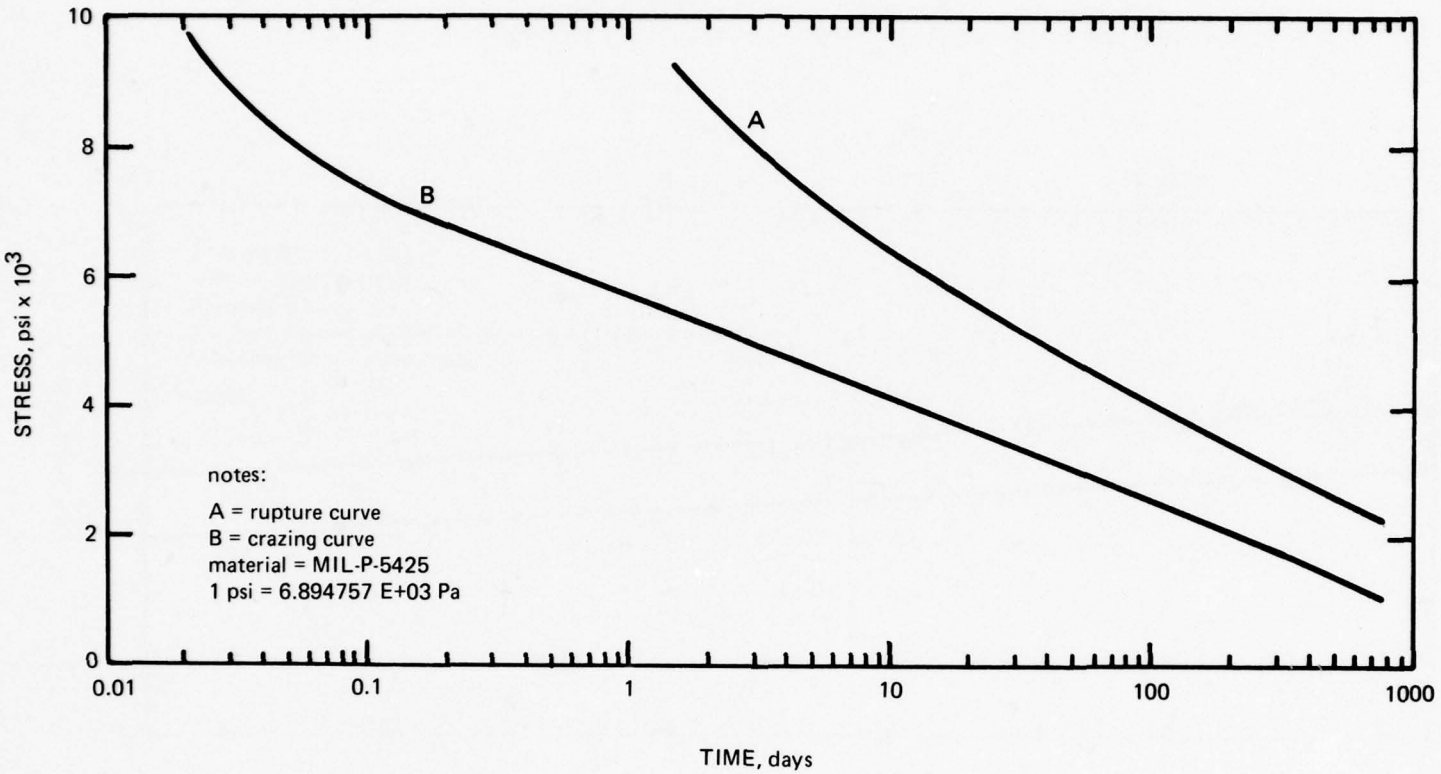

Figure 4.42. Rupture stress and initiation of surface crazing on acrylic plastic. Long-term sustained flexural loading in an outdoor environment (reference 4.1).

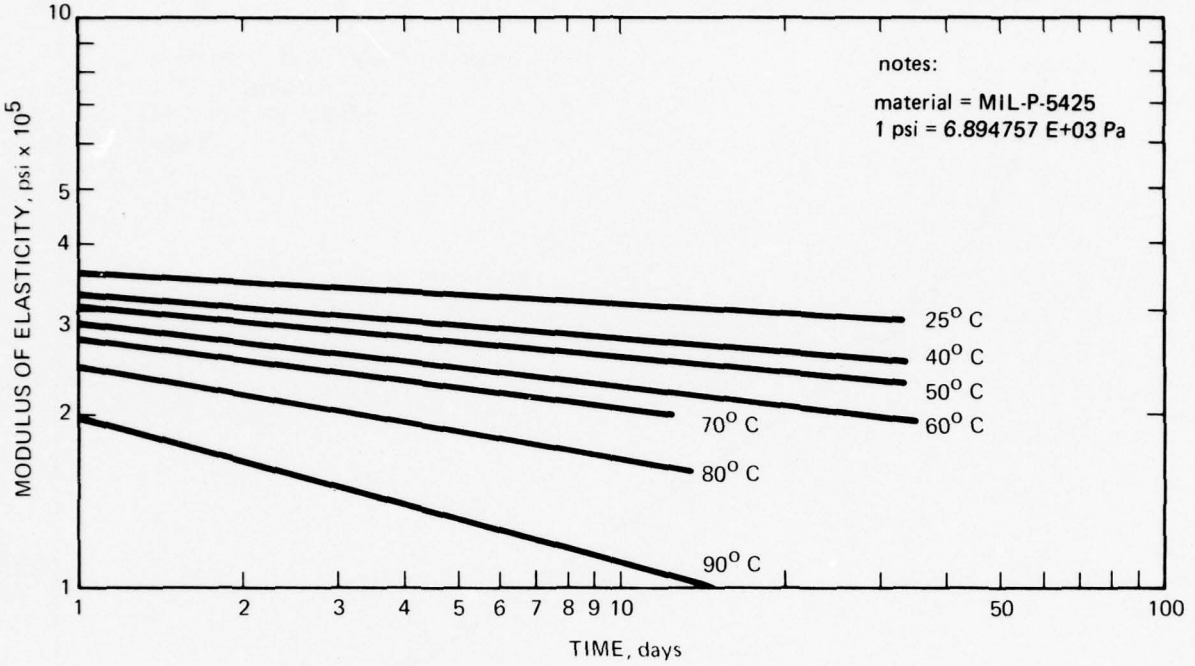

Figure 4.43. Effective modulus of acrylic plastic under long-term sustained flexural loading in a laboratory environment where the ambient temperature varies from 25 to 90° C (reference 4.10).

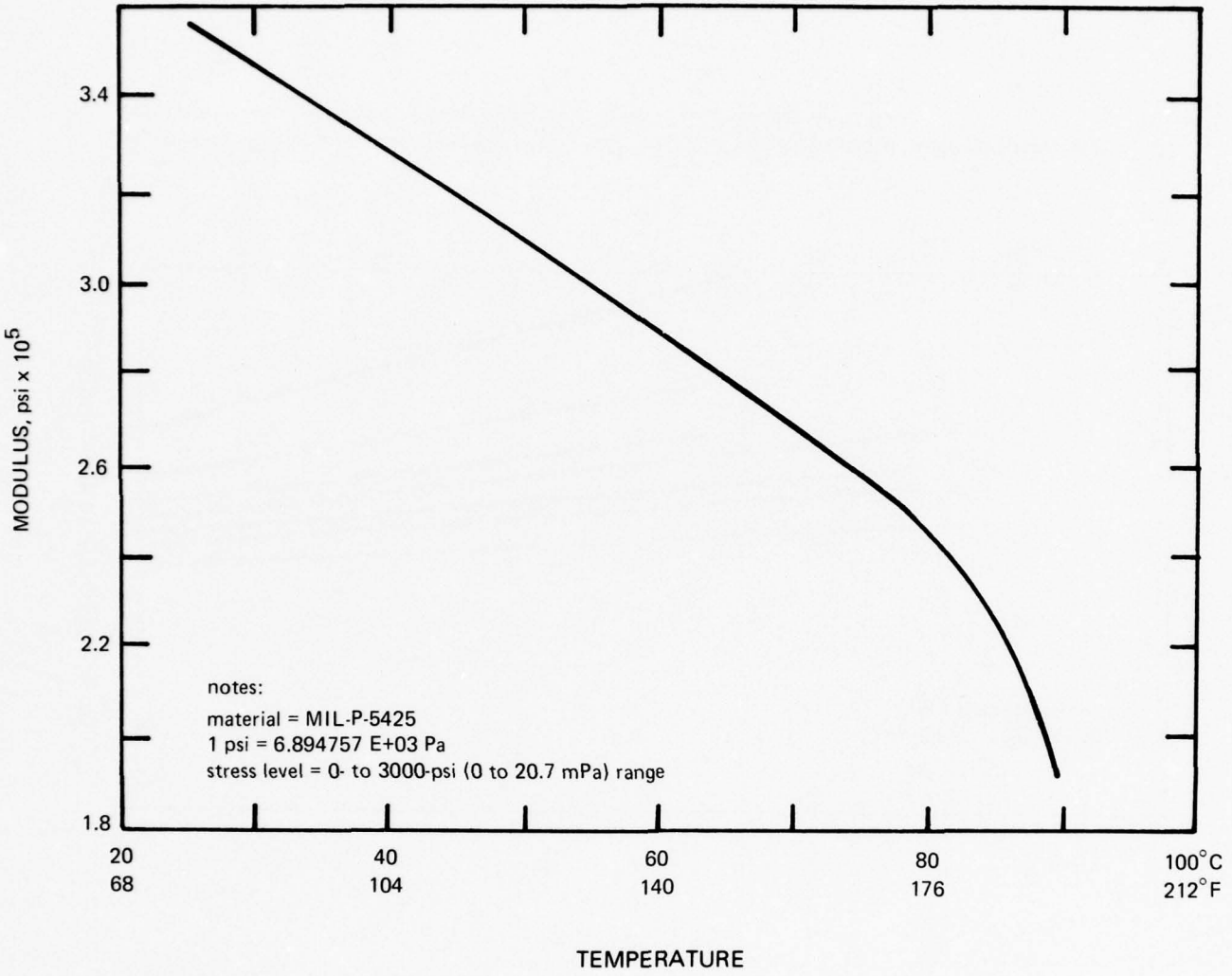

Figure 4.44. Effective modulus of acrylic plastic after 1 day of sustained flexural loading in a laboratory environment where the ambient temperature varies from 20 to 90° C (reference 4.10).

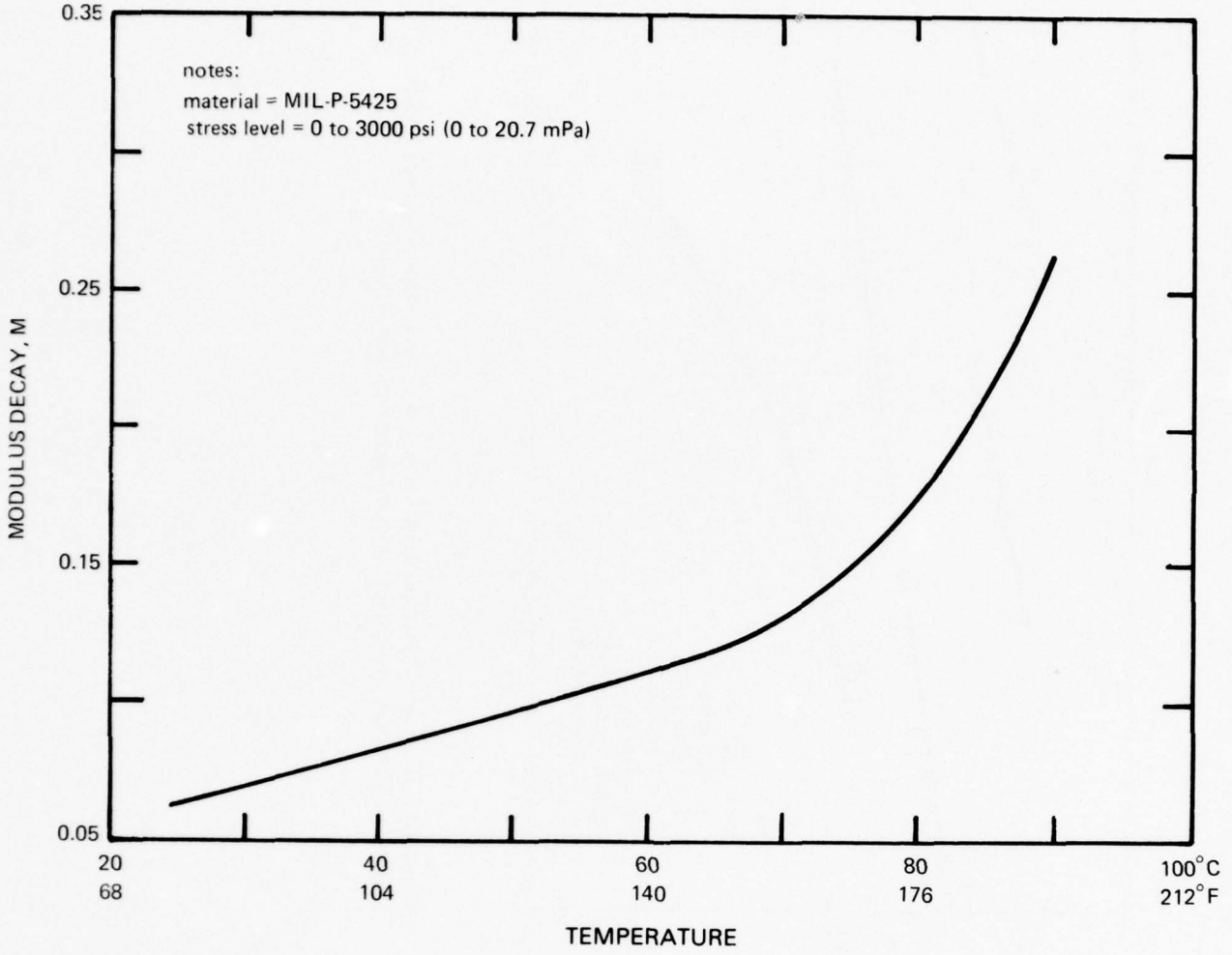

Figure 4.45. Decay of effective modulus of acrylic plastic (M) as a function of ambient test temperature (reference 4.10).

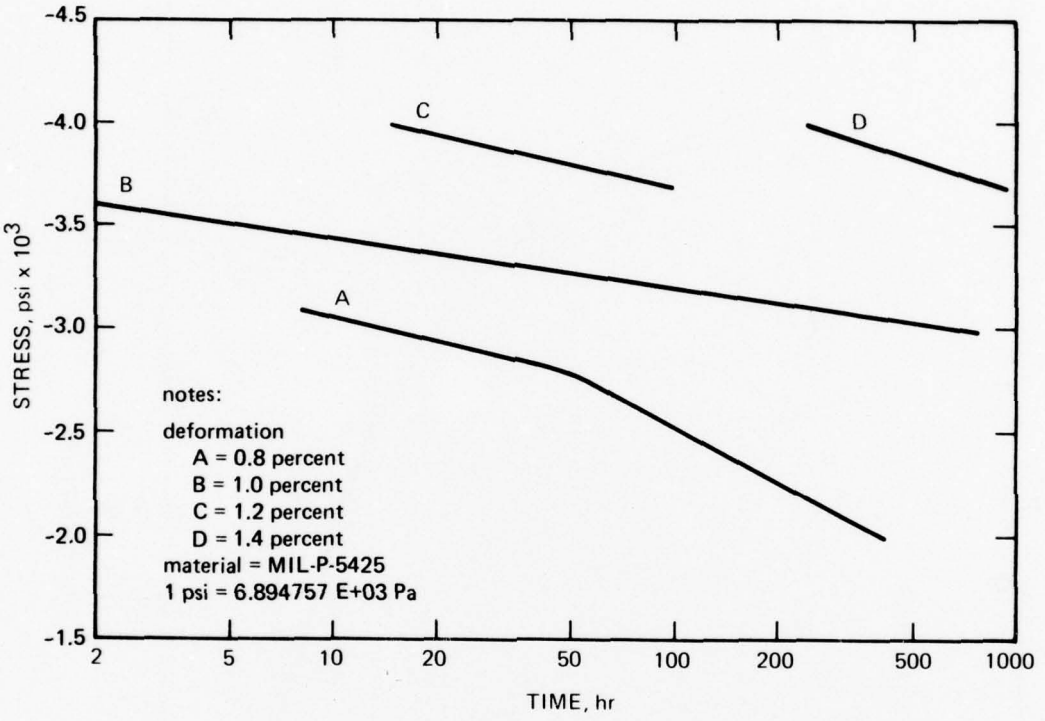

Figure 4.46. Behavior of acrylic plastic under long-term sustained uniaxial compression loading in a laboratory environment at room temperature (reference 4.1).

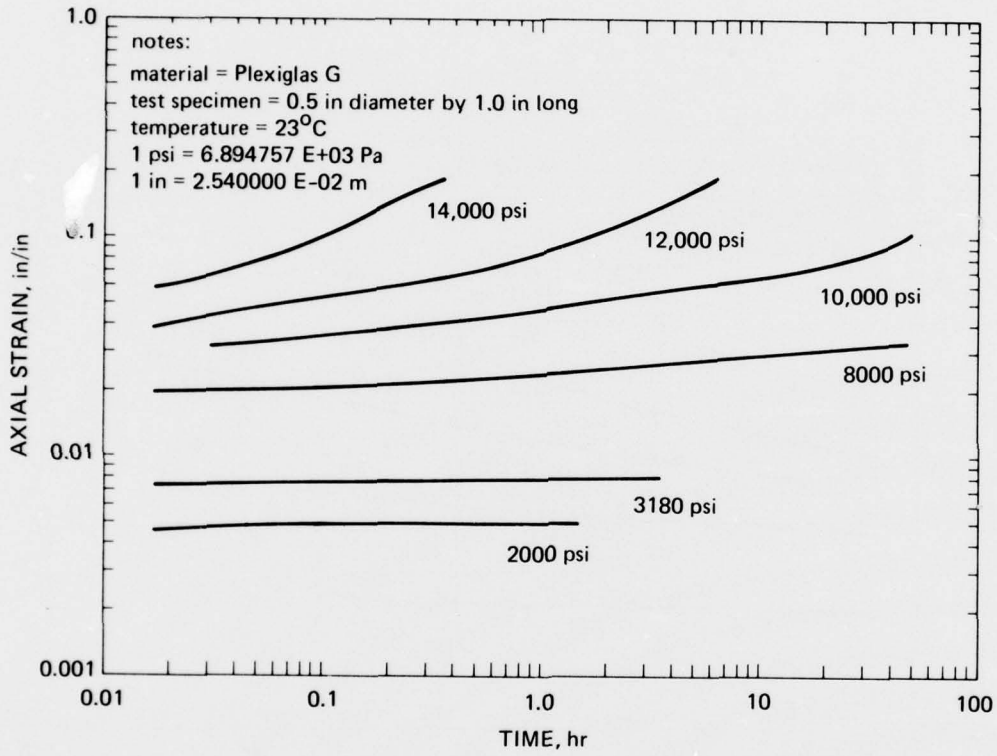

Figure 4.47. Axial strains in cylindrical test specimens of acrylic plastic under long-term sustained uniaxial compression loading in a laboratory environment at room temperature.

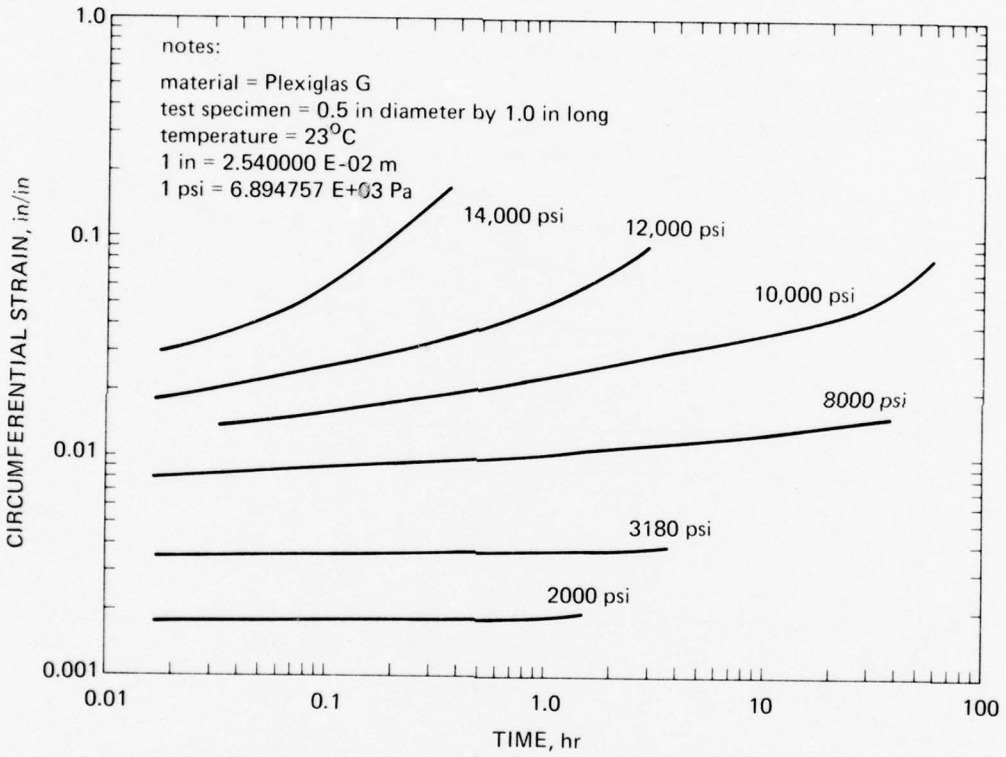

Figure 4.48. Circumferential strains to cylindrical test specimens of acrylic plastic under long-term sustained uniaxial compression loading in a laboratory environment at room temperature.

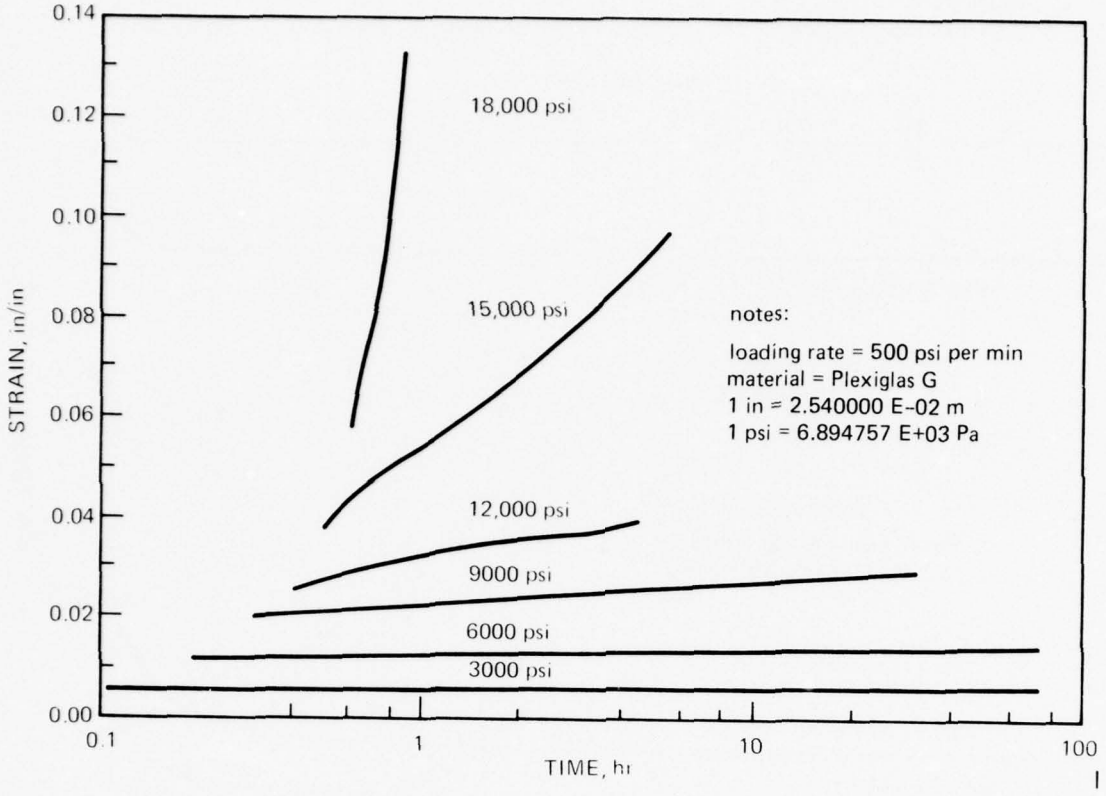

Figure 4.49. Axial strains in cylindrical test specimen of acrylic plastic under long-term sustained uniaxial compression loading in laboratory environment at 36°F (2°C) ambient temperature (reference 4.6).

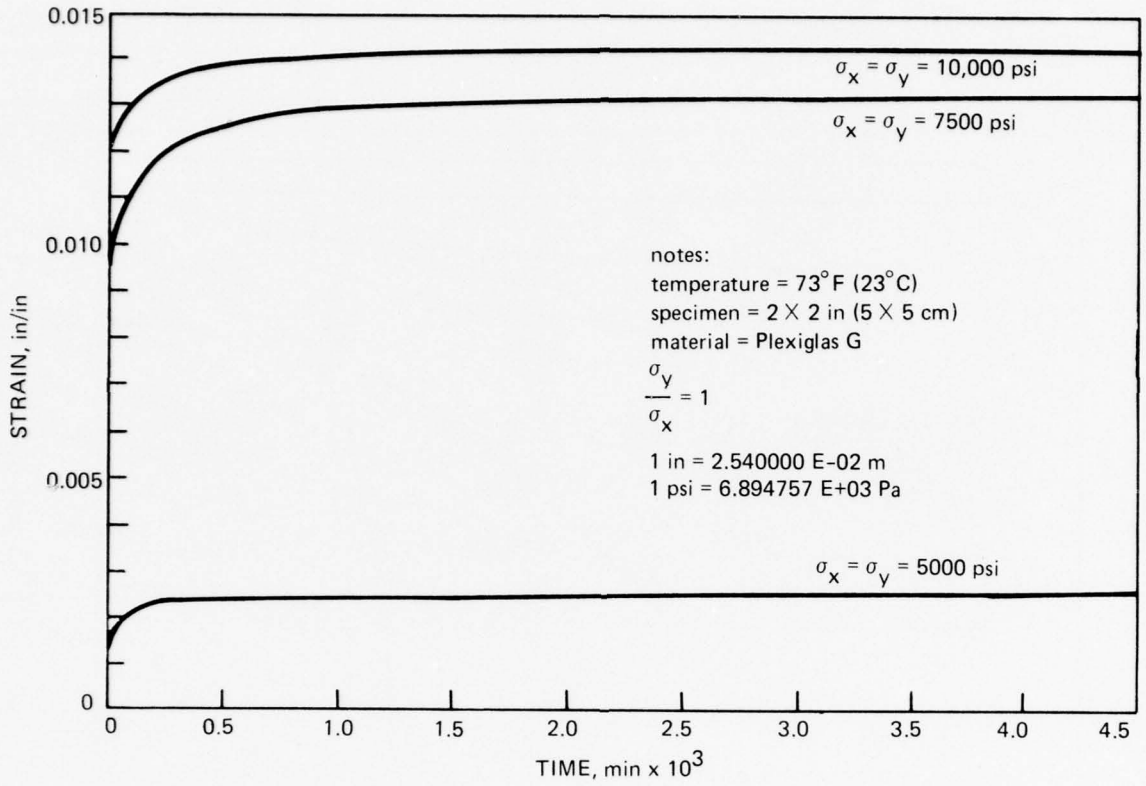

Figure 4.50. Creep of a cubical test specimens under long-term sustained biaxial compression loading in a laboratory environment at room temperature. The ratio of biaxial stresses acting along y and x axes is 1.

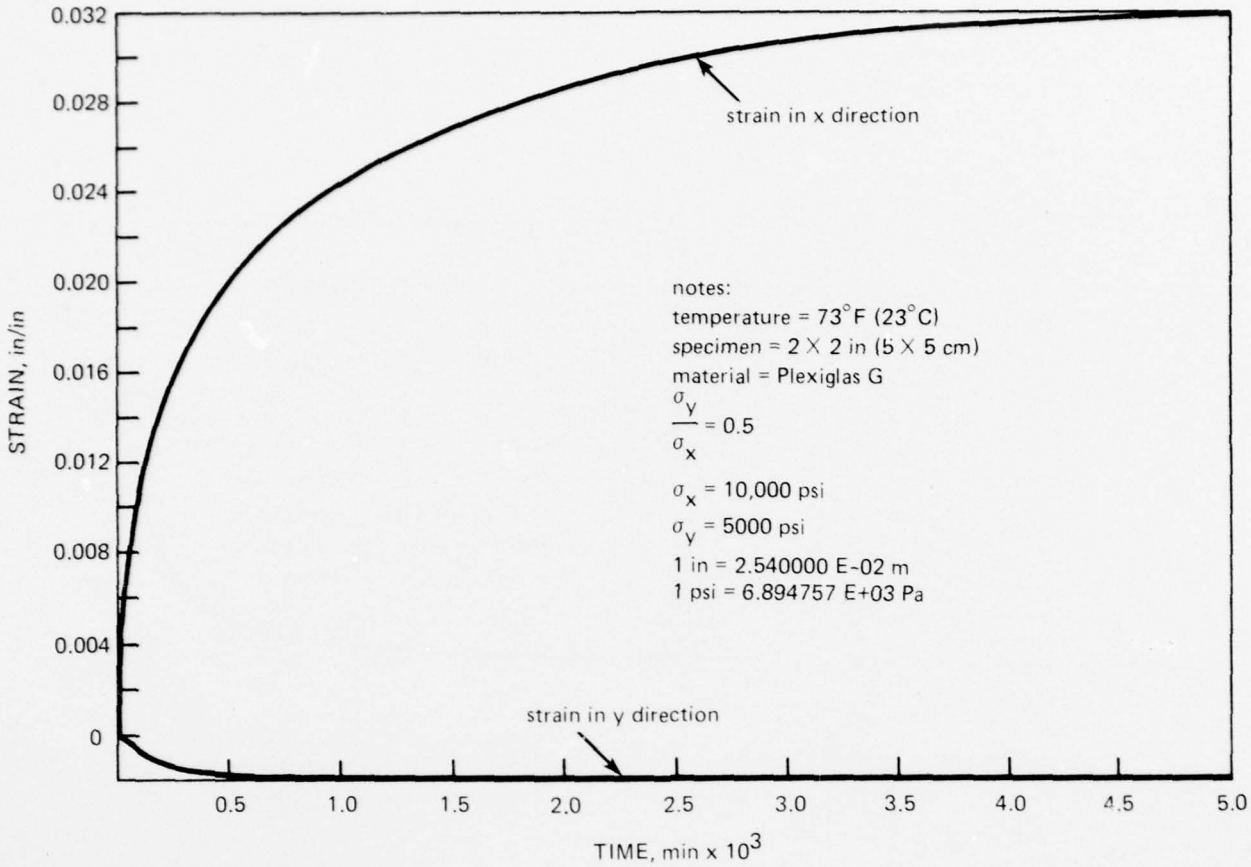

Figure 4.51. Creep of a cubical test specimen under long-term sustained biaxial compression loading in laboratory environment at room temperature. The ratio of biaxial stresses acting along y and x axes is 0.5.

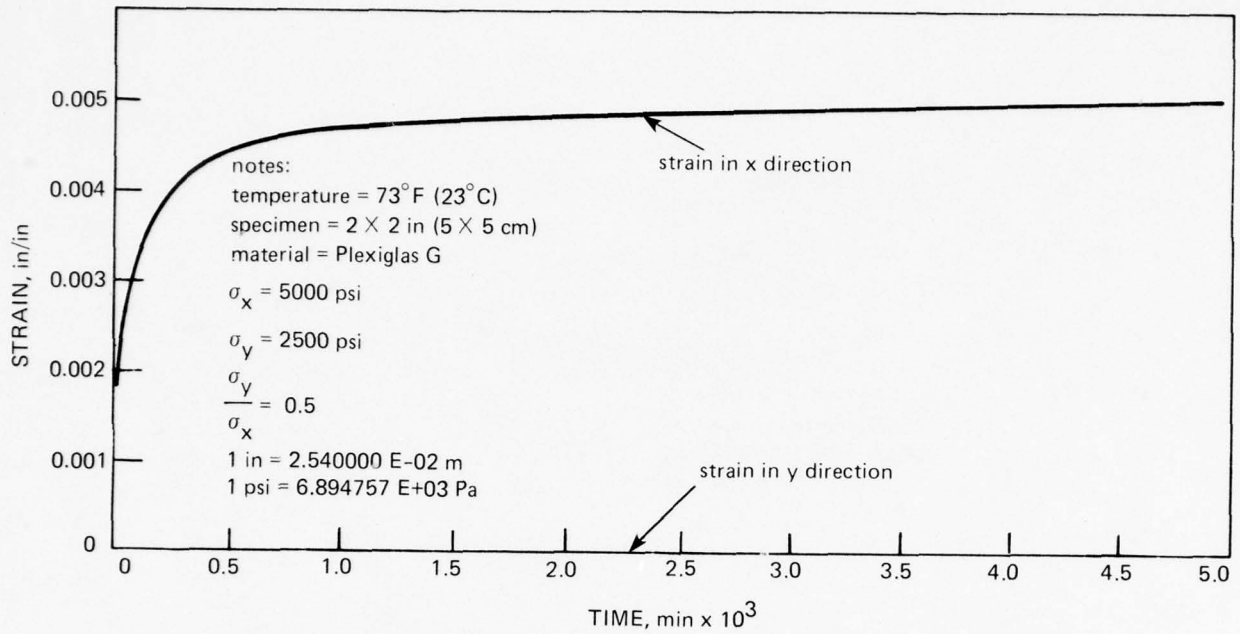

Figure 4.52. Creep of a cubical test specimen under long-term sustained biaxial compression loading in a laboratory environment at room temperature. The ratio of biaxial stresses acting along y and x axes is 2. There is no measurable strain in the y direction.

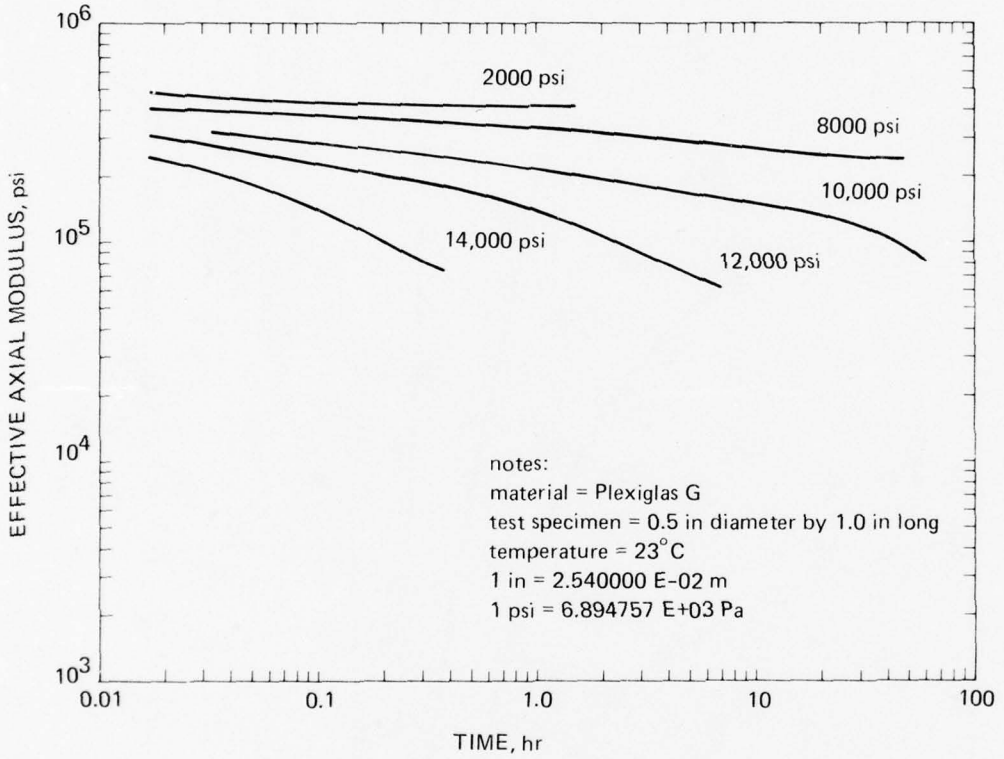

Figure 4.53. Effective modulus of acrylic plastic under long-term sustained uniaxial compression loading in a laboratory environment at room temperature.

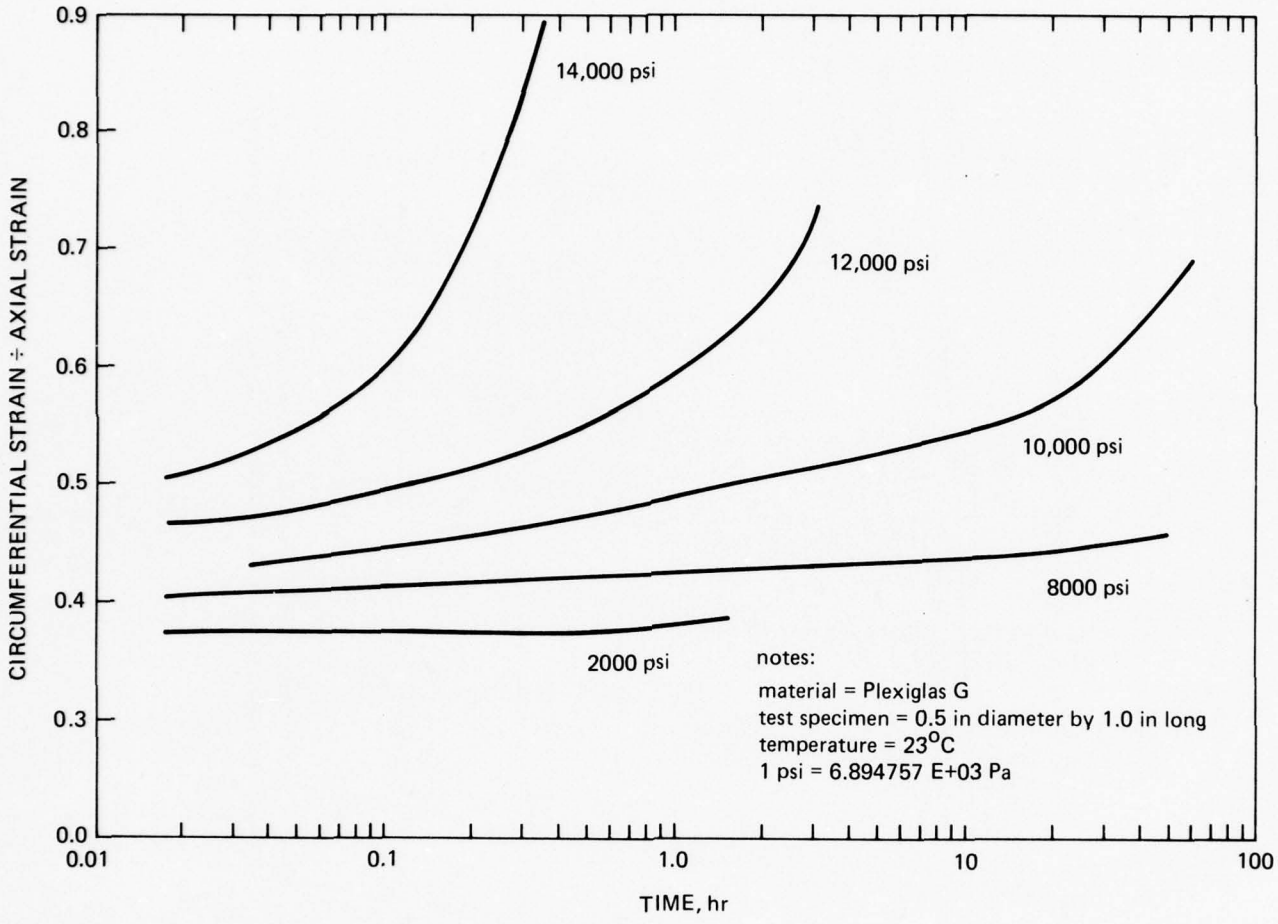

Figure 4.54. Poisson's ratio of cylindrical test specimens under long-term sustained uniaxial compression loading in a laboratory environment at room temperature.

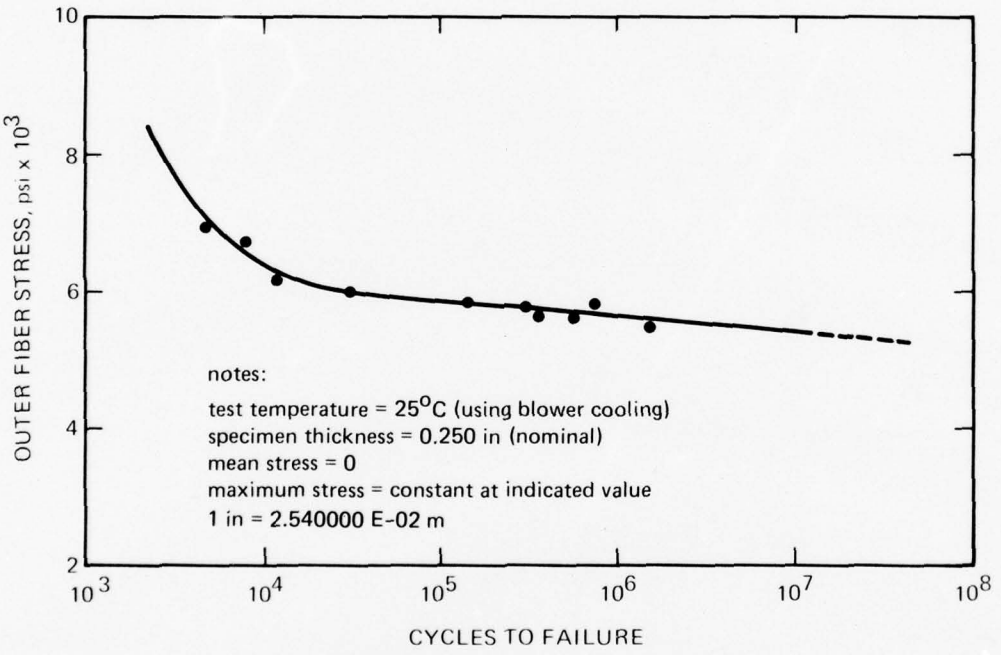

Figure 4.55. Flexural fatigue stress of acrylic plastic under rapid stress cycling rate (1800 stress reversals per minute) (reference 4.3).

SECTION 5. FOULING AND WEATHERING OF ACRYLIC PLASTIC . . . 5-1

5.1 INTRODUCTION . . . 5-1

5.2 FOULING . . . 5-1

5.3 WEATHERING . . . 5-4

5.4 SUBMERGENCE . . . 5-7

5.5 REFERENCES . . . 5-8

SECTION 5. FOULING AND WEATHERING OF ACRYLIC PLASTIC

5.1 INTRODUCTION

When using acrylic as an engineering material, it is imperative that the characteristics of the material, as well as its resistance to the ambient environment, be known. In the case of fouling, weathering, and long-term submergence, extensive data are not available and definitive statements cannot be made. However, some experimental data exist in all these areas, and on this basis some general observations can be made.

5.2 FOULING

Marine microorganisms attach themselves to all submerged surfaces and create a marine slime layer of bacteria, algae, and other microorganisms (reference 5.1). On this primary layer which acts as an inducement, the barnacle population begins to grow along with hydroids and other marine plants and animals. When attached, these organisms multiply at a rate up to 1,000,000 times faster than when free floating (reference 5.1). There are, however, some natural deterrents to the accumulation of fouling. Cold, excessive heat, salinity, pressure, pollution, and water movement all act to inhibit the growth of marine organisms. Fouling organisms decrease in variety and abundance with increased depth to about 100 feet (30.5 meters), and below 100 feet (30.5 meters) the fouling increases the closer the object is to the bottom (reference 5.2).*

Over a period of years, a large number of test specimens of various materials was lowered into the ocean to a maximum depth of 6800 feet (2072.6 meters) and left for periods of up to 5 years (references 5.3 through 5.7). When retrieved from the ocean, most of the fouling on the acrylic panels consisted of mud tubes made by tubeworms and the growth of various species of bryozoa, hydroids, barnacles, *anomiae,* and colonial tunicates. It was also discovered that numerous deep-to-shallow grooves were present on the acrylic (reference 5.8). These had been created when the material was placed in contact with the untreated wood and the borers had eaten through the wood and into the acrylic. In extruded acrylic, however, only a small number of borers penetrated into the plastic (reference 5.4). It seems reasonable to assume that while acrylic is probably not susceptible to biological deterioration in the deep ocean, it must not be placed in direct contact with untreated wood as it can be damaged to some extent by wood borers (reference 5.5).

While the agents of fouling do not actually damage the acrylic in a way that will cause structural failure, they do ruin its usefulness, since they reduce or destroy visibility. Dr. C. V. Metzler of the Naval Missile Center, Point Mugu, California, conducted a series of experiments to determine the rate of loss of visibility of acrylic in shallow water at the end of a pier. He found that after 8 hours there was no loss of visibility and no fouling; after 7

**For information on what happens at greater depths, the work of James S. Muraoka of the Civil Engineering Laboratory, Port Hueneme, California, is very valuable (references 5.3 through 5.10).*

days, a slight loss of visibility and fouling by algae; after 18 days, a complete loss of visibility and fouling by many different organisms (reference 5.2) (figure 5.1). Muraoka conducted a similar experiment, but in the open ocean at a depth of 120 feet (36.6 meters). He found that after 12 months exposure visibility through a clear acrylic panel was only fair and fouling consisted of hydroid growth; in 18 months the visibility was very poor (reference 5.8). There were several factors apparently involved in the different results of these two tests. First, the difference in depth: Metzler's specimens were at times as close as 15 feet (4.6 meters) to the surface. Second, Muraoka's tests were conducted in the open ocean while Metzler's were done from a pier located in calm water. Third, there were differences in the temperature ranges, water movement, and pollutants. Therefore, the best statement that can be generalized from these studies is that fouling does occur and that in a relatively short period of time an acrylic panel can become so fouled as to be virtually opaque.

This loss of visibility makes an acrylic window useless to its user. In the case of a submersible which may be in the water for only 4 to 6 hours a day and then rinsed off topside with fresh water, the windows will never become fouled. The specimen in figure 5.2 was placed in the ocean and rinsed off with fresh water once a day for 1 week. It was then continually submerged for 1 week, and visibility still remained quite good (refererce 5.2). When the window was rinsed with seawater rather than fresh water, visibility was destroyed within a 2-week period (figure 5.3). Therefore, if acrylic windows are to be subjected to prolonged continuous exposure, some method must be found to keep fouling organisms from attaching themselves to the windows.

Over the years various substances have been used in an attempt to provide an antifouling coating. Any antifouling material must be (1) highly toxic to the fouling organisms, (2) easily applied, (3) a clear material so that it will not affect the transparency of the acrylic, and (4) have a long toxic life (reference 5.10). In addition, the substance must not attack the acrylic. Most antifouling "paints," whether those used on ship bottoms or windows, wear off in 12 to 20 months (reference 5.1). In some cases a bacterial film may form a protective layer over the antifouling coating that is normally toxic to fouling animals, thereby affording a foothold for growth for these animals (reference 5.9).

The Organo-tin compound known as bis (tri-N-butyltin) oxide or simply TBTO appeared to be the most promising antifouling coating as it met all criteria for desirability (references 5.11, 5.2, and 5.10). Ames found that the best protection was afforded by using Farboil 207-2 to which 3 to 5 percent of TBTO was added. After 60 days of immersion, Ames found no fouling organisms, but there was a slight slime detritus film over the windows. However, visibility and transparency were still fair to good, and the windows could easily be cleaned by wiping with a soft cloth (reference 5.11) (figure 5.4). Metzler, in his shallow water tests, coated his windows with undiluted TBTO and found that there was no fouling for at least 2 weeks (reference 5.2) (figure 5.5).

After some inconclusive tests with antifouling agents, Dyckman and others decided that the only way the agents would work for prolonged periods would be if they were introduced directly into the surface of the acrylic (reference 5.2) or bound within a resinous polymer matrix (reference 5.1). Muraoka experimented with impregnating acrylic with a concentrated TBTO solution by placing the test specimens under hydrostatic pressure and thus attempting to force the TBTO inside the acrylic (reference 5.10). In his experiment, he had four series of panels. One set was untreated and was the control set. A second set was

simply dip-treated in a TBTO solution and allowed to dry in air. A third was put in a concentrated solution of TBTO and subjected to a hydrostatic pressure of 3000 pounds per square inch (20.68 megapascals) for 30 minutes. The fourth set was put in a concentrated solution of TBTO and subjected to a pressure of 10,000 pounds per square inch (68.9 megapascals) for 5 hours. Both sets 3 and 4 were drip dried, which left a sticky coating that distorted visual images. Therefore, some windows in the third set were cleaned with alcohol. All the sets were then placed in the ocean in approximately 20 feet (6 meters) of water about 5 feet (1.5 meters) off the bottom. After 9 days, the uncleaned treated panels in the third set showed very little growth and good visibility. After 29 days, these windows were completely covered and there was no visibility. The average temperature during this test was 60°F (15.5°C). For the dip-treated panels in the fourth set the results were slightly different. After 6 days, these windows were free of biological growth, but there was a slight reduction in visibility. After 18 days, there was no significant growth and visibility was very good. After 35 days the panels were covered with a fine film which significantly reduced visibility. The water temperature during this test averaged 64°F (17.8°C). While these tests are not conclusive, it seems reasonable to conclude that any application of TBTO protects the acrylic only during the early stages of exposure and for only a limited time (reference 5.10). In fact, some experiments indicate that no antifouling agent for acrylic windows has been successful for more than 20 days (reference 5.12).

This same conclusion also appears valid for strippable films which can be applied directly to the window. Metzler found that N. F. Cardarelli of B. F. Goodrich Company had developed a transparent polyvinyl chloride film impregnated with TBTO (reference 5.2). This film, like TBTO applied any other way, has a rather short life, but it has the advantage of easy replacement. It was used on the PX-15 when it floated for 3 months in the Gulf Stream in 1968. Muraoka found that a plastic film of PTFE tested for 5 years at 120 feet (36.6 meters), while covered with growth, could easily be stripped away and underneath the window would be as clean as when first placed in the ocean (reference 5.8). No cleaning of the window was necessary. Therefore, he believed that the film may have certain advantages over painted-on antifouling coatings.

It is apparent, however, that if an acrylic window is to be submerged for any appreciable period of time, for example, in a submerged habitat, then some antifouling measures other than those presently available must be employed. If the window is placed at diver depth, it is possible that a combination of painted-on TBTO, strippable film, and wiping could keep the window clean. At the greater depths, these approaches simply will not suffice.

When the Civil Engineering Laboratory at Port Hueneme, California, decided to build a concrete experimental habitat to test materials construction and deployment techniques at a depth of 600 feet (182.8 meters), a large spherical sector window of acrylic plastic was incorporated into the structure, although the habitat (SEACON I) was never to be manned. After submersion, the window would allow manned submersibles and unmanned robots not only to inspect the interior of the habitat for leakage but also to record photographically some data prominently displayed on instrumentation panels inside the vessel. While SEACON I was still in the planning stages, it became apparent that a new approach must be tried, if the window were to remain useful for the full 10-½ months SEACON I was to be on the ocean floor. Therefore, a special external fouling prevention system was designed, installed, and made operational. This system was composed of a window cover, a wiper brush

assembly, a lift bag attached to the window cover and wiper assembly, a solenoid valve to activate air for the lift bag, a 1/10-horsepower DC motor to rotate the brushes, and a chemical dispenser of TBTO installed in the window cover (reference 5.12). The window cover provided a stagnant area around the window's exterior, where the TBTO was to be continually leached from the chemical dispenser. When the inspection party inside a submersible wished to use the window for viewing, the solenoid valve was activated and air at 10 pounds per square inch (0.68 megapascal) above ambient pressure filled the bag. This caused the cover to rise, brought the brushes out of contact with the window, and gave the inspection party an unobstructed view through the window. When set on automatic, the DC motor rotated the wiper brushes for 2 minutes every 8 hours or, if on manual, for any desired time. It was planned that when the window cover was reclosed, the dispenser would introduce TBTO into the stagnant area around the window until the equilibrium of the TBTO solution was reached. However, the dispenser fell off and was lost while the habitat was being launched, and thus no chemical was used in the antifouling system. The wiper assembly was set on automatic and operated successfully throughout the entire 10-½ months of submersion in the ocean. The cover assembly was raised and lowered remotely by inspection parties 10 times during this same period. The wiper brushes performed beyond expectations. On the perimeter of the window where the wipers did not reach, there were hydroids and primary slime, but the action of the wipers apparently prevented the spread of the hydroids and a slime buildup (reference 5.12). As Metzler found previously, disturbing the environment appeared to reduce the rate of fouling markedly (reference 5.2). A photograph of this assembly is in figure 5.6.

It is obvious from this discussion that there is presently no easy method that can be readily employed to counteract fouling. However, it must be remembered that fouling does not structurally affect an acrylic window. It causes the window to become useless for its designed purpose, but once cleaned it can usually be reused. The worst case of fouling occurs when the window is submerged for extended periods of time, as in a habitat. It is recommended that more experimental approaches be investigated for preventing fouling of windows in stationary habitats, if their functional value is to be preserved over the habitat's projected operational life.

5.3 WEATHERING

Tests with weathering, like fouling, have produced only limited data. In a study done by Yustein, Winans, and Stark (references 5.13 and 5.14), transparent materials were subjected to weathering in various climatic locations. Of these materials, methyl methacrylate showed the least reduction in mechanical strength properties without any serious impairment of serviceability of the material after 5 years exposure. The test specimens were made from cast acrylic sheets with 1/8 inch (0.33 centimeter) nominal thickness. They were subjected to weathering in five different locations selected to typify a hot, wet climate; a hot, dry climate; a temperate climate; a subarctic climate; and an arctic climate. Table 5.1 shows the results of this test over a 3-year period.

In another 3-year study published by the Armed Forces Supply Support Center similar results were obtained (reference 5.15). The objective was to compare the changes in physical properties between materials exposed to various climates and those stored indoors. Results show that 3 years of indoor storage have almost as much effect on the mechanical properties of acrylic as does weathering in a temperate climate for the same time. Only in a

Table 5.1. Effects of weathering in various climates on acrylic plastic.*

Property	Panama	New Mexico	New York	Canada	Alaska
Tensile strength	Down slightly with period of exposure	Down slightly after most exposure	Down slightly	Cyclical	Cyclical
Flexural strength	Down slightly with period of exposure	No change	No change of any significance	Down slightly	Down slightly after long exposure
Light transmission	Up	No change	Down slightly	No change	No change
Haze	Up	Up	Up to 6 percent	Up slightly	Up slightly
Surface appearance	Yellowed some	Yellowed some	No change	No change	No change

*A 3-year study on 1/8-inch-thick (0.33 centimeter) test specimens (reference 5.14).

tropical climate was the deterioration of physical properties significant, approximately 10 percent per year (table 5.2).

In another study of weathering (reference 5.16), Rainhart and Schimmel gained access to a 4- by 12- by 1/8-inch (10 by 30 by 0.33 centimeters) piece of Plexiglas which had been mounted for 17 years and 18 months in a static test frame outside Albuquerque, New Mexico. They subjected the weathered panel to a series of tests and compared the results with those obtained from unweathered acrylic. The study showed that there had been a significant increase in the brittleness of the material. Furthermore, in the areas of flexural strength and maximum strain the study supported the data of Yustein, Winans, and Stark

Table 5.2. Effect of outdoor weathering and storage (2.5 to 3 years) on the tensile properties of MIL-P-5415 materials (reference 5.15).

Condition	Tensile Strength, 10^3 psi	Strain at Failure, percent	Modulus of Elasticity, 10^5 psi
Original	11.2	5.8	4.4
After 3 years of storage	10.4	5.8	4.1
After exposure to			
3 years of temperate climate	10.5	5.0	4.4
3 years of subarctic climate	9.2	3.9	4.6
2.5 years of dry, hot climate	9.6	3.6	4.4
2.5 years of tropical climate	7.5	2.2	4.4

that losses in these areas are a continuous and not a step function of time. The degree of embrittlement was shown by a 65-percent decrease in strain at rupture and a 51-percent decrease in flexural strength. In addition, there was a small but steady increase (7 percent) in the tangent modulus of elasticity over time. Of all properties measured, the optical transmission decreased the least: After the surface of the pitted acrylic specimen was repolished, its transmissivity was the same as that of an unweathered specimen.

By summarizing existing weather data, it can be stated that although acrylic plastic weathers it is a slow process which decreases the original tensile strength, flexural strength, and ductility by a few percent per year. It must be pointed out, however, that all the test specimens used in these experiments were extremely thin. Many authorities hypothesize that weathering is a surface effect. If this is true, then the action of ultraviolet rays, chemical attacks by pollutants such as ozone, and abrasion by dust particles, rain, and snow will have a marked effect on the results obtained when using thin specimens as test samples. These results would then not actually be applicable to windows or massive acrylic structures which are 10 to 40 times thicker than the test specimens. Therefore, the effects generated by the weathering tests may very well represent insignificant changes when applied to anything except 1/8-inch-thick (0.33 centimeter) specimens. Until data based on weathered 1- to 4-inch-thick (2.54 to 10.16 centimeters) acrylic specimens become available it is reasonable to assume that the published data from thin specimen studies are also applicable to thick sheets used for construction of windows in hyperbaric chambers.

The lack of tensile and flexural strength data for thick weathered acrylic is a minor inconvenience when compared with the total lack of data on changes in compressive strength. The latter could decrease a small amount, a large amount, or not at all. It could even conceivably increase with exposure as weathered acrylic is known to be more brittle than unweathered acrylic. Since all spherical and many conical frustum windows experience only compressive stresses, this information would be of great value. It is hoped that this lack of data on compressive strength of weathered acrylic will be rectified in the future by ASME, the sponsor of safety standards for acrylic viewports in hyperbaric chambers.

Another area of ignorance concerning the properties of weathered acrylic plastic deals with the synergistic effect between stresses and weathering. Sufficient exploratory data exist to indicate that the presence of tensile or flexural stresses in material exposed to weather accelerates its deterioration dramatically. The data are not available, however, that would permit quantification of this synergistic effect over 10 to 20 years. It would be of practical value to determine the effect of a compressive stress field on the rate of weathering, since many hyperbaric windows in service are in compression when pressurized. It is doubtful, however, whether such data will soon become available as the number of variables needing elucidation is large and complex: Not only must the effect of different principal stresses in a stress field be determined, but the effect of their magnitudes on the rate of weathering must also be quantitatively established. When one adds to this the variables represented by the duration and ambient temperatures of cyclic and sustained loading conditions, the real complexity of the problem facing the investigators of weathering becomes apparent.

Because of this complexity and the lack of definitive data on which to formulate quantified relationships between the deterioration of physical properties in weathered acrylic, length of exposure, magnitude of stresses, and type of loading, an empirical rule has been adopted by ASME (reference 5.17). This rule states that the useful life of acrylic

viewports in pressure vessels for human occupancy is 10 years. It is based on the conservative assumption that within 10 years even stressed acrylic in a tropical climate will retain more than 50 percent of its original load-carrying ability. Thus, the effective safety factor of acrylic viewports even in tropical service will decrease only from the original range of 3 to 4 to that of 1.5 to 2, which is still a marginally adequate value for manned service. When appropriate data from thick acrylic specimens become available, the service life of acrylic viewports may be extended to 15 or 20 years, saving the industry significant sums of money.

5.4 SUBMERGENCE

For specimens submerged for varying lengths of time, the data are much more comprehensive than for weathering. For example, the following results are available:

1. Specimens immersed in water for as long as 5 years do not undergo a significant chemical change (reference 5.18).

2. After investigation of windows from TRIESTE II, no deterioration in the material's mechanical properties was found and there was no indication of degradation of the viewing characteristics or quality (reference 5.19).

3. Plexiglas does not deteriorate with age (reference 5.20).

Acrylic, like other permeable materials, does absorb some water when subjected to prolonged exposure in the ocean. However, the results vary. In one test, 1/16-inch-thick (1.5 millimeters) specimens were placed in a 100-percent humidity environment and the water absorption was measured at 2 percent (reference 5.18). Another experiment with 1/4-inch-thick (6.3 millimeters) specimens that were immersed for 250 days led to a 2.2-percent absorption (reference 5.18). Muraoka found that his specimens which were left at 2370 feet (122 meters) in the open ocean for 1 year absorbed about 0.44-percent moisture if the specimen were of extruded acrylic and about 0.46-percent if it were made of cast acrylic (reference 5.7). If the specimen were left for 1 year at 6800 feet (2072 meters), the extruded acrylic absorbed only 0.35 percent and the cast acrylic 0.40 percent (reference 5.5). In tests conducted for 2 years at 5640 feet (1719 meters), Muraoka found moisture absorption for extruded acrylic to be 0.23 percent and for cast acrylic to be 0.51 percent (reference 5.6). It can be concluded that the maximum water absorption was 2.2 percent for extended immersion of these specimens. It should be emphasized, however, that all the specimens were extremely thin in comparison with actual windows or acrylic structures and that the effect of this thickness difference is unknown. It is believed, however, that thicker windows will absorb less than the values recorded, since only one face will be exposed to the water and only a small proportion of the total volume will thus be wetted.

These same general conclusions can be made regarding the hardness tests conducted with acrylic both before and after submergence. One series showed the hardness test of acrylic before exposure reading 90.0 on the durometer and 88.0 after 5 months at 600 feet (183 meters) (reference 5.12). Another showed a dry reading of 90.0 for cast acrylic and 82.0 after exposure for 2 years at 5640 feet (1719 meters) (reference 5.6). Whether this change can be attributed to the absorption of water, effects of pressure, or slight changes in mechanical properties is unclear. The fact remains that while some slight changes do occur they are not significant and can theoretically be disregarded when designing with acrylic.

In the area of other physical properties, acrylic test specimens of 1/4 and 1/8 inch thickness (0.6 and 0.3 centimeter) were placed at 2300 feet (701 meters) in the open ocean for 6-½ months in both flexed and relaxed positions. The results showed an insignificant increase in E (flexural modulus) and a decrease in tensile and compressive strengths (reference 5.21). However, all changes were less than 10 percent. In another experiment with 1/4- and 1/8-inch-thick (0.6 and 0.3 centimeter) specimens placed in 6780 feet (2067 meters) of water for 403 days the same results were obtained (reference 5.22). It thus seems reasonable to conclude that the physical properties of acrylic do not change rapidly or continually, even when subjected to long-term loading, in the greater depths of the ocean. However, it must again be realized that all test specimens tested to date have been very thin and that the results may not be completely applicable to acrylic structures or thick acrylic windows.

5.5 REFERENCES

5.1 Dyckman, E. J., and Montemarano, J. A., "New Comcepts in Antifouling Technology–Organometallic Polymers," *American Paint Journal,* August 20, 1973.

5.2 Naval Missile Center, Technical Memorandum TM-68-9, "Biological Fouling of Transparent Plastics," by C. V. Metzler.

5.3 Naval Civil Engineering Laboratory, Technical Report R-329, "Deep Ocean Biodeterioration of Materials – Part I: Four Months at 5,640 Feet," by James S. Muraoka, November 1964.

5.4 Naval Civil Engineering Laboratory, Technical Report R-393, "Deep Ocean Biodeterioration of Materials – Part II: Six Months at 2,340 Feet," by James S. Muraoka, August 1965.

5.5 Naval Civil Engineering Laboratory, Technical Report R-456, "Deep Ocean Biodeterioration of Materials – Part IV: One Year at 6,800 Feet," by James S. Muraoka, June 1966.

5.6 Naval Civil Engineering Laboratory, Technical Report R-495, "Deep Ocean Biodeterioration of Materials – Part V: Two Years at 5,640 Feet," by James S. Muraoka, November 1966.

5.7 Naval Civil Engineering Laboratory, Technical Report R-525, "Deep Ocean Biodeterioration of Materials – Part VI: One Year at 2,370 Feet," by James S. Muraoka, May 1967.

5.8 Naval Civil Engineering Laboratory, Technical Report R-810, "Biodeterioration and Fouling of Materials – Five Years at Depth of 120 Feet," by James S. Muraoka, May 1974.

5.9 Naval Civil Engineering Laboratory, Technical Report R-182, "The Effects of Marine Organisms on Engineering Materials for Deep Ocean Use," by James S. Muraoka, March 1962.

5.10 Naval Civil Engineering Laboratory, Technical Note N-1020, "Marine Fouling of Acrylic Plastics Pressure Treated with Organo-Tin Compound," by James S. Muraoka, February 1969.

5.11 General Dynamics, Electric Boat Division, "Final Report, NR-1 Ships Systems Developmental Test (NA-STS-02) – Viewport Marine Growth," by W. L. Ames, October 1968.

5.12 Civil Engineering Laboratory, Technical Report R-817, "Seafloor Construction Experiment, SEACON I," by T. R. Kretschmer *et. al.*, February 1975.

5.13 Yustein, S. E., Winans, R. R., and Stark, H. J., "Outdoor Weather Aging of Plastics Under Various Climatological Conditions," *American Society for Testing Materials Bulletin*, pp. 31–43, April 1951.

5.14 Yustein, S. E., Winans, R. R., and Stark, H. J., "Three Years' Outdoor Weather Aging of Plastics Under Various Climatological Conditions," *American Society for Testing Materials Bulletin*, pp. 29–29, February 1954.

5.15 Armed Forces Supply Support Center, Military Handbook-17, "Plastics for Flight Vehicles–Part II, Transparent Glazing Materials," 14 August 1961.

5.16 Sandia Laboratories, "Effect of Outdoor Aging on Acrylic Sheet," by L. G. Rainhart and W. P. Schimmel, Jr., September 1974.

5.17 American Society of Mechanical Engineers, *Safety Standard for Pressure Vessels for Human Occupancy*, ASME/ANSI PVHO-1, 1977.

5.18 Imperial Chemicals Industries Limited, Plastics Division, "The Properties of 'Perspex' Acrylic Materials."

5.19 Naval Ship Research and Development Center, "Material Characterization Studies of a Trieste II(DSV-1) Sphere Window After Deep Submergence Service," by Frank M. Schwartz, May 1972.

5.20 Willoughby, T. E., Letter to Mr. A. I. Snyder, Supervising Engineer, Pressure Vessel Department of Industrial Relations. Subject: Request for Permission to Use Non-Code Pressure Vessel of the Vickers Oxygen Chamber.

5.21 U. S. Naval Air Engineering Center, Report NAEC AML R-2260-C1, parts A and B, "Oceanographic Effects on Plastic Engineering Materials and Elastometic Materials," by H. J. Lee, January 1966.

5.22 U. S. Naval Air Engineering Center, Report NAEC AML R-2350 C-1, "Oceanographic Effects on Plastic Engineering Materials," by H. J. Lee, January 1966.

Figure 5.1. Untreated sample of 2.5-inch-thick (6.4 centimeters) acrylic plastic after continuous submersion for 2 weeks 9 feet (2.7 meters) below the sea surface in 33-feet-deep (10 meters) water off Pt. Mugu, California.

Figure 5.2. Untreated sample of 2.5-inch-thick (6.4 centimeters) acrylic plastic after 2 weeks cumulative submersion 18 feet (5.5 meters) below the sea surface in 33-feet-deep (10 meters) water off Pt. Mugu, California. Sample was removed each day during the first week and bathed briefly in fresh water. During the second week the sample was left undisturbed.

Figure 5.3. Untreated sample of 2.5-inch-thick (6.4 centimeters) acrylic plastic after 2 weeks cumulative submersion 18 feet (5.5 meters) below the sea surface in 33-feet-deep (10 meters) water off Pt. Mugu, California. Sample was removed each day during the first week and bathed briefly in seawater. During the second week the sample was left undisturbed.

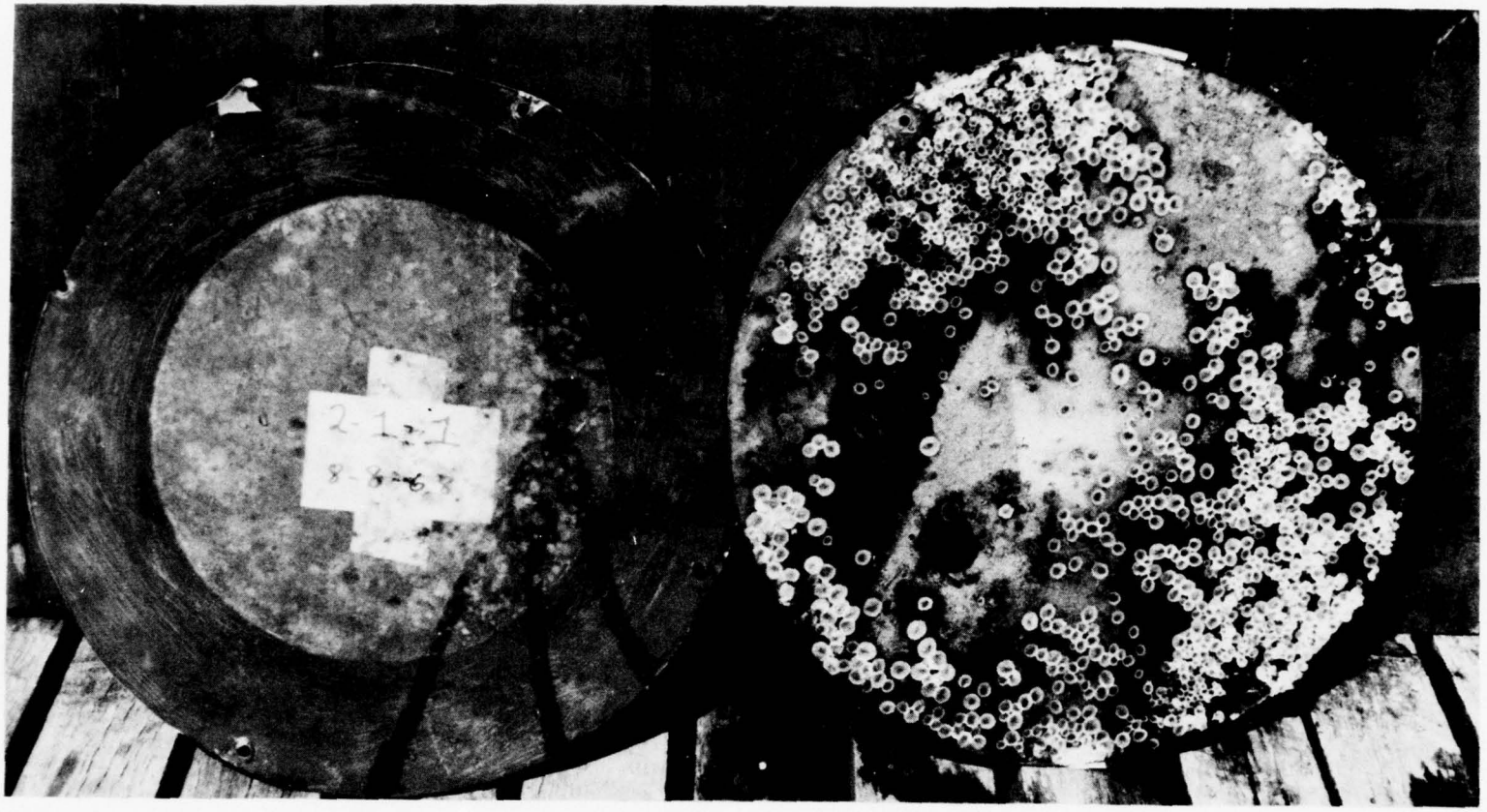

Figure 5.4. Acrylic plastic samples after continuous submersion for 2 months in Charlestown Pond, Rhode Island. Window on the left was coated with Farboil 207-2 (3-percent TBTO), while the one on the right was left untreated. The coated window was fouled only with algae film.

Figure 5.5. Sample of 2.5-inch-thick (6.4 centimeters) acrylic plastic treated with TBTO after continuous submersion for 2 weeks 11 feet (3.35 meters) below the sea surface in 33-feet-deep (10 meters) seawater off Pt. Mugu, California.

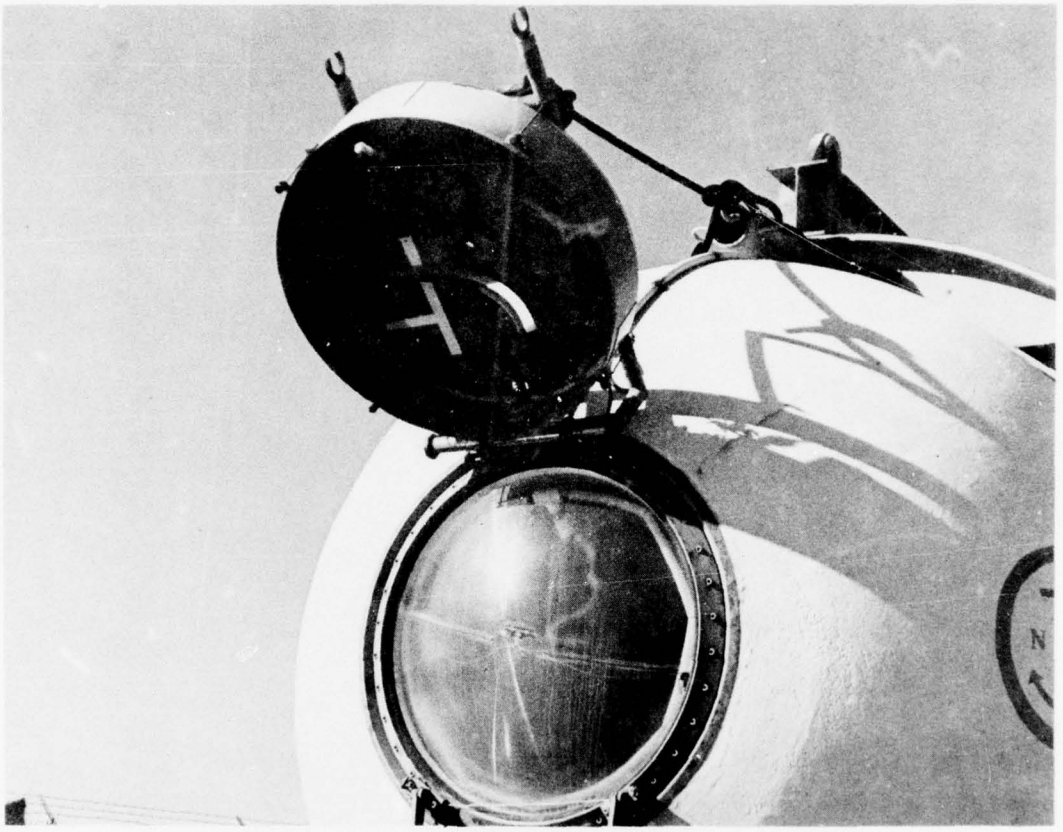

Figure 5.6. Viewport assembly of SEACON I habitat showing protective cover and wiper brushes for cleaning the window. The cover is raised only for brief periods of time when observations are performed by a submersible through the window.

SECTION 6. PRESSURE-RESISTANT WINDOWS . . . 6-1

6.1 INTRODUCTION . . . 6-1

6.2 WINDOW CLASSIFICATIONS . . . 6-1

6.2.1 Window Shapes . . . 6-2
6.2.2 Window Curvatures . . . 6-2
6.2.3 Bearing Surfaces . . . 6-2

6.3 SUMMARY . . . 6-3

SECTION 6.
PRESSURE-RESISTANT WINDOWS

6.1 INTRODUCTION

Because the pressure hulls of submersibles and hyperbaric chambers are traditionally made of opaque materials, there must be some provision for visibility from the interior of the opaque enclosure (figure 6.1). Windows made of transparent acrylic plastic basically satisfy this requirement (figure 6.2). Although they do not provide unhampered visibility, the field-of-view is in most cases adequate for the application. In cases where the field-of-view from a single window does not suffice, several windows can be grouped together (figure 6.3).

The incorporation of a window into a pressure hull is a complicated process that significantly increases the cost and weight of the finished hull. The reason is that the window mounting must secure [illegible] the window in place, and also serve as a reinforcement for the opening in the hull. The window-mounting assembly generally requires not only an extensive stress analysis but also fabrication within tight dimensional tolerances. Because the mounting must provide reinforcement for the opening in the hull without extensive deformation of the window seat, its large bulk increases the weight of the hull.

Since the cost of a finite-element stress analysis for a pressure hull with a window mounting is independent of the window's diameter and since the cost of fabricating the window-flange assembly does not increase in direct proportion with the window's diameter, a large diameter window is more cost-effective than several smaller ones that cover the same field-of-view. This is the reason for the trend to fewer, but larger, windows in opaque pressure hulls for human occupancy (figure 6.4).

6.2 WINDOW CLASSIFICATIONS

Windows are classified by the curvature of their viewing surface, shape of their circumference, and configuration of their bearing surface. Using the curvature of the viewing surface as a classification criterion, all windows can be classified as either plane or curved (figure 6.5). Windows with curved surfaces can be further subdivided according to the character of the curvature: spherical, aspherical, cylindrical, etc. Using the shape of the window's circumference as a classification criterion, the windows can be classified as round, square, rectangular, elliptical, triangular, etc (figure 6.6). The configuration of bearing surfaces allows the windows to be further classified into windows with conical, plane, toroidal, or spherical bearing surfaces (figure 6.7). When a window is described according to all of its classifications, it can be readily visualized. Thus, for example, a round window with plane viewing surfaces and a conical bearing surface is readily recognized as a conical frustum, the standard window for deep submergence applications.

6.2.1 Window Shapes

Only round windows are generally used in high-pressure applications. The round opening in the mounting flange distributes stresses uniformly around the circumference, thus minimizing the cross-section of the flange. Square, rectangular, or triangular windows are used very rarely because openings with straight edges in the mounting generate very high stress concentrations at the corners. Still, square or rectangular windows are popular for very low-pressure applications because of low fabrication and installation costs associated with rectangular mountings and straight edges (figure 6.8).

Rectangular windows wrapped around the hull in the form of cylindrical shell sectors are used only in limited applications, since the stress concentrations in the rectangular reinforcing flange permit application only at very low pressures. It is only when the cylindrical shell sector extends completely around the circumference of the pressure hull that it becomes attractive as a pressure-resistant window shape, i.e., the distribution of stresses becomes uniform and the shape and size of mounting flanges become amenable to economic fabrication. However, thick cylindrical windows have a serious drawback in the form of severe optical distortion along the longitudinal axis of the cylinder. Thus, because of their high cost and great optical distortion, they are used only rarely. A typical application is in the cylindrical conning towers of shallow submersibles where they provide the observer a 360-degree (6.28 radians) view around the periphery of the submersible (figure 6.9).

6.2.2 Window Curvatures

Because of the uniformity of stress distribution around the penetration in the pressure hull, window mounting, and body of the window, round windows with curved viewing surfaces, although of recent development, are beginning to predominate in high-pressure applications. The optimum shape is the spherical shell sector that both maximizes the structural response of the window to pressure loading by generating only compressive stresses in the acrylic and optimizes the magnitude of the undistorted field-of-view by acting as a wide-angle lens. Thus, spherical shell sector shapes have been used in the windows in the pilot's compartments of most submersibles with a 0- to 1000-meter depth capability (figure 6.10).

Windows with plane viewing surfaces are not as attractive for high-pressure applications as are those with curved surfaces because of the nonuniform distribution of stresses in the body of the window. The parallel plane surfaces cause the window to behave like a flat membrane under flexure. As a result, the low-pressure face is submitted to tensile stresses while the high-pressure face is subjected to compressive stresses of equal magnitude. Since acrylic plastic is very notch sensitive in a biaxial tensile stress field, the low-pressure face must be protected against the scratches and gouges that significantly lower the window's critical pressure.

6.2.3 Bearing Surfaces

To eliminate the presence of undesirable tensile stresses in windows with plane viewing surfaces for high-pressure service, the windows are provided with a conical bearing surface that superimposes a compressive radial stress on the plane viewing faces. This is particularly

effective for thick plane windows (t/D_i greater than or equal to 0.5), where the superimposed compressive radial stress is larger in magnitude than is the tensile stress on the low-pressure face, thus eliminating undesirable tensile stresses (figure 6.11). Plane windows are often found in low-prssure service without conical bearing surfaces, since for low t/D_i ratios the conical surfaces do not significantly decrease the tensile stresses but do increase the cost (figure 6.4). Conical bearing surfaces are also used on windows with spherical viewing surfaces, where their presence allows the spherical shell sector windows to behave like true sectors of a spherical shell under compression. By allowing the sectors to slide in the conical mountings, flexure stresses in the shell sectors are either completely eliminated or minimized. Conical bearing surfaces also improve the sealing ability of the window. Since a window with conical bearing surface acts like a pressure-energized conical plug in a matching conical mounting seat, it is a reliable solution for sealing under very high pressures.

However, the conical bearing surface is not without some drawbacks. The conical angles on both the window and the mounting flange must be precisely machined to insure proper contact between the bearing surfaces of the window and its seat, reliable sealing, and smooth displacement under pressure. Because of the appreciable "in-and-out" sliding displacement in the flange during repeated pressure cycling, fatigue shear cracks tend to appear on the bearing surfaces of the window sooner than on plane bearing surfaces, particularly when the latter are protected by bearing gaskets. Thus, windows with plane bearing surfaces resting on gaskets are found in those applications where a very long cyclic pressurization fatigue life is required.

Spherical and toroidal bearing surfaces provide no significant structural advantage over conical bearing surfaces. Since spherical and toroidal bearing surfaces are, except for very small sizes, difficult and expensive to fabricate, they have not been extensively used.

6.3 SUMMARY

The most effective pressure-resistant window configuration in terms of weight and field-of-view is considered to be a true spherical shell sector with conical bearing surfaces. The least desirable pressure-resistant window configuation is considered to be a plane rectangle, square, or triangle. Other window configurations fall between these two extremes. The actual choice must be based not only on structural requirements, but also on cost, field-of-view, optical performance, ease of installation, maintenance, and other operational requirements.

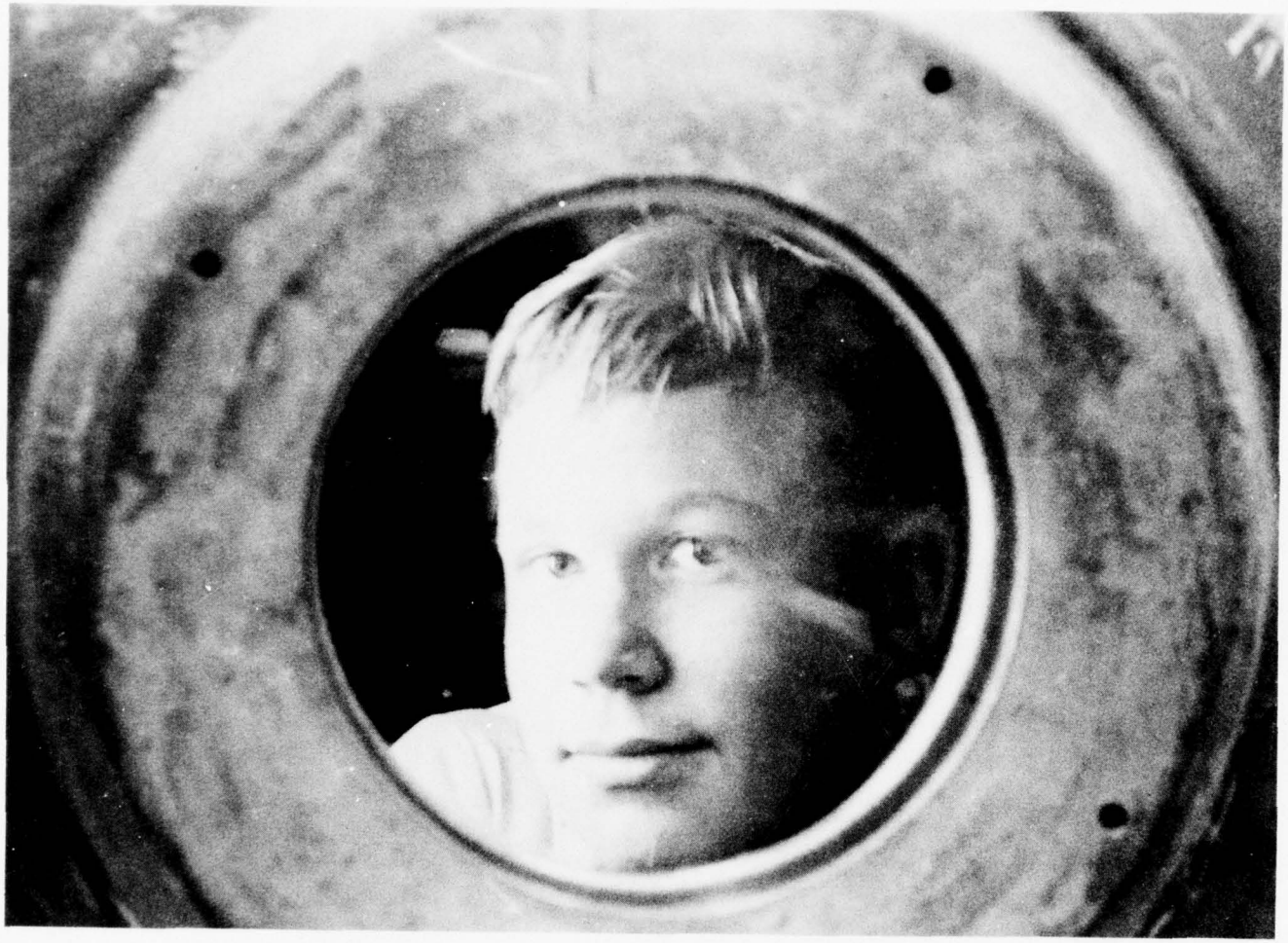

Figure 6.1. Typical size of a plane acrylic plastic window in a pressure vessel for human occupancy.

Figure 6.2. Window shapes, sizes, and bearing surface configurations developed by Navy engineers for hulls of submersibles, habitats, diving bells, and hyperbaric chambers.

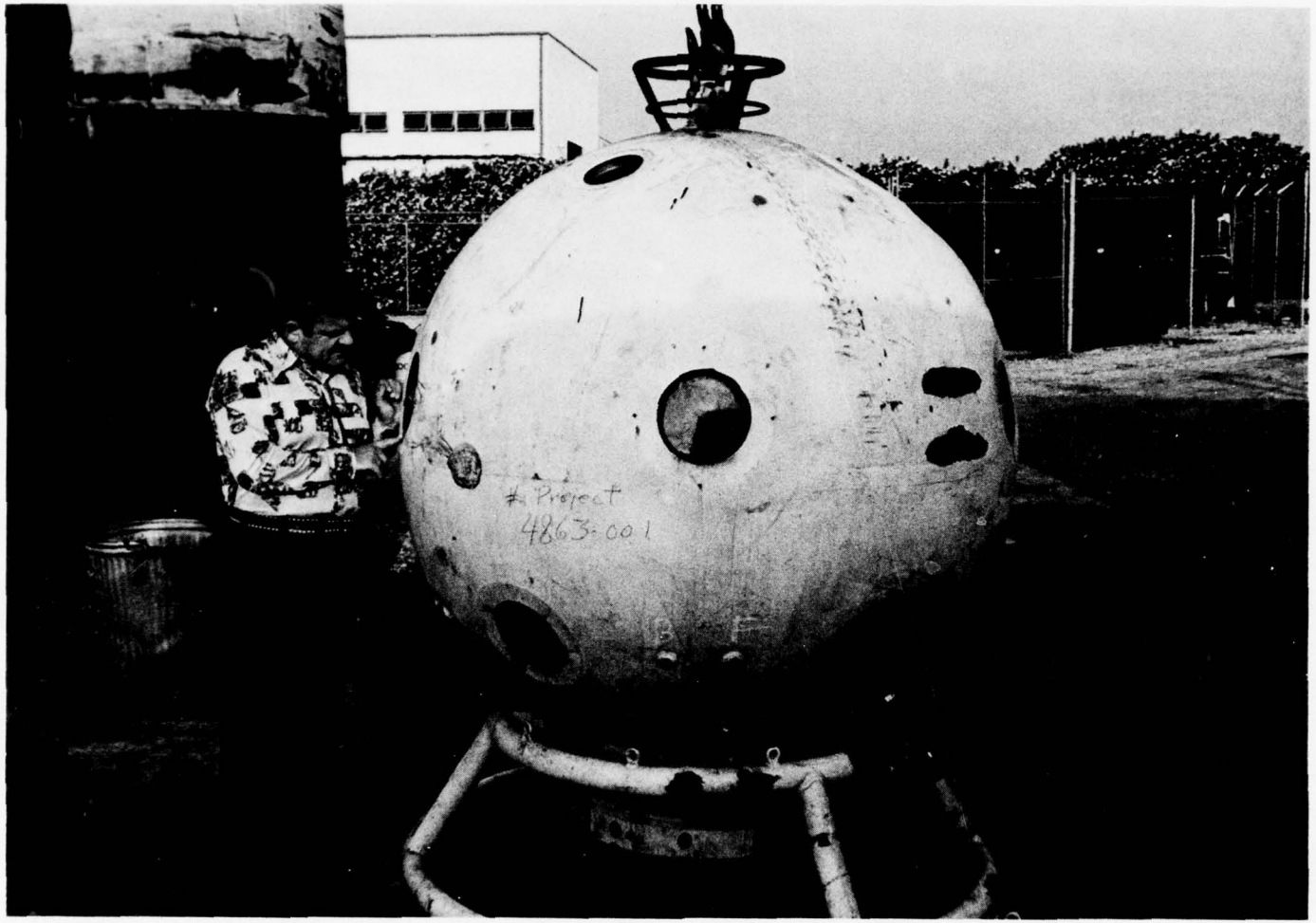

Figure 6.3. Typical multiple-plane window installation to provide visibility not afforded by a single-plane window.

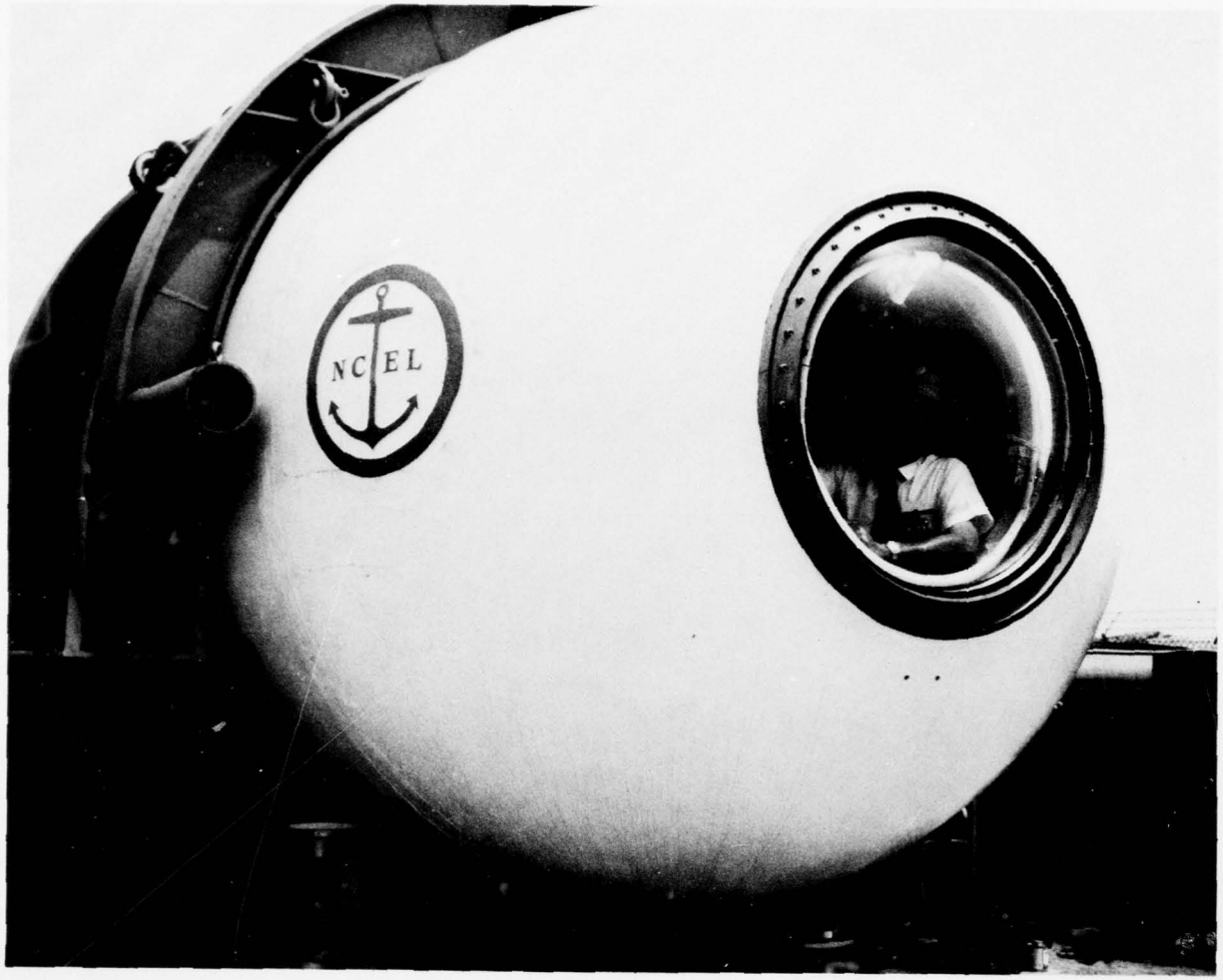

Figure 6.4. Typical spherical sector window in an undersea habitat. The panoramic visibility provided by the spherical sector window surpasses that of several plane windows at a fraction of their cost and weight.

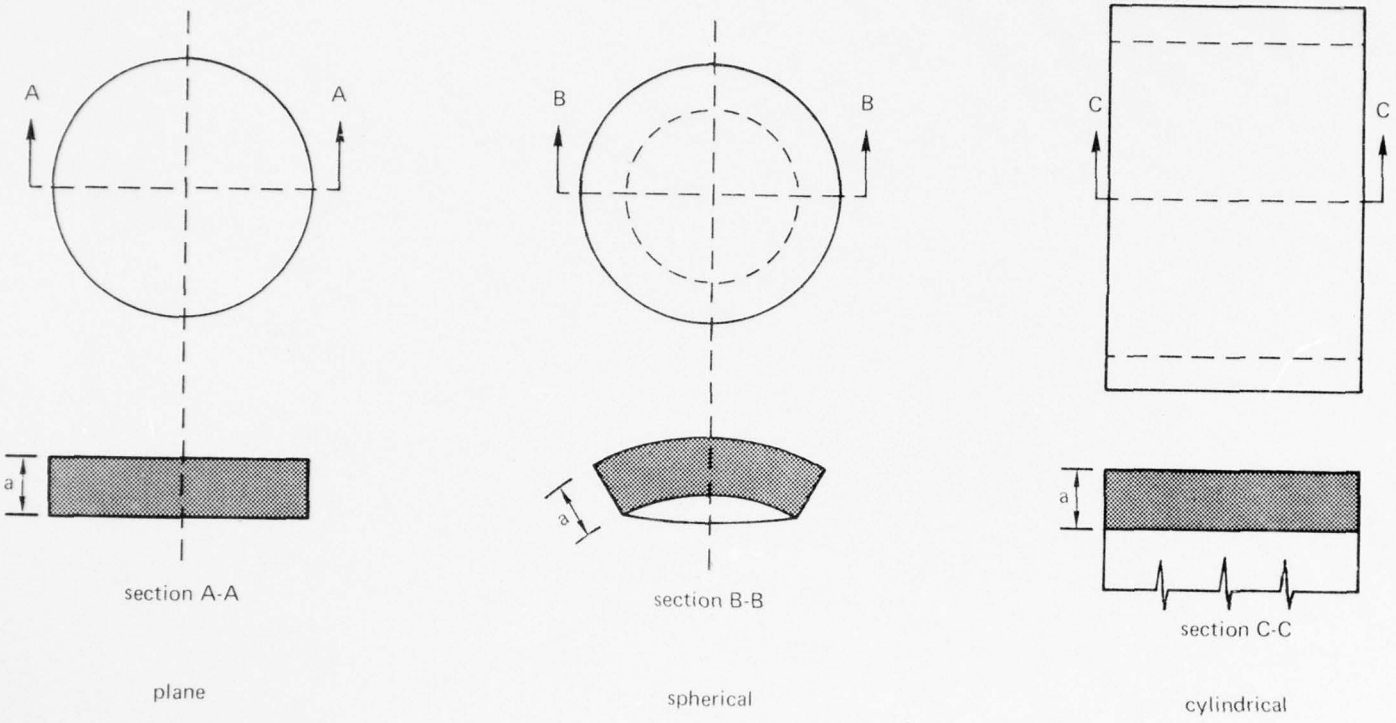

Figure 6.5. Common surface curvatures of pressure-resistant windows.

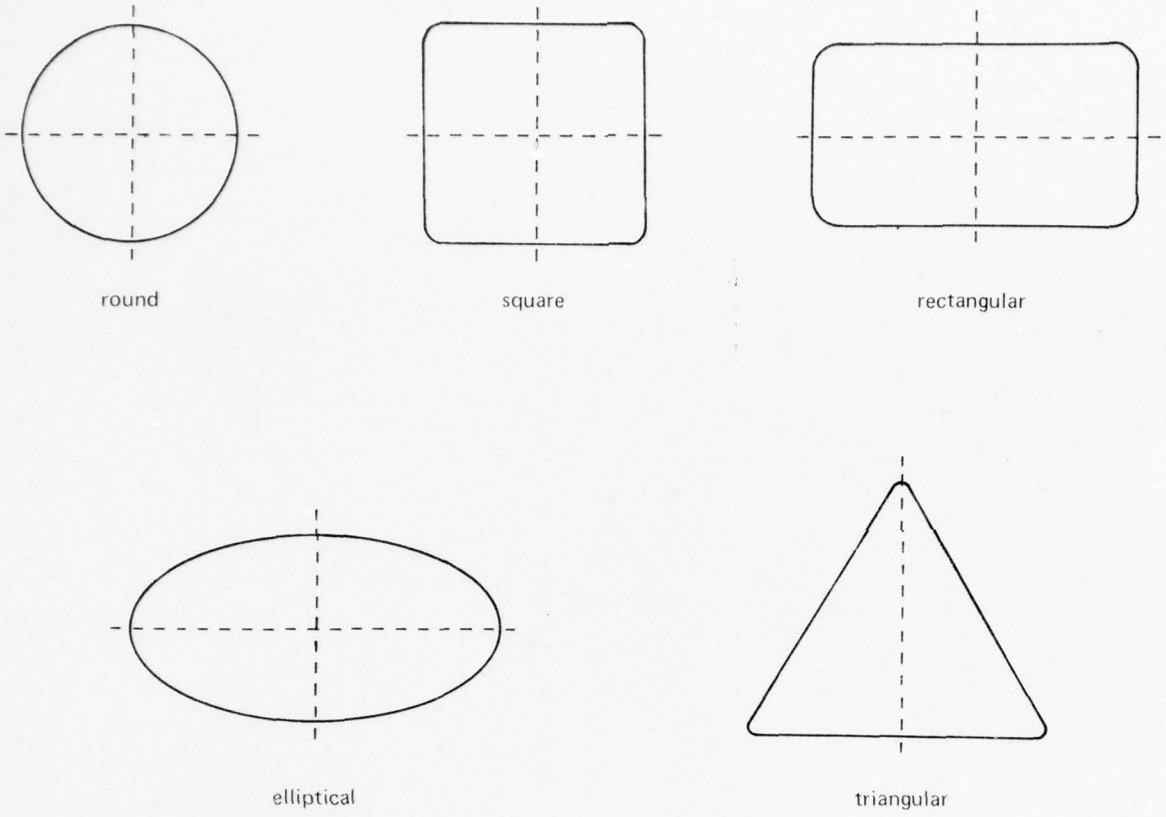

Figure 6.6. Common shapes of pressure-resistant windows. The triangular shape has been used only in outer space vehicles that are pressurized internally to less than 15 pounds per square inch (1 megapascal) for the comfort of the astronauts.

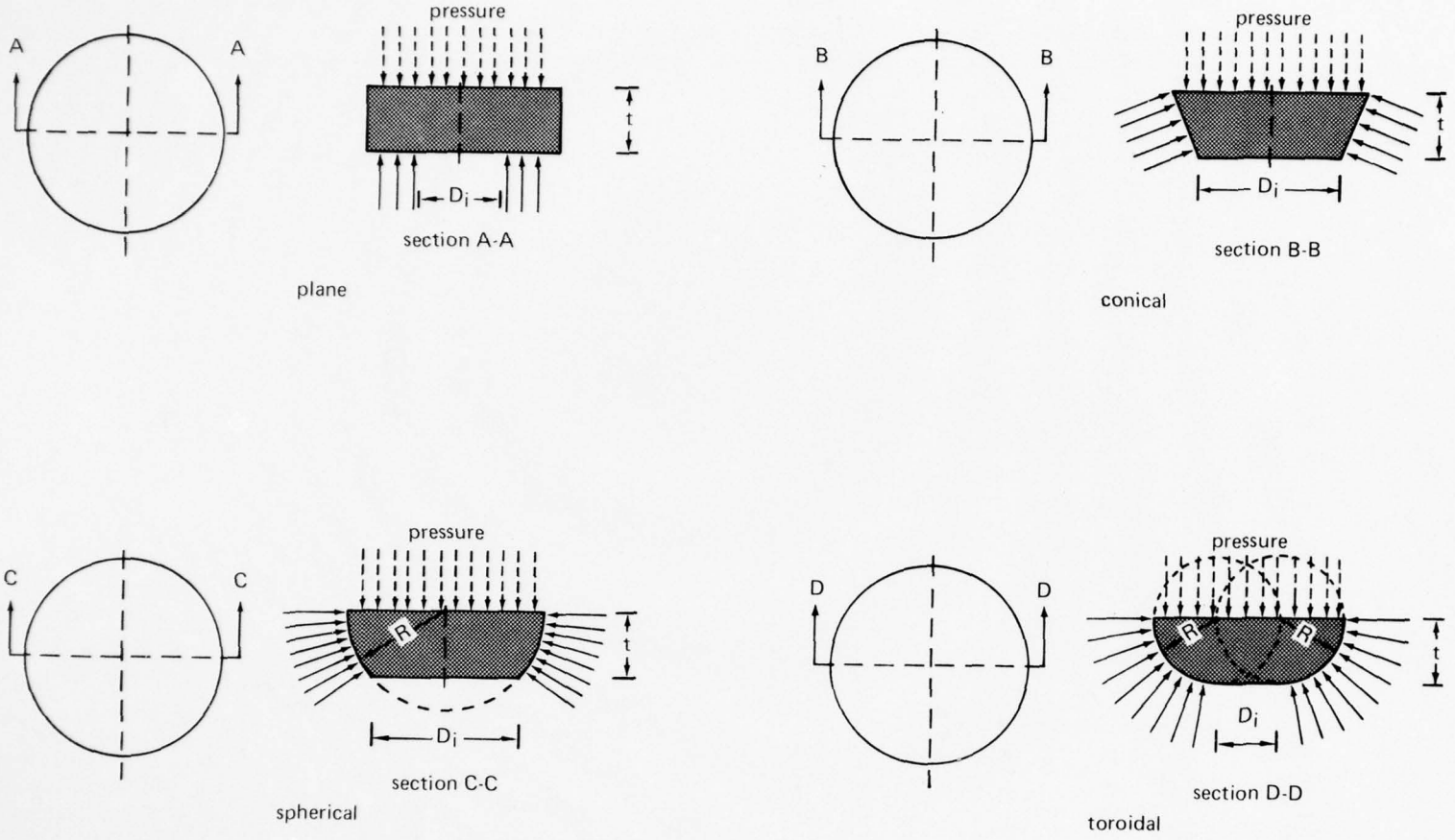

Figure 6.7. Bearing surfaces utilized on pressure-resistant windows. Although the illustration shows only bearing surfaces on plane disc windows, the same configurations can be applied to windows of other shapes and curvatures.

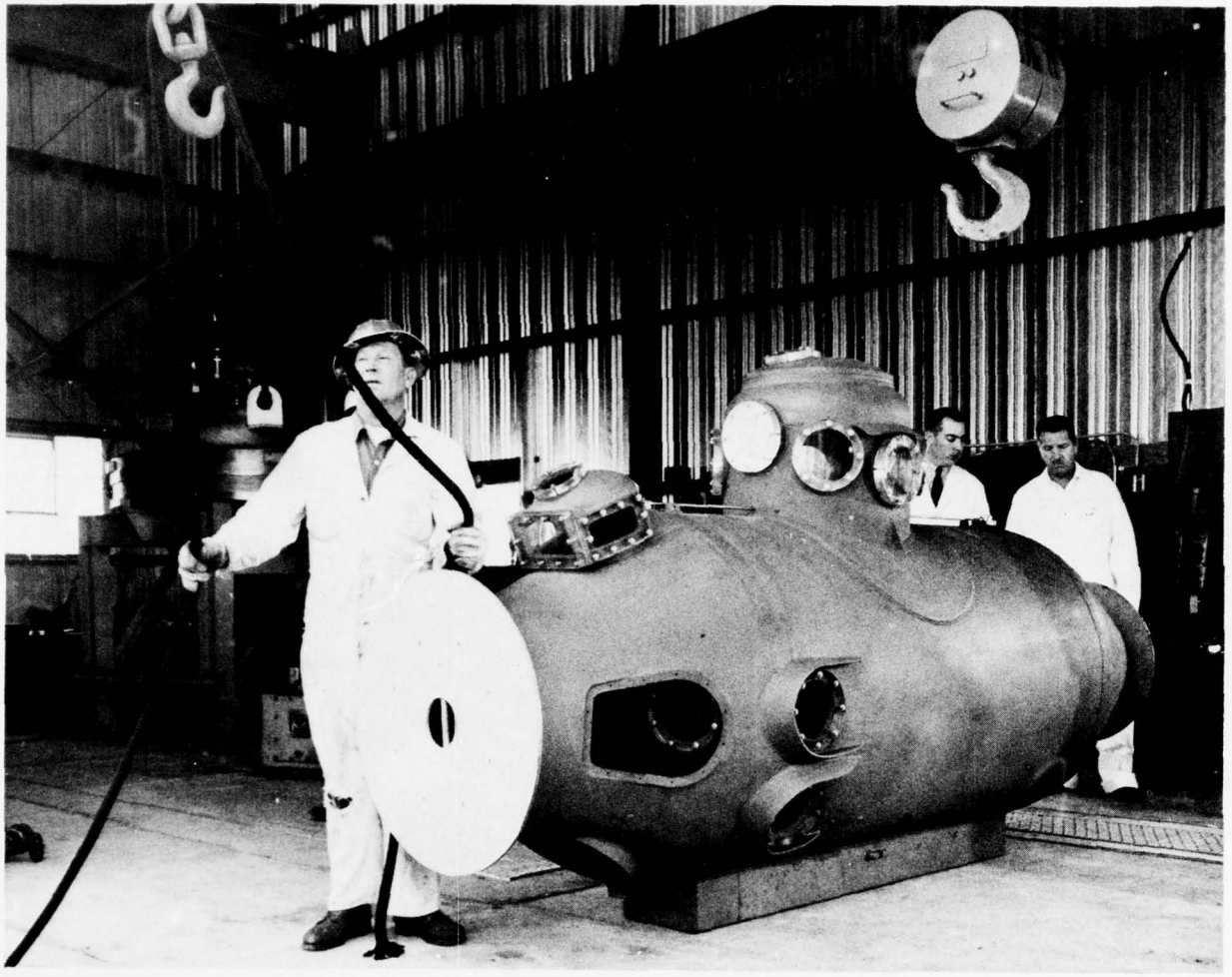

Figure 6.8. Typical application of round and rectangular plane windows in a shallow-depth submersible.

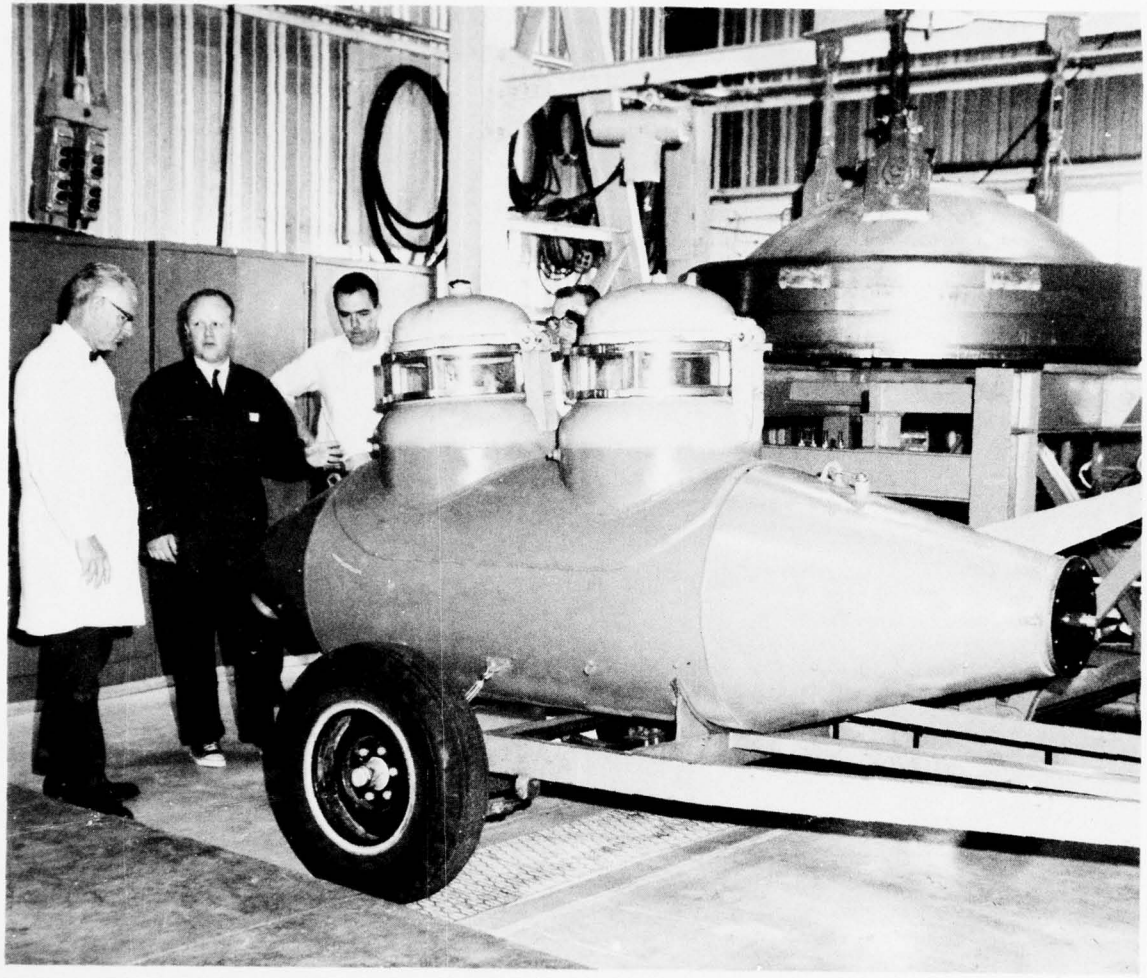

Figure 6.9. Typical application of cylindrical windows in the conning towers of a shallow-depth submersible.

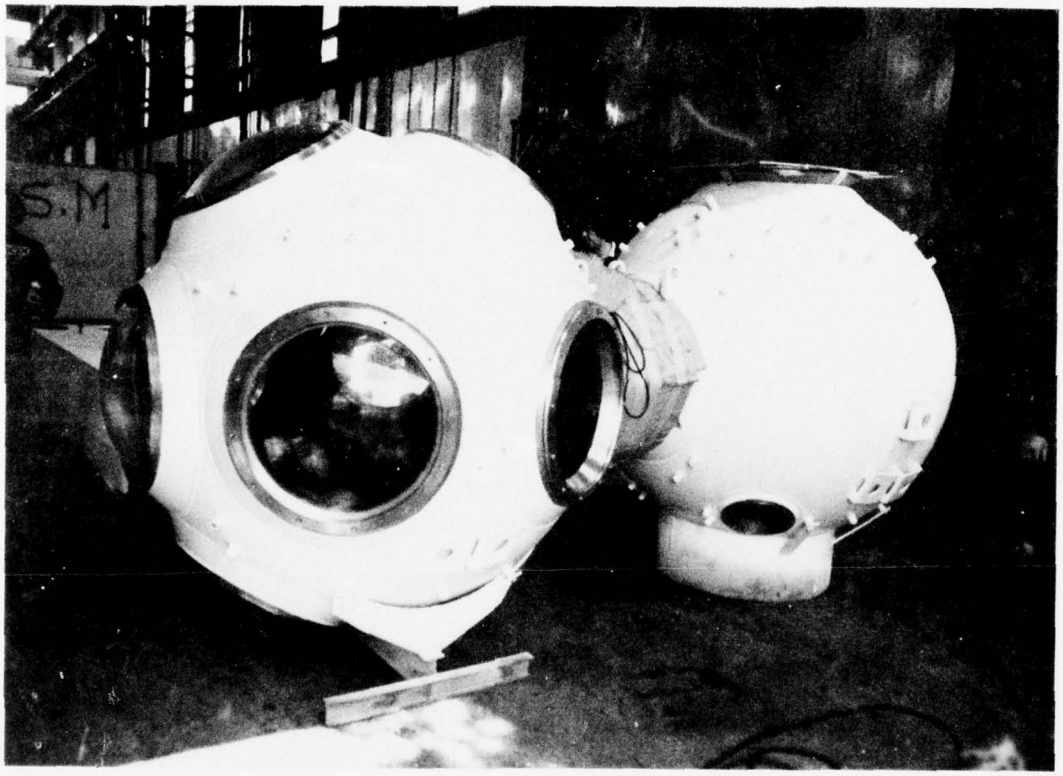

Figure 6.10. Typical multiple installation of spherical sector windows in the pilot's compartment of a submersible with a medium operational depth capability.

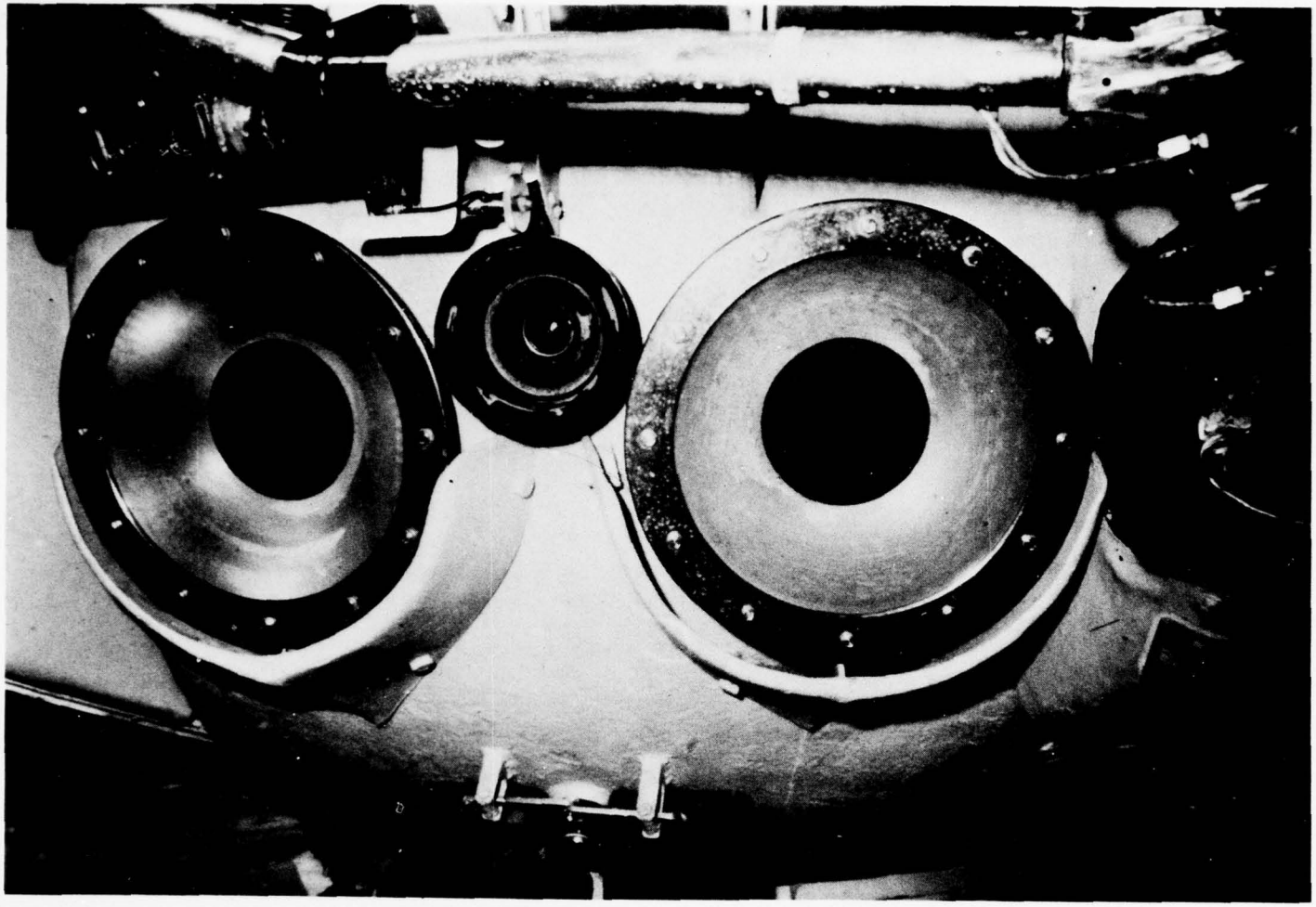

Figure 6.11. Typical application of round plane windows with conical bearing surfaces in a submersible with medium operational depth capability.

SECTION 7. PLANE DISC WINDOWS WITH FLAT BEARING SURFACES . . . 7-1

7.1 INTRODUCTION . . . 7-1

7.2 STRUCTURAL PERFORMANCE . . . 7-2

7.3 MODES OF FAILURE . . . 7-2

7.4 PREDICTION OF CRITICAL PRESSURES . . . 7-3

7.5 SEATING . . . 7-5

7.5.1 Bearing Support . . . 7-5
7.5.2 Bearing Gasket(s) . . . 7-5
7.5.3 Sealing . . . 7-6
7.5.4 Retainer Ring . . . 7-6
7.5.5 Window Mounting . . . 7-6

7.6 FABRICATION OF WINDOWS . . . 7-6

7.7 RESISTANCE TO IMPULSE AND POINT-IMPACT LOADING . . . 7-7

7.8 REFERENCES . . . 7-8

SECTION 7. PLANE DISC WINDOWS WITH FLAT BEARING SURFACES

7.1 INTRODUCTION

For several reasons the plane disc window configuration (figure 7.1) is the oldest design used for incorporation of pressure-resistant windows into pressure vessels for human occupancy (references 7.1 through 7.8):

1. The plane shape of the window surface lends itself to economical fabrication from sheets or plates of transparent materials. This is particularly true of glass which was used extensively in many early designs.

2. Because of the plane bearing surfaces on the window the seat on the mounting can also be plane, which permits machining to close flatness tolerances with common machine shop tools.

3. Sealing a plane window in its mounting against internal or external pressure poses no problems, since this can be easily done with a simple gasket fabricated from almost any available material. This feature in particular has made plane disc windows the standard design for two-way pressure vessels.

Presently, however, plane disc windows are not as popular as their low cost of fabrication and ease of installation would indicate, i.e., (1) the large mass of required mountings significantly increases the weight of the pressure hull and (2) the presence of tensile stresses on the low-pressure face of the window makes the window sensitive to crack initiation, particularly under hydrodynamic-impulse or point-impact loading. As a result, acrylic plastic plane disc windows are only rarely used outside two areas: (1) low-cost submersibles and hyperbaric chambers for pressure service less than 1000 pounds per square inch (6.89 megapascals) and (2) diving bells and personnel transfer capsules for pressure service less than 1000 pounds per square inch (6.89 megapascals), where the pressure hull is alternately subjected to external and internal pressurizations.

The only area where the popularity of plane disc window designs has significantly increased is in the chemical processing industry. Because of high temperature and corrosive liquid requirements, glass instead of acrylic plastic continues to be utilized. Since glass plane discs with flat bearing surfaces are several orders of magnitude less expensive than other glass window configurations, economic considerations have put this window design in a dominant position (references 7.6, 7.7, and 7.8). Because of stringent industrial fail-safe requirements, the inherent brittleness of massive glass windows has been compensated for in some designs with laminated construction, radial precompression of the window, or both. Similar modifications are, of course, also feasible for plane acrylic disc windows in pressure vessels for human occupancy. They have not been pursued actively, however, because of the associated penalties in additional weight and cost of the window-mounting assembly.

7.2 STRUCTURAL PERFORMANCE

The plane disc acrylic window with plane bearing surfaces reacts to hydrostatic loading applied to one of the faces as a flat, edge-supported, circular plate does under uniform loading (references 7.1 and 7.2). As a result, the face exposed to hydrostatic pressure goes into biaxial compression, while the opposite face goes into biaxial tension. The maximum stresses are found at the centers of the faces: positive on the low-pressure face and negative on the high-pressure face. Because the retaining ring tends to restrain the edge of the window from rotation during application of hydrostatic pressure, high stresses are also generated in the window near the edge of support (figure 7.2). The maximum compressive stress is generally somewhat larger than the maximum tensile stress, probably the result of radial compression of the window edge with hydrostatic pressure, radial contraction of the mounting, or both.

Because the ultimate tensile strength of acrylic plastic is approximately 50 percent lower than its compressive yield strength, cracking of the window generally starts at the center of the low-pressure face. The presence of scratches at the center of the low-pressure face can significantly decrease the critical pressure of the window because of the acrylic plastic's notch sensitivity (figures 7.3 and 7.4). For windows which are alternately pressurized from each side, protection of both faces against scratching becomes imperative. Because the window's edge is in compression it can tolerate with impunity rough surface finishes, scratches, and even O-ring grooves.

The magnitude of stresses at the centers of faces as well as the critical pressure of the window is a function of window thickness (t), diameter of the unsupported window area (D_i), and external diameter of the window (D_o) restrained by the retaining ring. Increasing the t/D_i ratio raises the critical pressure dramatically, while increasing the D_o/D_i ratio has only a limited effect. Experimental data indicate that the critical pressure of a window tested without a retaining ring is not affected by changes in the D_o/D_i ratio, if the ratio is greater than or equal to 1.25. How much further the D_o/D_i ratio can be decreased without causing the window to deform on the plane bearing surface is not known. In absence of data to the contrary the designer of flat disc windows is cautioned not to decrease the D_o/D_i ratio beyond 1.25, although designs do exist with a 1.12 ratio.

7.3 MODES OF FAILURE

Plane disc acrylic windows with plane bearing surfaces fail in either a flexure or shear mode, depending on the magnitude of their t/D_i ratios (references 7.1 and 7.2). Those with a ratio less than or equal to 0.4 fail in flexure while those with large t/D_i ratios fail primarly in shear. Since cracks initiated by tensile components of flexure stresses can in some cases propagate without further increases in service pressure, the failure of a thin, flat disc acrylic window can be catastrophic, i.e., there is no warning to the occupant of the vessel. This is not, however, valid for thick windows, where both the tensile and shear cracks can be heard and seen prior to catastrophic failure.

Because of the time- and temperature-dependent strength properties of acrylic plastic, plane disc windows can fail in short-term, long-term, or cyclic pressurization modes. Since the ultimate tensile strength of acrylic will decrease with duration of loading and increase in ambient temperature, the highest values for critical pressures were experimentally determined under short-term loading at low temperatures while the lowest values were found

under long-term loading at high ambient temperatures. Values during cyclic loading varied between those found at short- and long-term loadings, depending on the duration of individual pressure cycles, ambient temperature, and number of pressure cycles.

Regardless of type of loading, fracture was initiated in thin windows at the center of the low-pressure face (figure 7.5). The fracture assumed the shape of a star whose rays propagated towards the edge of window's bearing surface. If loading on the window was increased by additionally raising the pressure, the rays penetrated into the interior of the window until a conchoidal fracture surface in the shape of a cone was generated (figure 7.6). The size of the cone base equaled that of the unsupported window area, while the tip of the cone penetrated the center of the high-pressure surface (figure 7.7). The mode of failure appeared to be independent of ambient temperature, except for a given pressure loading the extent of fracture increased with ambient temperature (figure 7.8).

The initiation of fracture in thick windows differed only in one respect: The fracture of the window was initiated by a circumferential shear crack located at the edge of the unsupported low-pressure face (figure 7.9). The star-shaped crack only appeared if the pressure loading on the window was further increased. Because shear cracks predominate, the fracture surface in a failed window is cylindrical, distinctively different from the cone-shaped fracture surface observed in thin windows (figure 7.10).

7.4 PREDICTION OF CRITICAL PRESSURES

Although the ultimate strength of acrylic plastic under short- and long-term uniaxial tensile stresses is known, no reliable analytic or empirical relationship has been developed to allow confident prediction of the precise value of critical pressure for plane disc windows under short-term, long-term, or cyclic pressure loadings. As a result, all existing plane disc window designs must rely on experimental data.

The majority of existing data was generated by pressurizing model-scale windows to implosion under short-term loading conditions, while measuring their axial displacement (reference 7.1, 7.2, and 7.5). These data are extensive and general enough to cover the range of $0.05 \leqslant t/D_i \leqslant 0.65$ at ambient temperature (figures 7.11 and 7.12). Because the t/D_i and D_o/D_i ratios are dimensionless, critical pressures of model-scale windows can be used for directly predicting the critical pressures of full-scale windows with the same ratios. To predict the axial displacement of full-scale windows, however, one must multiply the displacement of the model-scale windows by the ratio of the diameters of the full-scale window to the model-scale window. For other ambient temperatures and loading conditions there are only very scattered data. On the basis of these data several relationships have been discovered which allow accurate prediction of the critical pressure of any plane disc acrylic window under long-term or cyclic loading conditions by using as few as five test specimens (figures 7.13, 7.14, and 7.15). The basic findings are

1. Crack growth is time and temperature dependent.
2. Test results are repeatable.
3. Cracks initiate at the same locations and produce fracture surfaces identical to those generated by short-term loading conditions.
4. Impending catastrophic fracture can be detected well in advance, since crack growth is very slow, except for very thin windows or windows loaded close to their short-term critical pressure (figure 7.16).

5. Axial displacement of the window's center at the moment of failure is the same for all loading conditions. This forms the basis of a simple failure warning system that uses an electric contact switch preset to close when the displacement of the window reaches 25 percent of projected displacement at failure. (The latter value is generally obtained in a short-term test to failure.)

The prediction of critical pressures under long-term or cyclic pressure loadings is based on the premise that critical pressure data points generated during long-term (figures 7.13 and 7.14) or cyclic (figure 7.15) loading tests will tend to fall on a straight line when plotted on log-log coordinates representing pressure and time (static fatigue) or pressure and number of cycles (cyclic fatigue). In this manner the critical pressure of a specific plane window design at, for example, 10,000 hours or 10,000 cycles, can be extrapolated from a minimum of five tests lasting less than 1000 hours. Model-scale windows can be used for the generation of these data, since the critical pressures of model-scale windows are the same as for full-scale windows with identical t/D_i and D_o/D_i ratios. Such data, however, have been generated for only a few t/D_i ratios and temperatures.

For t/D_i ratios and temperatures for which the static and cyclic fatigue data do not exist, the designer must either establish an experimental test program or utilize the existing short-term data at room temperature with appropriate conversion factors that consider the temperature and loading conditions likely to be encountered during operational service. This design approach significantly differs from the previous approach, i.e., the first experimentally proves that the static and cyclic fatigue properties of a given window design at predicted ambient temperatures are in excess of those required by service conditions, whereas the second uses empirical selection of adequate conversion factors to relate existing short-term data to projected service conditions.

In the experimental approach, the actual critical pressures under long-term and cyclic loadings are determined and subsequently compared to operational pressure, while in the empirical approach only the short-term critical pressure and the conversion factor are known. Based on the effectiveness and cost of the window-mounting assembly, the first approach is preferable as it allows optimization of the design for a given set of unique operational conditions. Because of the conservatism inherent to a conversion factor applicable to many diverse operational conditions, the second results in a less cost-effective, but much safer, design. Since the second approach bypasses expensive and lengthy experimental programs it has been selected by many designers in preference to the more precise, but also more expensive, method.

Because the selection of an appropriate conversion factor is generally beyond the capability of those not specializing in window design, they must use the conversion factors developed for such applications by professional engineering societies, pressure vessel classification societies, and government agencies. The factors in table 7.1 were developed through a joint effort of The American Society of Mechanical Engineers, Det Norske Veritas, U.S. Bureau of Shipping, U.S. Coast Guard, and the Naval Undersea Center. The factors are conservative for all applications, except where sustained loadings are in excess of 40,000 hours. In selecting these factors many design, fabrication, and service variables not usually considered by the designer were included.

Table 7.1. Conversion factors for acrylic plastic plane disc windows.

Operational Pressure Ranges	Temperature				
	50°F (10°C)	75°F (24°C)	100°F (38°C)	126°F (52°C)	151°F (66°C)
	Conversion Factors				
2500 psi (17.2 mPa)	5	6	8	10	16
5000 psi (34.5 mPa)	5	6	8	10	
7500 psi (51.7 mPa)	5	6			

7.5 SEATING

Plane disc acrylic windows require a mounting that not only provides bearing support to the window's low-pressure face but also retains it in place against compressed seals. If the window will see pressure service on both faces, the mounting must provide adequate support to both. Although there are many approaches feasible to the design of a successful mounting, all should have the following features (figure 7.17) to satisfy safety requirements of pressure vessels for human occupancy (section 15).

7.5.1 Bearing Support

The bearing support for the window's plane viewing surface should be flat to within 0.010 inch (0.25 millimeter) and have an external diameter with a ratio of at least D_o/D_i greater than or equal to 1.25. Discontinuities in the form of O-ring grooves should be avoided on the bearing surface of the mounting as they act as crack initiators in the window's bearing surface. The inner edge of the bearing support should have a radius of greater than or equal to 0.020 inch (0.5 millimeter) to avoid cutting into the flat window face(s) when under load. For two-way pressure service, bearing supports must be provided for both viewing surfaces of the window.

7.5.2 Bearing Gasket(s)

These should be slightly oversize, of at least 80-durometer hardness, and from 0.020 to 0.125 inch (0.5 to 3.2 millimeters) thick. To minimize lateral extension under compression they should be securely bonded with contact cement to the bearing support surface in the flange. If the window is subjected to two-way pressure service, a bearing gasket should also be bonded to the bearing support surface on the retainer ring. Since the gaskets function

as primary or secondary seals they should preferably be made from nonpermeable elastomeric material.

7.5.3 Sealing

The window should preferably be sealed with two seals whose sealing actions are independent of each other. The primary seal should be a gasket pressing against the high-pressure face of the window, while the secondary seal may be a radially compressed O-ring pressing against the circumference or a bearing gasket at the bearing support under the low-pressure face. To prevent lateral extrusion the gaskets should be bonded to the mounting. An elastomeric bearing gasket under the window can also be used as a secondary seal.

7.5.4 Retainer Ring

A flat retainer ring securely fastened to the mounting should be used to retain the window and compress those gaskets acting as seals. To avoid overcompressing the gaskets and to help during assembly, one surface on the retaining ring should, upon tightening of the screws, contact the mounting. If the window is exposed to pressure on either face, the retainer ring and screws should be placed on the side of the hull exposed to the higher pressure.

7.5.5 Window Mounting

The window cavity in the mounting should be sufficiently deep to accommodate the window and compressed gaskets without undue looseness or squeezing. The diameter of the cavity should provide snug fit for the window with its O-ring seal. Excessive clearance ($\geqslant$0.060 inch (1.5 millimeters)) between the edge of the window and the mounting will not only prevent the O-ring from sealing but will also lower the critical pressure of the window. Since the walls of the cavity serve as an integral component of the seals, they must be kept free of corrosion. Weld overlays of Monel, electroless nickel platings, or painting can prevent corrosion of the window cavity walls and the retaining ring surface in contact with the gasket.

The window mounting also serves as a reinforcement around the penetration in the hull. Thus contraction or expansion of the hull causes the mounting to change dimensionally. Since excessive rotation of the bearing surface ($>$ 0.5 degree (0.008 radian)) or excessive squeezing of the window by the mounting, if the initial clearance between the window and the seat is zero, can superimpose high radial compressive stresses on those stresses already induced by hydrostatic loading, both the radial squeeze and angular rotation should be considered during design. The radial compressive stress generated by squeezing the window should not exceed 1000 pounds per square inch (6.89 megapascals).

7.6 FABRICATION OF WINDOWS

Plane windows are generally made by machining discs from acrylic plastic sheets of appropriate thickness. Significant savings can be realized by selecting window thicknesses corresponding to standard sheet thicknesses (from 1/4 to 4 inches (0.6 to 10.2 centimeters) in increments of 1/4 inch (0.6 centimeter)). If the desired thickness can only be achieved by machining down a thicker sheet, it is mandatory that the machined flat surface (or surfaces) be machined to a 32-rms finish prior to sanding and polishing. This is necessary to eliminate

AD-A070 535 NAVAL UNDERSEA CENTER SAN DIEGO CA F/G 11/9
ACRYLIC PLASTIC VIEWPOINT FOR OCEAN ENGINEERING APPLICATIONS. V--ETC(U)
FEB 77 J D STACHIW
UNCLASSIFIED NUC-TP-562-VOL-1 NL

4 OF 5
AD
A070535

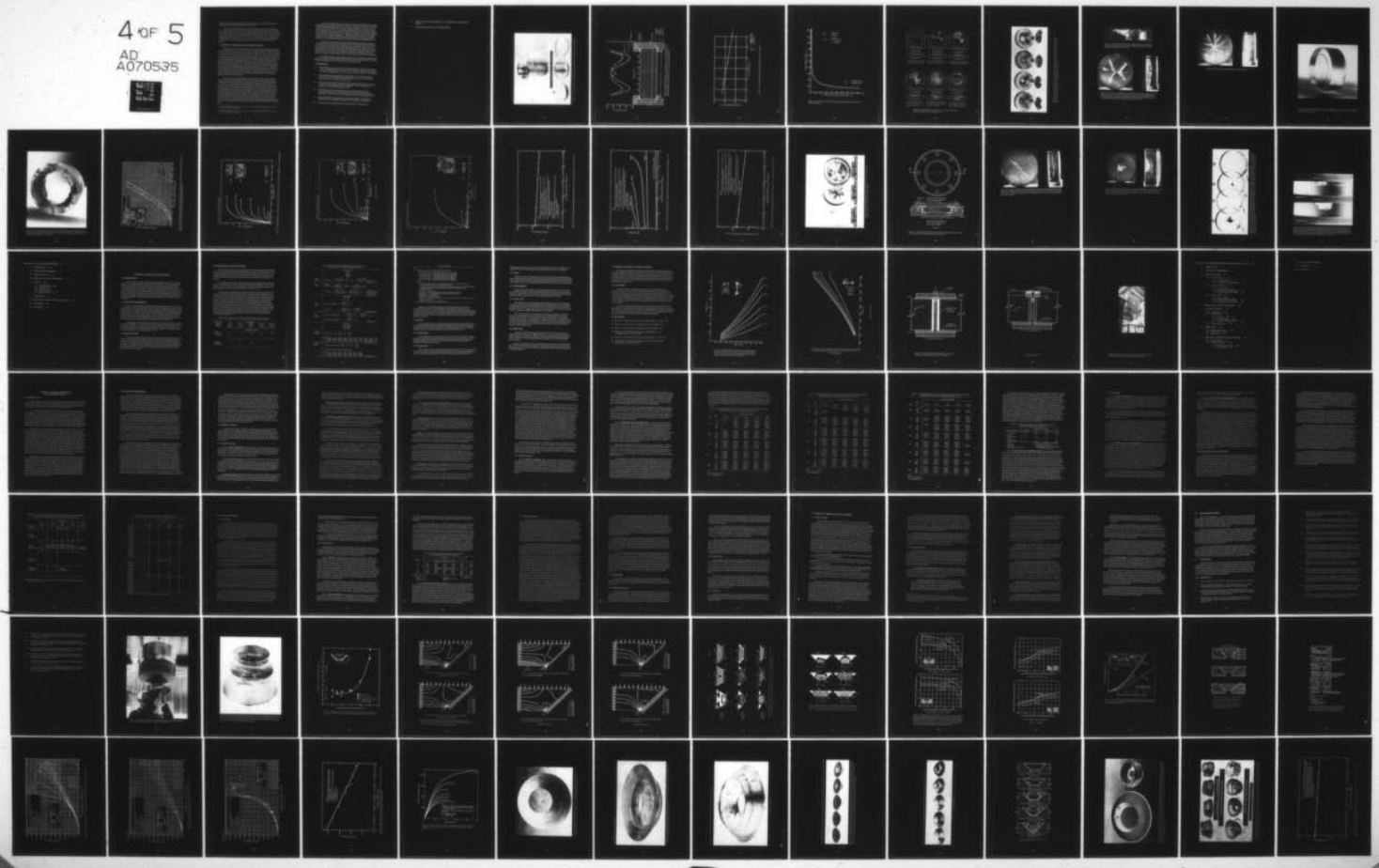

any stress risers on surfaces which will be subjected to tension. Failure to perform this function may result in premature failure of the window.

Annealing of machined windows must be performed at least once and preferably twice. The first process should be done on rough cut discs at sufficiently high temperatures (320 to 340°F (160 to 171°C)) to anneal them thoroughly and to stabilize them dimensionally (diameter shrinks 2.2 percent and thickness increases 4 percent). The second annealing should occur at low temperatures (170 to 212°F (77 to 100°C)) only when all machining and polishing operations have been completed. Because of massive shrinkage from the first annealing process, no dimensional changes occur during final annealing of the finished product.

7.7 RESISTANCE TO IMPULSE AND POINT-IMPACT LOADING

Pressurized plane disc windows are sensitive to impulse and point-impact loading because both generate dynamic tensile stresses which, when superimposed on the static tensile stresses generated by hydrostatic loading, cause the windows to fracture under low dynamic overpressures. The available experimental data are not sufficient to form conclusive findings in this area, but it appears that dynamic overpressures equal to or greater than 20 percent of the window's short-term static critical pressure will initiate fracture on the low-pressure face of a statically unpressurized window (reference 7.3). If the window is already presurized statically, the magnitude of dynamic overpressure required for fracture initiation on the low-pressure face is less (figure 7.18). Sufficient data are not available to permit the derivation of an empirical relationship between fracture initiation and the relative magnitudes of static and dynamic pressures simultaneously acting on the high-pressure face. A safe rule at the present time is to add the static pressure to the dynamic pressure and to use the sum of the combined pressures as effective overpressure. If the magnitude of effective overpressure is equal to or greater than 20 percent of the short-term static critical pressure, initiation of fracture can be expected.

There are less data for point-impact loading than for dynamic pressure loading. Available data indicate that plane disc windows are at least one order of magnitude less resistant to point-impact loading than spherical sector windows with the same t/D_i ratio. For example, it requires only approximately 300 foot-pounds (407 newton-meters) of kinetic energy* to initiate fracture in a 2-inch-thick (5 centimeters), flat disc acrylic window with a t/D_i ratio of 0.38 that is statically pressurized to 450 pounds per square inch (3.10 megapascals) on the impacted face (reference 7.4). If the impact** were applied to the low-pressure face of the same window statically pressurized to 450 pounds per square inch (3.10 megapascals), only 112 foot-pounds (152 newton-meters) of kinetic energy would be required to initiate fracture (figure 7.19) (reference 7.4). For this reason it is recommended that a plane disc window with a t/D_i ratio less than or equal to 0.38 be protected with an external guard or shield against point impacts that are generated during retrieval of an internally pressurized personnel transfer capsule aboard a rolling and pitching ship.

A 200-pound (91 kilograms) weight with 0.25-inch-radius (0.6 centimeter) point impacting at 10 feet per second (3.05 meters per second) on the high-pressure face.

**A 200-pound (91 kilograms) weight with a 0.75-inch-radius (1.9 centimeters) point impacting at 6 feet per second (1.8 meters per second) on the low-pressure face.*

The most promising approach to providing a transparent shield against point-impact loading is laminated window construction (reference 7.2), which consists of 0.25-inch-thick (0.6 centimeter) acrylic sheets bonded with a transparent elastomer to the high- and low-pressure faces (figures 7.20 and 7.21). By bonding the shield to the window, the shield is made shatterproof against minor impacts and the point loading on the shield is transmitted by the elastomer as dynamic pressure over a larger area of the window, thus eliminating the need for frequent cleaning of trapped dirt. Laminated shields also provide the structural component of the window sandwiched between shields with excellent protection against scratches, which can significantly decrease the critical pressure of the window (figure 7.4).

Experiments conducted by firing small caliber bullets against windows protected with laminated, 0.25-inch-thick (0.6 centimeter), acrylic shields show that such shielding is more than adequate to preserve the structural integrity of the load-carrying acrylic core sandwiched between two thin shields. Although shielding plane disc windows with acrylic sheets laminated to the window with elastomeric compounds is expensive (triples or quadruples the cost of the window), the resulting increase in impact resistance and protection against scratching of the load-carrying window core more than compensates for the increase.

For applications where minor impacts frequently occur, the laminated shields should be made from stretched acrylic (MIL-P-25690), as its resistance to crack initiation is an order of magnitude higher than that of utility-grade acrylic plastic (LP-391).

7.8 REFERENCES

7.1 Naval Civil Engineering Laboratory, Technical Report R527, "Windows for External or Internal Hydrostatic Pressure Vessels – Part II: Flat Acrylic Windows Under Short-Term Pressure Applications", by J. D. Stachiw, G. M. Dunn, and K. O. Gray, May 1976.

7.2 Naval Civil Engineering Laboratory, Technical Note N-1127, "Flat Disc Acrylic Plastic Windows for Man-Rated Hyperbaric Chambers at the U.S.N. Experimental Diving Unit," by J. D. Stachiw, November 1970.

7.3 Southwest Research Institute, Report 03-2406, "Resistance of Cylindrical Viewports to Pressures Emanating from Underwater Explosions," by B. W. VanZant, A. L. Schraeder, and R. C. DeHart, September 1968.

7.4 Naval Ship Research and Development Center, Letter Report 68-720-1262, "Structural Performance of Acrylic Windows for the Personnel Transfer Capsule MK2 Mod 0," by M. A. Krenzke, F. M. Schwartz, and G. D. Ward, September 1968.

7.5 Autonetics, Division of North American Aviation, Incorporated, Letter Report, "Pressure Effects on Plexiglas Circular Discs," by C. E. Bodey, 22 April 1965.

7.6 Chemical Engineering, "Sight Glass Worth Looking Into," 23 January 1961.

7.7 Pressure Products Company, Bulletin A-61, "See With Safety," Charleston, West Virginia.

7.8 Pittsburgh Testing Laboratory, Test Report 489962.

Figure 7.1. Acrylic plastic plane disc windows and mounting flange for evaluation under hydrostatic loading.

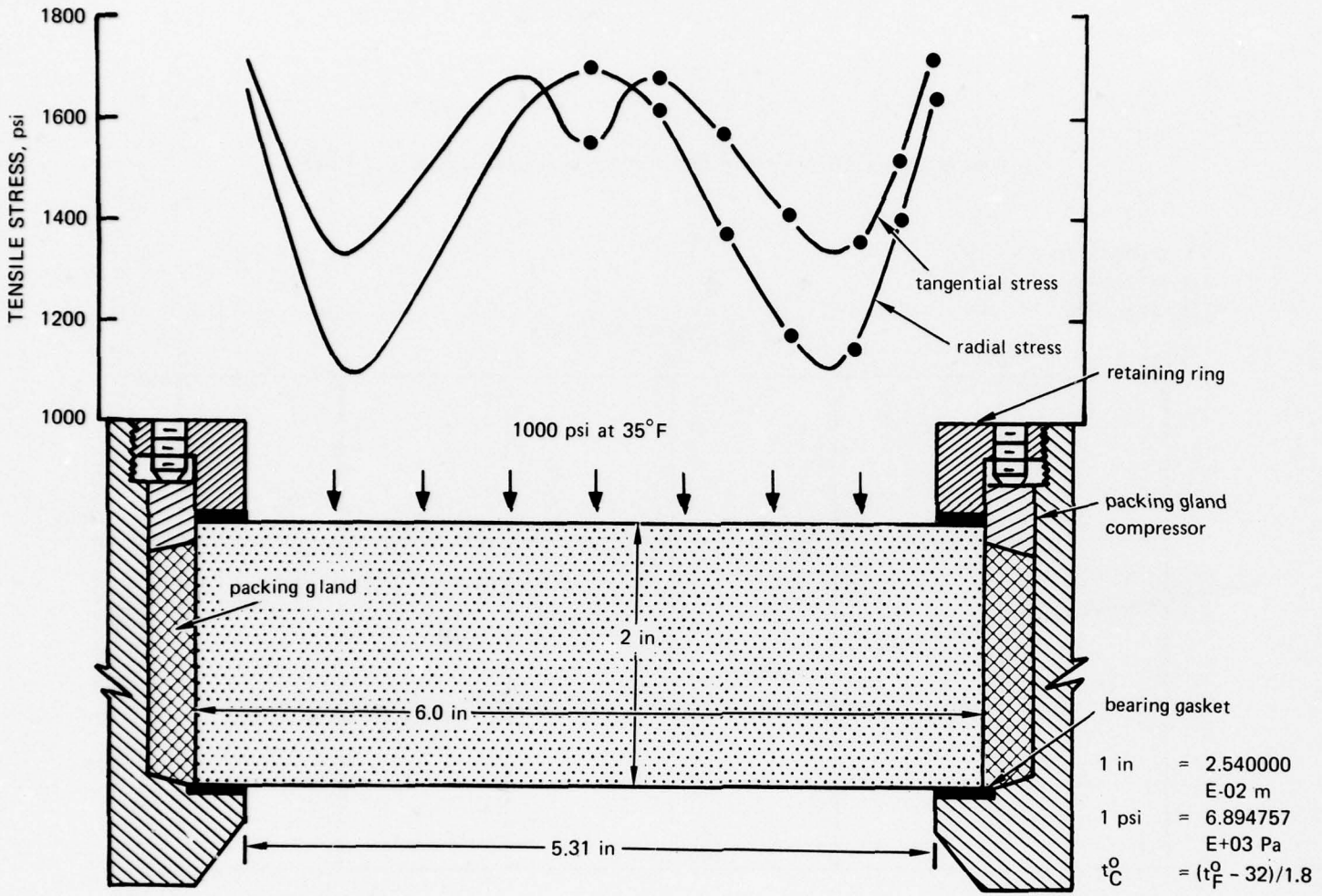

Figure 7.2. Distribution of stresses on the low-pressure face of a plane disc acrylic window ($t/D_i = 0.38$; $D_o/D_i = 1.14$; temperature = 32° F (0° C)). This type of mounting was developed by Pressure Products Company for use primarily with glass windows.

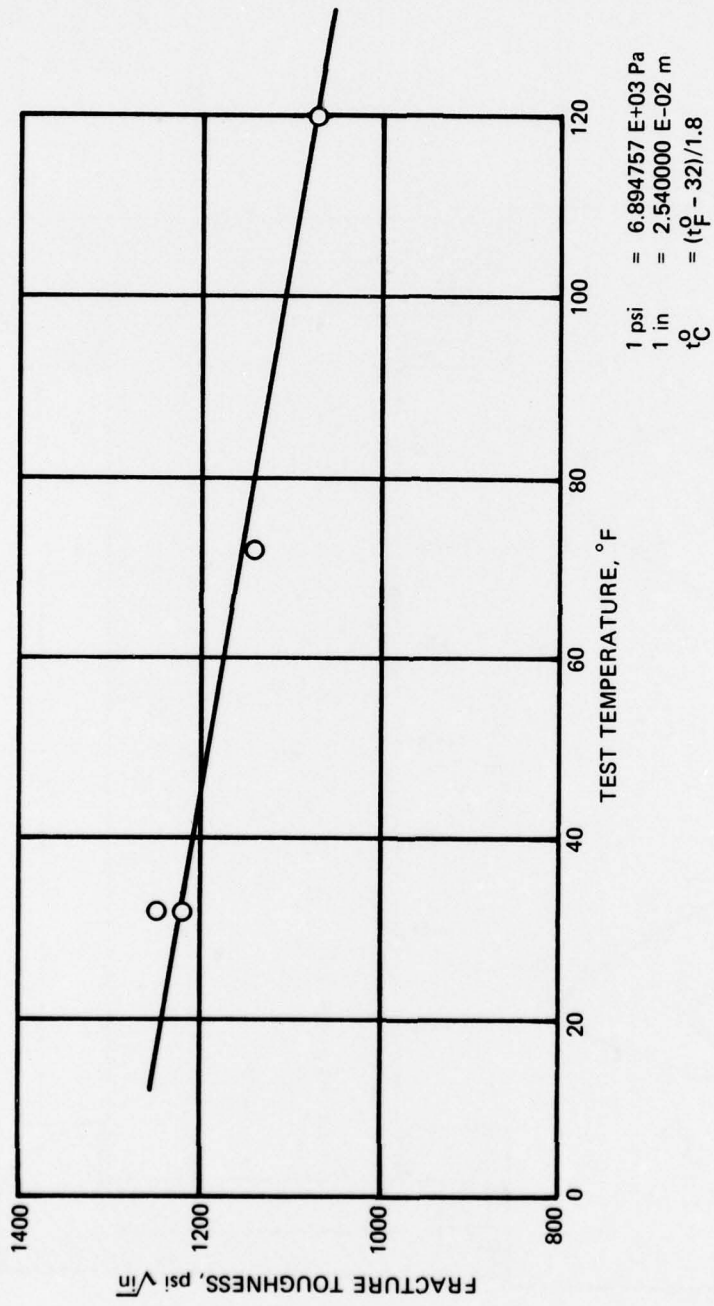

Figure 7.3. Fracture toughness of acrylic plastic from 20 to 120°F (-6.7 to +48.9°C).

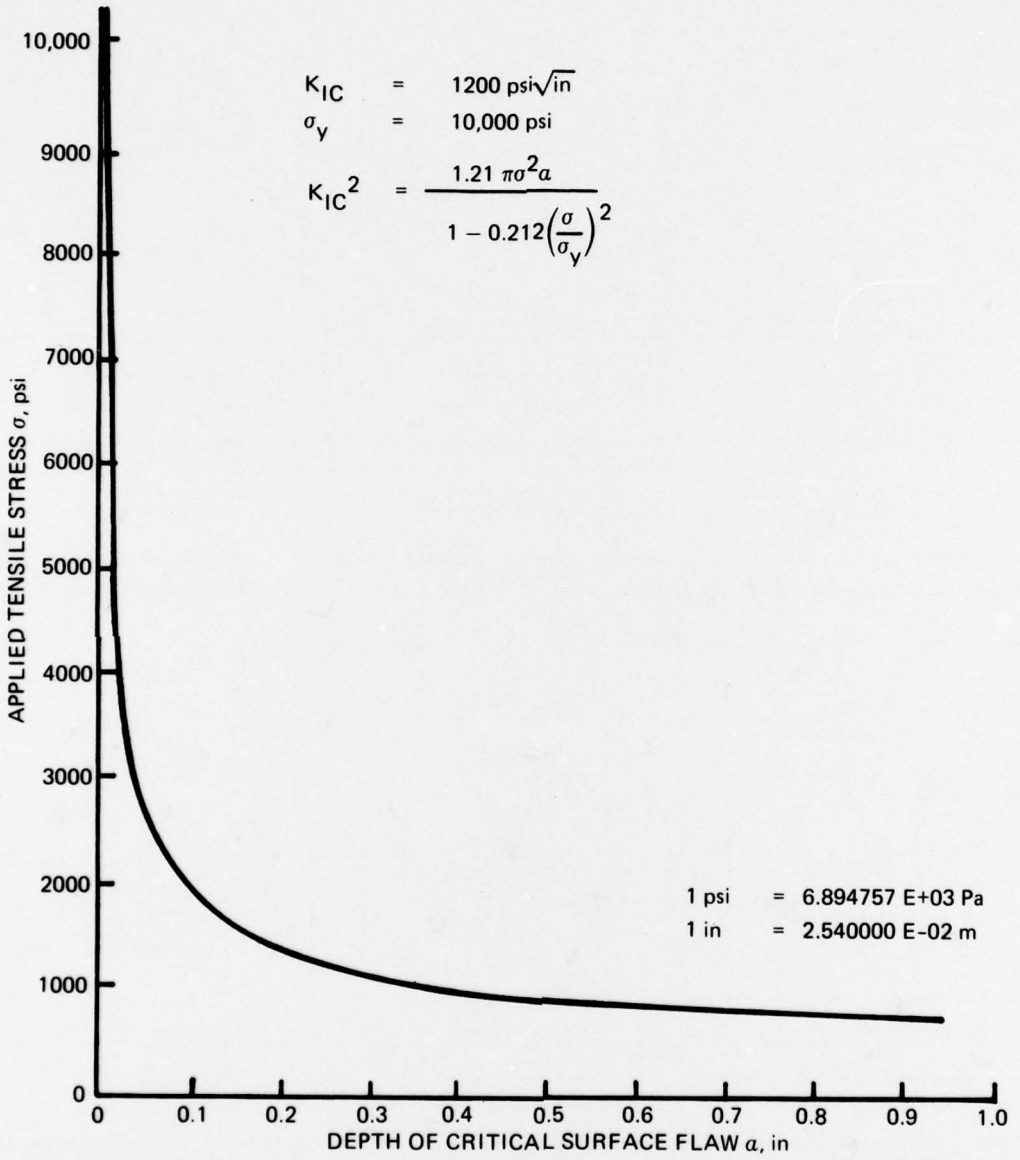

Figure 7.4. Critical flaw size for acrylic plastic under applied tensile stress at 45°F (7.2°C) ambient temperature.

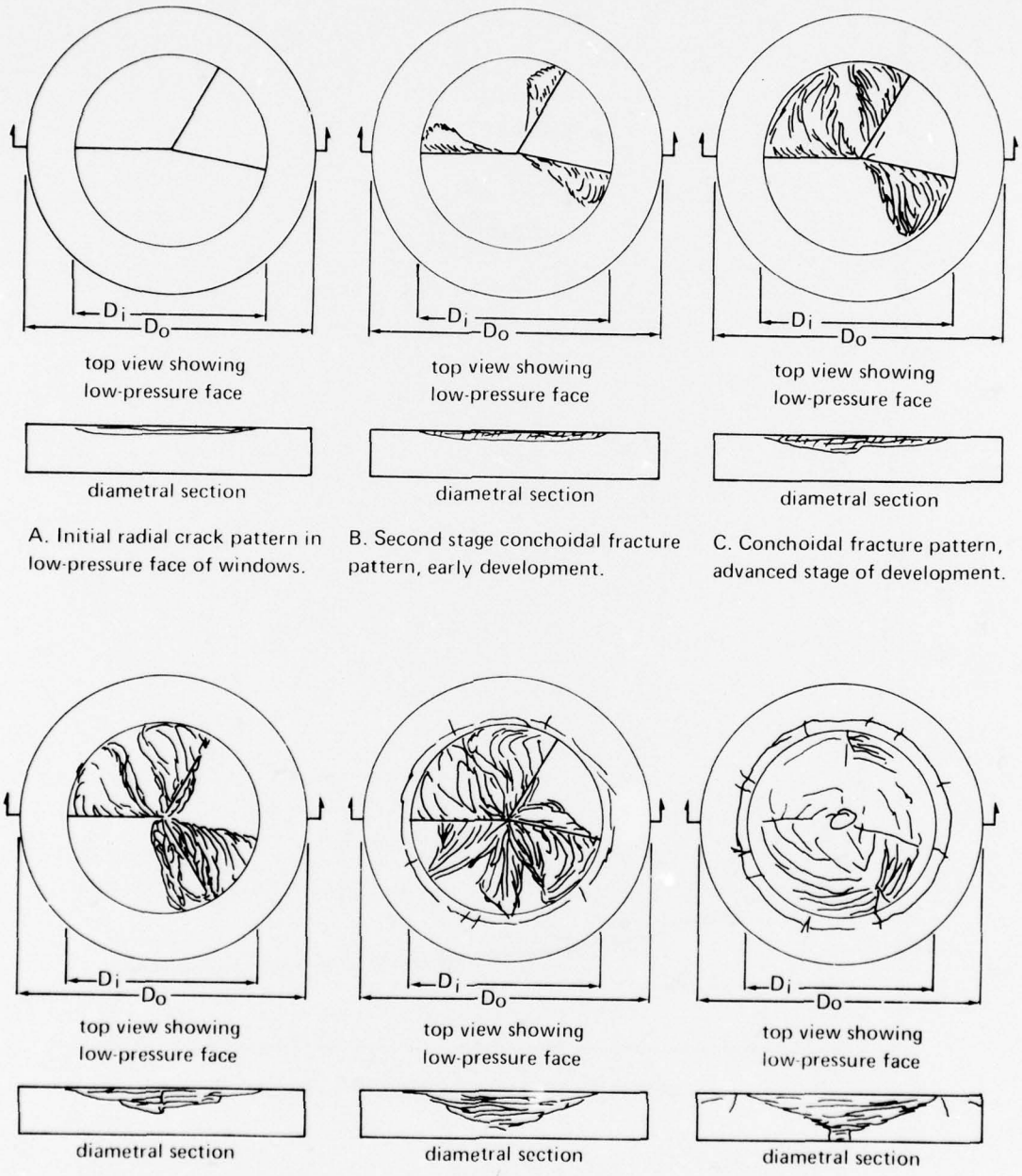

Figure 7.5. Fracturing process in a plane disc arcylic window under external hydrostatic loading ($t/D_i \leq 0.4$ and $D_o/D_i \leq 1.5$).

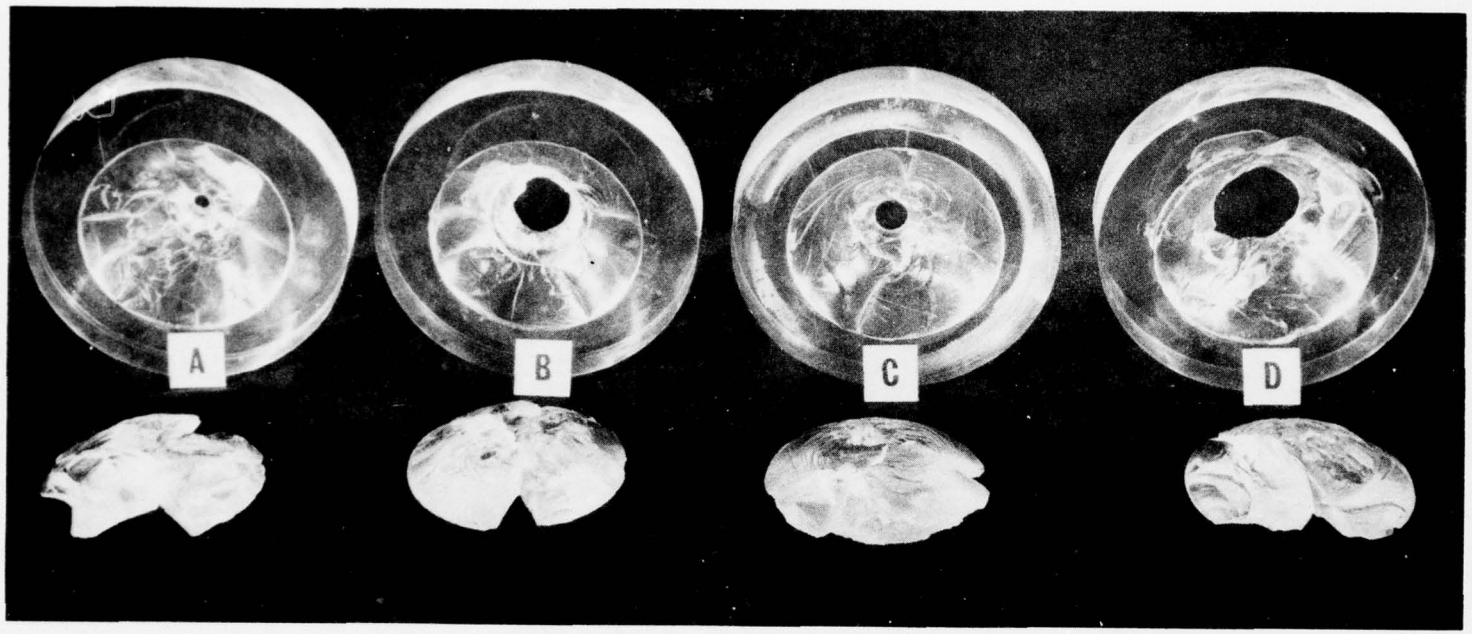

Figure 7.6. Typical cone-shaped flexure fracture surfaces on low-pressure faces of thin, plane disc plastic windows after short-term hydrostatic pressurization to implosion from 6100 to 6600 pounds per square inch (42.1 to 45.5 megapascals) ($t/D_i = 0.31$; $D_o/D_i = 1.5$; temperature = 75°F (23.8°C)).

Figure 7.7. Edge view of a plane disc acrylic window after short-term pressurization to failure ($t/D_i = 0.40$; $D_o/D_i = 1.5$; pressure = 13,000 pounds per square inch (89.6 megapascals); temperature = 72°F (22.2°C)).

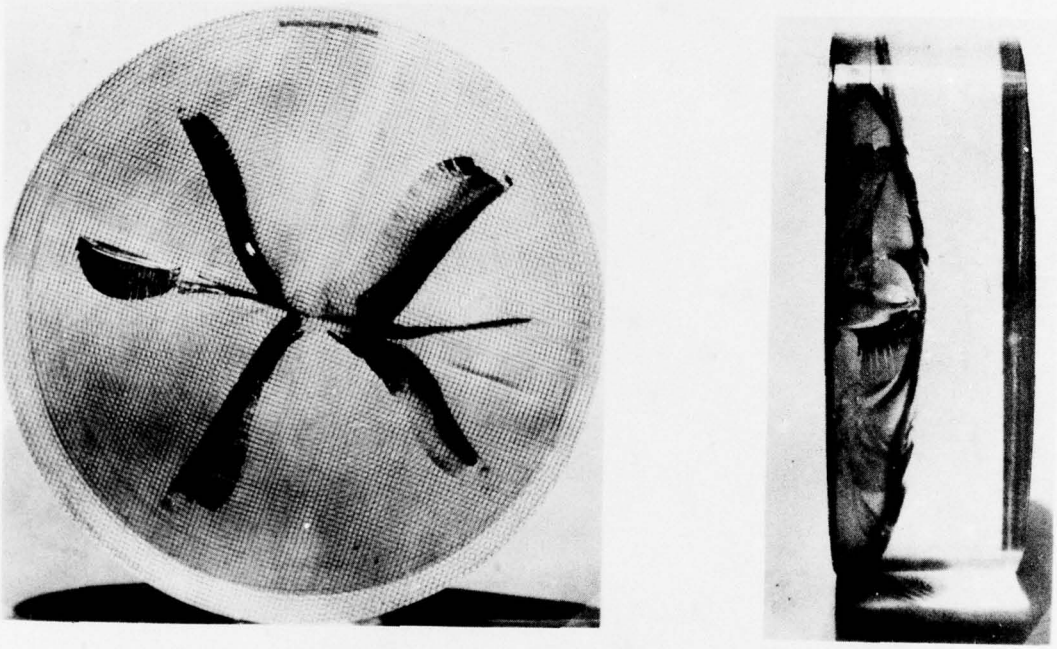

Figure 7.8. Fracture pattern in a plane disc acrylic window after short-term overpressurization ($t/D_i = 0.38$; $D_o/D_i = 1.14$; pressure = 4285 pounds per square inch (29.5 megapascals)). Low-pressure face is covered with 0.005-inch-deep (0.13 millimeter) machined notches on 0.05-inch (1.27 millimeters) centers. Part A. Overpressurization at 35°F (1.67°F).

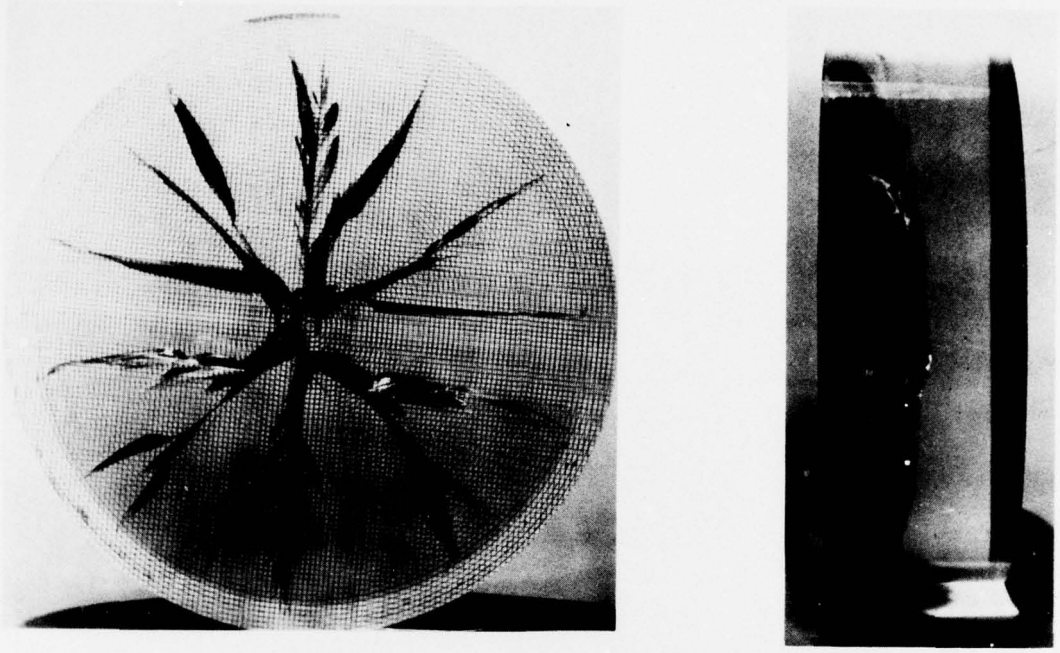

Figure 7.8. Continued. Part B. Overpressurization at 120°F (48.8°C).

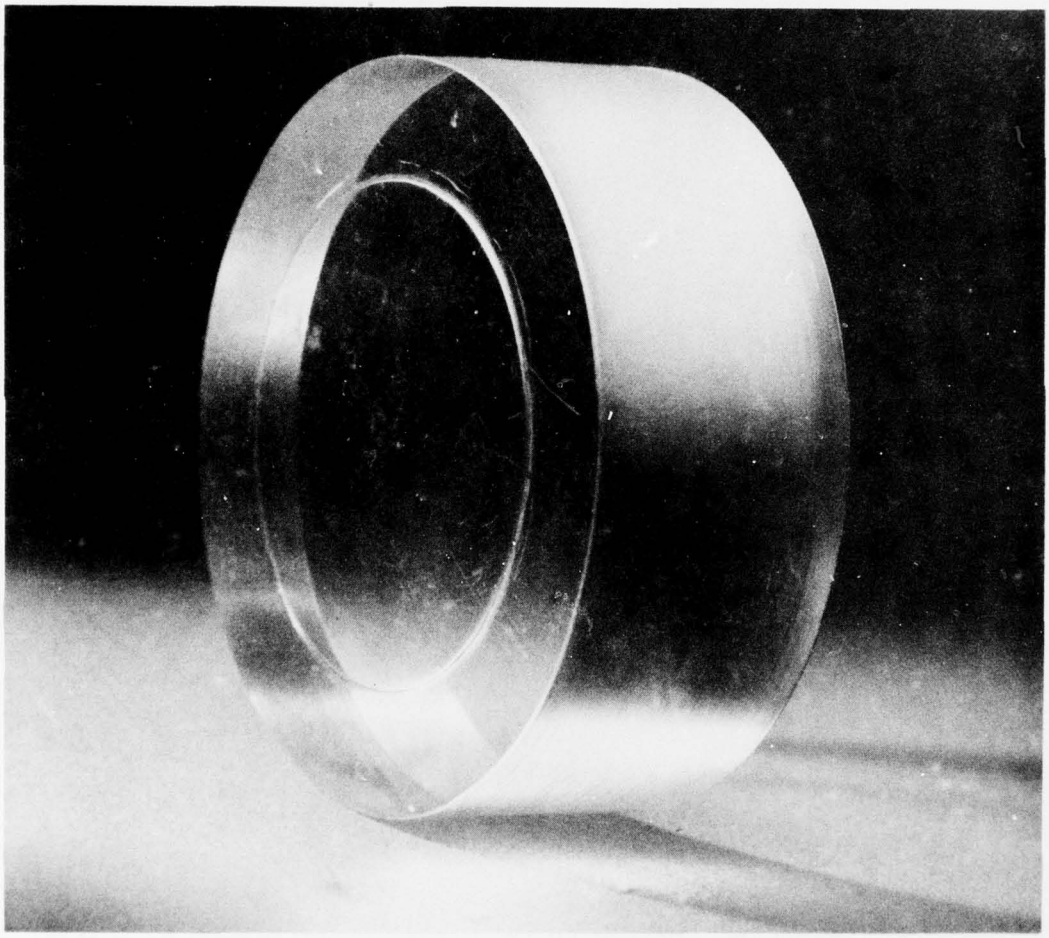

Figure 7.9. Initiation of shear cracks at the edge of the extrusion on the low-pressure face of a plane disc acrylic window ($t/D_i = 0.57$; $D_o/D_i = 1.5$; pressure = 16,200 pounds per square inch (111.7 megapascals); temperature = 67°F (19.4°C)).

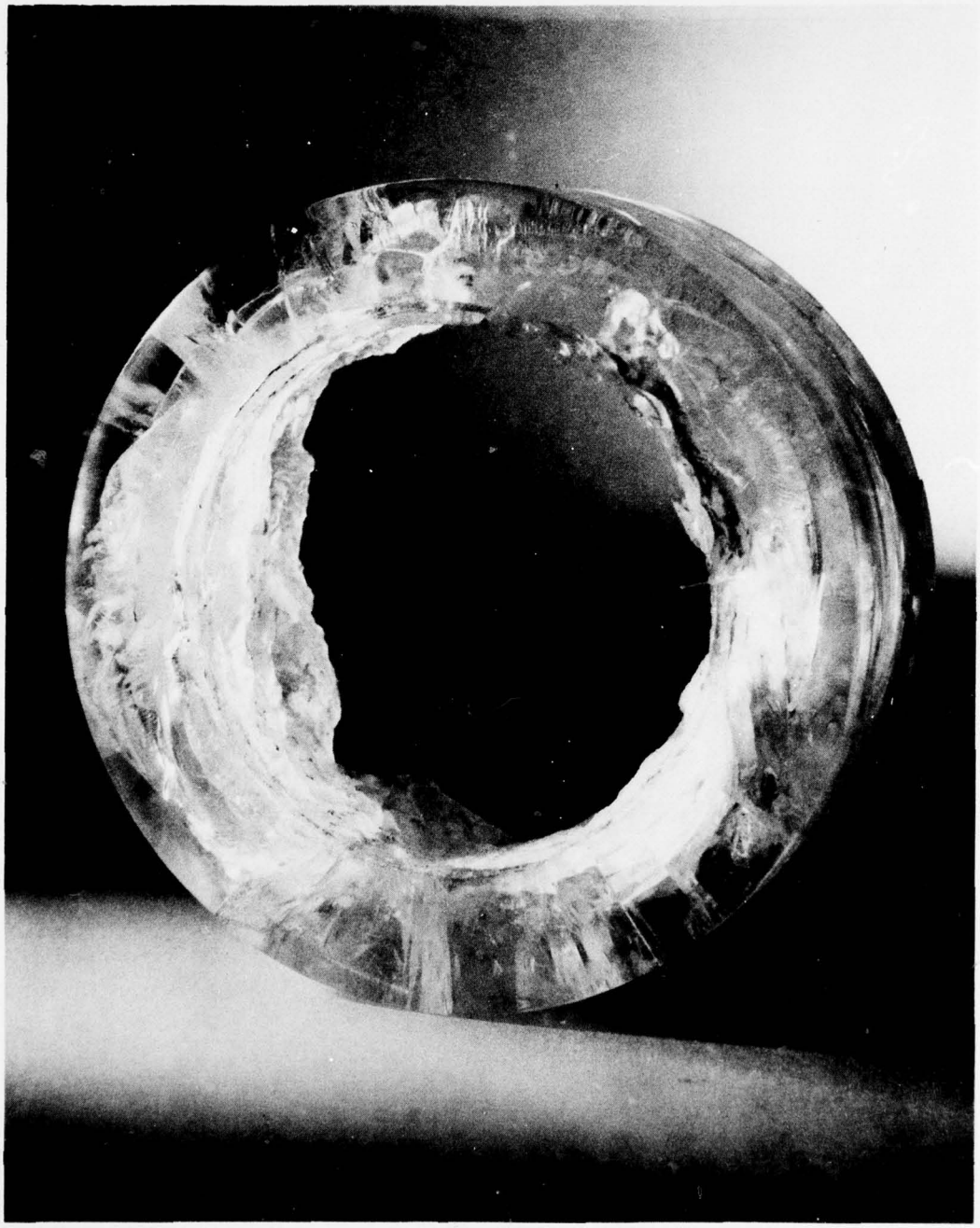

Figure 7.10. Typical cylindrical shear fracture surface in a thick plane disc acrylic window after short-term pressurization to implosion ($t/D_i = 0.85$; $D_o/D_i = 1.5$; pressure = 22,800 pounds per square inch (157.2 megapascals); temperature = 71°F (21.6°C)).

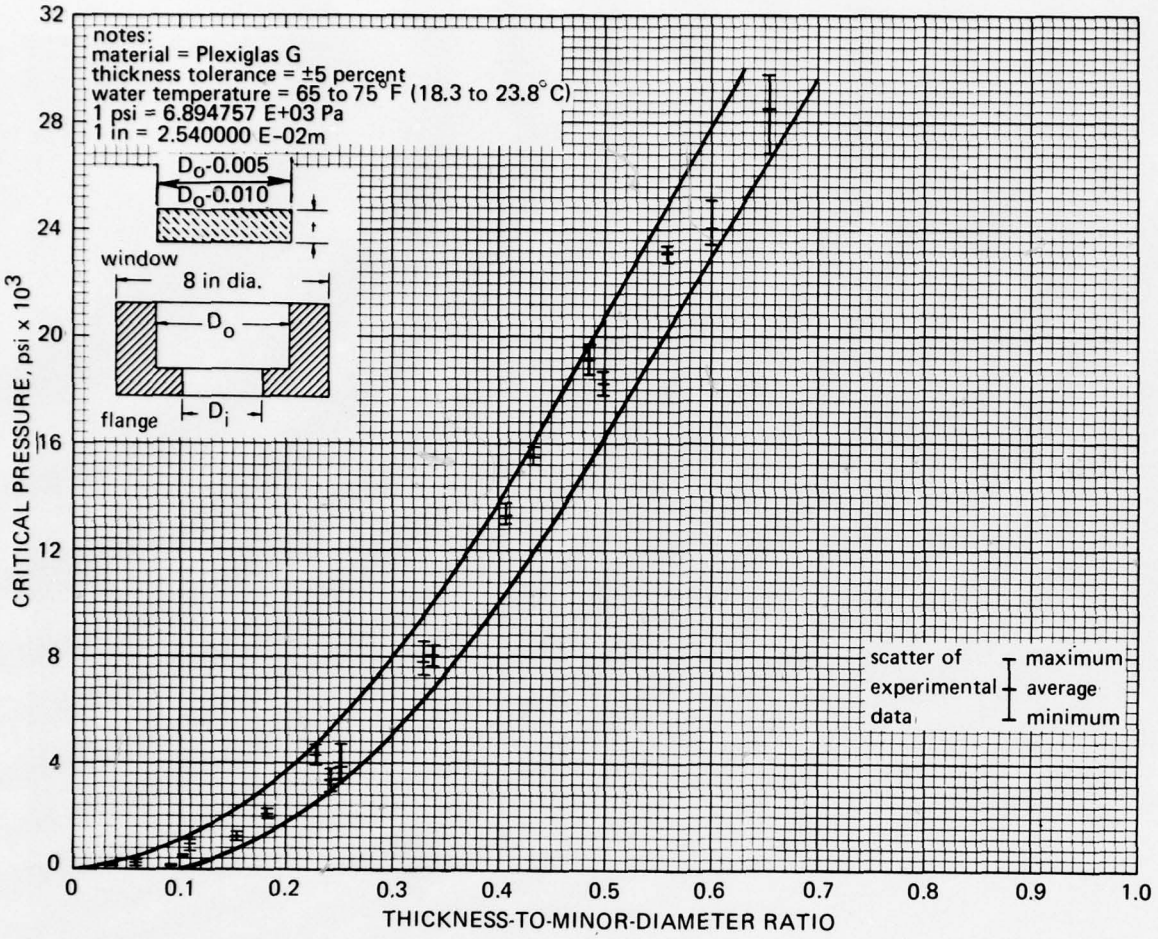

Figure 7.11. Critical pressures of plane disc acrylic windows under short-term hydrostatic loading (room temperature; $D_o/D_i = 1.5$; pressurization rate = 650 pounds per square inch (4.48 megapascals) per minute).

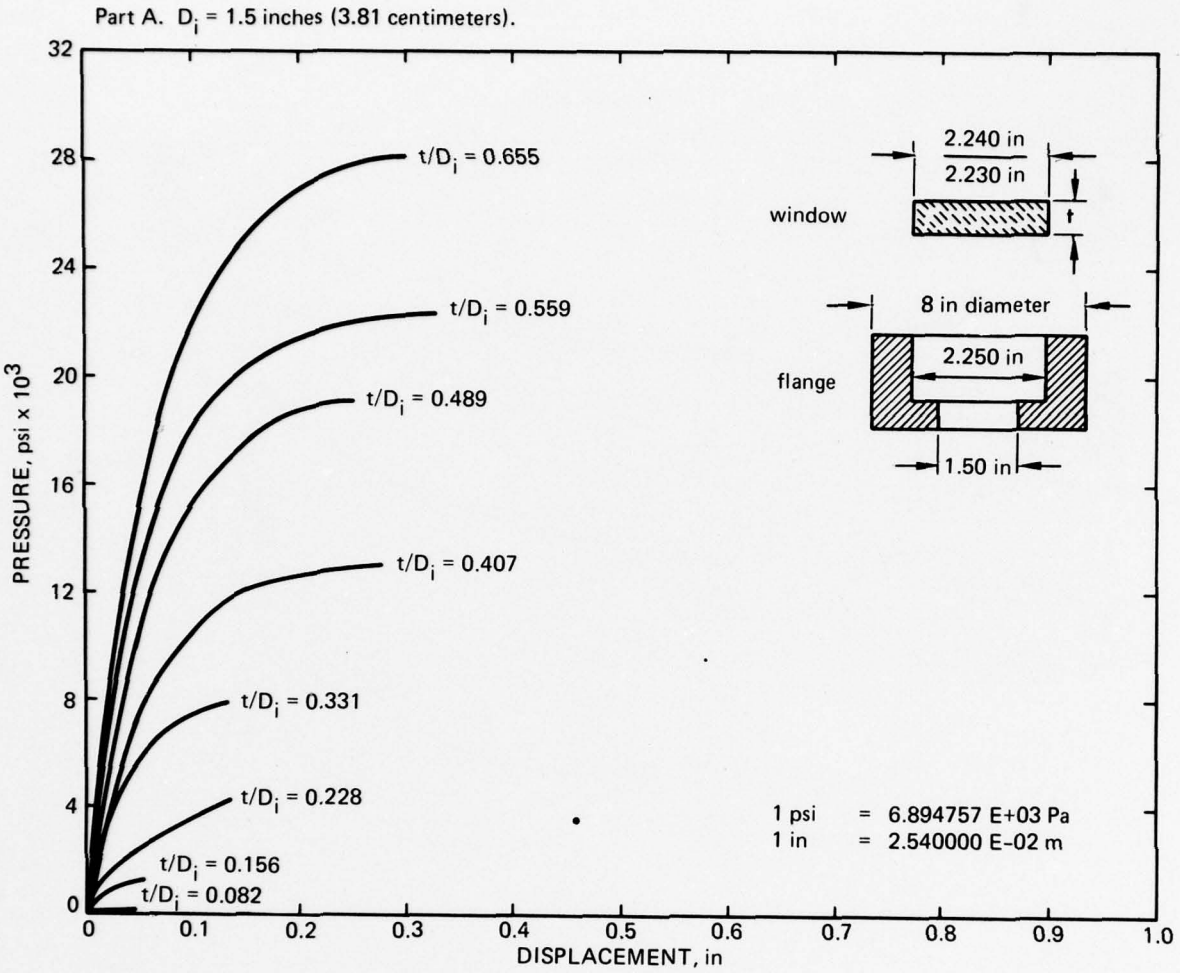

Figure 7.12. Axial displacement at center of acrylic plane disc window under short-term hydrostatic loading (D_o/D_i = 1.5; room temperature).

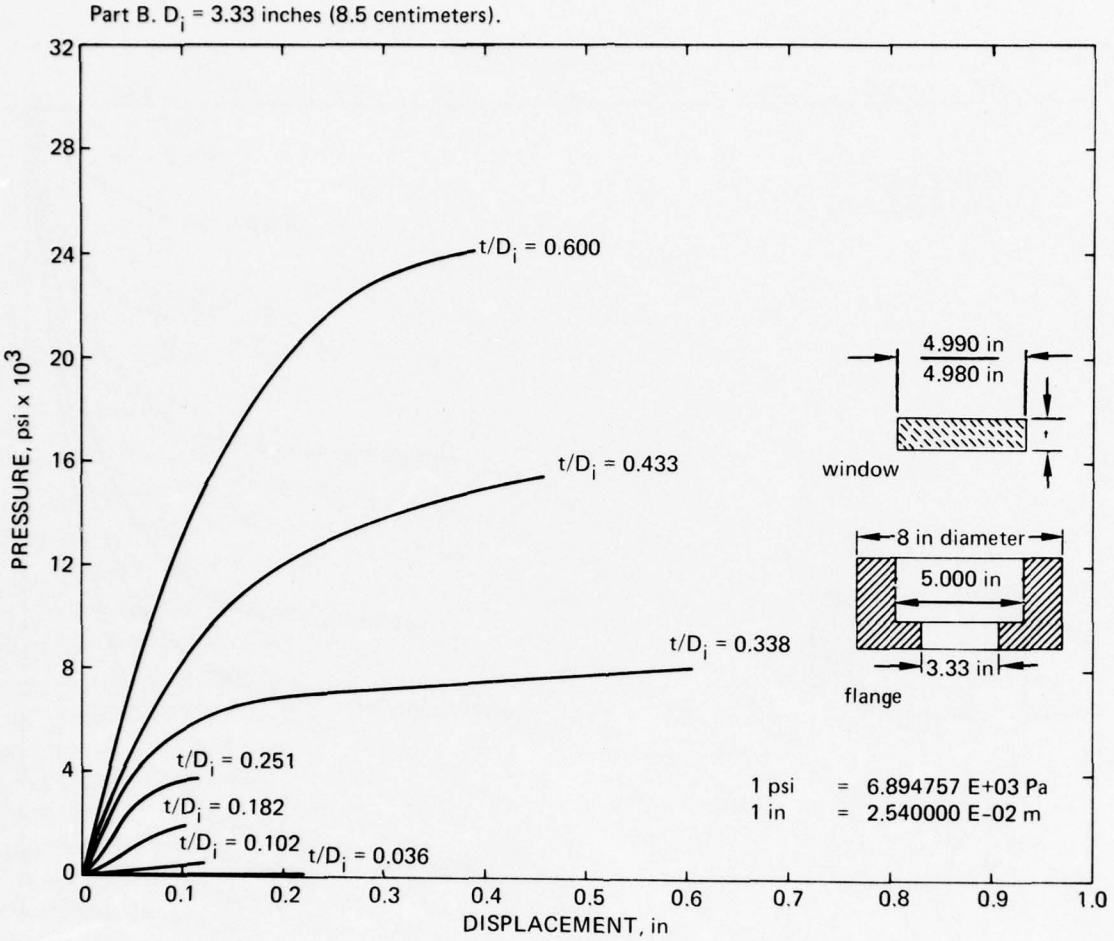

Figure 7.12. Continued.

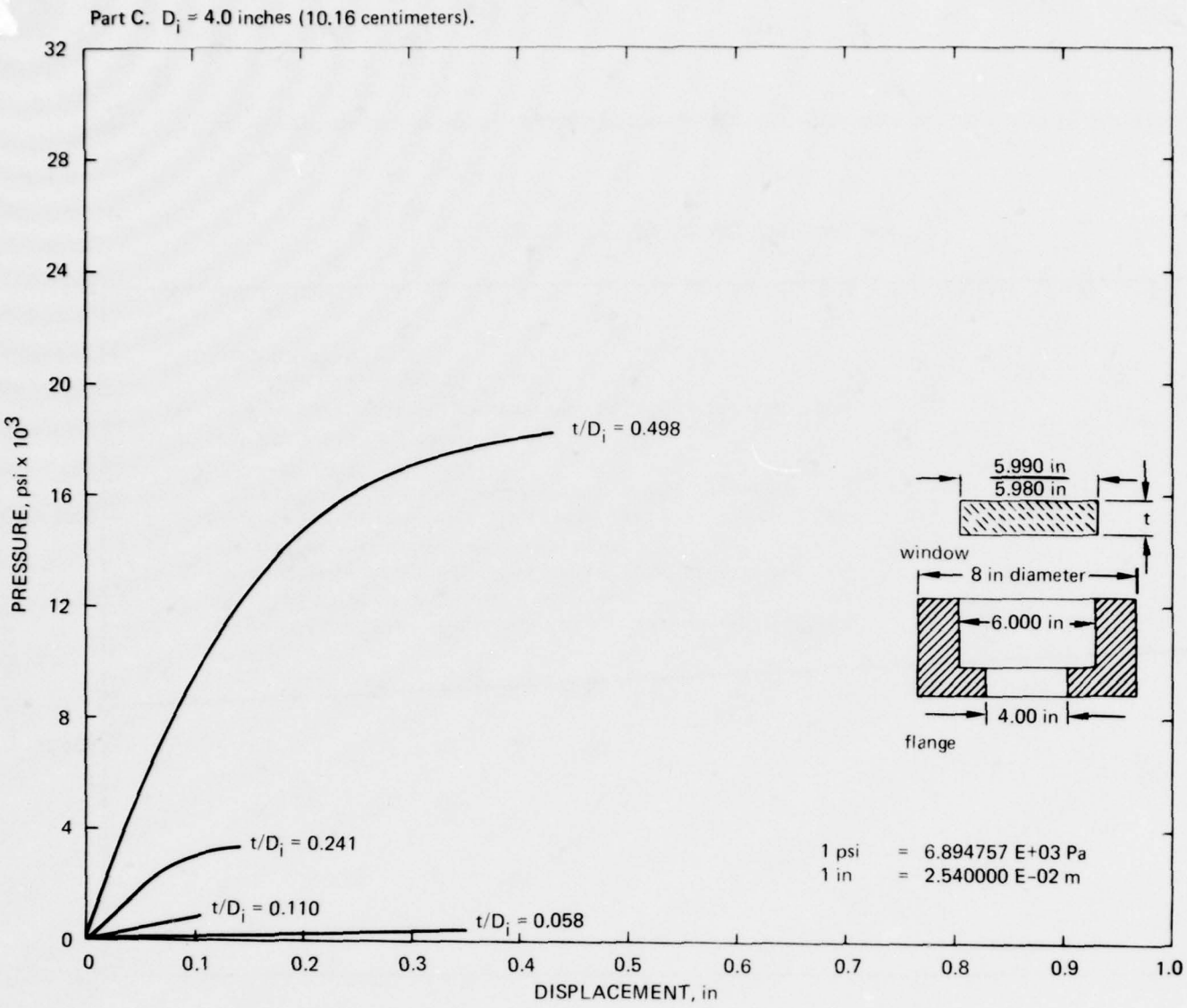

Figure 7.12. Continued.

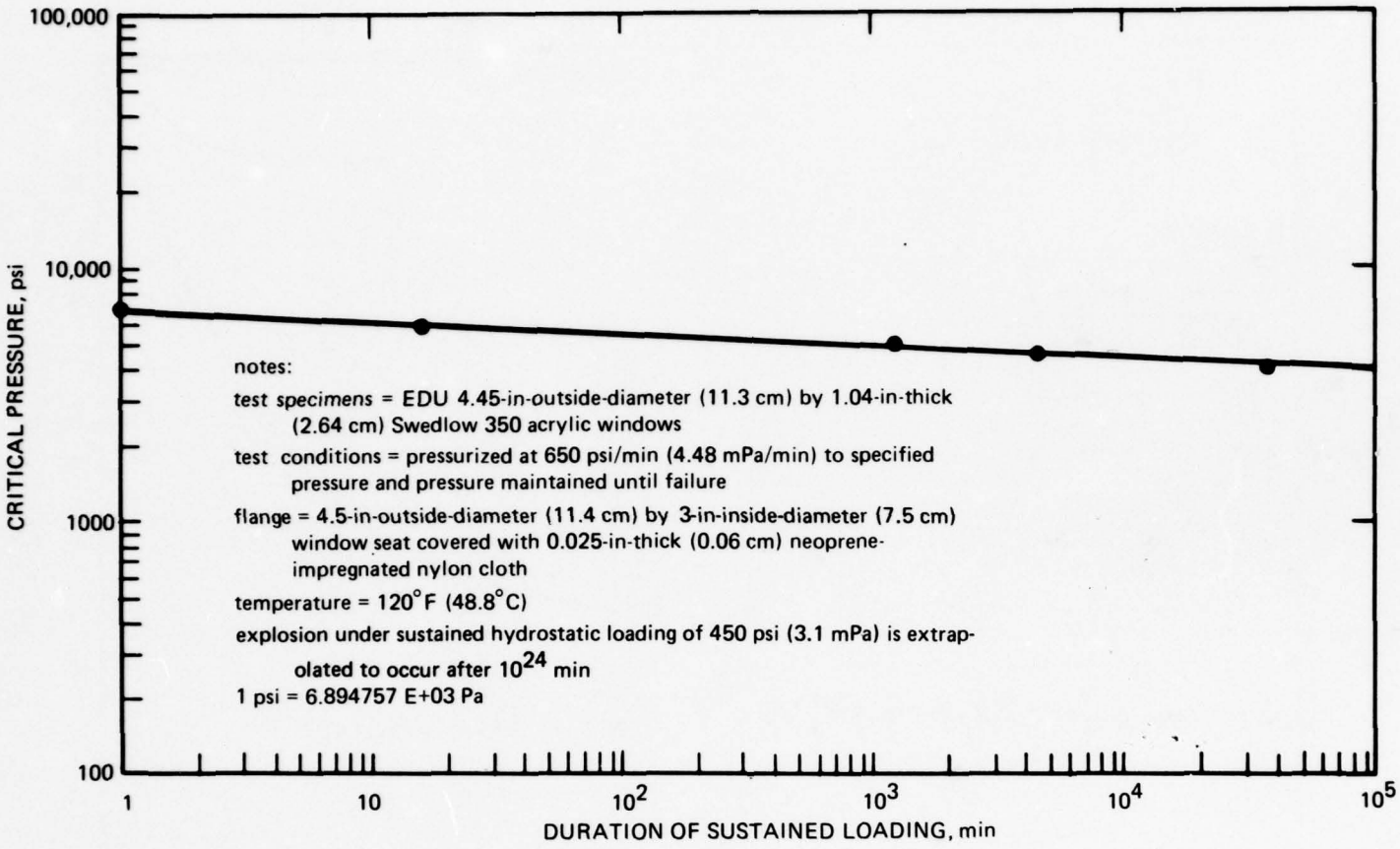

Figure 7.13. Effect of long-term pressure loading on critical pressure of plane disc acrylic windows ($t/D_i = 0.35$; $D_o/D_i = 1.48$).

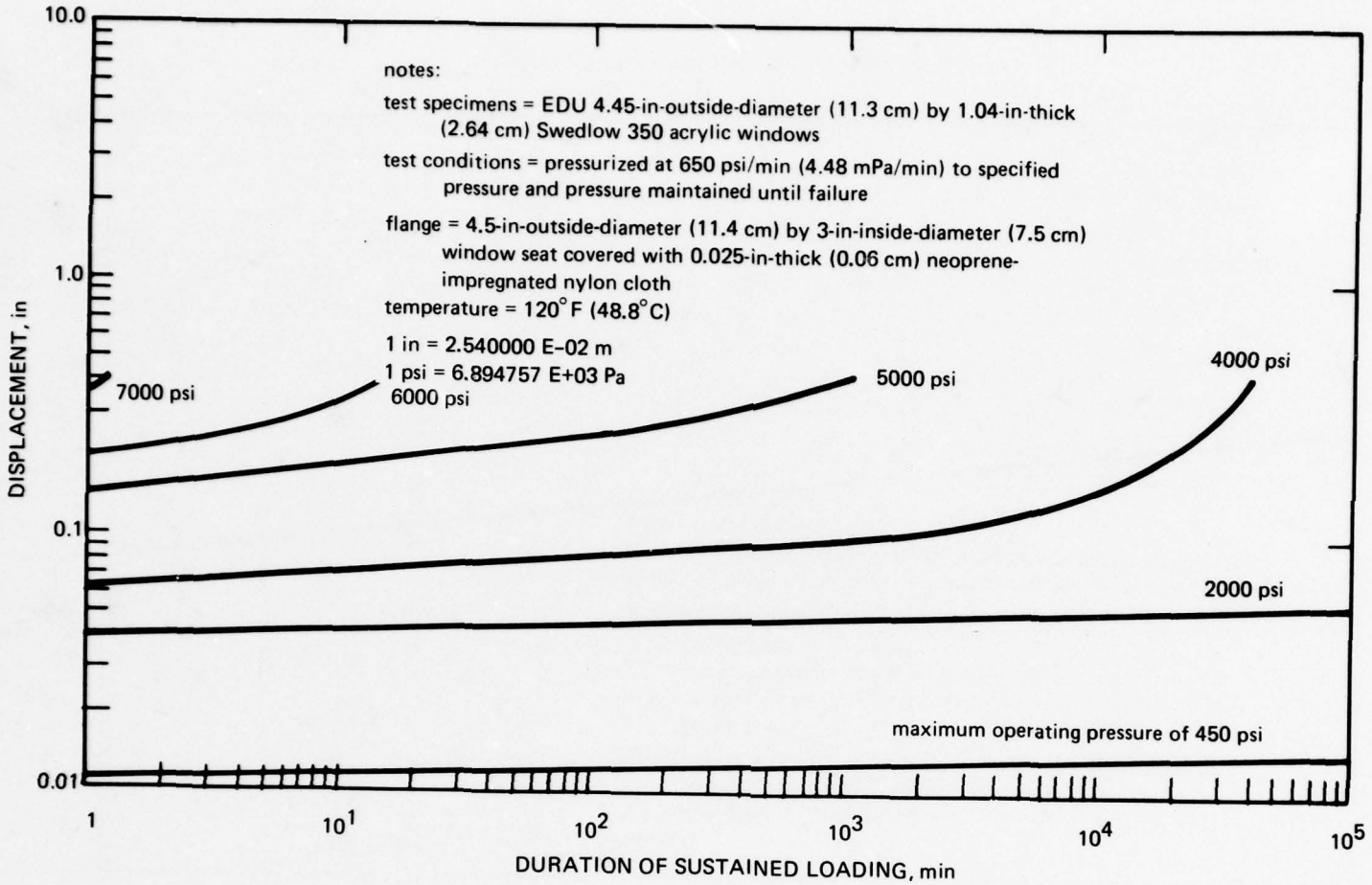

Figure 7.14. Effect of long-term pressure loading on axial displacements of plane disc acrylic windows ($t/D_i = 0.35$; $D_o/D_i = 1.48$).

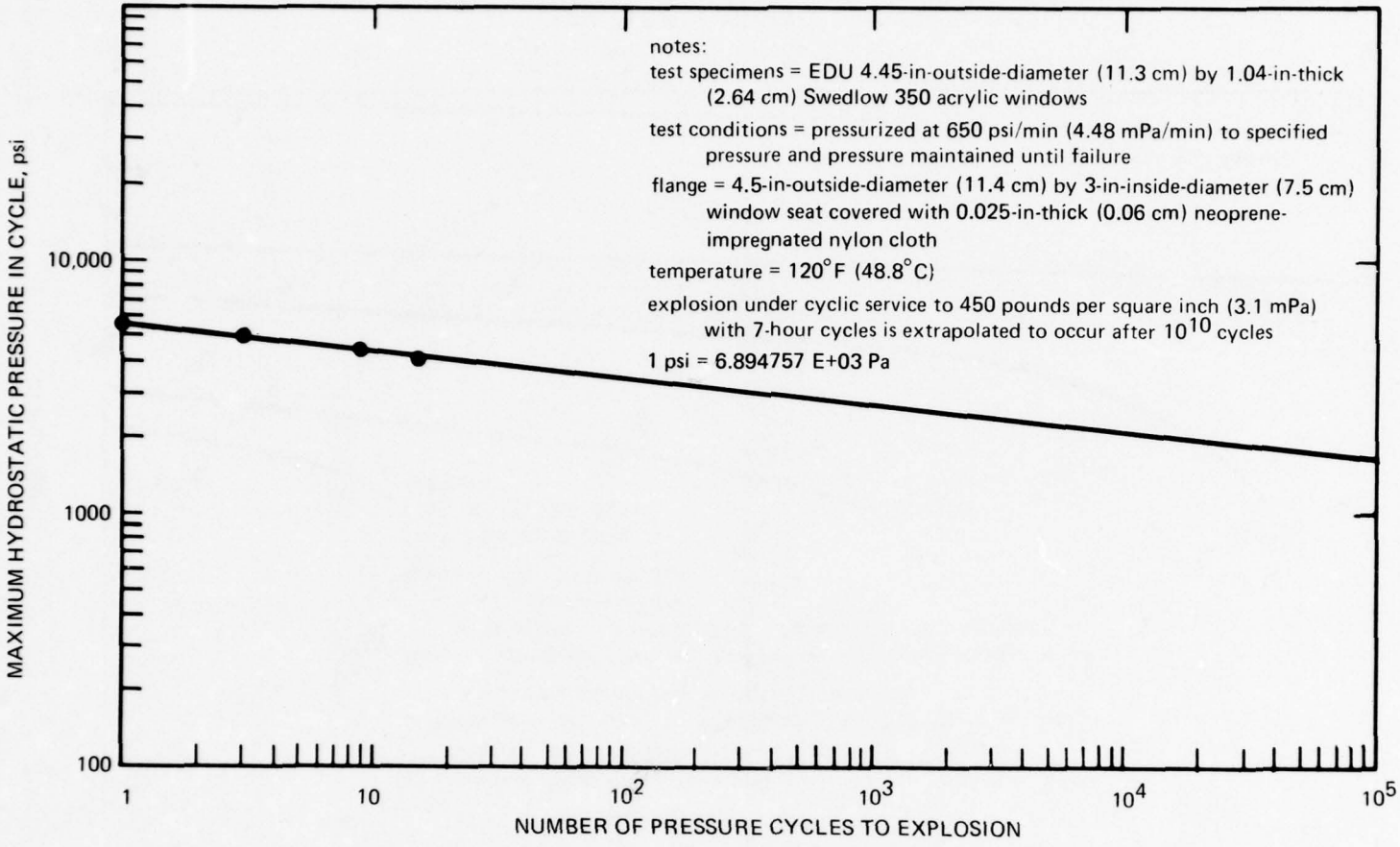

Figure 7.15. Effect of cyclic pressure loading on critical pressure of plane disc acrylic windows ($t/D_i = 0.35$; $D_o/D_i = 1.48$).

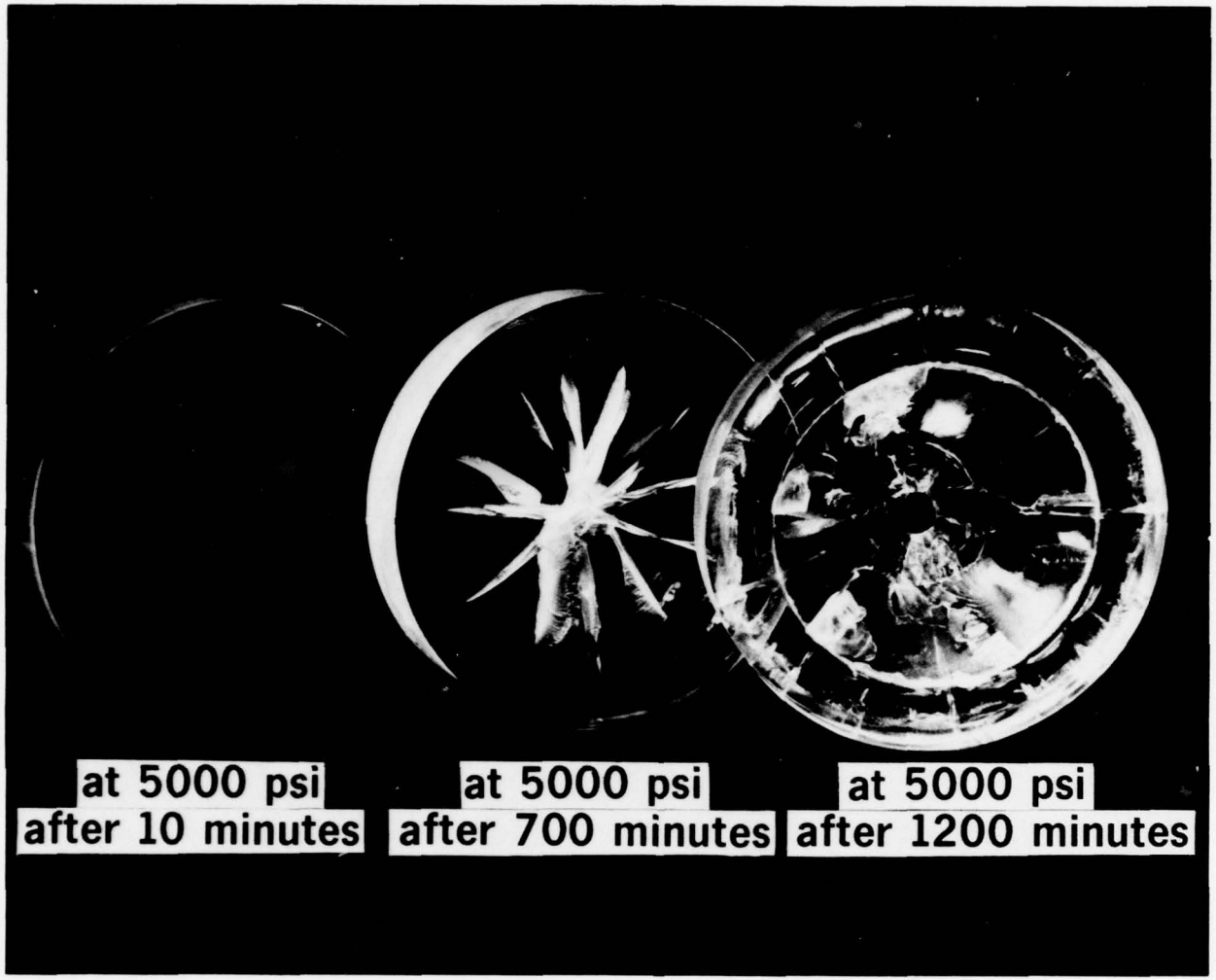

Figure 7.16. Effect of loading duration on extent of fracture in a flat disc acrylic window ($t/D_i = 0.35$; $D_o/D_i = 1.48$; temperature = 120°F (48.8°C)).

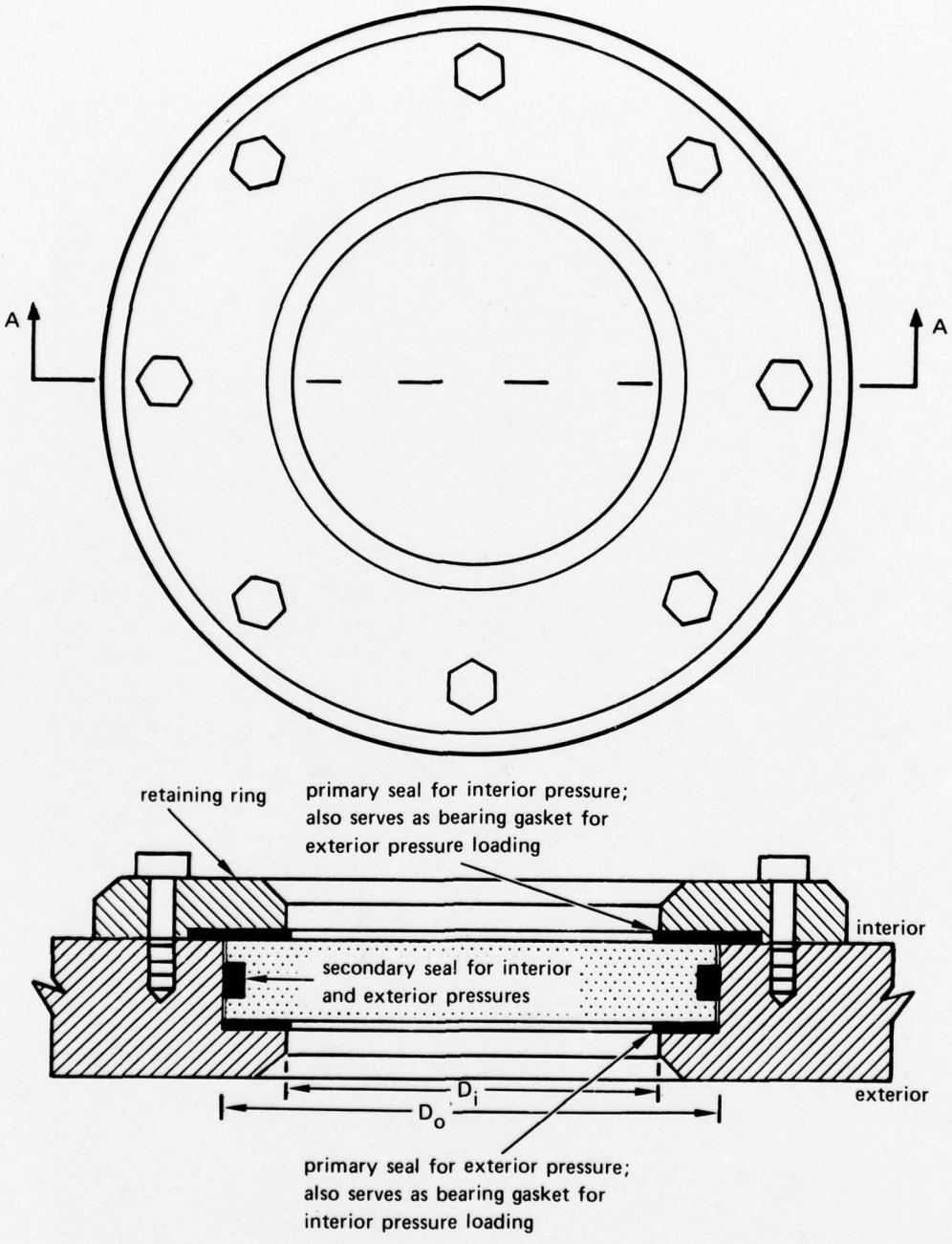

Figure 7.17. Typical design of a plane disc acrylic window-mounting assembly for a personnel transfer capsule for both internal and external pressure service.

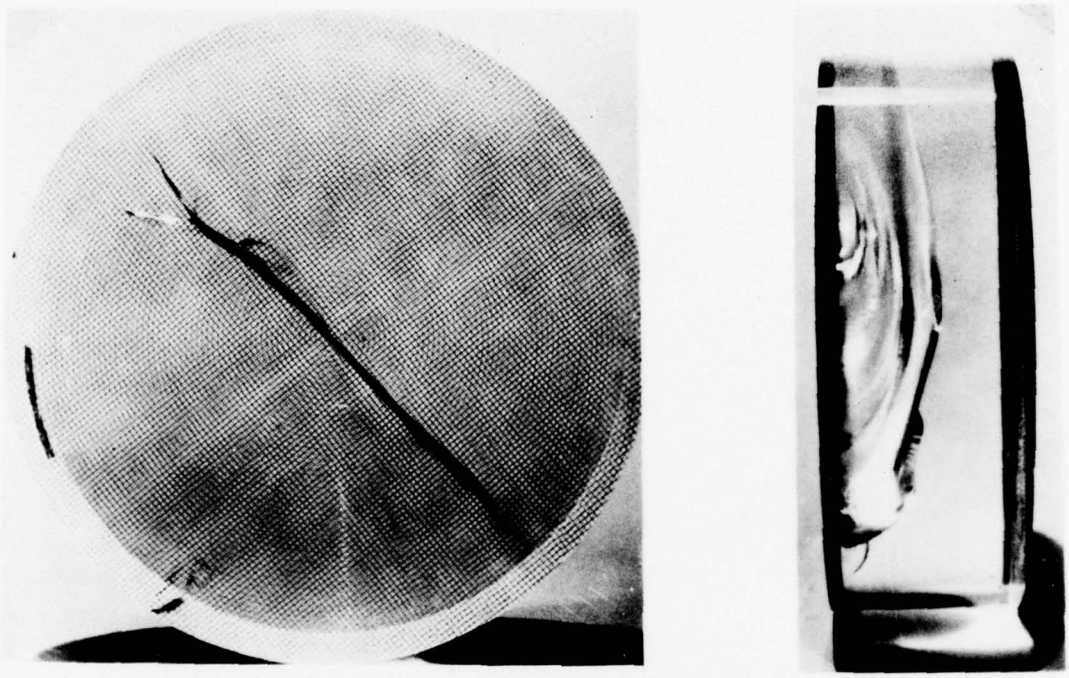

Figure 7.18. Fracture in low-pressure face of a plane disc acrylic window after being subjected to dynamic overpressure on high-pressure face of window ($t/D_i = 0.38$; $D_o/D_i = 1.14$; static pressure = 450 pounds per square inch (3.1 megapascals); dynamic pressure = 1200 pounds per square inch (8.3 megapascals); temperature = 55°F (13°C)).

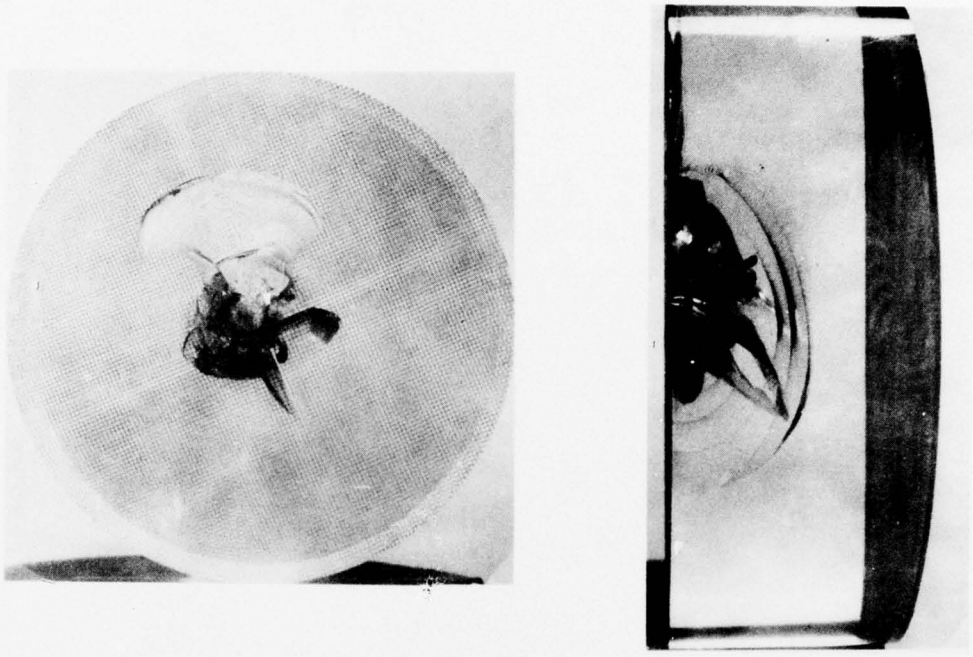

Figure 7.19. Fracture in low-pressure face of a flat disc acrylic window after being subjected to point-impact loading on low-pressure face ($t/D_i = 0.38$; $D_o/D_i = 1.14$; static pressure = 450 pounds per square inch (3.1 megapascals); 200 pounds (90.7 kilograms) at 6.1 feet per second (1.9 meters per second); temperature = 35°F (1.7°C)).

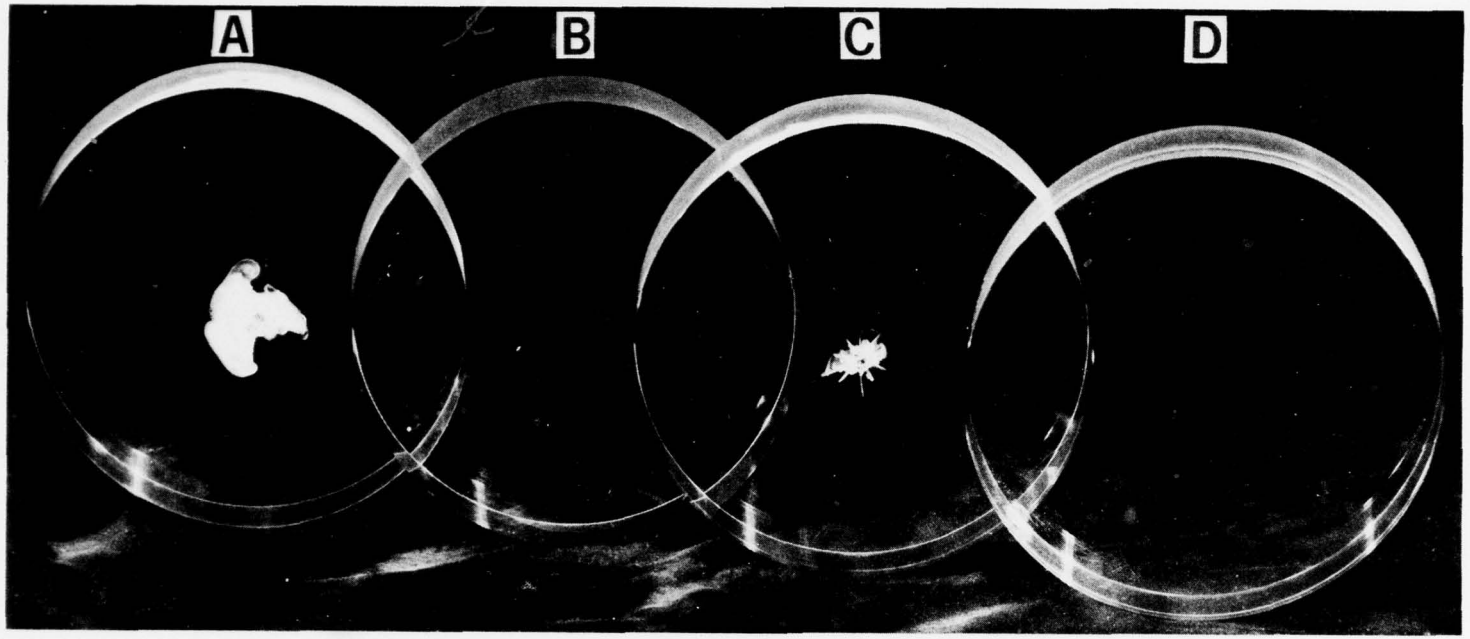

Figure 7.20. Extent of damage to surfaces of shielded and unshielded acrylic flat disc windows after being impacted by a .22-caliber long rifle bullet fired from 6 feet (1.8 meters). The 0.25-inch-thick (0.6 centimeter) acrylic shield is bonded with a 0.1-inch-thick (0.25 centimeter) elastomer layer to a 1.0-inch-thick (2.54 centimeters) window. Unshielded windows: A, after impact; B, before impact. Shielded windows: C, after impact; D, before impact.

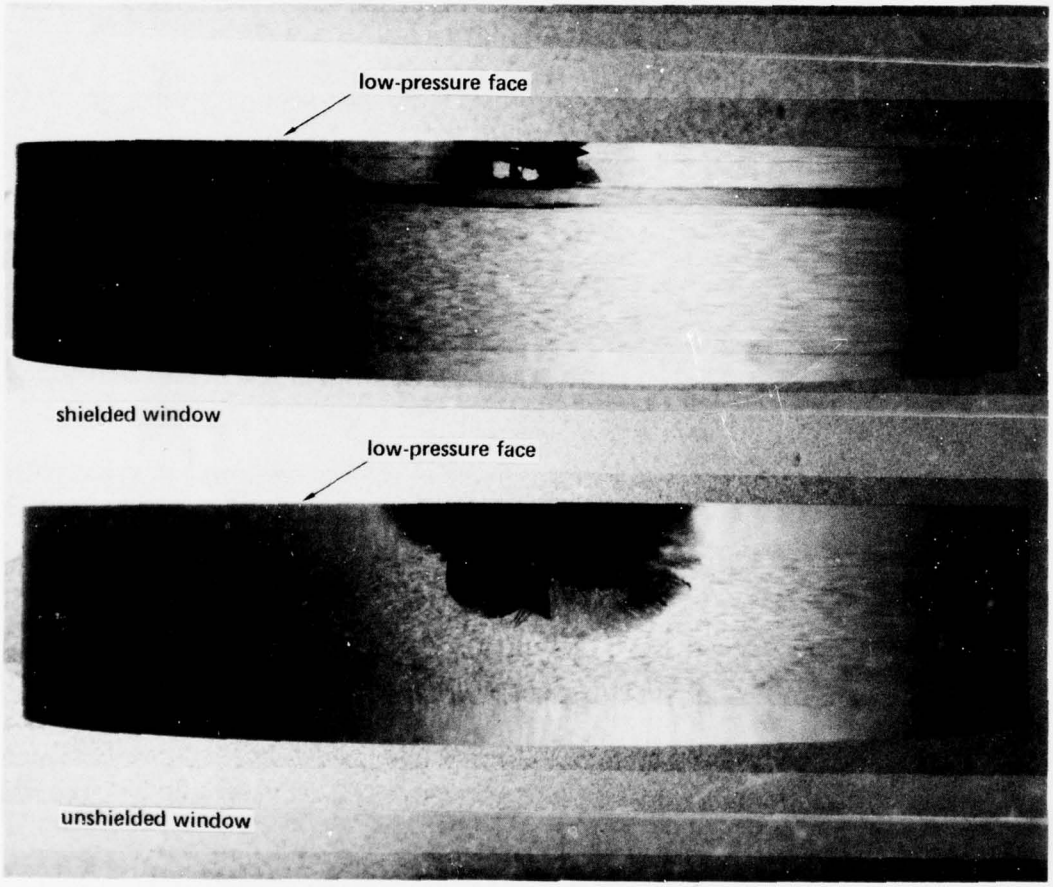

Figure 7.21. Depth of crack penetration in impacted windows of figure 7.20. Note that the crack was stopped by the elastometric layer between the shield and the structural member of the window, thus preserving the structural integrity of the window. This is not the case with the unshielded window which lost its structural integrity and would have exploded at one-tenth of its regular short-term critical pressure, if the window were pressurized on the opposite face to the impact.

SECTION 8. PLANE RECTANGULAR WINDOWS . . . 8-1

8.1 INTRODUCTION . . . 8-1

8.2 STRUCTURAL PERFORMANCE . . . 8-1

8.3 MODE OF FAILURE . . . 8-1

8.4 PREDICTION OF CRITICAL PRESSURES . . . 8-2

8.5 SEATING . . . 8-4

8.5.1 Bearing Support . . . 8-4
8.5.2 Bearing Gaskets . . . 8-4
8.5.3 Sealing . . . 8-5
8.5.4 Retaining Methods . . . 8-5
8.5.5 Window Cavity . . . 8-5

8.6 FABRICATION . . . 8-5

8.7 RESISTANCE TO IMPULSE AND POINT LOADING . . . 8-6

8.8 CONCLUSION . . . 8-6

8.9 REFERENCES . . . 8-6

SECTION 8. PLANE RECTANGULAR WINDOWS

8.1 INTRODUCTION

Plane rectangular windows are primarily used in aquaria, water tunnels, incubation chambers, and subsurface habitats. Their primary advantages are a very large undistorted field-of-view and the low cost of the window-mounting assembly. Because high tensile stresses are present at the center, edges of the seat, and corners of the low-pressure face, these windows are only cost-effective for pressures less than or equal to 15 pounds per square inch (0.1 megapascal). If the cost-effectiveness criterion is ignored, the usable range can probably be extended to about 30 pounds per square inch (0.2 megapascal). Pressures above this value usually require expensive massive custom castings, instead of inexpensive mass-produced acrylic sheets. Thus they cannot successfully compete in cost with spherical window shapes.

8.2 STRUCTURAL PERFORMANCE

Plane rectangular windows perform under hydrostatic loading as either a flat simply supported plate or as a flat plate with fixed edges. Because the soft gaskets under the retaining flange permit the window edge to flex, it is a reasonable assumption that the edge is free to rotate and thus the window reacts like a simply supported plate. Flexing the plate induces a biaxial tensile stress field in the low-pressure face and a biaxial compressive stress field in the high-pressure face. Because acrylic plastic is notch sensitive in tension, steps must be taken to protect the low-pressure face against scratches. On the other hand, the low stress level in the edges of the window allows even a sawed finish on those surfaces.

The magnitude of stresses at the center of the low-pressure face, as well as the critical pressure of the window, is a function of the window's thickness, width, and length. Because both width and length are very large compared with thickness, the restraining effect exercised by the mounting on the deflection of the window is negligible. As a result, the width of the bearing surface can be as small as $D_o/D_i = 1.04$.

8.3 MODE OF FAILURE

Since plane rectangular windows are generally used only in low-pressure service, their thickness-over-width ratios are usually less than 0.1. This causes them, like thin plane disc windows, to fail in flexure and in most cases without prior warning. Also similar to plane disc windows, the highest values of critical pressures are found under short-term loading and low ambient temperature, while the lowest values are encountered at long-term loading and high ambient temperatures. The value of critical pressure under cyclic pressure loadings falls between the two extremes.

8.4 PREDICTION OF CRITICAL PRESSURES

In the total absence of test data, the designer must either generate experimental data or rely on analytical calculations with appropriate safety factors. The simplified experimental approach that needs the smallest number of windows (minimum of five) to qualify a particular design requires only that the windows (full scale or model scale) be tested to catastrophic failure under short-term loading and that the data conversion factors in table 8.1 be applied.

For applications where the critical pressure under actual operating conditions must be known, several windows must be tested to destruction under simulated service conditions (long term, cyclic, or both) and their performance extrapolated by using the plotting technique discussed in section 7.4 (shown on figures 7.13, 7.14, and 7.15).

Critical pressures under different operational conditions cannot be precisely calculated because of the time- and temperature-dependent properties of acrylic plastic. It is relatively easy, however, to calculate the thickness of the window for the required operational pressure by the use of the analytic expression for rectangular plates, if a low working stress is selected. Using 570 pounds per square inch (3.9 megapascals) as the nominal maximum stress level, a family of design curves was plotted for the selection of aquarium window dimensions at temperatures less than or equal to 100°F (38°C) (figure 8.1). These design curves can be applied with a high level of confidence to the design of plane rectangular windows, providing the windows are not exposed to dynamic pressures or point-impact loading and the depth of scratches on the low-pressure face does not exceed 0.02 inch (0.05 centimeter). For operational pressures and window dimensions exceeding those in figure 8.1, it is feasible to apply the formulas in table 8.2 for the calculation of window thickness (references 8.1 through 8.6).

Table 8.1. Conversion factors for acrylic plastic plane rectangular windows.

Operational Pressure Ranges	Temperature				
	50°F (10°C)	75°F (24°C)	100°F (38°C)	126°F (52°C)	151°F (66°C)
	Conversion Factors				
2500 psi (17.2 mPa)	7	8	10	12	18
5000 psi (34.5 mPa)	7	8	10		

Table 8.2. Approximate formulas for calculation of maximum stresses in plane acrylic plastic windows under uniform hydrostatic loading (reference 8.1).

Edge Supported

elliptical, solid

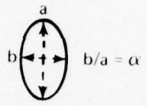

(at center) $s_b = -\dfrac{0.3125(2-\alpha)wb^2}{t^2} = \max s$ $\quad \max y = \dfrac{(0.146 - 0.1\alpha)wb^4}{Et^3}$ (for $\nu = 1/3$)

(reference 8.2)

Edge Fixed

(at edge) (span a) $s_a = \dfrac{3wb^2\alpha^2}{2t^2(3+2\alpha^2+3\alpha^4)}$ (span b) $s_b = \dfrac{3wb^2}{2t^2(3+2\alpha^2+3\alpha^4)} = \max s$

(at center) $s_a = -\dfrac{3wb^2(\alpha^2 m+1)}{4t^2(3+2\alpha^2+3\alpha^4)m}$ $s_b = \dfrac{-3wb^2(m+\alpha^2)}{4t^2(3+2\alpha^2+3\alpha^4)m}$ $\max y = -\dfrac{3w(m^2-1)b^4}{16m^2Et^3(6+4\alpha^2+6\alpha^4)}$

(reference 8.3)

All edges Fixed

square, solid

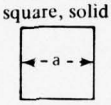

(at center of each edge) $s_a = \dfrac{0.308\,wa^2}{t^2} = \max s$

(at center) $s = -\dfrac{6w(m+1)a^2}{47mt^2}$ $\max y = -\dfrac{0.0138\,wa^4}{Et^3}$

(reference 8.4)

Edges Supported

(at center, on diagonal section) $s = -\dfrac{0.2214\,wa^2}{t^2}$ $\max y = -\dfrac{0.0443\,wa^4}{Et^3}$ ($\nu = 0.3$)

(at corners, on diagonal section) $s = -\dfrac{0.2778\,wa^2}{t^2} = \max s$

(reference 8.4)

All Edges Supported

rectangular, solid

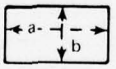

(at center) $\max s = s_b = \beta\dfrac{wb^2}{t^2}$ $\quad \max y = \alpha\dfrac{wb^4}{Et^3}$

a/b	1	1.2	1.4	1.6	1.8	2	3	4	5	∞
β	0.2874	0.3762	0.4530	0.5172	0.5688	0.6102	0.7134	0.7410	0.7476	0.7500
α	0.0444	0.0616	0.0770	0.0906	0.1017	0.1110	0.1335	0.1400	0.1417	0.1421

(reference 8.6)

All edges Fixed

(at centers of long edges) $s_b = \beta\dfrac{wb^2}{t^2} = \max s$ $\quad \max y = \alpha\dfrac{wb^4}{Et^3}$

where β and α may be found from the following table:

a/b	1	1.2	1.4	1.6	1.8	2	∞
β	0.3078	0.3834	0.4356	0.4680	0.4872	0.4974	0.5000
α	0.0138	0.0188	0.0226	0.0251	0.0267	0.0277	0.0284

(reference 8.6)

Table 8.2. Continued.

Notes:

1. Maximum design stresses for different ambient temperature ranges:

   32 to 50°F (0 to 10°C) = 1700 pounds per square inch (11.7 megapascals)
   32 to 75°F (0 to 24°C) = 1500 pounds per square inch (10.3 megapascals)
   32 to 100°F (0 to 38°C) = 1200 pounds per square inch (8.2 megapascals)
   32 to 125°F (0 to 52°C) = 1100 pounds per square inch (7.6 megapascals)
   32 to 150°F (0 to 66°C) = 900 pounds per square inch (6.2 megapascals)
   32 to 175°F (0 to 79°C) = 600 pounds per square inch (4.1 megapascals)

2. Notation:

   w: unit-applied load in pounds per square inch (1 pound per square inch = 6.894757 E+03 Pascals)
   t: thickness of plate in inches (1 inch = 2.540000 E-02 meters)
   s: unit stress at surface of plate in pounds per square inch (1 pound per square inch = 6.894757 E+03 Pascals)
   y: vertical deflection of plate from original position in inches (1 inch = 2.540000 E-02 meters)
   E: modulus of elasticity
   m: reciprocal of ν_r, Poisson's ratio
   positive sign for s: tension at upper surface and equal compression at lower surface
   negative sign for s: equal compression at upper surface and tension at lower surface
   positive sign for y: upward deflection
   negative sign for y: downward deflection
   subscripts r, t, a, and b used with s: radial direction, tangential direction, direction of dimension a, and direction of dimension b, respectively

3. All dimensions are in inches (1 inch = 2.540000 E-02 meters)

Scratches can be avoided by applying an abrasion-resistant coating to the low-pressure face or their effect can be mitigated by using laminated construction or pre-stretched acrylic material. Of these approaches, the application of abrasion-resistant coating is probably the most economical. For aquarium and habitat windows, it is best to apply the coating to both faces or frequent cleaning of the high-pressure face may destroy its optical value in several years.

8.5 SEATING

The mounting for plane rectangular windows requires basically the same features as the mounting for plane disc windows. Because of the large sizes and low operational pressures, however, larger dimensional tolerances and deflections under pressure can be allowed without detriment to the structural performance of the window (figure 8.2).

8.5.1 Bearing Support

The bearing support for the edges of the window need not be machined, if a flatness less than or equal to 0.125 inch (0.3 centimeter) can be achieved by other means. Welds joining the angles or channels that serve as bearing supports should be ground flush to eliminate point loading on the window.

8.5.2 Bearing Gaskets

These should be of 60- to 90-durometer hardness and from 0.125 to 0.250 inch thick (0.3 to 0.6 centimeter) to equalize the bearing stresses in a plane window pressing against an uneven seat in the mounting. To avoid extrusion, the gaskets should be bonded to the

bearing surface in the mounting. Since the bearing gasket also serves as a secondary seal it should be fabricated from elastomeric material and the joints bonded or vulcanized.

8.5.3 Sealing

Because of its large circumference and the unevenness of both the retaining flange and the window surface, sealing should be primarily done with room-temperature-vulcanizing silicone rubber squeezed into the annular space between the ege of the window and the wall of the window cavity. The bearing gasket underneath the window serves as a secondary seal.

8.5.4 Retaining Methods

A flat retainer flange bolted to the mounting should be used to retain the window. A soft elastomeric gasket is used below the retaining flange to equalize the contact pressure between the retainer flange and the window. The properties of the gasket under the retaining flange should be similar to those of the bearing gasket below the window.

8.5.5 Window Cavity

The window cavity in the mounting should have sufficient depth to accommodate the window and both compressed gaskets without undue looseness or squeezing. It should be dimensioned to allow for an annular space of 0.1- to 0.2-inch (0.25 to 0.5 centimeter) magnitude between the window and the cavity wall. Because the cavity wall serves as part of the seal, it should be sandblasted and painted prior to mounting.

The mounting also serves as a reinforcement around the penetration. Because of large window dimensions and the rectangularity of the opening, large deflections in the mounting can be expected. To avoid premature failure of the window, it is necessary to consider this during design. As a guideline it is recommended that the annular space between the edge of the window and the seat should never decrease to zero when the assembly is subjected to operational pressure and temperature and that rotation of the seat should never exceed 0.5 degree (0.008 radian).

8.6 FABRICATION

Large plane rectangular windows are generally sawed to size from commercially available, flat acrylic plastic sheets. Milling of the edges is not required, unless the window will be mounted in a machined seat (figure 8.3). Because sawing introduces large residual stresses into the edges of the window, annealing is mandatory to preclude initiation and growth of cracks.

Because of the large dimensions, annealing should be performed at low temperatures so that excessive shrinkage does not take place. Adequate annealing can be achieved, if the large window plates are heated to 185°F (85°C) for at least 24 hours while evenly supported in a horizontal position.

8.7 RESISTANCE TO IMPULSE AND POINT LOADING

Pressurized rectangular plane windows are very sensitive to dynamic pressure and point-impact loadings. Because of their large size and very low t/D_i ratios, protection with transparent shields is inappropriate, as it provides very little protection. If dynamic overpressures or impacts are expected during the projected life of the window, the only reasonable protection is to increase the thickness of the window during the design stage. This is particularly advised for windows in aquaria containing massive creatures, e.g., whales, porpoises, sharks, swordfish, etc.

8.8 CONCLUSION

Aquaria with large transparent panels have been built utilizing off-the-shelf, 48- by 60-inch (122 by 152.4 centimeters) acrylic plates with a thickness of 2 to 4 inches (5 to 10 centimeters). There is no need, however, to have the imagination of the architect fettered by the dimensions of commercially mass-produced acrylic plates, as plates of almost any conceivable size can custom cast. Custom-cast plates of 96 by 96 by 12 inches (244 by 244 by 30.5 centimeters) have been successfully produced, and larger sizes can be readily supplied by industry, if the customer is willing to pay the additional charge for the required tooling.

It can be successfully argued that from the cost-effectiveness viewpoint it is more economical to procure many small mass-produced panels instead of a few large custom-cast panels. There is no doubt, however, that the cost of mounting and sealing many small panels more than offsets the higher cost of the large custom panels. The panoramic vision of the large panels afforded to the spectator is then a valuable bonus feature.

8.9 REFERENCES

8.1 Roark, R. J., *Formulas for Stress and Strain,* McGraw Hill Co: New York, 1965.

8.2 Morley, A., *Strength of Materials,* Longmans, Green and Company, 1919.

8.3 Prescott, J., *Applied Elasticity,* Longmans, Green and Company, 1924.

8.4 Westinghouse Technical Night School Press, "Applied Elasticity," by S. Timoshenko and J. M. Lessells, 1925.

8.5 *Handbook of Engineering Fundamentals,* Wiley and Sons: New York, 1954.

8.6 Timoshenko, S., and Wionowsky-Krieger, S., *Theory of Plates and Shells,* McGraw-Hill Co.: New York, 1959.

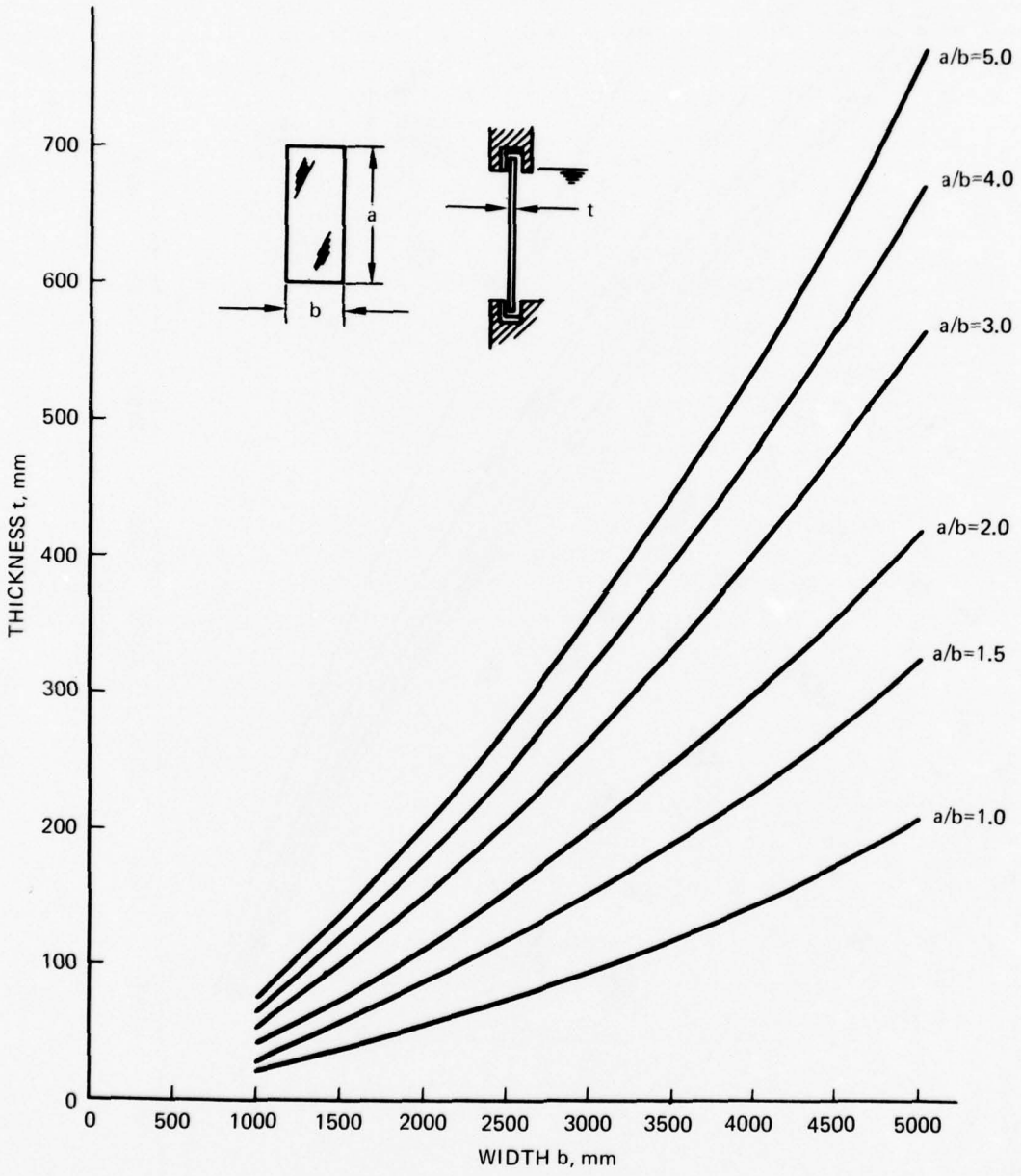

Figure 8.1. Required thickness of acrylic plastic in rectangular windows under hydrostatic loading. Note that the curves apply only to designs where the water level is never above the top edge of the window and the ambient temperature does not exceed 100°F (38° C).

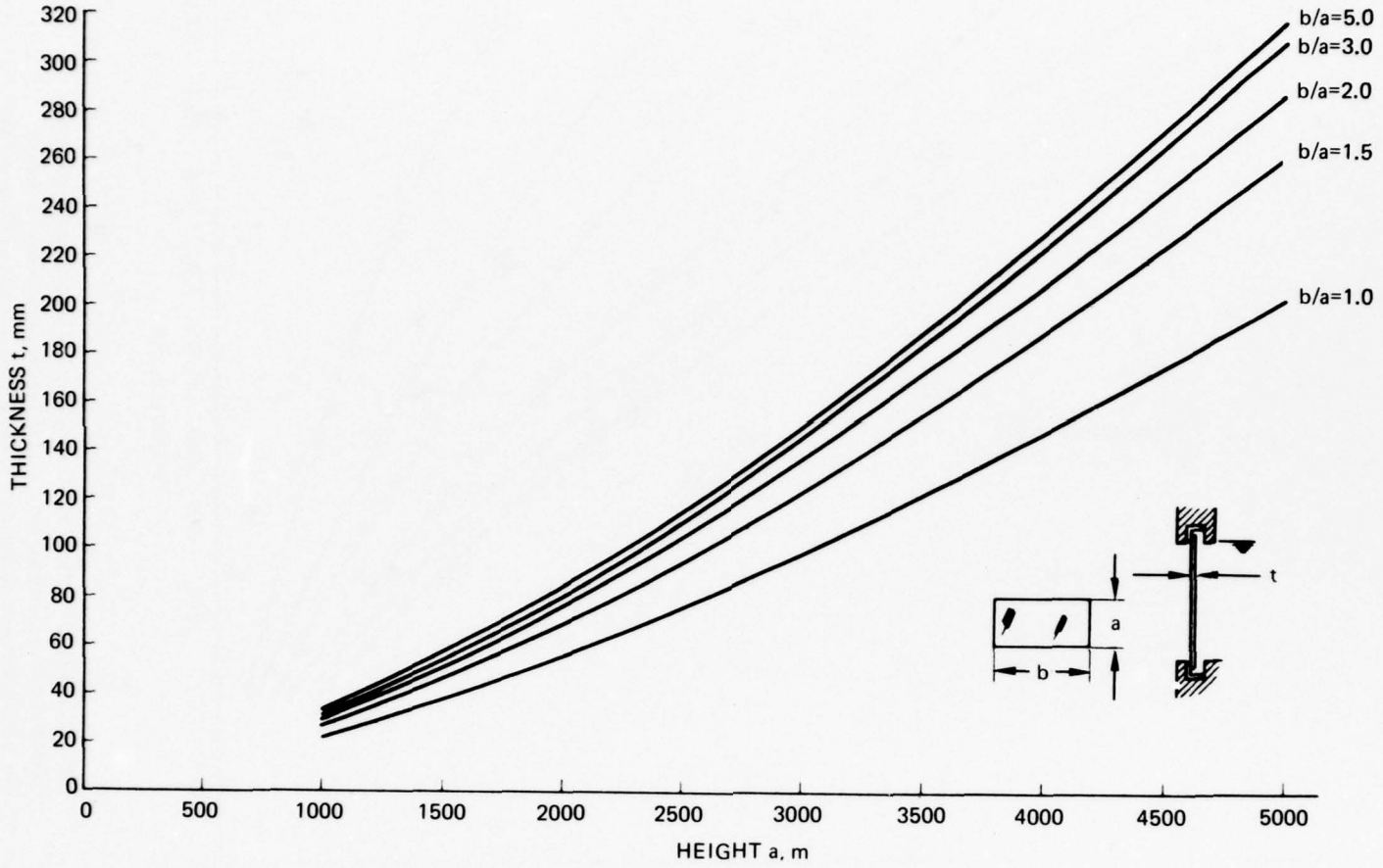

Figure 8.1. Continued.

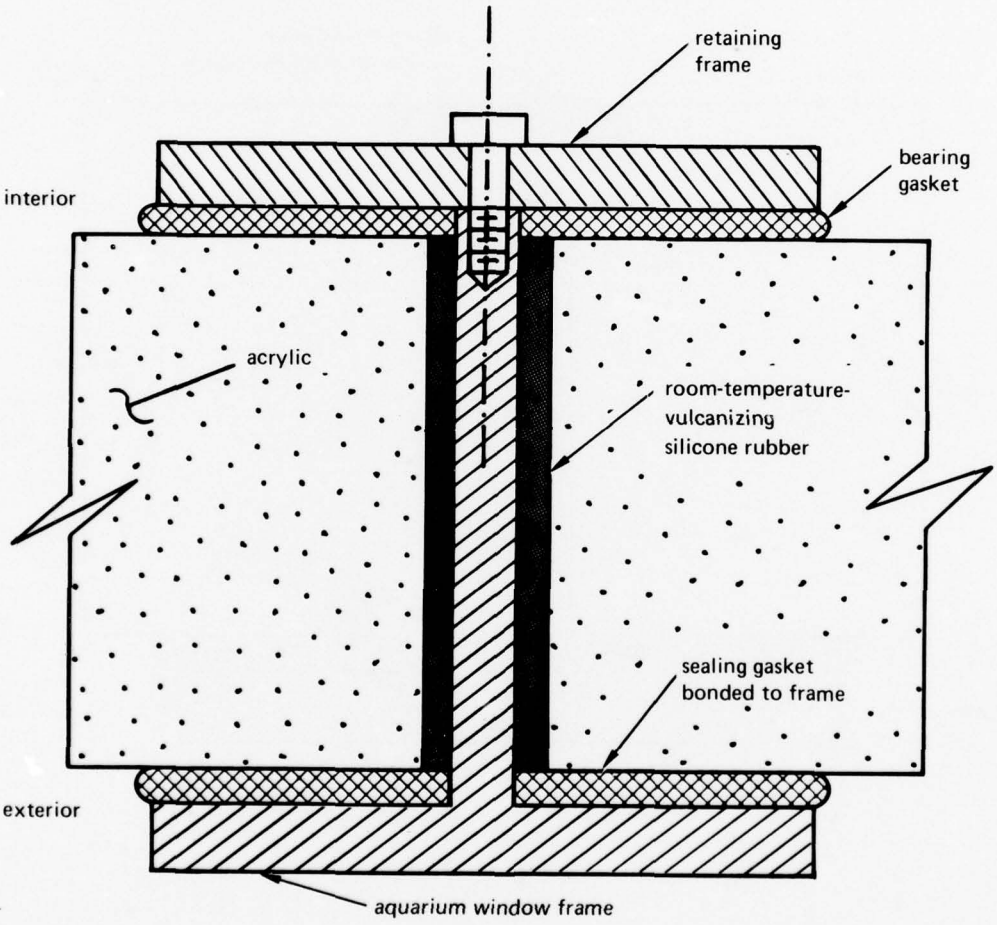

Figure 8.2. Typical mounting for aquarium windows. Note that the retaining bolts are located on the interior of the aquarium.

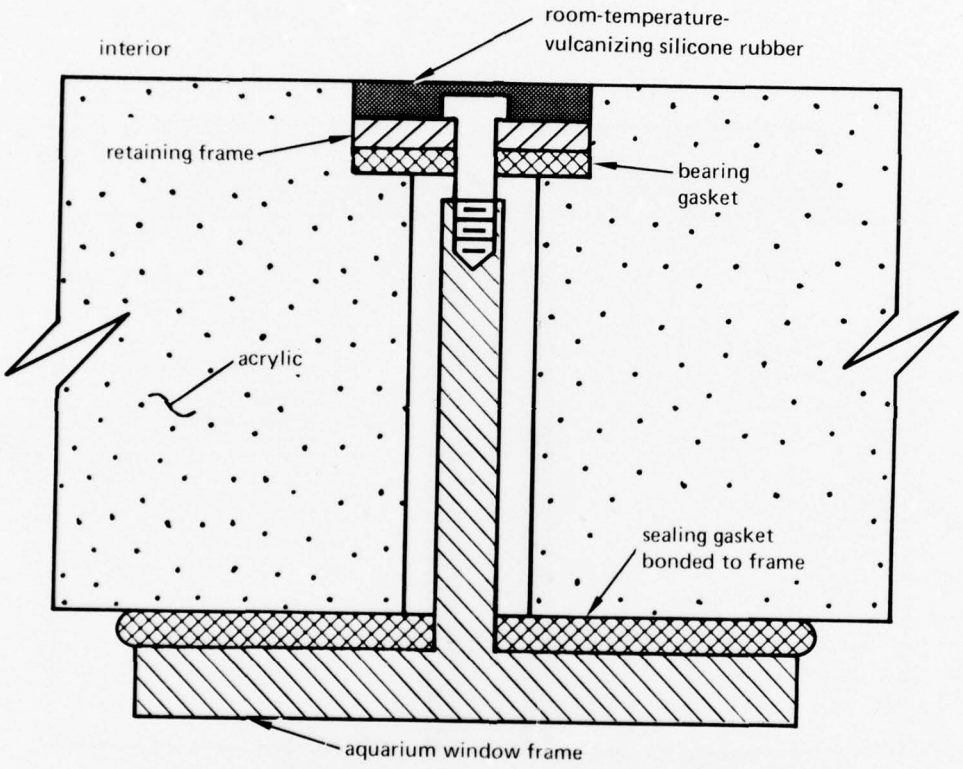

Figure 8.2. Continued.

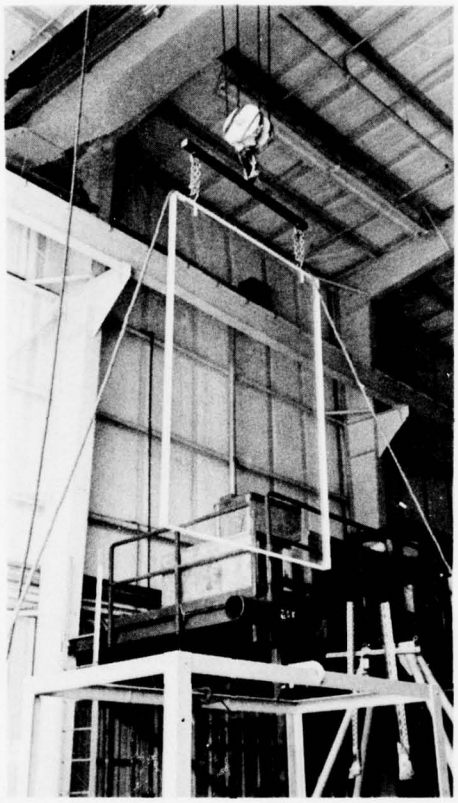

Figure 8.3. Placement of a 72- by 96-inch (183 by 244 centimeters) window with milled edges into an aquarium frame made from steel angles.

SECTION 9. PLANE DISC WINDOWS WITH CONICAL BEARING SURFACES . . . 9-1

9.1 INTRODUCTION . . . 9-1

9.2 STRUCTURAL PERFORMANCE . . . 9-2

9.3 MODES OF FAILURE . . . 9-3

9.3.1 Short-Term Loading . . . 9-3

9.3.1.1 Critical Pressure . . . 9-3
9.3.1.2 Displacement and Deformation . . . 9-5

9.3.2 Long-Term Loading . . . 9-6

9.3.2.1 Critical Pressure . . . 9-6
9.3.2.2 Displacement and Deformation . . . 9-7
9.3.2.3 Bearing Surface Deterioration . . . 9-11

9.3.3 Cyclic Loading . . . 9-12

9.3.3.1 Critical Pressure . . . 9-12
9.3.3.2 Displacement and Distortion . . . 9-12
9.3.3.3 Bearing Surface Deterioration . . . 9-13

9.4 PREDICTION OF CRITICAL PRESSURES . . . 9-13

9.5 SEATING OF WINDOWS . . . 9-17

9.5.1 Conical Angle . . . 9-17
9.5.2 Bearing Surfaces . . . 9-18

9.5.2.1 Friction . . . 9-18
9.5.2.2 Crack Initiation . . . 9-18
9.5.2.3 Rotation of Bearing Surfaces . . . 9-19

9.5.3 Sealing and Retaining . . . 9-20

9.6 FABRICATION . . . 9-21

9.6.1 Dimensional Tolerances . . . 9-21
9.6.2 Surface Finish . . . 9-22
9.6.3 Chamfering . . . 9-22

9.7 RESISTANCE TO IMPULSE AND POINT LOADING . . . 9-23

9.7.1 Impulse Loading . . . 9-23
9.7.2 Point-Impact Loading . . . 9-24

9.7.2.1 Resistance to Fracture . . . 9-24
9.7.2.2 Failure Mode . . . 9-26

9.8 NONSTANDARD WINDOWS . . . 9-27

9.9 CONCLUSION . . . 9-27

9.10 REFERENCES . . . 9-27

SECTION 9. PLANE DISC WINDOWS WITH CONICAL BEARING SURFACES

9.1 INTRODUCTION

Plane disc windows with conical bearing surfaces that resemble the shapes of conical frustums were introduced into the ocean engineering field by Professor A. Piccard in the late 1930s. Without the use of the conical frustum shape and acrylic plastic, deep submergence submersibles would probably not have developed as rapidly as they did.

The conical frustum shape and acrylic plastic work well as a unit for high-pressure service (figure 9.1). The shape makes it possible to (1) increase the field-of-view through a small penetration in a thick hull, (2) have a reliable seal against high pressure, and (3) improve the structural performance of a plane disc with a plane bearing surface. The acrylic plastic because of its inherent viscoelastic behavior allows the conical frustum to mold itself to the shape of the conical seat in the flange without the initiation of cracking at stress risers. It also keeps the stresses at a low level by allowing the conical frustum to act like a viscoelastic plug, whose axial position in the conical seat is a function of external pressure. Without such characteristic properties of viscoelastic plastic, a conical frustum window design would fail.

Attempts to use stronger, but more brittle, materials in conical frustums have failed. Both Professor A. Piccard (reference 9.1) and the author (reference 9.2) have attempted to use massive glass instead of acrylic plastic for conical frustum windows. By interposing a layer of compliant material between the steel seat and the glass bearing surface it was thought that a stress-riser free match between the two mating surfaces could be achieved, which would keep the stresses at an acceptable level. Unfortunately this did not prevent cracking in the window (figure 9.2). As subsequent finite-element stress analyses have shown, the conical frustum plug in a conical seat is inherently subject to very high, shape-induced, stress concentrations around its circumference near the edge of the low-pressure face, although both conical surfaces match perfectly. Because of these concentrations, the shear stresses in the glass are of such magnitude that tensile cracks are initiated in the glass during the relaxation phase of the first pressure cycle to which the window is subjected. The same stress risers also act upon the conical frustum made of acrylic plastic, but because of the material's viscoelasticity the peak stresses in the window's body are substantially less.

Because of advantages associated with the design of conical frustum acrylic windows, they enjoyed a virtual monopoly in man-rated pressure vessels from the late 1930s to the late 1960s. However, with operational requirements now calling for increased underwater visibility, spherical sector windows are beginning to replace them, except in those applications where either a small viewport is operationally acceptable or where very high-pressure requirements exist. Thus, conical frustums are presently used only where the operational requirements for viewports are less than 12 inches (30.5 centimeters) in diameter and the requirement for design pressure is in excess of 5000 pounds per square inch (34.5 megapascals). Since conical frustum windows economically satisfy these requirements they will remain a viable solution to the need for inexpensive, reliable, small diameter windows in pressure hulls used for human occupancy.

9.2 STRUCTURAL PERFORMANCE

Plane discs with conical bearing surfaces respond to hydrostatic loading on their high-pressure faces as do plane discs supported around their circumferences by inclined seats. Because the seat is at an angle to the plane faces of the disc, it produces vertical and radial reactions on the disc. Within the disc, the radial reaction force generates compressive radial strains which are superimposed on the strains produced by flexure. As a result of this superposition, the compressive stress at the center of the high-pressure face is higher than that on a plane disc with a plane bearing surface. Conversely the resultant stress at the center of the low-pressure face is either compressive or tensile; if tensile, it is lower than that on a plane disc with a plane bearing surface and an identical thickness-to-minor-diameter ratio.

Because of this interaction between membrane flexure and radial compression, it is feasible to design conical frustum windows that will not have tensile stresses on the low-pressure face, providing the windows are not subjected to dynamic pressure, point-impact loading, and static pressures above their design limits. The variables that determine the resultant principal stress are (1) the thickness-to-minor-diameter ratio (t/D_i), (2) the seat overhang ratio (D_i/D_f), and the angle of the conical seat (α). To eliminate tensile stress, the thickness-to-minor-diameter and seat overhang ratios are increased and the included conical angle of the seat is decreased (references 9.3 and 9.4). Consider the following examples. For a 90-degree (1.57 radians) included conical seat angle, the t/D_i ratio must be equal to or exceed 0.5 and the D_i/D_f ratio must exceed 1.06 (figure 9.3). For a 60-degree (1.04 radians) included angle, the minimum t/D_i ratio required is less than 0.5 and the D_i/D_f ratio must exceed 1.04. For a 120-degree (2.09 radians) angle, the minimum t/D_i ratio must be higher than 0.5 and the D_i/D_f ratio must exceed 1.1.

The interaction between membrane flexure, radial compression, and vertical shear not only decreases the magnitude of the tensile flexure stress component at the center of the low-pressure face and increases the compressive flexure stress component at the center of the high-pressure face, but it also generates very high compressive stress concentrations around the window's circumference at the edge of the low-pressure face (figure 9.4) (references 9.5 through 9.8). The stress riser generating these concentrations can be visualized as the reaction of the window's bearing surface to an attempted rotation of the window's edge in the flange seat because of membrane flexure. At a given pressure conical frustums with low t/D_i ratios tend to deflect more at the center than those with high ratios; thus the resulting stress concentrations are larger for windows with lower ratios. Also, since larger included angles provide a larger bearing surface for the window and decrease the magnitude of the radial reaction force by the seat, the stress concentrations at the low-pressure face are smaller for larger conical angles. By using photoelastic strain investigation techniques (references 9.3, 9.4, and 9.5), it has been shown that for a given pressure the magnitude of the stress concentration at the edge of the low-pressure seat is inversely related to the t/D_i ratio and seat angle and that the magnitude of the tensile stress on the low-pressure face is inversely related to the t/D_i ratio and directly related to the included conical angle (figures 9.5 and 9.6).

The magnitude of stresses in the conical frustum is also significantly influenced by friction between the window's bearing surface and the steel seat. Finite-element computer studies (references 9.6, 9.7, and 9.8) show that if two idealized cases – a window free to move without boundary restraint and a window totally restrained at the boundary – are compared, several interesting observations can be made: The peak compressive stress generated by the stress riser at the edge of the low-pressure face, as well as the principal compressive stresses at the center of the low- and high-pressure faces, is higher when the boundary restraint is absent (figure 9.4). This condition is advantageous for windows with a t/D_i ratio less than or equal to 0.5, i.e., prone to the presence of tensile stresses on the low-pressure face. Windows with a high t/D_i ratio (greater than or equal to 0.5) may, however, benefit from some boundary restraint, since this would tend to decrease the high compressive stresses in the windows. Viewports with conical frustum windows are between the extremes of fixed and free boundaries. For windows in greased steel seats with 32-rms finish, the experimentally measured stress distribution is close to the calculated case for the free boundary (figure 9.7) (references 9.6 and 9.8).

9.3 MODES OF FAILURE

Conical frustum windows, like other acrylic plastic windows, can fail under short-term, long-term, or cyclic loading conditions. Under short-term loading conditions, the physical properties of the material that determine the strength of the window are the short-term tensile and compressive strengths. Under long-term and cyclic pressure loadings, it is the viscoelastic and viscoplastic properties that determine the window's life. Since the window can be subjected to all three conditions during its operational life, all will be discussed in this section.

9.3.1 Short-Term Loading

9.3.1.1 CRITICAL PRESSURE. When subjected to short-term pressurization, the window deflects and axially displaces through the conical seat in the flange until catastrophic failure occurs. The magnitude of hydrostatic pressure required to cause failure depends on the window's nondimensional t/D_i ratio, conical seat angle, finish on the low-pressure face, seat overhang, and ambient temperature (see appendix B).

The nondimensional t/D_i ratio increases the resistance of the conical frustum window to failure (reference 9.10), although not in a linear manner. An increase in the ratio is always accompanied by an increase in critical pressure, until the ultimate compressive strength of acrylic plastic is reached, approximately 48,000 pounds per square inch (330.9 megapascals) at 70°F (21°C). This occurs in the hydrostatic pressure range of 40,000 to 50,000 pounds per square inch (275 to 344 megapascals), the exact magnitude depending upon ambient temperature.

The conical seat angle also increases the window's resistance to failure (reference 9.10), although not in a linear manner (figure 9.8). An increase in the angle is always accompanied by an increase in critical pressure, until the geometrically imposed limit of 180 degrees (3.1 radians) is reached. Most improvement occurs in the range of 30 to 90 degrees (0.052 to 1.57

radians). Additional increases in conical angle are followed only by minimal increases in critical pressure. For this reason, the 90-degree (1.57 radians) conical frustum is considered to be an optimized, cost-effective design where the field-of-view, structural performance, and cost have been properly balanced.

The finish on the low-pressure face is important to the critical pressure of windows with a t/D_i ratio less than 0.5, since such windows have tensile stresses at this location. The presence of even very shallow scratches (less than 0.01 inch (0.25 millimeter)) will significantly decrease the critical pressure of these windows. For windows with a t/D_i ratio greater than or equal to 0.5, scratches do not significantly reduce the critical pressure, as the low-pressure face is in compression and thus not sensitive to surface crack initiation.

The window seat overhang significantly influences the critical pressure (figure 9.9) (reference 9.11). Inadequate overhang ($D_i/D_f < 1$) drastically decreases the critical pressure, as it provides inadequate radial and axial support to the frustum cone that is extruded through the conical penetration in the hull (figure 9.10). Excess overhang ($D_i/D_f > 1$) allows the critical pressures to be maximized, but at the expense of the optical field-of-view.

For each conical angle and t/D_i ratio, there is only one D_i/D_f ratio at which the critical pressure is maximized at the least expense to the angle of optical view. For windows with $t/D_i \leq 0.35$, the required overhang is very small, since such windows primarily fail in membrane flexure without significant axial displacement through the conical seat. For windows with $t/D_i > 0.35$, the overhang required for maximization may be very large, since such windows primarily fail in shear after considerable extrusion through the conical seat.

Standard overhang is considered to be $D_i/D_f = 1$ as it simplifies the standardization of test data. Since the data in figure 9.8 were generated with $D_i/D_f = 1$, the values for critical pressure represent neither the maximum nor minimum that can be attained with conical frustum windows in seats whose overhang is selected on the basis of a particular window's t/D_i ratio and conical angle. Since the windows in actual service are provided with some positive overhang ($D_i/D_f > 1$) as required by operational requirements (section 15), the values for standard critical pressures are conservative and thus acceptable for design purposes.

To date the effect of seat overhang has been studied in detail only for 90-degree (1.57 radians) frustums (figure 9.11) (reference 9.11). Results show that the critical pressure for a particular window design can be increased by increasing the D_i/D_f ratio instead of the t/D_i ratio. The gain in critical pressure can be dramatic: For the 90-degree (1.57 radians) conical frustum with a t/D_i ratio of 0.4, the standard critical pressure can be increased more than 100 percent by increasing the D_i/D_f ratio from 1 to 1.5 (figure 9.11). However, this is not necessarily accompanied by an equivalent improvement in static or cyclic fatigue. There are indications that such improvement is insignificant or, at best, minor, as catastrophic failure under pressure cycling does not occur in the same mode as under short-term loading.

Ambient temperature influences the critical pressure significantly because of its effect on the tensile and compressive strengths of acrylic plastic (references 9.11 and 9.12). Because its effect has been shown to be fairly linear between 32 and 190°F (0 to 88°C), short-term critical pressures can be readily extrapolated from existing data (figures 9.12 and 9.13).

9.3.1.2 DISPLACEMENT AND DEFORMATION. When hydrostatic pressure is applied to a conical frustum it flexes, displaces axially, and deforms either sequentially or simultaneously, depending on its t/D_i and D_i/D_f ratios, conical angle, and ambient temperature. Since it is difficult to separate the individual effects generated by flexure, axial displacement, and plastic deformation, they are generally lumped under the term of axial displacement, which is measured by a dial indicator resting against the center of the low-pressure face.

Axial displacement of the conical frustum is a stepless function of pressure and temperature for any given window (figure 9.14) (references 9.10, 9.11, and 9.12). At lower ambient temperatures and pressures, the relationship between pressure and displacement is linear; at higher ambient temperatures and pressures, it is nonlinear with the displacement increasing at a much higher rate than the pressure. Immediately preceding failure, the displacement increases without any further increase in pressure, indicating the yield of the material in the window.

Detailed data relating displacement to short-term pressure are in appendix B. When utilizing experimentally obtained displacement data, it must be remembered that the magnitude of displacement is not only related to the nondimensional ratios of t/D_i and D_i/D_f, but also to D. For this reason it is necessary to use a linear scaling factor when extrapolating the axial displacement of a model-scale test specimen to a full-scale operational window.

Axial displacement is important in the design of conical seats in flanges for conical frustums. Without knowing the actual values of axial displacement, it is virtually impossible to design a conical seat with the proper overhang (D_i/D_f). For a given pressure level, displacement is generally the smallest under short-term loading and the highest under long-term loading. On this basis, displacement under short-term design loading could be neglected, if it were not for the fact that most accidental overpressurizations are of a short-term nature, making the short-term axial displacement data applicable (appendix B). However, if the long-term axial displacement at design pressure is larger than under the short-term overpressurization, the former then becomes the controlling factor in sizing the seat overhang.

Deformation of windows prior to catastrophic failure varies in character and magnitude with the window's t/D_i and D_i/D_f ratios, included seat angle, and ambient temperature. However, there is still sufficient similarity between the modes of failure to give them the structural behavior characteristics of a single family.

Conical frustums with low t/D_i ratios ($t/D_i \leq 0.35$) fail in simple membrane flexure in a manner similar to plane disc windows with plane bearing surfaces (section 7). The first indication that the membrane flexure has exceeded the tensile strength of acrylic is a

star-shaped crack located at the center of the low-pressure face (figure 9.15). Additional pressure causes the disc to flex which propagates the cracks farther into the body, resulting in a conchoidal fracture (section 7). By way of summary it can be stated that the conchoidal fracture is characterized by a conical fracture surface which simultaneously intersects the conical bearing surface of the window around the circumference of the low-pressure face and the central area of the high-pressure face (figure 9.16).

Conical frustums with high t/D_i ratios ($t/D_i > 0.35$) fail primarily in shear rather than simple membrane flexure, although a significant amount of membrane flexure is still present in the $0.35 < t/D_i < 0.5$ range. Because of the higher ratios, the conical frustums flex only a small amount and the majority of axial displacement comes from a plastic extrusion through the minor opening in the conical seat. The formation of a plug-like extrusion on the low-pressure face, whose diameter equals that of the minor opening in the flange, is accompanied by the formation of a crater-like depression in the center of the high-pressure face (figure 9.17). After the depression and the extrusion reach a certain magnitude, the stress reaches such magnitude that circumferential cracks are initiated on the bearing surface of the window. An additional increase in pressure causes one of the cracks to propagate into the window's body until a conical fracture surface that intersects the high-pressure face at the edge of the depression is formed (figure 9.18). Any further axial displacement caused by a pressure increase is limited to the central portion of the window, while the separated outer shell of the window remains stationary in the conical seat. As the pressure is increased, the central portion of the window extrudes and the crater deepens at a faster rate, since the remaining bearing surface is much smaller. Finally the body of the remaining window above the opening becomes so thin that a secondary fracture cone originating at the throat of the window seat and penetrating the high-pressure face at the center of the crater is formed, a process that finally causes the window to leak (figure 9.19).

The locations of the initiation of the primary and secondary conical fractures vary with the t/D_i ratio and conical angle. The effects of higher ambient temperature on deformation are to increase the plasticity and decrease the tensile and compressive strengths of the material. As a result, the magnitudes of the crater and the extrusion become much larger before fracture is initiated, although the overall ability of the window to withstand pressure without failure decreases (figure 9.20).

9.3.2 Long-Term Loading

9.3.2.1 CRITICAL PRESSURE. When a conical frustum window is subjected to sustained pressure loading of a given magnitude, it will continue to displace and deform until catastrophic failure takes place or it will displace and deform for a short period of time and then for all practical purposes cease to do so. The first response is termed static fatigue. It is observed in all sustained pressurizations (figures 9.21 and 9.22) with the exception of those where the window is subjected to a sustained pressure whose magnitude is only a very small fraction of its short-term critical pressure, i.e., less than 1/10 of short-term critical pressure.

The static fatigue of any window can be described in terms of three variables: pressure, time, and ambient temperature. Experimental data on static fatigue, plotted on pressure and time coordinates, can be used to predict the time to failure of any window, if the magnitude of sustained pressure and the ambient temperature are known. However, such data do not exist because of the high cost of generating such information. As a result the designer must conduct an experimental program with either full- or model-scale specimens to determine the static fatigue properties of a particular conical frustum design.

Adequate data do exist, however, to guide the designer in the selection of structural characteristics for the window. For example, the static fatigue of a conical frustum window improves with increases in the t/D_i and D_i/D_f ratios and the conical angle, while it degrades with increases in temperature and the duration of the loading (references 9.13 through 9.16). For a few windows, the static fatigue life at sustained pressure levels of 20,000, 10,000, and 5000 pounds per square inch (137.8, 68.9, and 34.5 megapascals) and room temperature has also been established (appendix B).

9.3.2.2 DISPLACEMENT AND DEFORMATION. Conical frustum acrylic plastic windows flex, axially displace, and deform under long-term loading in a manner identical to that which occurs under short-term loading (figure 9.23). The only difference is how the displacement and deformation of the window are achieved: Under short-term loading, the continuous increase in hydrostatic loading increases the magnitude of displacement and deformation, while under long-term loading it is the duration of the loading which causes the increase. For example, a conical frustum window under sustained loading may react to a hydrostatic pressure of 10,000 pounds per square inch (68.9 megapascals) after 0, 10, and 100 minutes of sustained loading in the same manner as the identical window would under pressures of 10,000, 12,000, and 15,000 pounds per square inch (68.9, 82.7, and 103.4 megapascals) during short-term pressurization.

Magnitudes of displacement and deformation under sustained loading vary with the t/D_i and D_i/D_f ratios, conical angle, and ambient temperature in a manner similar to that found under short-term loading. Thus to minimize the axial displacement and distortion of the window, a conical frustum design with the highest t/D_i and D_i/D_f ratios and conical angles, allowed by tradeoff studies that consider the weight and size of the viewport assembly, should be selected.

Axial displacement and distortion under sustained loading are in many respects more important considerations than critical pressure during the design phase, i.e., before the window fails catastrophically it will lose its value as an operational window. Fortunately extensive experimental data exist on axial displacement, the result of three, definitive, long-term studies conducted at sustained pressure levels of 20,000, 10,000 and 5000 pounds per square inch (137.8, 68.9, and 34.5 megapascals) (see appendix B and references 9.13, 9.14, and 9.15). Because the test programs used five test specimens for each t/D_i ratio and included angle, the resulting displacement curves are not only reliable, but they also provide insight into the range of displacements obtained from five identical windows tested under the same conditions (figures 9.24 and 9.25). The spread of displacement readings between individual test specimens with the same t/D_i ratios was generally less than 20 percent of the mean

value, which indicates good reproducibility of experimental data, particularly when it is considered that temperatures during the sustained loading varied by as much as 10 percent. The applicability of existing experimental data can be extended beyond 1000 hours by plotting the axial displacements on log-log coordinates as a function of time (tables 9.1, 9.2, and 9.3). Since the resulting plots represent straight lines, they can be easily extrapolated by any desired amount. Extrapolations beyond 10 years are not recommended, however, as significant deterioration of physical properties in the material can be expected after this time (section 5).

Table 9.1. Average axial displacements of conical frustum acrylic windows during sustained loading at 5000 pounds per square inch (34.5 megapascals) (reference 9.15).

t/D_i	Time, hr	Included Conical Angle				
		30 deg	60 deg	90 deg	120 deg	150 deg
0.375	1	0.345 in	0.036 in	0.028 in	0.026 in	0.026 in
	10	–	0.042 in	0.032 in	0.029 in	0.029 in
	100	–	0.048 in	0.040 in	0.034 in	0.036 in
	500	–	0.062 in	0.044 in	0.039 in	0.041 in
	1000	–	0.072 in	0.047 in	0.041 in	0.044 in
0.500	1	0.074 in	0.025 in	0.024 in	0.020 in	0.023 in
	10	0.086 in	0.028 in	0.025 in	0.021 in	0.024 in
	100	0.100 in	0.030 in	0.027 in	0.024 in	0.026 in
	500	0.106 in	0.031 in	0.028 in	0.025 in	0.027 in
	1000	0.112 in	0.032 in	0.030 in	0.028 in	0.028 in
0.625	1	0.054 in	0.024 in	0.023 in	0.021 in	0.015 in
	10	0.056 in	0.025 in	0.024 in	0.021 in	0.016 in
	100	0.058 in	0.027 in	0.026 in	0.023 in	0.017 in
	500	0.058 in	0.028 in	0.027 in	0.024 in	0.018 in
	1000	0.059 in	0.029 in	0.028 in	0.025 in	0.019 in
0.750	1	0.042 in.	0.022 in	0.020 in	0.016 in	0.017 in
	10	0.046 in	0.023 in	0.021 in	0.016 in	0.018 in
	100	0.048 in	0.023 in	0.022 in	0.018 in	0.019 in
	500	0.049 in	0.024 in	0.023 in	0.018 in	0.020 in
	1000	0.050 in	0.025 in	0.023 in	0.019 in	0.021 in
1.000	1	0.040 in	0.020 in	0.023 in	0.014 in	0.018 in
	10	0.040 in	0.021 in	0.023 in	0.015 in	0.019 in
	100	0.041 in	0.021 in	0.024 in	0.016 in	0.020 in
	500	0.041 in	0.022 in	0.024 in	0.017 in	0.021 in
	1000	0.042 in	0.023 in	0.024 in	0.017 in	0.022 in

Notes:
1 deg = 1.745 329 E-02 rad
1 in = 2.540 000 E-02 m

Table 9.2. Average axial displacements of conical frustum acrylic windows during sustained loading at 10,000 pounds per square inch (68.9 megapascals) (reference 9.14).

t/D_i	Time, hr	Included Conical Angle				
		30 deg	60 deg	90 deg	120 deg	150 deg
0.500	1	not applicable	0.146 in	0.062 in	0.050 in	0.050 in
	10		–	0.102 in	0.066 in	0.064 in
	100		–	–	0.195 in	0.194 in
	500		–	–	–	–
	1000		–	–	–	–
0.625	1	0.180 in	0.057 in	0.046 in	0.036 in	0.032 in
	10	0.197 in	0.066 in	0.047 in	0.038 in	0.038 in
	100	0.340 in	0.076 in	0.054 in	0.045 in	0.041 in
	500	0.524 in	0.081 in	0.058 in	0.049 in	0.045 in
	1000	–	0.084 in	0.062 in	0.053 in	0.048 in
0.750	1	0.120 in	0.052 in	0.042 in	0.035 in	0.031 in
	10	0.126 in	0.059 in	0.044 in	0.036 in	0.033 in
	100	0.133 in	0.065 in	0.048 in	0.039 in	0.038 in
	500	0.138 in	0.069 in	0.051 in	0.041 in	0.039 in
	1000	0.140 in	0.071 in	0.052 in	0.042 in	0.040 in
0.875	1	0.085 in	0.046 in	0.038 in	0.034 in	0.030 in
	10	0.092 in	0.048 in	0.038 in	0.035 in	0.030 in
	100	0.103 in	0.055 in	0.044 in	0.036 in	0.035 in
	500	0.106 in	0.055 in	0.044 in	0.039 in	0.037 in
	1000	0.108 in	0.057 in	0.045 in	0.040 in	0.038 in
1.000	1	0.076 in	0.042 in	0.033 in	0.030 in	0.028 in
	10	0.078 in	0.043 in	0.035 in	0.030 in	0.029 in
	100	0.078 in	0.048 in	0.042 in	0.034 in	0.034 in
	500	0.081 in	0.052 in	0.043 in	0.038 in	0.036 in
	1000	0.082 in	0.053 in	0.044 in	0.039 in	0.037 in
1.250	1	0.074 in	0.041 in	0.032 in	0.029 in	0.027 in
	10	0.076 in	0.041 in	0.034 in	0.029 in	0.028 in
	100	0.077 in	0.047 in	0.041 in	0.034 in	0.033 in
	500	0.077 in	0.051 in	0.042 in	0.037 in	0.035 in
	1000	0.079 in	0.053 in	0.043 in	0.038 in	0.036 in

Notes:
1 deg = 1.745 329 E-02 rad
1 in = 2.540 000 E-02 m

Table 9.3. Average axial displacements of conical frustum acrylic windows during sustained loading at 20,000 pounds per square inch (137.8 megapascals) (reference 9.13).

t/D_i	Time, hr	Included Conical Angle				
		30 deg	60 deg	90 deg	120 deg	150 deg
0.025	1	not applicable	not applicable	not applicable	not applicable	not applicable
	100					
	500					
	1000					
0.750	1	not applicable	0.308 in	0.118 in	0.098 in	0.074 in
	100		0.610 in	0.256 in	0.163 in	0.149 in
	500		0.755 in	0.360 in	0.320 in	0.310 in
	1000		0.825 in	0.408 in	0.395 in	0.380 in
0.875	1	0.708 in	0.141 in	0.090 in	0.087 in	0.071 in
	100	–	0.213 in	0.146 in	0.122 in	0.099 in
	500	–	0.260 in	0.196 in	0.144 in	0.124 in
	1000	–	0.328 in	0.238 in	0.160 in	0.145 in
1.000	1	0.504 in	0.126 in	0.080 in	0.082 in	0.060 in
	100	0.726 in	0.165 in	0.124 in	0.109 in	0.081 in
	500	0.946 in	0.186 in	0.151 in	0.130 in	0.092 in
	1000	–	0.204 in	0.167 in	0.137 in	0.101 in
1.250	1	0.285 in	0.112 in	0.075 in	0.068 in	
	100	0.324 in	0.156 in	0.099 in	0.089 in	not applicable
	500	0.345 in	0.168 in	0.108 in	0.101 in	
	1000	0.485 in	0.183 in	0.118 in	0.109 in	
1.500	1	0.212 in	0.108 in	0.073 in	0.062 in	
	100	0.246 in	0.138 in	0.099 in	0.080 in	not applicable
	500	0.256 in	0.150 in	0.105 in	0.093 in	
	1000	0.275 in	0.160 in	0.115 in	0.103 in	
1.750	1	0.210 in	0.102 in	0.072 in	0.062 in	
	100	0.236 in	0.130 in	0.097 in	0.080 in	not applicable
	500	0.244 in	0.142 in	0.108 in	0.085 in	
	1000	0.255 in	0.148 in	0.112 in	0.090 in	
2.000	1	0.196 in	0.099 in	0.070 in	0.061 in	0.051 in
	100	0.223 in	0.127 in	0.089 in	0.082 in	0.068 in
	500	0.230 in	0.136 in	0.096 in	0.092 in	0.075 in
	1000	0.238 in	0.143 in	0.103 in	0.097 in	0.077 in

Notes
1 deg = 1.745 329 E-02 rad
1 in = 2.540 000 E-02 m

For conical frustum viewports to be used as optical elements for underwater cameras, it is not only important to know how much the window displaces in the conical seat towards the camera, but also how much the low- and high-pressure faces depart from their original plane configurations. The departure from a thick plane lens becomes very marked as the window approaches failure (figures 9.26 and 9.23B). Unfortunately, the change of the plane disc into a lens with an optically noticeable, concave, high-pressure face and a convex, low-pressure face occurs even at pressures for which the windows are rated operationally safe (figure 9.27) (reference 9.16). Thus the designer should know how much the conical frustum departs from an ideal plane disc. The published data on this subject are meager (figure 9.26), and the designer must either perform a finite-element strain analysis of the design prior to construction or fabricate one and measure the changes in the window's curvature. This would best be accomplished by optical means or, if not possible, by closely spaced electrical or mechanical displacement indicators. Because of the large expense involved, neither is often used. It is important to note, however, that regardless of whether the experimental or analytical approach is used the results are comparable, particularly if the assumption is made that the window is free to slide in its seat (table 9.4).

Table 9.4. Low-pressure face displacements per 1000-pound-per-square-inch (6.89 megapascals) linear range (reference 9.6).

Type of Displacement	$\delta_z/a \times 10^3$ at Locations			
	r/a = 0.0	r/a = 0.5	r/a = 0.9	r/a = 1.0
Experimental	4.60	4.04	2.50	1.54
Analytic (free boundary)	4.52	3.93	2.38	1.41
Analytic (fixed boundary)	3.51	2.82	1.06	0.00

Notes:
$t/D_i = 0.46$
$D_i/D_f = 1.06$
temperature = 75°F (23.8°C)
pressure = 0 to 5000 psi (0 to 34.5 mPa)
a = radius of low-pressure face
r = radial distance to a point on low-pressure face measured from its center

9.3.2.3 BEARING SURFACE DETERIORATION. Besides axial displacements and distortions, another important factor that must be considered in the selection of the t/D_i and D_i/D_f ratios and conical angle for a given window is the deterioration of the conical bearing surface. Because of shear stresses the conical bearing surface will craze and crack with time. The cracks will ultimately propagate through the body of the window and form a conical fracture surface identical to the one observed in windows under short-term loading. It is interesting to note that the extent of surface cracking on the conical bearing surface varies primarily with the conical angle. Thus, if the t/D_i and D_i/D_f ratios, pressure, duration of loading, and temperature are held constant, the extent of bearing area near the low-pressure face covered with cracks and the depth of crack penetration will vary inversely with the conical angle (figure 9.28). This indicates that one can locate stress risers, like O-ring grooves, with greater impunity in the bearing surface near the window's high-pressure face when the conical angle is large. A general rule is that the shear cracks in the bearing surface of conical frustums extend only about 80, 40, 20, 10, and 5 percent of the bearing surface's length measured from low-pressure faces for 30-, 60-, 90-, 120-, and 150-degree (0.52, 1.04, 1.57, 2.09, and 2.61 radians) windows, respectively.

9.3.3 Cyclic Loading

9.3.3.1 CRITICAL PRESSURE. When subjected to cyclic pressure loading, a conical frustum acrylic plastic window will, if cycled long enough to some elevated pressure, fail catastrophically because of the cyclic fatigue of the material. The number of cycles required to produce catastrophic failure depends on the magnitude of maximum pressure during the loading phase of the cycle, duration of the loading and relaxation phases, and ambient temperature. Failure will occur sooner if the pressure is high, loading phase long, relaxation phase short, and ambient temperature high.

The same geometrical parameters apply to the design of conical frustum windows with a high cyclic fatigue capability as to conical frustum windows with a high static fatigue capability or high short-term critical pressure, i.e., the t/D_i and D_i/D_f ratios and conical angle should be as large as possible.

Little published data are available on the cyclic fatigue life on conical frustum windows (references 9.12 and 9.17), and the designer must conduct an experimental program if the cyclic fatigue of the design must be known. However, the available data have established that when critical pressures of identical conical frustum test specimens are plotted as a function of the number of pressure cycles on log-log coordinates a linear graph results (figure 9.29) and that the maximum pressure during a cycle should be less than 25 percent of the short-term critical pressure for the same window, if a cyclic fatigue life in excess of 10,000 cycles is to be expected with confidence. The linearity of the graph makes it possible to extrapolate the critical pressures from the few specimens that failed at a low number of cycles to a much larger number of cycles. Extrapolation beyond 10 years is not recommended, however, since the strength of acrylic plastic deteriorates significantly after 10 years.

9.3.3.2 DISPLACEMENT AND DISTORTION. During cyclic pressure loading, the conical frustum flexes, displaces, and distorts in a manner similar to that found during long-term pressure loading. The primary difference is the magnitude of strains, displacement, and distortion. During the first pressure cycle, the conical frustum behaves as it does under long-term loading at the same pressure, temperature, and duration. The strains and displacements begin to differ during the second cycle. The difference becomes more pronounced as the number of cycles increases until the window fails. It is interesting to note that the difference between the structural responses in each cycle becomes less as the cycling progresses. In general, the difference between the first and succeeding cycles is a function of the temperature and the relationship between the maximum cyclic pressure and the window's short-term critical pressure. As a rule, if the cyclic pressure is more than 50 percent of the short-term critical pressure the difference between structural responses during the first and succeeding cycles is significant, while if the cyclic pressure is less than 25 percent of the short-term critical pressure the difference is minor (figures 9.30 and 9.31).

When the magnitudes of the strains and displacements during a loading phase after some number of cycles are compared with those from a sustained loading of the same total loading duration, those under cyclic loading are smaller. If the length of the loading phase in each cycle is equal to the relaxation phase, then the increase in displacement caused by

cycling creep is only about 10 to 20 percent of the sustained loading creep measured at the number of hours equal to the total of all pressure cycle durations.

9.3.3.3 BEARING SURFACE DETERIORATION. The conical bearing surface develops circumferential shear cracks similar to those found during short- and long-term pressure loadings. If the number and the depth of the cracks on the bearing surface of pressure-cycled windows are compared with those from windows subjected to sustained loading, the sum of loading phase durations must be an order of magnitude larger than that of the uninterrupted sustained loading before the depth and number of cracks reach equal magnitude.

Published data (references 9.3, 9.6, 9.8, 9.12, and 9.16) on the initiation of cracks on the bearing surface under cyclic pressure loading are very limited for two reasons: (1) it requires more manpower to unlock the pressure vessel frequently and inspect the windows for bearing cracks than it does to instrument the window for the detection of only catastrophic failure and (2) the appearance of surface bearing cracks precedes catastrophic failure by hundreds, and sometimes thousands, of pressure cycles and thus is not as an important criterion in design as is catastrophic failure (figure 9.32). Furthermore, detection of the first crack on the bearing surface is of a qualitative nature, while detection of catastrophic failure is not. This does not mean that the appearance of cracks on the bearing surface should be ignored. To the contrary, the appearance of many deep (greater than 0.1 inch (0.25 centimeter)) circumferential cracks is an indication that the cyclic fatigue life of the window will expire in the near future and that replacement windows must be ordered. How much cyclic fatigue life remains can be approximately ascertained by reinspecting the cracks on the bearing surface after it has been subjected to several additional pressure cycles and noting the increase in crack depth. When inspecting the windows, care must be taken not to confuse circumferential shear cracks with axial scratches and gouges formed when the soft acrylic surface slides on the hard metal. The presence of these marks is natural, and does not indicate expiring fatigue life. These axial scratches and gouges will be particularly numerous near the low-pressure face, where the bearing pressure between the mating acrylic and steel surfaces is the highest.

9.4 PREDICTION OF CRITICAL PRESSURES

To determine a safe conical frustum design for a given working pressure, the designer must consider both the projected service parameters at which the window will operate and the structural capabilities of the selected design. The service parameters that must be known are (1) maximum ambient temperature at design pressure, (2) maximum expected overpressurization caused by human error or equipment malfunction, (3) longest expected duration of a single sustained loading at design pressure, and (4) desired fatigue life at design pressure for pressure cycles with known loading and relaxation phases. The structural capabilities that must be known are defined by the (1) critical pressure under short-term pressurization at design temperature, (2) static fatigue, i.e., duration of sustained loading that will cause the window to fail catastrophically under design pressure and temperature, and (3) cyclic fatigue, i.e., number of cycles at design pressure that will cause the window to fail catastrophically at design temperature.

Knowing both the projected service parameters and structural capabilities, the designer can compare them and then either reject or accept the design. This is, of course, the ideal approach to the selection of a cost-optimized, safe design. To date there has been only one study (reference 9.12) in which all structural parameters for a chosen design were experimentally established prior to placing it in service (1000 pounds per square inch (6.89 megapascals) and 150°F (66°C)). The primary reason for the lack of such data is the cost and long time frame; for example, the study in reference 9.12 lasted 1 year and cost approximately $30,000 (see figures 9.13, 9.14, 9.21, 9.22, and 9.33). Other reasons involve proprietary data and classified applications.

Faced with the absence of published data, the designer can either initiate a study to determine the structural parameters inherent in the design or follow standard design procedures based on the cumulative experience of the ocean engineering community. The standard approach (section 15) will not produce a design that is cost-optimized for a given set of service parameters. It will, however, produce a design rapidly and economically that will satisfy most service requirements with an adequate margin of safety. Since this procedure has been discussed in detail in section 7, it will only be summarized in this section.

The standard procedure for windows with a design pressure less than 10,000 pounds per square inch (68.9 megapascals) is based on the postulate that the static and cyclic fatigues of acrylic plastic windows are related to their short-term critical pressures by a set of conversion factors (table 9.5), whose magnitudes are functions of ambient temperature and expected static and cyclic fatigue requirements of standard designs. The magnitude of conversion factors is based on a requirement for a maximum of 10,000 pressure cycles, where the sum of loading phases does not exceed 40,000 hours, or a single sustained loading, where the length does not exceed 40,000 hours. The conversion factors also provide approximate safety margins of 300, 100, and 50 percent against short-term, long-term, and cyclic pressure loadings, respectively, at design pressure and temperature. These safety margins are present only in windows in prime condition; age, surface deterioration, accidental overpressurizations, and cumulative number of hours in service decrease the margins to zero in about 10 years, the projected maximum life of standard windows.

For design pressures larger than 10,000 pounds per square inch (68.9 megapascals), the procedure is to select the dimensions of the conical frustum from a set of designs, whose performances have been established. Because of limitations inherent with acrylic plastic, the conversion factors for these designs (table 9.6) are less than those for a design pressure less than 10,000 pounds per square inch (68.9 megapascals). As a result, the safety margins are even less. However, all windows designed on the basis of data in table 9.6 have performed satisfactorily in the range of 10,000 to 20,000 pounds per square inch (68.9 to 137.8 megapascals) without premature failure.

Table 9.5. Conversion factors for acrylic plastic conical frustum windows designed for pressures less than 10,000 pounds per square inch (68.9 megapascals).

Operational Pressure	Temperature				
	50°F (10°C)	75°F (24°C)	100°F (38°C)	126°F (52°C)	151°F (66°C)
	Conversion Factor*				
2500 psi (17.2 mPa)	5	6	8	10	16
5000 psi (34.5 mPa)	4	5	7	9	4500 psi (31 mPa)
7500 psi (51.7 mPa)	4	5			
10,000 psi (68.9 mPa)	4	5	8000 psi (55.2 mPa)		

conversion factors for these pressures must be interpolated between upper and lower values

*These conversion factors apply only to short-term critical pressures experimentally obtained in flanges with $D_i/D_f = 1$ at an ambient temperature of 75°F (24°C).

Table 9.6. Conversion factors for acrylic plastic conical frustum windows designed for pressures in excess of 10,000 pounds per square inch (68.9 megapascals).

Operational Pressure	t/D_i*	Temperature, 50°F (10°C) D_i/D_f			
		60 deg (1.04 rad)	90 deg (1.57 rad)	120 deg (2.09 rad)	150 deg (2.61 rad)
11,000 psi (75.86 mPa)	1.0	↑	↑	↑	↑
12,000 psi (82.73 mPa)	1.1	↑	↑	↑	↑
13,000 psi (89.63 mPa)	1.2	↑	↑	↑	↑
14,000 psi (96.53 mPa)	1.3	↑	↑	↑	↑
15,000 psi (103.45 mPa)	1.4	1.13	1.17	1.23	1.69
16,000 psi (110.34 mPa)	1.5	↑	↑	↑	↑
17,000 psi (117.24 mPa)	1.6	↑	↑	↑	↑
18,000 psi (124.14 mPa)	1.7	↑	↑	↑	↑
19,000 psi (131.03 mPa)	1.8	↑	↑	↑	↑
20,000 psi (137.93 mPa)	1.9	1.20	1.26	1.53	2.48
		Temperature, 75°F (24°C)			
11,000 psi (75.86 mPa)	1.1	↑	↑	↑	↑
12,000 psi (82.73 mPa)	1.2	↑	↑	↑	↑
13,000 psi (89.63 mPa)	1.3	↑	↑	↑	↑
14,000 psi (96.53 mPa)	1.4	↑	↑	↑	↑
15,000 psi (103.45 mPa)	1.5	1.13	1.17	1.23	1.69
16,000 psi (110.34 mPa)	1.6	↑	↑	↑	↑
17,000 psi (117.24 mPa)	1.7	↑	↑	↑	↑
18,000 psi (124.14 mPa)	1.8	↑	↑	↑	↑
19,000 psi (131.03 mPa)	1.9	↑	↑	↑	↑
20,000 psi (137.93 mPa)	2.0	1.20	1.26	1.53	2.48

*t/D_i values can be used only for service at ambient temperatures less than 75°F (24°C)

9.5 SEATING OF WINDOWS

9.5.1 Conical Angle

Conical frustums require seats with precisely matched conical bearing surfaces. Since this can only be done by handlapping the window inside the seat, the cost is prohibitive. For this reason, extensive experiments have been conducted to establish the effect of angular mismatch between the window's bearing surface and the seat (reference 9.5). On the basis of these data, it can be postulated that a mismatch of less than 1 degree (0.02 radian) has no significant effect on the short-term critical pressure. There is no question, however, that an angular mismatch of less than 1 degree (0.02 radian) has a significant effect on the magnitude of stresses at the center and edge of the low-pressure face (figures 9.34 and 9.35) in the elastic range of elastic plastic.

If the gap between the window and the seat is maximum at the low-pressure face, then the positive flexure stress component at the center of the low-pressure face and the negative flexure stress component at the center of the high-pressure face are increased. At the same time, the compressive radial stress component is decreased at the center of the low-pressure face and increased at the center of the high-pressure face. The principal stress at the center of the low-pressure face then becomes more positive (larger) for t/D_i values less than or equal to 0.5 and less negative (smaller) for values greater than 0.5 when compared with windows that have been precision lapped into their seats, i.e., ideal windows. Thus for windows with a t/D_i ratio less than or equal to 0.5 the gap at the low-pressure face is undesirable since it increases the resultant tensile stress at the center of the low-pressure face, while for windows with a t/D_i ratio greater than 0.5 the gap is desirable since it decreases the magnitude of peak compressive stress found on the bearing surface near the low-pressure face (reference 9.22).

If the gap is maximum at the high-pressure face, then the radial compressive stress component is increased at the center of the low-pressure face and decreased at the center of the high-pressure face. The flexure stress components on the low-pressure and high-pressure faces remain approximately the same as they do for an ideal window. The principal stress at the center of the low-pressure face then becomes less positive (smaller) for t/D_i values less than or equal to 0.5 and more negative (larger) for values greater than 0.5 when compared with ideal windows. Thus for windows with t/D_i ratios less than or equal to 0.5 the gap at the high-pressure face is desirable since it decreases the resultant stress at the center of the low-pressure face, while for windows with ratios greater than 0.5 the gap is undesirable since it increases the peak compressive stress on the bearing surface near the low-pressure face.

These problems are overshadowed by the effects of the angular mismatch on the low-pressure seal. A large clearance between the high-pressure face and the seat makes it difficult to seal the face with gaskets or O-rings while the window is under radial or axial compression. For this reason, a large clearance is considered operationally unacceptable, although it generates a favorable stress field in cones with t/D_i ratios less than or equal to 0.5. Clearance at the low-pressure face poses no problem in sealing and is acceptable.

Because of these sealing problems two courses of action are recommended for windows with large gaps at the high-pressure face.

1. For frustums with t/D_i ratios greater than 0.5, the machining tolerance for the included angle should be positive, i.e., the angle should be larger than or equal to the nominal value, while for the associated seat in the flange the tolerance should be negative, i.e., the angle should be smaller than or equal to the nominal value. The magnitude of machining tolerance on the included angle in both cases should not surpass 0.25 degree (0.004 radian), resulting in a possible maximum angular mismatch of 0.5 degree (0.008 radian).

2. For frustums with t/D_i ratios less than or equal to 0.5, the machining tolerances for the included angle should be positive, the same as for the associated seat in the flange. In addition, the magnitude of the tolerance should not surpass 0.25 degree (0.004 radian), resulting in a possible maximum angular mismatch of 0.25 degree (0.004 radian).

9.5.2 Bearing Surfaces

The bearing surfaces on both the acrylic plastic conical frustum and the steel seat have a significant influence on the frustum's stress field and the initiation of cracking on the frustum's bearing surface. This is caused by the roughness of the metallic seat surface which determines not only the coefficient of friction between the acrylic plastic and the metal, but also serves as a stress riser for the initiation of surface shear cracks.

9.5.2.1 FRICTION. Friction between a fine-machined (32 rms) acrylic frustum and a metallic seat depends on both the finish of the seat and the presence or absence of a lubricating agent. For a dry seat, the friction increases with the roughness of the metallic surface and the hydrostatic pressure acting on the conical frustum (figure 9.36A). The coefficient of friction is quite large even for polished ($\tan \beta = 0.35$ on 8 rms) or ground ($\tan \beta = 0.45$ on 20 rms) steel surfaces. This indicates that for fine-machined seat surfaces, typical of most window installations, the coefficient of friction exceeds 0.5. For a lubricated seat, the difference in coefficients for polished and ground surfaces is much less than for dry surfaces (figure 9.36B). Since most operational conical frustum windows are well lubricated prior to installation, it is not necessary to polish the steel seat surface, i.e., the 0.15 coefficient of friction for a lubricated ground surface is only minimally higher than the 0.1 coefficient for a lubricated polished surface.

A photoelastic study of stress fields in conical frustums resting on ground and polished seats has shown that there is no significant difference between the magnitude or distribution of stresses, regardless of whether the seats are dry or lubricated (figure 9.37). This is not the case, however, if the seat is made rougher by machining rather than by polishing or grinding. The increase in friction and the change in stress magnitude have not been quantified, only their effect on initiation of surface shear cracks has been experimentally observed.

9.5.2.2 CRACK INITIATION. Crack initiation on the bearing surface of the acrylic conical frustum depends to a large degree on the roughness and condition of the steel seat. The presence of circumferential grooves for containment of single or multiple O-rings is detrimental and cracks will initiate sooner in the acrylic bearing surface than if the grooves

were absent (figures 9.38 and 9.39). However, if only low surface ridges and grooves (less than 250 rms) caused by machining in a lathe are present, the roughness of the surface is beneficial.

Since data are only fragmentary, a general relationship between the degree of roughness and crack initiation cannot presently be made. However, based on experiments (reference 9.6) using 90-degree (1.57 radian) conical frustums ($t/D_i = 0.59$ and $D_i/D_f = 1.06$), it can be tentatively postulated that an increase in roughness from polished (8 rms) to rough machined (125 rms) surfaces is beneficial for conical frustums with t/D_i ratios greater than 0.5. In this particular experiment, 15 well lubricated windows were rapidly pressure cycled five times to 88 percent of their short-term critical pressure. Only the windows pressurized in a seat with 125-rms surface roughness completed the test without cracks in the bearing surface and a minimum amount of permanent plastic deformation (table 9.7). All others had cracks, whose depths were inversely related to the roughness of the seat (figures 9.40 and 9.41). The data from this experiment also substantiate the findings of a finite-element stress analysis (section 9.2), which postulated that boundary restraint is beneficial for windows with t/D_i ratios greater than 0.5, as it tends to decrease the magnitudes of peak compressive stresses on the bearing surface near the low-pressure face and axial displacement.

Table 9.7. Deformations of model-scale viewports after five short-term pressure cycles to 20,000 pounds per square inch (137.8 megapascals).

Flange Finish, rms	Set Number					Average
	1	2	3	4	5	
	Low-Pressure Face Permanent Extrusion, in					
125	0.025	0.030	0.038	0.037	0.025	0.031
63	0.064	0.055	0.069	0.080	0.058	0.065
32	0.070	0.060	0.078	0.085	0.064	0.071
	High-Pressure Face Depression Depth, in					
125	0.004	0.005	0.008	0.007	0.003	0.005
63	0.029	0.015	0.032	0.036	0.016	0.026
32	0.035	0.035	0.023	0.042	0.026	0.033

Notes

$D = 1.06$ in (2.7 cm)
$t = 0.62$
$\alpha = 90$ deg (1.57 rad)
$t/D_i = 0.59$
temperature = 70°F (21°C)
$D_i/D_f = 1.06$
1 in = 2.540000 E-02 m

9.5.2.3 ROTATION OF BEARING SURFACES. The rotation of bearing surfaces on the steel seat, caused by forces transmitted from the hull to the seat flange, also affects the distribution and magnitude of stresses in the conical frustum window (figure 9.42), as the rotation changes the magnitude of the seat's included angle (reference 9.20). The result is similar to the angular mismatch between the frustum and seat (see section 9.5.1 and reference 9.18). In this particular case, the seat was supported in such a way that the application of the pressure tended to decrease the angle of the seat. As expected from theoretical considerations, this increased the bending moment and the magnitude of flexure stress components in the conical frustum. Because of the effect that seat rotation has on the magnitude of stresses, care must be taken to not have the rotation exceed 0.5 degree (0.008 radian), unless the designer plans to achieve well defined change in stress distribution.

9.5.3 Sealing and Retaining

Sealing of conical frustums is generally accomplished with both low- and high-pressure seals (figure 9.43, designs A and D). The low-pressure seal utilizes either a thick elastomeric gasket atop the high-pressure face or an O-ring wedged between the chamfered edge of the high-pressure face, the bearing surface of the seat, and the steel retaining ring. The high-pressure seal utilizes the grease trapped between the conical frustum and the seat. This arrangement is generally considered very satisfactory, as the most reliable high-pressure seal known is the tightly wedged frustum, while the less reliable low-pressure seal must only keep the window from leaking at very low pressure (less than 50 pounds per square inch (0.35 megapascal)) during pressurization and depressurization procedures. The only difficulty is that during very long sustained loading the window may creep so much axially that upon depressurization it may not return enough to compress the gasket or wedge seal properly against the retaining ring and some leakage will take place at low pressure.

This problem can be eliminated during the design process by providing sufficient mechanical precompression for the seals at 0 pound-per-square-inch (0 megapascal) ambient pressure. Thus, even during the maximum duration of sustained loading at design pressure, there will be sufficient compression on the seals to prevent leakage around the window during rapid depressurization of the pressure vessel. (The magnitude of recommended precompressions is in section 15.) For conical frustums with a t/D_i ratio less than or equal to 0.5 this is probably the best currently available design. However, for those with a ratio greater than 0.5 other seal designs can be used because of the increased window thickness. Two of the more common ones use O-rings, but not as wedge seals. The unique features of these seals (designs B and E) are (1) they seal at both low and high pressures regardless of the window's axial displacement under pressure and (2) the O-ring groove is machined in the conical frustum. Both features are operationally valuable, since the window can have both the O-ring and the bearing contact as high-pressure seals and the O-rings come assembled with the window and do not depend on selection and fitting in the field by unqualified personnel. Of the two O-ring seals, the one on the bearing surface (design E) is more positive, since it depends on the axial displacement of the O-ring rather than radial compression and it requires a less complex seat in the flange. It also has the capability of relieving any buildup of pressure acting on the low-pressure face during depressurization. Its major drawback is that unless the groove is located near the high-pressure face and is properly machined, it will serve as a crack initiator in the window. However, locating the groove within 0.3t distance from the high-pressure face and providing the bottom of the groove with generous radii (0.025 to 0.05 inch (0.06 to 0.12 centimeter)) will eliminate this problem. The other seal utilizing an O-ring in radial compression (design B), although more expensive to incorporate into the viewport assembly, has several good features that make it desirable for some applications: Because it is not located in the bearing surface the O-ring groove does not act as a crack initiator and because the O-ring is in radial compression it also seals against any pressure acting against the low-pressure face of the window. This latter feature is sometimes desirable, as some deep-diving submersibles build up slight internal pressure during the dive and the windows should not act like poppet valves when reaching the ocean surface during ascent. Several windows with this sealing system have performed successfully at 20,000-pounds-per-square-inch (138 megapascals) service (figure 9.44).

The satisfactory operation of seals using O-rings as wedge seals (design D), radial seals (design B), or axial seals (design E) requires that the surface of the seat be rust-free and possess at least a 32-rms finish. Rust will cause the seals to leak, while excessive surface roughness will cause the seals to abrade and loose their sealing ability after only a few pressure cycles. The seating surface can be kept rust-free for short periods of time (less than 1 year) by a liberal application of the proper grease (if greases other than DC-4 silicone are used it is necessary to check for their compatibility with acrylic plastic) or by painting them and subsequently sanding them smooth. The only long-term solution is to use a Monel weld overlay and machine it smooth. In some cases, thick electroless nickel plating has given good service for extended periods of time, but its life is usually only a little better than that of a painted seat (less than 5 years).

For proper operation, all seal designs require a window retainer that applies axial force before the hydrostatic pressure reaches sufficient magnitude to take over this function. The window retainer, typically a bolted-on ring, relies either on an elastomeric gasket or a circular leaf spring to apply pressure uniformly along the circumference of the high-pressure face. In addition, either the gasket or the spring is required to compensate for the dimensional tolerances on the window's thickness which cause it to seat either too high or too low in the seat.

In some designs (A and D), the elastomeric gasket under the retainer ring also serves as a low-pressure seal. In these cases, the compression of the gasket or O-ring must be sufficient to exert a sealing action, even when the window has axially displaced under pressure. Where the gasket or O-ring does not serve as a low-pressure seal, only sufficient compression is necessary to seat the window properly. The retainer ring must have sufficient rigidity to prevent its deformation when the screws are tightened around its circumference. This generally requires a thickness of at least 0.125 inch (0.32 centimeter) in windows with a major diameter of less than 12 inches (30.5 centimeters) and 0.25 inch (0.64 centimeter) for those with a major diameter in excess of 12 inches (30.5 centimeters). To prevent overcompression of gaskets the retainer ring must be able to bottom against the flange when fully tightened.

9.6 FABRICATION

Acrylic plastic conical frustums require the same material and fabrication quality assurance as any other acrylic plastic window used for manned pressure vessels (see sections 7 and 15). Three requirements which apply specifically to conical frustums will be discussed in this section.

9.6.1 Dimensional Tolerances

These must be specified so that the window will fit into the seat without any difficulty or loss of sealing ability, i.e., the diameter of the high-pressure face must be kept within very tight dimensional tolerances or the window will not seal properly at the high-pressure face where the low-pressure seal is located. The effect of variation in the diameter can basically be compensated for by selecting a design where the edge of the high-pressure face is chamfered to receive an O-ring for axial compression. The thickness of the window must be

dimensioned from the high-pressure face, and the diameter of the low-pressure face becomes only a reference dimension. Since both the high-pressure face and the window thickness are easy to measure in the machine shop, no problems should be encountered with the diameter of the low-pressure face being of proper size, if the included angle has been kept within the specified angular tolerance.

The effect of angular deviation from the nominal angle on the distribution of stresses in the window and practical approaches to specifying angular tolerances were discussed in section 9.5.1 and will not be repeated. What does require reiteration, however, is the fact that a well equipped machine shop can turn conical frustums on a lathe to an angular tolerance of $\pm < 0.1$ degree (0.002 radian), a major diameter tolerance of $\pm < 0.01$ inch (0.02 centimeter), and a thichness of $\pm < 0.01$ inch (0.02 centimeter).

Since an acrylic plastic window changes dimensions significantly in comparison to its steel seat during a temperature change, it is important to determine beforehand at what temperature the window should perfectly fit the seat and at what temperature and humidity the window's dimensions are to be measured in the machine shop. Since there are no shops that consistently maintain an ambient temperature lower than 70°F (21°C) or higher than 80°F (27°C), it is recommended that the dimensions on the drawings be stated and that the measurements be performed at 75°F (24°C) and 50-percent relative humidity, although their nominal dimensions are calculated for a design temperature differing from 75°F (24°C).

9.6.2 Surface Finish

A high quality surface finish is important for the low-pressure face of windows with t/D_i ratios less than or equal to 0.5, as the principal stresses at the center of the low-pressure face are positive. In windows with a t/D_i ratio greater than 0.5, the fine finish required on the low-pressure face is only for optical purposes, since the principal stresses at the center of the low-pressure face are negative. The finish on the high-pressure face is only a function of optical requirements because this face is not subjected to tensile stresses during hydrostatic loading.

There can be no stress risers on the bearing surface in the circumferential direction, since this is the orientation of the shear cracks found on this surface. The particular risers to be avoided are the machining marks that result from turning in a lathe. Unless these are eliminated by very fine turning (32 rms) or fine sanding, the static and cyclic fatigue lives of the window will be significantly shortened. The window must also be annealed to eliminate residual stresses generated by machining and polishing operations (figure 9.45). (For proper annealing procedures, see section 15.)

9.6.3 Chamfering

Chamfering the high-pressure face's circumference is beneficial for measurement of that dimension as well as for subsequent handling during installation of the window in the steel seat. Several designs exist that use the resulting chamfer for containment of the O-ring seal (figure 9.43D).

9.7 RESISTANCE TO IMPULSE AND POINT LOADING

9.7.1 Impulse Loading

Conical frustums of acrylic plastic with $0.5 \leqslant t/D_i \leqslant 1.0$ and a 90-degree (1.57 radians) included conical angle fracture under dynamic impulse loading generated by underwater explosions in a 40 to 70°F (4.4 to 21°C) ambient environment at a peak overpressure equal to approximately 20 percent of the short-term critical pressure (references 9.17, 9.19, and 9.22). Static pressure superimposed on the dynamic peak overpressure has no significant effect, if the static pressure does not exceed approximately 25 percent of the short-term critical pressure. Both model- and full-scale windows perform in an identical manner when the t/D_i and D_i/D_f ratios and included conical angles are the same. What the quantitative effect of dynamic impulse loading is on a window with a t/D_i ratio less than 0.5, greater than or equal to 1.0, or an included angle less than 90 degrees (1.57 radians) is not known. The effects of static pressures in excess of 25 percent of short-term critical pressure or ambient temperatures in excess of 70°F (21°C) on the dynamic peak overpressure required to initiate fracture in the windows are also not known. Based on theoretical considerations, however, reasonably reliable predictions can be made of the performance of windows with different t/D_i ratios and included angles tested at higher ambient pressures or temperatures under dynamic impulse loading:

1. Conical angles differing from 90 degrees (1.57 radians) cause windows to perform like 90-degree (1.57 radians) conical frustums.

2. t/D_i ratios less than 0.5 make windows less resistant to dynamic pressure than conical frustums with $0.5 \leqslant t/D_i \leqslant 1.0$, while t/D_i ratios larger than 1.0 make windows more resistant to dynamic pressures.

3. Ambient temperatures in the –40 to +40°F (–40 to +4.4°C) range cause windows to perform like those in the +40 to +70°F (+4.4 to +21°C) range, while temperatures from +70 to +150°F (+21 to +65°C) make them less resistant to dynamic pressures.

4. Ambient static pressure in the 25- to 50-percent range of short-term critical pressures causes windows with a t/D_i ratio less than or equal to 0.5 to fail at a lower dynamic peak overpressure and those with a ratio greater than 0.5 to fail at a higher dynamic peak overpressure.

The fracture of conical frustum windows under dynamic pressure impulse loading is initiated at the low-pressure face and progresses to the high-pressure face. If the dynamic peak overpressure is only high enough to initiate fracture (approximately 17 percent of short-term critical pressure), the resulting damage generally consists of a conical surface on the low-pressure face with the apex of the cone pointing toward the high-pressure face (figure 9.46); however, the window is still capable of withstanding static design pressure without leaking. If the dynamic peak overpressure is high enough to produce catastrophic failure of the window (greater than or equal to 25 percent of the short-term critical pressure), the resulting damage consists not only of spalling on the low-pressure face but also of several radial cracks that initiate at the center of the window, radiate toward the edges, and penetrate the entire thickness of the window (figure 9.47).

In general, it appears that the resistance of conical frustums to explosive-generated dynamic overpressures is about the same as that for circular discs with plane bearing surfaces (section 7). It would thus appear that the conical bevel angle has no, or at most very little, effect on the performance of plane acrylic discs under dynamic pressure loading. The explanation may be that the pressure is applied so rapidly (a rate of approximately 30×10^6 pounds per square inch per second (0.21×10^6 megaspascal)) that the beneficial viscoelastic wedging action of the frustum in the conical seat cannot occur and the frustum reacts to the rapidly applied dynamic pressure like a simple plane circular disc.

If there is any advantage to conical frustums for dynamic pressure applications, it is their performance under ambient static pressure while being subjected to dynamic overpressure. For plane discs with plane bearing surfaces the effect of ambient static pressure is always detrimental; for conical frustums with a t/D_i ratio greater than or equal to 0.5 it is either neutral or positive; and for conical frustums with a t/D_i ratio less than 0.5 the effect is probably the same as it is for plane discs with plane bearing surfaces.

9.7.2 Point-Impact Loading

Conical frustum acrylic plastic windows fracture when impacted on their high- or low-pressure faces with a hard object. Because point-impact loading occurs more frequently on the high-pressure face than on the low-pressure face, it has been the subject of several experimental studies (references 9.3, 9.7, and 9.17). The results of studies in which the impact is applied at right angles to the high-pressure face show that the magnitude of kinetic energy required to initiate fracture is a function of the thickness, t/D_i ratio, ambient temperature, ambient hydrostatic pressure, impact velocity, window diameter (D_i), impactor diameter, and location of impact.

9.7.2.1 RESISTANCE TO FRACTURE. Because of the many experimental variables, the studies were limited to the following: 90-degree (1.57 radians) included angle; thickness-to-minor-diameter ratio of $0.4 \leqslant t/D_i \leqslant 1.0$; impact velocity of 4 to 20 feet per second (1.2 to 6 meters per second); temperature of 38 to 70°F (3.3 to 21°C); and impactor diameter of 0.25 to 1.125 inches (0.64 to 2.85 centimeters).*

> The velocity of the impactor from 4 to 20 feet per second (1.2 to 6 meters per second) appears to have no effect on the magnitude of kinetic energy required to fracture a window.** The point at which velocity influences the magnitude of the kinetic energy required for fracture is not known; there are indications, however, that it occurs at velocities higher than 50 but less than 1000 feet per second (15 to 305 meters per second).

---

*The impactor is shaped like a hemisphere whose apex contacts the surface of acrylic windows.

**Fracture under point-impact loading is defined as the loss of sealing ability. Hertzian cracks on the high-pressure face in the immediate vicinity of point of impact appear at much lower impact energies than those at which the window fractures. However, because they do not decrease the short-term critical pressure of the window or cause it to leak, they are considered to be structurally insignificant.

The impactor diameter significantly affects the magnitude of the kinetic energy required for fracturing the conical frustum window (figure 9.48), if the diameter of the impactor is less than 0.5 D_i (reference 9.17). As the impactor diameter increases so does the kinetic energy required to fracture a window with the same t/D_i ratio and D_i. An interesting relationship appears to exist between the diameter of the impactor and the diameter of the window when the t/D_i ratio is kept constant, i.e., the kinetic energy required for fracture can be represented on semilog coordinates as a linear function of diameter, if the ratio of the impactor diameter to window diameter remains constant at 0.25 (figure 9.49). By using this relationship experimental data generated with model-scale windows can be extrapolated to full-scale windows with the same t/D_i ratio, if the diameter of the impactor is scaled with the diameter of the window to maintain the constant ratio of 0.25.

Ambient pressure influences the kinetic energy required for fracturing a conical frustum window (figure 9.50) (references 9.6 and 9.17). Increased ambient pressure raises the kinetic energy required to fracture windows with a t/D_i ratio greater than or equal to 0.5. Although experimental data do not exist for impacts on windows with ratios less than 0.5, it is postulated that the presence of static ambient pressure will lower the kinetic energy required for initiation of fracture because the static pressure generates additional tensile stresses on the low-pressure face where fracture originates.

The thickness-to-minor-diameter ratio has a significant effect on kinetic energy, if the window diameter is kept constant (figure 9.51) (reference 9.6). This indicates that the energy appears to be related to thickness, rather than the t/D_i ratio of the conical frustum window, except when the ratio is less than 0.5. This postulate is substantiated by comparing the approximately equal kinetic energies required to fracture two 2-inch-thick (5 centimeters) conical frustums: (1) $t/D_i = 1.0$, impactor diameter = 0.5 inch (1.27 centimeters), and D_i = 2 inches (5 centimeters) and (2) $t/D_i = 0.5$, impactor diameter = 0.5 inch (1.27 centimeters), and D_i = 4 inches (10.16 centimeters).

Ambient temperature from 38 to 70°F (3.3 to 21°C) has no significant effect. On the basis of known fracture toughness, Izod impact strength, and tensile strength for acrylic plastic from –40 to +150°F (–40 to +66°C), it can be postulated that temperatures from –40 to +40°F (–40 to +4.4°C) will also have no effect, while those from +70 to +150°F (+21 to +66°C) may decrease the magnitude of the required kinetic energy.

The location of impact on the high-pressure face has a very significant effect on the magnitude of kinetic energy required for fracture. As long as the point of impact is located on the high-pressure face within the circle directly above the low-pressure face, the amount of kinetic energy required for fracture

initiation remains constant. Moving the center of impact outside that circle decreases the required magnitude. The most vulnerable location on the conical frustum window to point impact is in the immediate vicinity of the retainer ring's edge.

The resistance of conical frustum windows to point-impact loading appears to be approximately the same as that of plane disc windows with plane bearing surfaces and a t/D_i ratio less than 0.5. Since there are no impact data for plane disc windows with plane bearing surfaces and t/D_i ratios greater than or equal to 0.5, it is not feasible to make a meaningful comparison in this range. It is expected, however, that the resistance to impact will be higher than that of plane disc windows with plane bearing surfaces and that this improvement will increase with increases in the t/D_i ratio.

In general, it appears that the impact resistance of conical frustums, similar to plane disc windows with plane bearing surfaces, is not adequate to withstand impacts generated during typical at-sea operations. Thus, a submersible moving at 1 knot (0.5 meter per second) or being hoisted aboard its support ship with a deck-mounted crane generates more kinetic energy than conical frustums with $t < 4.0$ inches (10.2 centimeters) can absorb without fracture ($<$ 500 foot-pounds) ($<$ 678 newton-meters). For this reason, they should be considered as fragile and wherever possible be protected by a transparent impact shield bonded with a transparent elastomer to the high-pressure face or an external bumper.

9.7.2.2 FAILURE MODE. A conical frustum window with $0.5 \leqslant t/D_i \leqslant 1$ impacted at the center of its high-pressure face fails by spalling on the low-pressure face and the formation of star-shaped fracture planes radiating from the point of impact to the circumference of the face (figure 9.52) (reference 9.17). The spalling takes the form of a conical fracture surface whose apex is towards the point of impact on the high-pressure face, and the circumference of the fracture cone coincides with the edge of the low-pressure face.

Off-center impacts produce fracture patterns different in appearance from those produced by a central impact. The spalling does not take the form of a regular fracture cone, and instead of star-shaped fracture planes there are several irregular fractures propagating to the edge of the high-pressure face (figure 9.53). The fracture mode of conical frustums impacted on the high-pressure face under ambient static pressure does not differ substantially from those observed on windows under zero ambient pressure (figure 9.54). In addition, the fracture pattern does not change significantly when the surfaces of the window are scored to simulate sharp surface scratches.

If the impact is not severe enough to initiate fracture, full hertzian cracks will be observed on the high-pressure face at the edge of the hemispherical impact indentation. Repeated impacts on the same location with insufficient kinetic energy to initiate fractures do not cause the hertzian cracks to propagate, and for this reason they are not considered as fracture initiation on the window under impact loading.

9.8 NONSTANDARD WINDOWS

There are many applications in which window design considerations demand a small outer diameter while operational requirements demand conical bearing surfaces with a large included angle. The only way to reconcile these conflicting requirements is to eliminate the sharp edge of the window with a deep chamfer. Since a chamfer decreases the area of the conical bearing surface of the window, care must be taken in design to keep the magnitude of the chamfer within a structurally acceptable range.

Extensive data exist on the structural performance of plane disc windows with conical bearing surfaces equipped with shallow chamfers, i.e., ℓ/t less than 0.06, where ℓ is the width of the chamfer measured along the window's axis of revolution. Only scattered data have been generated for conical frustums with very deep chamfers. Thus an empirical relationship between ℓ/t and short- and long-term critical pressure cannot be established at this time. Sufficient data exist, however, to guide the designer in the selection of chamfers that will significantly decrease the outside diameter of the window without any measurable decrease in structural performance (figure 9.55).

For conical frustum windows with an included conical angle equal to or in excess of 90 degrees (1.57 radians), the width of the chamfer should not exceed $\ell/t = 0.5$. It is not known how wide the chamfer may be for windows with angles less than 90 degrees (1.57 radians) without a significant decrease in structural performance. Still, it can be assumed with reasonable confidence that chamfers with less than $\ell/t = 0.25$ can be tolerated by such windows without an increase in critical pressure under short- and long-term loading.

9.9 CONCLUSION

Plane disc windows with conical bearing surfaces fabricated from acrylic plastic are the most reliable windows known today for withstanding hydrostatic pressures from −15 to 20,000 pounds per square inch (0.1 to 138 megapascals). Because of their excellent performance and reliable sealing, they are preferred by designers for all applications, except where panoramic visibility is the primary design requirement. It can be thus stated that the window invented by Professor Auguste Piccard has successfully withstood the test of time as an excellent solution to a difficult problem.

9.10 REFERENCES

9.1 Piccard, Auguste, *Earth, Sky and Sea.* Oxford University Press: New York, 1956.

9.2 Naval Civil Engineering Laboratory, "Exploratory Evaluation of Glass Conical Frustum Windows Under Hydrostatic Loading," by J. D. Stachiw, 1965

9.3 Allied Research Associates, Incorporated, Technical Report ARA 350-3, "Tests of Acrylic Deep Submergence Windows Under Simulated Operational Conditions," by R. Winter and J. Pozerycki, September 1968.

9.4 Allied Research Associates, Incorporated, Technical Report ARA 315-10, "An Experimental Investigation of Deep Submergence Windows," by R. Winter, October 1966.

9.5 Allied Research Associates, Incorporated, Technical Report ARA 315-7, "A Photoelastic Investigation of Deep Submergence Windows," by R. Winter and H. Becker, May 1966.

9.6 Naval Civil Engineering Laboratory, Technical Report R-675, "Stress Analysis of a Conical Acrylic Viewport," by M. R. Snoey and J. D. Crawford, April 1970.

9.7 Naval Ship Research and Development Center, Report 3167, "The Structural Performance of Acrylic Viewports for Deep Submersibles," by F. M. Schwartz, August 1969.

9.8 Naval Civil Engineering Laboratory, Technical Report R-686, "Structural Design of Conical Acrylic Viewports," by M. R. Snoey and M. G. Katona, June 1970.

9.9 Naval Ship Research and Development Center, Report 2944, "Evaluation of Full Scale DSRV-1 Acrylic Windows Under External Pressure," by M. A. Krenzke, et al., January 1969.

9.10 Naval Civil Engineering Laboratory, Technical Report R-512, "Windows for External or Internal Hydrostatic Pressure Vessels; Part I, Conical Acrylic Windows Under Short-Term Pressure Application," by J. D. Stachiw and K. O. Gray, January 1967.

9.11 Naval Civil Engineering Laboratory, Technical Report R-773, "Windows for External or Internal Hydrostatic Pressure Vessels; Part VII, Effect of Temperature and Flange Configurations on Critical Pressure of 90-Degree Conical Acrylic Windows Under Short-Term Loading," by J. D. Stachiw and J. R. McKay, August 1972.

9.12 Stachiw, J. D., and Gray, K. O., "Procurement of Safe Viewports for Hyperbaric Chambers," *ASME Transactions/Journal of Engineering for Industry*, November 1971.

9.13 Naval Civil Engineering Laboratory, Technical Report R-645, "Windows for External or Internal Hydrostatic Pressure Vessels; Part IV, Conical Acrylic Windows Under Long-Term Pressure Application of 20,000 psi," by J. D. Stachiw, October 1969.

9.14 Naval Civil Engineering Laboratory, Technical Report R-708, "Windows for External or Internal Hydrostatic Pressure Vessels; Part V, Conical Acrylic Windows Under Long-Term Pressure Application of 10,000 psi," by J. D. Stachiw and W. A. Moody, January 1970.

9.15 Naval Civil Engineering Laboratory, Technical Report R-747, "Windows for External or Internal Hydrostatic Pressure Vessels; Part VI, Conical Acrylic Windows Under Long-Term Pressure Application of 5,000 psi," by J. D. Stachiw and K. O. Gray, June 1971.

9.16 Southwest Research Institute, Report 03-2704-11, "Deep Star 20,000 Window Proof Pressure and Qualification Tests," by E. M. Briggs, et al., May 1971.

9.17 Naval Ship Research and Development Center, Letter Serial 69-720-687, "Evaluation of DSRV-1 Acrylic Windows Under Dynamic Loading," by J. J. Mecholsky and F. M. Schwartz, June 1969.

9.18 Allied Research Associates, Incorporated, Technical Report No. ARA-F-271-5, "Photoelastic Investigation of Stresses in a Penetrated Hemisphere," by H. Hamilton and H. Becker, December 1964.

9.19 Naval Electronics Laboratory, Technical Memorandum 933, "Explosive Effect on Manned Submersible Viewports," by A. J. Schlosser, May 1966.

9.20 Vasta, J., et al., "Structural Problems in Penetrated Spheres Under Pressure," AIAA Paper No. 66-709, *AIAA/USN 2nd Marine Systems and ASW Conference,* Long Beach, California, August 1966.

9.21 J. W. Manor. Observation Windows of the Deep Submersible ALVIN. *Journal of Ocean Technology,* Vol. 1, No. 1. 1966.

9.22 Southwest Research Institute, Technical Report N00600-68-C-1427, "Resistance of Conical Viewports to Underwater Explosions and Implosions," by B. W. Vanzant, et al., January 1969.

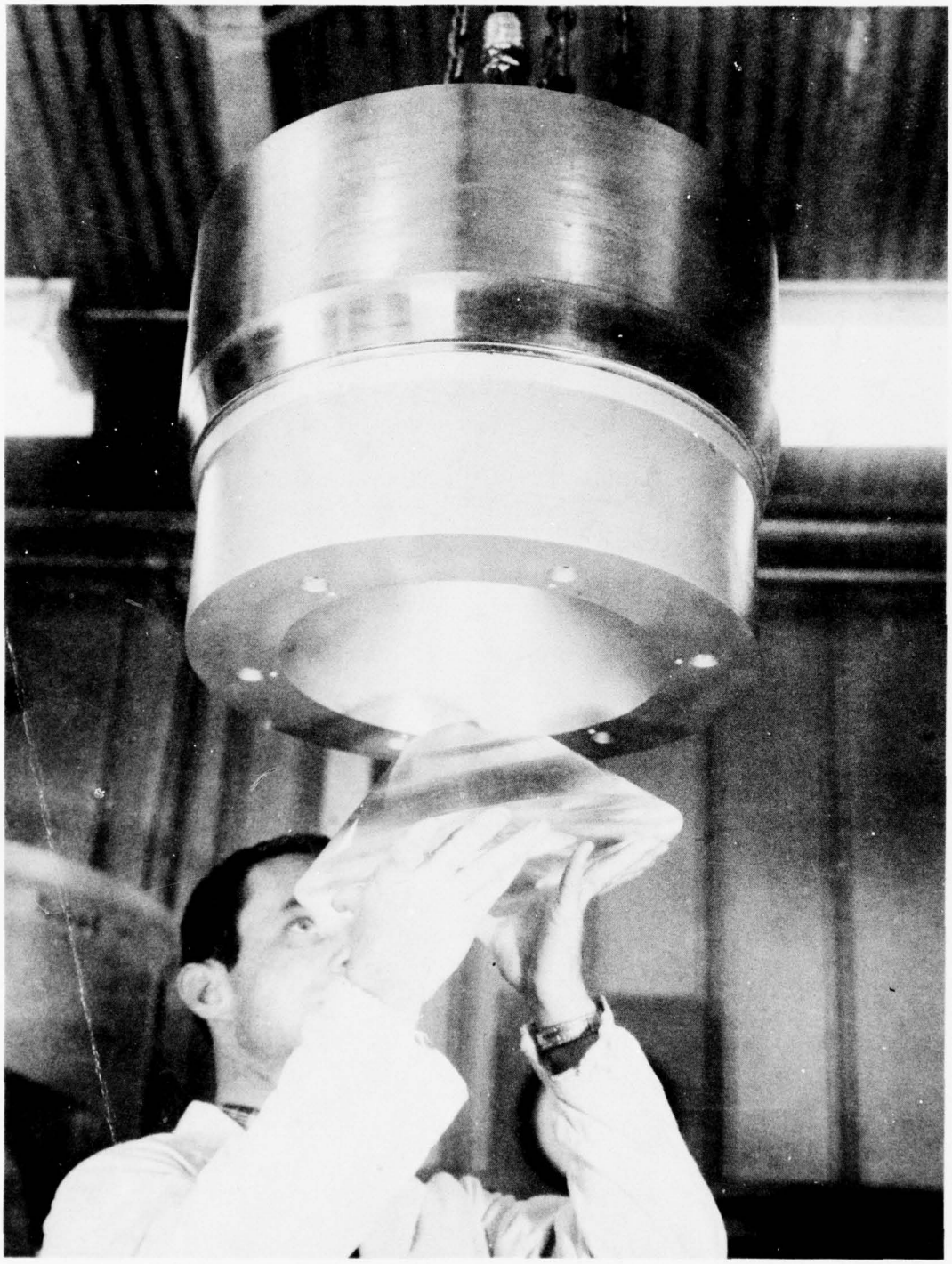

Figure 9.1. Acrylic plastic conical frustum window being placed in its seat for evaluation under hydrostatic pressure. Evaluation is done inside a deep ocean simulator.

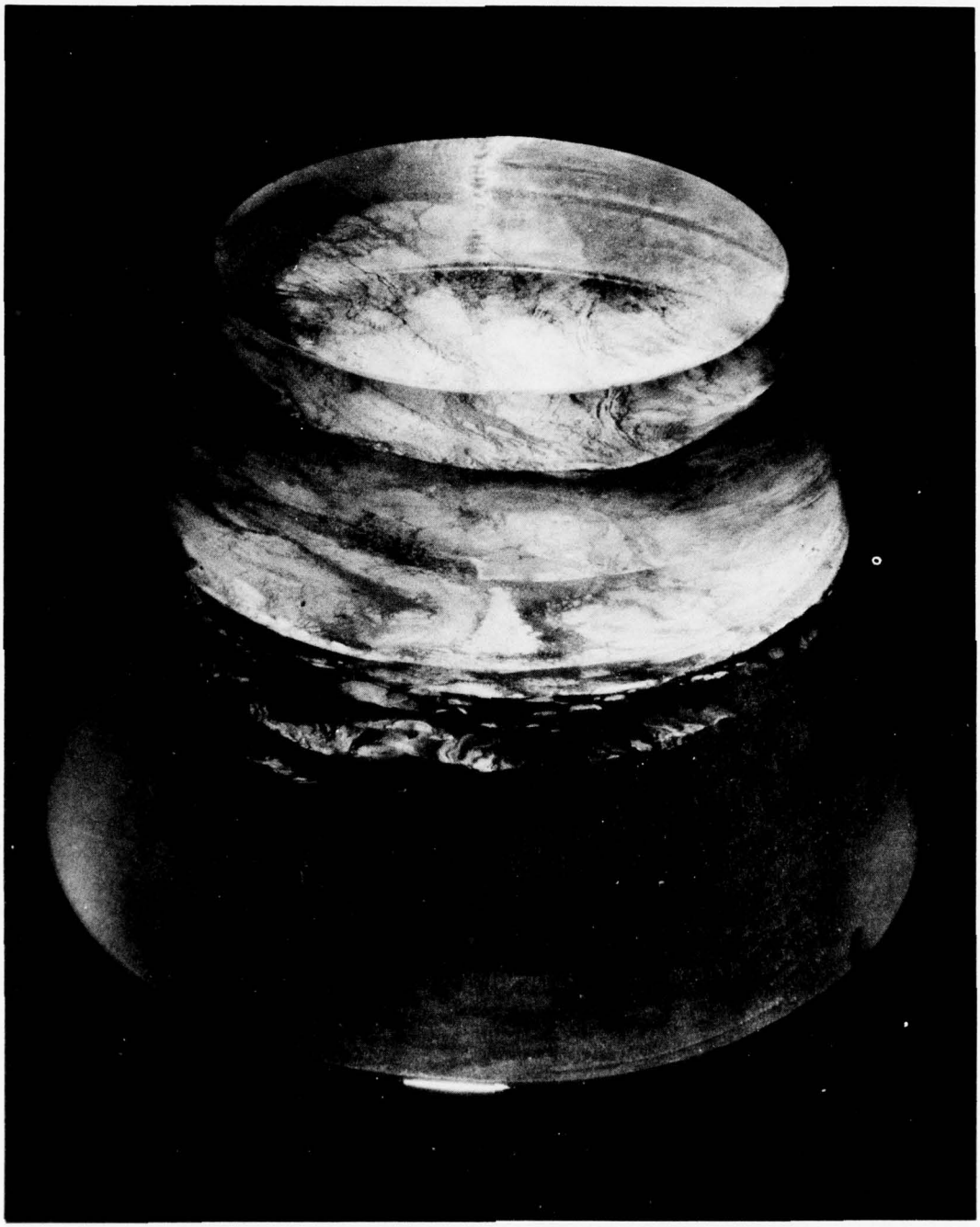

Figure 9.2. Glass conical frustum window after hydrostatic pressurization to 10,000 pounds per square inch (68.9 megapascals). At many locations the circumferential cracks on the bearing surface penetrated to the center of the window. A nylon bearing sleeve was used around the window to eliminate stress concentrations (t/D_i = 1.5 and conical angle = 30 degrees (0.52 radian)).

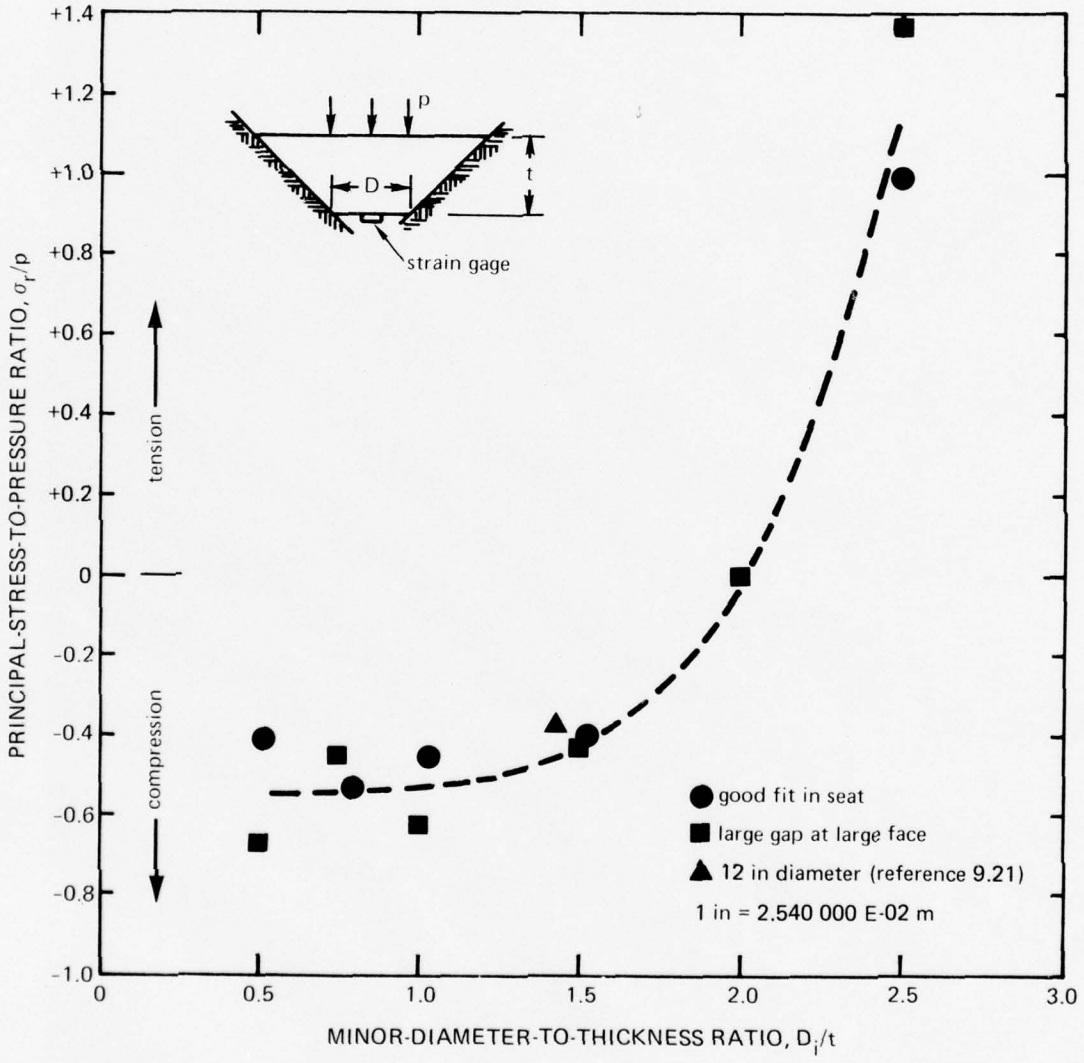

Figure 9.3. Principal stress at center of low-pressure face as a function of window diameter and thickness. The stress becomes negative only when t/D_i is greater than 0.5 (reference 9.4).

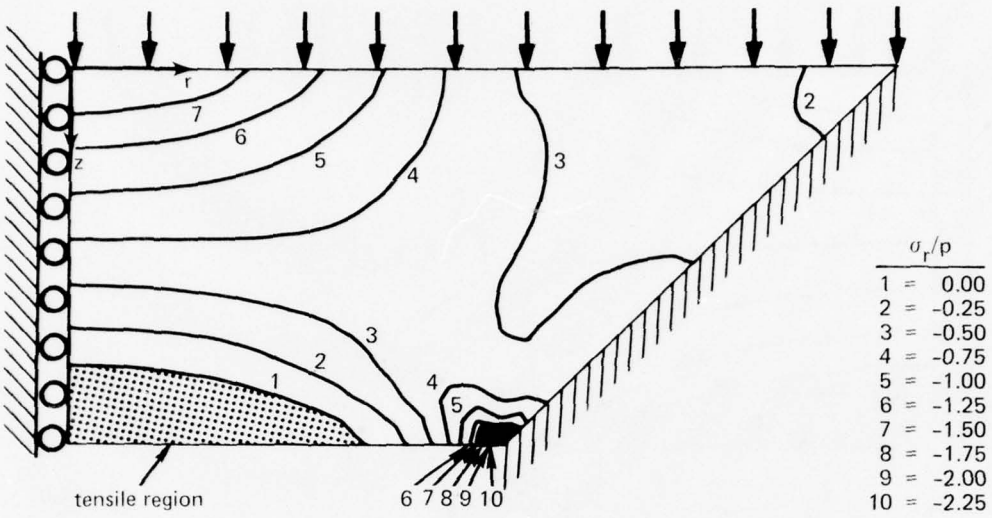

Part A. Radial stress (σ_r) for a fixed boundary (pressure = 1000 pounds per square inch (6.89 megapascals)).

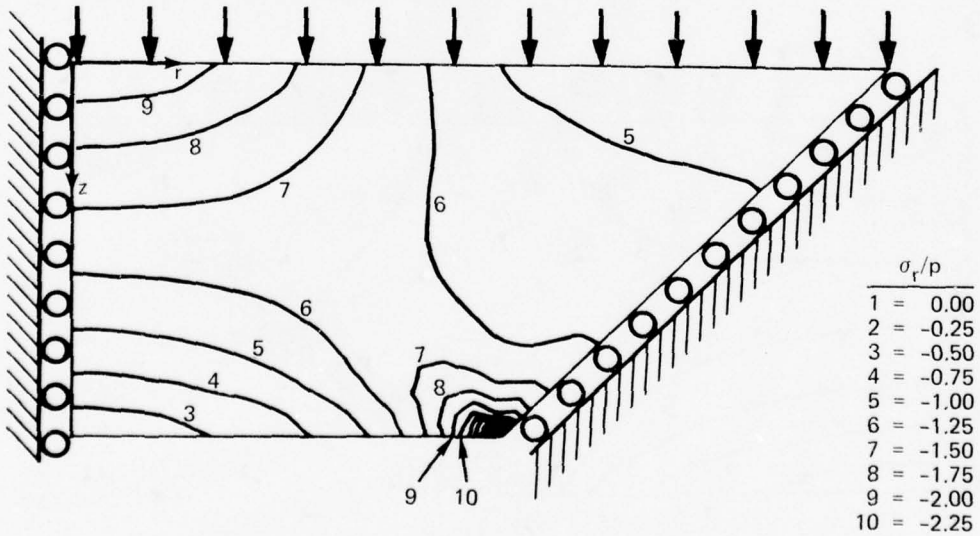

Part B. Radial stress (σ_r) for a free boundary (pressure = 1000 pounds per square inch (6.89 megapascals)).

Figure 9.4. Distribution of stresses in a 90-degree (1.57 radians) conical frustum with the t/D_i ratio equal to 0.46 and the D_i/D_f ratio greater than 1.0. Distribution was plotted on the basis of a finite-element computer program (reference 9.6).

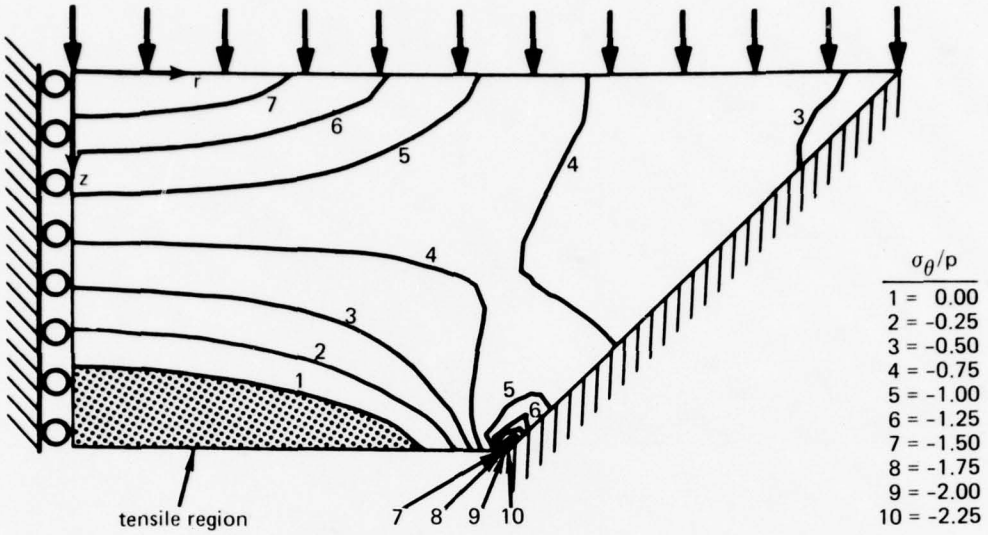

Part C. Circumferential stress (σ_θ) for a fixed boundary (pressure = 1000 pounds per square inch (6.89 megapascals)).

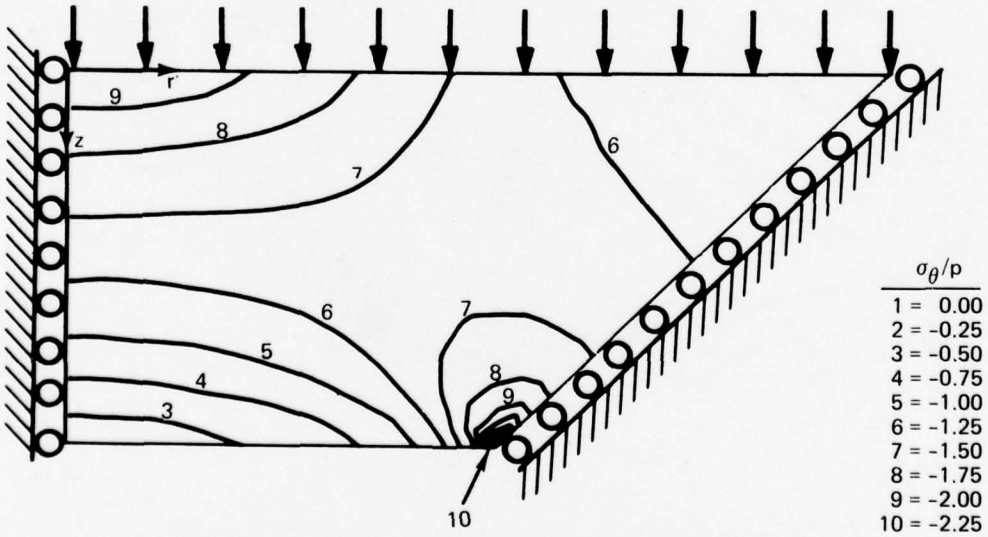

Part D. Circumferential stress (σ_θ) for a free boundary (pressure = 1000 pounds per square inch (6.89 megapascals)).

Figure 9.4 Continued.

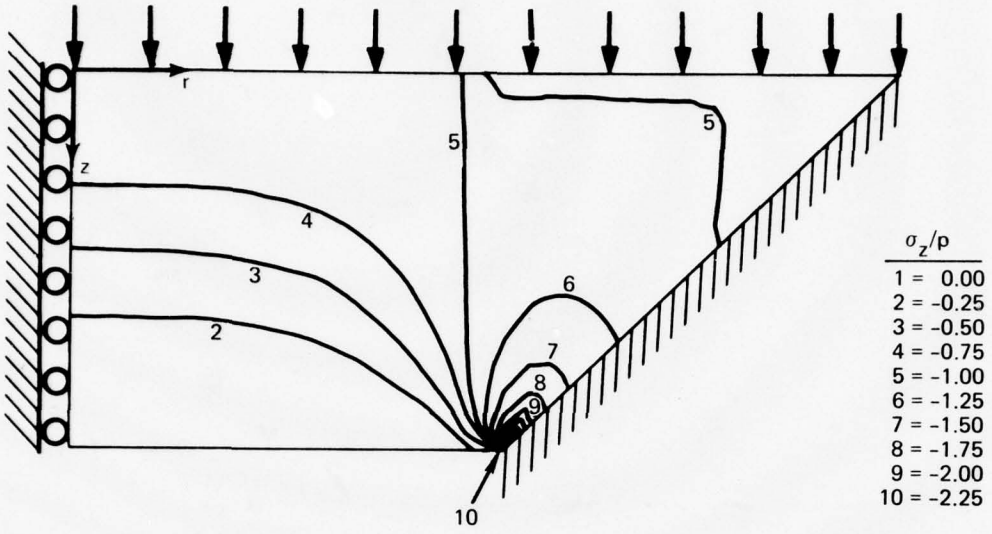

Part E. Axial stress (σ_z) for a fixed boundary (pressure = 1000 pounds per square inch (6.89 megapascals)).

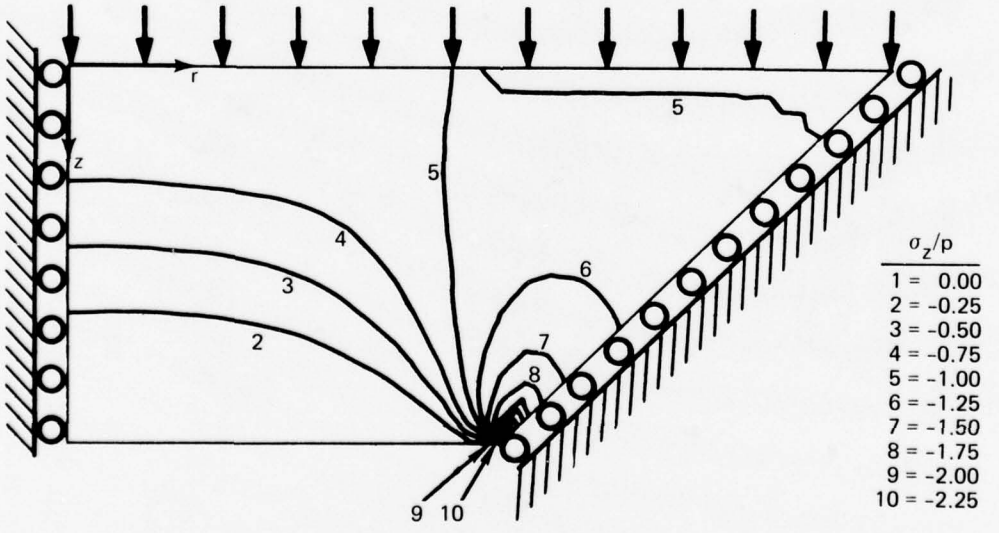

Part F. Axial stress (σ_z) for a free boundary (pressure = 1000 pounds per square inch (6.89 megapascals)).

Figure 9.4. Continued.

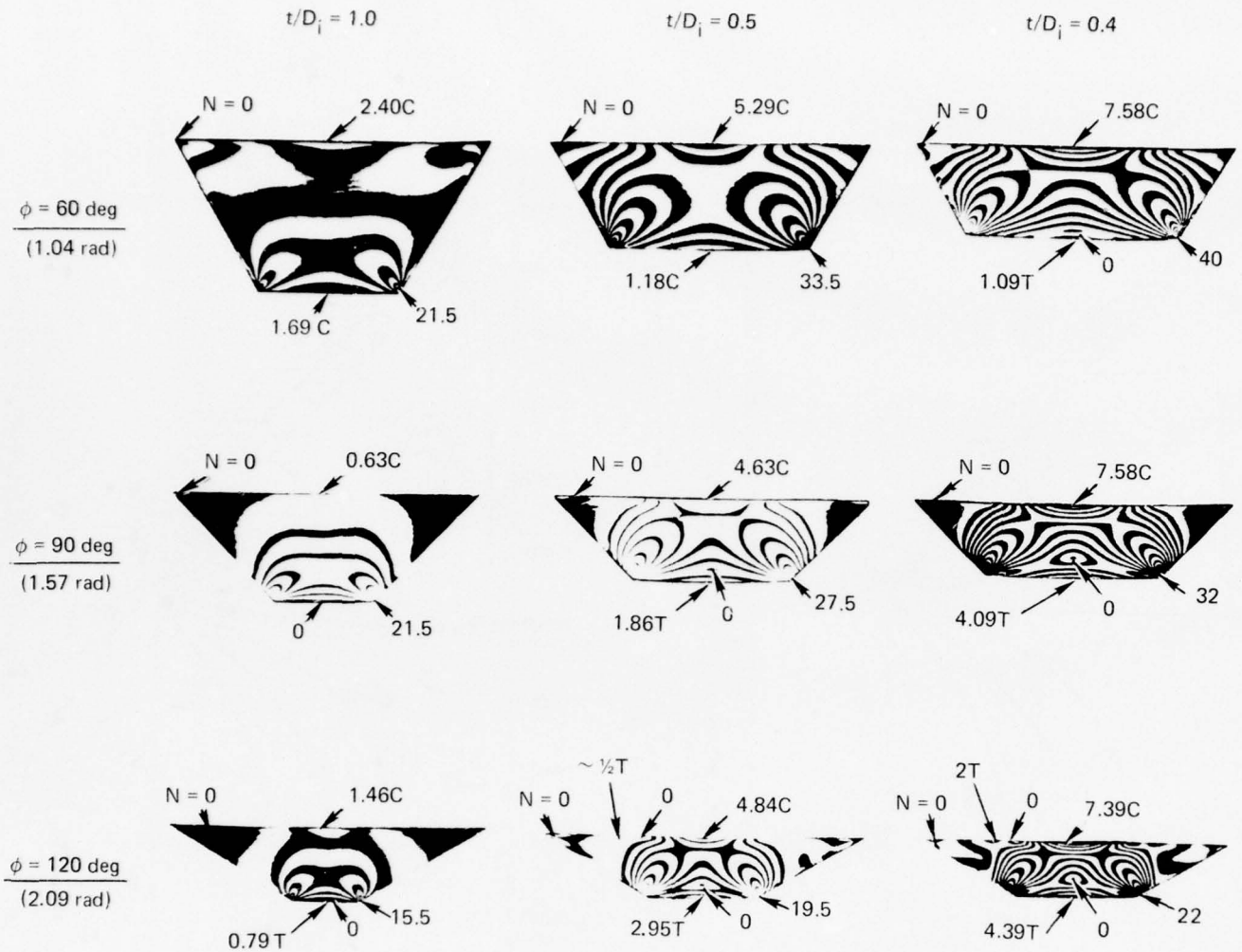

Figure 9.5. Magnitude and location of peak stresses as functions of t/D_i ratio and included conical angle. The isochromatic fringe patterns were generated in epoxy test specimens subjected to the same pressure loading (reference 9.5).

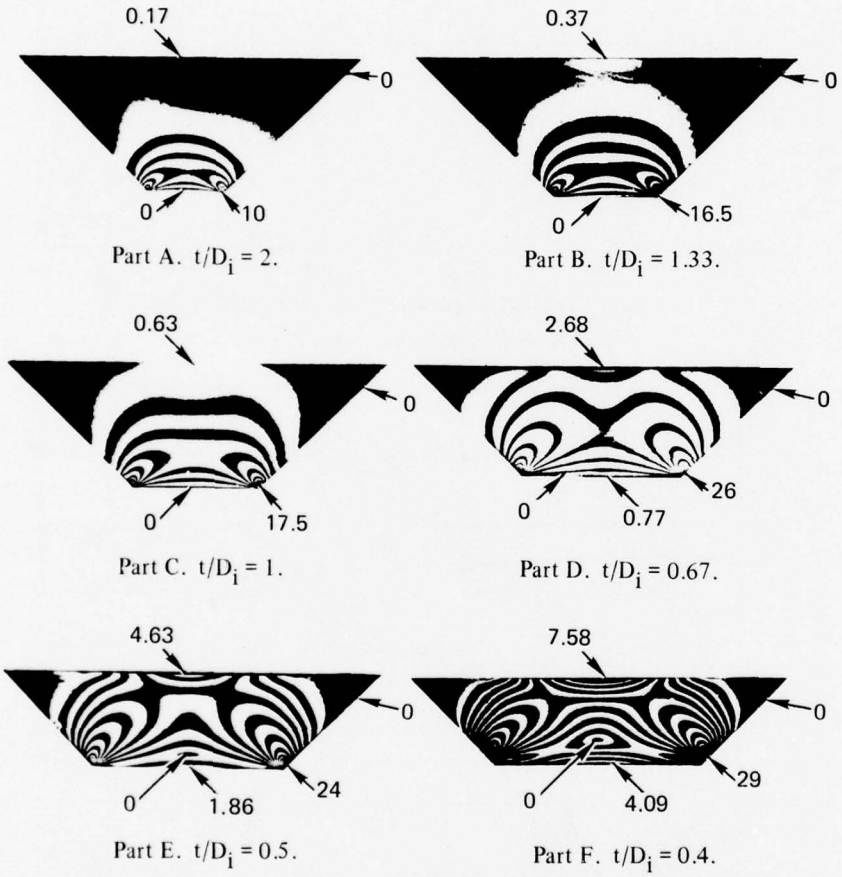

Figure 9.6. Magnitude and location of peak stresses in 90-degree (1.57 radians) conical frustums as functions of their t/D$_i$ ratios. The isochromatic fringe patterns were generated in epoxy test specimens subjected to the same pressure loading (reference 9.5).

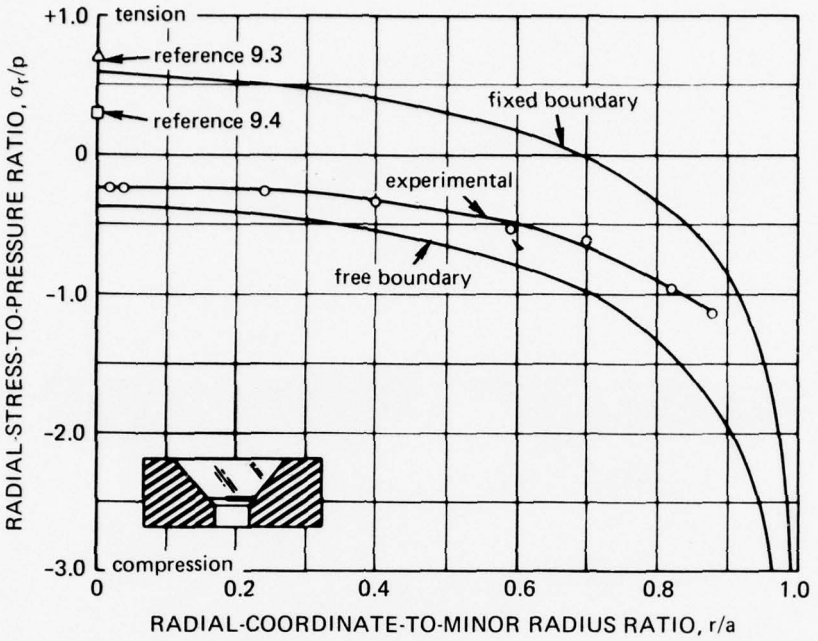

Part A. Radial stress on minor radius.

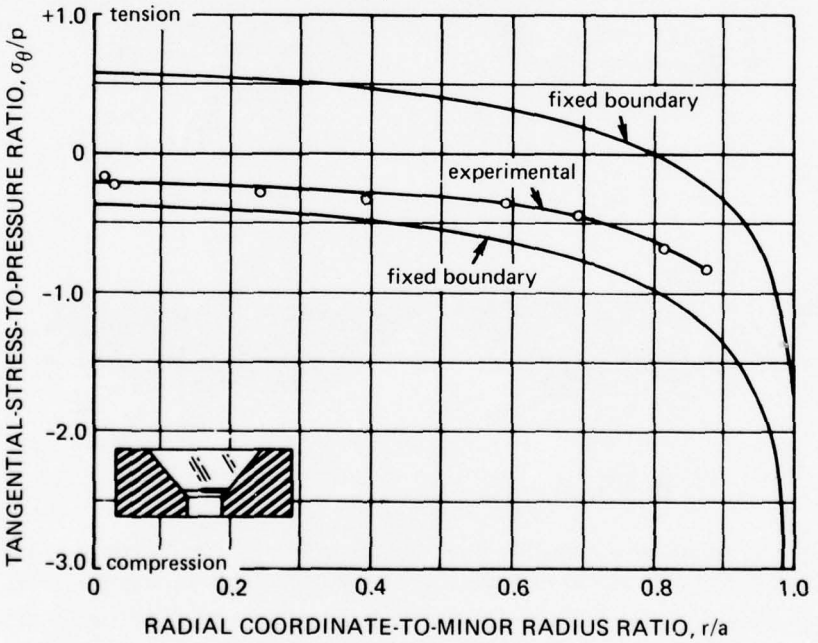

Part B. Tangential stress on minor radius.

Figure 9.7. Comparison of stresses calculated on the basis of a finite-element computer program with experimentally measured stresses. The stresses were measured experimentally by electric resistance straingages. (Conical angle = 90 degrees (1.57 radians); $t/D_i = 0.46$; $D_i/D_f = 1.06$; temperature = 75°F (24°C); and pressure = 5000 pounds per square inch (34.4 megapascals).) The measured stresses are between the calculated values, based on fixed- and free-boundary assumptions (reference 9.6).

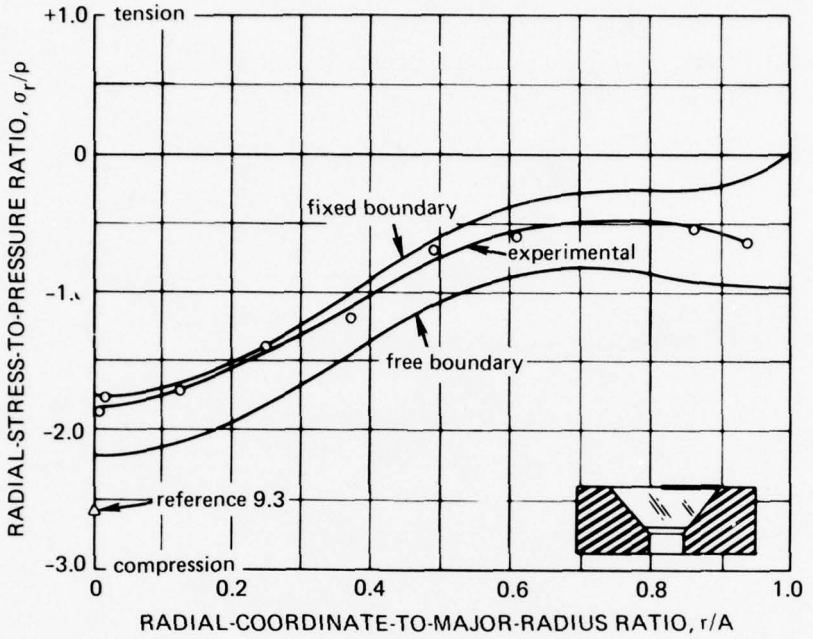

Part C. Radial stress on major radius.

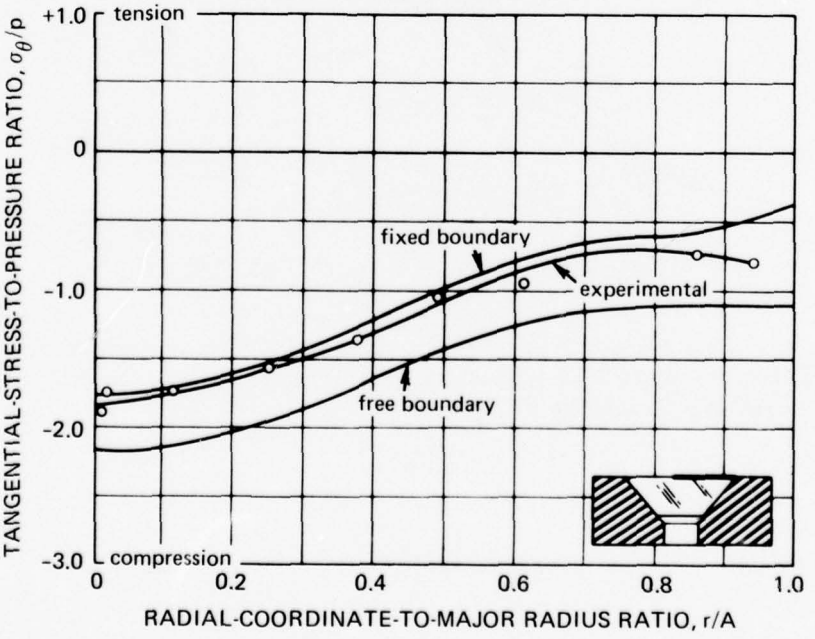

Part D. Tangential stress on major radius.

Figure 9.7. Continued.

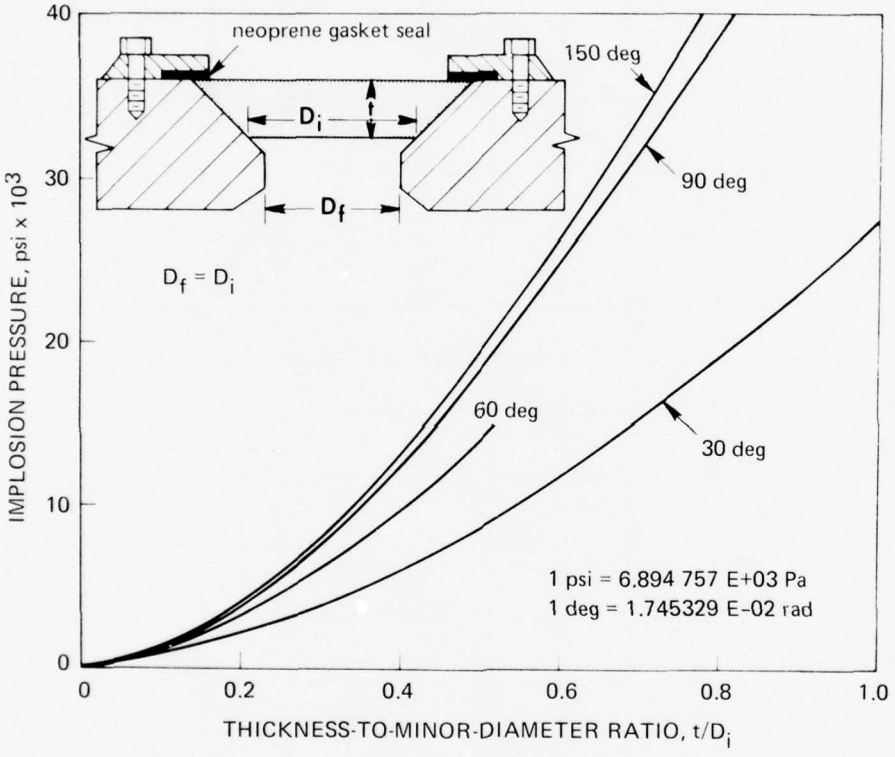

Figure 9.8. Short-term critical pressures of conical frustums tested to destruction at a rate of 650 pounds per square inch (4.48 megapascals) per minute. $D_i/D_f = 1.0$ at ambient room temperature (reference 9.10).

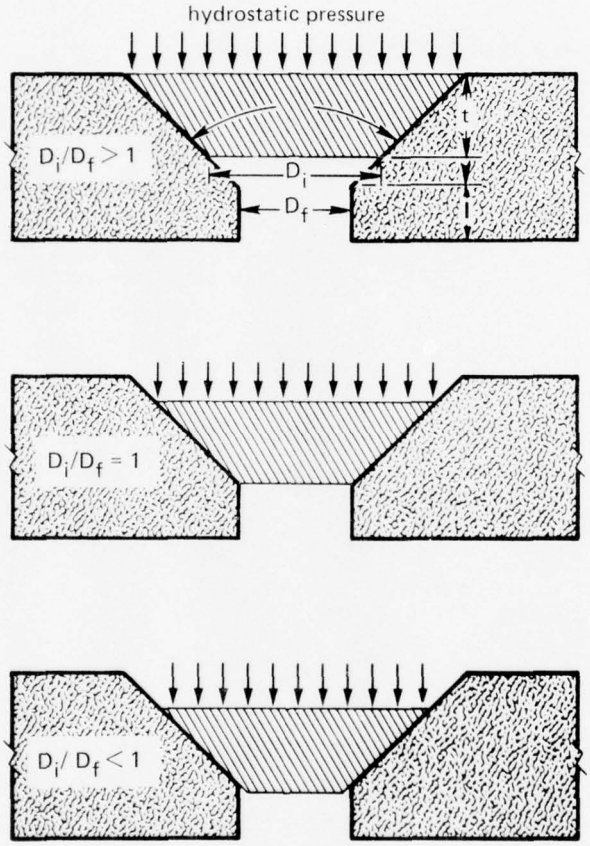

Figure 9.9. Seat overhang as a function of D_i/D_f ratio.

Short-term critical pressure is maximized where $D_i/D_f > 1.0$ and minimized where $D_i/D_f < 1.0$.

$D_i/D_f = 1.0$ is considered to be the standard test arrangement for comparison of critical pressures generated by windows with different t/D_i ratios and included angles (reference 9.11).

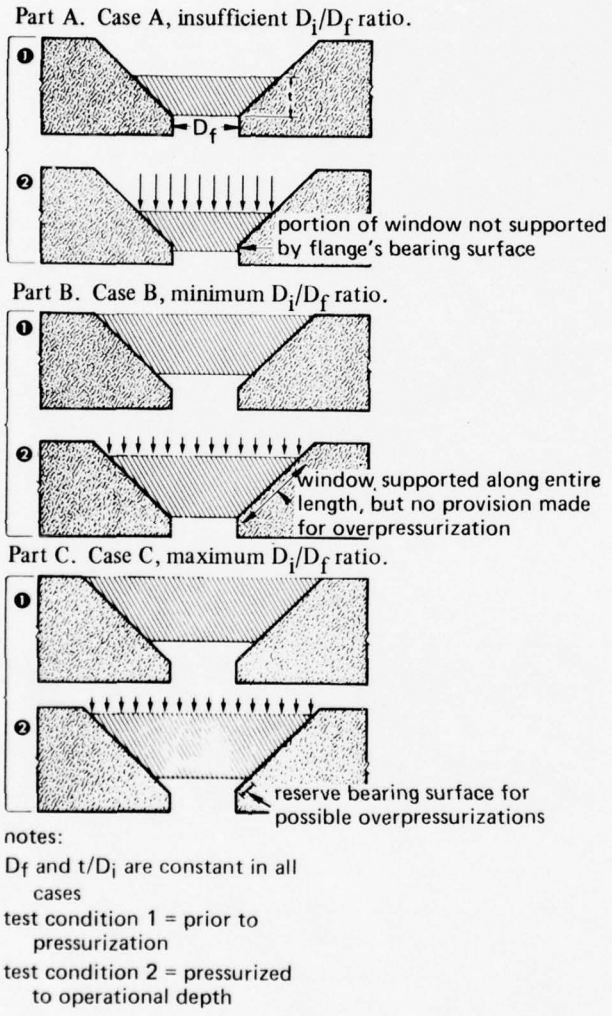

Figure 9.10. Typical axial displacements of conical frustums in seats with overhangs in the range of $1.0 \leq D_i/D_f < 2.0$. For operational windows, case B is recommended (reference 9.11).

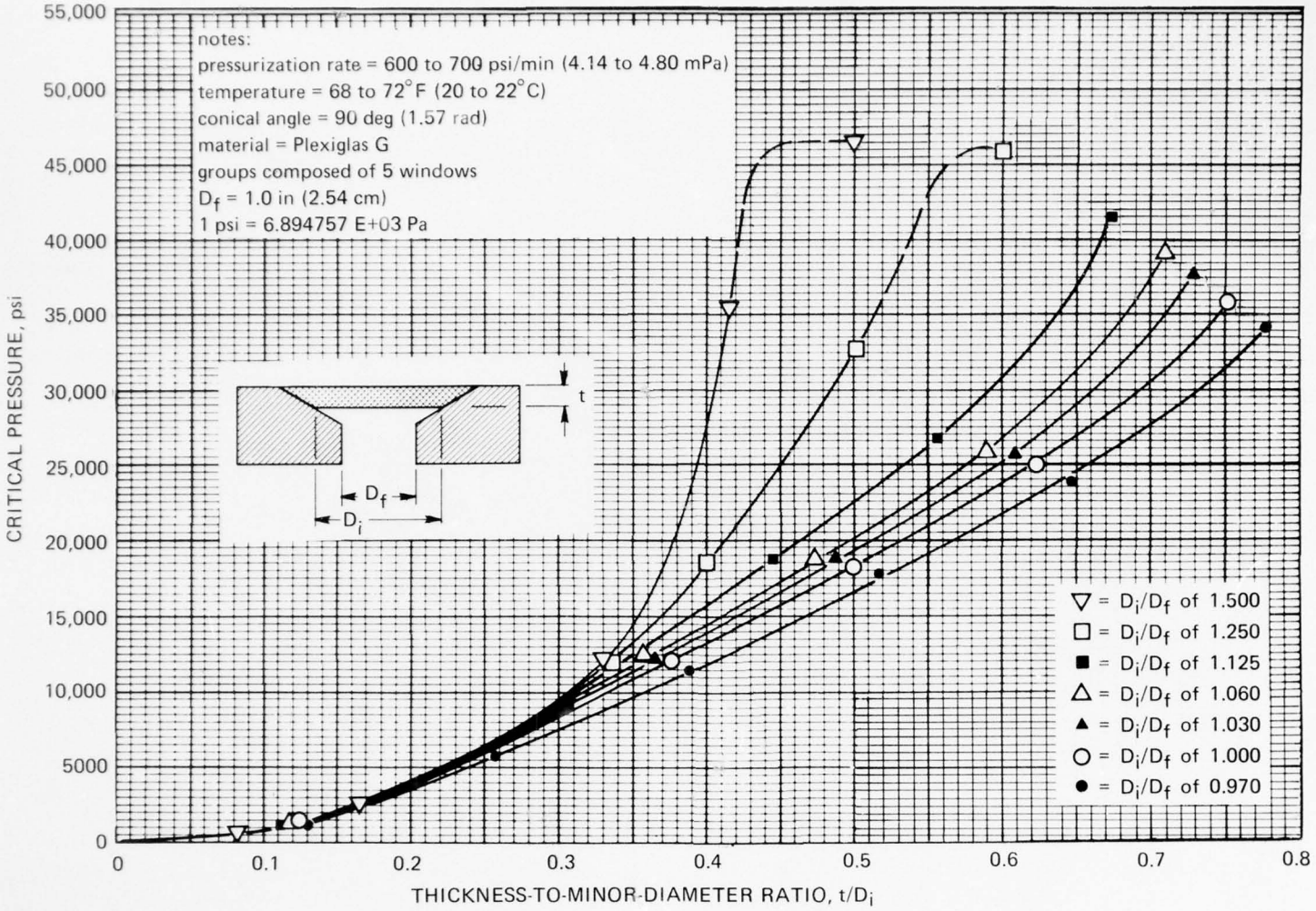

Figure 9.11. Effect of D_i/D_f ratio on short-term critical pressure for 90-degree (1.57 radians) conical frustums (reference 9.11).

Part A. $D_i/D_f = 1.0$.

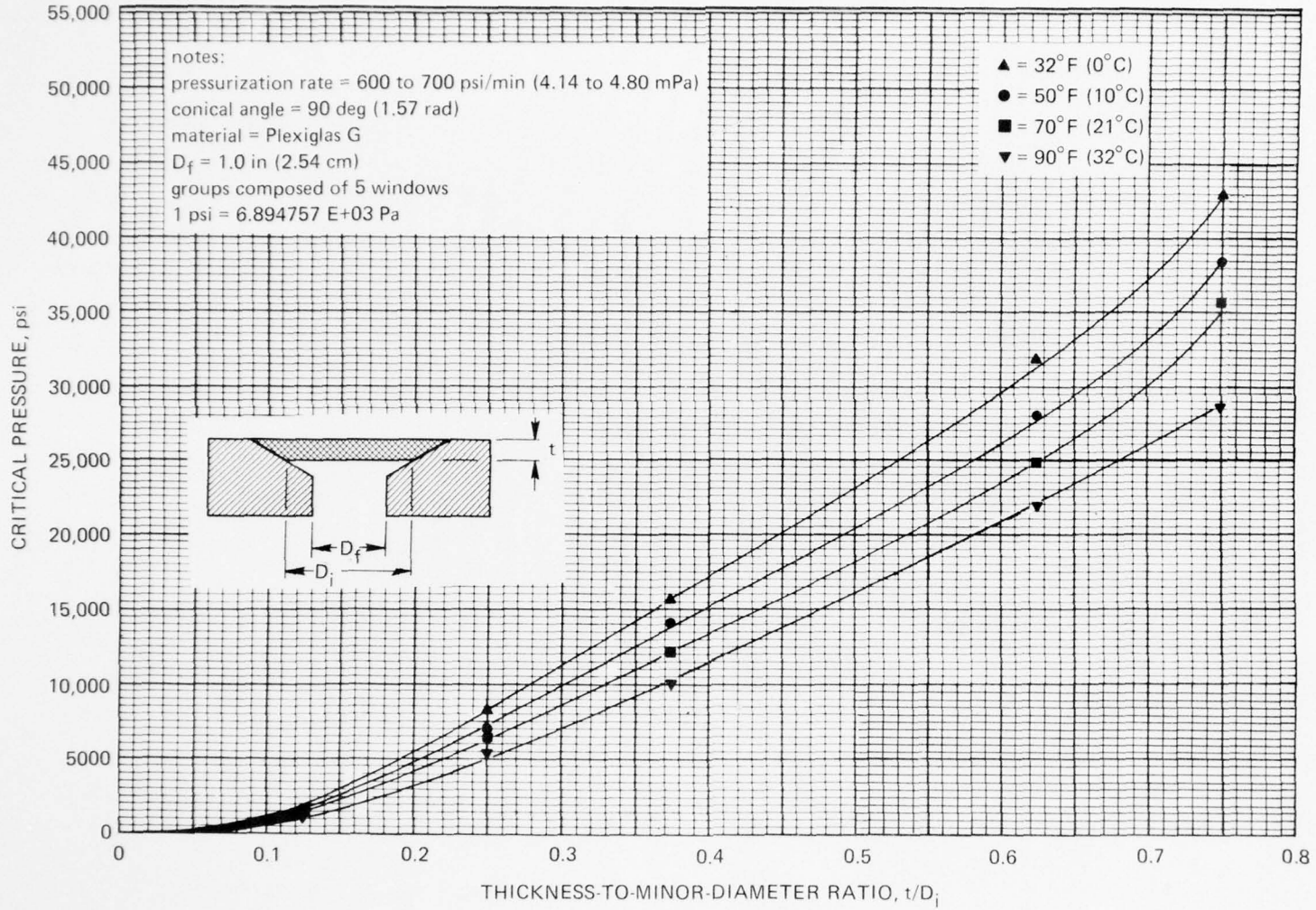

Figure 9.12. Effect of temperature on short-term critical pressure of 90-degree (1.57 radians) conical frustums located in a standard seat (reference 9.11).

Part B. $D_i/D_f = 1.5$.

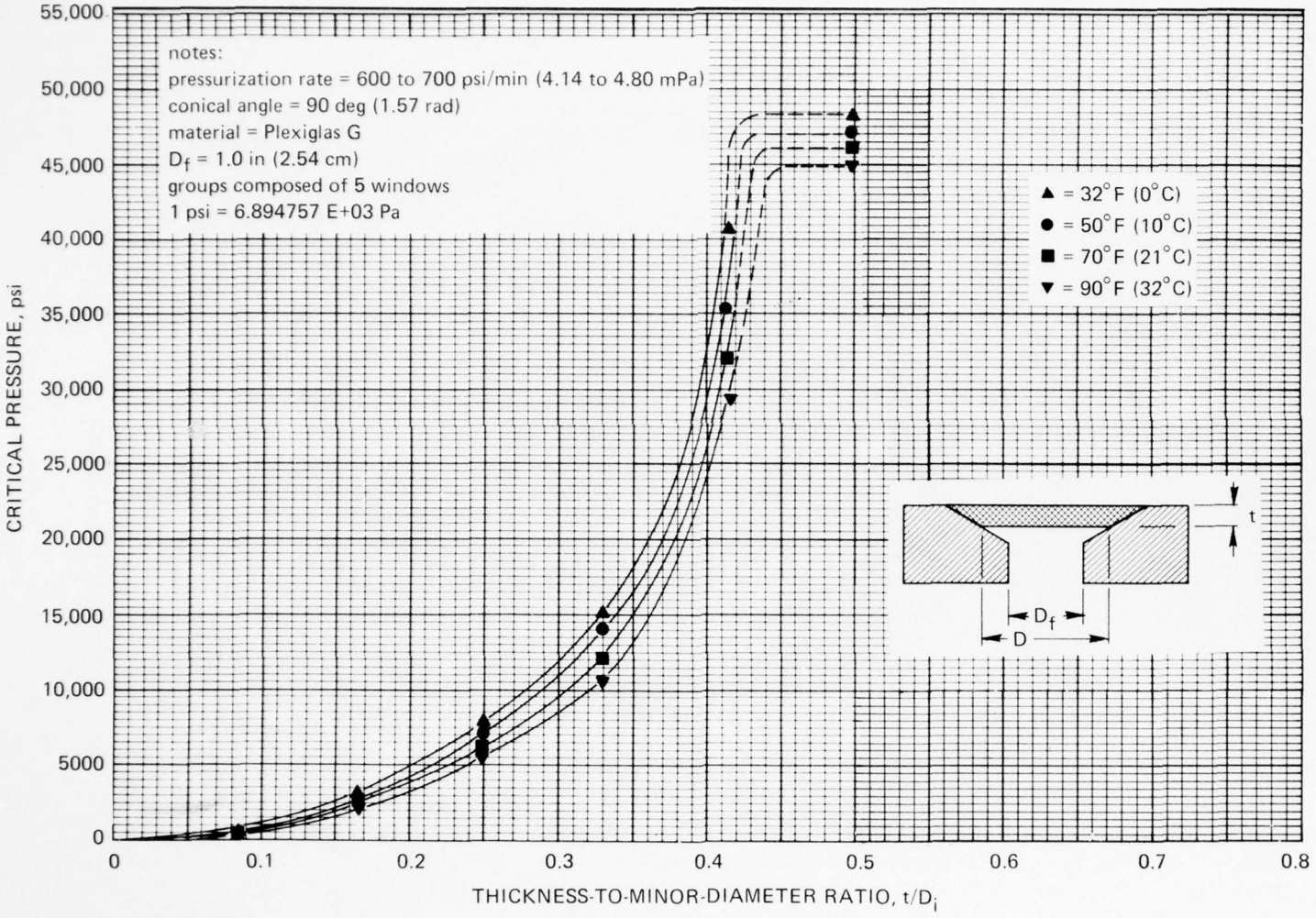

Figure 9.12. Continued.

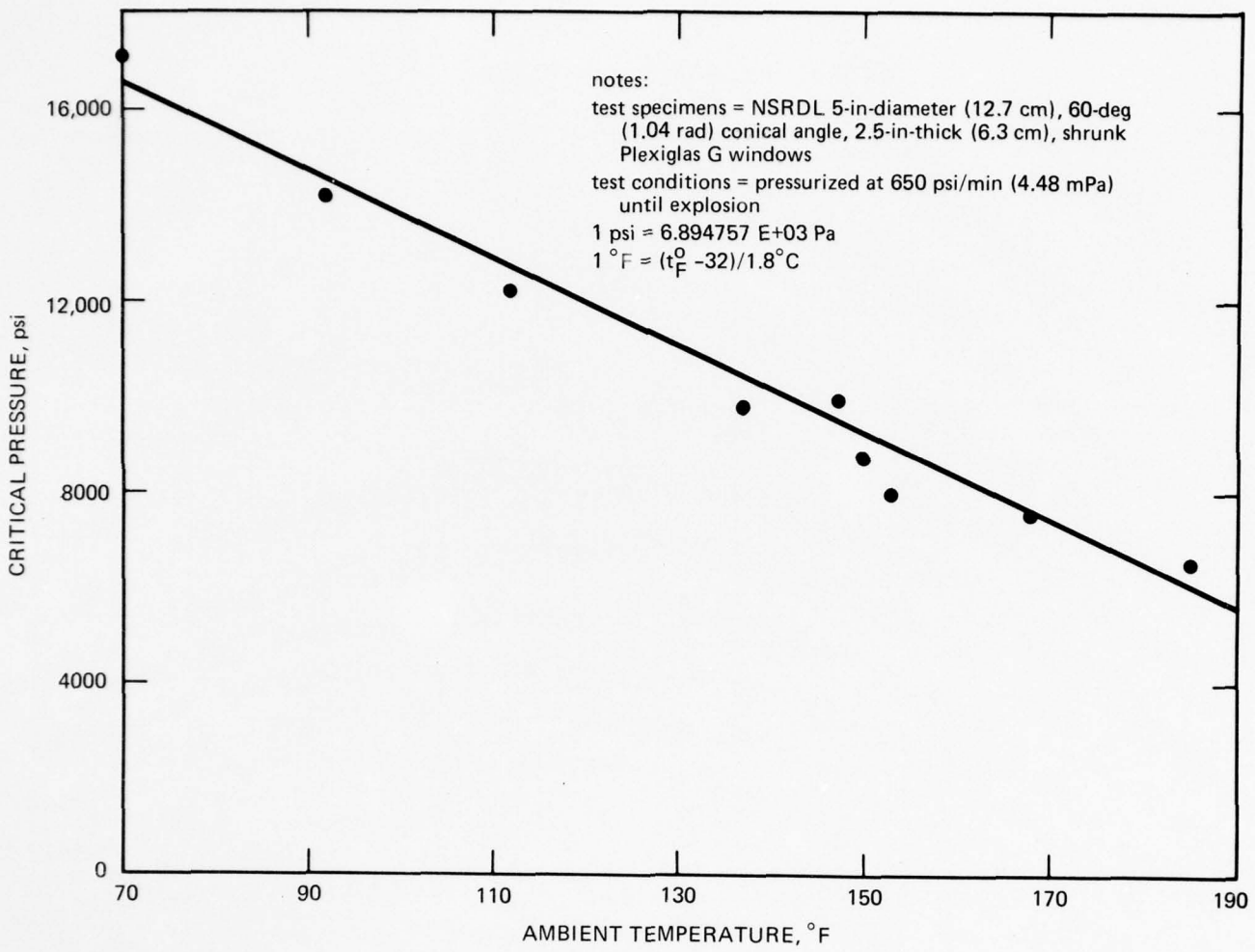

Figure 9.13. Effect of temperature on short-term critical pressure for 60-degree (1.04 radians) conical frustums with a t/D_i ratio of 0.5 located in a seat with a D_i/D_f ratio of 1.04 (reference 9.12).

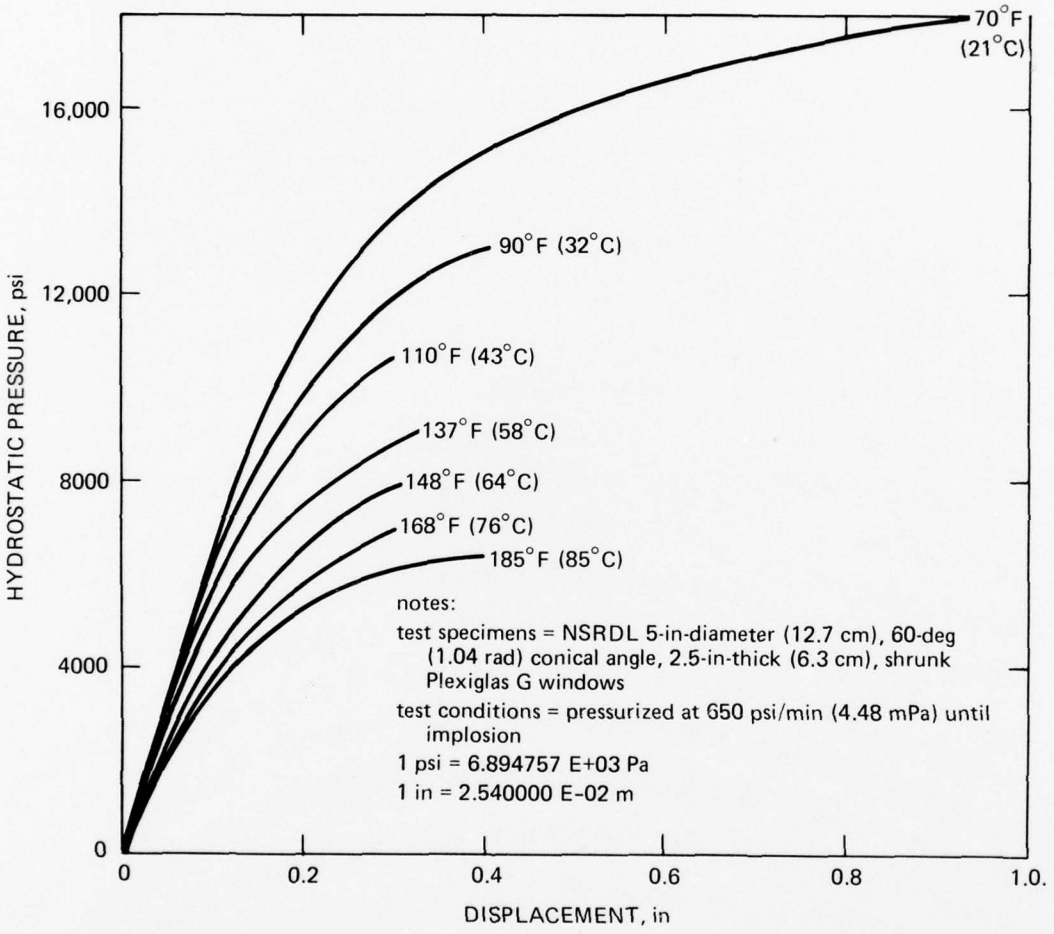

Figure 9.14. Effect of temperature on short-term displacement for 60-degree (1.04 radians) conical frustums with a t/D_i ratio of 0.5 located in a seat with a D_i/D_f ratio of 1.04 (reference 9.11).

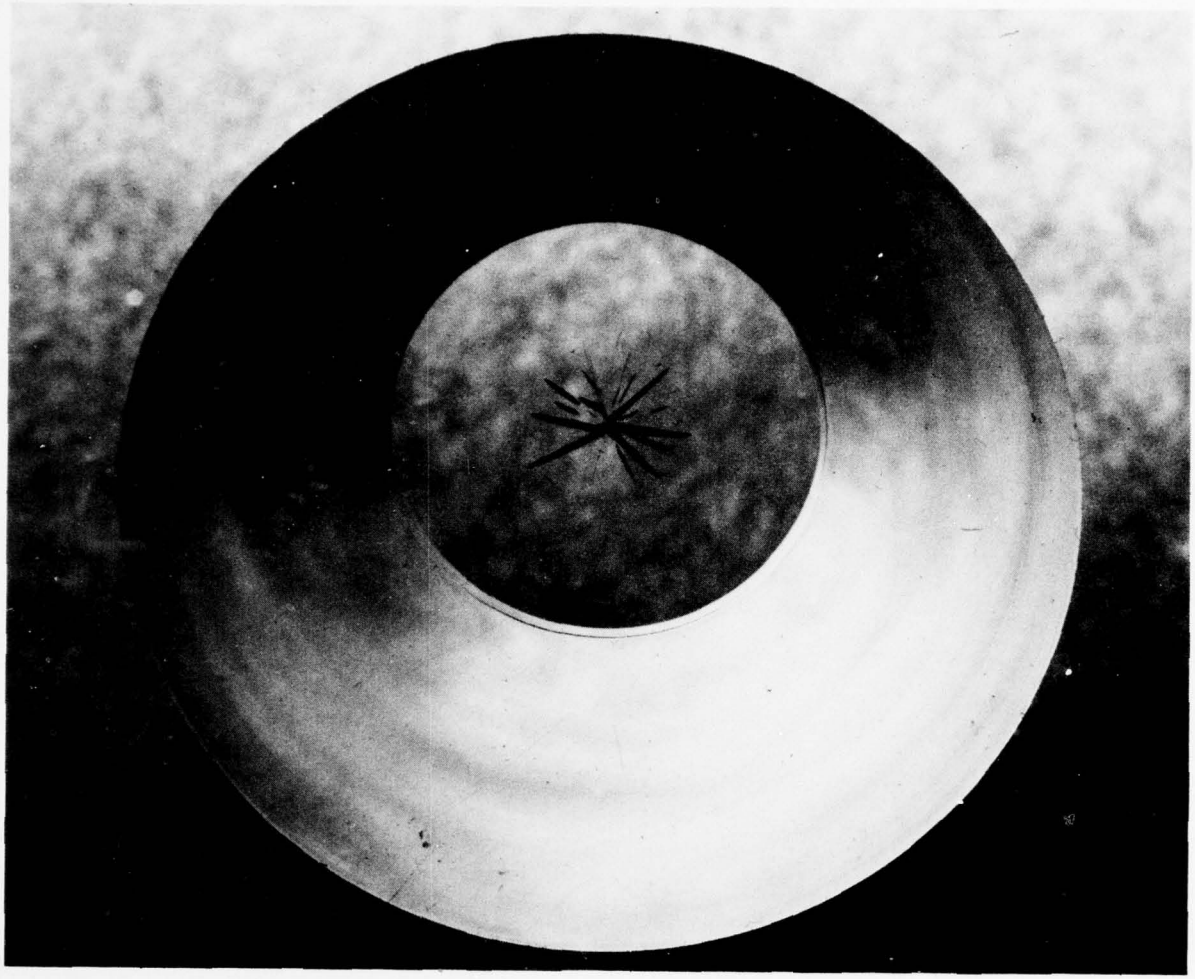

Figure 9.15. Initiation of membrane flexure fracture in thin conical frustums under hydrostatic loading ($t/D_i = 0.125$; conical angle = 90 degrees (1.57 radians); ambient room temperature; low-pressure face (reference 9.11).

Part A. High-pressure face; note small opening.

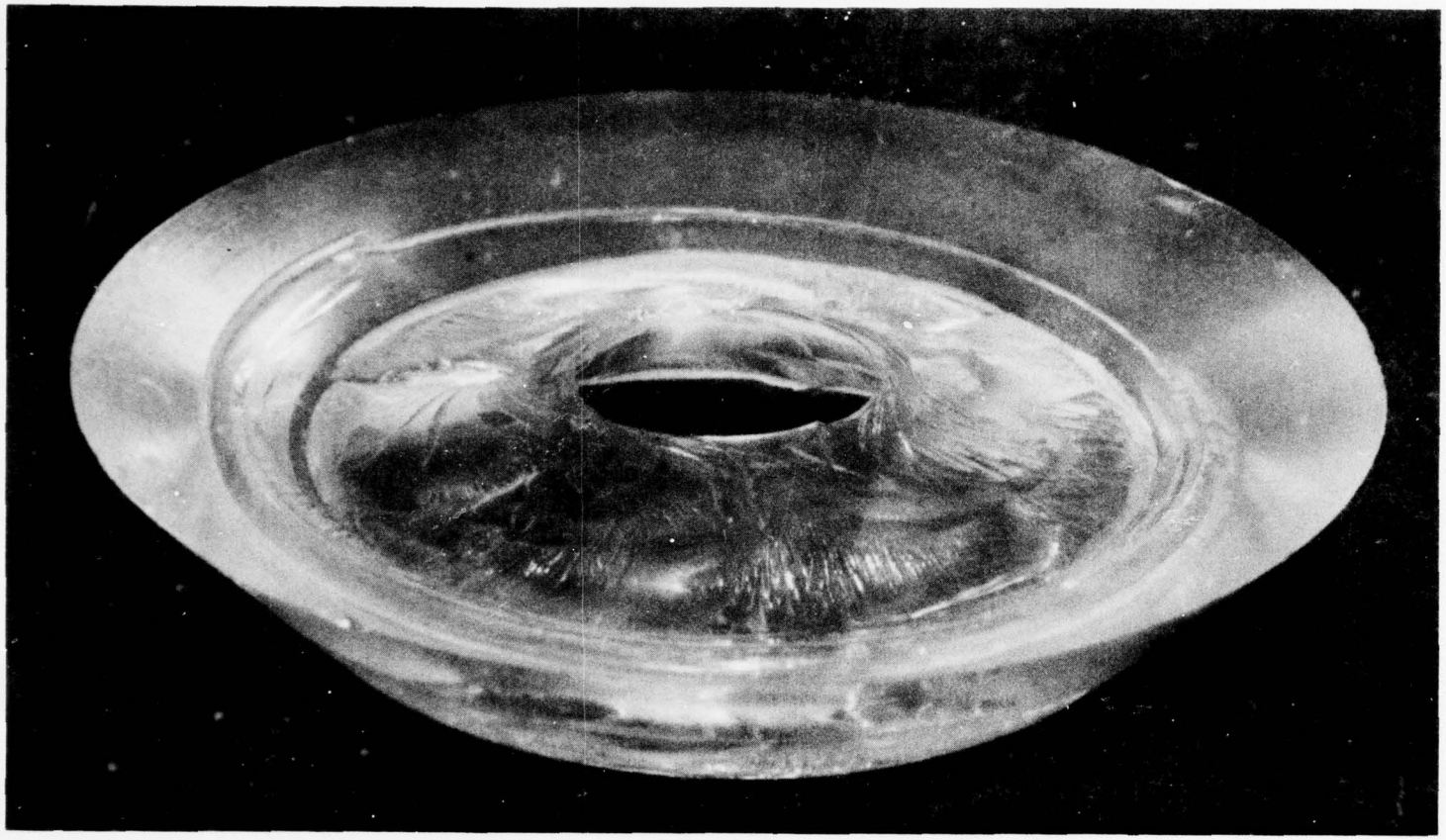

Figure 9.16. Typical conchoidal fracture surface caused by membrane flexure in conical frustums with $0.125 < t/D_i \leq 0.35$ ($t/D_i = 0.25$; conical angle = 90 degrees (1.57 radians); ambient room temperature).

Part B. Low-pressure face; note that diameter of fracture surface is equal to diameter of low-pressure face.

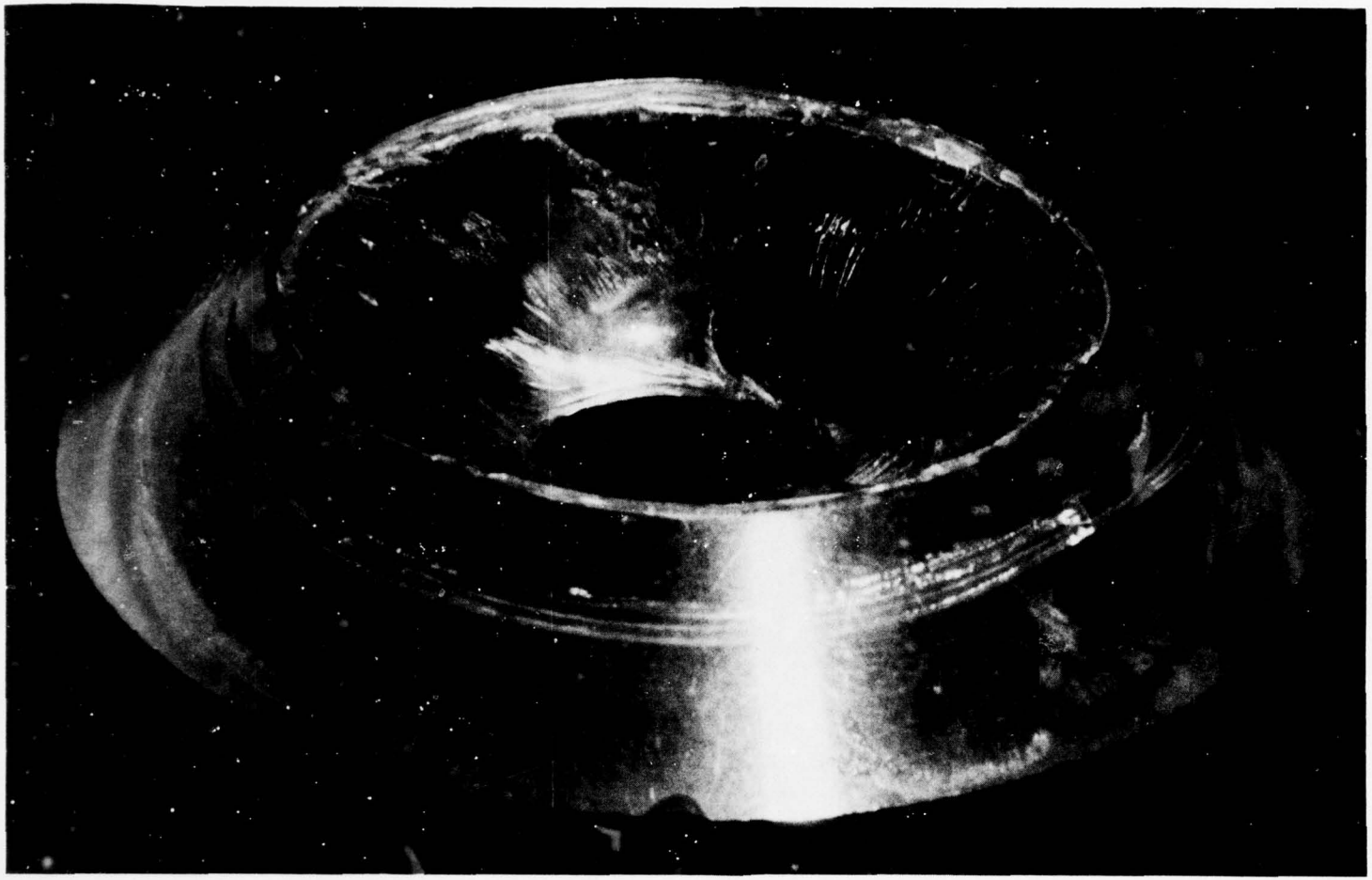

Figure 9.16. Continued.

Part A. High-pressure face; note how the crater becomes progressively deeper as the window approaches the formation of the conical fracture surface.

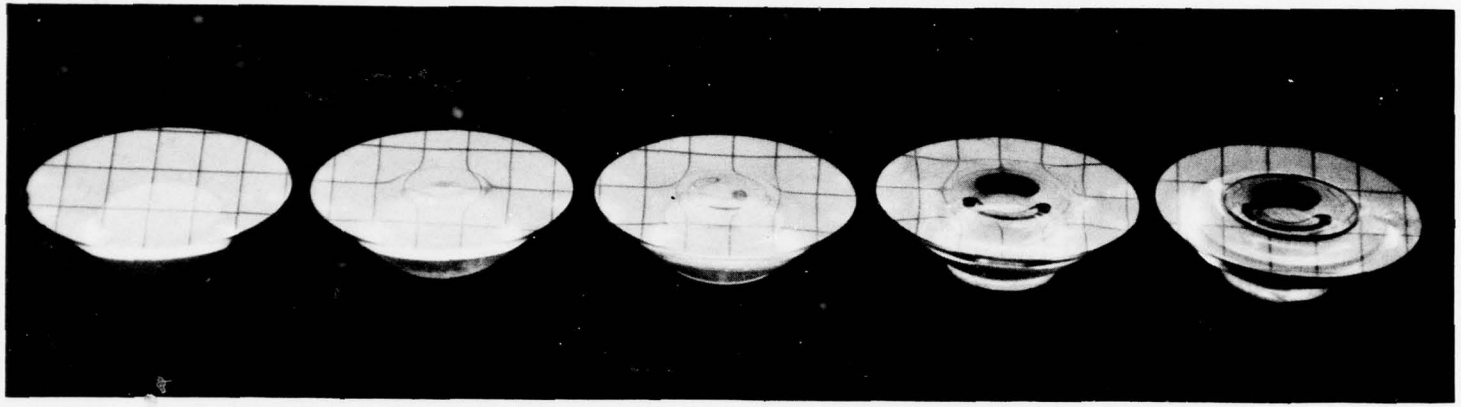

Figure 9.17. Conchoidal shear fracture of thick conical frustums with a t/D_i ratio > 0.35 ($t/D_i = 0.625$; conical angle = 90 degrees (1.57 radians); tested at 32, 50, 70, and 90°F (0, 10, 21, and 32°C) to 20,000 pounds per square inch (137.8 megapascals)). The different temperatures have the same effect as sustained loading of different durations or different magnitudes of pressure under short-term loading.

Part B. Low-pressure face; note the progressive formation of a plug-like extrusion until the conical fracture surface is formed.

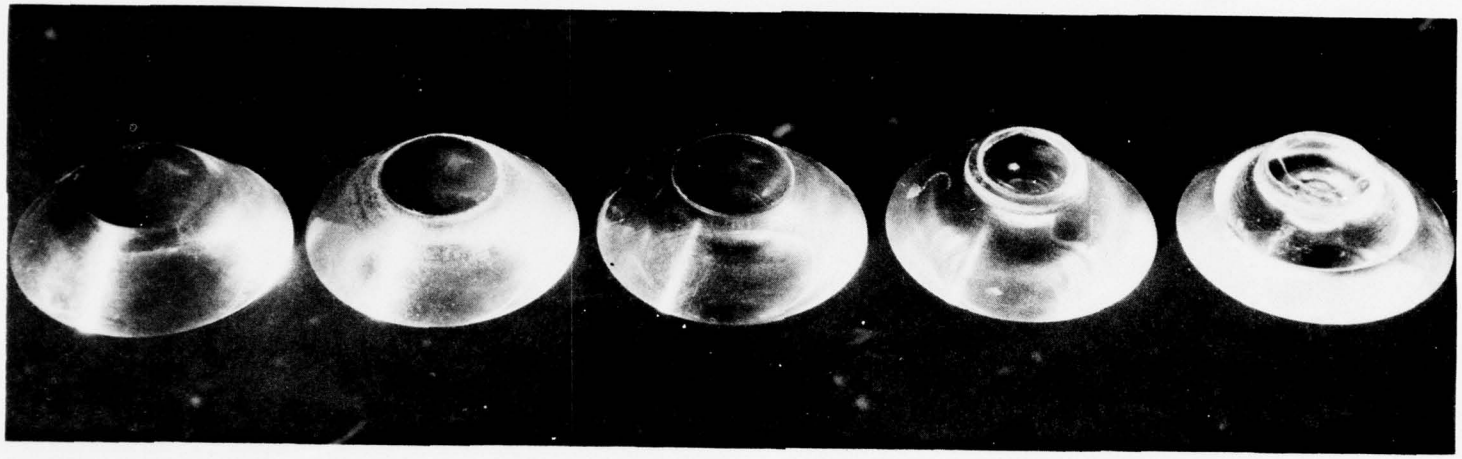

Figure 9.17. Continued.

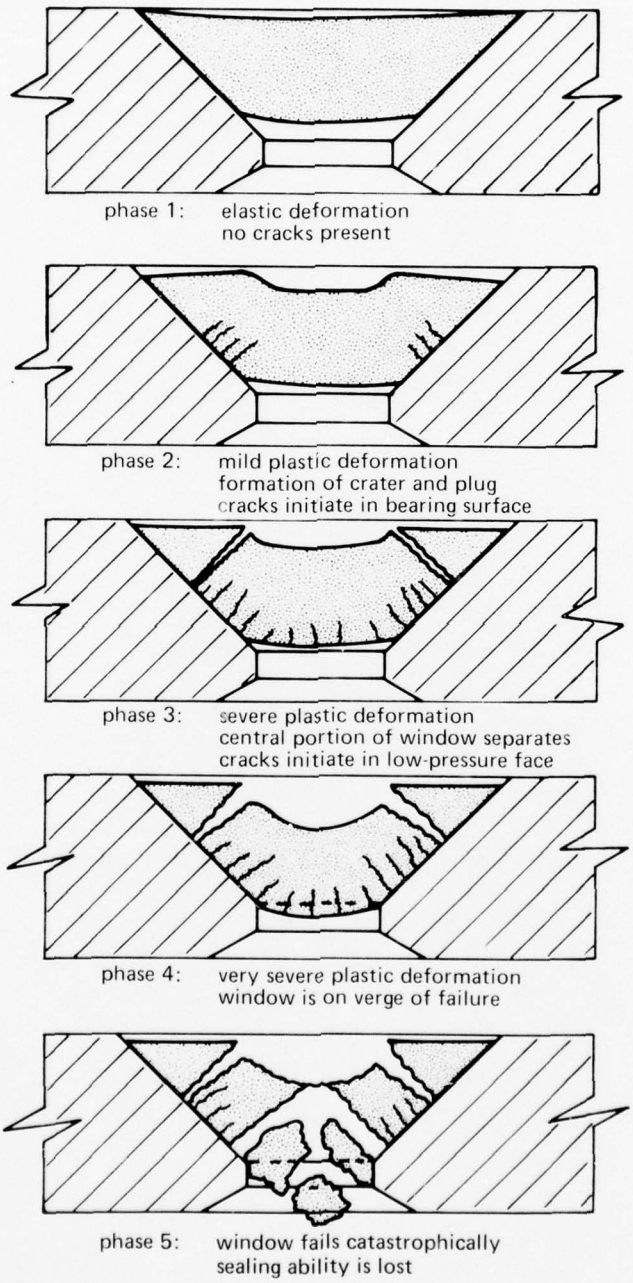

Figure 9.18. Fracture formations in thick conical frustums with $t/D_i > 0.35$.

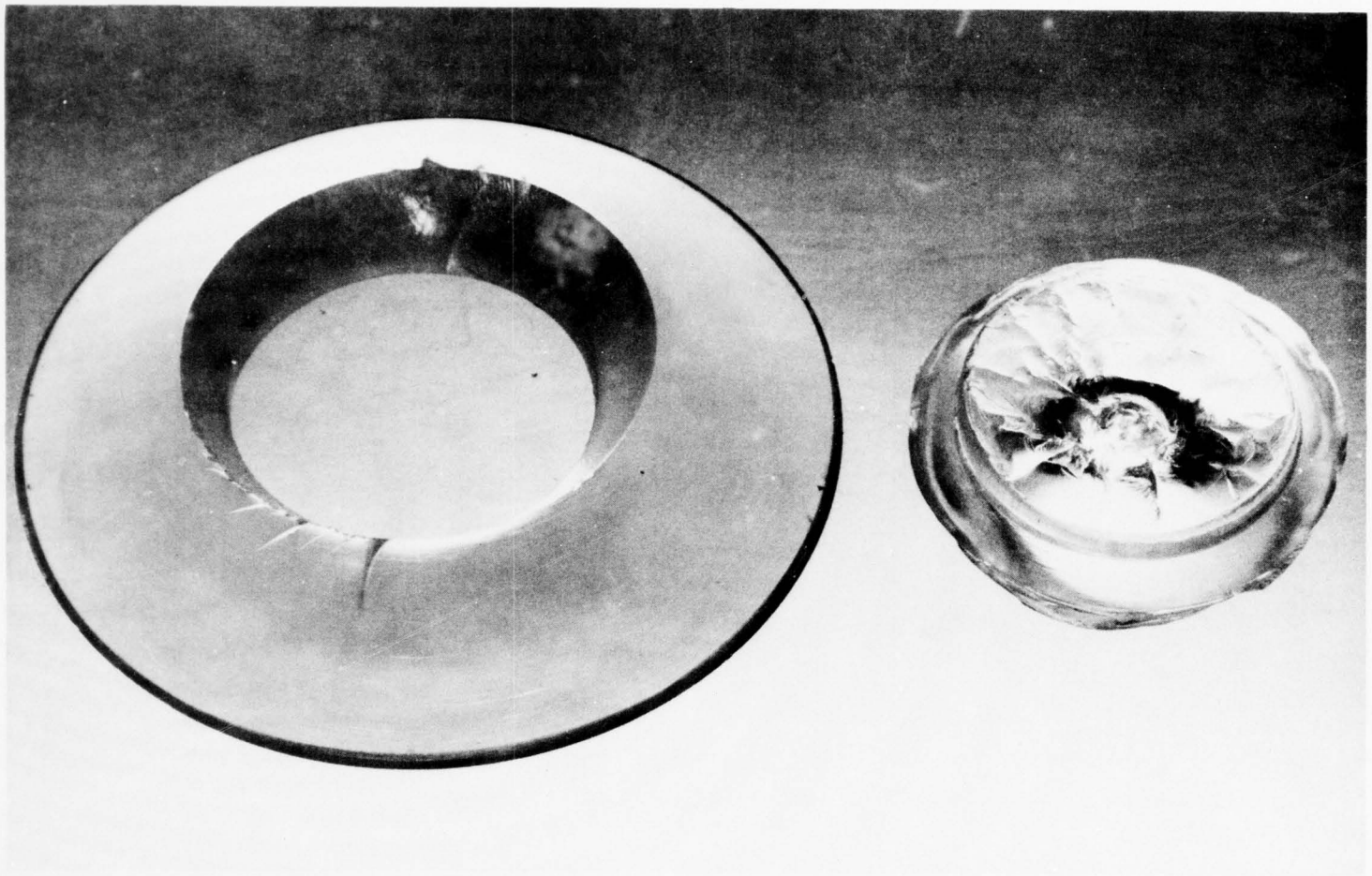

Figure 9.19. Conical shear fracture in body of thick frustum. Conchoidal fracture surface was formed after separation of the central portion of the window from the main body. After the central portion extruded farther with the formation of a long plug on the low-pressure face and a deep crater on the high-pressure face, a conchoidal fracture cone formed on the low-pressure face. Note that the opening through which the water entered is small (reference 9.12).

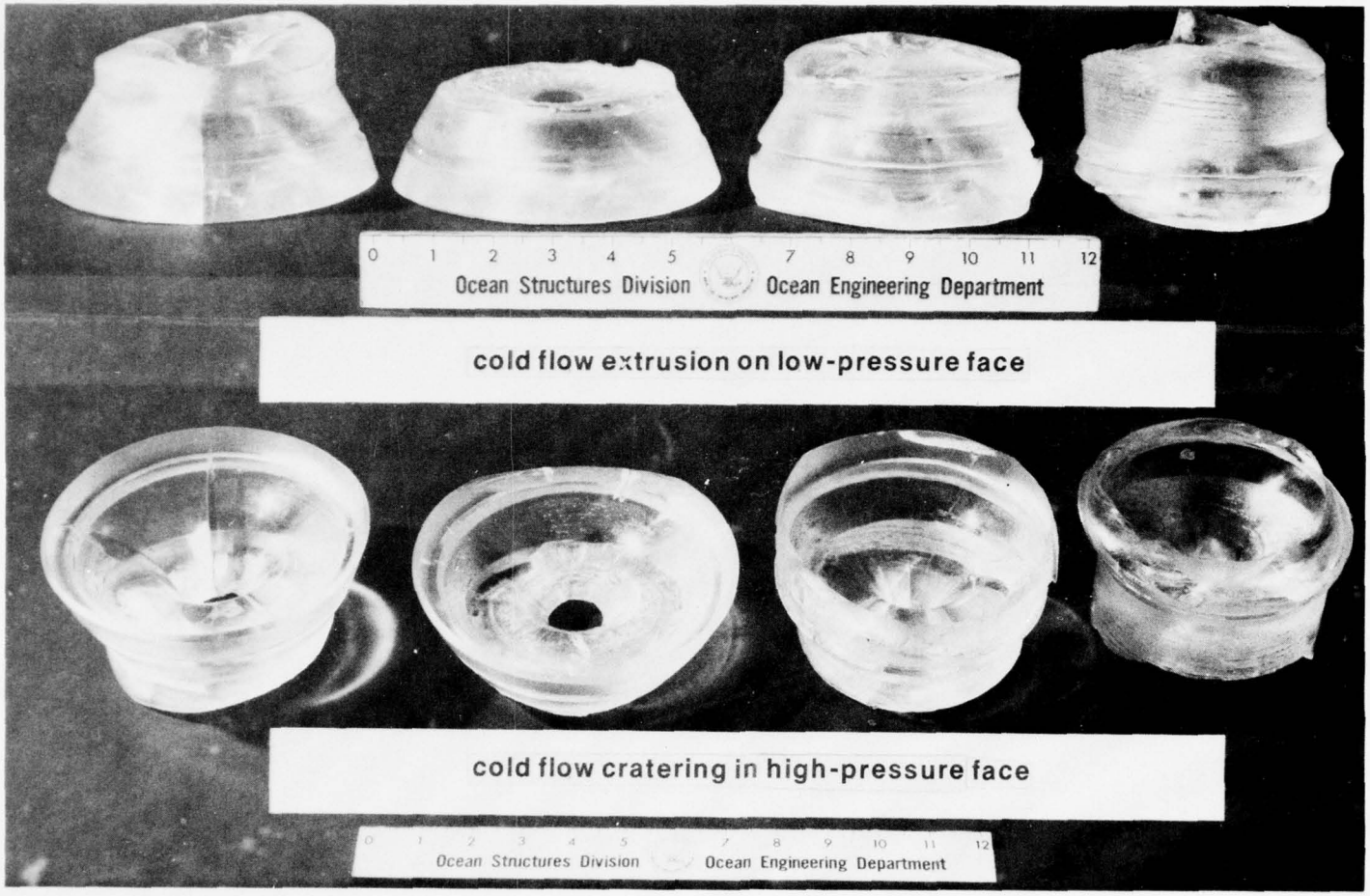

Figure 9.20. Typical shear cone fractures in thick frustums tested under sustained hydrostatic loading at an elevated ambient temperature ($t/D_i = 0.5$; $D_i/D_f = 1.04$; temperature = 150°F (66°C)). Note the extensive plastic deformations that are typical of acrylic plastic frustums operating at elevated temperatures (reference 9.12).

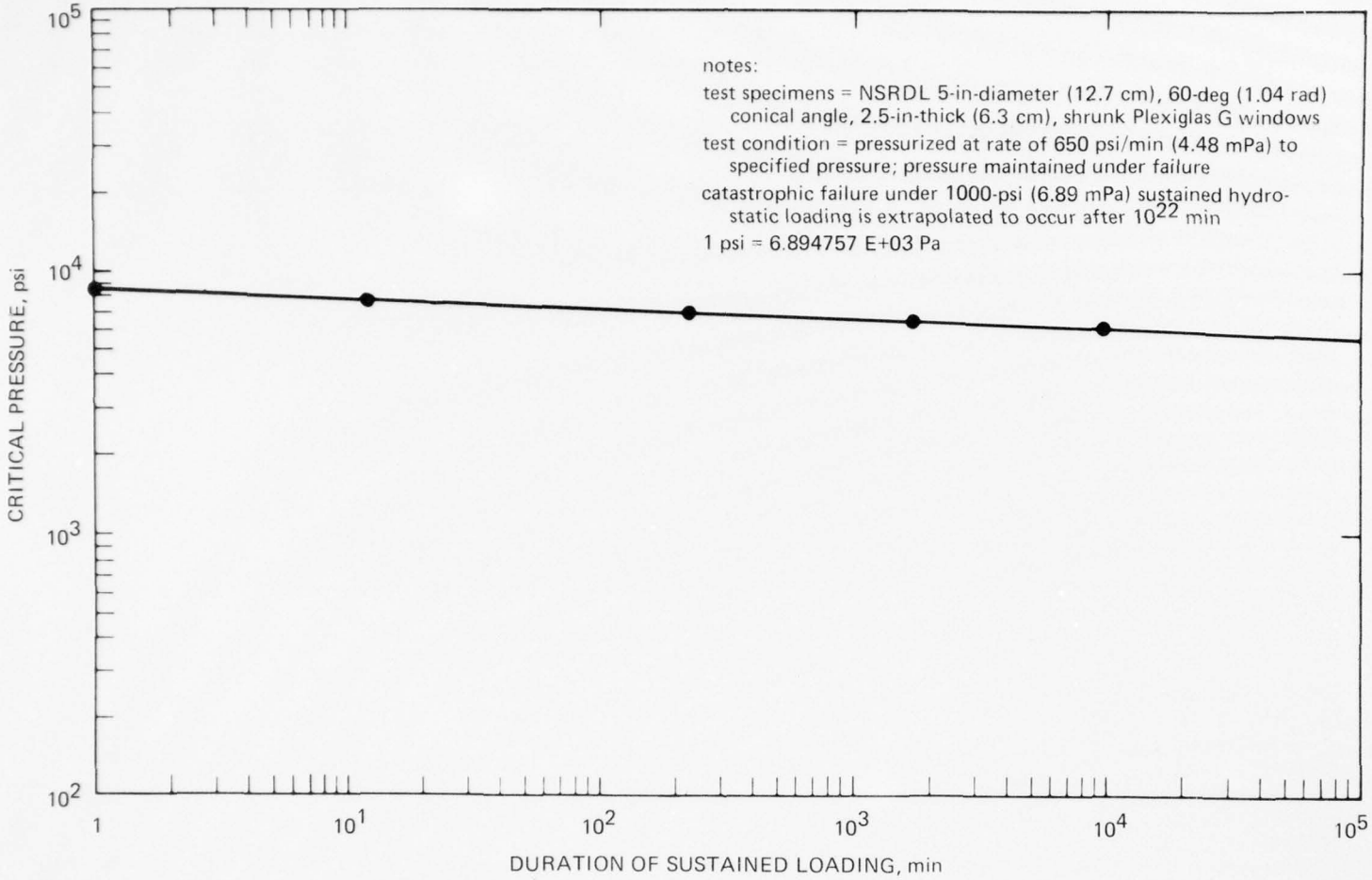

Figure 9.21. Static fatigue of a conical frustum ($t/D_i = 0.5$; $D_i/D_f = 1.04$; temperature = 150°F (66°C)). Note linearity of graph, which makes it easy to extrapolate existing data for future designs (reference 9.12).

AD-A070 535 NAVAL UNDERSEA CENTER SAN DIEGO CA F/G 11/9
ACRYLIC PLASTIC VIEWPOINT FOR OCEAN ENGINEERING APPLICATIONS. V--ETC(U)
FEB 77 J D STACHIW
UNCLASSIFIED NUC-TP-562-VOL-1 NL

5 OF 5
AD
A070535

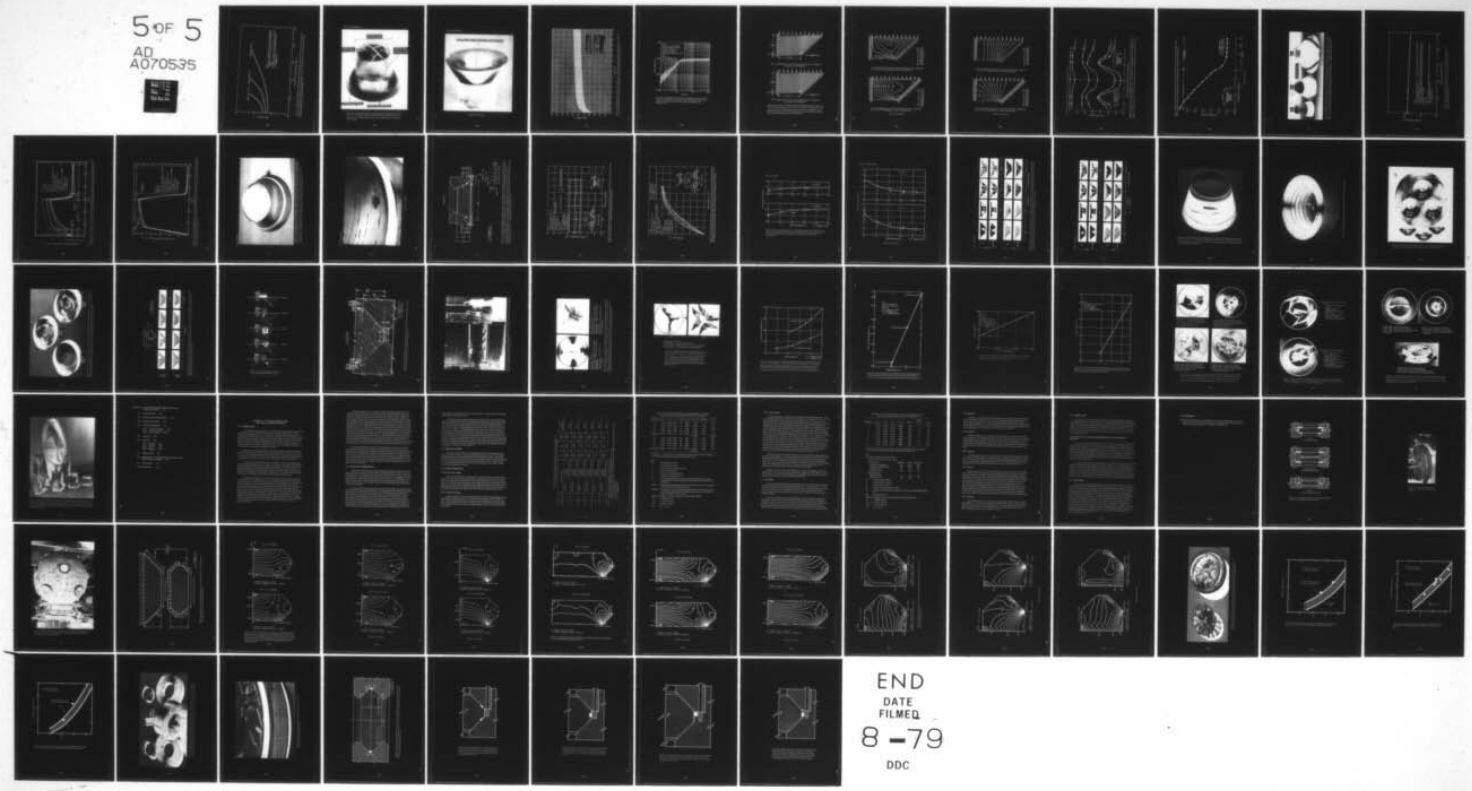

END
DATE
FILMED
8-79
DDC

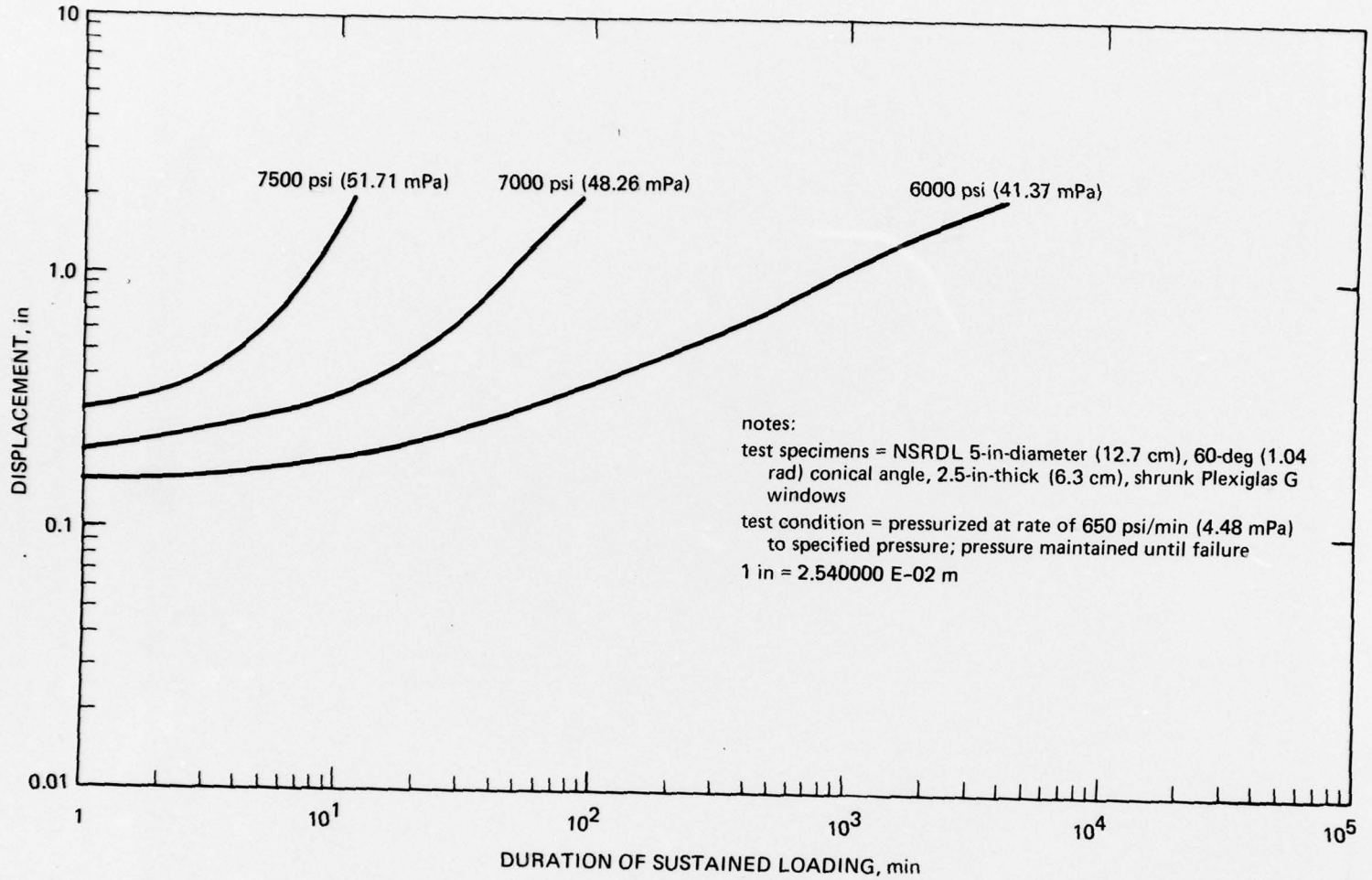

Figure 9.22. Typical axial displacements of conical frustums under sustained loading at an elevated temperature ($t/D_i = 0.5$; $D_i/D_f = 1.04$; temperature = 150°F (66°C)). Note that all test specimens failed only after an axial displacement of a certain magnitude was achieved, although all were pressurized to different levels (reference 9.12).

Part A. Low-pressure face.

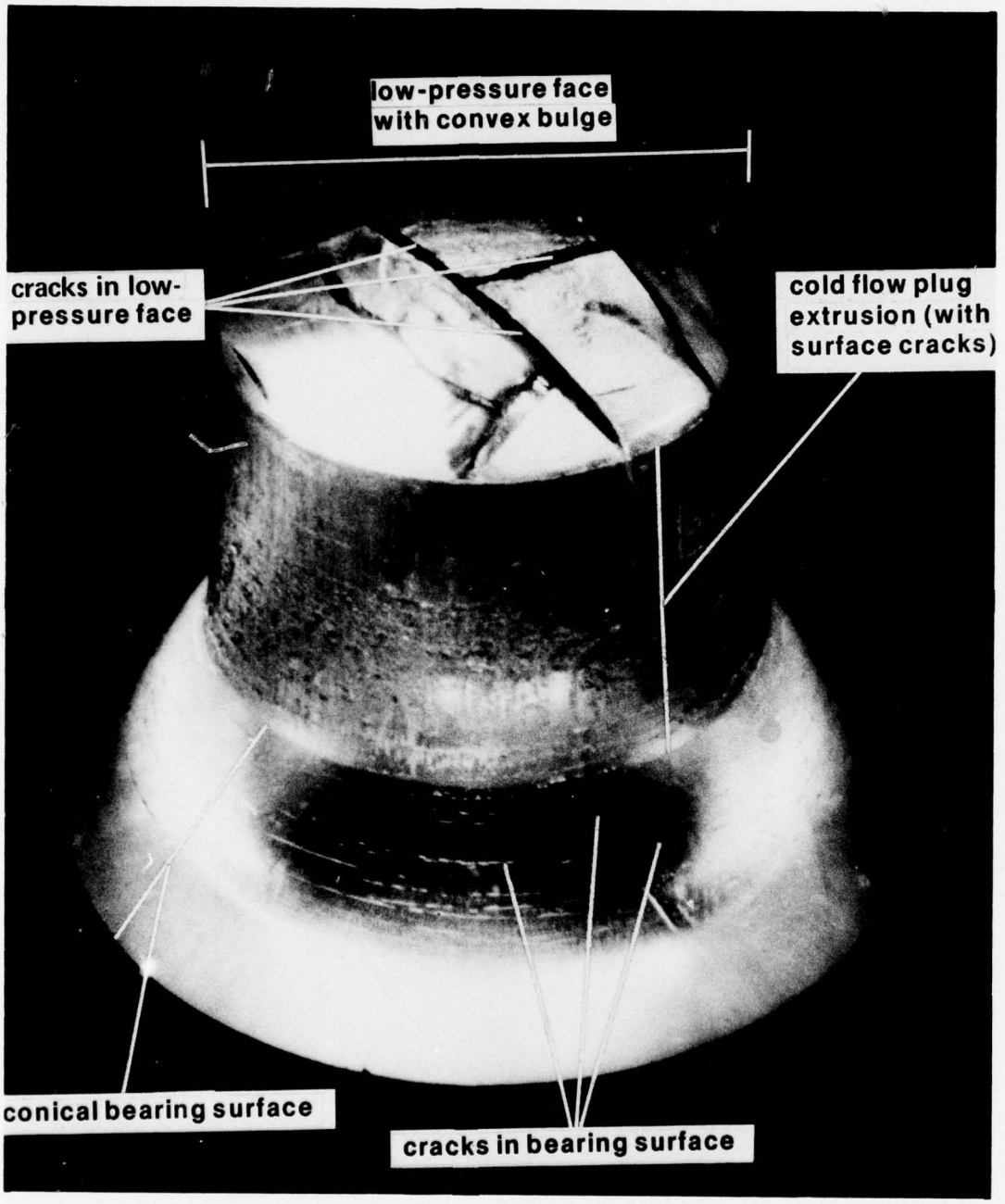

Figure 9.23. Large-scale deformation of conical frustum under sustained pressure loading ($t/D_i = 0.75$; conical angle = 60 degrees (1.04 radians); $D_i/D_f = 1$; temperature = 70°F (21°C); pressure = 20,000 pounds per square inch (137.8 megapascals); w = 1000 hours) (reference 9.12).

Part B. High-pressure face.

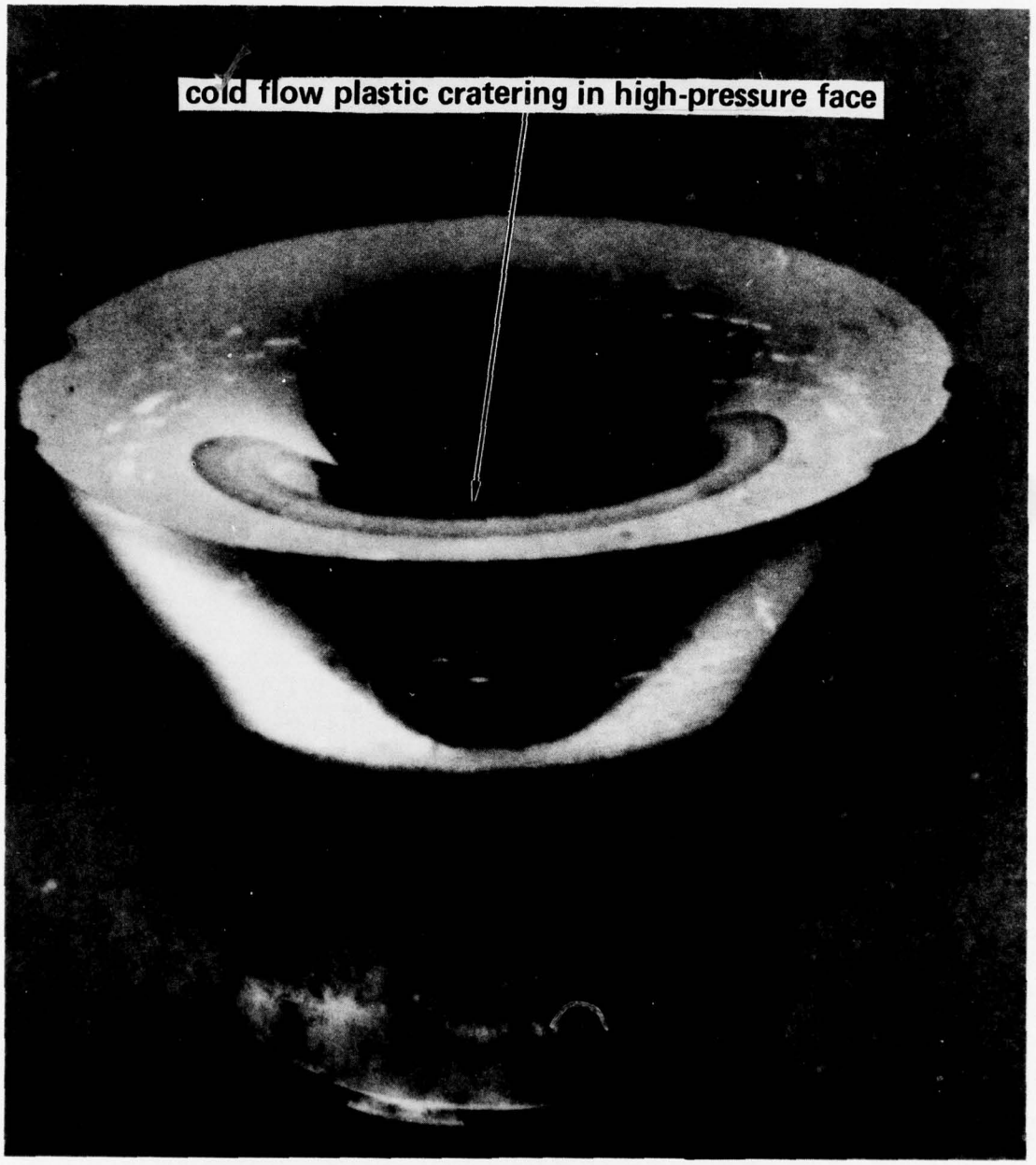

Figure 9.23. Continued.

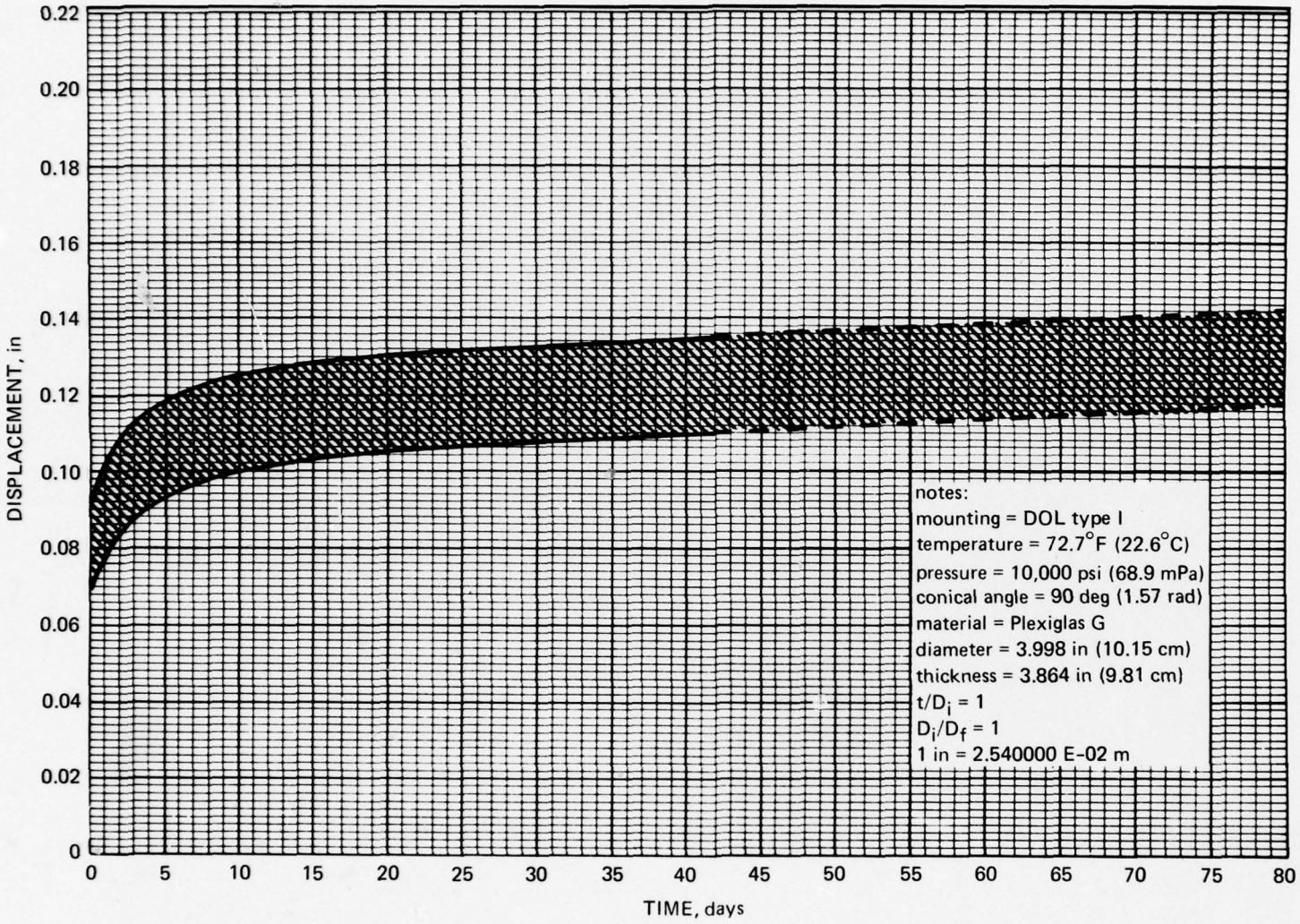

Figure 9.24. Axial displacements for a group of five identical conical frustum windows under sustained pressure loading at ambient room temperature. Although the rate of displacement is initially large, it decreases to a manageable level (reference 9.14).

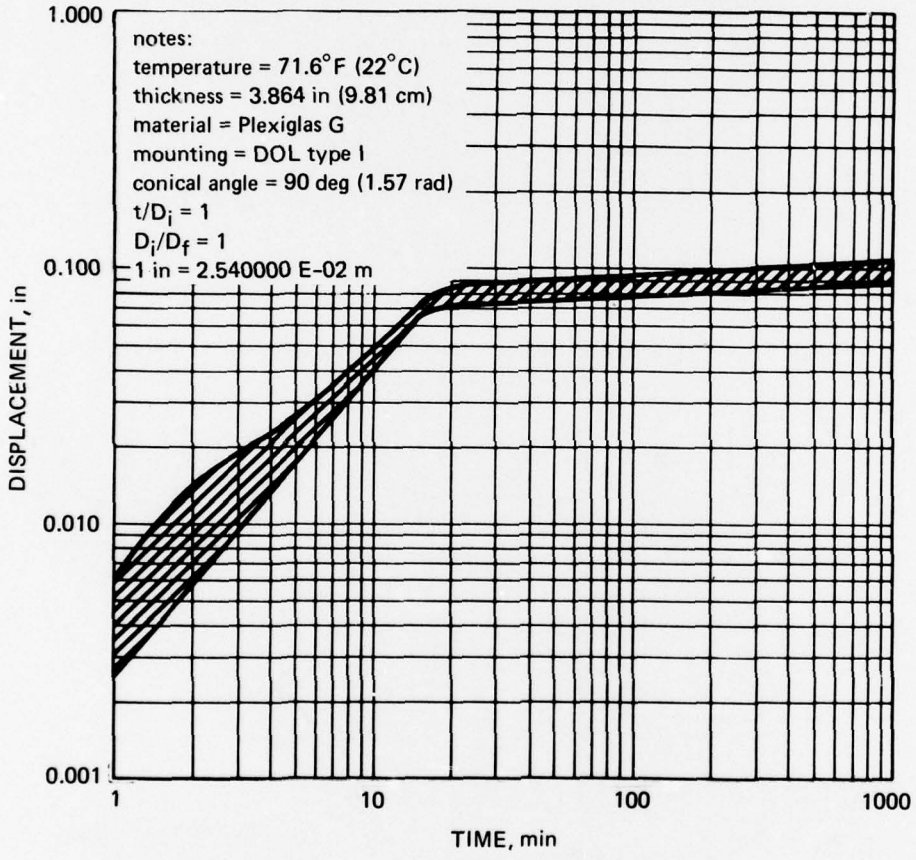

Figure 9.25. Axial displacements of conical frustums plotted on log-log coordinates. Once the sustained pressure level has been reached, the displacement can be represented by a linear graph, a feature which is useful for extrapolation of data (reference 9.14).

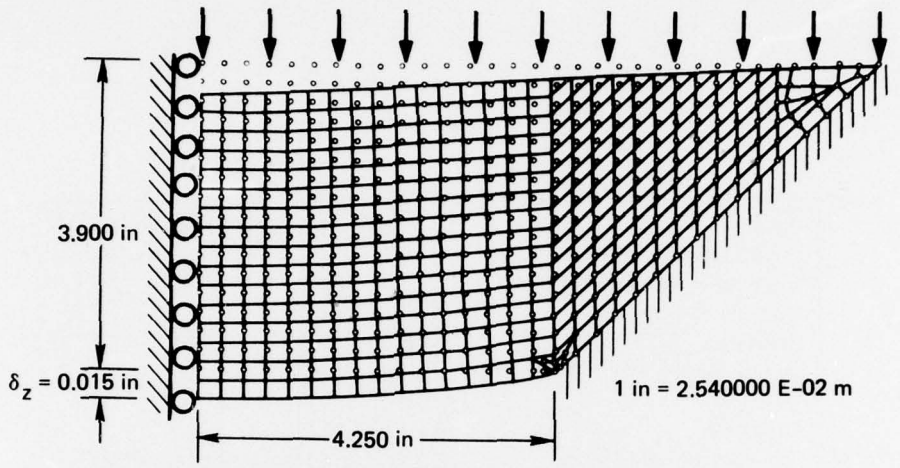

Part A. Displaced shapes of viewports, fixed boundary (pressure = 1000 pounds per square inch, 6.89 megapascals).

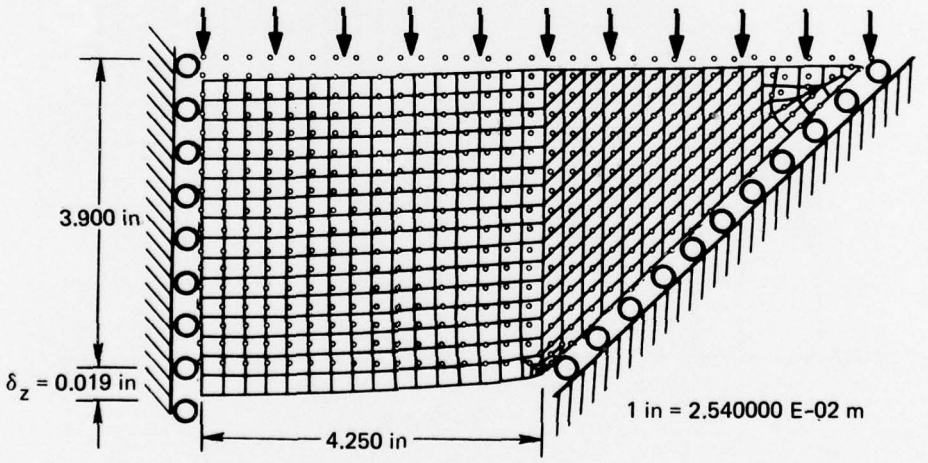

Part B. Displaced shapes of viewports, free boundary (pressure = 1000 pounds per square inch, 6.89 megapascals).

Figure 9.26. Displacements of a thick conical frustum window calculated on the basis of a finite-element computer program (t/D_i = 0.46; D_i = 8.50; D_i/D_f = 1.06; temperature = 75°F (23.8°C), pressure = 0 to 5000 pounds per square inch (0 to 34.5 megapascals)). The displacements calculated on the basis of free-boundary conditions are significantly larger than those based on fixed-boundary conditions (reference 9.6).

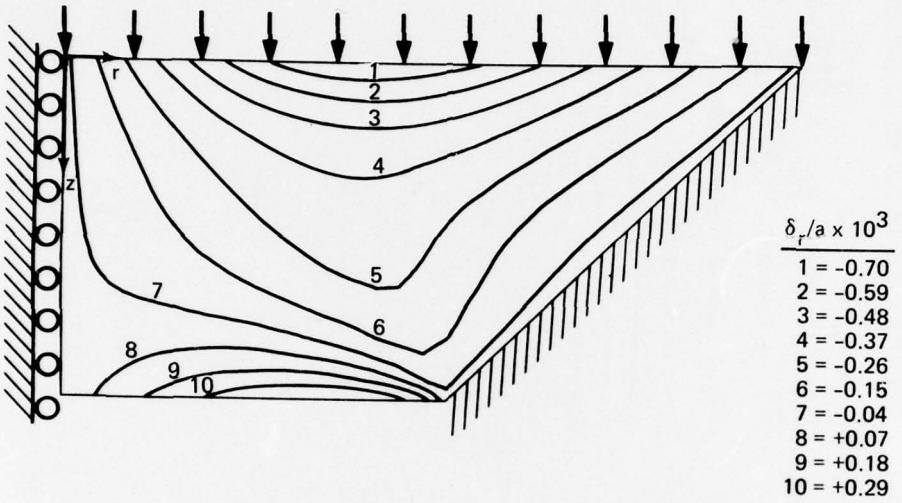

Part C. Radial displacement contour plots, fixed boundary (pressure = 1000 pounds per square inch, 6.89 megapascals); a = radius of low-pressure face.

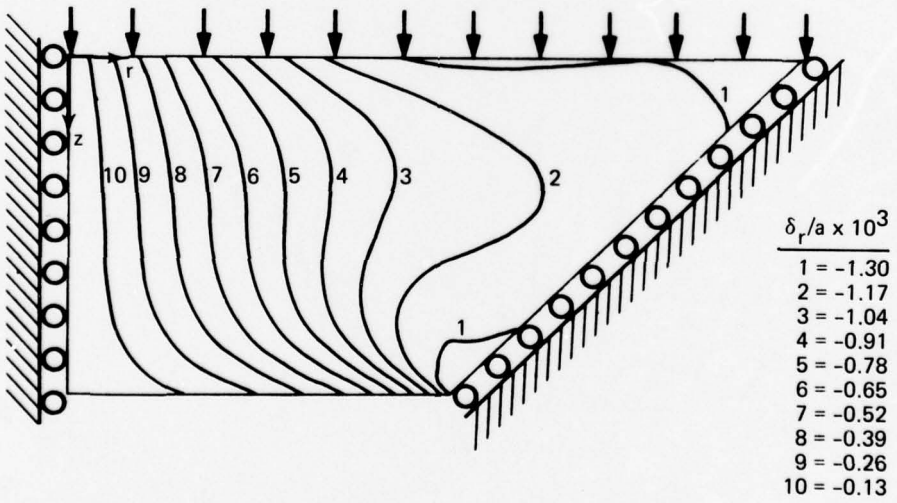

Part D. Radial displacement contour plots, free boundary (pressure = 1000 pounds per square inch, 6.89 megapascals); a = radius of low-pressure face.

Figure 9.26. Continued.

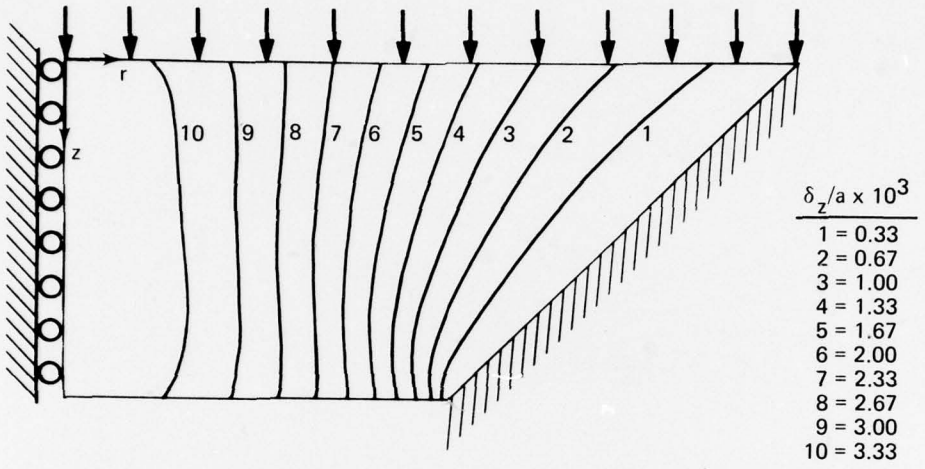

Part E. Axial displacement contour plots, fixed boundary (pressure = 1000 pounds per square inch, 6.89 megapascals); a = radius of low-pressure face.

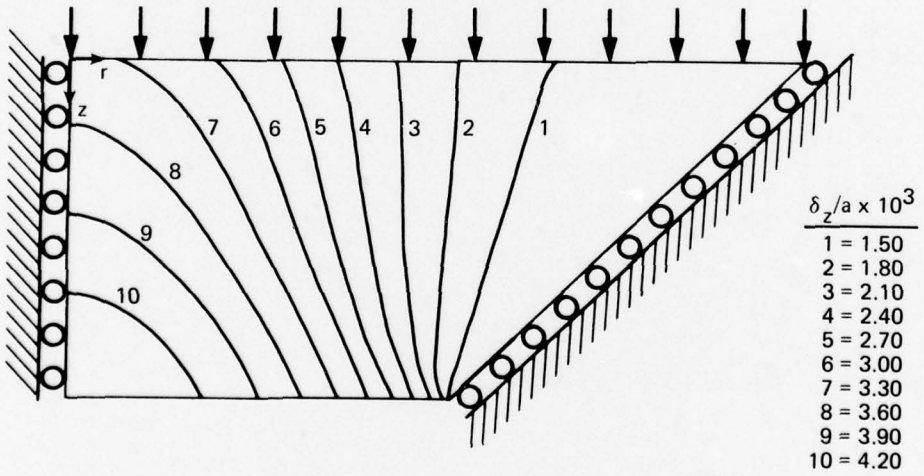

Part F. Axial displacement contour plots, free boundary (pressure = 1000 pounds per square inch, 6.89 megapascals); a = radius of low-pressure face.

Figure 9.26. Continued.

Part A. High-pressure face; note formation of ridge around crater-like depression.

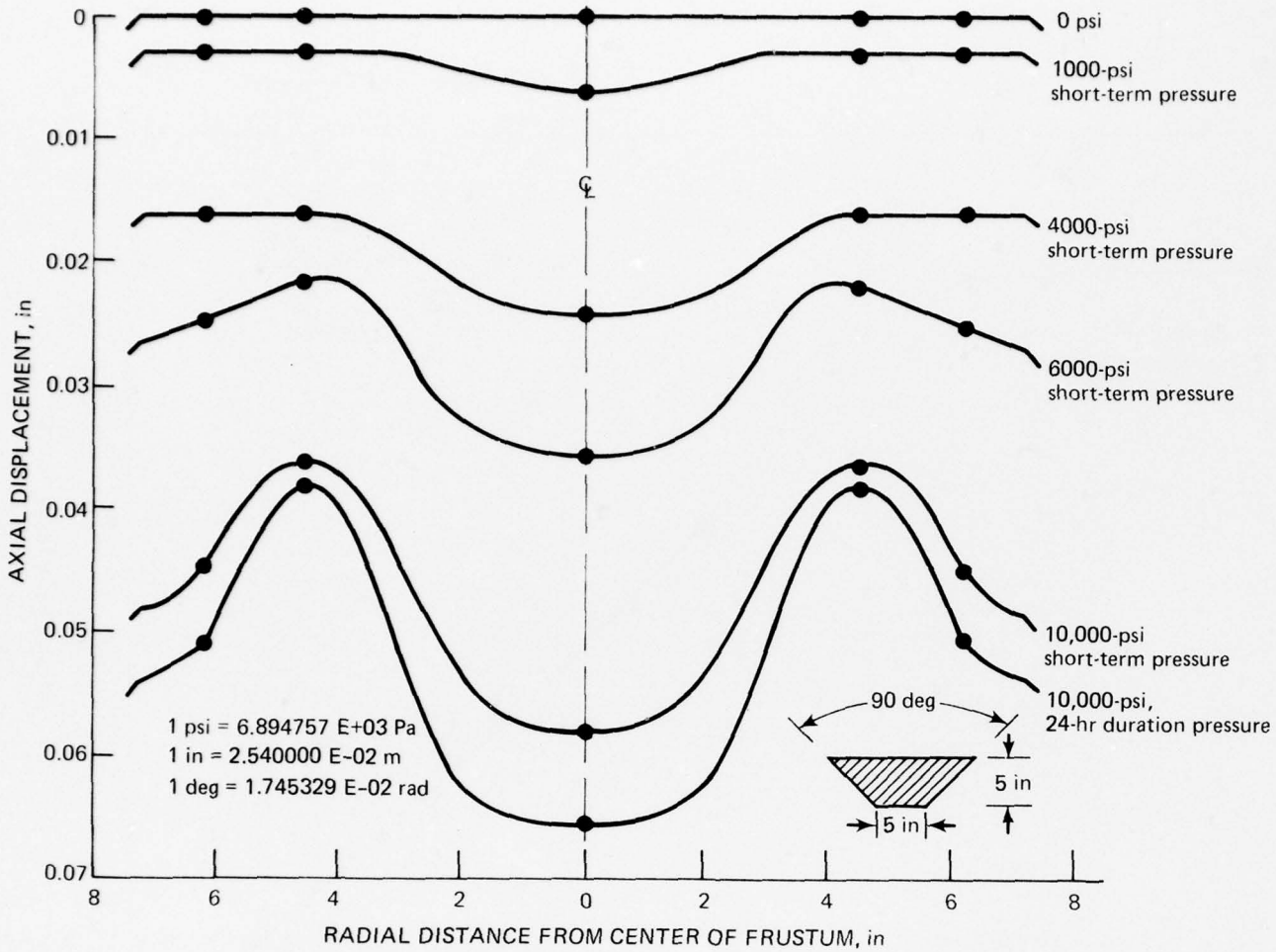

Figure 9.27. Deflection and total axial displacement of thick conical frustum window under sustained loading at design pressure of 10,000 pounds per square inch (68.9 megapascals). ($t/D_i = 1$; $D_i = 5$ inches (12.7 centimeters); $D_i/D_f = 1.67$; conical angle = 90 degrees (1.57 radians); temperature = 70°F (21°C); short-term critical pressure = 50,000 pounds per square inch (344.7 megapascals).)

Part B. Low-pressure face; note that the axial displacement measured at the center of the low-pressure face is approximately 100 percent higher than that of the high-pressure face, emphasizing the plug-like extrusion of the conical frustum.

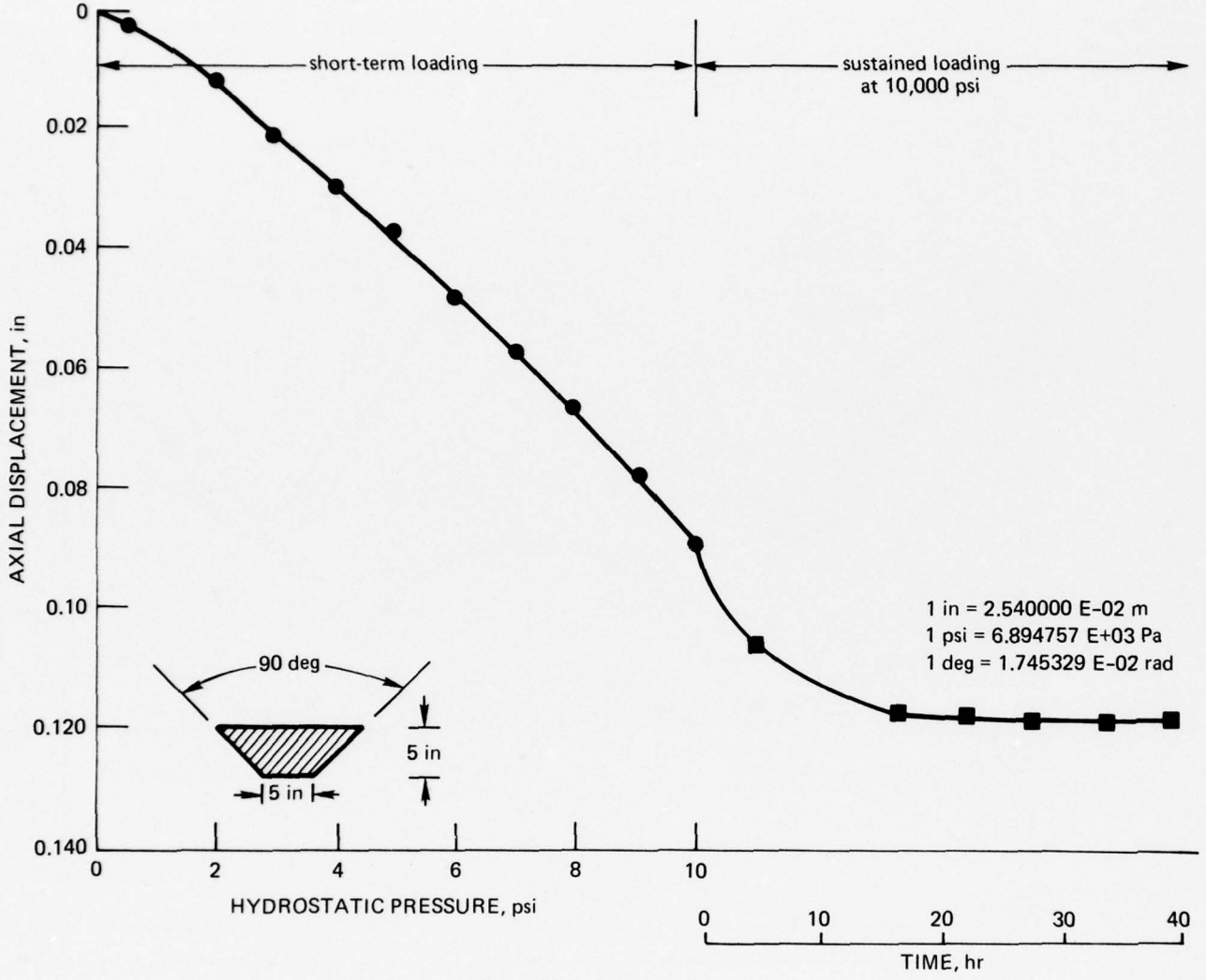

Figure 9.27. Continued.

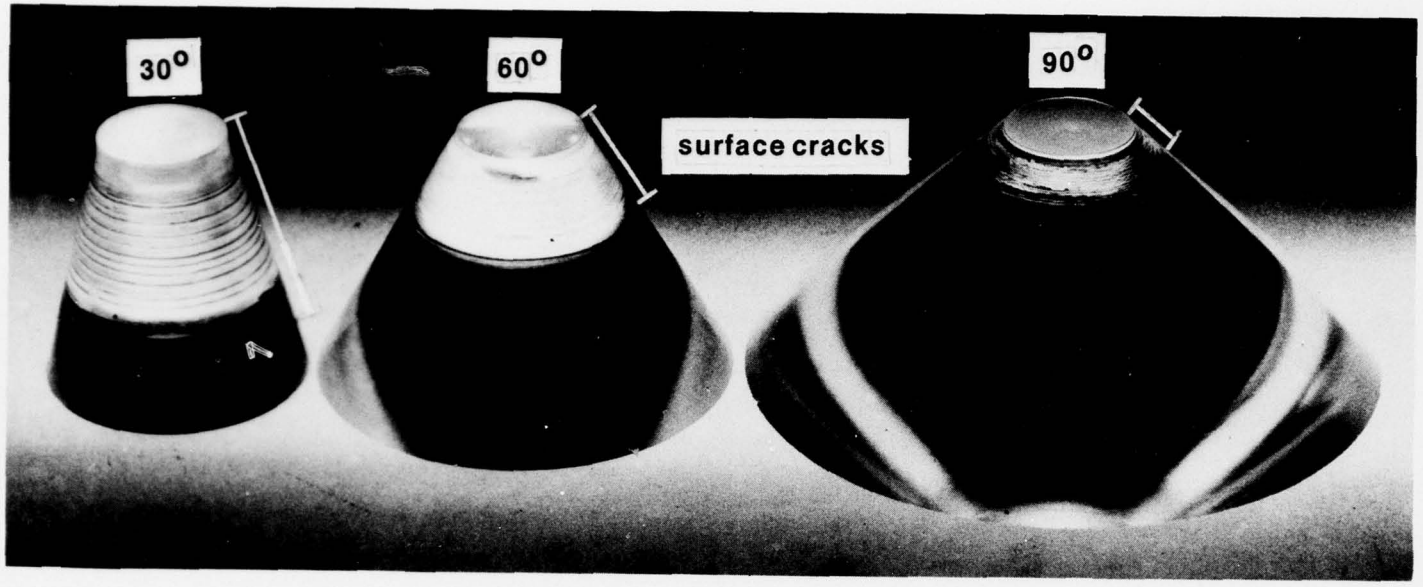

Figure 9.28. Distribution and severity of cracks on conical frustum's bearing surface after sustained pressure loading ($t/D_i = 1.75$; $D_i/D_f = 1.0$; temperature = 75°F (24°C); pressure = 20,000 pounds per square inch (137.8 megapascals); w = 1000 hours). Note that the cracks on the 30-degree (0.52 radian) frustum are more numerous and deeper than those on the 90-degree (1.57 radians) window (reference 9.13).

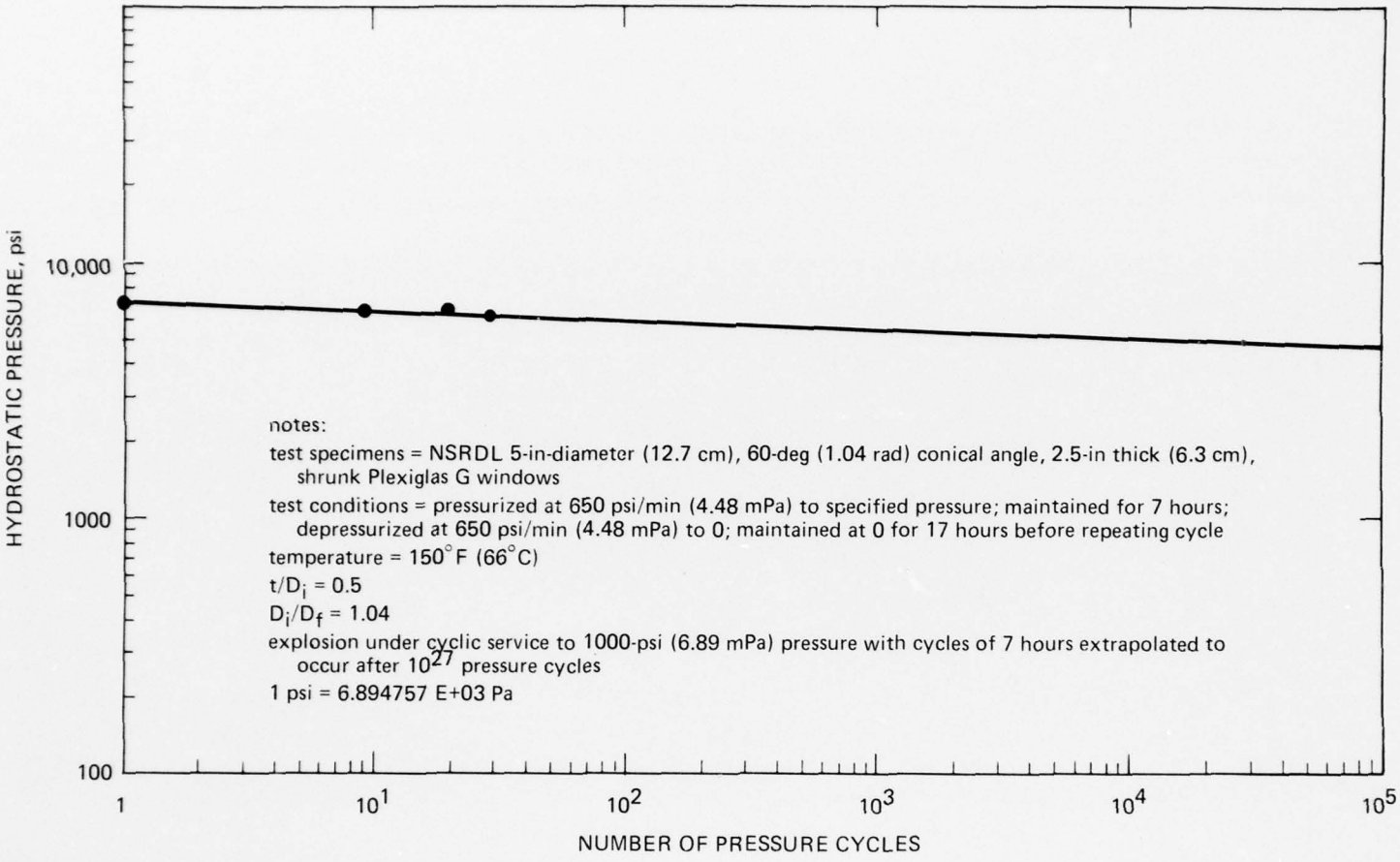

Figure 9.29. Typical cyclic fatigue of conical frustum window. Note that the relationship between the number of pressure cycles and the catastrophic failure pressure is represented by a straight line on log-log coordinates (reference 9.12).

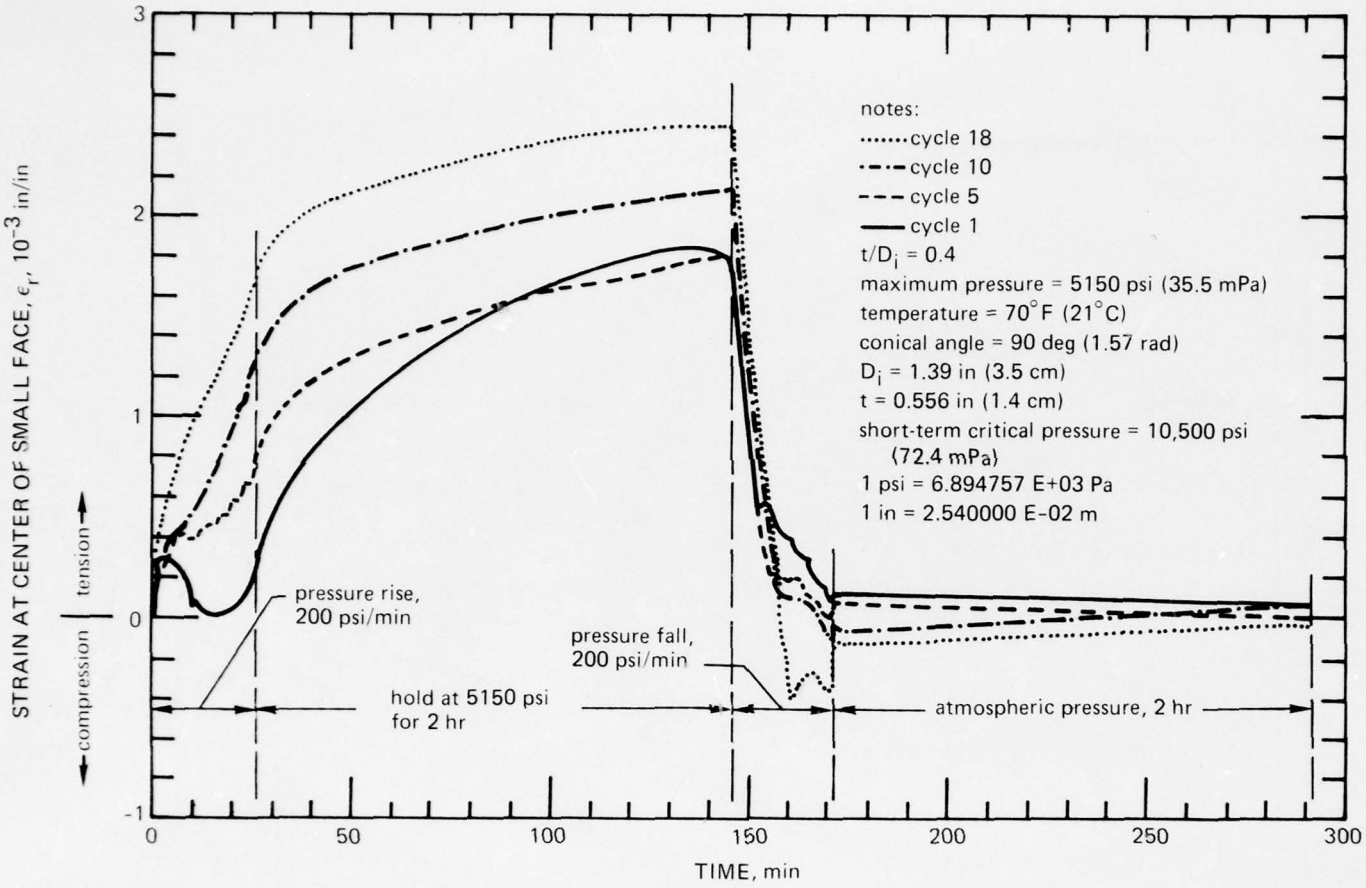

Figure 9.30. Increase in strain of a conical frustum window with repeated cyclic pressurizations to approximately 50 percent of its short-term critical pressure. As the pressure cycling progresses, the residual compressive stresses begin to appear during relaxation (reference 9.3).

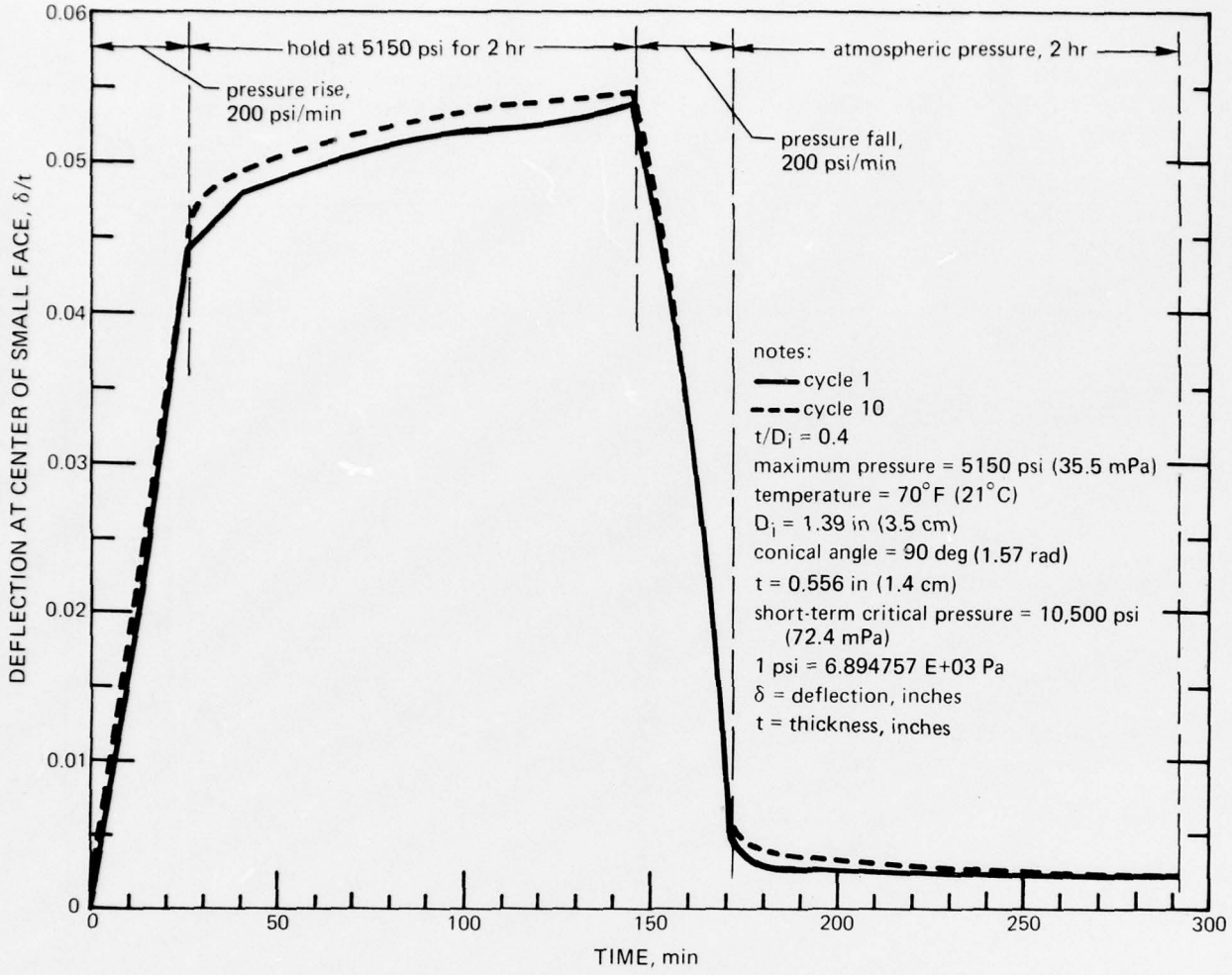

Figure 9.31. Increase in axial displacement of a conical frustum window with repeated cyclic pressurizations to approximately 50 percent of its short-term critical pressure. There is permanent deformation in the window after the first cycle, as the center of the low-pressure face does not return to its original position (reference 9.3).

Part A. Overall view.

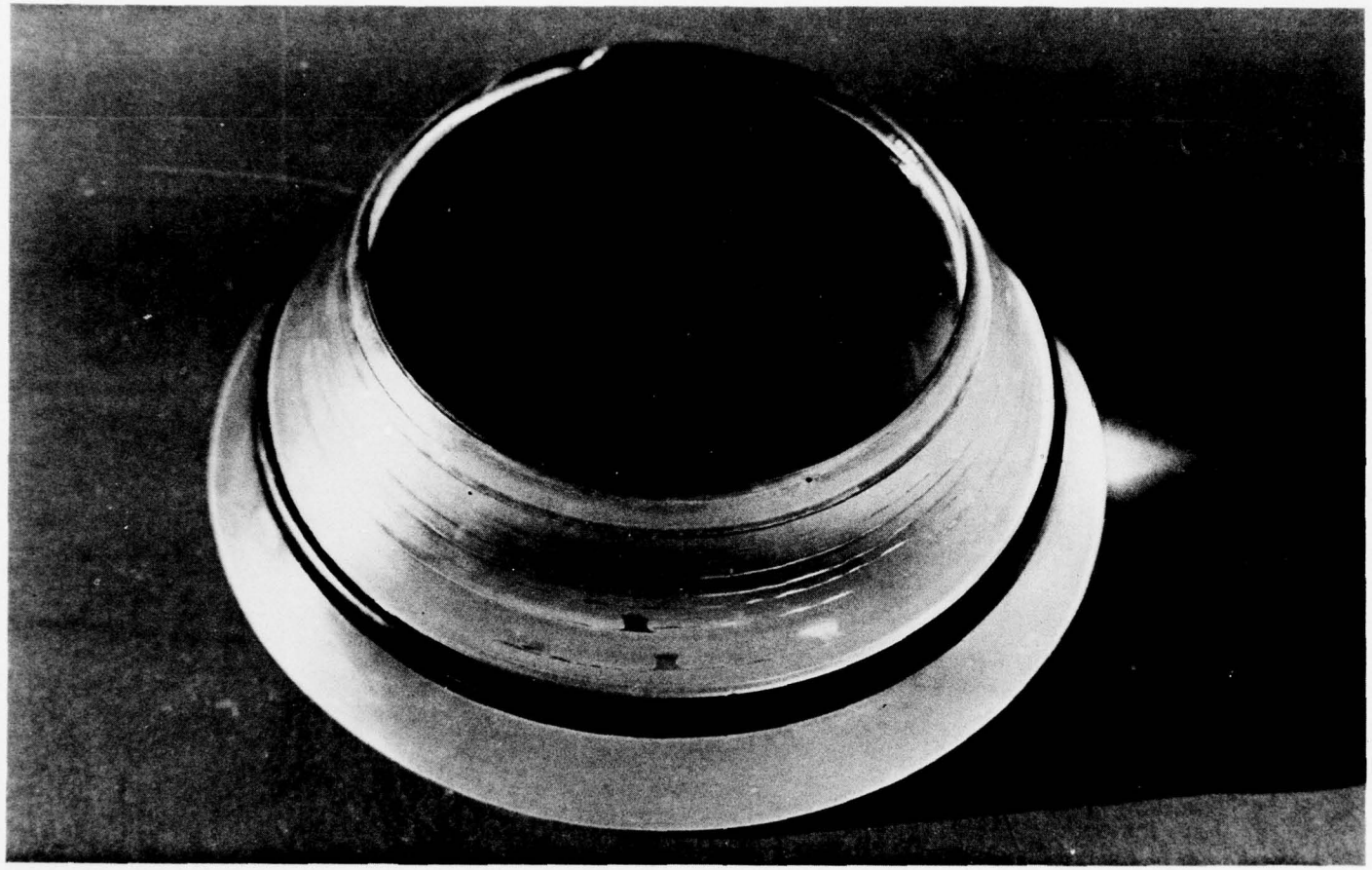

Figure 9.32. Cyclic fatigue cracks in a conical frustum window after 100 pressure cycles to 30 percent of its short-term critical pressure (temperature = 150°F (66°C); $t/D_i = 0.5$; conical angle = 60 degrees (1.04 radians); $D_i/D_f = 1.04$; maximum pressure = 5000 pounds per square inch (34.5 megapascals); short-term critical pressure = 17,000 pounds per square inch at 75°F (24°C). The O-ring groove did not act as a crack originator because it was located close to the high-pressure face (reference 9.12).

Part B. Close-up view.

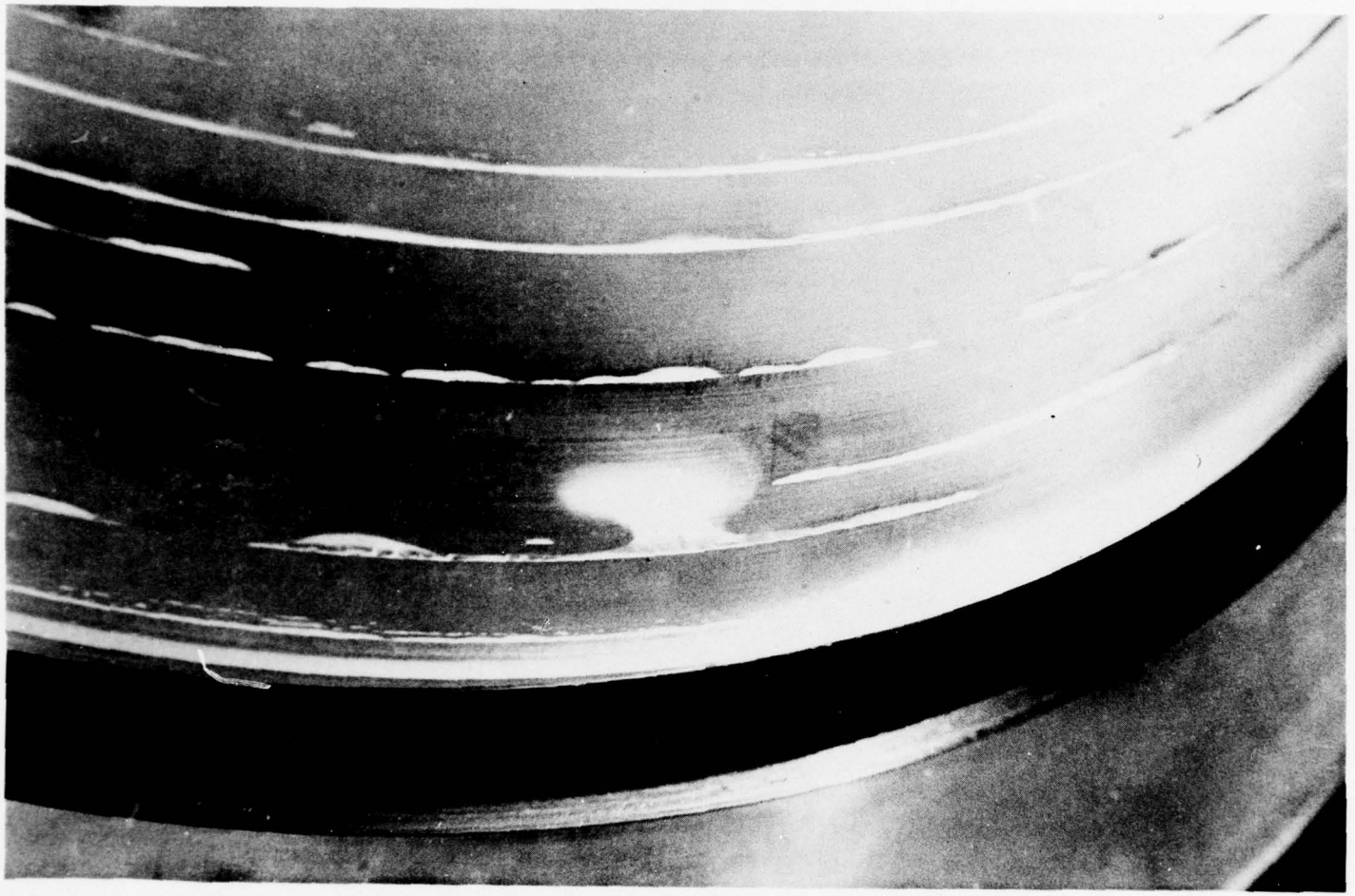

Figure 9.32. Continued.

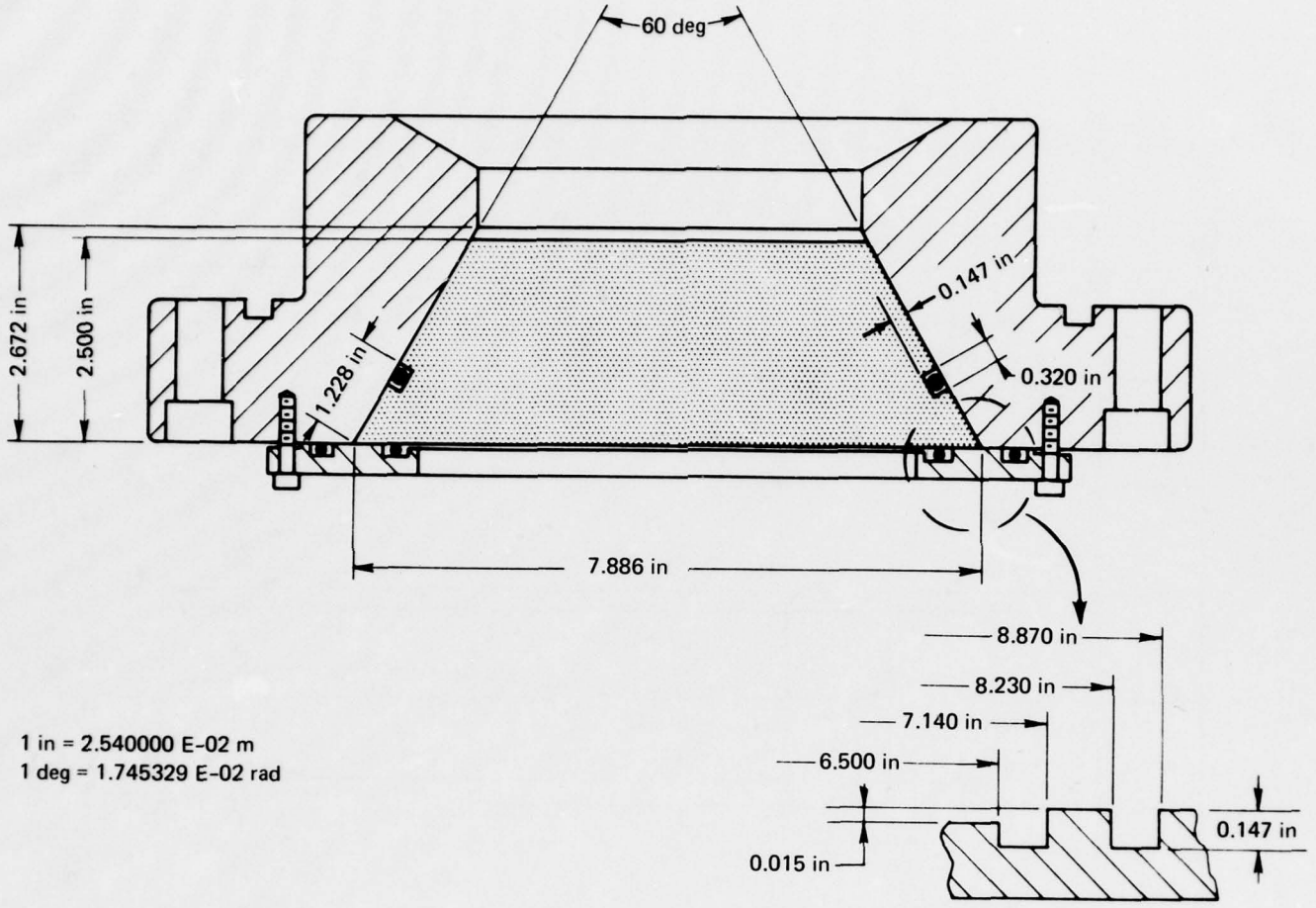

Figure 9.33. Conical frustum window assembly that was extensively evaluated prior to installation in the NCSL deep-ocean test facility ($t/D_i = 0.5$; conical angle = 60 degrees (1.04 radians); $D_i/D_f = 1.04$; temperature = 150°F (66°C); design pressure = 1000 pounds per square inch (6.89 megapascals); short-term critical pressure = 17,000 pounds per square inch at 75°F (24°C). The short-term critical pressure is shown in figure 9.13; the short-term displacement in figure 9.14; the static fatigue in figure 9.21; displacement under long-term loading in figure 9.22; and cyclic fatigue in figure 9.29 (reference 9.12).

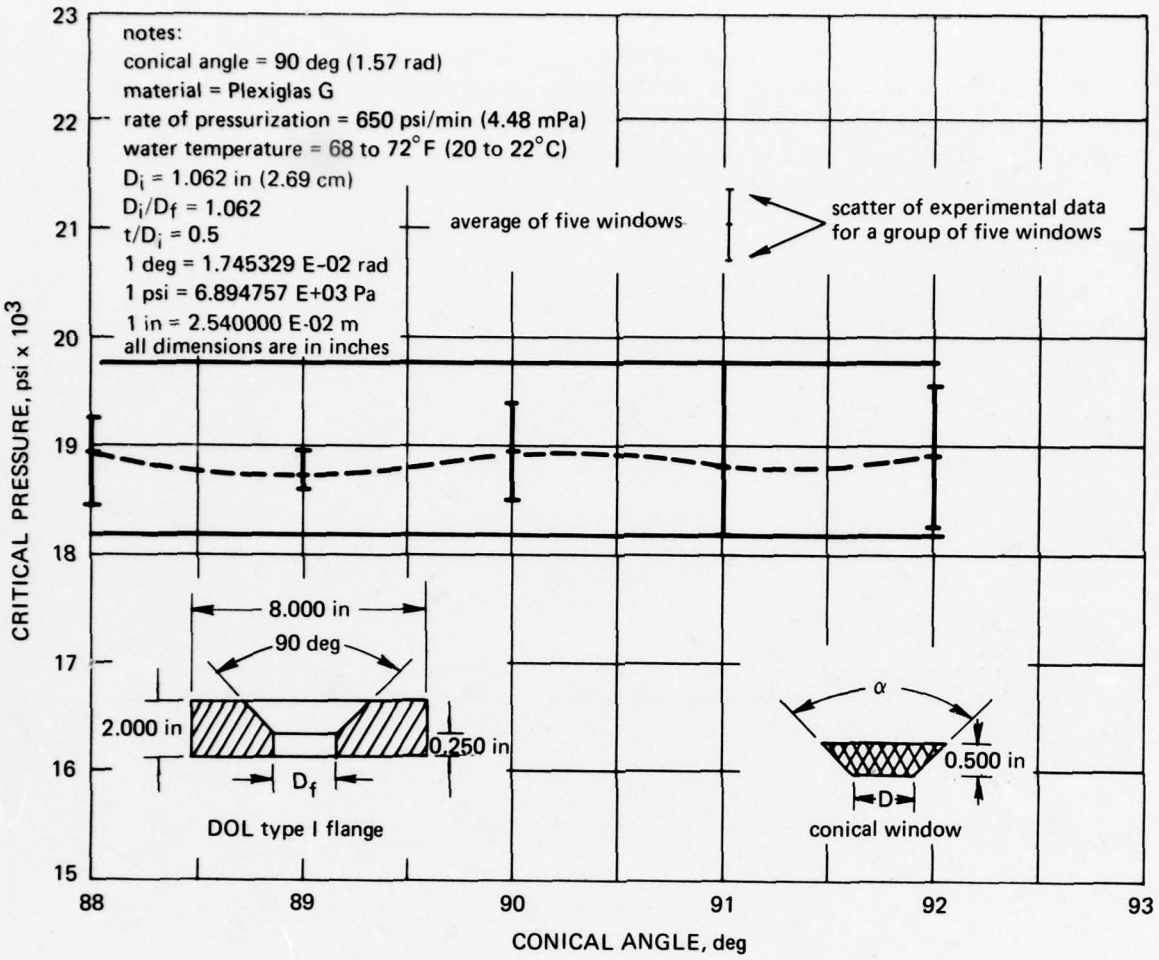

Figure 9.34. Effect of angular mismatch between the conical frustum and the conical seat in the flange on the short-term critical pressure. Note that the effect of a ±2-degree (0.003 radian) mismatch is insignificant.

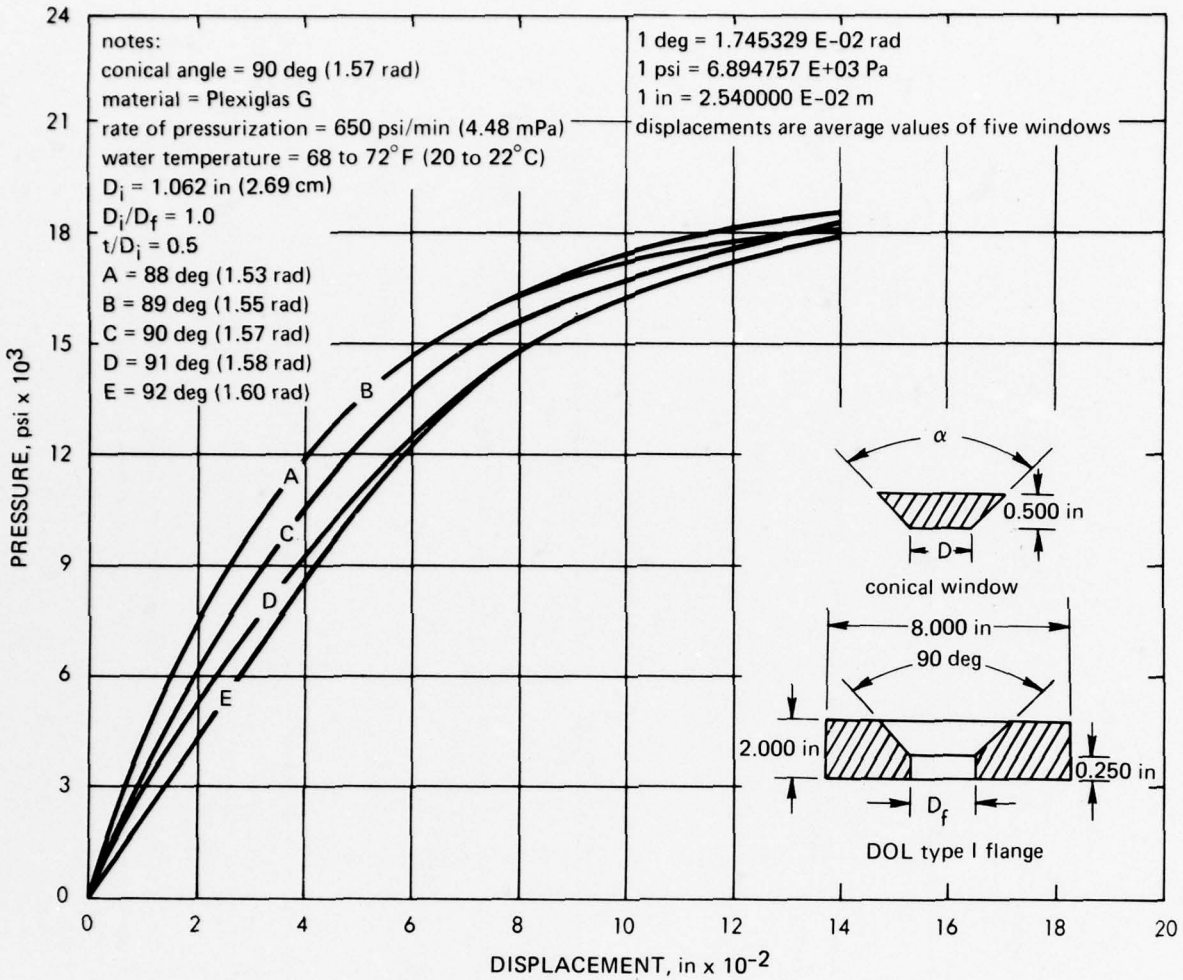

Figure 9.35. Effect of angular mismatch between conical frustum and the conical seat on the axial displacement under short-term loading. Note that the axial displacement increases with the magnitude of the negative mismatch (less than 90 degrees (1.57 radians)) and decreases with the magnitude of the positive mismatch (more than 90 degrees (1.57 radians)).

Part A. Dry surfaces.

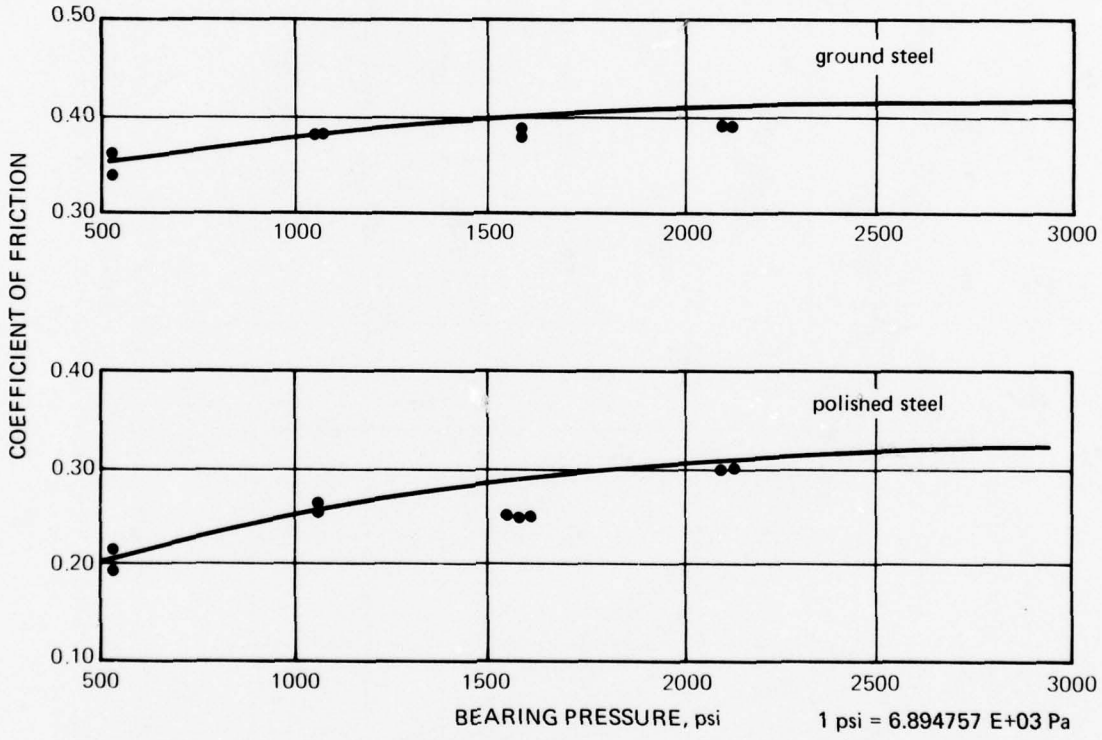

Figure 9.36. Effect of bearing pressure on the coefficient of friction between acrylic plastic and bearing surfaces with 8- and 20-rms finishes. At bearing pressures in excess of 3000 pounds per square inch (20.7 megapascals), the coefficient of friction assumes a constant value (reference 9.18).

Part B. Lubricated surfaces.

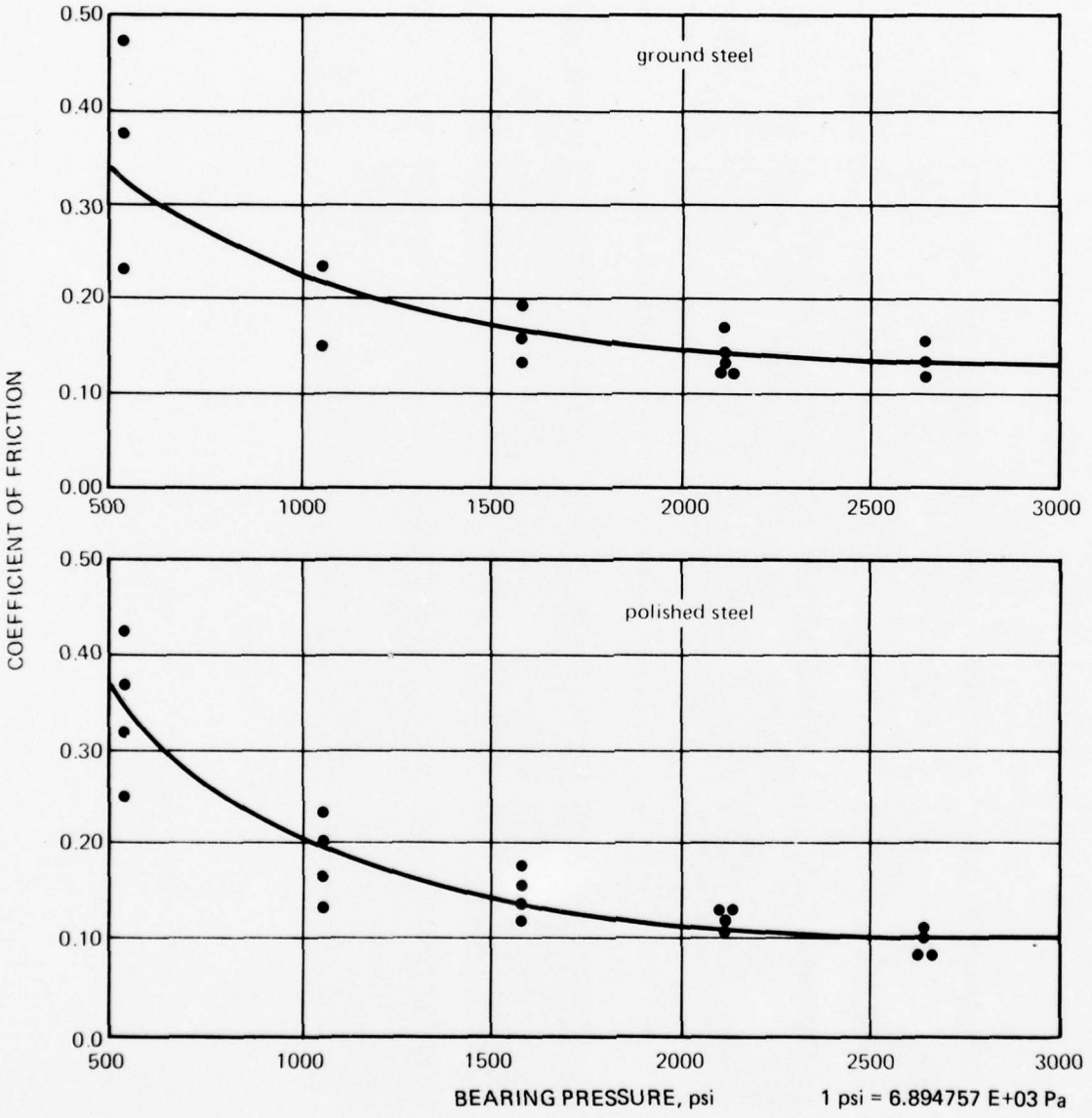

Figure 9.36. Continued.

Part A. 8-rms finish.

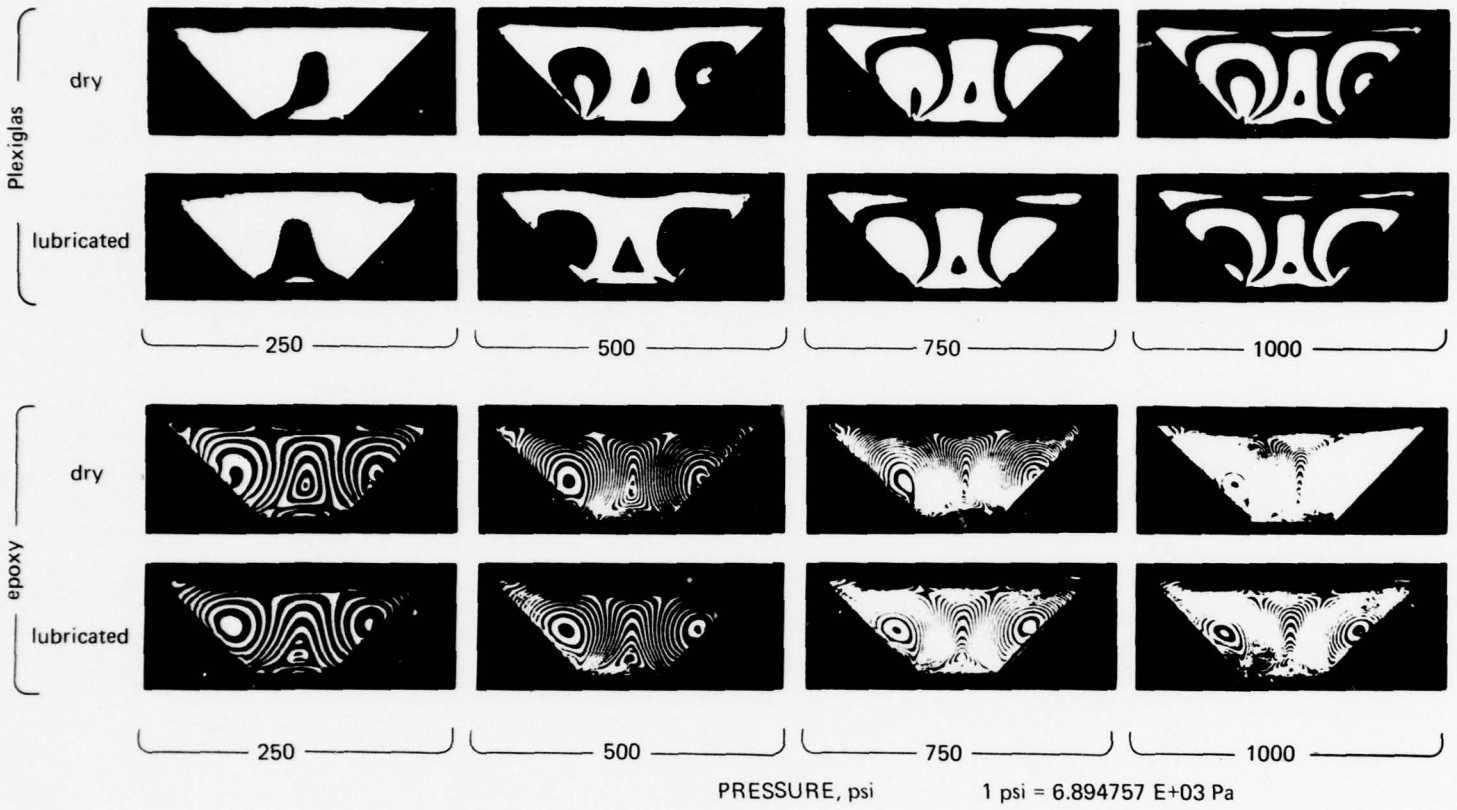

Figure 9.37. Effect of seat bearing surface condition on the distribution and magnitude of stresses in two-dimensional models of conical frustums under simulated hydrostatic pressure loading. There is no significant difference between the dry and lubricated seats in the number or location of photoelastic fringe concentrations (reference 9.18) ($t/D_i = 0.5$; $\alpha = 90$ degrees (1.57 radians)).

Part B. 20-rms finish.

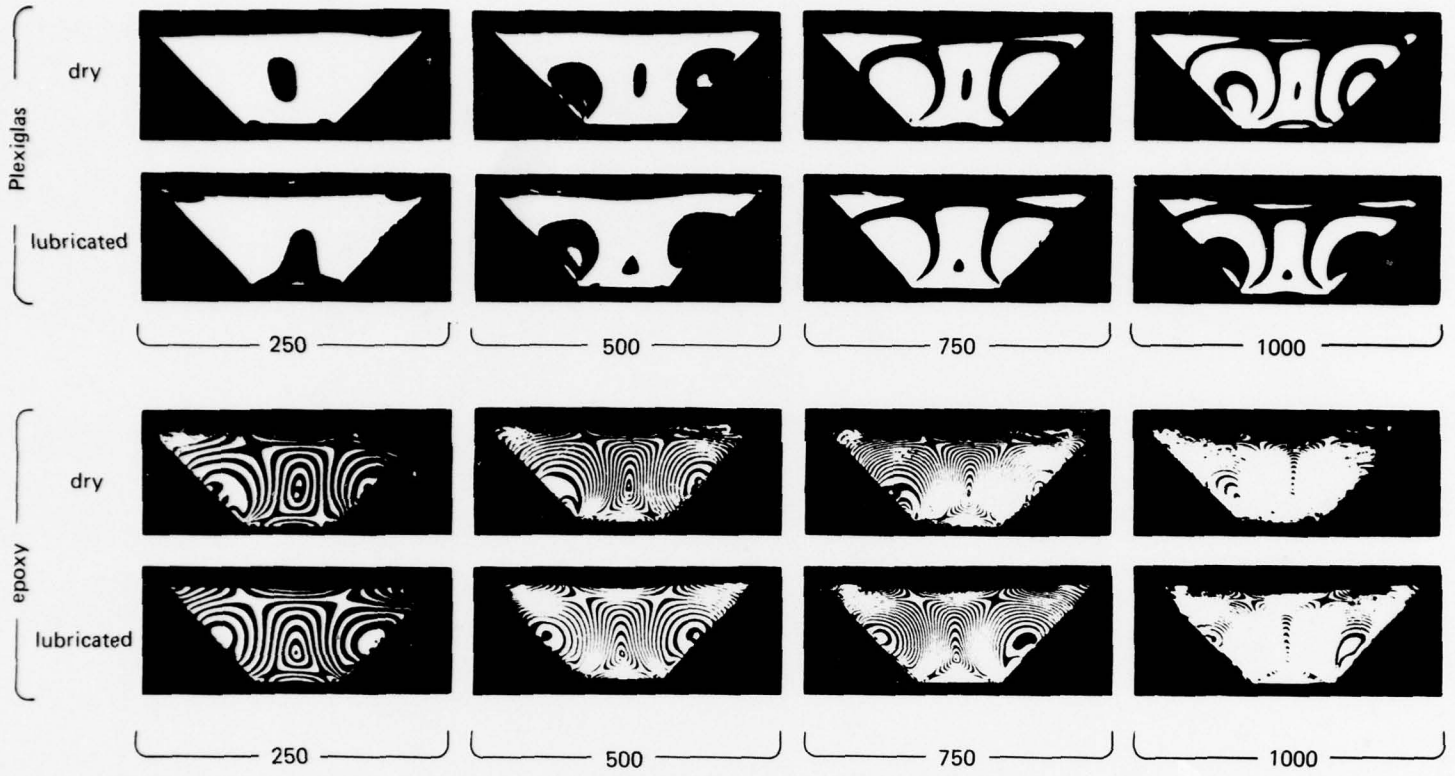

Figure 9.37. Continued.

Figure 9.38. Effect of O-ring grooves in the flange seat on the initiation of bearing cracks in acrylic plastic conical frustums (t/D_i = 1.0; conical angle = 37 degrees (0.65 radian); pressure = 10,000 pounds per square inch (68.9 megapascals); temperature = 75°F (24°C)). The location of the cracks corresponds to the location of the O-ring grooves in figure 9.39.

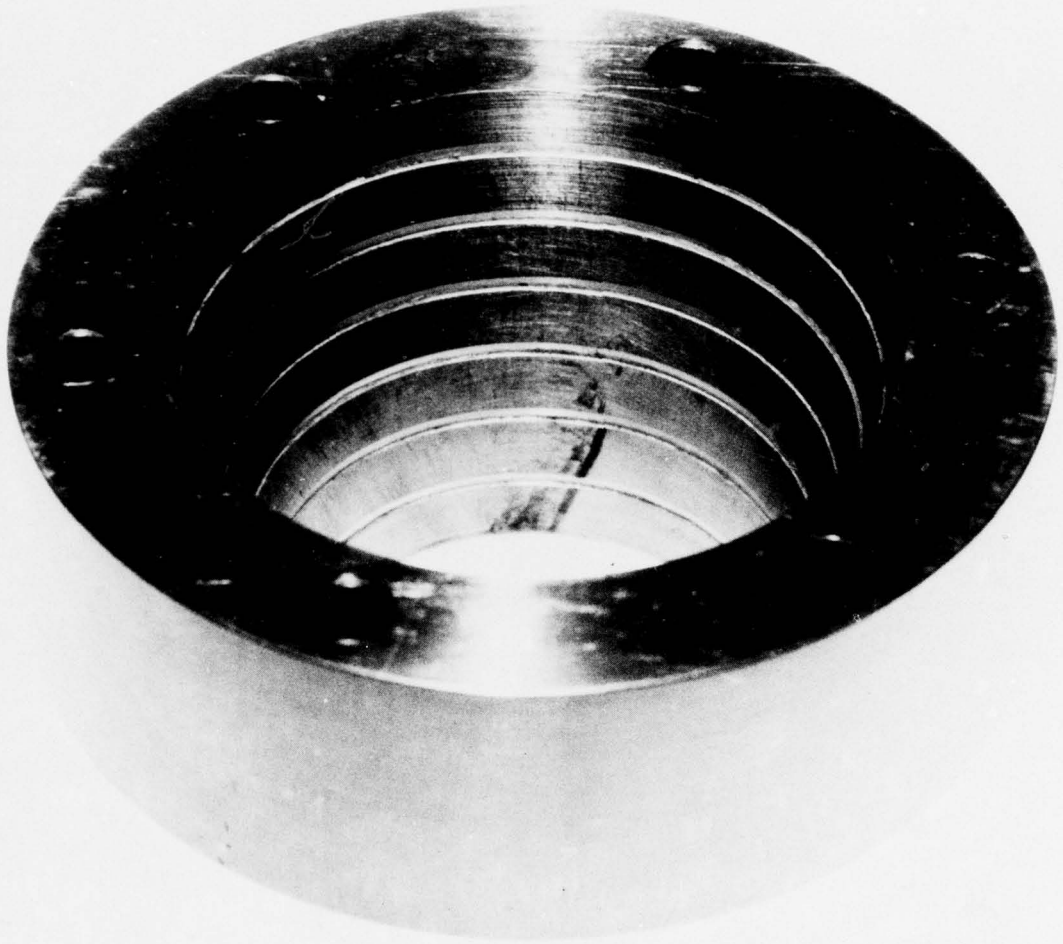

Figure 9.39. Seat with multiple O-ring grooves that generated the bearing cracks in figure 9.38.

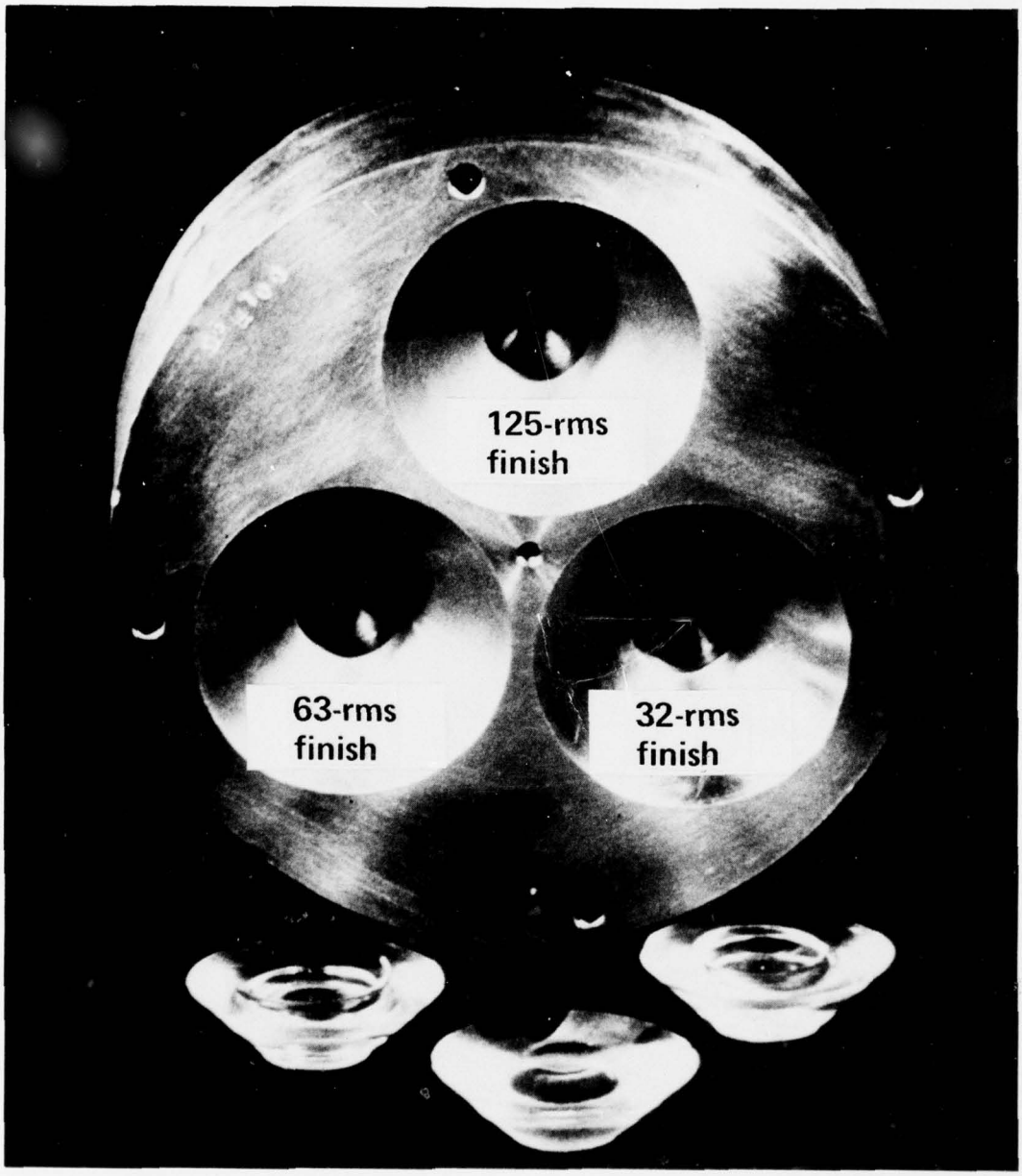

Figure 9.40. Test fixture used to evaluate the effect of the flange seat surface finish on the initiation of cyclic fatigue cracks in conical bearing surfaces of conical frustums.

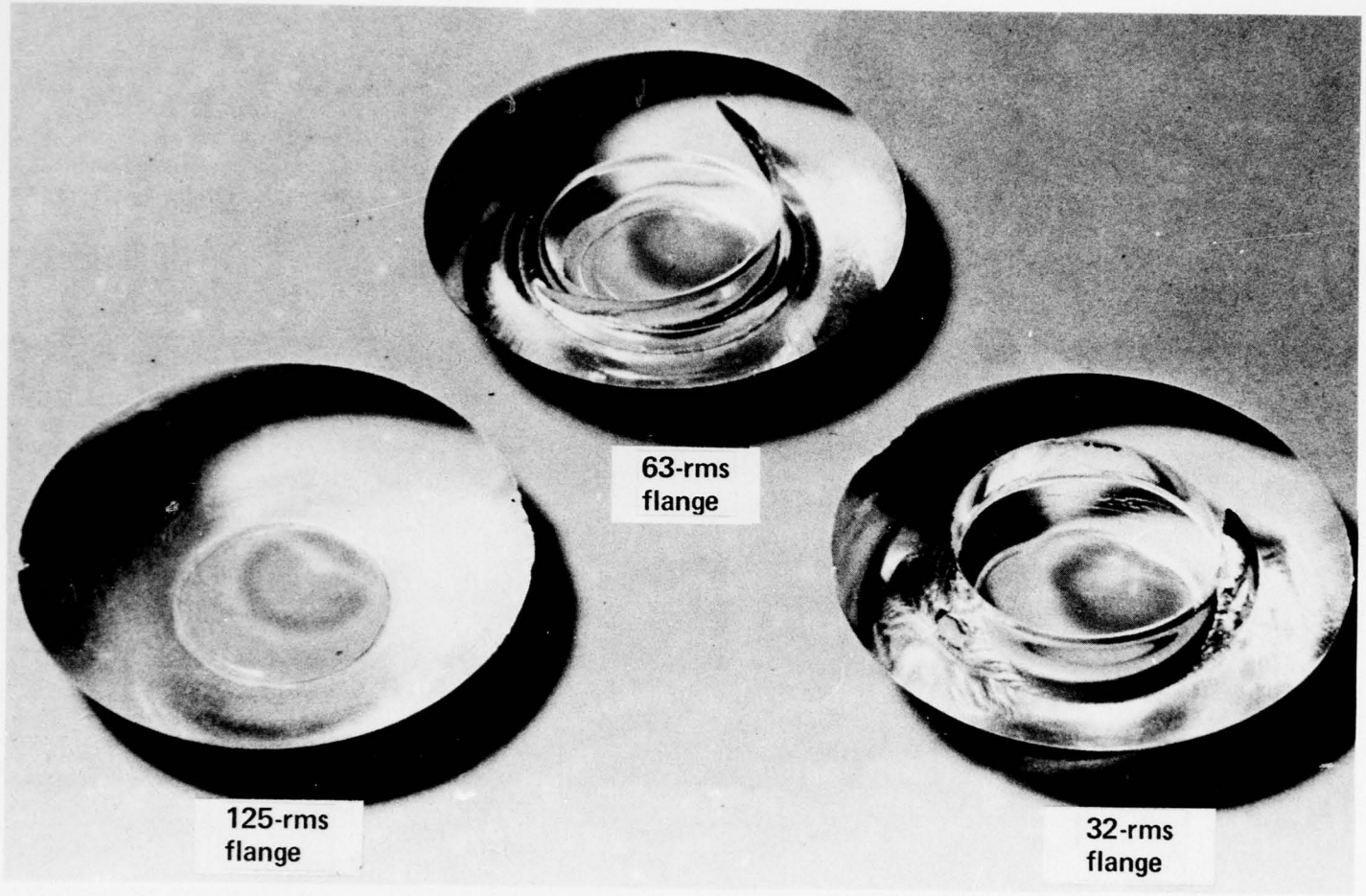

Figure 9.41. Effect of the seat surface finish on the cyclic fatigue of conical frustums (t/D_i = 0.59; temperature = 70°F (21°C); pressure = 0 to 23,000 pounds per square inch (0 to 158.6 megapascals); conical angle = 90 degrees (1.57 radians)). Note that the window tested in the seat with a 125-rms finish is free of cracks, while the one tested in the seat with the 32-rms finish has failed (reference 9.6).

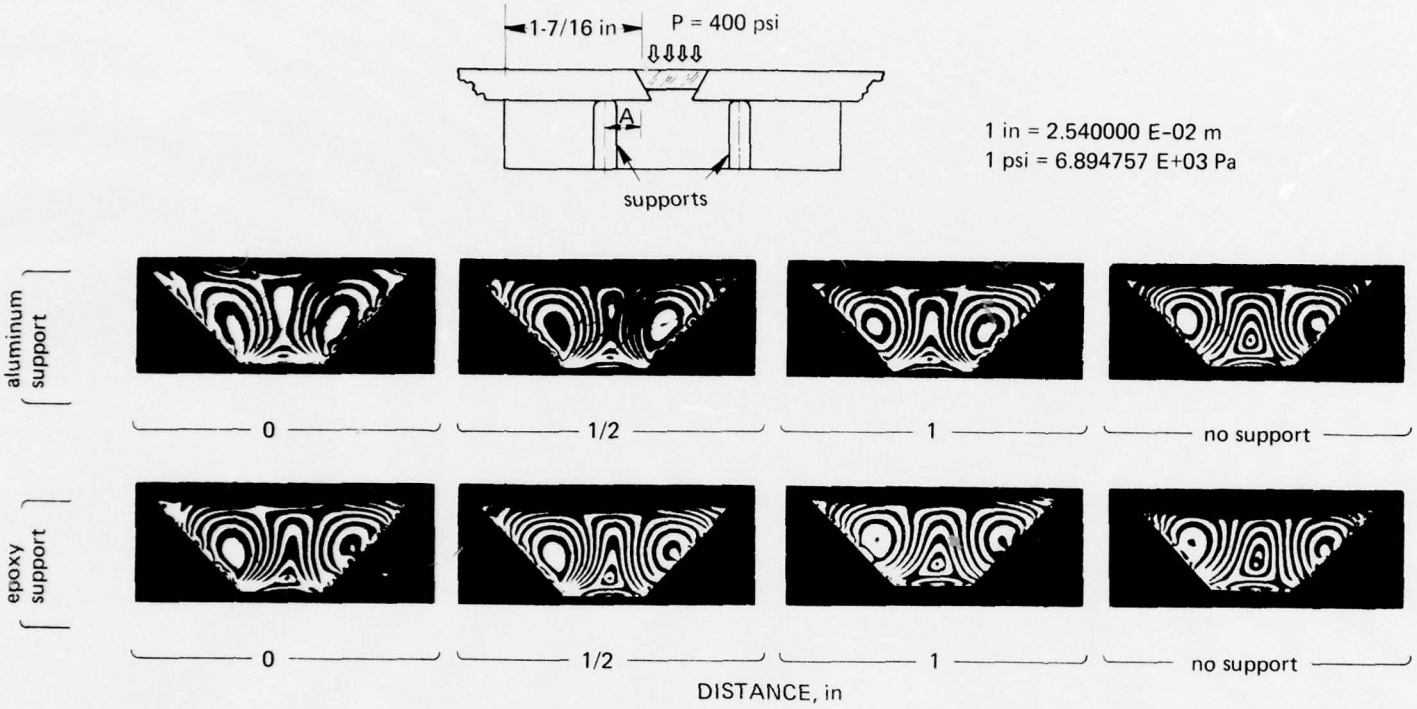

Figure 9.42. Effect of seat surface rotation on the magnitude and location of stresses in two-dimensional models of conical frustums under simulated hydrostatic loading. The number of photoelastic fringe concentrations at the center of the low-pressure face increases with increases in the seat surface rotation (reference 9.18).

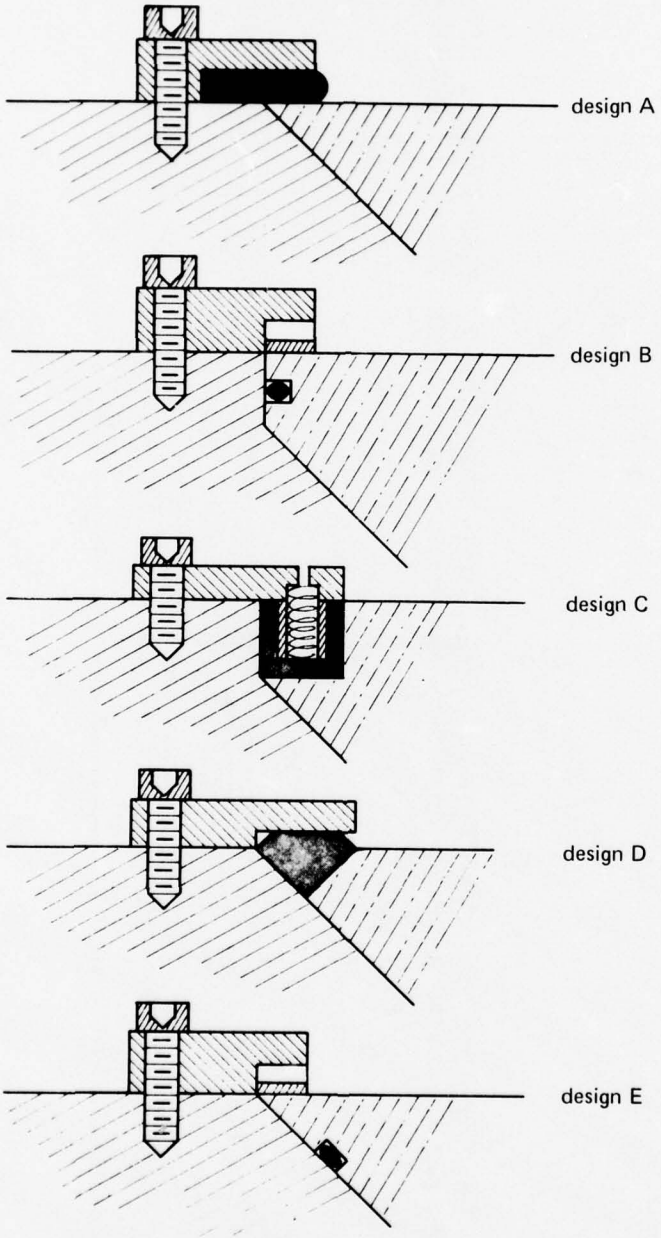

Figure 9.43. Typical seal designs for acrylic plastic frustums under external hydrostatic loading.

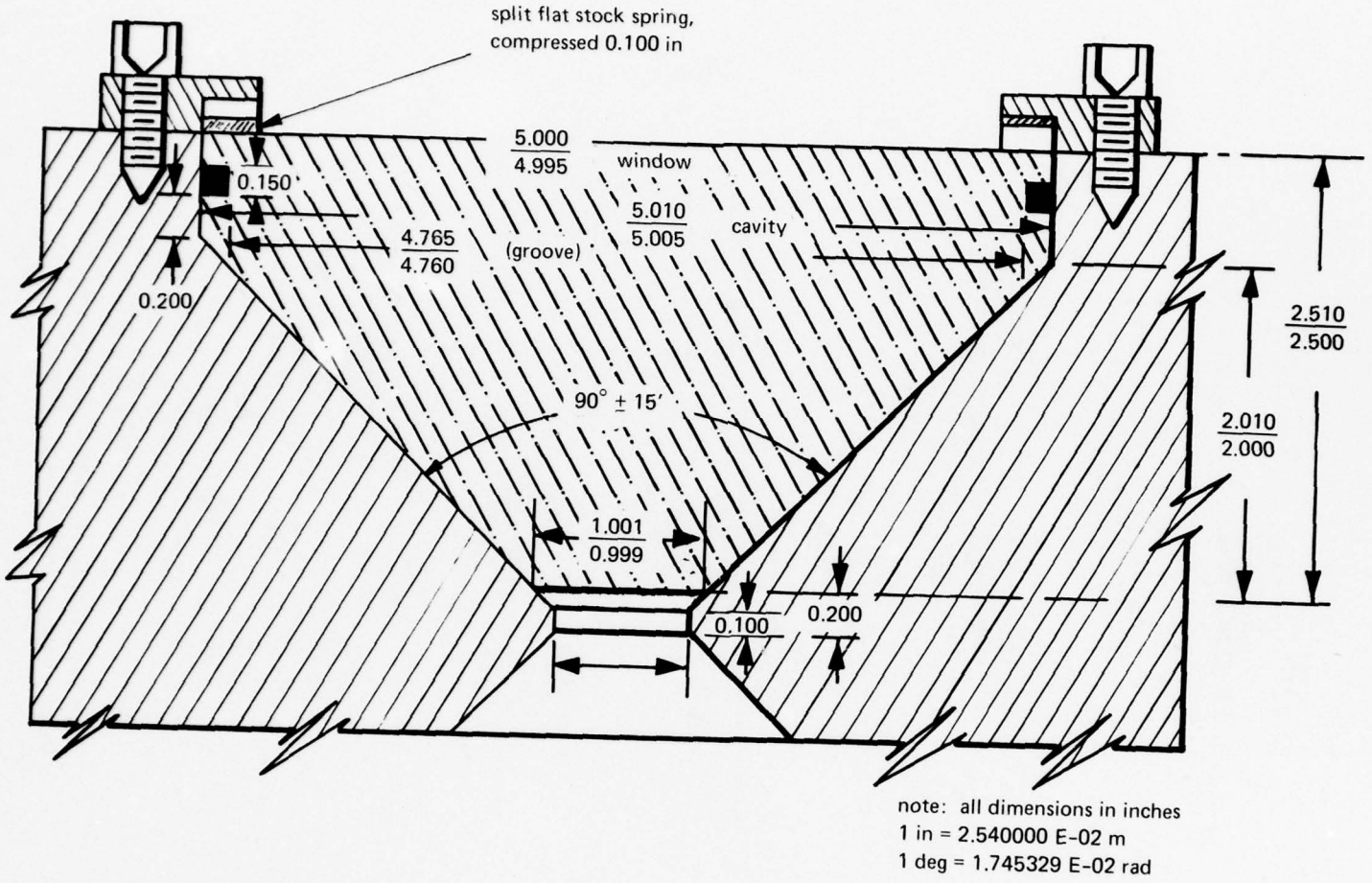

Figure 9.44. Existing seal design for conical frustum window at sustained loading of 20,000 pounds per square inch (138 megapascals) and ambient room temperature (reference 9.13).

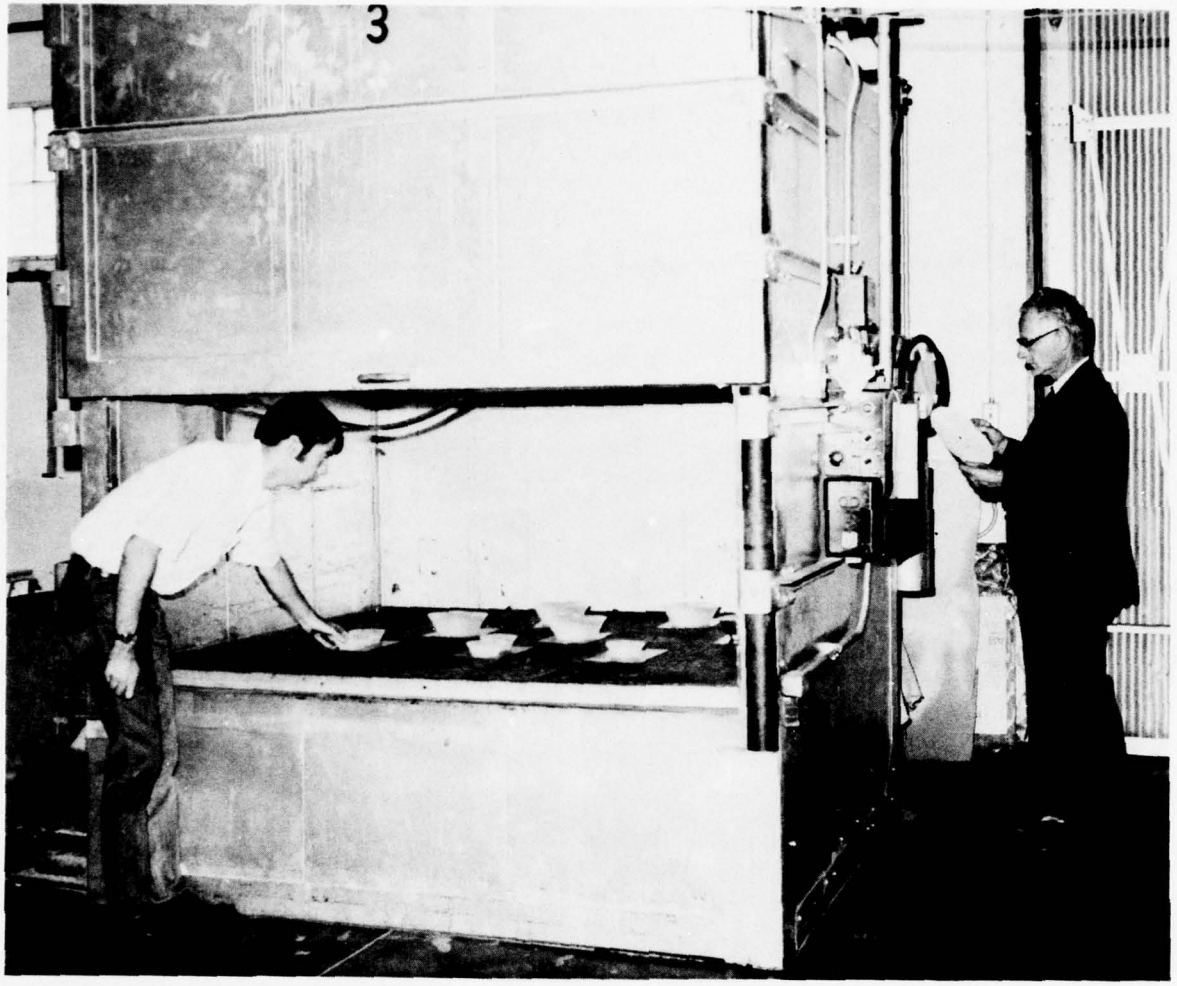

Figure 9.45. Annealing acrylic plastic conical frustum windows at the conclusion of the fabrication process. Temperature chart serves as a permanent record of the annealing cycle.

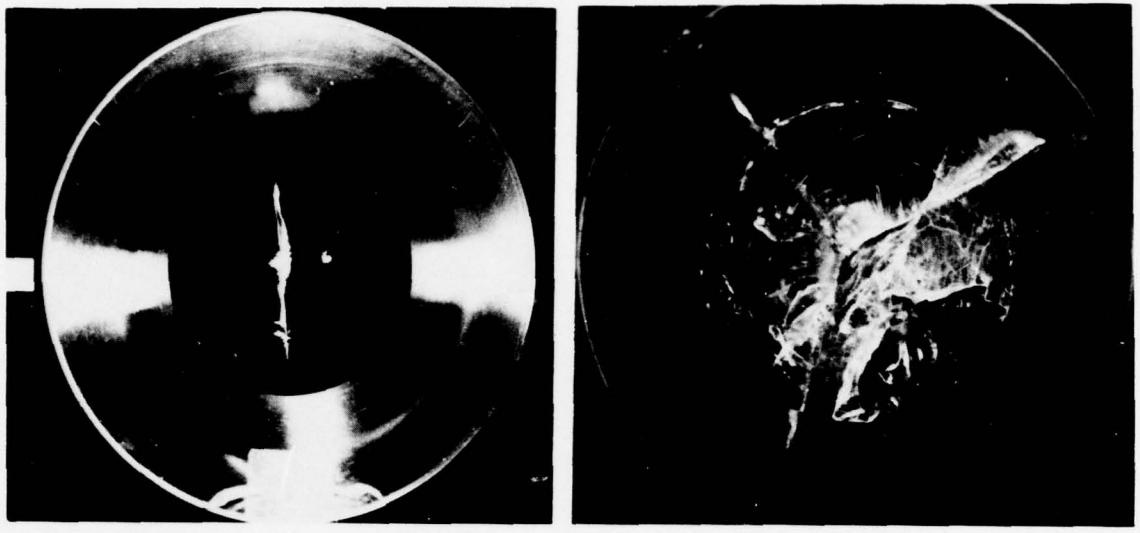

charge weight = 8.5 grams
standoff distance = 18 inches (45.7 centimeters)
peak overpressure = 3200 pounds per square inch (22 megapascals)
hydrostatic pressure = 0 pound per square inch (0 megapascal)

charge weight = 8.5 grams
standoff distance = 18 inches (45.7 centimeters)
peak overpressure = 3200 pounds per square inch (22 megapascals)
hydrostatic pressure = 2700 pounds per square inch (18.6 megapascals)

Figure 9.46. Results of dynamic pressure impulse loading on acrylic plastic conical frustums with identical dimensions ($t/D_i = 0.5$; conical angle = 90 degrees (15.7 radians); temperature = 54°F (12.2°C); and short-term critical pressure = 18,000 pounds per square inch (124 megapascals)). Note the presence of radial cracks on the low-pressure face that are initiated by a peak dynamic overpressure equal to 0.18 X short-term critical pressure (reference 9.17).

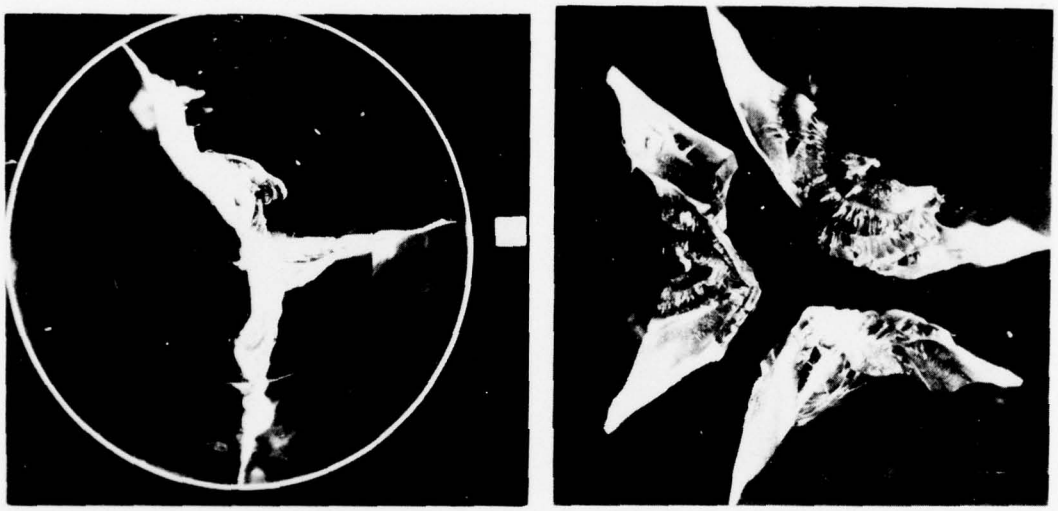

inside outside

charge weight = 14.6 grams
standoff distance = 12 inches (30.5 centimeters)
peak overpressure = 6200 pounds per square inch (42.8 megapascals)
hydrostatic pressure = 0 pound per square inch (0 megapascal)

Figure 9.47. Results of dynamic pressure impulse loading on acrylic plastic conical frustum (t/D_i = 0.5; conical angle = 90 degrees (1.57 radians); temperature = 54°F (12.2°C); and short-term critical pressure = 18,000 pounds per square inch (124 megapascals)). Note that the radial cracks initiating on the low-pressure face have completely penetrated the body of the window subjected to a peak dynamic overpressure equal to 0.35 × short-term critical pressure (reference 9.17).

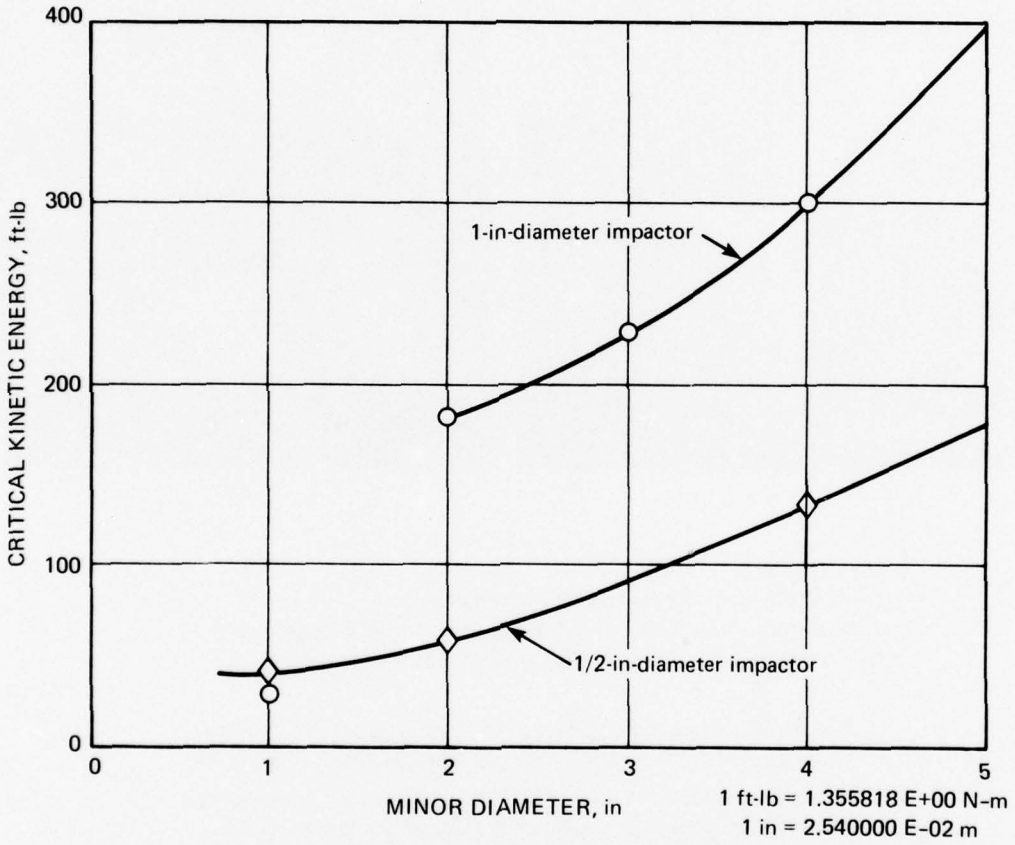

Figure 9.48. Effects of thickness, window diameter, and size of impactor on critical kinetic energy required to fracture 90-degree (1.57 radians) conical frustum windows with $t/D_i = 0.5$ at ambient 0-pound-per-square-inch (0 megapascal) pressure and 70°F (21°C) temperature. The larger and thicker windows are more impact resistant although the t/D_i ratio remains the same, and the impactors with greater radii require greater kinetic energy to fracture the window (reference 9.17).

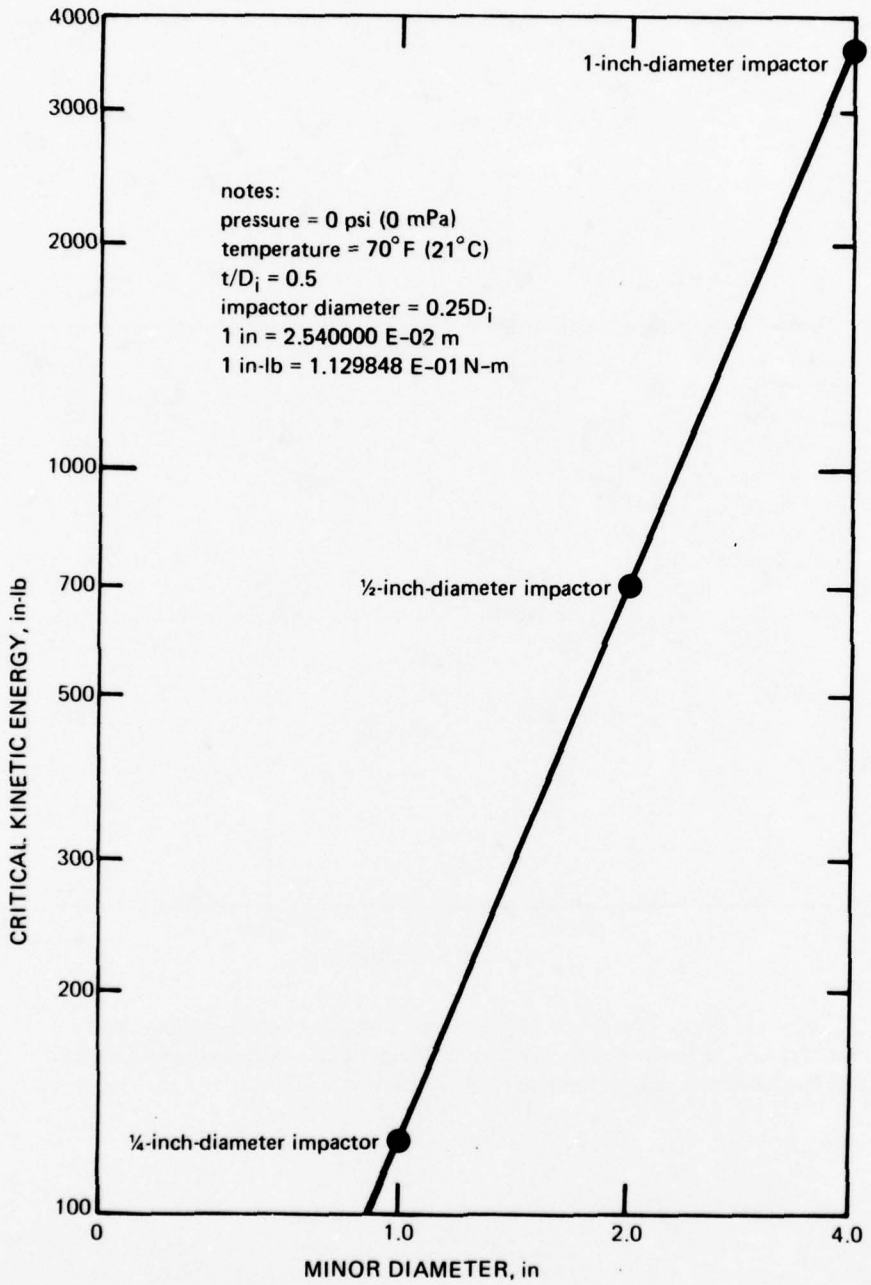

Figure 9.49. Plotting technique for extrapolating critical kinetic energies obtained with model-scale conical frustum test specimens to full-scale windows with the same t/D_i ratio. Note that the impactor diameter must always be equal to 0.25 D_i (reference 9.17).

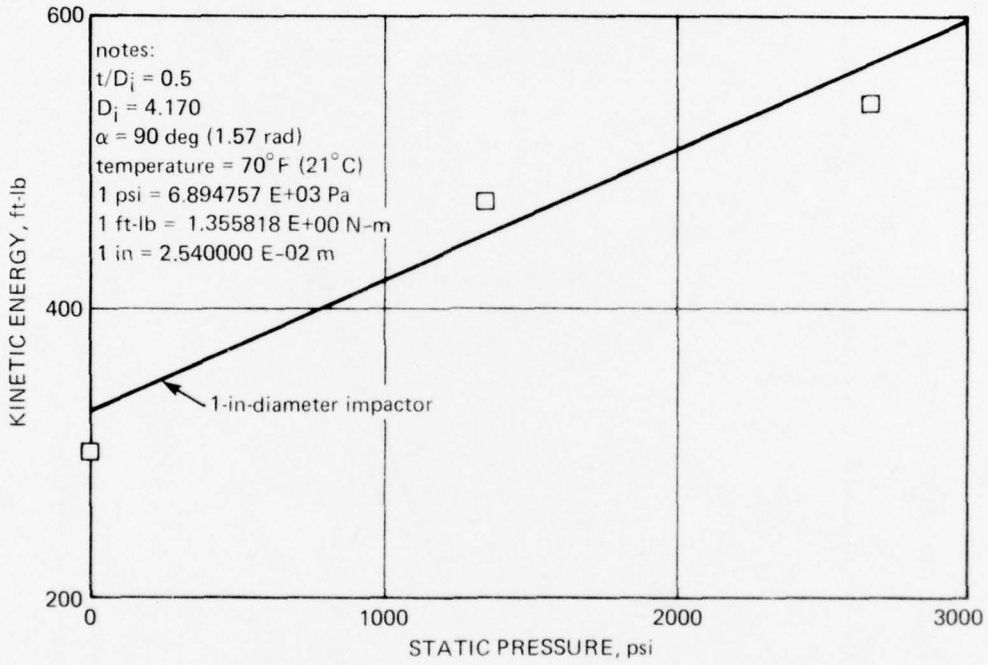

Figure 9.50. Effect of ambient static pressure on critical kinetic energy required to fracture conical acrylic plastic frustums. Note that the increase in pressure makes the frustums more impact resistant (reference 9.7).

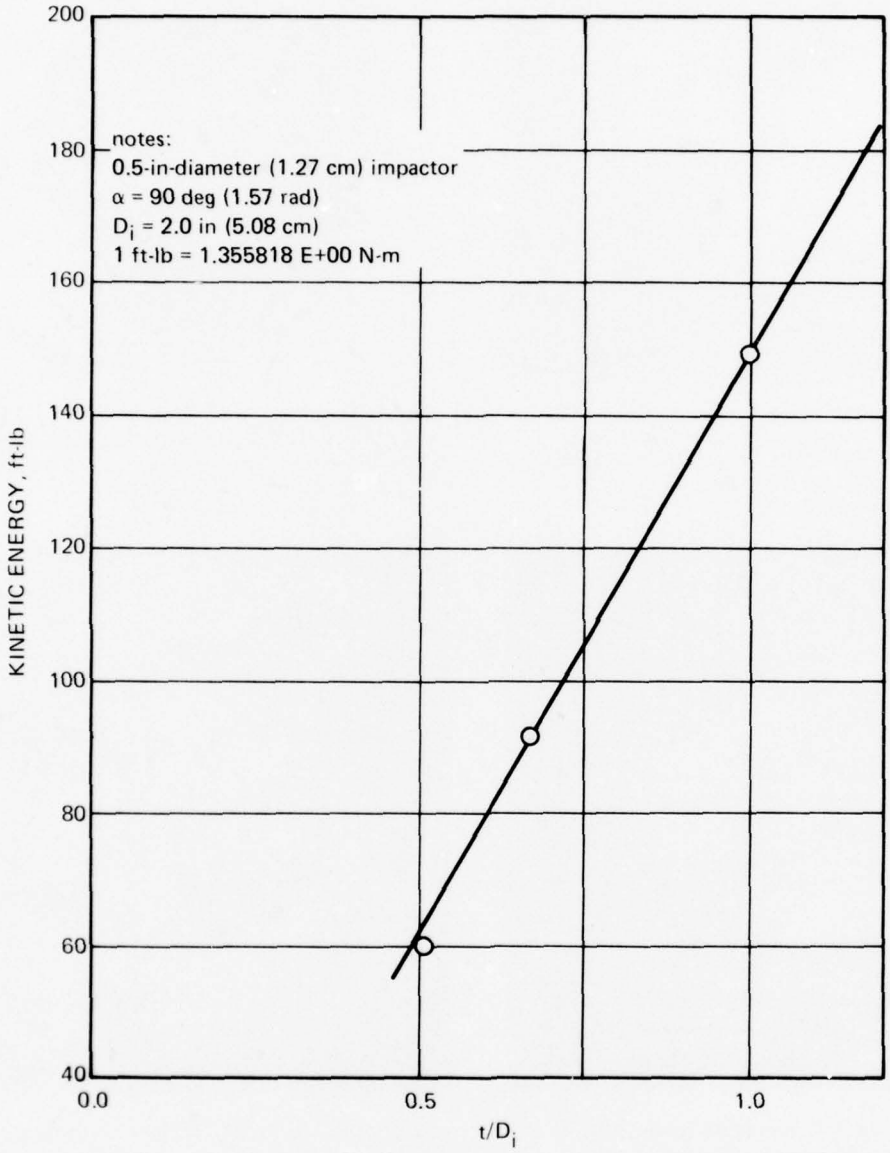

Figure 9.51. Effect of thickness on the impact resistance of conical frustums. Because the diameters of all windows are the same, the increase in impact resistance must be a function of thickness alone and not the t/D_i ratio (reference 9.7).

projectile radius = 0.125 inch (0.32 centimeter)
projectile weight = 50 pounds (22.7 kilograms)
pressure = 0 pound per square inch (0 megapascal)
critical velocity = 3.7 feet per second
(1.12 meters per second)

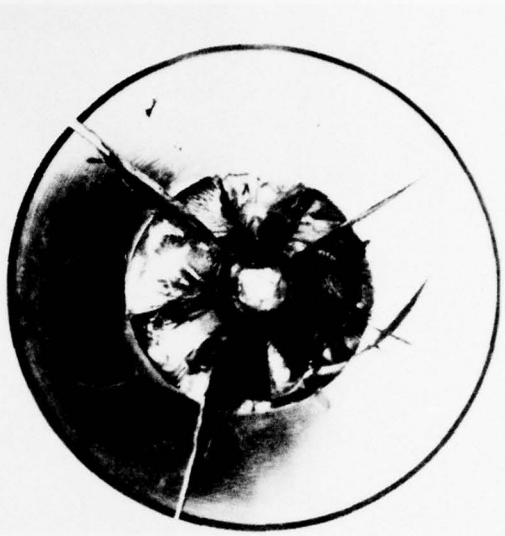

projectile radius = 0.25 inch (0.64 centimeter)
projectile weight = 50 pounds (22.7 kilograms)
pressure = 0 pound per square inch (0 megapascal)
critical velocity = 7.3 feet per second
(2.22 meters per second)

projectile radius = 0.375 inch (0.95 centimeter)
projectile weight = 50 pounds (22.7 kilograms)
pressure = 0 pound per square inch (0 megapascal)
critical velocity = 6.6 feet per second
(2 meters per second)

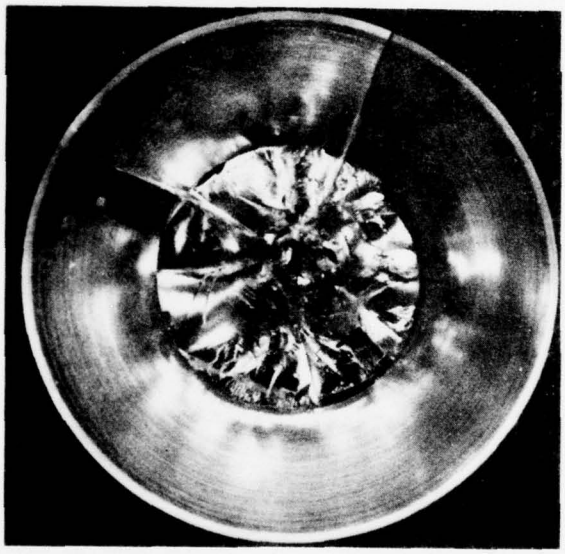

projectile radius = 0.5 inch (1.27 centimeters)
projectile weight = 50 pounds (22.7 kilograms)
pressure = 0 pound per square inch (0 megapascal)
critical velocity = 6.1 feet per second
(1.86 meters per second)

Figure 9.52. Fracture patterns in identical, acrylic plastic, 90-degree (1.57 radians) conical frustums impacted centrally on the high-pressure face with spherical projectiles of different diameters (t/D_i = 0.5, D_i = 1 inch (2.54 centimeters), temperature = 70°F (21°C)). Note the star-shaped cracks and spalling on the low-pressure face originating directly below the point of impact (reference 9.17).

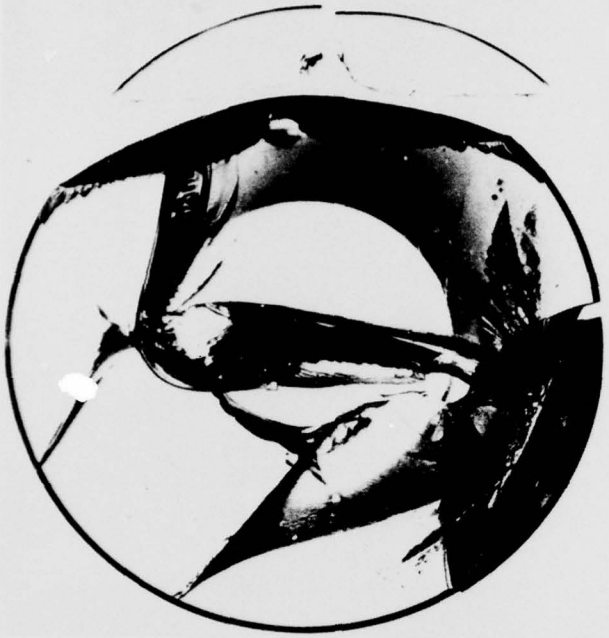

4-inch-inside diameter (10.2 centimeters) window
- 1-inch (2.54 centimeters) off-center impact
- *projectile radius* = 0.25 *inch* (0.64 centimeter)
- projectile weight = 100 pounds (45.4 kilograms)
- pressure = 15 pounds per square inch (0.1 megapascal)
- critical velocity = 5.8 feet per second (1.77 meters per second)

2-inch-inside diameter (5.08 centimeters) window
- 1.5-inch (3.81 centimeters) off-center impact
- projectile radius = 0.25 inch (0.64 centimeter)
- projectile weight = 100 pounds (45.4 kilograms)
- pressure = 15 pounds per square inch (0.1 megapascal)
- critical velocity = 4.1 feet per second (1.25 meters per second)

Figure 9.53. Fracture patterns in acrylic plastic 90-degree (1.57 radians) conical frustums impacted off-center on the high-pressure face with spherical projectiles. Note that an off-center impact does not create a star-shaped crack as a central impact does (reference 9.17).

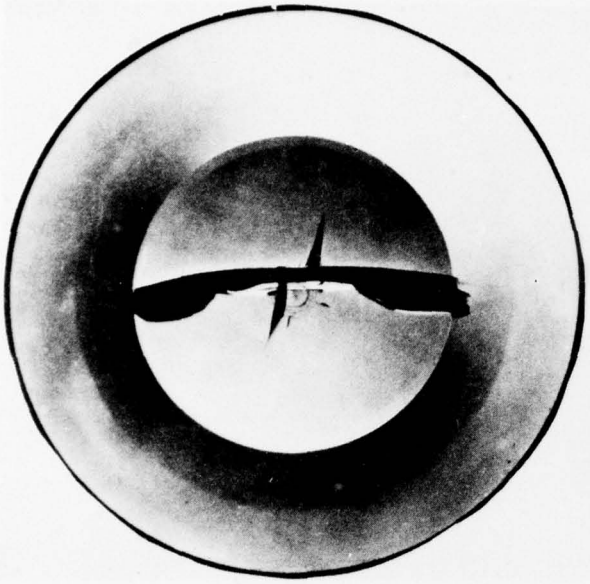

projectile radius = 0.5 inch (1.27 centimeters)
projectile weight = 200 pounds (90.7 kilograms)
pressure = 2667 pounds per square inch (18.4 megapascals)
critical velocity = 12.9 feet per second (3.9 meters per second)

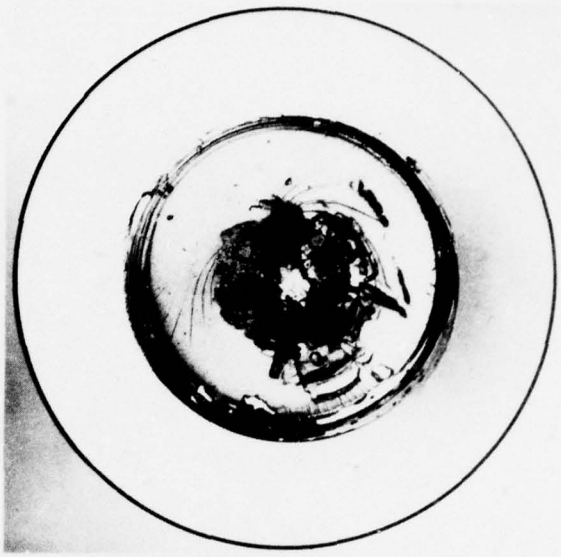

projectile radius = 0.5 inch (1.27 centimeters)
projectile weight = 100 pounds (45.4 kilograms)
pressure = 0 pound per square inch (0 megapascal)
critical velocity = 12.6 feet per second (3.84 meters per second)

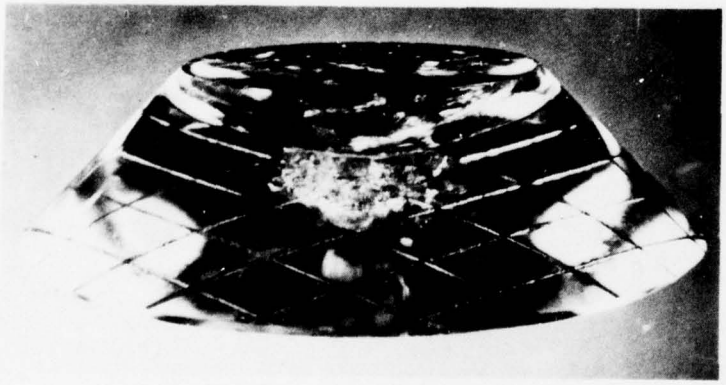

projectile radius = 0.5 inch (1.27 centimeters)
projectile weight = 200 pounds (90.7 kilograms)
pressure = 2667 pounds per square inch (18.4 megapascals)
critical velocity = 12.9 feet per second (3.9 meters per second)

Figure 9.54. Fracture patterns in acrylic plastic, 90-degree (1.57 radians), conical frustum windows centrally impacted on high-pressure face ($t/D_i = 0.5$, $D_i = 4$ inches (10.2 centimeters), temperature = 70°F (21°C)). Note that it requires significantly more kinetic energy to initiate fracture in a window under high ambient static pressure (reference 9.17).

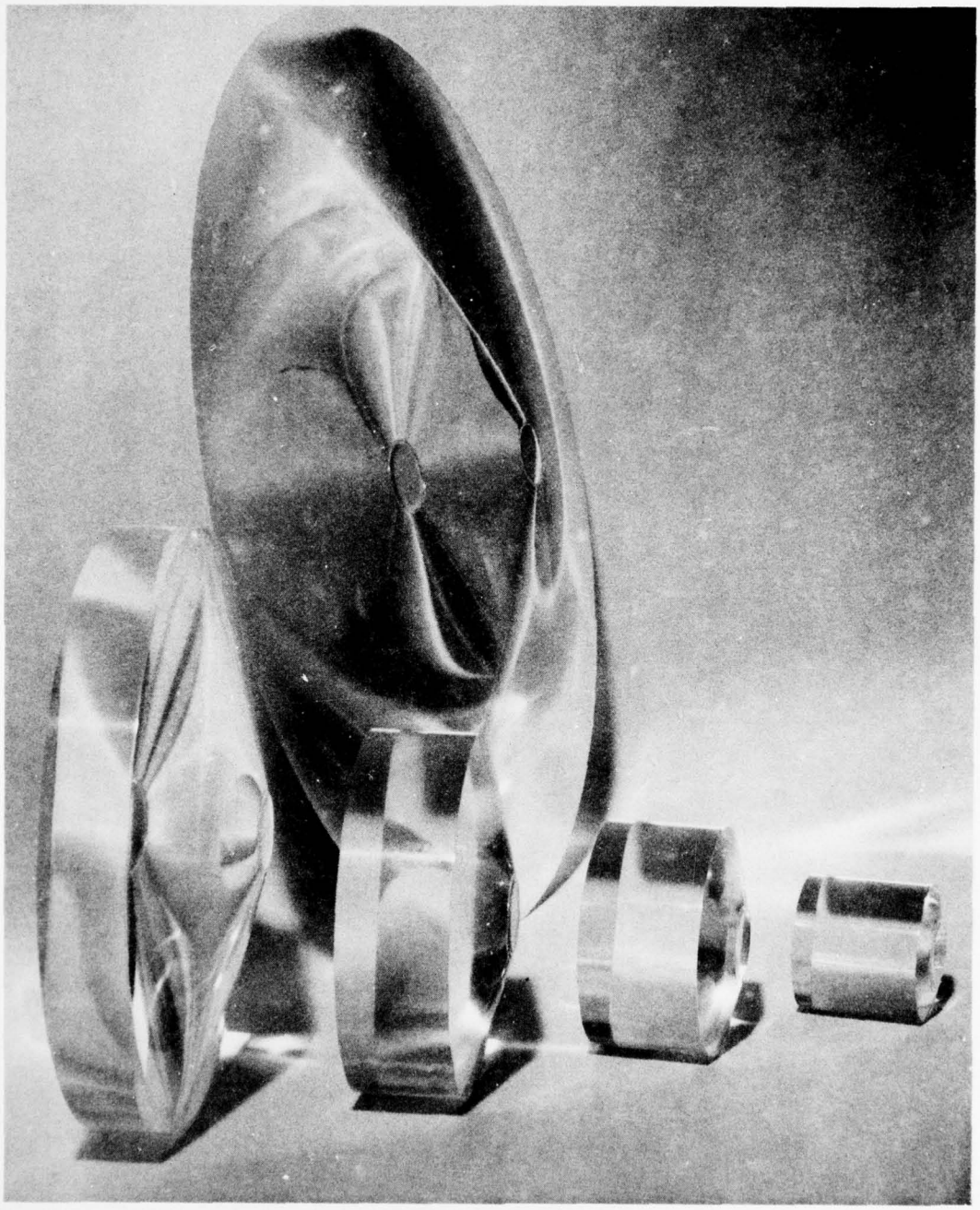

Figure 9.55. Series of conical frustums with 150-degree (2.08 radians) included angle and $t/D_i = 2$ whose edges have been modified by chamfers. The chamfers have a width of $\ell/t = 0.52, 0.72, 0.85, 0.92$, and 0.03. The axial displacement of all windows after 78 hours of sustained loading under 20,000 pounds per square inch (138 megapascals) and ambient room temperature was in the 0.068- to 0.077 inch (0.172 to 0.196 millimeter) range.

SECTION 10. PLANE DISC WINDOWS WITH TWIN CONICAL BEARING SURFACES . . . 10-1

10.1 INTRODUCTION . . . 10-1

10.2 STRUCTURAL PERFORMANCE . . . 10-2

10.3 MODES OF FAILURE . . . 10-3

10.4 CRITICAL PRESSURES . . . 10-3

10.4.1 Short-Term Loading . . . 10-3
10.4.2 Long-Term Loading . . . 10-3
10.4.3 Cyclic Loading . . . 10-6

10.5 SEATING . . . 10-6

10.6 SEALING . . . 10-8

10.6.1 Design A . . . 10-8
10.6.2 Design B . . . 10-8
10.6.3 Design C . . . 10-8
10.6.4 Design D . . . 10-8

10.7 FABRICATION . . . 10-9

10.8 RESISTANCE TO UNDERWATER EXPLOSIONS AND POINT-IMPACT LOADING . . . 10-9

10.9 CONCLUSION . . . 10-9

10.10 REFERENCE . . . 10-10

SECTION 10. PLANE DISC WINDOWS WITH TWIN CONICAL BEARING SURFACES

10.1 INTRODUCTION

As discussed in section 9, plane disc windows with a single conical bearing surface are extensively used for both high- and low-pressure loadings, if the pressure is always applied to the high-pressure face of the window. If pressure is applied intentionally or accidentally to the low-pressure face, the window tends to lift from its conical seat in the flange and only the restraint exercised by the retaining ring keeps it from being ejected. Since the edge of the window contacting the retaining ring is very thin, even a very low pressure will shear the edge of the high-pressure face. Because of this characteristic a plane disc window with a single conical bevel cannot serve successfully in a pressure vessel subjected to both external and internal pressures.

Pressure vessels which are designed for both internal and external pressure service require viewports that can withstand and seal off pressure applied to either face. This imposes a special requirement upon the design of the viewport. To date, three types of viewports have been developed for manned service with usage depending on operational requirements (figure 10.1). All are acceptable from structural and operational viewpoints.

The three designs differ significantly in acquisition, cost, bulk, and weight, characteristics which are of great interest to operators of diving bells, personnel transfer capsules, and submersibles with diver lockout capability. Of the three, the costliest, bulkiest, and heaviest assembly is the one that uses two plane discs with single conical bearing surfaces placed back-to-back in the mounting flange. The least expensive, but medium in bulk and weight, uses the single plane disc with plane bearing surfaces. The lightest and least bulky, but of medium cost, utilizes the plane disc with twin conical bearing surfaces.

The most obvious approach is to place two conical frustum windows back-to-back, but this design has several disadvantages. The chief problem is that two metal supporting frames must be used, each thicker than the two lenses. The additional cost of the lenses and frames is significant, and the additional weight can be even more important. When the objective is to have a positively buoyant bell, each pound of bell weight above a set amount must be offset by external flotation. Since existing syntactic foams are about half the specific gravity of water, 1 pound (0.45 kilogram) is added to the dry weight of the bell for each pound of buoyancy. This additional weight must then be accounted for when considering the dynamic loading on the padeyes, lift wire, winch, and bell launch-and-recovery equipment on the deck of the boat or platform. Another problem is that water invariably manages to get between the lenses. The resultant fogging and corrosion can in a short time decrease visibility through the viewport to the point where it loses any value as an observation window.

By using a design with only a single disc window with plane bearing surfaces, the weight and bulk disadvantage can be reduced and fogging eliminated. Plane acrylic discs with plane bearing surfaces were used in early designs for relatively shallow depths, but because of the presence of high tensile stresses in service and the subsequent thickness of acrylic required to reduce them, the weight saving in the window-flange assembly was nominal. Sealing problems also occurred because of the requirement for hard gaskets on both sealing-bearing surfaces. What finally gave the third design, the plane disc with twin conical bearing surfaces, its advantages was its superior structural performance and positive sealing capability (figure 10.2). This structural superiority over the competing window is derived from the twin conical bearing surfaces that superimpose radial compression on the pressure-generated flexure moment in the disc. As a result, radial compressive stress is superimposed upon the tensile component of the flexure stress. Thus the magnitude of principal tensile stress in the center of the low-pressure face on the twin-beveled disc is always lower than in a disc with plane bearing surfaces. As one increases the t/D_i ratio of twin-beveled plane discs, the magnitude of tensile stress decreases until it disappears completely ($t/D_i \geqslant 0.5$). This is not the case in plane discs with plane bearing surfaces, where the principal tensile stresses on the low-pressure face cannot be eliminated by increasing the magnitude of t/D_i ratio.

The fact that the tensile stress in a twin-beveled plane disc is always less than in a disc with plane bearing surfaces has significant structural value, since the lower tensile stresses make the window more resistant to point-impact and dynamic overpressure loadings. In this respect the viewport with a twin-beveled plane disc window behaves like the viewport with two single-beveled disc windows, except that it is half the cost, weight, and bulk. It is this combination of low cost, low weight, low bulk, and decreased magnitude (or total absence if $t/D_i > 0.5$) of tensile stresses that makes viewports with these windows so attractive to designers, fabricators, and operators of pressure vessels for internal and external pressure service (figure 10.3).

10.2 STRUCTURAL PERFORMANCE

A plane disc window with twin conical bearing surfaces behaves under pressure basically as a plane disc window does with a single conical bearing surface. Because of the conical bearing surface, the principal strain at the center of the low-pressure face is positive for t/D_i less than 0.5 and negative for t/D_i greater than or equal to 0.5. Its magnitude is approximately the same as the principal strain measured at the center of the low-pressure face on a plane disc with a single conical bearing surface and the same included conical angle and t/D_i ratio for two reasons: (1) the same resistance to bending moment and (2) the presence of the same radial forces.

The major difference between plane disc windows with a single conical bearing surface and those with twin conical bearing surfaces lies in the magnitude of bearing stresses acting on the conical bevel. These stresses in the plane disc with twin conical bearing surfaces are higher because the surface area of the bearing surface is less than half of that on windows with a single conical bevel (figure 10.4). Since the magnitude of bearing stresses on the conical surface varies with distance from the low-pressure face, the loss of the bearing surface between the high-pressure face and the midplane of the window does not double the bearing stresses on the remaining bearing surface, but only increases them insignificantly (compare figure 10.5 with figure 9.4). Because this increase is insignificant, the fatigue life of the bearing surface on a window with twin conical bevels is about the same as that of a

bearing surface on a window with a single conical bevel, i.e., cracks will not appear significantly sooner on the bearing surface.

A finite-element stress analysis performed for a range of t/D_i ratios in plane discs with twin conical bearing surfaces shows that like plane discs with a single conical bearing surface the magnitude of the peak bearing stress for a given hydrostatic loading does not decrease with an increase in the t/D_i ratio at the same rate as the maximum compressive stress does at the center of high-pressure face (figures 10.5, 10.6, and10.7 and table 10.1) (reference 10.1). Because of this phenomenon, the crack-free cyclic fatigue life of plane disc windows with twin conical bearing surfaces decreases with an increase in t/D_i ratio, if the windows are pressure cycled in all cases at the same fraction of the window's short-term critical pressure. For this reason the conversion factors of table B2 in section 15 are, in terms of crack-free cyclic bearing surface life, overly conservative for low t/D_i ratios and somewhat marginal for high t/D_i ratios. However, since for low t/D_i ratios the catastrophic failure is not initiated at the bearing surface, but at the center of low-pressure face, the conservatism of conversion factors for bearing surface cracking does not make thin windows overdesigned in comparison to thick windows.

10.3 MODES OF FAILURE

Plane disc windows with twin conical bearing surfaces fail in the same manner as plane disc windows do with a single conical bearing surface (figure 10.8). Thin windows fail primarily in flexure, while thick ones fail by the formation of a shear surface in the shape of a cone whose apex intersects the center of the high-pressure face while the diameter of the low-pressure face intersects the conical bearing surface. Because of this, both the faces and conical bearing surfaces must be free of crack initiators, e.g., scratches, O-ring grooves, machining marks, or crazing.

10.4 CRITICAL PRESSURES

10.4.1 Short-Term Loading

Under short-term loading, critical pressures of plane discs with twin conical bearing surfaces for many t/D_i ratios and included angles are about the same as they are for plane discs with a single conical bearing surface, if the included angle and t/D_i ratio are the same (table 10.2). For this reason, all empirical curves relating short-term critical pressure to the t/D_i ratio and included angle of plane discs with a single conical surface can be used with a high degree of confidence for predicting the critical pressures of plane discs with twin conical bearing surfaces (table 10.2, figures 10.9, 10.10, and 10.11, and sections 9 and 15).

10.4.2 Long-Term Loading

Experimental data do not exist for plane windows with twin conical bearing surfaces under long-term pressure loading. For this reason it is not definitely known whether the critical pressures and displacements are the same as they are for plane disc windows with a single conical bearing surface. However, based on the fact that the short-term critical pressures and displacements are the same, it is highly probable that they are also equal for long-term loading.

Table 10.1. Peak stresses and displacements calculated for typical acrylic plastic discs with twin conical bearing surfaces under short-term hydrostatic loading.

α, deg	t/D_i	Boundary Condition		σ_x, psi	σ_y, psi	σ_{hoop}, psi	Axial displacement, in
90	0.23	fixed edge	σ, maximum	2204.5	1404.3	2204.5	
			σ, minimum	-5261.2	-6611.3	-5261.2	
			displacement, maximum				0.0534
		free-sliding edge	σ, maximum	1299.3	260.0	1299.3	
			σ, minimum	-5992.7	-5792.1	-5344.6	
			displacement, maximum				0.0512
90	0.46	fixed edge	σ, maximum	588.8	8.9	588.8	
			σ, minimum	-2595.6	-2818.7	-2595.6	
			displacement, maximum				0.0185
		free-sliding edge	σ, maximum	-342.9	9.5	-308.5	
			σ, minimum	-2469.3	-2335.5	-2469.3	
			displacement, maximum				0.0196
90	1.00	fixed edge	σ, maximum	157.1	-6.4	156.5	
			σ, minimum	-1571.7	-1872.6	-1571.7	
			displacement, maximum				0.0109
		free-sliding edge	σ, maximum	-394.8	17.4	-537.2	
			σ, minimum	-1788.0	-1736.9	-1857.2	
			displacement, maximum				0.0142

Notes:
1. Hydrostatic pressure is applied only to one face of the window.
2. All calculated values are valid only for short-term pressurization at 75°F (24°C).
3. Physical constants for acrylic plastic are E = 444,000 pounds per square inch (3061 megapascals) and Poisson's ratio = 0.4.
4. 1 deg = 1.745329 E-02 rad.
5. 1 psi = 6.894757 E+03 Pa.
6. 1 in = 2.540000 E-02 m.

Table 10.2. Experimental evaluation of twin-beveled plane disc windows under short-term pressure loading at ambient room temperature.*

Specimen	D_o, in	t/D_i	ℓ/t	α, deg	P_{cf}, psi	STCP, psi	$STCP/P_{cf}$	T, °F
9	3.520	0.230	0.250	90	5000	5640	1.128	70.0
10	3.720	0.320	0.250	90	9000	10,640	1.180	69.5
11	4.020	0.317	0.120	90	9000	9300	1.030	72.0
12	3.250	0.423	0.120	90	13,600	13,780	1.010	74.0
13 through 18	10.310	0.308	0.116	90	8800	9400 (average)	1.070	72.0 (average)
19	3.820	0.210	0.250	120	3000	4605	1.535	69.0
20	4.130	0.290	0.250	120	7000	9455	1.350	70.0
21	3.337	0.260	0.250	60	5000	6540	1.308	69.0
22	3.461	0.355	0.250	60	8000	9455	1.180	69.0
23 through	10.500	0.363	0.250	90	10,500	>10,000 (average)	1.000	74.0

* If $STCP/P_{cf} > 1$, the critical pressures of the twin beveled plane disc windows exceed the minimum critical pressures of single bevel disc windows with identical t/D_i ratios.

Notes:

D_o = major diameter, inches.

t = overall thickness, inches.

ℓ = width of cylindrical surface, inches.

D_i = minor diameter, inches.

α = included conical angle, degrees.

T = ambient test temperature, °F.

P_{cf} = experimentally determined, average catastrophic failure pressure of an equivalent window with a single bevel and identical t/D_i and α, pounds per square inch.

STCP = experimentally determined short-term critical pressure of the test specimen with twin bevels, pounds per square inch.

$STCP/P_{cf}$ = relationship between experimentally established short-term critical pressure of test specimen with twin bevels and the catastrophic failure pressure of equivalent windows with twin bevels.

Material: Plexiglas G satisfying requirements of ANSI/ASME PVHO-1.

1 in = 2.540000 E-02 m.

1 deg = 1.745329 E-02 rad.

1 psi = 6.894757 E+03 Pa.

$1^{\circ}_{C} = (t^{\circ}_{F} - 32)/1.8$.

10.4.3 Cyclic Loading

Experimental data exist only for three t/D_i ratios and included angles ($t/D_i = 0.26$, $\alpha = 60$ degrees (1.04 radians); $t/D_i = 0.23$, $\alpha = 90$ degrees (1.57 radians); $t/D_i = 0.21$, $\alpha = 120$ degrees (2.09 radians)) under cyclic pressure loading (table 10.3). For these values, the ultimate fatigue life of a plane disc window with twin conical bearing surfaces appears to be essentially the same as it is for plane disc windows with a single conical bearing surface. Whether this is also true for other t/D_i ratios and included angles is not positively known. It can be postulated that the fatigue life of discs with twin conical bevels is probably either the same or a little less than it is for discs with a single bevel for the entire range of t/D_i ratios and included angles, although the bearing stresses in the conical surface are somewhat higher. The reasons appear to vary with the magnitude of the t/D_i ratio. At low t/D_i ratios ($\leqslant 0.25$), cyclic fatigue failure is caused by a crack initiated at the center of the low-pressure face; thus the higher bearing stresses have only an insignificant effect on the magnitude of crack-initiating stress at the center of the face. At intermediate and high t/D_i ratios, however, failure is caused by the formation of a conical shear fracture surface initiated on the conical bearing surface at approximately midheight of the window. The removal of material from the window by the second conical bevel that otherwise would shear off during formation of primary conical shear fracture eliminates formation of the primary, but not secondary, fracture cones (formation of these fractures was discussed in section 9.3.1.2).

Since the formation of the secondary fracture cone is generally accompanied by loss of pressure sealing ability, it is only at this point that the window is considered to have failed. Because this cone probably forms after the same number of pressure cycles, regardless of whether the disc has a single or twin conical bevel, its ultimate fatigue life is probably the same. This, of course, does not mean that fatigue cracks may not form sooner on the bearing surface of windows with a single bevel, it only means that catastrophic failure will not. Experimental verification of these postulates remains to be performed.

There is no doubt, however, that O-ring grooves cannot be incorporated into the bearing surface, as is the case with discs equipped with a single bevel (figure 10.12). The use of O-ring grooves will initiate the formation of a conical shear surface, as the locations of the groove and of the shear cone base coincide (figure 10.13).

10.5 SEATING

The precautions discussed in section 9 for plane discs with a single conical bevel must be used when seating discs with twin conical bearing surfaces. In some respects the seating of windows with twin conical bearing surfaces requires closer machining tolerances for both the window and the seat, i.e., the window must not only be securely restrained against pressures applied to either side, but it also must seal reliably regardless of the side to which pressure is applied.

The seat in the flange and the retaining ring must provide adequate overhang (D_i/D_f), regardless of which side of the window is pressurized (figure 10.14). The magnitude of overhang, in absence of any other data, should be based on data generated by testing plane discs with a single conical bevel (see sections 9 and 15 and appendix B). However, the designer should treat these values as minima, since the displacement of plane disc windows with twin conical bevels may in many cases be somewhat larger than that for conical frustums.

Table 10.3. Experimental evaluation of twin-beveled plane disc windows under cyclic pressure loading at ambient room temperature.*

Specimen	D_o, in	t/D_i	ℓ/t	P_{cr}, psi	DP, psi	P_{cr}/DP (CF)	α, deg
1	3.520	0.230	0.250	3000	500	6	90
2	3.720	0.320	0.250	6000	500	12	90
3	3.737	0.308	0.116	5500	500	11	90
4	3.616	0.308	0.250	5500	500	11	90
5	3.337	0.260	0.250	3000	500	6	60
6	3.461	0.355	0.250	6000	500	12	60
7	3.820	0.210	0.250	3000	500	6	120
8	4.130	0.290	0.250	6000	500	12	120

* There was a total absence of cracks or surface crazing at the conclusion of 1000 pressure cycles, indicating that the cyclic fatigue life of these windows exceeded 10,000 cycles.

Notes:

Description of Pressure Cycling Program

Total number of pressure cycles = 1000

Pressure phases	Minimum	Average	Maximum
Pressure at beginning, psi	490	554.6	600
Pressure at termination, psi	250	502.9	730
Duration, hours	2	6.8	58
Temperature, °F	60	74.8	92
Relaxation phases			
Duration, hours	2	6.3	36
Temperature, °F	60	74.8	90

D_o = major diameter, inches.

t = overall thickness, inches.

D_i = minor diameter, inches.

ℓ = width of cylindrical surface, inches.

P_{cr} = short-term critical pressure, calculated on the basis of ANSI/ASME PVHO-1, psi

DP = design pressure, psi.

Material = Plexiglas G satisfying requirements of ANSI/ASME PVHO-1.

1 in = 2.540000 E-02 m.

1 psi = 6.894757 E+03 Pa.

1 deg = 1.745329 E-02 rad.

$1^\circ_C = (t^\circ_F - 32)/1.8$

10.6 SEALING

Plane disc windows with twin conical bearing surfaces require a special seal for satisfactory performance. The design must not only perform satisfactorily against pressure acting on either side of the window, but also when the pressures acting on the window are almost equal in magnitude, e.g., a lockout chamber during lockout of divers at design depth. Several designs have been developed for this application and experimentally evaluated either in the laboratory or in service (figures 10.15, 10.16, 10.17, and 10.18).

10.6.1 Design A

Design A (figure 10.15) is considered the least desirable from both structural and sealing viewpoints. The O-ring grooves in the conical bearing surfaces serve as crack initiators and thus significantly lower the cyclic fatigue life of the window. Furthermore, because of the difference in the temperature expansion coefficients, it is very difficult to keep both O-rings under axial compression through a wide range of temperatures and service pressure loading scenarios. Once the precompression on O-rings is lost, the window assembly will leak.

10.6.2 Design B

Design B (figure 10.16) is very satisfactory for sealing, but only partially satisfactory structurally. The O-ring groove in the vertical edge of the window's circumference is not as bad a stress riser as it is in design A. However, under an adequately high stress level, it will serve as a crack initiator. This will generally occur only at a pressure level above the rated working pressure, but still significantly below the short-term critical pressure level.

10.6.3 Design C

Design C (figure 10.17) is the most satisfactory. It does not serve as a crack initiator in the window, and it also allows for looser machining tolerances of the window thickness because the O-ring is under radial compression augmented by axial squeezing. It will seal adequately even when the window has displaced axially from its neutral position. Since the O-ring relies for its sealing action on the initial radial and axial compressions, care must be taken during design to allow for radial contraction of the acrylic window because of the -40°F (-40°C) external ambient temperature experienced by diving systems in arctic environments prior to their submersion in the +28°F (-2°C) Arctic Ocean. The oversized windows will cause some difficulties when they are mounted in the chamber at room temperature, unless the windows are precooled to at least -40°F (-40°C) prior to assembly. Considerable care must also be exercised in the selection of materials for the O-rings, as many of the standard materials loose their elastomeric properties at such low temperatures.

10.6.4 Design D

From sealing and structural viewpoints, design D (figure 10.18) is about as satisfactory as design C. It is, however, less desirable from fabrication, assembly, and maintenance viewpoints. The bottom of the deep O-ring groove is not easily visible even when the window and O-ring are removed, which makes incipient rusting and pitting hard to detect. Even if rusting is detected, it is very difficult to remove.

10.7 FABRICATION

Fabrication of plane disc windows with twin conical bearing surfaces is easier to accomplish than it is for conical frustums, as the cylindrical area around the circumference of the window allows it to be held in the chuck of a lathe without special tooling. The same angular tolerances must be maintained during machining as they are for plane discs with a single bevel. The dimensional tolerance on the major diameter of the window, however, must be tighter than for conical frustums to ensure proper radial compression of the O-ring between the outer diameter of the window and the inside surface of the seat even at low operational temperatures.

10.8 RESISTANCE TO UNDERWATER EXPLOSIONS AND POINT-IMPACT LOADING

There are presently no experimental data on the performance of plane disc windows with twin conical bearing surfaces when subjected to underwater explosions and point-impact loadings. However, it can be postualted with a high degree of confidence that the window behaves like a conical frustum window. This postulate is based on the fact that the short-term critical pressure of plane discs with twin conical bearing surfaces is the same as it is for plane discs with a single conical bearing surface. Since failures of windows under point-impact loading and underwater explosions are short-term phenomena, there is no reason to believe that the response of discs with twin conical bevels will differ from that of discs with single conical bevels.

It is also believed that discs with twin bevels are probably better suited to resist point impacts or underwater explosions than are discs with a single level. Under point-impact loading the twin-beveled disc should be more impact resistant, since only the thickest area of tne disc is exposed to impact while the vulnerable thin edge of the disc is protected by the metallic seat. The resistance to underwater explosions should also be higher because the dynamic overpressure can only act on a small central area on the high-pressure face. Still, in absence of any experimental data to confirm this postulate, it is prudent to assume that the resistance of discs with twin bevels does not exceed that of discs with a single conical bevel.

10.9 CONCLUSION

The maximum safe operational pressure of plane disc windows with twin conical bearing surfaces and a cylindrical sealing surface with a width of $l/t \leqslant 0.25$ can be specified on the basis of design criteria developed in the ANSI/ASME PVHO-1 Safety Standard for plane disc windows with a single conical bearing surface (section 15). The t/D_i ratio depends on the magnitude of the specified design pressure (safe maximum operational pressure), design temperature, and included conical angle. Depending on the value of the design temperature, different conversion factors are selected for calculating the required short-term critical pressure (table B2 in appendix A of the ANSI/ASME PVHO-1 Safety Standard). For example, a design pressure of 500 pounds per square inch (3.45 megapascals) at 75°F (24°C) calls for a conversion factor of 6, which results in a specified short-term critical pressure of 3000 pounds per square inch (20.7 megapascals) (500 X 6 = 3000). Once the short-term critical pressure is calculated, then the minimum t/D_i ratio needed to meet this requirement is determined by using the design curves in figures B3 and B4 in appendix A of the ANSI/ASME PVHO-1 Safety Standard. In this case the t/D_i ratio (90-degree (1.57 radians) included angle) is 0.23.

10.10 REFERENCE

10.1 Stachiw, J. D., Smith, N. E. and Burnside, O. H., "Structural Performance of Acrylic Plastic Plane Disc Windows with Twin Conical Bearing Surfaces," American Society of Mechanical Engineers, Paper No. 77-WA/OcE-1, December 1977.

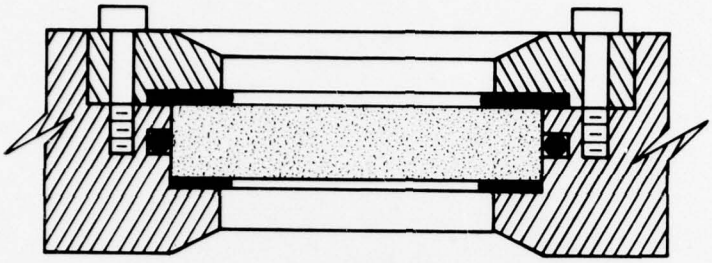

plane disc
with plane bearing surfaces

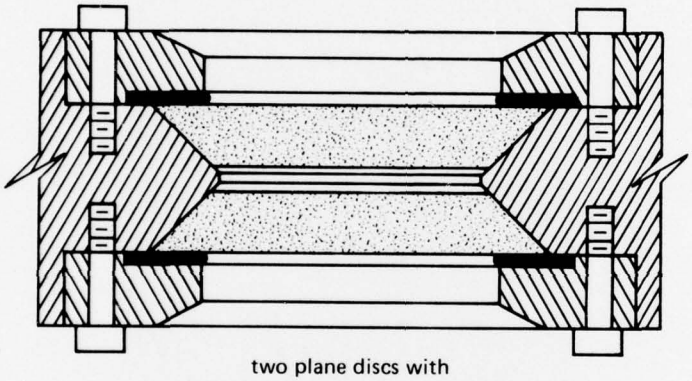

two plane discs with
single conical bearing surfaces

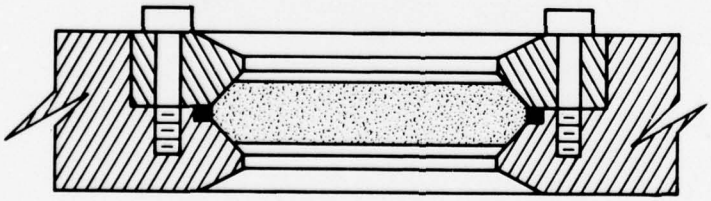

plane disc
with twin conical bearing surfaces

Figure 10.1. Proven design concepts for viewports in pressure hulls subjected to both internal and external pressures.

Figure 10.2. Typical twin beveled plane disc window, i.e., window with twin conical bearing surfaces.

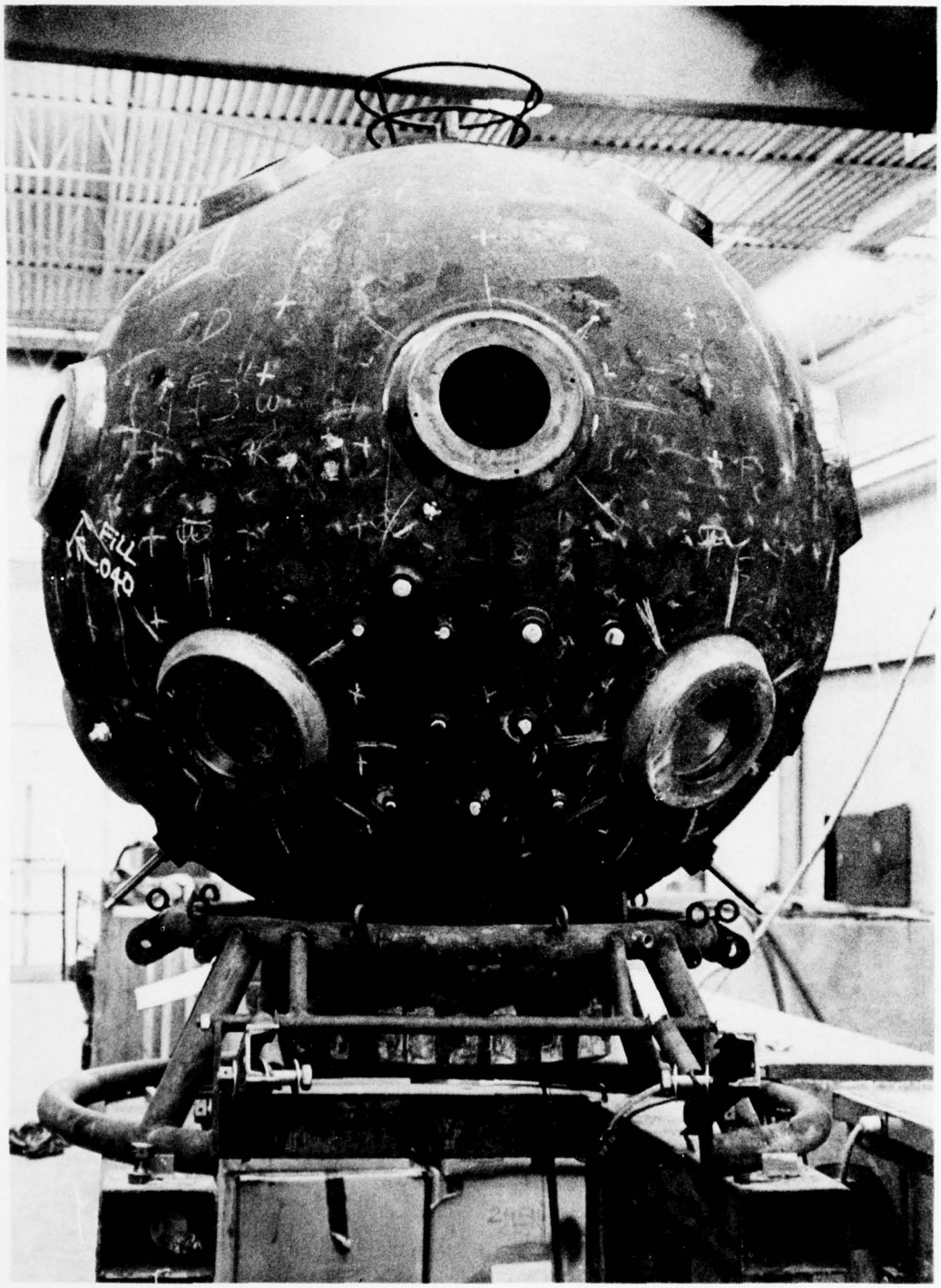

Figure 10.3. Typical diving bell with twin-beveled plane disc windows. Built by Southwest Research Institute for the Sub-Sea International. Note the small bulk of mountings for 8-inch-diameter (20 centimeters) viewports.

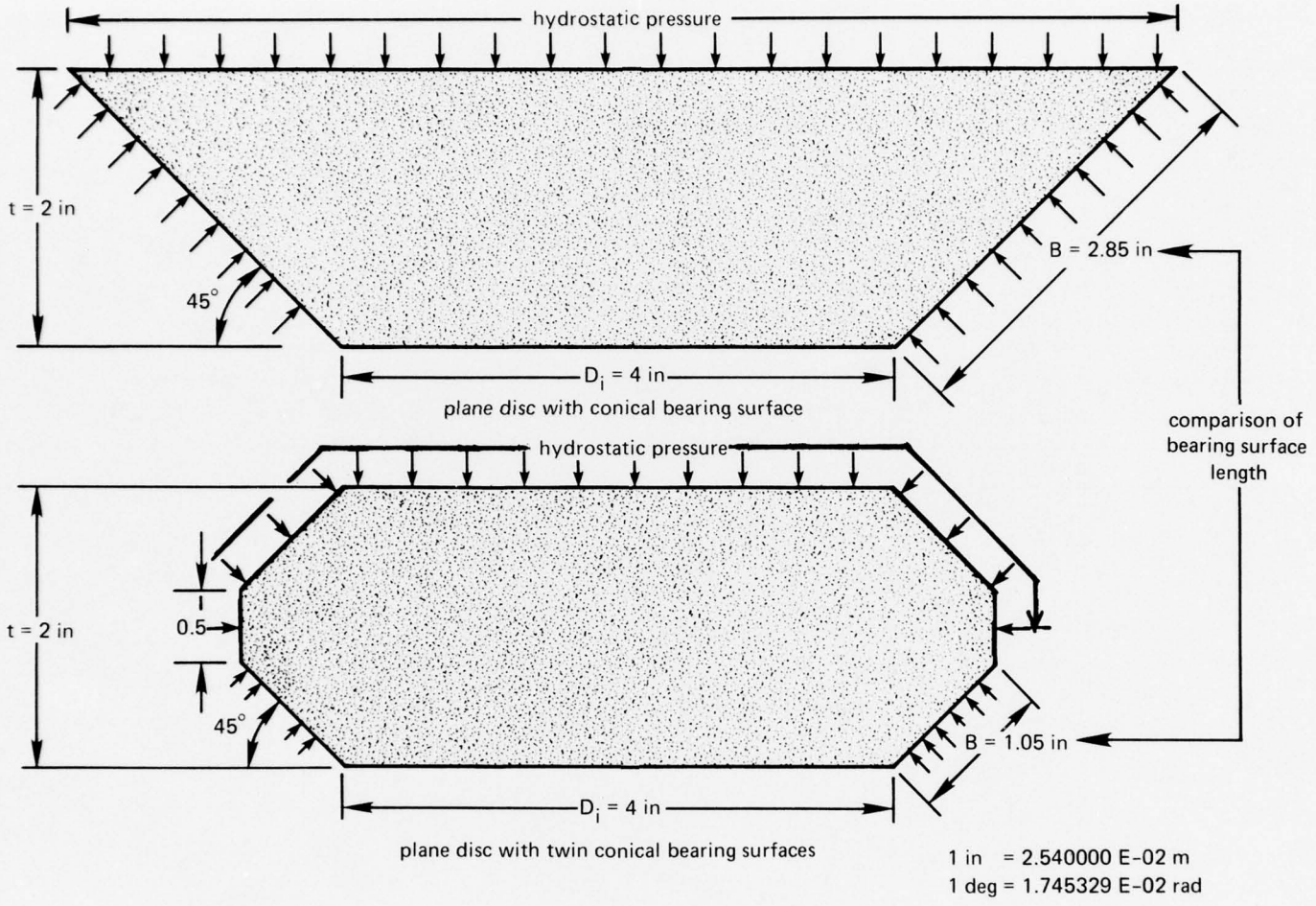

Figure 10.4. Comparison of two windows with $t/D_i = 0.5$. Note that the bearing surface of the twin-beveled window is less than 50 percent of the single-beveled window.

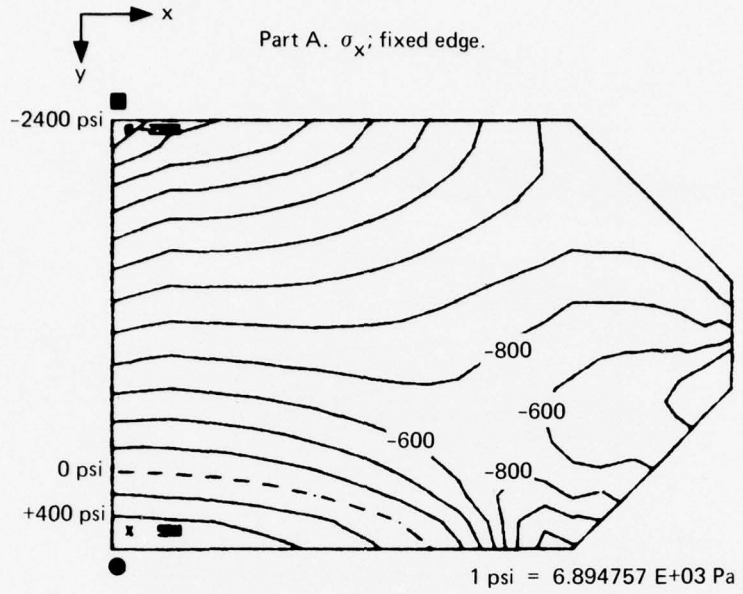

p = 1000 psi; stress contour = 200 psi
● maximum = 588.8 psi; ■ minimum = -2595.6 psi

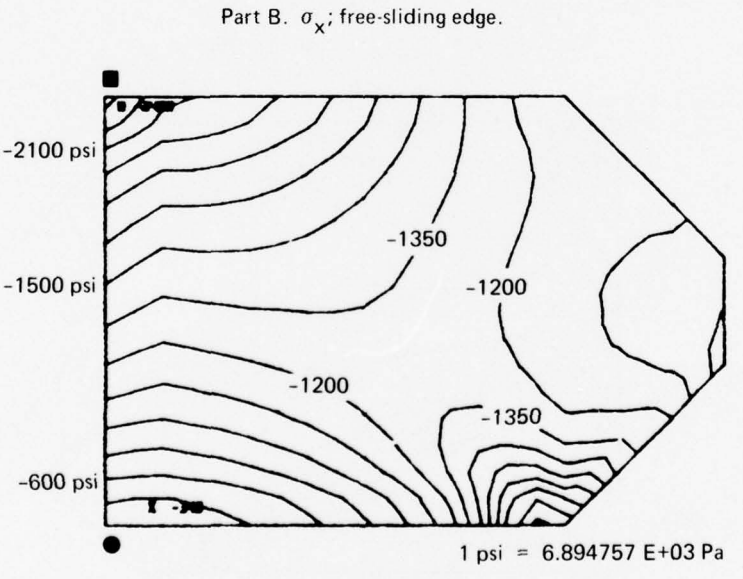

p = 1000 psi; stress contour = 150 psi
● maximum = -342.9 psi; ■ minimum = -2469.3 psi

Figure 10.5. Results of finite-element stress analysis for a twin-beveled plane disc with a 90-degree (1.57 radians) included conical angle and $t/D_i = 0.46$. Note that two boundary conditions which bracket the actual interaction between the bearing surface on the window and the mounting seat were used in the analysis. Compare the values of maximum stresses with those for single-beveled plane discs with identical dimensions.

Part C. σ_{hoop}; fixed edge.

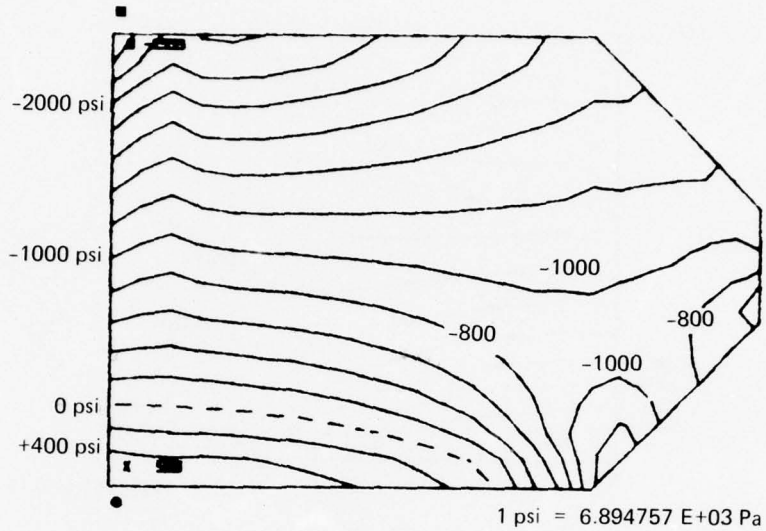

1 psi = 6.894757 E+03 Pa

p = 1000 psi; stress contour = 200 psi

● maximum = 588.8 psi; ■ minimum = - 2595.6 psi

Part D. σ_{hoop}; free-sliding edge.

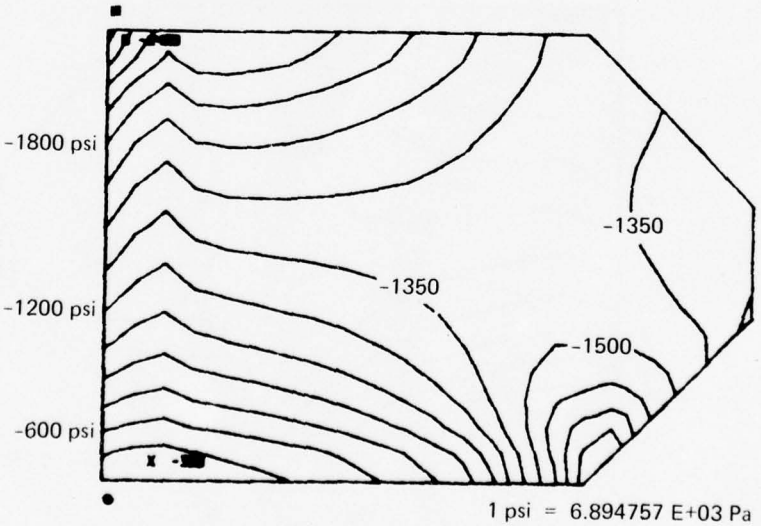

1 psi = 6.894757 E+03 Pa

p = 1000 psi; stress contour = 150 psi

● maximum = -308.5 psi; ■ minimum = -2469.3 psi

Figure 10.5. Continued.

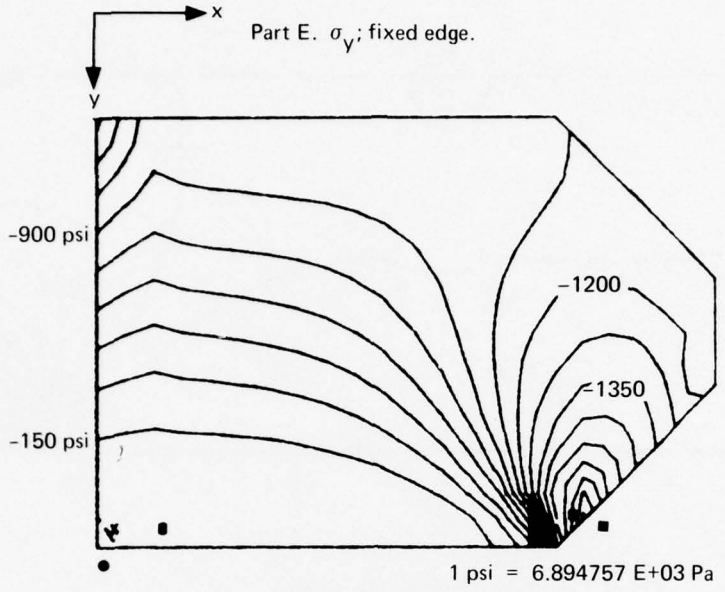

p = 1000 psi; stress contour = 150 psi
● maximum = 8.9 psi; ■ minimum = -2818.7 psi

Part F. σ_y; free-sliding edge.

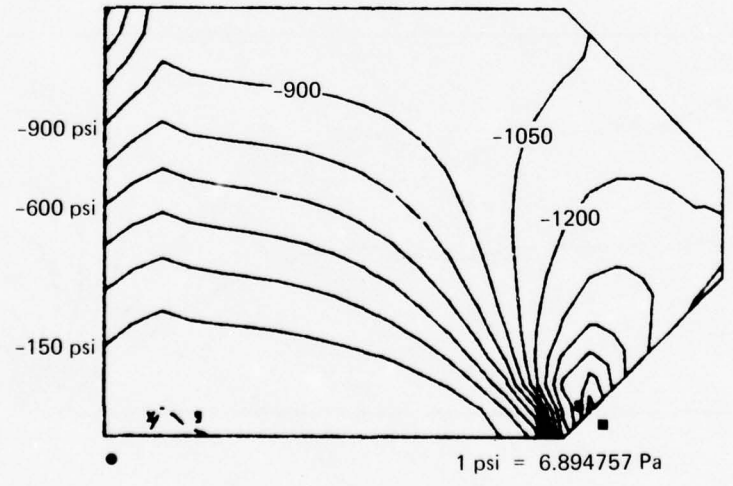

p = 1000 psi; stress contour = 150 psi
● maximum = 9.5 psi; ■ minimum = -2335.5 psi

Figure 10.5. Continued.

Part A. σ_y; fixed edge.

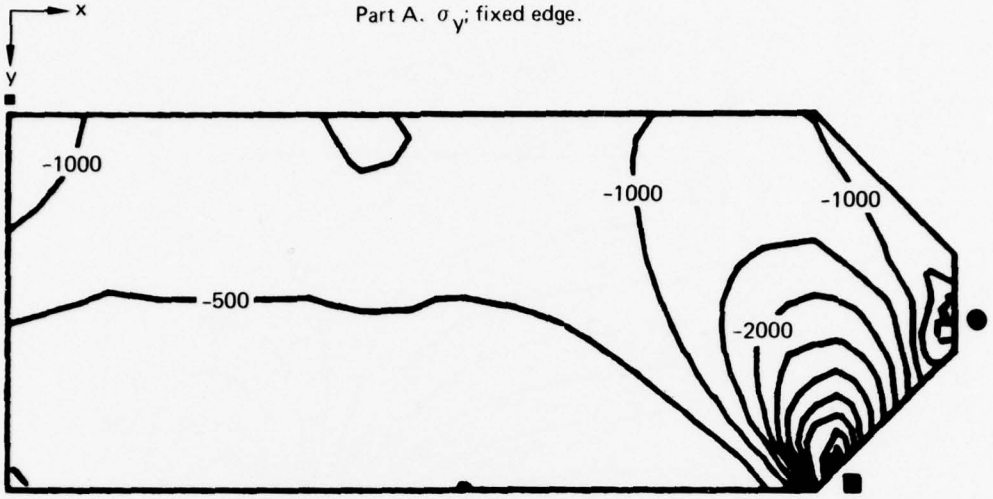

1 psi = 6.894757 E+03 Pa

p = 1000 psi; stress contour = 500 psi
● maximum = +1404.3 psi; ■ minimum = -6611.3 psi

Part B. σ_y; free-sliding edge.

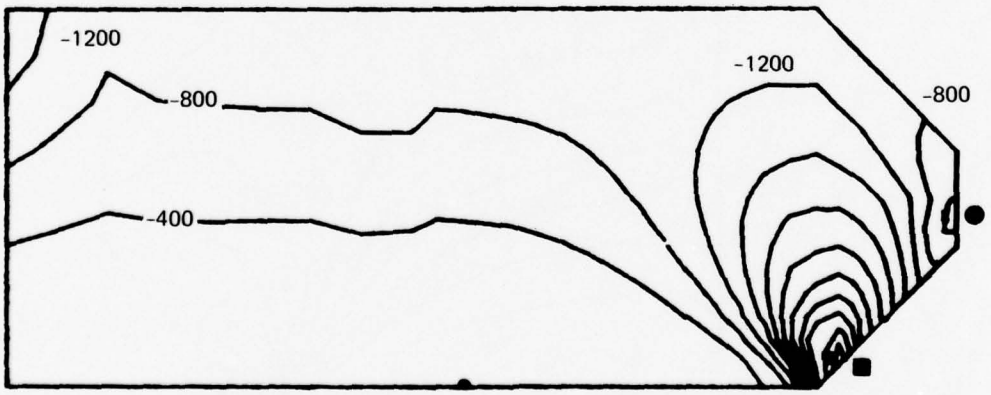

1 psi = 6.894757 E+03 Pa

p = 1000 psi; stress contour = 400 psi
● maximum = 260 psi; ■ minimum = -5792.1 psi

Figure 10.6. Results of finite-element stress analysis for a twin-beveled plane disc with a 90-degree (1.57 radians) included conical angle and $t/D_i = 0.23$.

Part C. σ_x; fixed edge.

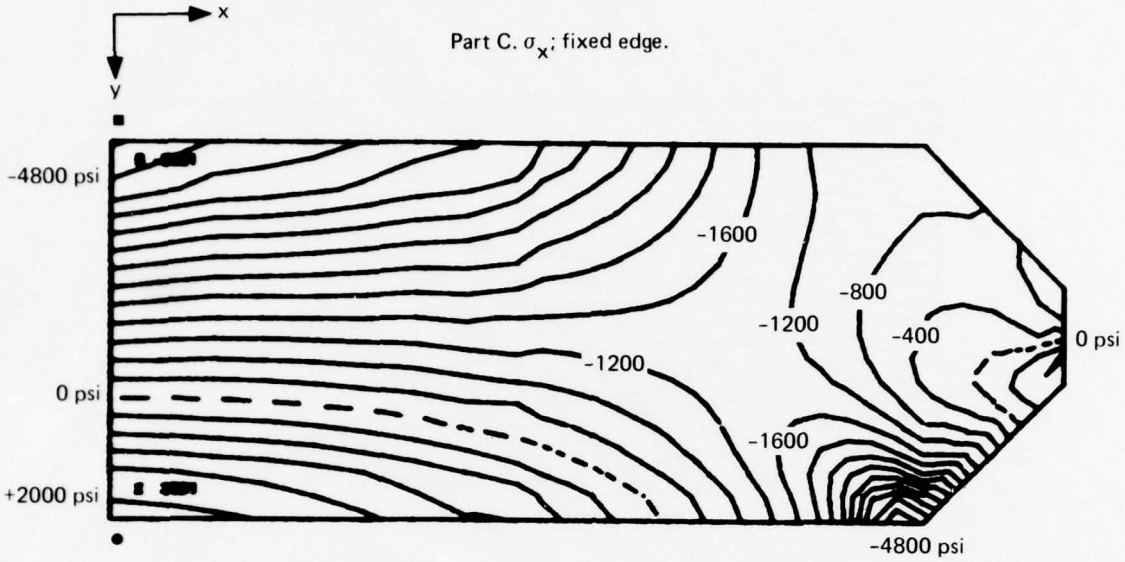

1 psi = 6.894757 E+03 Pa

p = 1000 psi; stress contour = 400 psi

● maximum = 2204.5 psi; ■ minimum = -5261.2 psi

Part D. σ_x; free-sliding edge.

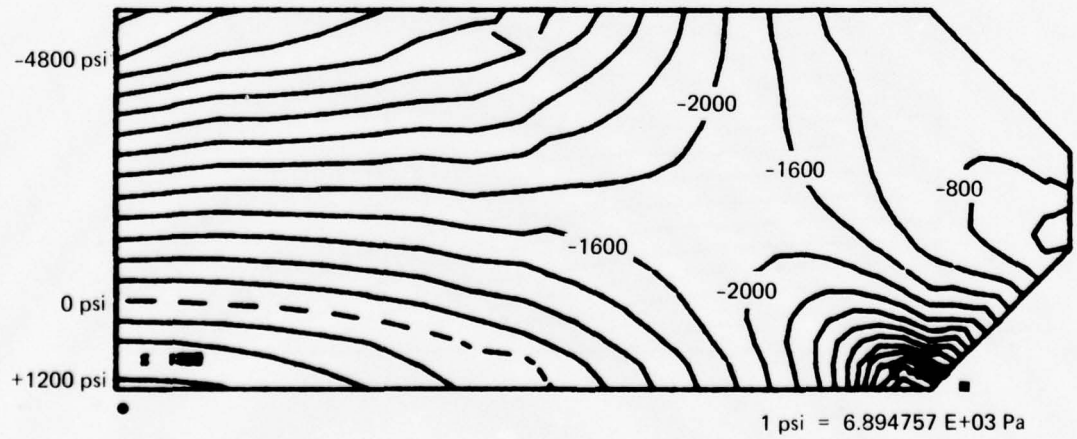

1 psi = 6.894757 E+03 Pa

p = 1000 psi; stress contour = 400 psi

● maximum = 1299.3 psi; ■ minimum = -5992.7 psi

Figure 10.6. Continued.

Part E. σ_{hoop}; fixed edge;

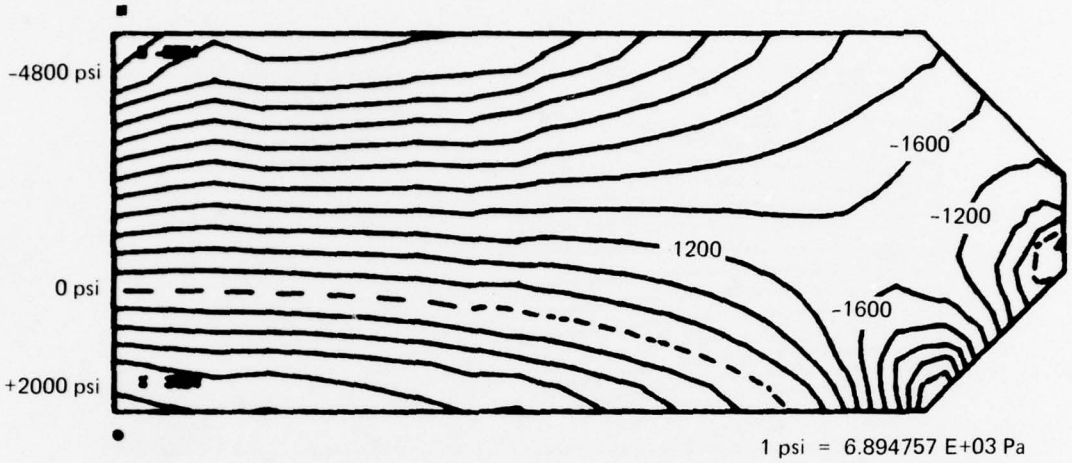

1 psi = 6.894757 E+03 Pa

p = 1000 psi; stress contour = 400 psi
● maximum = 2204.5 psi; ■ minimum = -5261 psi

Part F. σ_{hoop}; free-sliding edge.

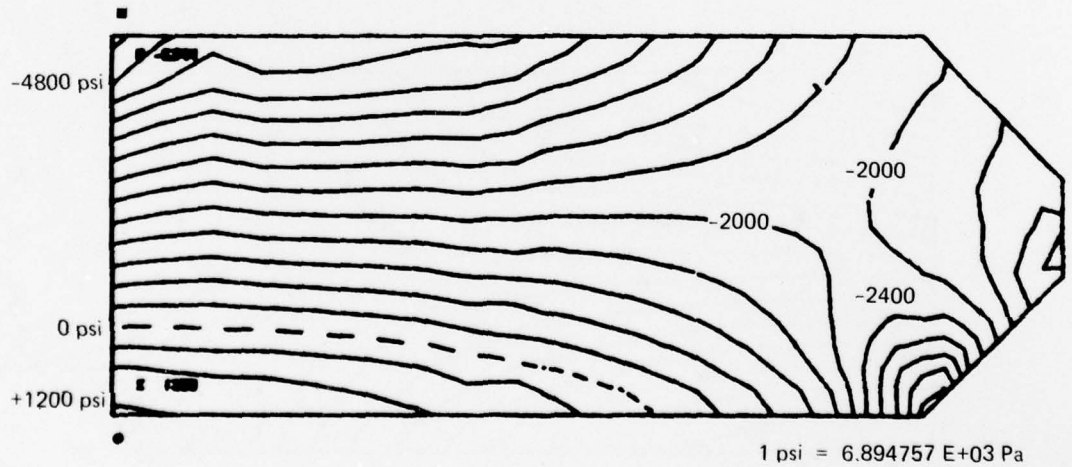

1 psi = 6.894757 E+03 Pa

p = 1000 psi; stress contour = 400 psi
● maximum = 1299.3 psi; ■ minimum = -5344.6 psi

Figure 10.6. Continued.

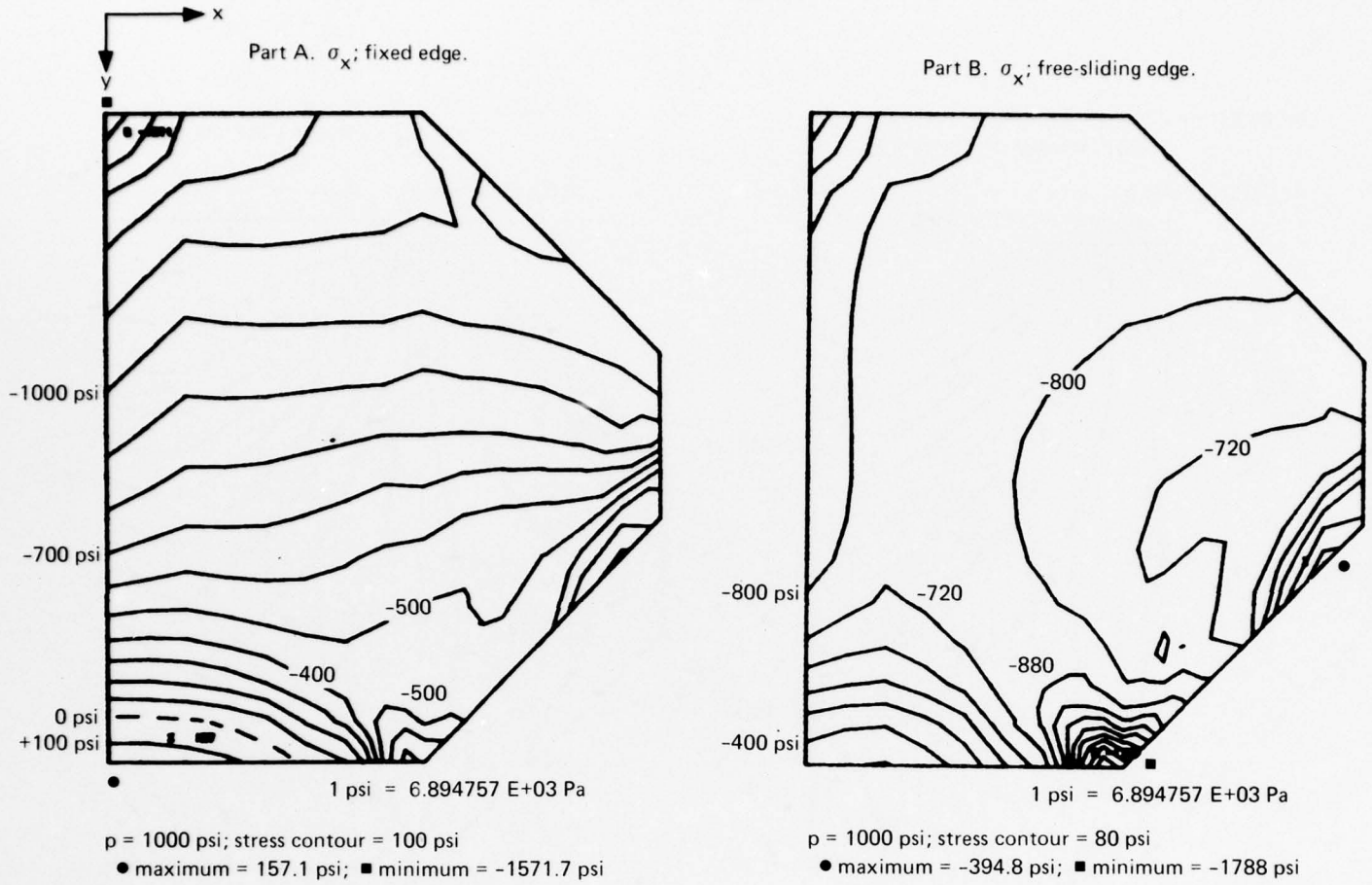

Figure 10.7. Results of finite-element stress analysis for a twin-beveled plane disc with a 90-degree (1.57 radians) included conical angle and $t/D_i = 1.0$.

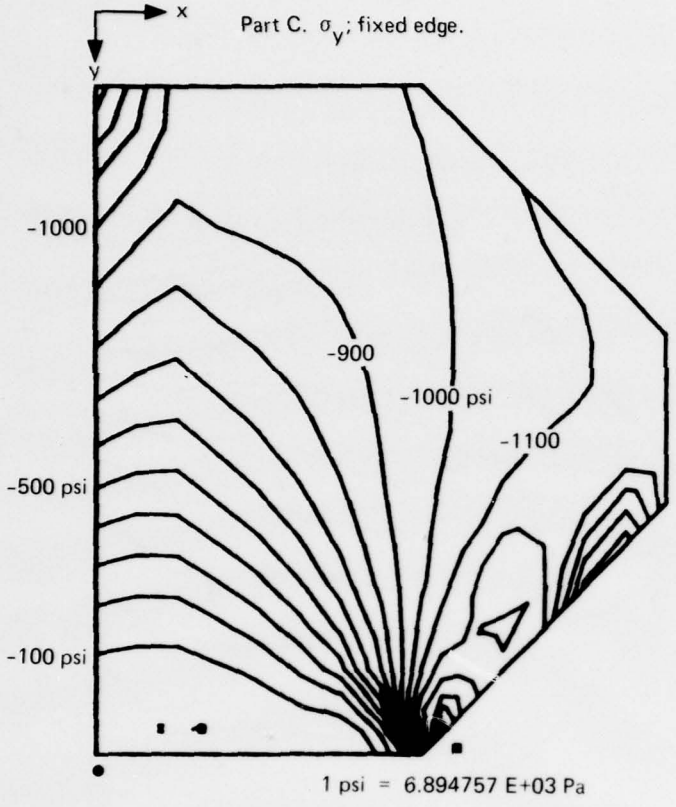

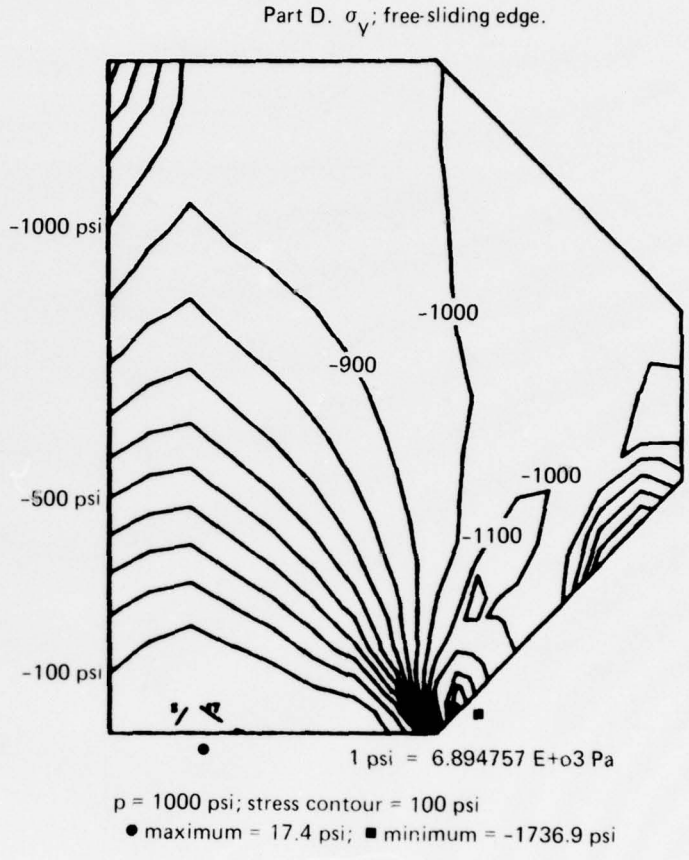

Figure 10.7. Continued.

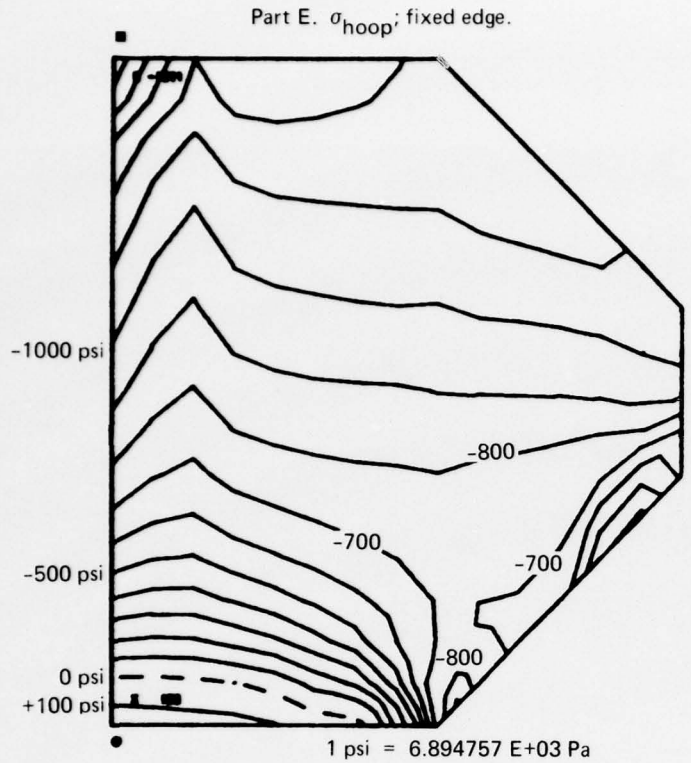

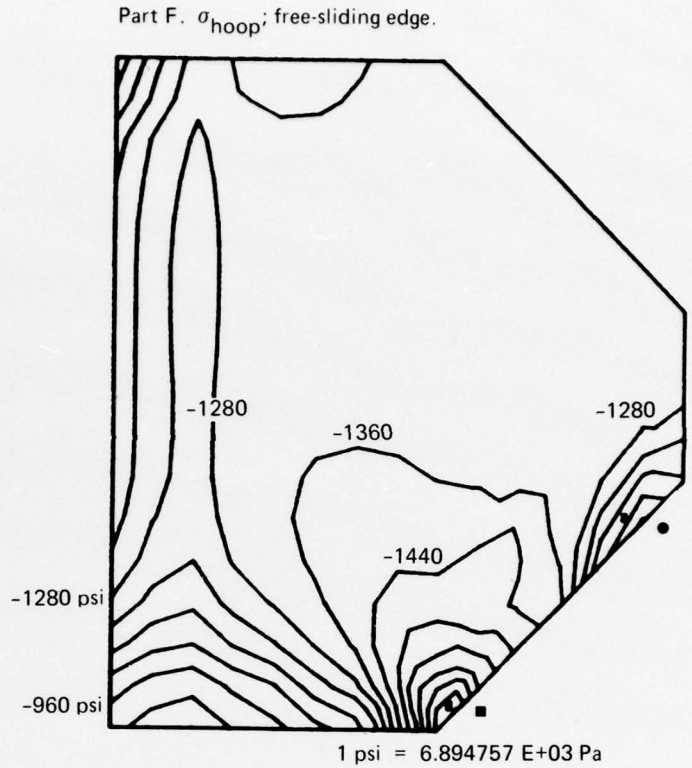

Figure 10.7. Continued.

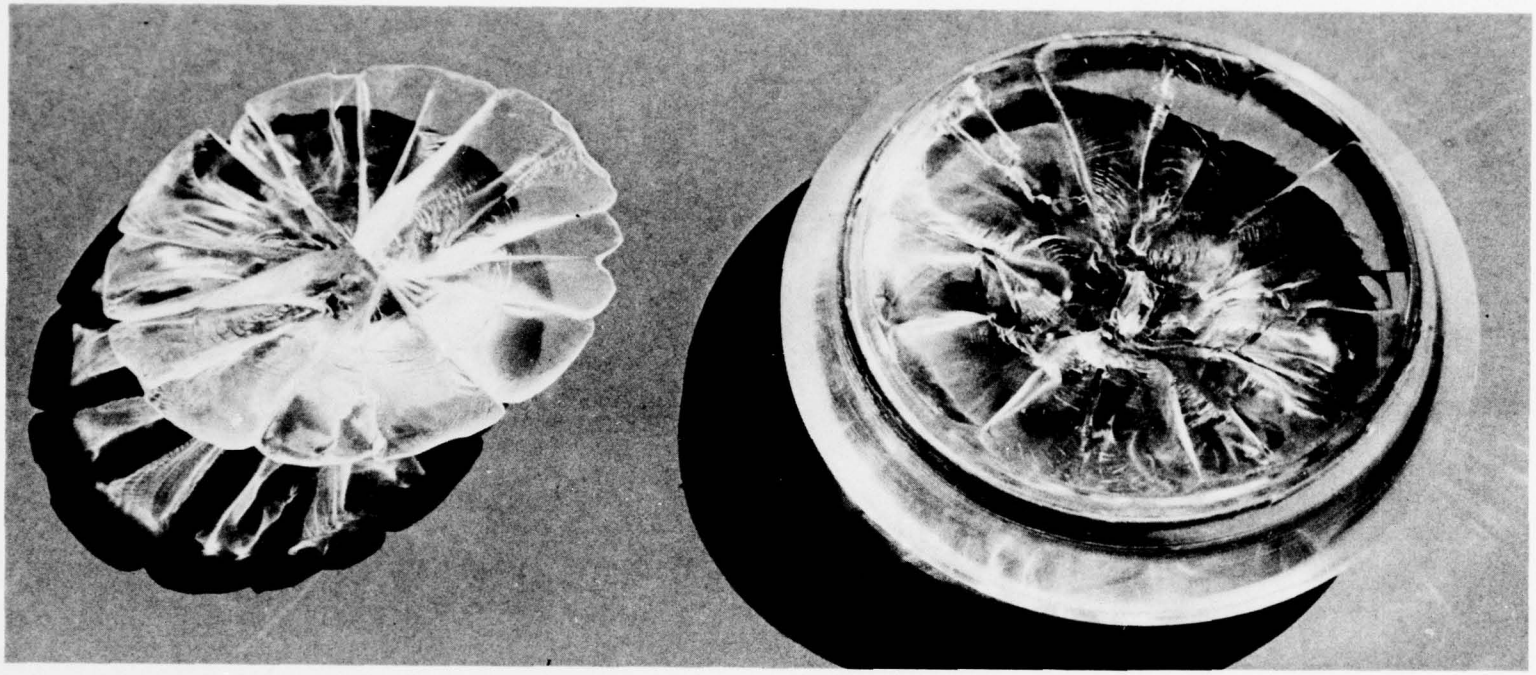

Figure 10.8. Fracture surface on a twin-beveled plane disc after short-term hydrostatic loading to fracture initiation (t/D_i = 0.32; D_o = 4 inches (10 centimeters); test pressure = 9300 pounds per square inch (64 megapascals).

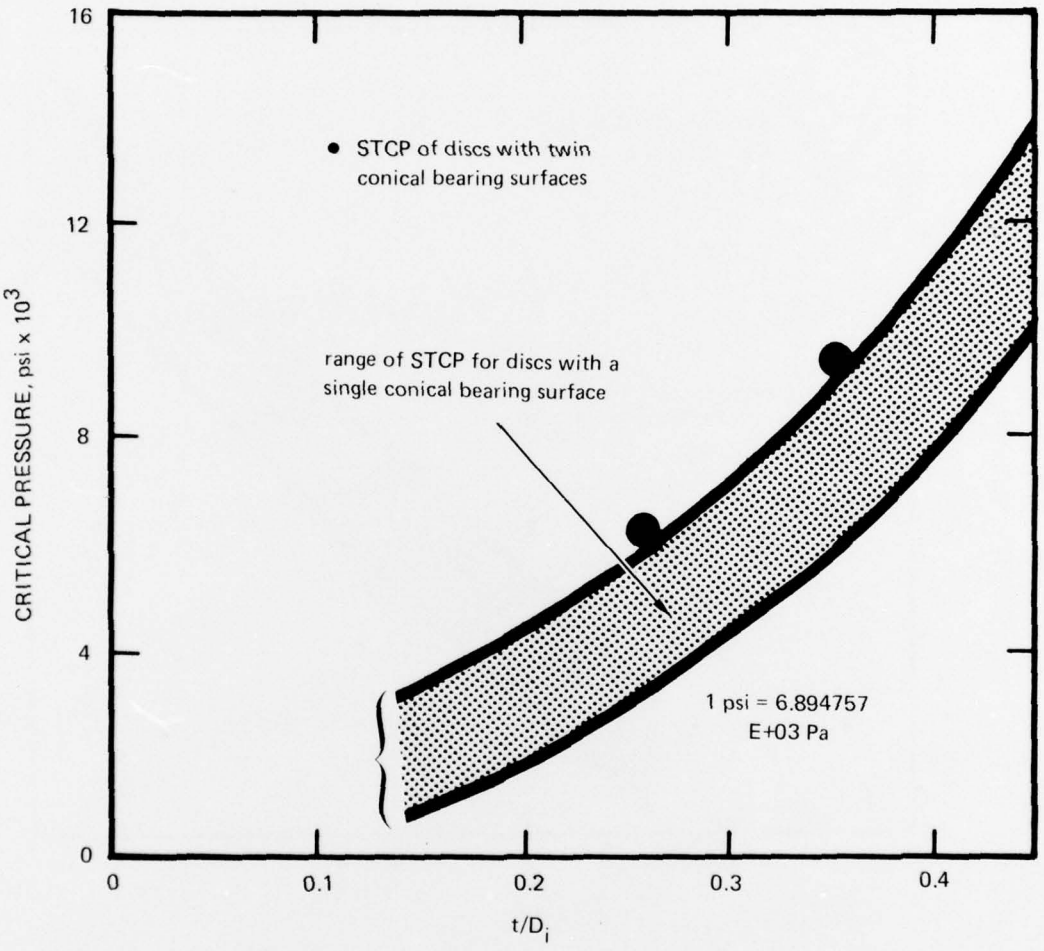

Figure 10.9. Comparison of short-term critical pressures (STCP) for discs with single and twin conical bearing surfaces with 60-degree (1.04 radians) included angle.

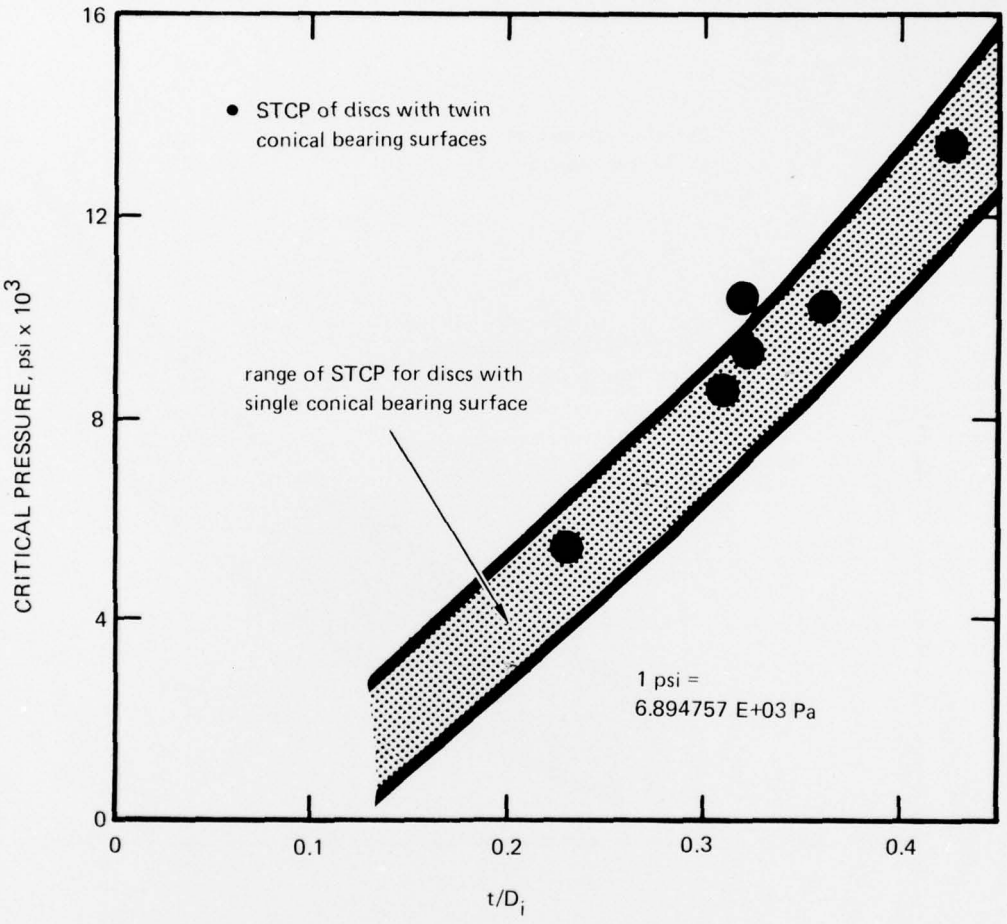

Figure 10.10. Comparison of short-term critical pressures (STCP) for discs with single and twin conical bearing surfaces with 90-degree (1.57 radians) included angle.

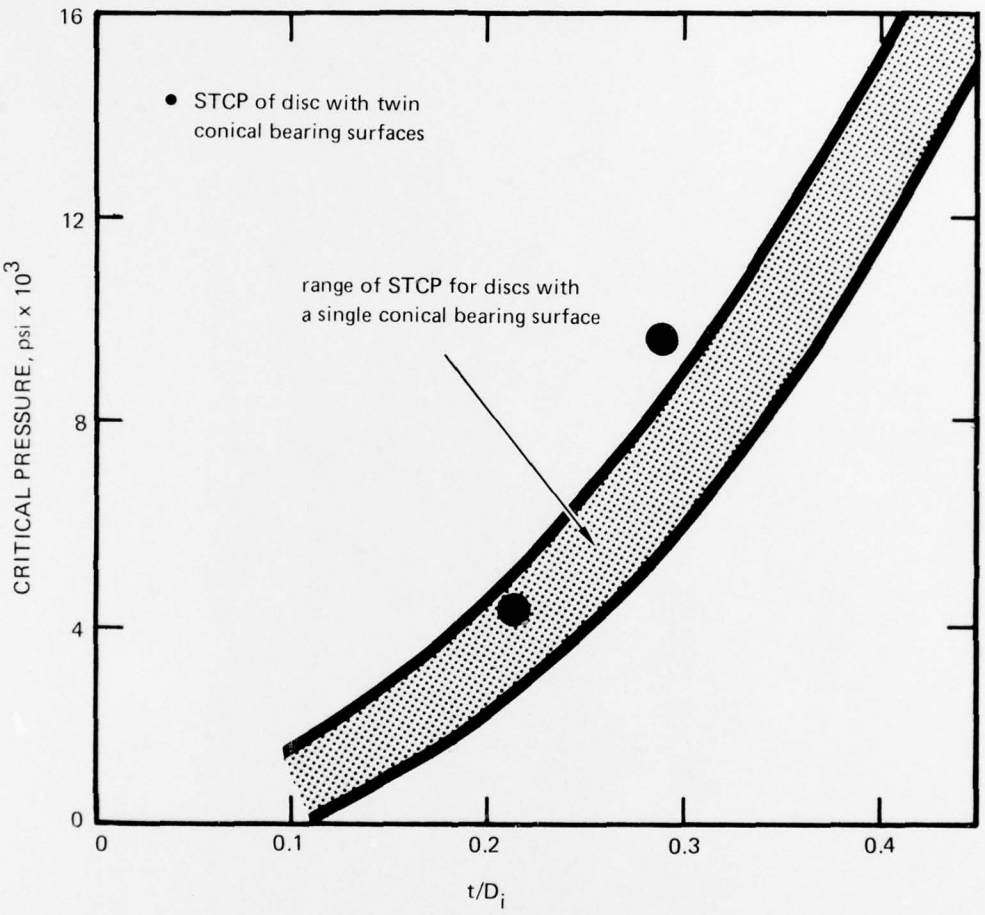

Figure 10.11. Comparison of short-term critical pressures (STCP) for discs with single and twin conical bearing surfaces with 120-degree (2.09 radians) included angle.

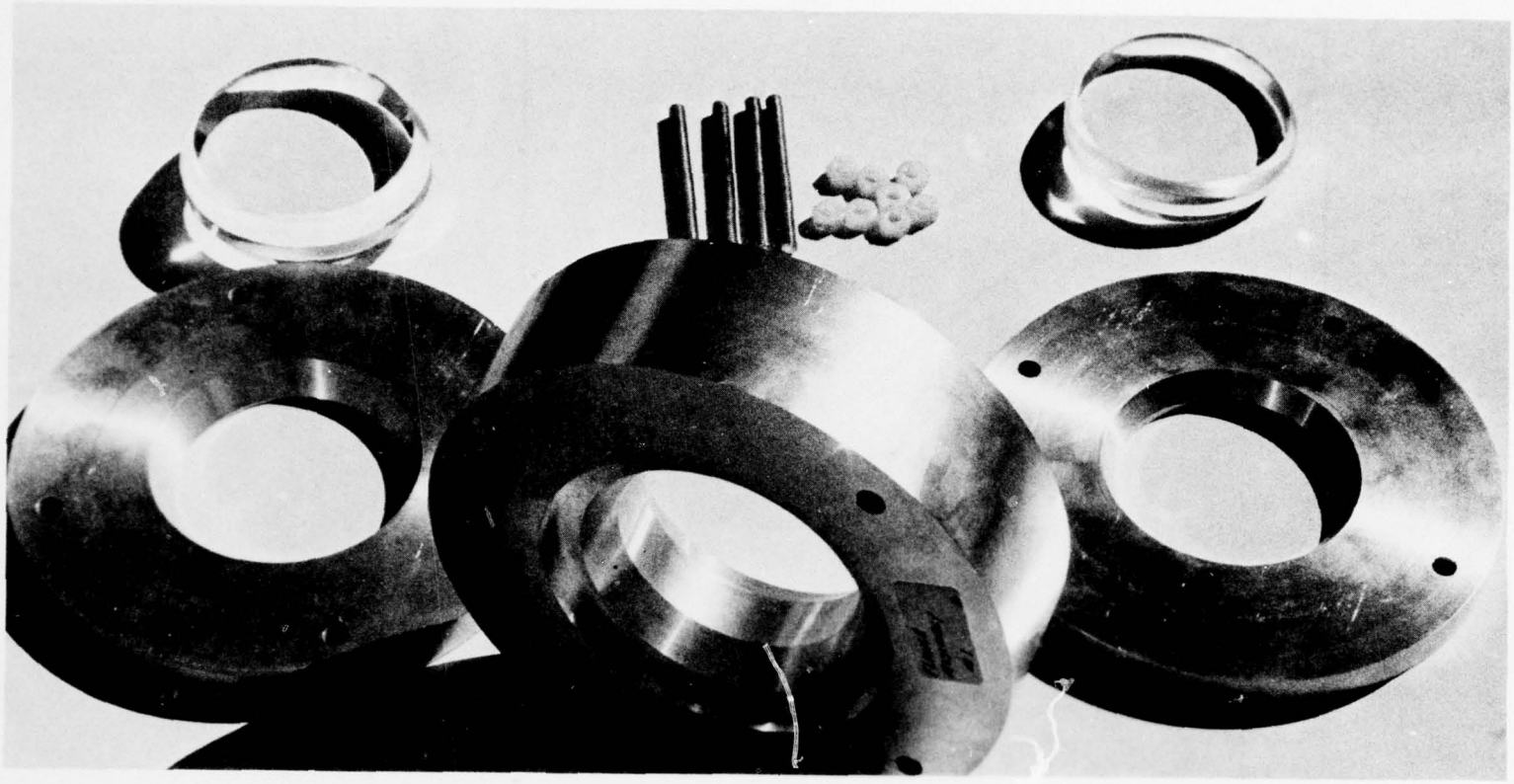

Figure 10.12. Mounting used for pressure cycling of plane discs with twin conical bearing surfaces. Two discs were tested back-to-back with an air space between them. The seal was similar to the one in figure 10.16. No cracks were observed on the bearing surfaces after 1000 8-hour pressure cycles to 500 pounds per square inch (3.45 megapascals) at 75°F (24°C).

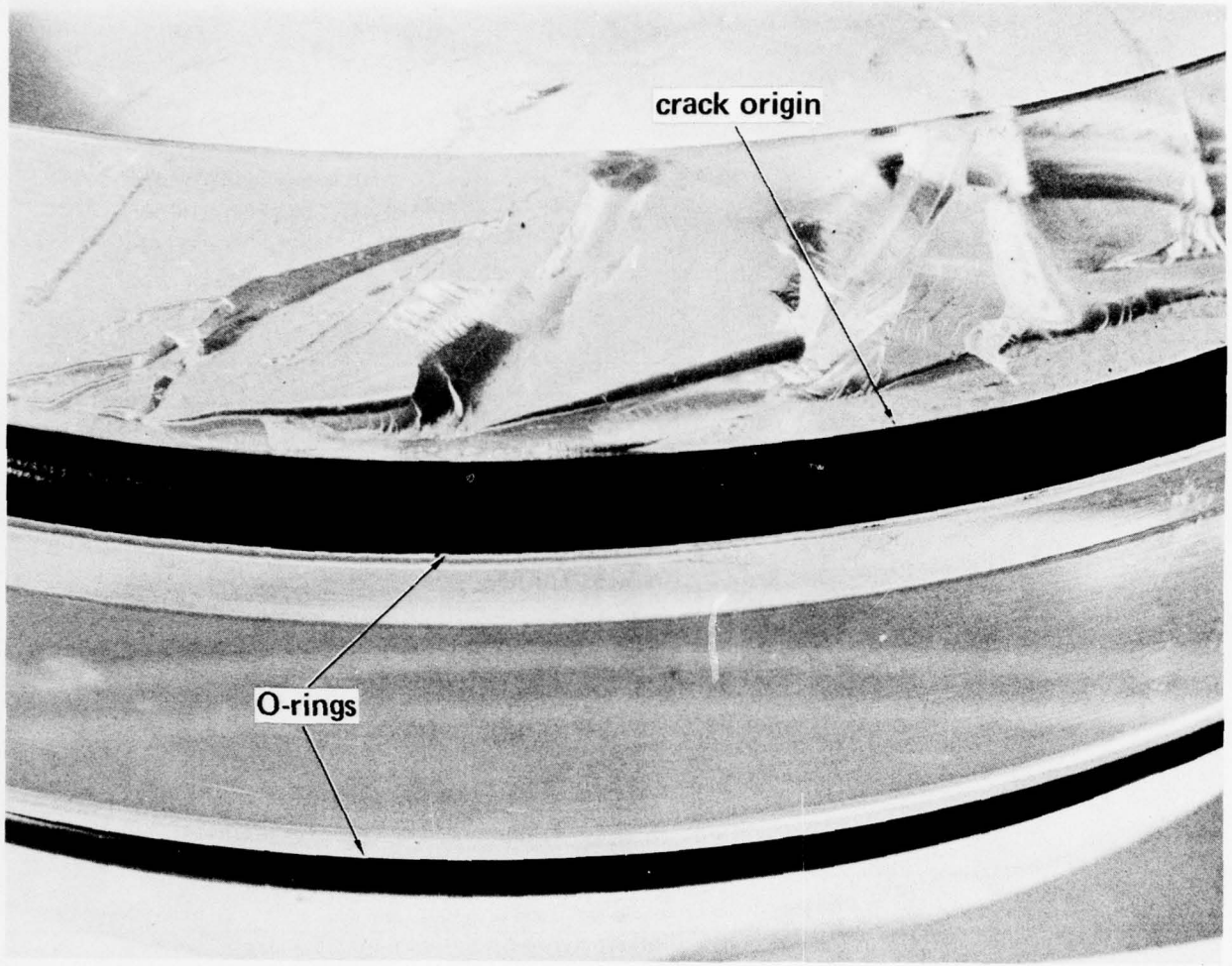

Figure 10.13. Plane disc with twin-beveled bearing surfaces showing fractures initiated by the O-ring grooves in the bearing surfaces.

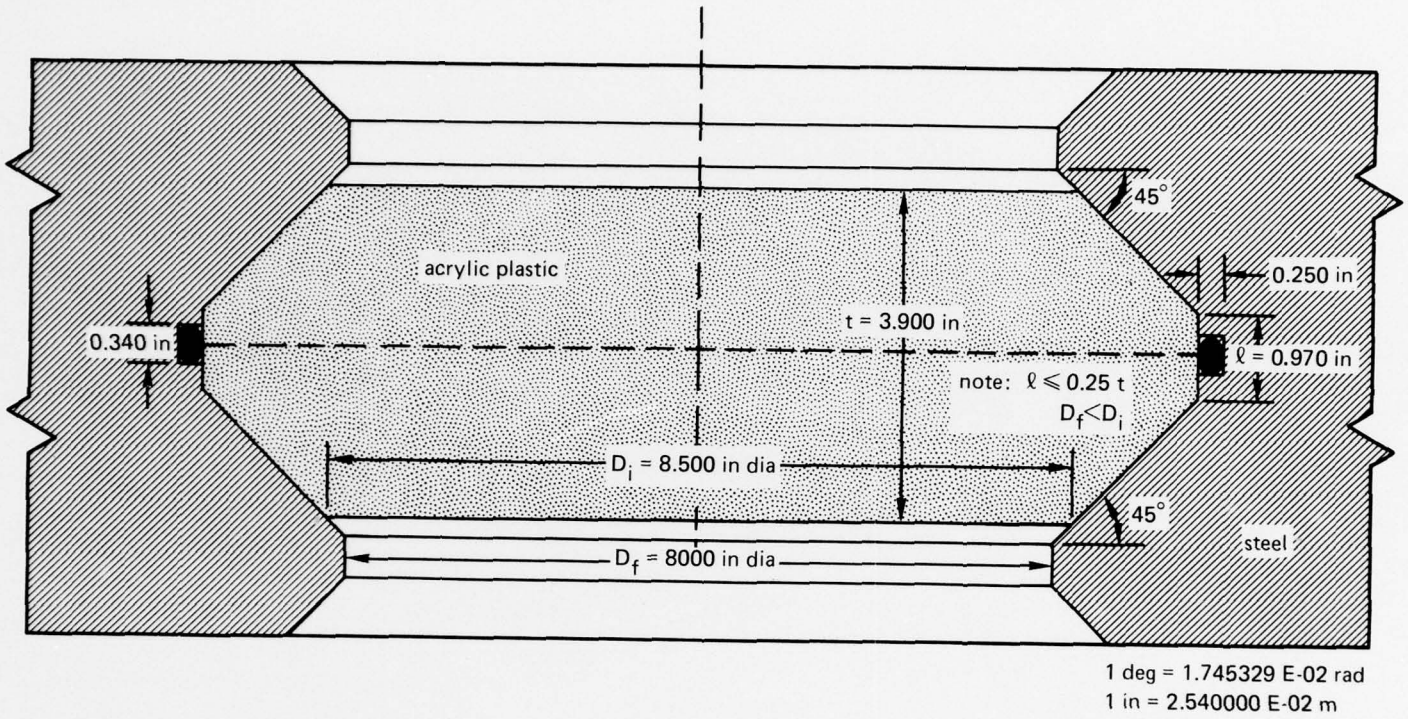

Figure 10.14. Viewport with twin-beveled plane disc window for 1600-pound-per-square-inch (11 megapascals) service in the 0 to 120°F (-18 to 49°C) temperature range. Note the seat overhang on the mounting flange to provide support to the axially displacing window ($t/D_i = 0.46$).

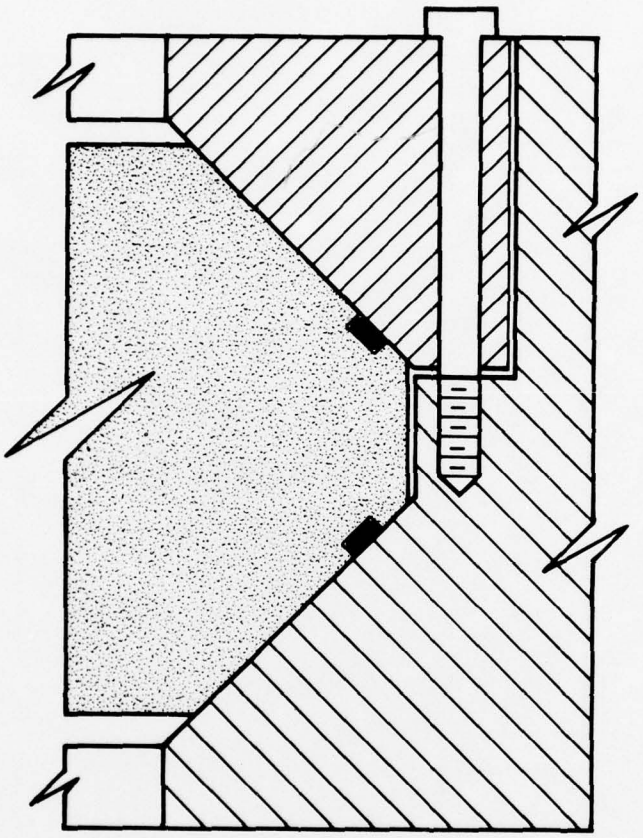

Figure 10.15. Sealing arrangement for twin-beveled discs using axially compressed O-rings located in the grooves on the bearing surfaces of the window. This is not a recommended design, as the O-ring grooves in the bearing surfaces significantly decrease the fatigue life of the window.

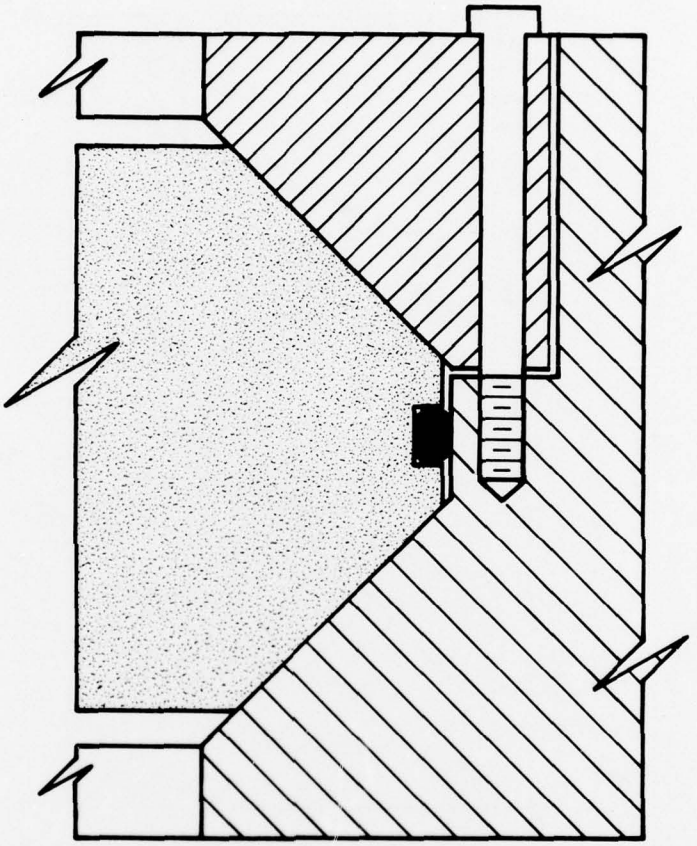

Figure 10.16. Sealing arrangement for twin-beveled discs using a radially compressed O-ring located in a groove on the cylindrical surface of the window. This design is only marginally acceptable, as the deep O-ring groove will initiate cracks if the window is accidentally overpressurized in service.

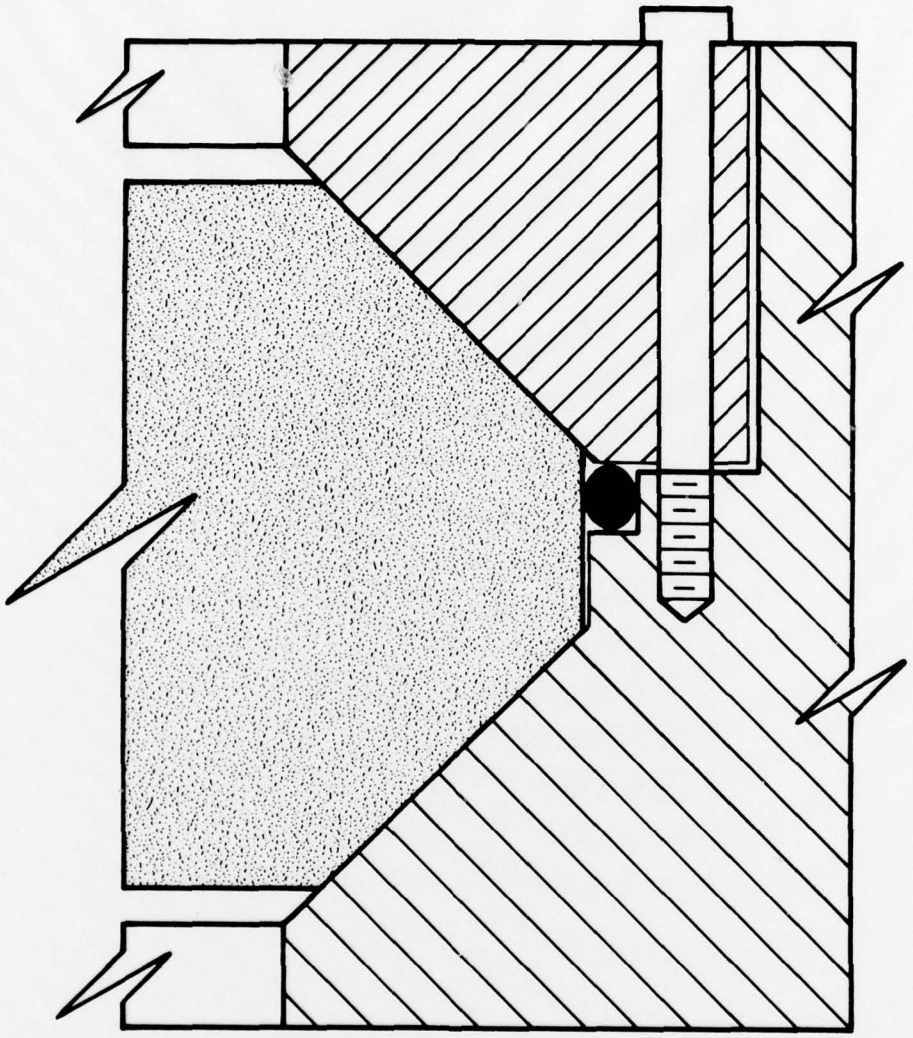

Figure 10.17. Sealing arrangement for twin-beveled discs using a radially and axially compressed O-ring located on a ledge of the cylindrical surface in the mounting. This design is recommended, as it provides very positive sealing without decreasing the fatigue life of the window.

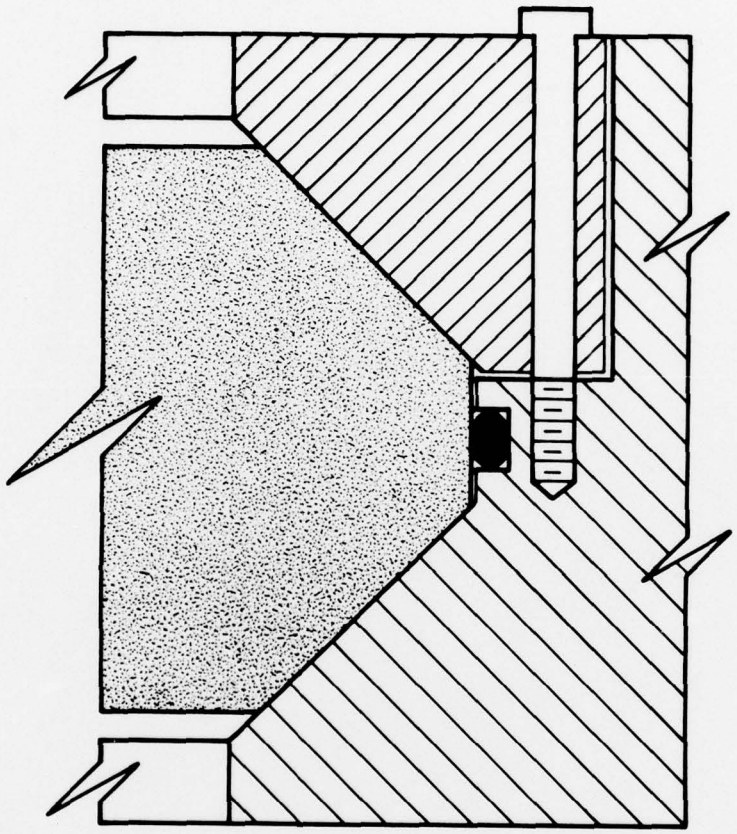

Figure 10.18. Sealing arrangement for twin-beveled discs using a radially compressed O-ring located in a groove machined into the cylindrical surface of the mounting. This design is acceptable because the O-ring groove does not decrease the fatigue life of the window. Inaccessibility to the bottom of the groove makes it difficult to clean out the rust during scheduled maintenance overhauls of the viewport assembly.